Volume 178 Number 1

THE BIOLOGICAL BULLETIN

FEBRUARY, 1990

Published by the Marine Biological Laboratory

THE
BIOLOGICAL BULLETIN

PUBLISHED BY
THE MARINE BIOLOGICAL LABORATORY

FEBRUARY, 1990

Printed and Issued by
LANCASTER PRESS, Inc.
PRINCE & LEMON STS.
LANCASTER, PA

THE BIOLOGICAL BULLETIN

THE BIOLOGICAL BULLETIN is published six times a year by the Marine Biological Laboratory, MBL Street, Woods Hole, Massachusetts 02543.

Subscriptions and similar matter should be addressed to Subscription Manager, THE BIOLOGICAL BULLETIN, Marine Biological Laboratory, Woods Hole, Massachusetts 02543. Single numbers, $25.00. Subscription per volume (three issues), $57.50 ($115.00 per year for six issues).

Communications relative to manuscripts should be sent to Michael J. Greenberg, Editor-in-Chief, or Pamela L. Clapp, Managing Editor, at the Marine Biological Laboratory, Woods Hole, Massachusetts 02543. Telephone: (508) 548-3705, ext. 428. FAX: 508-540-6902.

POSTMASTER: Send address changes to THE BIOLOGICAL BULLETIN, Marine Biological Laboratory, Woods Hole, MA 02543.

Second-class postage paid at Woods Hole, MA, and additional mailing offices.
ISSN 0006-3185

INSTRUCTIONS TO AUTHORS

The Biological Bulletin accepts outstanding original research reports of general interest to biologists throughout the world. Papers are usually of intermediate length (10–40 manuscript pages). Very short papers (less than 9 manuscript pages including tables, figures, and bibliography) will be published in a separate section entitled "Notes." A limited number of solicited review papers may be accepted after formal review. A paper will usually appear within four months after its acceptance.

The Editorial Board requests that manuscripts conform to the requirements set below; those manuscripts that do not conform will be returned to authors for correction before review.

1. ***Manuscripts.*** Manuscripts, including figures, should be submitted in triplicate. (Xerox copies of photographs are not acceptable for review purposes.) The original manuscript must be typed in no smaller than 12 pitch, using double spacing (*including* figure legends, footnotes, bibliography, etc.) on one side of 16- or 20-lb. bond paper, 8½ by 11 inches. Please, no right justification. Manuscripts should be proofread carefully and errors corrected legibly in black ink. Pages should be numbered consecutively. Margins on all sides should be at least 1 inch (2.5 cm). Manuscripts should conform to the *Council of Biology Editors Style Manual*, 4th Edition (Council of Biology Editors, 1978) and to American spelling. Unusual abbreviations should be kept to a minimum and should be spelled out on first reference as well as defined in a footnote on the title page. Manuscripts should be divided into the following components: Title page, Abstract (of no more than 200 words), Introduction, Materials and Methods, Results, Discussion, Acknowledgments, Literature Cited, Tables, and Figure Legends. In addition, authors should supply a list of words and phrases under which the article should be indexed.

2. ***Title page.*** The title page consists of: a condensed title or running head of no more than 35 letters and spaces, the manuscript title, authors' names and appropriate addresses, and footnotes listing present addresses, acknowledgments or contribution numbers, and explanation of unusual abbreviations.

3. ***Figures.*** The dimensions of the printed page, 7 by 9 inches, should be kept in mind in preparing figures for publication. We recommend that figures be about 1½ times the linear dimensions of the final printing desired, and that the ratio of the largest to the smallest letter or number and of the thickest to the thinnest line not exceed 1:1.5. Explanatory matter generally should be included in legends, although axes should always be identified on the illustration itself. Figures should be prepared for reproduction as either line cuts or halftones. Figures to be reproduced as line cuts should be unmounted glossy photographic reproductions or drawn in black ink on white paper, good-quality tracing cloth or plastic, or blue-lined coordinate paper. Those to be reproduced as halftones should be mounted on board, with both designating numbers or letters and scale bars affixed directly to the figures. All figures should be numbered in consecutive order, with no distinction between text and plate figures. The author's name and an arrow indicating orientation should appear on the reverse side of all figures.

4. ***Tables, footnotes, figure legends, etc.*** Authors should follow the style in a recent issue of *The Biological Bulletin* in preparing table headings, figure legends, and the like. Because of the high cost of setting tabular material in type, authors are asked to limit such material as much as possible. Tables, with their headings and footnotes, should be typed on separate sheets, numbered with consecutive Roman numerals, and placed after the Literature Cited. Figure legends should contain enough information to make the figure intelligible separate from the text. Legends should be typed double spaced, with consecutive Arabic numbers, on a separate sheet at the end of the paper. Footnotes should be limited to authors' current addresses, acknowledgments or contribution numbers, and explanation of unusual abbreviations. All such footnotes should appear on the title page. Footnotes are not normally permitted in the body of the text.

5. ***Literature cited.*** In the text, literature should be cited by the Harvard system, with papers by more than two authors cited as Jones *et al.*, 1980. Personal communications and material in preparation or in press should be cited in the text only, with author's initials and institutions, unless the material has been formally accepted and a volume number can be supplied. The list of references following the text should be headed Literature Cited, and must be typed double spaced on separate

pages, conforming in punctuation and arrangement to the style of recent issues of *The Biological Bulletin*. Citations should include complete titles and inclusive pagination. Journal abbreviations should normally follow those of the U. S. A. Standards Institute (USASI), as adopted by BIOLOGICAL ABSTRACTS and CHEMICAL ABSTRACTS, with the minor differences set out below. The most generally useful list of biological journal titles is that published each year by BIOLOGICAL ABSTRACTS (BIOSIS List of Serials; the most recent issue). Foreign authors, and others who are accustomed to using THE WORLD LIST OF SCIENTIFIC PERIODICALS, may find a booklet published by the Biological Council of the U.K. (obtainable from the Institute of Biology, 41 Queen's Gate, London, S.W.7, England, U.K.) useful, since it sets out the WORLD LIST abbreviations for most biological journals with notes of the USASI abbreviations where these differ. CHEMICAL ABSTRACTS publishes quarterly supplements of additional abbreviations. The following points of reference style for THE BIOLOGICAL BULLETIN differ from USASI (or modified WORLD LIST) usage:

A. Journal abbreviations, and book titles, all underlined (for *italics*)

B. All components of abbreviations with initial capitals (not as European usage in WORLD LIST *e.g. J. Cell. Comp. Physiol.* NOT *J. cell. comp. Physiol.*)

C. *All* abbreviated components must be followed by a period, whole word components *must not* (*i.e. J. Cancer Res.*)

D. Space between all components (*e.g. J. Cell. Comp. Physiol.*, not *J.Cell.Comp.Physiol.*)

E. Unusual words in journal titles should be spelled out in full, rather than employing new abbreviations invented by the author. For example, use *Rit Vísindafjélags Islendinga* without abbreviation.

F. All single word journal titles in full (*e.g. Veliger, Ecology, Brain*).

G. The order of abbreviated components should be the same as the word order of the complete title (*i.e. Proc.* and *Trans.* placed where they appear, not transposed as in some BIOLOGICAL ABSTRACTS listings).

H. A few well-known international journals in their preferred forms rather than WORLD LIST or USASI usage (*e.g. Nature, Science, Evolution* NOT *Nature, Lond., Science, N.Y.; Evolution, Lancaster, Pa.*)

6. ***Reprints, page proofs, and charges.*** Authors receive their first 100 reprints (without covers) free of charge. Additional reprints may be ordered at time of publication and normally will be delivered about two to three months after the issue date. Authors (or delegates for foreign authors) will receive page proofs of articles shortly before publication. They will be charged the current cost of printers' time for corrections to these (other than corrections of printers' or editors' errors). Other than these charges for authors' alterations, *The Biological Bulletin* does not have page charges.

Reference: *Biol. Bull.* **178**: 1–9. (February, 1990)

The Role of Arachidonic Acid and Eicosatrienoic Acids in the Activation of Spermatozoa in *Arenicola marina* L. (Annelida: Polychaeta)

M. G. BENTLEY[1]*, S. CLARK[2], AND A. A. PACEY[1]

[1]*Gatty Marine Laboratory, University of St. Andrews, St Andrews, Fife, KY16 8LB, Scotland, U.K., and* [2]*Dove Marine Laboratory and Department of Biology, University of Newcastle upon Tyne, Newcastle upon Tyne, NE1 7RU, U.K.*

Abstract. Partial purification of a sperm maturation factor (SMF) in the intertidal polychaete *Arenicola marina* has implicated arachidonic acid, an arachidonic metabolite, or a similar substance as the active factor from the prostomium. The effects of a number of 20-carbon fatty acids on inactive spermatozoa are investigated, and this reveals that only arachidonic acid and 8,11,14-eicosatrienoic acid cause sperm activation. The use of argentation thin-layer chromatography to separate fatty acids with varying degrees of unsaturation reveals a component in prostomial lipid extract, which co-migrates with eicosatrienoic acids. Investigations using cyclooxygenase and lipoxygenase result in a loss of sperm-activating properties of both prostomial extract and fatty acids. The use of cyclooxygenase and lipoxygenase inhibitors has no effect. Bovine serum albumin (BSA) reduces the sperm activating properties of both fatty acids and prostomial extract in a dose-dependant way. Additional purification procedures using: (a) organic solvents and aqueous buffers and (b) ODS silica cartridges, demonstrate that the active fraction of prostomial extract co-elutes at every step with the 8,11,14-eicosatrienoic acid standard. Gas chromatography of methyl esters of prostomial lipid extract reveals the presence of a peak with an identical retention time to the methyl ester of authentic 8,11,14-eicosatrienoic acid standard. The results described here provide strong evidence that the active SMF in prostomial homogenate is not a fatty acid metabolite but the parent acid 8,11,14-eicosatrienoic acid. These results could only be made unequivocal by full structural analysis using mass spectrometry and NMR following capillary gas-liquid chromatography.

Received 28 August 1989; accepted 30 November 1989.

* To whom all correspondence should be addressed.

Introduction

Arenicola marina is a common intertidal polychaete. Its reproductive cycle is annual, with most populations found around the coasts of the British Isles spawning in the autumn or early winter (Howie, 1959). The reproductive biology of this species has been reviewed by Howie (1984). In both sexes, gamete proliferation occurs in the gonads, and early germ cells are released into the coelomic fluid where gametogenesis proceeds (Ashworth, 1904; Newell, 1948). Females approaching maturity are characterized by many oocytes that have completed vitellogenesis but are arrested in prophase of meiosis I; maturing males have many sperm morulae (Howie, 1959). Sperm morulae are plates of several hundred fully differentiated immotile spermatozoa, which are bound together at both the head and distal ends of the flagella (Newell, 1948; Bentley 1985, 1986a, b; Bentley and Pacey, 1989).

Spawning in both male and female *Arenicola marina* is a direct consequence of the maturation of the gametes. The maturation of the oocytes (entry into metaphase of meiosis I), and the breakdown of the sperm morulae to free-swimming spermatozoa, results in the immediate shedding of these from the ciliated funnels of the nephromixia (Howie, 1961b, c). Oocytes mature by the action of a maturation hormone (Howie, 1963, 1966) from the prostomium, which induces germinal vesicle breakdown *in vitro* (Meijer and Durchon, 1977). The dissociation of the sperm morulae in males is also brought about

by a prostomial maturation hormone (sperm maturation factor) (Howie, 1963, 1966), which is a lipid (Howie, 1961a; Bentley, 1985).

Bentley (1985) began purifying the sperm maturation factor (SMF) using thin-layer chromatography, indicating that it was a relatively polar lipid. Lipids recovered from the TLC plates were tested for SMF activity in an *in vitro* assay. Biological activity was recovered from areas of the TLC plates where a number of pharmacologically active, non-steroid lipids are found. Further TLC studies led Bentley (1986a) to suggest that SMF may be a metabolite of the 20-carbon polyunsaturated fatty acid—arachidonic acid. Arachidonic acid (5,8,11,14-eicosatetraenoic acid) is one of a number, and probably the most important, of 20-carbon polyunsaturated fatty acids that are naturally occurring precursors of a wide range of extremely biologically active compounds. These include the prostaglandins, HETE's (hydroxy-eicosatetraenoic acids), and leukotrienes. Roles for these compounds have been identified in a wide range of vertebrates and invertebrates. Their roles in invertebrates have been recently reviewed (Stanley-Samuelson, 1987) and we will not discuss them further here. However, it should be noted that arachidonic acid is metabolized by starfish oocytes (Meijer and Guerrier, 1984; Meijer *et al.*, 1984; Meijer *et al.*, 1986), and that this results in the breakdown of the germinal vesicle prior to fertilization.

In light of the information available on the chemical nature of SMF, the present investigation examines in detail the possible role of arachidonic acid and the related 8,11,14-eicosatrienoic acid in the activation of spermatozoa in *Arenicola marina*.

Materials and Methods

Gravid individuals of *Arenicola marina* were collected by digging in sand during low water of spring tides at St. Andrews Bay, Fife, Scotland, and Fairlie Sands, Ayrshire, Scotland. Specimens were maintained individually in seawater at 5°C in the laboratory until use. Sperm samples for bioassay use were removed from the coelomic cavity as described previously (Bentley and Pacey, 1989). *In vitro* assays of sperm morula suspensions were performed as described by Bentley (1985).

Preparation of prostomial lipid extracts

Prostomial lipid extracts were prepared from mature specimens of *Arenicola marina*. The prostomia were removed using iridectomy scissors, and were homogenized using an MSE Soniprep 150 ultrasonic disintegrator at 0°C. The lipid fraction was partitioned from the sample using an equal volume of chloroform:methanol (2:1 v/v). The organic layer from several extractions was removed, pooled, and dried over anhydrous sodium sulphite. The samples were then concentrated by removing the solvent mixture in a rotary evaporator. The dried lipid residues were redissolved in methanol before being assayed for biological activity or used in subsequent analytical procedures.

Thin-layer chromatography (TLC)

A sample of total lipid was applied to 20 × 20 × 0.25 cm pre-coated silica gel F_{254} TLC plates (Merck) using a 100 μl disposable micropipette. Prior to applying the sample, the plates were cleaned of any lipid contaminants by running the blank plate, in the solvent system to be used, for its full length. After allowing the solvent to evaporate, the plate was activated in an oven at 120°C for 30 min. The solvent system used was the upper phase of: ethyl acetate:2,2,4-trimethylpentane:acetic acid:water (45:25:10:50 v/v) (Salmon and Flower, 1982) and the plates were run in a vertical chamber until the solvent front had moved 12 cm up the plate. The solvent was then allowed to evaporate from the plate in a fume cupboard, and the spots were visualized by spraying the plate with 10% phosphomolybdic acid in ethanol. A second plate was run simultaneously with the above, but was not sprayed with phosphomolybdic acid. Areas corresponding to the visualized spots on the first TLC plate were scraped off the plate and the lipids eluted in methanol and tested for biological activity as described above.

Argentation TLC

A sample of total prostomial lipid was spotted on to two further activated TLC plates impregnated with 5% $AgNO_3$ in acetone (see Christie, 1982). The plates were developed as for the TLC described above. Free fatty acid standards were also applied to the plates. When the solvent front had reached the 12-cm mark, the plates were removed, the solvent evaporated, and the plates washed with distilled water to remove the $AgNO_3$. One of the plates was sprayed with phosphomolybdic acid and the second plate was used for recovering the lipids for bioassay.

In vitro *assay of 20-carbon fatty acids*

Free fatty acids: eicosanoic, 11-eicosenoic, 11,14-eicosadienoic, 8,11,14-eicosatrienoic acid, 11,14,17-eicosatrienoic, 5,8,11,14-eicosatetraenoic (arachidonic), and 5,8,11,14,17-eicosapentaenoic acids, were obtained from Sigma Chemical Co., and 1×10^{-2} *M* stock solutions prepared in HPLC grade methanol (BDH). For use in bioassay, aliquots of these stock solutions were diluted 100 fold to give a final free acid concentration of 1×10^{-4} *M* and a negligible residual solvent concentration. Double dilutions of the free acids were then used to de-

termine the biological activity of each acid in the activation of spermatozoa *in vitro*.

Effect of cyclooxygenase and lipoxygenase pathway inhibitors

Stock solutions (10 m*M*) of the cyclooxygenase inhibitors aspirin, indomethacin, and tolazoline, were prepared in TFSW (triple filtered seawater). A 1-m*M* solution of butylated-hydroxytoluene, a lipoxygenase inhibitor, was also prepared. Prostomia were then homogenized in solutions of each inhibitor before bioassay for SMF activity. Control experiments were carried out in which the inhibitors of cyclooxygenase or lipoxygenase were added to prostomial extract after homogenization, or TFSW prior to bioassay. This permits the distinction to be made between metabolism of fatty acid substrate by the prostomial homogenate and metabolism by the spermatozoa themselves.

Incubation of biologically active fatty acid with cyclooxygenase and lipoxygenase

(A) Arachidonic acid was incubated with fresh bovine lung homogenate to obtain products from the cyclooxygenase pathway as described by Powell (1982). One gram of bovine lung tissue was homogenized on ice in 5 ml 0.05 *M* Tris-HCl buffer, pH 7.4. One ml of the homogenate was incubated with arachidonic acid at a final concentration of 1×10^{-2} *M* at 37°C for 5 min. The reaction was terminated by adding 5 ml ethanol, then adding 16 ml H_2O, and centrifuging at $400 \times g$ for 10 min. The supernatant was removed and assayed for biological activity.

(B) One-ml aliquots each containing 1.8 mg (*c.* 250,000 units) of soybean lipoxygenase was incubated with arachidonic acid at a final concentration of 5×10^{-3} *M* at 25°C for 15 min. After incubation, the reaction was terminated by heating, the extract was centrifuged, and the supernatant was assayed for biological activity. Incubations containing denatured lipoxygenase and lacking lipoxygenase were also carried out.

Incubation of prostomial extract with lipoxygenase

One-ml aliquots each containing the equivalent of 0.36 prostomium were incubated with 1.8 mg (*c.* 250,000 units) of lipoxygenase, for 60 min at 20°C. After incubation, the reaction was stopped and the sample treated as described above. Incubations containing denatured lipoxygenase and lacking lipoxygenase were carried out in parallel.

Incubations of biologically active fatty acid with BSA

Prostomial homogenate and 8,11,14-eicosatrienoic acid were bioassayed in the presence of dissolved BSA (bovine serum albumin). BSA solutions were freshly prepared in TFSW to give a final concentration in the assay of 0, 100, 1000 $\mu g \cdot ml^{-1}$, and 10 $mg \cdot ml^{-1}$, respectively.

Extraction of SMF by organic solvents and aqueous buffers

Extraction of SMF from biologically inactive lipid constituents of prostomial extracts were carried out as described by Jouvenaz *et al.* (1970) and Van Dorp (1971). This allows larger quantities of starting material to be purified, and permits the separation of free fatty acids from their often biologically active, but extremely labile, metabolites. This procedure involves the initial preparation of ethanolic lipid extract, washing the residue with ethanol:diethyl ether (1:1 v/v), followed by adding saline. The extract is then reduced in volume to 2.5 ml, acidified to pH 4 with citric acid, and contaminating lipids removed with petroleum ether. The remaining lipids are then taken up into ethyl acetate concentrated to about 5 ml total volume. Tris buffer (1.5 ml, pH 7.8) is then added to take up any prostaglandins present. All the organic and aqueous fractions obtained throughout this procedure were bioassayed for SMF activity.

Extraction of SMF on ODS silica cartridges

Freshly prepared prostomial homogenate and free fatty acid standards were separately applied to pre-wet Sep-Pak® C_{18} Cartridges (Waters Associates) in 10% aqueous ethanol with the pH adjusted to 4.0 using a 1-*M* stock solution of citric acid. The Sep-Pak® was prewetted using 2 ml of methanol followed by 5 ml of H_2O before applying the sample or standard. Fractions were partitioned using the following solvent mixtures (Powell, 1982): aqueous ethanol (20 ml, 10%), 20 ml H_2O, 10 ml petroleum ether, 10 ml petroleum ether:chloroform (65:35 v/v), and 10 ml methyl formate. The Sep Pak® was regenerated using 10 ml of 80% aqueous ethanol. The fraction obtained using each solvent was collected and prepared for bioassay as described above.

Gas-liquid chromatography of prostomial lipids

Prostomial lipid extracts were prepared as described above, and methylated using a method modified from Christie (1982). The sample was dissolved in 1 ml of dichloromethane, and refluxed for 2 h with 2% methanolic H_2SO_4. After cooling, 4 ml of saturated NaCl was added, and the fatty acid methyl esters extracted with 2 ml petroleum ether (40°–60°C). GC analysis was performed using a Hewlett Packard 5890A gas chromatograph fitted with a flame ionisation detector. Samples were separated on a capillary non-polar column (fused silica, 25 m $\times$ 0.25 mm i.d., 0.12 df, CP-Sil 5CB) following on-col-

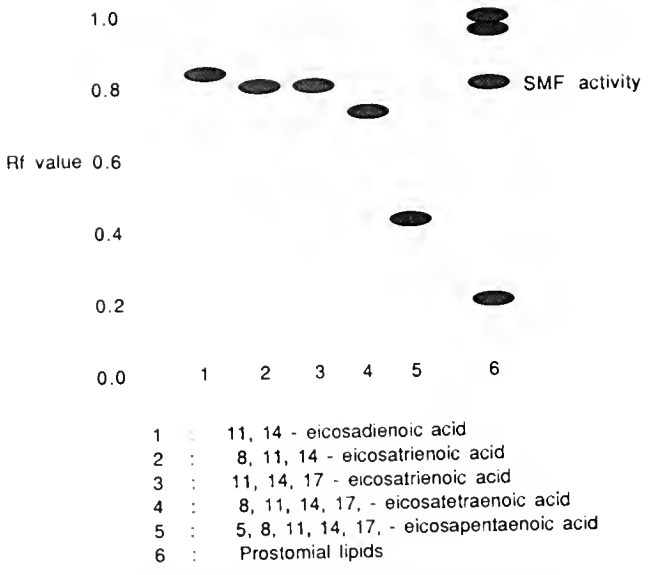

Figure 1. Separation of 20-carbon fatty acids (spots 1 to 5 with 2, 3, 3, 4, and 5 double bonds, respectively) and prostomial lipids by argentation thin-layer chromatography. The fatty acid standards with the greatest degree of saturation interact least with the silver nitrate on the TLC plate and therefore migrate furthest. The prostomial lipid extract shows a spot with an identical Rf value to the eicosatrienoic acids. This spot, when scraped off a washed plate, shows sperm maturation factor (SMF) activity *in vitro*.

umn injection. A linear thermal gradient program from 90°–300°C at 20°C·min^{-1} was used with helium as the carrier gas (25 cm·s^{-1}).

Results

Analysis of prostomial lipid extract and C20 fatty acids by TLC

TLC on activated silica gel plates, using the upper phase of: ethyl acetate:2,2,4-trimethylpentane:acetic acid:water (45:25:10:50 v/v) as a solvent, allows the separation of C20 fatty acids from their metabolites. The biological activity associated with prostomial lipid samples is associated with a region of the TLC plate that is identical to the position where free fatty acids are found (Rf 0.78–0.82). This chromatographic separation cannot distinguish between fatty acids with varying degrees of unsaturation.

Argentation TLC (using the same solvent system and TLC plates impregnated with 5% $AgNO_3$) allows fatty acids of the same carbon number to be separated according to the number of double bonds in the molecule. Figure 1 illustrates the results of this separation. SMF activity was recovered from a region of the plate which corresponds to the position of the C20:3 acids (8,11,14-eicosatrienoic acid and 11,14,17-eicosatrienoic acid). This technique is unable to separate these two isomers because they are identical in their degree of unsaturation.

Sperm activation by C20 fatty acids

In vitro bioassay of eicosanoic, 11-eicosenoic, 11,14-eicosadienoic, 8,11,14-eicosatrienoic acid, 11,14,17-eicosatrienoic, 5,8,11,14-eicosatetraenoic (arachidonic), and 5,8,11,14,17-eicosapentaenoic acids for the ability to induce sperm activation showed that both 8,11,14-eicosatrienoic acid and arachidonic acid displayed biological activity. The results are summarized in Table I. Concentration ranges for biological activity of 8,11,14-eicosatrienoic acid and arachidonic acid are based on nine replicate experiments producing mean minimum concentrations required for a response of 4.47×10^{-5} *M* and 2.28×10^{-4} *M*, respectively. These data indicate that 8,11,14-eicosatrienoic acid is about five times more active in this system than in arachidonic acid.

Studies of cyclooxygenase and lipoxygenase pathways

The preparation of prostomial extract in the presence of inhibitors of cyclooxygenase activity (aspirin, indomethacin, tolazoline) or lipoxygenase (butylated hydroxytoluene) did not effect the SMF activity of the extract. Aspirin at concentrations of 5 m*M* and 10 m*M* caused sperm lysis (the reasons for this are not clear, but this effect is unlikely to be related to the cyclooxygenase inhibitory property of the aspirin). These results suggest that there is no conversion of parent fatty acid to a biologically active metabolite via either the cyclooxygenase or lipoxygenase pathway. However, polychaete enzymes metabolizing fatty acids may differ from vertebrate cyclooxygenases and lipoxygenases, and substances used as inhibitors may not effect enzyme activity. Quercetin, another lipoxygenase inhibitor, could not be used in this

Table I

Sperm activation by C20 fatty acids

Fatty acid	Activity	Threshold concentration for activation (Mean ± S.E.; n = 9)
A eicosanoic	−	
B 11-eicosenoic	−	
C 11,14-eicosadienoic	−	
D 8,11,14-eicosatrienoic	+	$4.47 \pm 1.46 \times 10^{-5}$ *M*
E 11,14,17-eicosatrienoic	−	
F 5,8,11,14-eicosatetraenoic	+	$2.28 \pm 1.78 \times 10^{-4}$ *M*
G 5,8,11,14,17-eicosapentaenoic	−	
H TFSW control	−	

Table II

The effects of cyclooxygenase and lipoxygenase on sperm activation by C20 fatty acids

	Activity	Threshold concentration for activation
a. Incubation with cyclooxygenase		
Arachidonic acid incubated with bovine lung cyclooxygenase	−	
Arachidonic acid	+	$1.25 \times 10^{-5} M$
Bovine lung homogenate (cyclooxygenase)	−	
TFSW	−	
b. Incubation with lipoxygenase		
Arachidonic acid incubated with soybean lipoxygenase	+	$2.5 \times 10^{-3} M$
Arachidonic acid	+	$4.0 \times 10^{-5} M$
Soybean lipoxygenase	−	
TFSW	−	

study because of a non-specific effect on spermatozoa, which will be reported elsewhere.

Incubation of arachidonic acid with bovine lung homogenate (cyclooxygenase) or soybean lipoxygenase was carried out to examine whether there was (a) a reduction, (b) enhancement, or (c) the same level of sperm activation after converting the fatty acid substrate to metabolites. Table II shows that both incubation with bovine lung homogenate and soybean lipoxygenase brought about a reduction in the fatty acid incubate's ability to activate spermatozoa. This suggests that the fatty acid has been largely converted to cyclooxygenase and lipoxygenase metabolites, which cannot activate the spermatozoa. Thin layer chromatographic analysis of the incubates confirm that most of the fatty acid is converted during incubation (Fig. 2). Thin layer chromatography of prostomial homogenate shows that most of the fatty acid remains unmetabolized. This indicates that the fatty acid is not normally converted to a metabolite by endogenous polychaete enzymes, which may be outcompeted for substrate during incubations with exogenous cyclooxygenase or lipoxygenase.

Incubation of prostomial homogenate with soybean lipoxygenase results in a total loss of SMF activity. This indicates the conversion of a fatty acid in the prostomial homogenate to non-active metabolites, and also suggests that it is this fatty acid component of the prostomial homogenate that causes sperm activation *in vitro*.

Incubations of 8,11,14-eicosatrienoic acid and prostomial extract with BSA

BSA (bovine serum albumin) was incubated with 8,11,14-eicosatrienoic acid and prostomial homogenate to investigate the possible interference of BSA on the ability of both the fatty acid and prostomial extract to activate spermatozoa of *Arenicola marina*. It has long been known that fatty acids interact strongly with serum albumin (Goodman, 1958). Figure 3 shows that the ability of both 8,11,14-eicosatrienoic acid and prostomial homogenate to activate spermatozoa is markedly reduced by the addition of BSA. This evidence lends further support to the suggestion that it is a fatty acid component of the prostomial homogenate that causes sperm activation *in vitro*.

Further purification of SMF from prostomial homogenate

Figure 4 shows the purification steps employed for the purification of SMF from crude prostomial homogenate, using the method developed by Jouvenaz *et al.*, (1970) and Van Dorp (1971) for the extraction of prostaglandins from biological tissues. The figure also traces the biological activity through the purification steps. SMF activity is finally recovered in an ethyl acetate fraction.

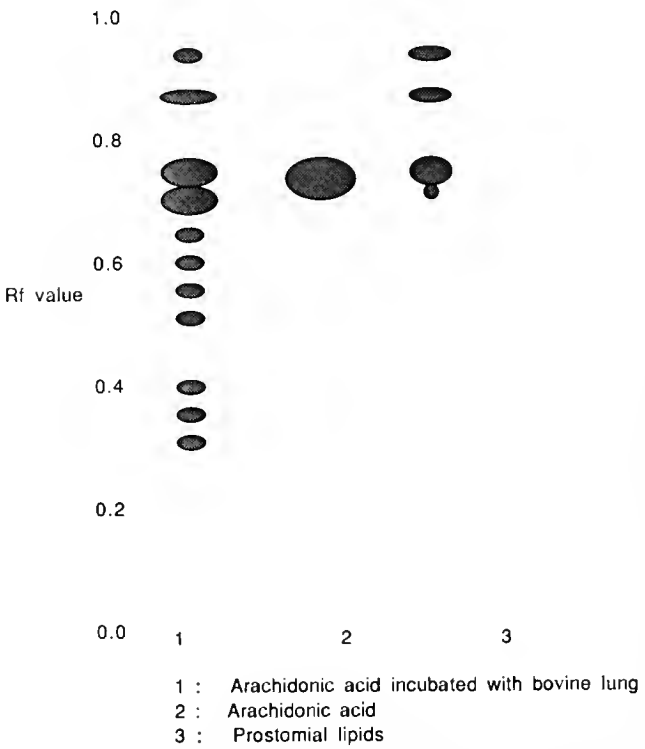

Figure 2. TLC analysis of prostomial lipids, arachidonic acid, and arachidonic acid following incubation with cyclooxygenase. Arachidonic acid can be seen at an Rf value of about 0.78. The cyclooxygenase products are clearly visible with Rf values lower than that of arachidonic acid itself. Prostomial lipid extract shows no spots which correspond to cyclooxygenase products, and which may have arisen as a result of action by endogenous cyclooxygenases.

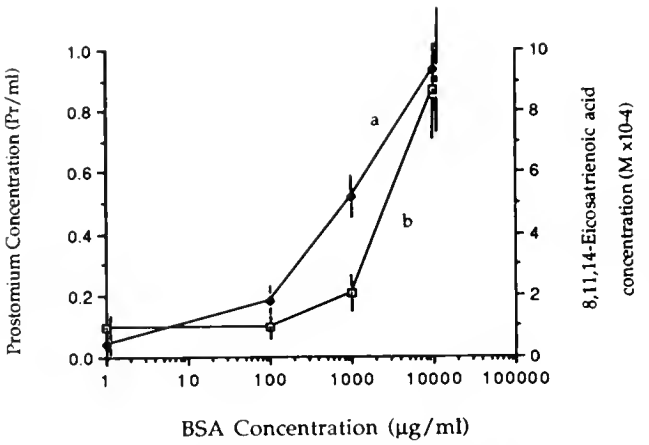

Figure 3. Minimum concentrations of (a) 8,11,14-eicosatrienoic acid, and (b) prostomial homogenate required to bring about sperm activation in the presence of bovine serum albumin (BSA). The fatty acid concentration, or the concentration of prostomial extract required to bring about sperm activation *in vitro*, increases with the concentration of dissolved BSA. Data shown are the mean (±SE) minimum concentrations required to bring about sperm activation in three replicated experiments.

Prostaglandins remain in the pH 7.8 Tris buffer and would be recovered only in an ethyl acetate fraction from Tris buffer at pH 4.0. This indicates that SMF activity is not recovered with prostaglandins but is recovered in the fatty acid fraction.

A parallel approach to the purification of SMF has been carried out using Sep-Pak® cartridges and a succession of aqueous and organic solvents. Table III shows that SMF activity is recovered in the same fractions as the 8,11,14-eicosatrienoic acid standard.

Gas chromatographic analysis of prostomial lipids

The results of separation of methyl esters of prostomial lipid extracts are shown in Figure 5. Three peaks with retention times corresponding to methyl esters of 5,8,11,14-eicosatetraenoic acid (8.72 min), 8,11,14-eicosatrienoic acid (8.81 min), 11,14,17-eicosatrienoic acid (8.93 min), can be identified. This clearly indicates the presence of 8,11,14-eicosatrienoic acid in prostomial lipid extracts obtained from prostomia showing SMF activity *in vitro*.

Discussion

The results obtained from thin layer chromatography of prostomial total lipid extracts described above showed that SMF activity co-migrated with 20-carbon fatty acid standards. In particular, it is associated with eicosatrienoic acids (demonstrated by argentation TLC). The bioassay of C20 fatty acids show that only two of the fatty acids tested brought about the activation (dissociation of the morulae and the acquisition of motility) *in vitro*: arachidonic and 8,11,14-eicosatrienoic acids. Arachidonic acid, while capable of activating spermatozoa, does not co-migrate with prostomial SMF in the argentation TLC. Clearly, then, arachidonic acid and SMF are not the same substance. All eicosatrienoic acids co-migrate in this TLC system but only 8,11,14-eicosatrienoic acid causes sperm activation *in vitro*. While 8,11,14-eicosatrienoic acid co-migrates with SMF, and has biological activity identical to SMF, this is insufficient evidence to propose that they are the same.

Arachidonic acid, 8,11,14-eicosatrienoic acid, and eicosapentaenoic acid are all naturally occurring 20-carbon fatty acids that differ in the number of double bonds, having 4, 3, and 5 double bonds, respectively. They are all precursors for a range of pharmacologically active molecules, the eicosanoids. Each of these three fatty

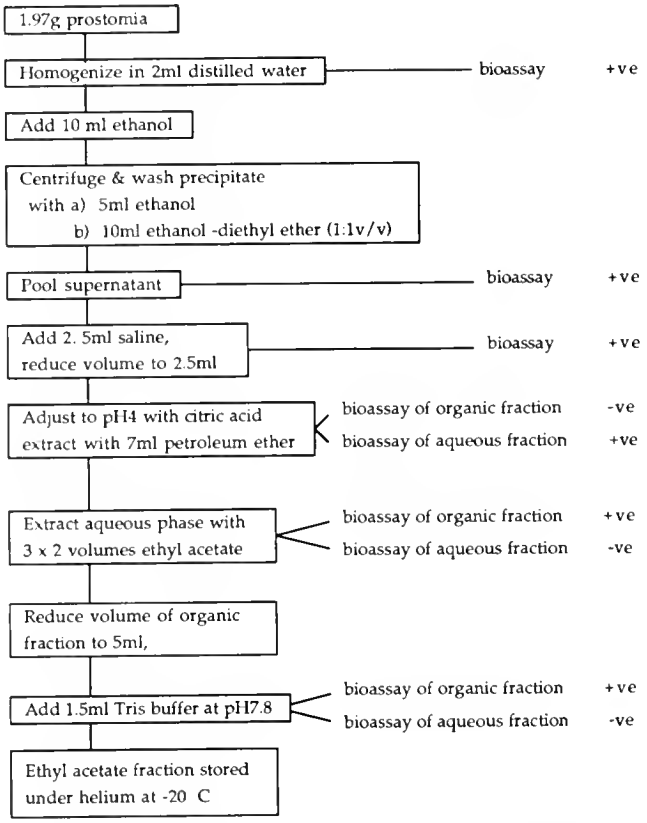

Figure 4. Extraction procedure used for sequential purification of sperm maturation factor (SMF) using organic solvents and aqueous buffers (after Jouvenaz *et al.*, 1970). Following each purification step, aqueous and organic phases were dried under helium, resuspended, and tested for their ability to activate sperm *in vitro*. The response is represented here as +ve or −ve, where +ve indicates the presence of SMF activity evidenced by sperm morula breakdown and the presence of free-swimming spermatozoa, and −ve indicates no activation of spermatozoa.

Table III

Purification of prostomial SMF on ODS silica cartridges

Eluent from cartridge	Activity of prostomium extract	Activity of 8,11,14-eicosatrienoic acid
1. 20 ml 30% ethanol	–	–
2. 20 ml H_2O dist.	–	–
3. 10 ml petroleum ether:chloroform (65:35 v/v)	+	+
4. 10 ml methyl formate	+	+
5. 10 ml 80% ethanol	–	–

acids gives rise to a series of prostaglandins (PGs): arachidonic acid, which is the best known and probably the most important, is converted to series 2 PGs; 8,11,14-eicosatrienoic acid is converted to series 1 PGs. Eicosapentaenoic acid, which is the most important C20 fatty acid in marine organisms, gives rise to series 3 PGs.

The use of the principal enzymes involved in the metabolism of the fatty acids to their respective prostaglandins (cyclooxygenase) and other metabolites (lipoxygenase) combined with the use of selective inhibitors permits the possible pathways involved to be elucidated. Evidence shown above, by using bovine lung homogenate and soybean lipoxygenase, which both caused a marked reduction of SMF activity of prostomial homogenate, suggests strongly that a fatty acid present in prostomial homogenate is responsible for the SMF activity. The use of inhibitors of cyclooxygenase and lipoxygenase suggests that there is no conversion of fatty acid in prostomial homogenate to metabolite(s), which may have potent biological activity as previously suggested (Bentley, 1986a).

Compared to other invertebrate groups, notably the insects, and the Crustacea, little is known of the chemical nature of polychaete hormones. To date, no hormone from polychaete tissues has been completely purified or its structure elucidated. Grothe *et al.* (1987) identified catecholamines in the nervous system of *Ophryotrocha puerilis,* which may have an endocrine related function. Numerous vertebrate-like peptides have been identified in the nervous system of polychaetes (Dhainaut-Courtois *et al.,* 1985), but functions have yet to be ascribed to these putative hormones. The possible action of a fatty acid as a hormone may seem unlikely,

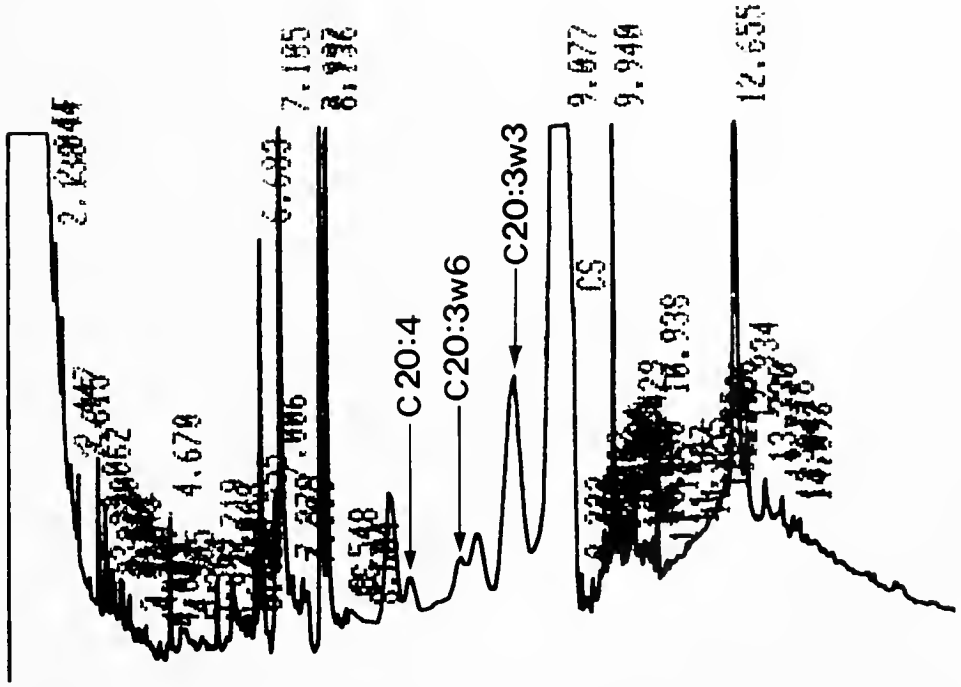

Figure 5. Gas chromatograph of fatty acid methyl esters (FAMEs) of biologically active prostomial lipids showing identified peaks corresponding to 5,8,11,14-acid (C20:4), 8,11,14-eicosatrienoic acid (C20:3w6), and 11,14,17-eicosatrienoic acid (C20:3w3) with retention times of 8.72 min, 8.81 min, and 8.93 min, respectively. These peaks correspond in absolute retention times, and relative distances to FAME standards of the three acids.

but the certain presence in the prostomium of *Arenicola marina* of a fatty acid that acts on distant target cells (sperm morulae in the coelomic fluid) may well be an example of such a "hormone." Its hormonal role is further supported by the cyclical nature of its appearance in prostomial extracts. Bentley (1985) showed that SMF activity of prostomial extracts is maximal around the breeding season of given populations and is non-existent during the post-spawning period.

Fatty acids and prostaglandins are present in a wide range of lower animals (Srivastava and Mustafa, 1984; Stanley-Samuelson, 1987). These essential fatty acids and their metabolites also have an effect on many aspects of reproduction in marine invertebrates. The endocrine control of oocyte maturation in asteroid echinoderms is now well understood and involves the action of a peptide gonad-stimulating substance (GSS), 1-methyl adenine, and an intracellular maturation-promoting factor (MPF) (see Giese and Kanatani, 1987 for review). One-methyl adenine acts on the oocytes to bring about maturation. However, Meijer *et al.* (1986) demonstrated that arachidonic acid mimics the action of 1-methyl adenine on starfish oocytes *in vitro*. It is possible that 1-methyl adenine acts as a "second messenger" or that the arachidonic acid mimics some hitherto unidentified fatty acid.

A tri-hydroxy metabolite of arachidonic acid has been identified as the hatching factor in the barnacle *Semibalanus* (*Balanus*) *balanoides* (Clare *et al.*, 1982, 1985; Holland *et al.*, 1985). Prostaglandins also cause spawning of the abalone, *Haliotis rufescens*, and the mussel, *Mytilus edulis* (Morse *et al.*, 1977).

Pharmacologically active metabolites of arachidonic and related fatty acids are characteristically short-lived substances produced close to, or at, their site of action. The parent fatty acids are often metabolized by the target cells themselves. This may occur at the cell surface or intracellularly. Typically this metabolism occurs as a result of the action of lipoxygenases or cyclooxygenase (PG synthetase). The precise nature of the enzymes may vary between phyla, and there is evidence that those found in some invertebrates (*e.g., Lymnaea stagnalis*) may be different to those occurring in vertebrates (Clare *et al.*, 1986). In the starfish oocyte, arachidonic acid is converted to HETEs at the plasma membrane (Meijer *et al.*, 1986). It may be that 8,11,14-eicosatrienoic acid is metabolized by the sperm morulae of *Arenicola marina* and this will be investigated by the use of radiolabeled precursors. The maturation of starfish oocytes by arachidonic acid is inhibited in a dose-dependent manner by the presence of BSA, however, maturation induced by 1-methyl adenine (the natural inducer) is not. The activation of spermatozoa of *A. marina* by prostomial extract or 8,11,14-eicosatrienoic acid are both inhibited in a similar dose-dependent manner by BSA. This may be further evidence to suggest that the fatty acid from the prostomium, causing sperm activation in *A. marina*, is a primary inducer rather than a "second messenger."

Purification procedures, followed by structural analysis, must be performed to identify the chemical nature of any endocrine substance with certainty. For example, the barnacle hatching factor was identified by organic extraction and subsequent GC-MS analysis (Holland *et al.*, 1985). One of the problems often encountered is obtaining sufficient starting material for purification. The separation procedures described in this paper show that SMF of *Arenicola marina* has identical chromatographic properties to 8,11,14-eicosatrienoic acid, and that 8,11,14-eicosatrienoic acid is present in the fatty acid component of prostomial extract. The use of bonded-phase C18 cartridges as a purification stage should permit sufficient quantities of SMF to be extracted to complete mass spectrometrical analysis.

Acknowledgments

The authors gratefully acknowledge the support of a Royal Society European Programme Fellowship to M.G.B., under the tenure of which this work was commenced; the award of support from the Royal Society Browne Fund to S.C.; and the award of an SERC postgraduate studentship to A.A.P. The authors also thank Prof. F. D. Gunstone and Mr. K. Black (Department of Chemistry, University of St. Andrews) for their assistance with GC analysis.

Literature Cited

Ashworth, J. H. 1904. *Arenicola. Mem. Liverpool Mar. Biol. Comm.* **11:** 1–118.

Bentley, M. G. 1985. Sperm maturation response in *Arenicola marina* L.: an *in vitro* assay for sperm maturation factor and its partial purification. *Int. J. Invertebr. Reprod. Dev.* **8:** 139–148.

Bentley, M. G. 1986a. Sperm maturation in Polychaeta. Pp 215–220 in *Advances in Invertebrate Reproduction, Vol. 4*, M. Porchet, J-C. Andries and A. Dhainaut, eds. Elsevier, Amsterdam.

Bentley, M. G. 1986b. Ultrastructure of experimentally induced sperm maturation in *Arenicola marina* L. P. 492 in *Advances in Invertebrate Reproduction, Vol. 4*, M. Porchet, J-C. Andries, and A. Dhainaut, eds. Elsevier, Amsterdam.

Bentley, M. G., and A. A. Pacey. 1989. A scanning electron microscopical study of sperm development and activation in *Arenicola marina* (L.) *Int. J. Invertebr. Reprod. Dev.* **15:** 211–219.

Christie, W. W. 1982. *Lipid Analysis.* Pergamon Press, Oxford. 207 pp.

Clare, A. S., R. van Elk, and J. H. M. Feyen. 1986. Eicosanoids: their biosynthesis in accessory sex organs of *Lymnaea stagnalis* (L.). *Int. J. Invertebr. Reprod. Dev.* **10:** 125–131.

Clare, A. S., G. Walker, D. L. Holland, and D. J. Crisp. 1982. Barnacle egg hatching: a novel role for a prostaglandin like compound. *Mar. Biol. Lett.* **3:** 113–120.

Clare, A. S., G. Walker, D. L. Holland, and D. J. Crisp. 1985. The hatching substance of the barnacle *Balanus balanoides* (L.). *Proc. R. Soc. Lond. B* **224:** 131–147.

Dhainaut-Courtois, N., M.-P. Duhois, G. Tramu and M. Masson. 1985. Occurrence and coexistence in *Nereis diversicolor* O. F. Müller (Annelida Polychaeta) of substances immunologically related to vertebrate neuropeptides. *Cell Tissue Res.* **242:** 97–108.

Giese, A. C., and H. Kanatani. 1987. Maturation and spawning. Pp 252–329 in *Reproduction in Marine Invertebrates, Vol 9, General Aspects: Seeking Unity in Diversity,* A. C. Giese, J. S. Pearse, and V. B. Pearse, eds. Blackwell Scientific Publications, Palo Alto, CA, and Boxwood Press, Pacific Grove, CA.

Goodman, DeW. S. 1958. The interaction of human serum albumin with long chain fatty acid anions. *J. Am. Chem. Soc.* **80:** 3892–3898.

Grothe, C., K. Seidl, and H.-D. Pfannenstiel. 1987. Cytochemical and Biochemical characterisation of neurosecretory material in the brain of an annelid, *Ophryotrocha puerilis* (Polychaeta). *Gen. Comp. Endocrinol.* **68:** 1–5.

Holland, D. L., J. East, K. H. Gibson, E. Clayton, and A. Oldfield. 1985. Identification of the hatching factor of the barnace *Balanus balanoides* as the novel eicosanoid 10,11,12-trihydroxy 5,8,14,17-eicosatetraenoic acid. *Prostaglandins* **29:** 819–830.

Howie, D. I. D. 1959. The spawning of *Arenicola marina* (L). I. The breeding season. *J. Mar. Biol Assoc. U. K* **38:** 395–406.

Howie, D. I. D. 1961a. The spawning of *Arenicola marina* (L). II. Spawning under experimental conditions. *J. Mar. Biol. Assoc. U. K* **41:** 127–144.

Howie, D. I. D. 1961b. The spawning of *Arenicola marina* (L.) III. Maturation and shedding of the ova. *J. Mar. Biol. Assoc. U. K* **41:** 771–783.

Howie, D. I. D. 1961c. Spawning mechanisms in the male lugworm. *Nature* **192:** 1100–1101.

Howie, D. I. D. 1963. Experimental evidence for the humoral stimulation of ripening of the gametes and spawning in the polychaete *Arenicola marina* (L.) *Gen. Comp. Endocrinol.* **3:** 660–668.

Howie, D. I. D. 1966. Further data relation to the maturation hormone and its site of secretion in *Arenicola marina* Linnaeus. *Gen. Comp. Endocrinol.* **6:** 347–361.

Howie, D. I. D. 1984. The reproductive biology of the lugworm, *Arenicola marina* (L.) Pp. 247–263 in *Polychaete Reproduction,* A. Fischer and H.-D. Pfannenstiel, eds. Fortschritte der Zoologie, Band 29, Gustav-Fischer-Verlag, Stuttgart, New York.

Jouvenez, D. H. Nugteren, R. K. Beerthuis, and D. A. Van Dorp. 1970. A sensitive method for the determination of prostaglandins by gas chromatography with electron capture detection. *Biochim. Biophys. Acta* **202:** 231–234.

Meijer, L., and M. Durchon. 1977. Contrôle neurohormonal de la maturation ovocytaire chez *Arenicola marina* (Annélide Polychète). Etude *in vitro*. *C. R. Acad. Sc. Paris* **285:** 377–380.

Meijer, L., and P. Guerrier. 1984. Maturation and fertilization in starfish oocytes. *Int. Rev. Cytol.* **86:** 129–196.

Meijer, L., P. Guerrier, and J. Maclouf. 1984. Arachidonic acid, 12- and 15-hydroxyeicosatetraenoic acids, eicosapentaenoic acid and phospholipase A_2 induce starfish oocyte maturation. *Dev. Biol.* **106:** 368–378.

Meijer, L., J. Maclouf, and R. W. Bryant. 1986. Arachidonic acid metabolism in starfish oocytes. *Dev. Biol.* **114:** 22–33.

Morse, D. E., H. Duncan, N. Hooker, and A. Morse. 1977. Hydrogen peroxide induces spawning in molluscs with activation of prostaglandin endoperoxide synthetase. *Science* **196:** 298–300.

Newell, G. E. 1948. A contribution to our knowledge of the life history of *Arenicola marina* (L.). *J. Mar. Biol. Assoc. U. K* **27:** 554–580.

Powell, W. S. 1982. Rapid extraction of arachidonic acid metabolites from biological samples using octadecylsilyl silica. Pp. 467–477 in *Methods in Enzymology, Vol. 87,* W. E. M. Lands and W. L. Smith, eds. Academic Press, Inc., New York.

Salmon, J. A., and R. J. Flower. 1982. Extraction and thin layer chromatography of arachidonic acid metabolites. Pp. 477–493 in *Methods in Enzymology, Vol. 87,* W. E. M. Lands and W. L. Smith, eds. Academic Press, Inc., New York.

Srivastava, K. C., and T. Mustafa. 1984. Arachidonic acid metabolism and prostaglandins in lower animals. *Mol. Physiol.* **5:** 53–59.

Stanley-Samuelson, D. W. 1987. Physiological roles of prostaglandins and other eicosanoids in invertebrates. *Biol. Bull.* **173:** 92–109.

Van Dorp, D. A. 1971. Recent developments in the biosynthesis and the analyses of prostaglandins. Pp. 181–195 in *Prostaglandins, Vol. 180,* P. W. Ramwell and J. E. Shaw, eds. *Ann. N. Y. Acad. Sci.*

Reference: *Biol. Bull.* **178:** 10–20. (February, 1990)

Development of Nerve Cells in Hydrozoan Planulae: III. Some Interstitial Cells Traverse the Ganglionic Pathway in the Endoderm

VICKI J. MARTIN

Department of Biological Sciences, University of Notre Dame, Notre Dame, Indiana 46556

Abstract. Hydrozoan planulae of *Pennaria tiarella* possess migratory stem cells—interstitial cells—that are capable of self renewal and can differentiate into either ganglionic nerve cells or nematocytes. The commitment and differentiation of a subpopulation of larval endodermal interstitial cells to the neural pathway were examined using light immunocytochemistry and transmission electron microscopy. Embryos of different ages, from 8 to 96 h, were tested for their ability to bind rabbit antiserum raised to the neuropeptide FMRFamide. A subpopulation of interstitial cells in the anterior endoderm of the planula begins to express a FMRFamide-like antigen between 48 and 72 h postfertilization. Concurrent with this endodermal interstitial cell expression, a subset of ectodermal ganglionic cells with FMRFamide-like immunoreactivity appears in the anterior end of the planula. Ultrastructural examination of the interstitial cell population in the anterior planular endoderm, at 48 h in development, indicates that, based upon morphology, there are at least three subsets of interstitial cells in this region: undifferentiated interstitial cells, interstitial cells traversing the nematocyte differentiation pathway, and interstitial cells traversing the neural differentiation pathway. The endodermal interstitial cells entering the neural pathway form a Golgi complex, electron-dense droplets, dense cored vesicles, and microtubules. Neurite formation does not occur in the endoderm; rather, neurites are only found in association with ectodermal ganglionic cells. Furthermore, planulae lack fully differentiated endodermal neurons. This study demonstrates that, during embryogenesis, some interstitial cells destined for neural differentiation are committed in the endoderm before their emigration to the ectoderm, begin to express cytochemical and morphological features of neural differentiation while in the endoderm, and migrate to the ectoderm as neuroblasts.

Received 5 June 1989; accepted 17 November 1989.

Introduction

The hydrozoan planula larva is an especially good system with which to examine the commitment and differentiation of cells during development: the number of cell types in the larva is small; their arrangement is simple; and neither the variety nor the arrangement of larval cells are very far from those of the adult (Martin and Thomas, 1980; Martin *et al.*, 1983; Thomas *et al.*, 1987; Martin, 1988a, b, c).

The hydrozoan planula contains a population of migratory undifferentiated cells: interstitial cells. Interstitial cells are capable of self-renewal, and can differentiate into either ganglionic nerve cells or nematocytes (Martin and Thomas, 1981a, b; Martin, 1988a). Interstitial cells arise in the endoderm, later migrate into and populate the ectoderm, and eventually differentiate into the two classes of cells (Martin and Archer, 1986). Do the interstitial cells (1) migrate as uncommitted cells and become committed by some sort of positional cues upon arrival in the ectoderm, or (2) are committed before they leave the endoderm, and migrate into the ectoderm to complete differentiation? The second alternative is correct for nematocytes, (Martin and Archer, 1986), and in this paper I show that it is also correct for neurons (*i.e.*, ganglionic cells).

This research describes a series of histological experiments designed to determine whether interstitial cells in a hydrozoan planula develop neuronal characteristics (ganglionic features) before arriving at their final destination in the ectoderm. The numbers and locations of in-

terstitial cells and ganglionic cells in hydrozoan embryos of different ages were determined by light microscopy and transmission electron microscopy (TEM). The ability of these embryos to bind a rabbit antiserum raised to the neuropeptide FMRFamide [such immunoreactivity has been demonstrated in planular sensory cells (Martin, 1988b)] was tested to determine whether the antigen is expressed by ganglionic cells or interstitial cells differentiating along the ganglionic pathway. Anti-FMRFamide was used in this study because when it is applied to cnidarians, the peptides bound are likely to be related to pGlu-Gly-Arg-Phe-amide, which is present in large amounts in nervous systems of adult anthozoans and probably also in hydrozoans and scyphozoans (Graff and Grimmelikhuijzen, 1988). The planular results show that a subpopulation of interstitial cells in the anterior endoderm of 48 h planulae expresses morphological and cytochemical features of ganglionic cell differentiation. Thus, at least some interstitial cells for the neural differentiation pathway are committed in the endoderm and actually traverse the ganglionic pathway in the endoderm.

Materials and Methods

Mature colonies of *Pennaria tiarella* were collected from pier pilings in Morehead City, North Carolina. Fronds from male and female colonies were placed together in the dark at 6:00 pm. At 9:00 pm the bowls were returned to the light and, within an hour, early cleavage embryos were found in the bottoms of the dishes. Embryos were collected, placed in small finger bowls of filtered seawater, and reared at 23°C.

Embryos of seven different ages: 8-, 10-, 16-, 24-, 48-, 72-, and 96-h, were prepared for transmission electron microscopy. Animals were fixed for 1 h in 2.5% glutaraldehyde, pH 7.4, in 0.2 *M* phosphate buffer. They were subsequently postfixed for 1 h in 2% osmium tetroxide (pH 7.2, in 1.25% sodium bicarbonate), dehydrated in an ethanol series, infiltrated, and embedded in Spurr's embedding medium. Serial thick and thin sections were cut with a Porter-Blum MT-2B ultramicrotome. Thick sections were mounted on gelatin-coated slides, stained with 0.5% toluidine blue in 1% sodium borate, and examined with a Zeiss research microscope. Thin sections were placed on 150-mesh copper grids and stained with 3.5% uranyl acetate in ethanol followed by lead hydroxide. Grids were examined and photographed with a Hitachi H-600 transmission electron microscope.

Wholemounts and paraffin sections of the selected embryonic stages were tested for their ability to bind a rabbit antiserum raised to FMRFamide (Immuno Nuclear Corporation). Twenty-four-hour planulae, treated for 2 h with 0.2% colchicine in seawater and subsequently allowed to recover for 24 h, were also exposed to the FMRFamide antiserum. Such colchicine treatment eliminates the entire interstitial cell system *i.e.*, interstitial cells, nematoblasts, nematocytes, and ganglionic cells (Martin and Thomas, 1981b).

To visualize the binding of FMRFamide antiserum on wholemounts, the procedure presented by Martin (1988b) was followed with some modifications. Animals were fixed for 1 h in 10% formalin in seawater and subsequently washed 3 times, for 15 min each, in 10 m*M* phosphate-buffered saline (PBS, pH 7.2). Incubation with the FMRFamide antiserum was for 1–4 h, with the primary antibody diluted 1:200 with 10 m*M* PBS, pH 7.2, containing 0.1% sodium azide, 0.3% Triton X-100, and 2% fetal calf serum. Incubations were carried out with planulae in lid-covered 96 well tissue culture plates placed on a rotating shaker platform set at 60 rpm. At the end of the first incubation period, the primary antibody was removed, and animals were washed 3 times, for 15 min each, in 10 m*M* PBS, pH 7.2. Incubation with the second antibody was for 1 h in fluorescein isothiocyanate (FITC)-conjugated goat anti-rabbit immunoglobin (Boehringer Mannheim). The FITC-tagged antibody was diluted 1:120 in 10 m*M* PBS, pH 7.2, containing 0.1% sodium azide, 0.3% Triton X-100, and 10% fetal calf serum. The second incubations were also done in 96 well plates rotated at 60 rpm. After the second incubation, animals were washed for three 15-minute changes in 10 m*M* PBS, pH 7.2. Wholemounts were examined for fluorescently labeled cells with a Zeiss microscope equipped with epifluorescence.

To visualize binding of FMRFamide antiserum to paraffin sections of embryos, samples fixed in formalin were dehydrated through an alcohol series, infiltrated and embedded in paraffin, and serially sectioned at 8 μm. Nine sections were mounted in the center of a glass slide, three rows one above the other, and each row containing three sections. Slides were rehydrated to distilled water, and the sections were surrounded by an outer ring of vacuum grease. Grease application was done in a moist chamber to prevent the sections from drying. FMRFamide antiserum was placed in the grease-created wells, thus immersing the sections. The slides were placed in a covered moist chamber and rotated at 20–40 rpm for 1–4 h. PBS rinses and incubation in the second antibody were carried out in the moist chamber. After incubation, the grease was removed from the slides; the sections were covered with mineral oil and examined for fluorescently labeled cells.

Binding specificity of the FMRFamide antiserum was determined by preincubating a 1:200 dilution of the antiserum with 10 μg/ml synthetic FMRFamide (Peninsula Lab) for 24 h at 4°C before using it to stain the embryos.

Results

Mature planula (72–96 h postfertilization)

The mature planula consists of an ectoderm, an acellular mesoglea, and an endoderm (Fig. 1). The ectoderm contains epithelial cells (epitheliomuscular, glandular, and sensory), interstitial cells, and their derivatives (nematoblasts, nematocytes, and ganglionic cells), whereas, the endoderm has gastrodermal epithelial cells, interstitial cells, and nematoblasts. Interstitial cells, nematoblasts, nematocytes, and ganglionic cells are easily identified in planular tissue at the light microscopic level (Figs. 1–3). Interstitial cells—small round cells measuring 7.5 μm in diameter—contain a centrally located nucleus with one to several nucleoli. They possess few cytoplasmic organelles and are scattered among the epithelial cells in both the ectoderm and the endoderm along the entire anterior-posterior axis of the planula (Fig. 2). Nematoblasts (developing nematocytes) range from 10 to 12.5 μm in diameter and have distinctive dark- or light-staining capsules (Figs. 1, 2). Each capsule houses a nematocyst thread that may possess barbs and spines. Nematoblasts are located in both the ectoderm and the endoderm and are mostly confined to the anterior and middle two-thirds of the planular axis. Mature nematocytes are found only at the ectodermal surfaces of planulae and exhibit the same distribution pattern as that of the nematoblasts. Ganglionic cells are 5 μm in diameter, exhibit a spindle shape, and are positioned all along the planular anterior-posterior axis at the base of the ectoderm just above the mesoglea (Fig. 3). The ganglionic perikaryon, its long axis oriented parallel to the mesoglea, contains a Golgi complex, microtubules, mitochondria, electron-dense droplets, and dense cored vesicles. Neurites project from either side of the cell bodies and form an extensive ectodermal neural plexus above the mesoglea (Figs. 3, 4). Such neurites are filled with microtubules, mitochondria, electron-dense droplets, and dense cored vesicles (Fig. 4). Electron-dense droplets and dense cored vesicles are found exclusively in differentiating and full-differentiated nerves. The endoderm lacks ganglionic cells and a neural plexus.

Interstitial cells and nematoblasts are migratory, whereas, nematocytes and ganglionic cells are not (Martin and Archer, 1986). These migratory cells move as single cells, and migration has been observed from the endoderm to the ectoderm and, once in the ectoderm, up and down the planular axis.

FMRFamide-like immunoreactivity is detected in a subpopulation of ganglionic cells in the planular ectoderm at 72 h postfertilization, just before metamorphosis (Fig. 5). Such immunopositive nerve cells are located at the base of the ectoderm above the mesoglea and are confined to the anterior head and anterior sides of the plan-

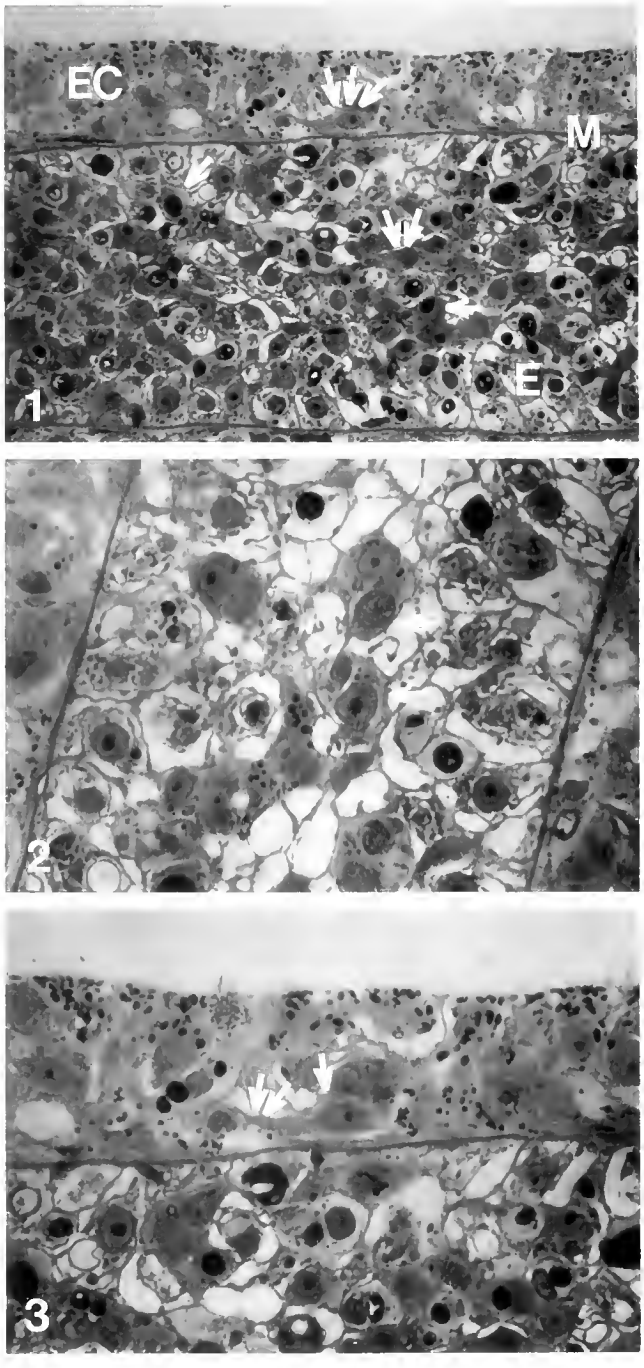

Figure 1. Longitudinal section of a 72 h planula showing ectoderm (EC), mesoglea (M) and endoderm (E). Endodermal nematoblasts (single arrow) and interstitial cells (double arrows) and an ectodermal ganglionic cell (triple arrows) are visible. ×250.

Figure 2. Endodermal interstitial cells (arrows) in a 72 h planula. Each cell contains a large nucleus with a prominent nucleolus and few other cytoplasmic organelles. ×620.

Figure 3. Ectodermal ganglionic cell (arrow) in a 72 h planula. The cell body is oriented parallel to the mesoglea and neurites (double arrows) extend from each side of the perikaryon. ×620.

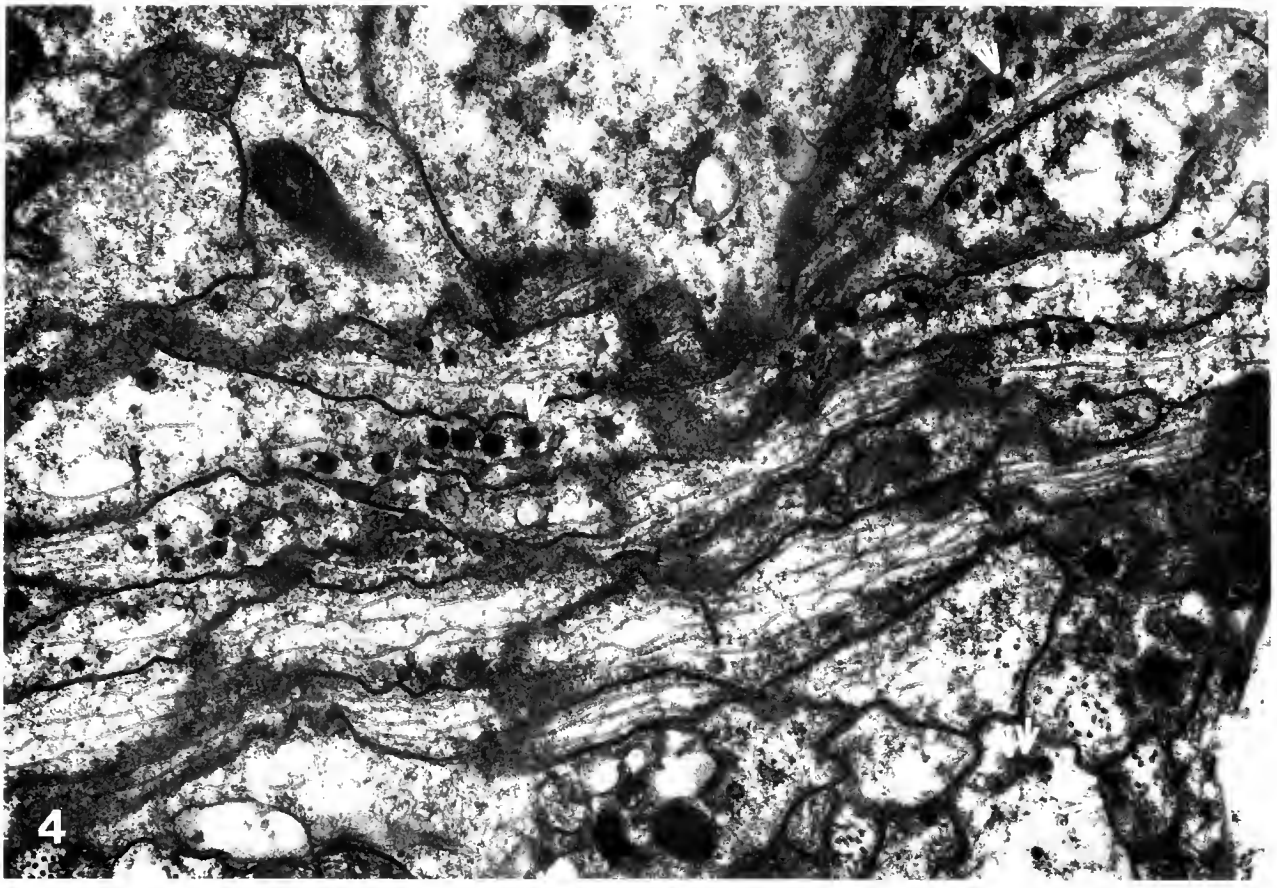

Figure 4. Ectodermal neurites of ganglionic cells. These neurites form a plexus just above the mesoglea and are rich in microtubules, mitochondria, electron-dense droplets (single arrows) and dense cored vesicles (double arrows). ×19,000.

ula. Cell bodies of the immunopositive ganglionic cells are stained, whereas their neurites (processes) are not. Nematoblasts and nematocytes do not produce the FMRFamide-like peptide, as indicated by their lack of staining. Furthermore, the majority of planular interstitial cells do not stain with the antibody. There is, however, a small subset of interstitial cells in the anterior endoderm of 72-h planulae that does express a FMRFamide-like peptide. Such positive cells first produce the neuropeptide at 48 h in development and are described below (see *Forty-eight hour planula*).

Figure 5. Wholemount of a 72 h planula. A subpopulation of ganglionic cells (arrow) in the ectoderm of the planula exhibits FMRFamide-like immunoreactivity. Such ectodermal ganglionic cells are confined to the anterior head and anterior sides of the planula. ×200.

Gastrulating embryo (8–10 h postfertilization)

Embryos gastrulate between 8–10 h postfertilization resulting in the formation of an immature, 10-h planula. This young planula consists of an ectoderm, an acellular mesoglea, and an endoderm (Figs. 6, 7). The ectoderm contains epithelial cells (dark-staining epitheliomuscular cells and light-staining glandular cells) and is devoid of interstitial cells, nematoblasts, nematocytes, and ganglionic cells. The endoderm consists of an outer epithelial layer of gastrodermal cells surrounding a central core of tightly packed interstitial cells (Figs. 6, 7). This core of interstitial cells extends the entire length of the planular

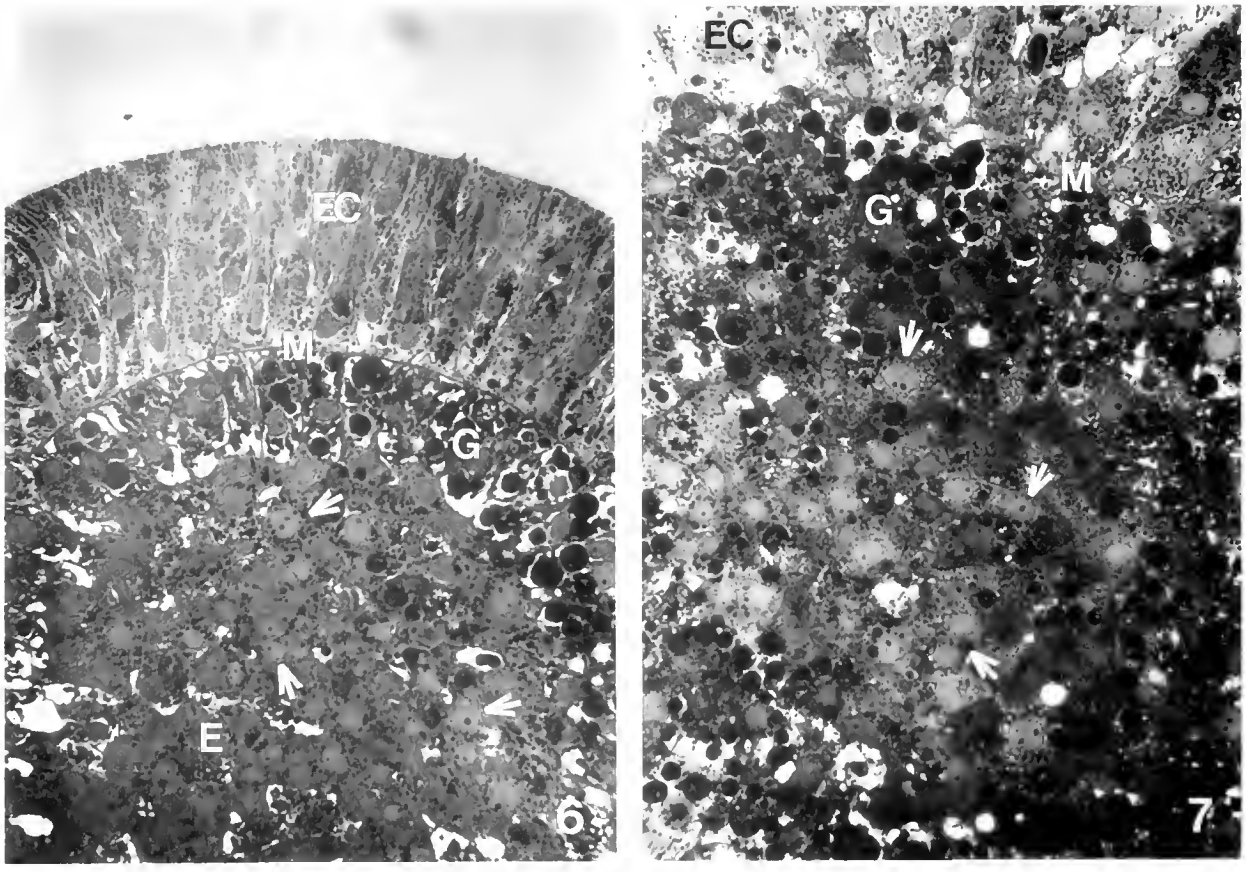

Figure 6. Cross section of a 10-h planula. The embryo consists of an ectoderm (EC), an acellular mesoglea (M), and an endoderm (E). The endoderm is composed of an outer columnar epithelial layer (G) surrounding a central core of lightly staining interstitial cells (arrows). The ectoderm contains epitheliomuscular cells (dark-staining cells) and glandular cells (light-staining cells), but is devoid of interstitial cells, nematoblasts, nematocytes, and ganglionic cells. × 320.

Figure 7. Endodermal region of a 10-h planula. Clusters of interstitial cells (arrows) occupy the central endoderm. EC, ectoderm; G, epithelial layer of endoderm; M, mesoglea. × 320.

anterior-posterior axis. These lightly staining, oval-shaped interstitial cells possess a large, centrally located nucleus with one to several nucleoli. Dark-staining granules occupy the cytoplasm of these young interstitial cells, however, such granules disappear as the cells mature. Interstitial cells of late planulae possess few granules (see Fig. 2).

Interstitial cells traverse the nematocyte differentiation pathway in the endoderm (see Figs. 1, 2, 8). Such cells are distinguished by the appearance of either a dark- or light-staining nematocyst capsule. The capsule enlarges to an extent that it displaces the nucleus to one side of the cell. A few endodermal nematoblasts, confined to the anterior and middle two-thirds of the endoderm, have been observed in the 10-h planula. Interstitial cells traversing the neural differentiation pathway have not been seen in the immature planula.

Interstitial cells and nematoblasts emigrate as single cells from the endoderm to the ectoderm. Interstitial cells migrate out from all locations along the planular endodermal axis, whereas outward nematoblast migration is confined to the anterior and middle endodermal regions. Interstitial cells and nematoblasts first appear in the planular ectoderm at 14 h postfertilization (Martin and Archer, 1986). Their ectodermal distribution corresponds to their above-mentioned migration patterns.

Immature planulae (10 h) do not express a FMRF-amide-like antigen as indicated by their lack of staining.

Young planula (24 h postfertilization)

By 24 h, the planular ectoderm contains epithelial cells (epitheliomuscular, glandular, and sensory), interstitial cells, nematoblasts, a few nematocytes, and ganglionic cells; the endoderm has gastrodermal epithelial cells, interstitial cells, and nematoblasts. Both interstitial cells

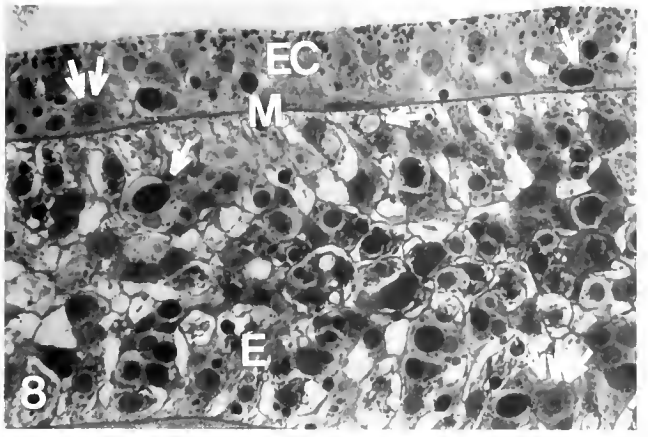

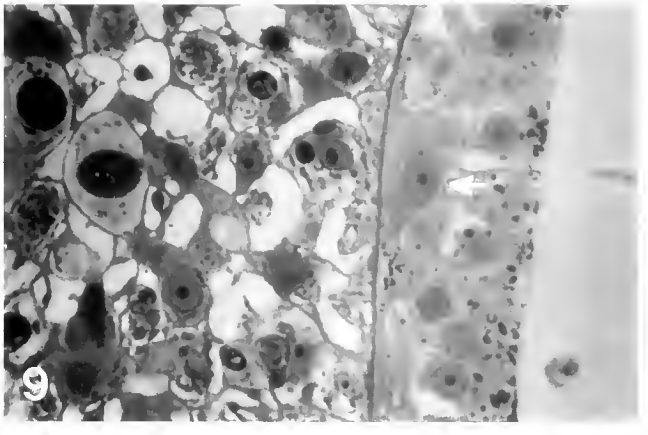

Figure 8. Longitudinal section of a 24-h planula. Differentiating nematoblasts (single arrows) are visible in both the endoderm (E) and the ectoderm (EC). A young ganglionic cell (double arrows) is seen at the base of the ectoderm above the mesoglea (M). Its neurites are not yet fully formed. Triple arrows, endodermal interstitial cells. ×250.

Figure 9. Ectodermal ganglionic cell (arrow) in a 24 h planula. Note its spindle shape and extending neurites. ×620.

and ganglionic cells occupy the entire anterior-posterior axis of the planula, whereas, nematoblasts and nematocytes are confined to the anterior and middle regions of the animal (Figs. 8, 9). In the ectoderm, ganglionic cells and nematoblasts are positioned in close proximity to the mesoglea, and interstitial cells are located slightly above these cells (*i.e.*, toward the outer ectodermal surface). In the endoderm, interstitial cells and nematoblasts may be found in the central core or out closer to the mesoglea. As planulae mature (24–96 h) the numbers of ectodermal and endodermal interstitial cells, ectodermal and endodermal nematoblasts, ectodermal nematocytes, and ectodermal ganglionic cells increase.

At 24 h, the nervous system begins to form (Martin, 1988a, b). This neural system is entirely ectodermal and consists of ganglionic cells (interstitial cell derivatives) and sensory cells (epithelial derivatives). Ganglionic cells form a neural plexus composed of cell bodies and their neurites; this plexus extends the entire length of the planula and is located just above the mesoglea (Fig. 9). These ganglionic cells have originated from interstitial cells that have migrated from the endoderm to the base of the ectoderm. Once in this ectodermal position, they elaborated morphological features characteristic of ganglionic cell differentiation. Interstitial cells traversing the ganglionic pathway in the endoderm have not been observed at this stage. Sensory cells first arise in the anterior end of the planula (later in development they appear all along the length of the planula) and extend from the free surface of the planula to the ganglionic plexus where they insert neurites into the plexus (Martin, 1988b).

Twenty-four hour ganglionic cells do not produce a FMRFamide-like peptide, however, the sensory cells do (Martin, 1988b). The FMRFamide-like peptide is first observed in the apices of sensory cells and only later in their mid to basal regions. FMRFamide-like positive sensory cells are observed throughout the remaining larval period (Figs. 10, 11). Interstitial cells and nematoblasts lack immunostaining at this stage, as does the entire endoderm.

Forty-eight hour planula

The distribution of interstitial cells and their progeny in the 48-h planula is similar to that observed in the 24-h planula. By 48 h, the numbers of these cells have dramatically increased in both germ layers.

At 48 h, a subpopulation of interstitial cells in the anterior endoderm begins to express a FMRFamide-like antigen (Figs. 10, 11). These positive-staining interstitial cells are found exclusively in the anterior-most endodermal region of the planula and are present in the central endodermal core and in the outer endodermal periphery (Figs. 10, 11). Depending upon the plane of section, the FMRFamide-positive interstitial cells exhibit either a mesenchymal shape or an oval morphology. Interstitial cells located in the mid to posterior endodermal regions do not express the FMRFamide-like peptide, as indicated by an absence of staining (Fig. 12). Just after the endodermal appearance of these FMRFamide-like positive interstitial cells, a few immunopositive ganglionic cells are detected in the ectoderm above the mesoglea confined to the anterior head and anterior sides of the planula. Their cell bodies are stained whereas their neurites are not. This is a full day after ganglionic cells first appear in the planular ectoderm. Nematoblasts and nematocytes do not stain for the FMRFamide-like peptide at this stage.

Between 48 and 72 h, the number of immunopositive endodermal interstitial cells and immunopositive ectodermal ganglionic cells increase. Their distribution is limited to the anterior end of the planula.

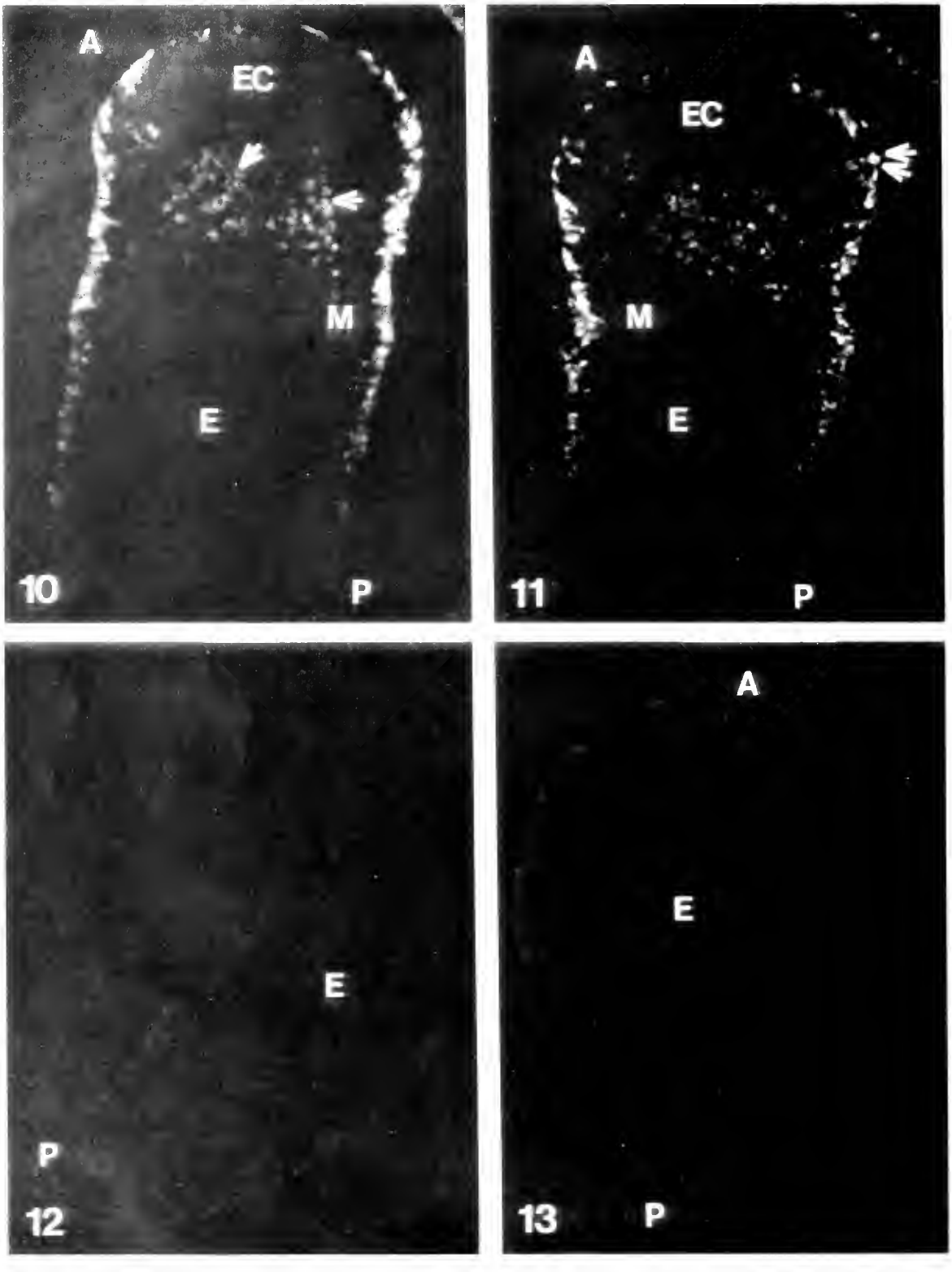

Figure 10. Longitudinal paraffin section of a 48-h planula. A subpopulation of interstitial cells (arrows) in the anterior endoderm of the planula begins to express a FMRFamide-like antigen at this stage in development. A, anterior; E, endoderm; EC, ectoderm; M, mesoglea; P, posterior. × 250.

Figure 11. Longitudinal paraffin section of a 48-h planula. This section is taken from a deeper region of the same planula shown in Figure 10. A subset of interstitial cells in the anterior endoderm expressing a FMRFamide-like antigen is visible, as are FMRFamide-positive sensory cells (double arrows). A, anterior; E, endoderm; EC, ectoderm; M, mesoglea; P, posterior. × 250.

Ultrastructural examination of interstitial cells in the anterior endoderm of 48-h planulae indicates that, based upon morphology, at least three subsets of interstitial cells are found in this region: undifferentiated interstitial cells, interstitial cells traversing the nematocyte differentiation pathway (nematoblasts), and interstitial cells traversing the ganglionic differentiation pathway (neuroblasts) (Figs. 14–19). All three subpopulations can be found in the central endodermal core and at the periphery of the endoderm. These three subsets are also found in older planulae (72 h) in the same endodermal position. Undifferentiated interstitial cells are characterized by a centrally located nucleus with a nucleolus, and a cytoplasm containing free ribosomes, a few mitochondria, and a few segments of rough endoplasmic reticulum (Fig. 14). These interstitial cells, as of yet, show no specific organelles indicative of a particular differentiation pathway. Interstitial cells committed to the nematocyte differentiation pathway have a cytoplasm rich in rough endoplasmic reticulum and form a distinctive nematocyst capsule (Fig. 15). This capsule is in close proximity to the nucleus and often displaces it to one side of the cell. Interstitial cells undergoing neural differentiation (ganglionic cell pathway) form a Golgi complex, electron-dense droplets, dense cored vesicles, and microtubules (Figs. 16–19). These electron-dense droplets and dense cored vesicles occupy the cell bodies of the developing endodermal ganglionic cells and are morphologically identical to the droplets and vesicles found in the ectodermal ganglionic cell bodies and neurites (see Figs. 4, 16, 17, 18, and 19). These developing endodermal neuroblasts do not form neurites in the endoderm, as neurites have only been observed in the ectoderm of the planula.

Colchicine-treated embryos

Embryos treated with colchicine and subsequently allowed to recover for one to two days lack all interstitial cells and their differentiated progeny (ganglionic cells, nematoblasts, neuroblasts, and nematocytes) (Martin and Thomas, 1981a). When such epithelial planulae are exposed to FMRFamide antiserum, they show no immunostaining (Fig. 13). There are no immunopositive interstitial cells, immunopositive neuroblasts, or immunopositive ganglionic cells.

Discussion

Research presented here, as well as past work (Martin and Archer, 1986), indicates that at least some larval interstitial cells are committed within the endoderm to the differentiation of either nerve cells or nematocytes. These restricted cells enter a differentiation pathway in the endoderm, and most probably migrate as nematoblasts or neuroblasts to a position in the ectoderm where differentiation is completed. This process probably accounts for the spatial distribution of the interstitial cell system in the larval ectoderm.

With regard to ganglionic cell formation, this study demonstrates a subpopulation of anterior endodermal interstitial cells that shows early signs of neural cytochemical differentiation by expressing a FMRFamide-like antigen. Concurrent with the appearance of these immunopositive interstitial cells, TEM indicates that a subset of interstitial cells in the same anterior endodermal region develops morphological features indicative of neural differentiation: formation of a Golgi complex, electron-dense droplets, dense cored vesicles, and microtubules. This subset of interstitial cells probably includes the FMRFamide-positive interstitial cells.

Furthermore, a subset of FMRFamide-positive ganglionic cells appears in the anterior ectoderm between 48–72 h. Because this occurs just after the endodermal appearance of the immunopositive interstitial cells, and because both populations are confined to the same anterior head region, the immunopositive interstitial cells have probably migrated to the base of the ectoderm where they differentiated into ganglionic cells. Alternatively, the interstitial cells traversing the neural pathway in the endoderm might never migrate to the ectoderm but simply remain and complete their differentiation, or die, in the endoderm. The alternative is unlikely because the planular endoderm lacks fully differentiated ganglionic cells [*i.e.*, they do not form neurites in the endoderm; neurite formation constitutes the last step in ganglionic cell differentiation (Martin, 1988a)], and TEM studies reveal no signs of degenerating cells in the endoderm at any stage of planular development.

The movements of interstitial cells, nematoblasts, and neuroblasts in planulae appear to be coordinated, as evidenced by their final placement within the ectoderm. Interstitial cells, which divide and possibly remain as stem cells, migrate out from all regions of the endoderm and distribute themselves along the whole planular axis in the ectoderm. Developing nematoblasts emigrate from the endoderm in a specific region of the planula (anterior to mid endoderm) and concentrate in an ectodermal area extending from the anterior end of the planula to the

Figure 12. Paraffin section of the posterior (P) region of a 48 h planula. The posterior endoderm (E) is devoid of FMRFamide-positive interstitial cells. ×250.

Figure 13. Paraffin section of a mature "recovered" colchicine-treated planula. Such epithelial planulae lack FMRFamide-like activity as indicated by the absence of staining. ×250.

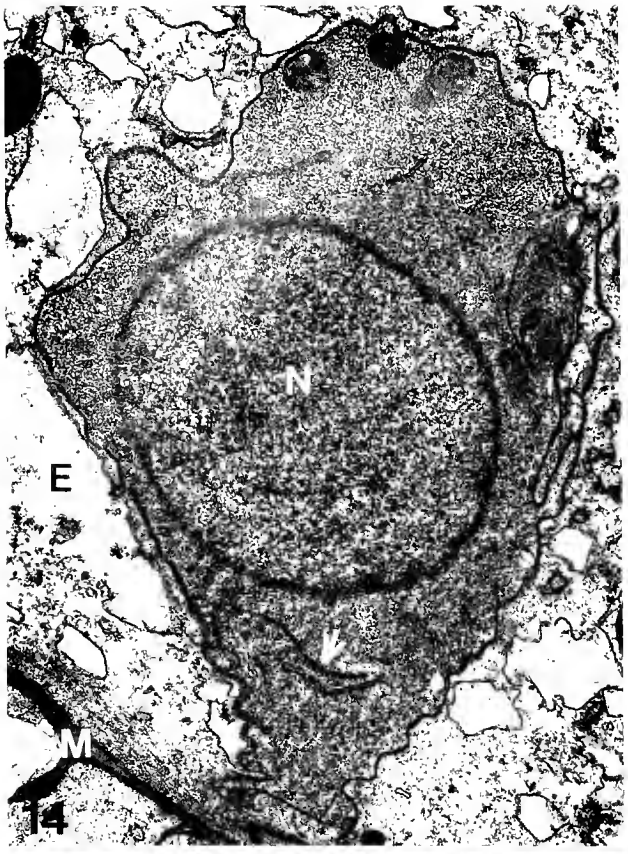
N
E
M
14

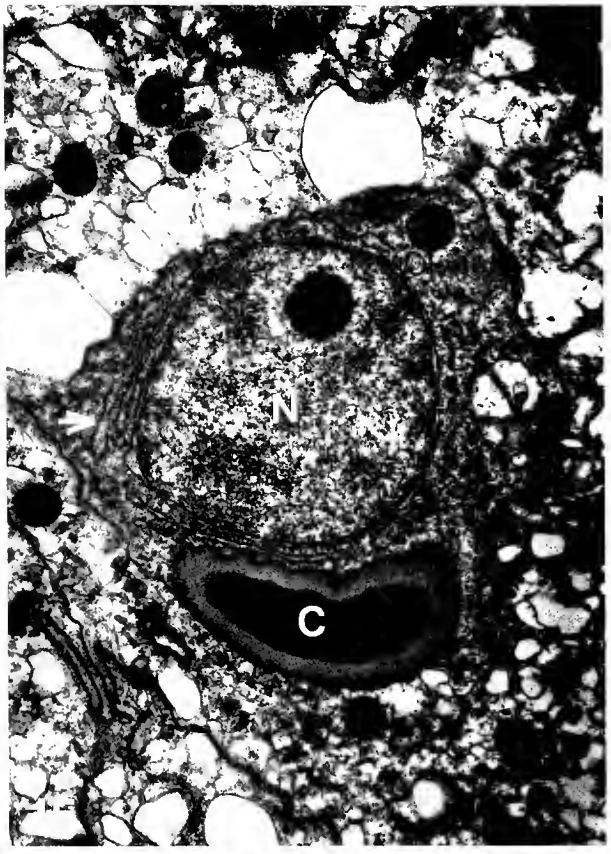
N
C

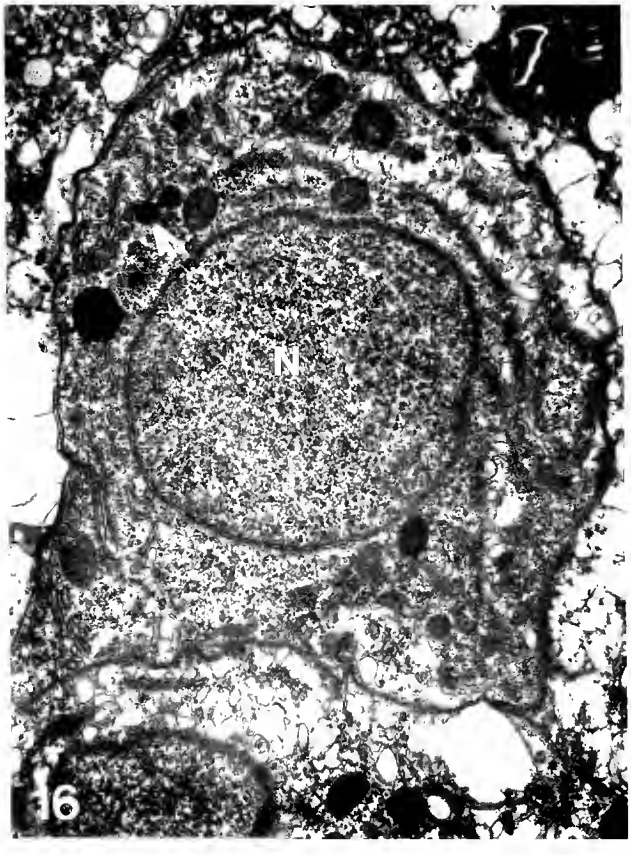
N
16

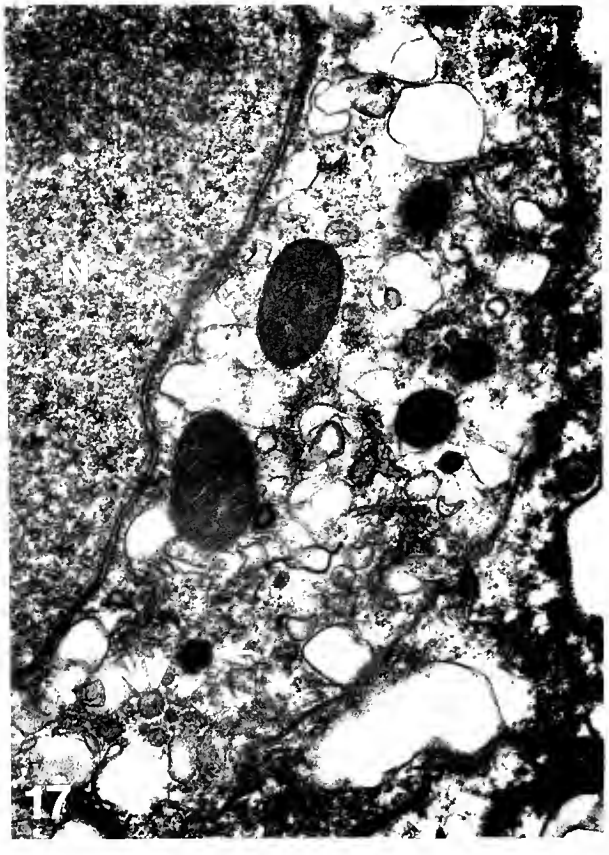
N
17

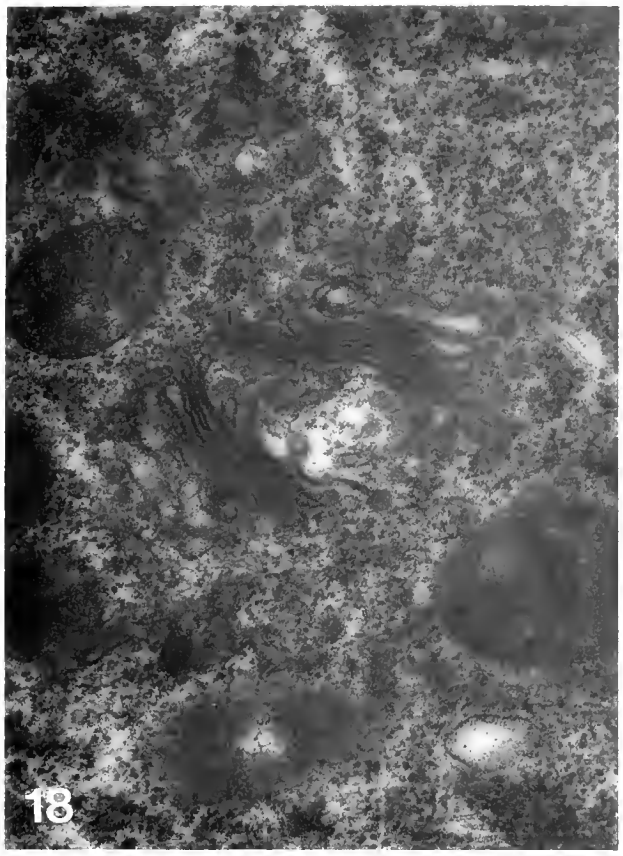

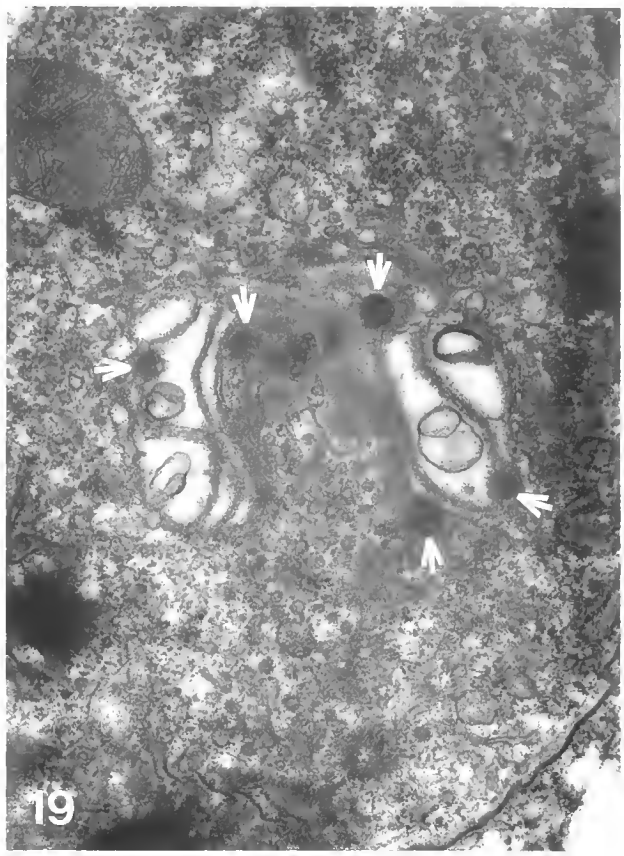

Figure 18. Golgi region of a "neural" endodermal interstitial cell in a 48 h planula. Several mitochondria and microtubules are seen in close proximity to the Golgi. × 37,400.

Figure 19. Electron-dense droplets (arrows) in the Golgi region of a developing endodermal ganglionic cell. Such droplets are characteristic of neural differentiation. × 20,400.

mid-region of the planula. Interstitial cells destined to form ganglionic cells migrate out from all regions of the central endoderm and are evenly distributed along the planular anterior-posterior axis in the ectoderm. Since the interstitial cells and their progeny exhibit a rather precise positioning within the ectoderm, some mechanism of directed migration may be operating in the planula. The FMRFamide findings support the notion of directed migration. FMRFamide-positive endodermal interstitial cells and FMRFamide-positive ectodermal

Figure 14. Endodermal interstitial cell in the anterior region of a 48-h planula. This undifferentiated cell contains a centrally located nucleus (N), a few segments of rough endoplasmic reticulum (arrow), a few mitochondria, and numerous free ribosomes. Although not visible in this plane of section, the interstitial cell also contains a prominent nucleolus. This interstitial cell has migrated from its site of origin in the central endoderm to the outer endoderm (E) and is in close proximity to the mesoglea (M). × 14,400.

Figure 15. Developing nematoblast in the anterior endoderm of a 48-h planula. Interstitial cells traversing the nematocyte differentiation pathway are characterized by the appearance of large amounts of rough endoplasmic reticulum (arrow) and by the formation of a nematocyst capsule (C). Such cells eventually emigrate to the ectoderm. N, nucleus. × 10,800.

Figure 16. Interstitial cell traversing the neural differentiation pathway in the anterior endoderm of a 48-h planula. Such interstitial cells committed to the ganglionic pathway form small electron-dense droplets (arrows) and dense cored vesicles (see Fig. 17), develop a Golgi (see Fig. 18), and accumulate microtubules in their cytoplasm (see Fig. 18). These cells do not develop neurites in the endoderm. N, nucleus. × 9,600.

Figure 17. Developing ganglionic cell in the endoderm of a 48-h planula. The cytoplasm of the differentiating interstitial cell becomes filled with electron-dense droplets (single arrow) and dense cored vesicles (double arrows). Similar droplets and vesicles are abundant in the cell bodies and the neurites of ectodermal ganglionic cells (see Fig. 4). N, nucleus. × 21,600.

ganglionic cells are confined to the same anterior head region of the late planula. As stated previously these positive interstitial cells probably emigrated to the ectoderm and formed the positive ganglionic cells. The fact that the FMRFamide-positive ganglionic cells are confined to a specific region in the ectoderm and not distributed at random suggests directed migration.

Acknowledgments

This research was supported by National Science Foundation Grants DCB-8702212, Career Advancement Award DCB-8711245, and DCB-8942149.

Literature Cited

Graff, D., and C. J. P. Grimmelikhuijzen. 1988. Isolation of <Glu-Gly-Leu-Arg-Trp-NH_2 (Antho-RWamide II), a novel neuropeptide from sea anemones. *FEBS Lett.* **239:** 137–140.

Martin, V. 1988a. Development of nerve cells in hydrozoan planulae: I. Differentiation of ganglionic cells. *Biol. Bull.* **174:** 319–329.

Martin, V. 1988b. Development of nerve cells in hydrozoan planulae: II. Examination of sensory cell differentiation using electron microscopy and immunocytochemistry. *Biol. Bull.* **175:** 65–78.

Martin, V. 1988c. Development of the interstitial cell system in a marine hydrozoan polyp. *Am. Zool.* **28:** 95A.

Martin, V., and W. Archer. 1986. Migration of interstitial cells and their derivatives in a hydrozoan planula. *Dev. Biol.* **116:** 486–496.

Martin, V., and M. Thomas. 1980. Nerve elements in the planula larva of the hydrozoan *Pennaria tiarella*. *J. Morphol.* **166:** 27–36.

Martin, V., and M. Thomas. 1981a. The origin of the nervous system in *Pennaria tiarella* as revealed by treatment with colchicine. *Biol. Bull.* **160:** 303–310.

Martin, V., and M. Thomas. 1981b. Elimination of the interstitial cells in the planula larva of the marine hydrozoan *Pennaria tiarella*. *J. Exp. Zool.* **217:** 303–323.

Martin, V., F.-S. Chia, and R. Koss. 1983. A fine-structural study of metamorphosis of the hydrozoan *Mitrocomella polydiademata*. *J. Morphol.* **176:** 261–287.

Thomas, M., G. Freeman, and V. Martin. 1987. The embryonic origin of neurosensory cells and the role of nerve cells in metamorphosis in *Phialidium gregarium* (Cnidaria, Hydrozoa). *Int. J. Invert. Rep. Dev.* **11:** 265–287.

Reference: *Biol. Bull.* **178:** 21–24. (February, 1990)

Putative Immunological Influence Upon Amphibian Forelimb Regeneration. II. Effects of X-Irradiation on Regeneration and Allograft Rejection

RAYMOND E. SICARD AND MARY F. LOMBARD

Department of Pediatrics, Rhode Island Hospital, Providence, Rhode Island 02903, and Department of Biology, Regis College, Weston, Massachusetts 02193

Abstract. Influence of the immune system on epimorphic regeneration of amphibian limbs has been suggested but not proved. The present investigation explored this hypothesis by examining the effects of x-irradiation on forelimb regeneration and rejection of skin allografts. Two kRad x-irradiation was provided either to a single limb or as whole-body irradiation to intact newts (with 1 limb shielded). Complete suppression of regeneration was observed when limbs to be amputated were irradiated directly. In addition, irradiated limbs displayed severe and protracted inflammation, with total resorption of the affected limbs in 85% of the cases. Moreover, delays in both the rate of forelimb regeneration and allograft rejection were found in animals receiving whole-body irradiation. However, in these cases neither forelimb regeneration nor allograft rejection were suppressed. These observations diffuse the challenge raised by irradiation studies to the notion of possible immunological influence on epimorphic regeneration. Moreover, the delays observed in both regeneration rate and allograft rejection following whole-body irradiation are consistent with possible interaction between the immune system and the regenerating limb. Nevertheless, confirmation that such interaction occurs and is integral to epimorphic regeneration must await further investigations.

Introduction

Epimorphic regeneration of lost appendages in vertebrates is accomplished by a mass of dedifferentiated tissues—the regeneration blastema. This mass of tissue is derived at the site of amputation (Butler, 1935; Brunst and Cheremetieva, 1936; Butler and O'Brien, 1942). Although it has been well-established that the blastema is not produced by an accumulation of blood cells, an influence of the immune system on the progress of regeneration has been suggested (Prehn, 1970). This hypothesis arose because of perceived similarities between sarcomas and the regeneration blastema. In essence, this hypothesis considers that immunostimulation might promote blastemal growth just as mild immunostimulation promotes the growth of certain sarcomas (Prehn, 1970, 1972; Prehn and Lappé, 1971).

The validity of this hypothesis has yet to be either confirmed or refuted conclusively. Nevertheless, several studies have demonstrated effects on the progress of regeneration of substances that might have altered immunological status (Sicard, 1981; Schotté and Sicard, 1982; and Sicard and Laffond, 1983). These experiments employed chemical interventions and assessed their impact on forelimb regeneration but not on immunological function. More recent investigations have examined parameters of immunological status (Sicard and Lombard, 1989). One of these studies disclosed modified responsiveness to T-cell mitogens during epimorphic regeneration (diminished responsiveness during dedifferentiation and blastema formation; augmented responsiveness during proliferative stages) but not following nonamputational trauma. Another study observed reciprocal effects of graft rejection and forelimb regeneration. That is, regeneration rate could be accelerated or delayed when combined with allograft challenge, depending upon the temporal relationship between both operations. Similarly, the rate of allograft rejection could be altered by events of epimorphic regeneration.

Although the results of these previous investigations

Received 30 December 1988; accepted 30 November 1989.

are consistent with immunological influence on epimorphic regeneration, they cannot yet prove that such influence occurs. On the other hand, the studies that established that the blastema is of local origin (Butler, 1935; Brunst and Cheremetieva, 1936; Butler and O'Brien, 1942) might present a formidable challenge to this notion. If whole-body irradiation rendered the subjects immunoincompetent, their subsequent regeneration of forelimbs occurred without immunological influence. However, if the animals retained immunocompetence, then regeneration occurred against a background of potential immunological influence. The absence of specific mention of increased morbidity or mortality in irradiated animals by earlier investigators leads us to the conclusion that immunocompetence was at least adequate to meet challenges of infection in these animals. Nevertheless, this requires verification.

The present investigation was undertaken to confront this potential challenge to the hypothesis that the immune system might influence the initiation and progress of epimorphic regeneration. This investigation employed x-irradiation as the means of intervention and assessed its effects both on forelimb regeneration and immune status (skin allograft rejection). Documentation of an impaired immune response (*i.e.*, delayed graft rejection) in the absence of an effect on forelimb regeneration would challenge or refute the immunostimulation hypothesis as it applies to epimorphic regeneration. On the other hand, demonstration of intact immunocompetence (*i.e.*, essentially normal allograft rejection) in irradiated newts regenerating amputated forelimbs removes the challenge presented by these earlier studies. However, it cannot establish that the immune system plays a role in epimorphic regeneration.

Materials and Methods

Animals

Adult newts (*Notophthalmus viridescens*), obtained from Tennessee, were maintained in glass bowls in Holtfreter's solution at 21 ± 2°C. Two control groups were established: (1) regenerating controls and (2) allograft controls. These groups received no treatment other than amputation or a skin graft and marked the "normal" rate of regeneration or graft rejection. Irradiations and surgical manipulations were performed on newts anesthetized in 0.1% aqueous methane tricaine sulfonate (MS-222).

Irradiation

Initial treatment consisted of x-irradiation. Experimental animals were divided into two groups, one receiving whole-body irradiation, except for a shielded limb, and a second group in which only one limb was irradiated. Total irradiation was either 2 kRad (whole-body and limb) or 2.2 kRad (whole body only). Irradiation was provided using a Picker-Gemini 320 kV industrial x-ray unit equipped with an aluminum filter. Output intensities of 125 or 160 kV were employed for 17.5 min to yield 2 and 2.2 kRad irradiation, respectively. Animals were positioned 15 cm from the source and radiation was administered dorsally. Shielding was provided by a 6 mm thickness of lead plate.

Table I

Effect of irradiation on forelimb regeneration

Treatment	Suppressed or aborted[1]	Mid-bud[2]	Palette	Digital
None	0/15	23 ± 4	33 ± 4	42 ± 4
2 kRad whole body (shielded limb)	3/10	22 ± 2	47 ± 12*	53 ± 10*
2 kRad irradiated limb	13/13**	>76**	—	—

[1] Number of cases/total number within group.
[2] Mean number of days ± 1 S.D.
* $P < 0.01$; ** $P < 0.001$.

Skin grafts

Subsequently, one group of nontreated newts and two groups of newts receiving whole-body irradiation received skin allografts. These animals were used to assess effects of irradiation in cellular immunity. Reciprocal allografts consisted of small pieces of skin, approximately 2 mm^2, implanted into wound sites created by removal of skin used as grafts for other animals. Thus each newt served as both a donor and a recipient. In addition, a small group of control and irradiated animals received autografts.

Amputations

The remaining control and irradiated animals were used to evaluate effects on regeneration. All regeneration groups were subjected to unilateral forelimb amputation through the distal stylopodium. In all instances, any portions of humerus extending beyond the wound surface were carefully trimmed.

Results and Discussion

Effects on regeneration

Regeneration occurred among all control animals and progressed to the early digital stage in approximately 42 days (Table I). Whole-body irradiation suppressed regeneration of shielded limbs in 3 of 10 newts and significantly ($P < 0.01$) slowed the rate of regeneration among

Table II

Effect of irradiation on graft rejection

Treatment	Retained skin graft[1]	Interrupted circulation[2]	Loss of pigment	Rejection
Autografts:				
None	3/3	>76	—	—
2 kRad	3/3	>76	—	—
Allografts:				
None	3/14	12 ± 1	18 ± 8	27 ± 7
2 kRad	1/12	18 ± 6*	24 ± 6	33 ± 10
>2 kRad	0/10	19 ± 7*	30 ± 6*	36 ± 6*

[1] Number of cases/total number within group.
[2] Mean number of days ± 1 S.D.
* $P < 0.05$.

the remainder (Table I). Thus, there was an adverse effect on forelimb regeneration of whole-body irradiation.

In contrast to the results of the shielded-limb group, irradiation of limbs caused total suppression of regeneration in all cases. This is in complete accord with observations from other laboratories (reviewed in Wallace, 1981). Moreover, irradiation of the limbs led to severe and persistent inflammation and ultimately to resorption of the limbs in 85% of the cases. These events appeared strikingly reminiscent of those described by Schotté and Butler (1941) in larval *Ambystoma* following limb denervation and by Butler (1933) in larval *Ambystoma* following irradiation. These investigators ascribed the resorption phenomenon to a failure of dedifferentiation to stop and the progressive stages of regeneration to commence. They inferred that apparent resorption of the stump occurred because of an inability to retain an appendage of dedifferentiated tissues. However, the aggravated initial inflammation followed by loss of pigmentation, and subsequent resorption of soft tissues observed in this study resembled more the rejection of a foreign graft (Cohen, 1966). The extent to which this similarity can be pursued and its implications are the objects of additional studies.

Effects on allograft rejection

Skin autografts were tolerated by those few control and irradiated animals used for that purpose (Table II). In addition, rejection of skin allografts occurred in 11 of 14 controls and 21 of 22 irradiated animals (Table II). However, the rate of rejection appeared to be sensitive to irradiation. In particular, irradiation above 2 kRad significantly delayed ($P < 0.05$), but did not suppress, allograft rejection. These results suggest that irradiation affected the immunological status of the newts; however, at the dosages used, this effect did not cripple the newts' immune system.

Demonstration of delays in the rate of regeneration of shielded limbs of otherwise whole-body irradiated animals suggest that one or more factors outside of the amputation site had been adversely affected by irradiation. To this observation, the resorption of amputated irradiated limbs presents an intriguing counterpoint. Furthermore, the persistence of inflammation and subsequent erosion (resorption) of the stump seems reminiscent of graft rejection. Therefore, it is tempting to suggest that the factors extrinsic to the limb that were affected by irradiation are associated with the immune system. In fact, the occurrence of both of these manifestations is consistent with interactions between the immune system and the amputated limb.

Speculations

Similarities between these data and previous observations of limb resorption following irradiation (Butler, 1933) or limb denervation (Schotté and Butler, 1941) in larval *Ambystoma* prompt the speculation: Following amputation, dedifferentiation of local tissues occurs. If dedifferentiated cells are stabilized and activated (*e.g.*, by neurotrophic factors), they modulate immunological expression favoring blastema formation and possibly contributing to promoting blastemal growth. However, if stabilization and activation does not occur, presumptive blastemal cells are eliminated by activated immunological defenses (Prehn, 1970; Coleman *et al.*, 1989). Moreover, the absence of a pool of accumulating blastema cells (*e.g.*, following irradiation) might lead to limb resorption in a futile attempt to establish such a pool.

Conclusions

The design of this investigation does not enable the means through which x-irradiation induced the particular effects observed to be known with certainty; consequently, alternative interpretations of our observations might be equally tenable. Nevertheless, the results of this investigation demonstrate that regeneration of shielded forelimbs by newts otherwise receiving whole-body irradiation occurs in animals that are still immunocompetent, at least in terms of allograft rejection. In addition, these data suggest that x-irradiation can affect the expression of epimorphic regeneration through central, as well as local, effects. Furthermore, this impairment of regeneration appears to occur in parallel to retardation of the rate of allograft rejection. Consequently, a relationship between immunological expression and epimorphic regeneration is suggested. Moreover, these results remove the potentially devastating challenge to this hypothesis presented by earlier investigations of limb regeneration in which x-irradiation was used.

Acknowledgments

The technical assistance of Kara Anderson, Katherine Costello, and Laurie Peluso is gratefully acknowledged.

Literature Cited

Brunst, V. V., and E. A. Cheremetieva. 1936. Sur la perte locale du pouvoir régénérateur chez le triton et l'axolotl causée par l'rradiation avec les rayons x. *Arch. Zool. Exptl. Gen.* **78:** 57–67.

Butler, E. G. 1933. The effects of x-radiation on the regeneration of the forelimb of *Amblystoma* larvae. *J. Exp. Zool.* **65:** 271–316.

Butler, E. G. 1935. Studies on limb regeneration in x-rayed *Amblystoma* larvae. *Anat. Rec.* **62:** 295–307.

Butler, E. G., and J. P. O'Brien. 1942. Effects of localized x-radiation on regeneration of the urodele limb. *Anat. Rec.* **84:** 407–413.

Cohen, N. 1966. Tissue transplantation immunity in the adult newt, *Diemictylus viridescens*. II. The rejection phase: first- and second-set allograft rejections and lack of sexual dimorphism. *J. Exp. Zool.* **163:** 173–190.

Coleman, R., M. Lombard, R. Sicard, and N. Rencricca. 1989. *Fundamental Immunology.* Unit 8: Cancer and Transplantation. Wm. C. Brown Publishers, Dubuque, IA. Pp. 427–504.

Prehn, R. T. 1970. Immunosurveillance, regeneration, and oncogenesis. *Progr. Exp. Tumor Res.* **14:** 1–24.

Prehn, R. T. 1972. The immune reaction as a stimulator of tumor growth. *Science* **176:** 170–171.

Prehn, R. T., and M. Lappé. 1971. An immunostimulation theory of tumor development. *Transplant. Rev.* 7: 26–54.

Schotté, O. E., and E. G. Butler. 1941. Morphological effects of denervation and amputation of limbs in urodele larvae. *J. Exp. Zool.* **87:** 279–322.

Schotté, O. E., and R. E. Sicard. 1982. Cyclophosphamide-induced leukopenia and suppression of limb regeneration in the adult newt, *Notophthalmus viridescens*. *J. Exp. Zool.* **222:** 199–202.

Sicard, R. E. 1981. The effects of putative immunological manipulations upon the rate of limb regeneration in adult newts, *Notophthalmus viridescens*. *IRCS Med. Scis.* **9:** 692–693.

Sicard, R. E., and W. T. Laffond. 1983. Putative immunological influence upon amphibian forelimb regeneration. I. Effects of several immunoactive agents on regeneration rate and gross morphology. *Exp. Cell Biol.* **51:** 337–344.

Sicard, R. E., and M. F. Lombard. 1989. Epimorphic regeneration and the immune system. Pp. 107–119 in *Recent Trends in Regeneration Research*. V. Kiortsis, S. Koussoulakos, and H. Wallace, eds. Plenum Publ. Corp., New York.

Wallace, H. 1981. *Vertebrate Limb Regeneration.* Wiley and Sons, Chichester.

Reference: *Biol. Bull.* **178:** 25–32. (February, 1990)

Correlation of Abnormal Radular Secretion with Tissue Degrowth During Stress Periods in *Helisoma trivolvis* (Pulmonata, Basommatophora)

DAVID A. SMITH[1] AND W. D. RUSSELL-HUNTER[2,3]

[1]*Wabash College, Department of Biology, Crawfordsville, Indiana 47933;* [2]*Syracuse University, Department of Biology, Syracuse, New York 13244-1270; and* [3]*Marine Biological Laboratory, Woods Hole, Massachusetts 02543*

Abstract. Laboratory experiments on starvation stress in *Helisoma trivolvis* elucidate a relationship between modifications of radular secretion and tissue degrowth resulting from stress. Tissue losses in starved adults ranged from 4.5% at 40 days to 27.7% at 160 days, with negligible mortality (<2%). Modifications in radular secretion that paralleled tissue loss involved not only abnormal secretion of individual teeth and of tooth rows, but especially an increased "packing" of radular rows per unit ribbon length. Radular length remained constant during experimental trials, however the mean number of tooth rows increased by almost 47% after 120 days of food deprivation. Radular patterns reflecting degrowth observed in these experiments were paralleled in radulae taken from overwintered animals sampled from natural populations. Rates of radular turnover averaged between 2.3% new growth per day (43 days to turnover) and 4.0% new growth per day (25 days to turnover). Radular samples could provide for *post hoc* detection of recent periods of tissue degrowth in snails, just as evidence of longer periods of tissue degrowth can be detected in the shells of long-lived bivalves.

Introduction

Natural populations of aquatic molluscs can experience tissue loss during winter. This phenomenon involves complex shifts in metabolism and has been called "degrowth" (Russell-Hunter, 1985). Previous reports have demonstrated that physiological stress, both short-term and of longer duration, can temporarily affect radular secretion (Isarankura and Runham, 1968; Kerth, 1971; Fujioka, 1985; Smith, 1987). The laboratory experiments reported here were designed to clarify the relationship between abnormal radular secretion and concurrent tissue degrowth resulting from starvation stress. Applied to field populations, these observations could provide an independent (short-term) method for detecting periods of starvation that had occurred shortly before sampling. This would complement the long-term detection of stress-induced degrowth based on "oversized" shells (Russell-Hunter *et al.,* 1984), or on modified catabolism (Russell-Hunter *et al.,* 1983). The Ramshorn snail of eastern North America, *Helisoma trivolvis* (Say, 1817), was particularly suitable for these experiments because it performs well in laboratory culture, and because recent studies have documented not only the biometry and mechanics of its radula (Smith, 1987, 1988, 1989), but also its actuarial bioenergetics, including its capacity for degrowth (Russell-Hunter and Eversole, 1976; Russell-Hunter *et al.,* 1983, 1984).

Detailed analysis of radula-tooth biometry in *Helisoma* has shown significant levels of interpopulation variation in this species (Smith, 1987, 1989). As with similar studies on Lymnaeid pulmonates by Berrie (1959) and Hunter (1975), in *Helisoma* there are no observable ecophenotypic effects on tooth shape. Despite this constancy (within individuals, and within populations) more general aspects of radular secretion, including the number and density of tooth rows, can be modified by environmental stress. Short exposures to near-freezing temperatures will produce a zone of modified tooth rows on the radula ribbon (Isarankura and Runham, 1968; Kerth, 1971; Fujioka, 1985; Smith, 1987), and longer exposures to the stress of starvation will produce "bunching" or "packing" of radular rows, as described below.

Received 6 July 1989; accepted 14 November 1989.

Work on the bioenergetics of tissue degrowth in *Helisoma* is also cognate to these experiments. Held in the laboratory in a metabolic framework simulating that of natural overwintering, a representative cohort of *Helisoma* showed a 50% loss of tissue biomass (involving perhaps 20% loss of protein) with only 10% mortality over 132 days (Russell-Hunter and Eversole, 1976). Metabolic shifts during the degrowth process were studied by Russell-Hunter *et al.* (1983) using nearly concurrent assessments of oxygen consumption and of nitrogenous excretion. There was a clearly controlled differential catabolism of protein resources during degrowth. One of the first quantitative reports of direct field evidence for tissue degrowth during winter is for natural populations of *Helisoma trivolvis* and of *Lymnaea palustris* in central New York state (Russell-Hunter *et al.*, 1984).

The existence of all these recent reports not only made stocks of *Helisoma* appropriate for these experiments, but also made it likely that a history of recent degrowth could be detected by detailed examination of the radula. In field studies this might come to parallel evidence (Clark, 1976; Mallet *et al.*, 1987; Peterson *et al.*, 1985) of longer periods of degrowth and regrowth which can be detected in the shells of long-lived bivalves.

Materials and Methods

Helisoma trivolvis is one of the more common gastropod molluscs of central New York state. This euryoecic, pulmonate snail is found primarily in eutrophic environments including lakes, ponds, streams, farm ponds, and drainage ditches. Mature adults used for laboratory analysis of tissue degrowth were taken from a small pond in Ithaca, New York (76°22.96′W, 42°25.78′N). To study the effects of overwintering on radula secretion, as well as the patterns of radular regrowth during early spring, snails were sampled in April and May, 1985, from four additional field sites (Eaton Reservoir, 75°42.27′W, 42°51.10′N; Meadowbrook Pond, 76°07.08′W, 43°01.59′N; Otter Pond, 76°32.83′W, 43°09.52′N; and Silver Lake, Remsen, 75°08.19′W, 43°20.97′N).

Methods used to quantify tissue degrowth were modified from those of Russell-Hunter and Eversole (1976), and protocols for radula preparation are detailed by Smith (1987). To initiate an investigation of tissue degrowth, more than 400 adult snails were collected at the Ithaca field site in October 1985. This sample reflects the natural variation in a single generation of *Helisoma* as it moves into winter conditions. All shells were measured with dial calipers (±0.1 mm) for maximum shell diameter (MD). On the basis of MD, individuals were then divided into three size classes: <14.0, 14.1–16.9, and >17.0 mm. Two individuals from each class were then cultured together in translucent plastic beverage cups (n = 6 per container) in approximately 400 ml of filtered pond water. At this time, groups, each containing six snails, were randomly designated (using Japanese icosahedral dice) as "fed" or "starved" experimentals or as baseline controls. Fed animals were provided fresh lettuce for the duration of the experiment; starved animals were starved for 120 days and then fed lettuce for the last 40 days of the trial. The experiment was run in a B.O.D. chamber at 8°C. Cold fluorescent lights illuminated the cultures on a 14L/10D cycle. Cups were cleaned, and provided with fresh, filtered, water each week.

Samples were taken at 0, 40, 80, 120, and 160 days both for analysis of tissue degrowth and for radular preparations. Of 264 animals used in this study, 72 were designated controls and 192 were experimentals. Of these 192, 144 were used for tissue analysis and 48 were used for estimating radular degrowth. At 40-day intervals, samples of 18 snails from each treatment were assessed for shell and tissue dry weight. Individuals were oven dried at 65°C, treated with an excess of 8.5% HNO_3 (12% v/v nitric acid), washed, and then redried, giving two dry weights, whole snail and tissue, and, by subtraction, a value for dissolved calcium carbonate. Tissue degrowth was then calculated as the difference between actual tissue dry weight (TDW) and that predicted from initial tissue-to-shell regressions established at the start of the trial (TDWp).

To determine the effects of food deprivation on radular secretion, 6 specimens from each of the above treatments were sampled every 40 days. Individuals were sacrificed in boiling water and removed from their shells. The buccal mass of each individual was removed, softened in saturated KOH for 2–5 seconds, and transferred to distilled water. Radulae were then removed with fine forceps, placed onto clean glass slides, arranged, and covered with coverglasses. Preparations were then held in distilled water for 24 hours, dehydrated in 70% EtOH and air dried. New coverglasses and mounting fluid were then applied. Abnormal radular secretion was quantified by first dividing each radula into three equal sectors on the basis of overall length. The total number of tooth rows per sector was then counted.

To study the natural patterns of return to normal radular secretion following overwinter stress, adult *Helisoma* were collected in early spring at four field sites. Sampling continued until evidence of abnormal secretion (row-packing) was no longer present. Radular growth rates were calculated as length of new growth as a fraction of ribbon length.

Methods used to study radular turnover in the laboratory follow Isarankura and Runham (1968). Pond water was cooled to approximately 1°C. Snails were placed in this bath for 24 hours. Individuals were then returned to room temperature (18°C) and were provided fresh lettuce. Individuals were sacrificed daily until regions of radular malformation were absent.

Table I

Tissue degrowth in Helisoma trivolvis

A.	40 d	80 d	120 d	160 d
Fed	−1.9 ± 1.63	−6.5 ± 1.41	−8.7 ± 1.50	−11.3 ± 1.91
Unfed	−2.2 ± 1.54	−8.6 ± 1.62	−13.1 ± 1.69	−14.6 ± 1.80
B.	40 d	80 d	120 d	160 d
Fed*	−3.5 ± 2.58	−11.0 ± 2.46	−15.7 ± 2.29	−19.0 ± 3.05
Unfed**	−4.5 ± 2.57	−15.6 ± 3.44	−23.8 ± 2.05	−27.7 ± 2.83

* ANOVA $F_{3,68} = 7.438$, $P < 0.001$

** ANOVA $F_{3,68} = 13.878$, $P < 0.001$

Data were subject to arcsin-square root transformation before analysis.

A. Change in tissue dry weight in milligrams (as TDW-TDWp, n = 18) over 160 days. B. Change in tissue dry weight as a percentage of predicted tissue dry weight [((TDW-TDWp)/TDWp)·100, n = 18], over 160 days.

Results

At the start of the laboratory trial 72 control individuals had been sacrificed. For these, analysis showed that tissue dry weight (mg) related to shell dry weight (mg) as TDW = 0.254·SDW + 1.335 (r = 0.956, n = 72, $P < 0.001$). With each set of known values of SDW, this relationship was then used as a predictor of TDW. The deviation of predicted (TDWp) from expected TDW for each individual was used as an indicator of tissue growth or of tissue degrowth. These values for each of four sampling periods are set out in Table I. Two-hundred and sixty-four individuals began the trial; four died (<2%) and were replaced with parallel experimental animals. Tissue degrowth clearly occurred by 80 days in both sets of experimental animals, and this had nearly doubled by 160 days (Table I). Degrowth over 160 days of food deprivation ranged from 4.5% tissue loss at 40 days to 27.7% tissue loss at 160 days. These values correspond to 2.2 mg below predicted tissue dry weight and 14.6 mg below TDWp, respectively. Degrowth in animals belonging to the fed treatment ranged from 3.5% at 40 days to 19.0% at 160 days. Levels of tissue loss in fed and unfed treatments did not differ ($P > 0.05$) at 40 and at 80 days. At 120 and at 160 days, however, treatments did show significantly different mean levels of degrowth (t_{120} days = 2.414, n = 36, $P < 0.05$; t_{160} days = 2.098, n = 36, $P < 0.05$).

Tissue degrowth in the experimental snails was paralleled by abnormal radular secretion (Fig. 1). This was manifest not only in malformations of individual radular rows (including smaller lateral, marginal, and rachidian teeth; irregular lateral, marginal, and rachidian teeth; and missing marginal teeth), but also, and most consistently, by an increased number of radular rows (packing) per unit ribbon length. Radular length remained constant during experimental trials, however the mean number of tooth rows increased by almost 47% after 120 days of food deprivation (Table IIa). Observations showed this increase was associated with the generative (posterior) end of the radular ribbon. Although secretory activity of the odontoblasts continued during the trial, secretion by the membranoblasts (which produces lengthening of the radula ribbon) proceeded at a much reduced relative rate (Fig. 2). [The precise mechanism of post-secretory radular transport remains uncertain. The topic has been reviewed by Runham (1963), Mischor and Märkel (1984), and Mackenstedt and Märkel (1987).] This differential activity of odontoblasts and of membranoblasts resulted in an increased density of tooth rows at the posterior end of the radula ribbon (Fig. 2). During the last 40 days of the trial (refeeding), radular transport was restored and the proper pattern of radular secretion was again established (Table IIb). Once a normal pattern of secretion was established, the region between the tightly compressed rows (generated during stress) and the normally deposited rows (generated during refeeding) provided a marker which could be used to quantify radular turnover rates either in experimental or in natural populations.

Patterns of abnormal radular secretion observed in the laboratory were paralleled in radulae taken from animals sampled from five field sites (Fig. 3). Weekly sampling in early spring allowed a unique opportunity to estimate radular growth and turnover rates under natural conditions. Values among five sites ranged between 3–4% new growth per day. This figure corresponds to approximately 5–7 rows per day, and to 225–315 teeth per day. Radulae from Meadowbrook Pond showed the slowest turnover (2.3% growth/day, 43 days to turnover) while radulae from Ithaca turned over most rapidly (4.0%/day, 25 days to turnover). Radulae from the other three sites turned over in approximately 30 days (Eaton, 2.9%/day, 34 days turnover; Otter, 3.6%/day, 28 days turnover, Remsen, 3.5%/day, 29 days turnover). These rate data agree with laboratory trials, which showed ribbon turnover in 30 days at room temperature. Field rates also agree with those determined by Isarankura and Runham (1968) who reported average radular production of approximately 3.2 rows per day (minimum 0.5, maximum 7.5, average minimum 2.8, average maximum 4.2 rows/day) for a variety of molluscs including *Helix* and *Lymnaea*. At one field site (Ithaca) the progress of return to normal radular secretion correlated with changes in tissue regrowth (as tissue/shell) (r = 0.937, n = 5, $P < 0.05$) indicating that radular growth is associated with increases in early spring tissue biomass.

Discussion

There is no doubt that, for *Helisoma trivolvis* at least, our experimental conditions closely match those of over-

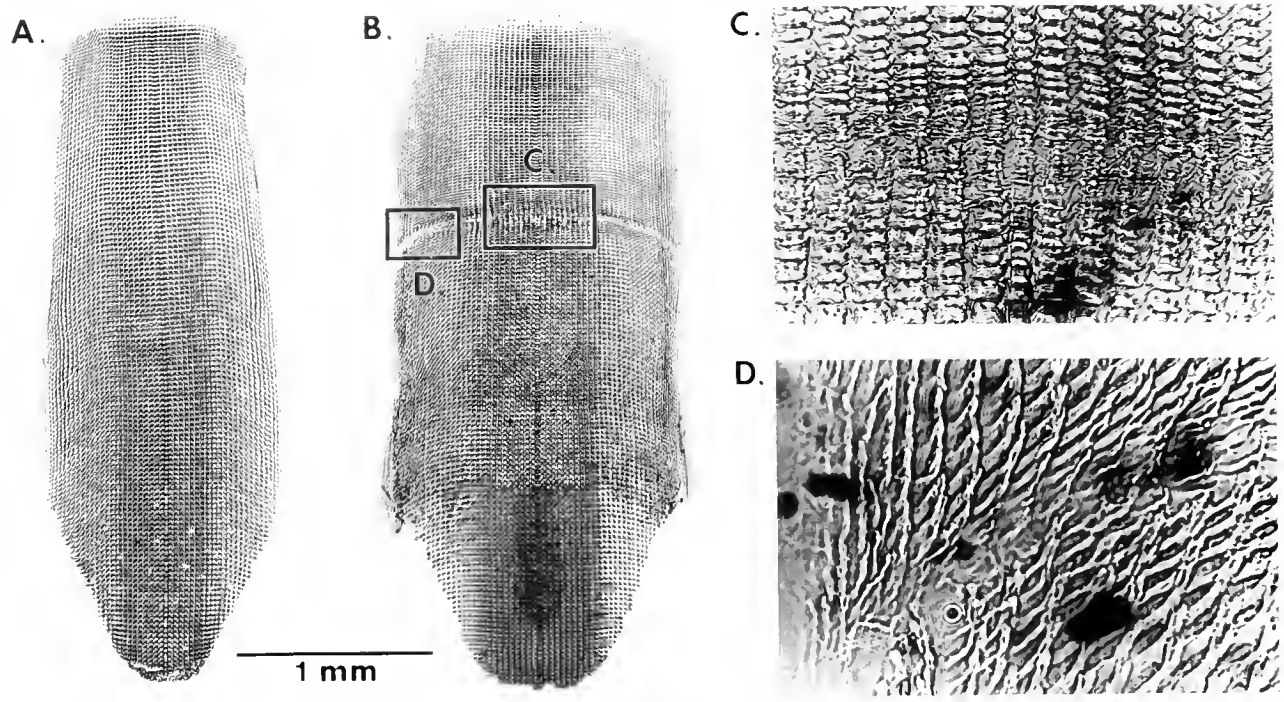

Figure 1. Untouched photographs to show radular malformations in *Helisoma*. A. Normal radula. B. Radula after 75 days of food deprivation. In both A and B, the most recently secreted radular rows are at the top of each photograph, and the rows in use are near the bottom. C. Enlarged view of rachidian and lateral-tooth region from B. Note lateral tooth malformations and row packing. D. Enlarged view of marginal-tooth region from B. Note that marginal teeth are absent from the region of degrowth.

wintering in natural populations. Degrowth in three field populations measured by Russell-Hunter *et al.* (1984) showed average losses in tissue biomass of 24.7%, 28.3%, and 41.3%. The maximum loss of 27.7% over 160 days in these experiments is appropriate.

The results of the present investigation confirm that the physiological stress of starvation in *Helisoma* results not only in tissue degrowth but also in concurrent changes in radular secretion. The significance of this concurrence is twofold, involving first, possible insight into the fundamental control mechanisms of stress response in molluscs, and second, the possibility (for applied studies) of *post hoc* detection, in natural populations, of earlier periods of starvation or similar stress. Before reviewing these two aspects, however, it is necessary to set out certain strengths and weaknesses in laboratory starvation experiments.

In general, quantitative studies of any kind of stress on

Table II

Modification of radular secretion in Helisoma trivolvis

A.	0 d	40 d	80 d	120 d	160 d
Length (mm)*	2.7 ± 0.04	2.9 ± 0.16	2.7 ± 0.17	2.7 ± 0.19	2.4 ± 0.29
Total rows**	138 ± 1.9	169 ± 9.4	192 ± 9.8	202 ± 13.7	194 ± 27.1
Rows/mm***	52 ± 0.9	59 ± 1.3	70 ± 2.0	77 ± 4.1	82 ± 9.7

* ANOVA $F_{4,20} = 0.707$, $P > 0.5$, **ANOVA $F_{4,20} = 3.072$, $P < 0.05$, ***ANOVA $F_{4,20} = 6.724$, $P < 0.01$.

B.	0 d	40 d	80 d	120 d	160 d
Anterior	34.6 ± 0.40	30.6 ± 0.51	28.8 ± 0.92	26.0 ± 1.48	31.4 ± 3.23
Middle	32.2 ± 0.37	29.2 ± 0.97	27.6 ± 0.40	24.4 ± 1.17	32.8 ± 4.89
Posterior	33.2 ± 0.49	40.6 ± 0.87	43.4 ± 1.03	49.2 ± 2.25	36.2 ± 2.82
Row number	138 ± 1.9	169 ± 9.4	192 ± 9.8	202 ± 13.7	194 ± 27.1

A. Basic statistics for abnormal radular secretion in unfed snails over 160 days (n = 5). B. Sector analysis as percent per sector based on total number of rows (average total on last line).

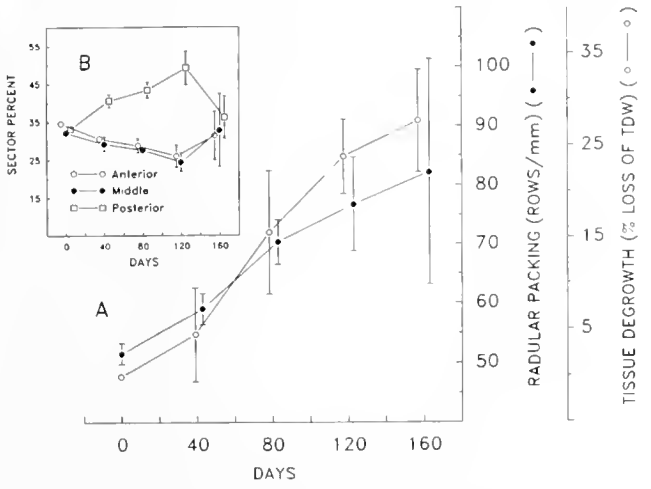

Figure 2. Patterns of radular modification and tissue degrowth in laboratory stocks of *Helisoma trivolvis*. Main plot (A) shows correlation of tissue degrowth and abnormal radular secretion. Insert plot (B) shows pattern of radular packing (see text for further explanation). Vertical bars are 95% confidence limits of each mean.

animals in laboratory culture must not involve high rates of mortality. Our survivorship rate (>98%) in the experimental groups is clearly satisfactory. Evidence of degrowth in snails and in other shelled molluscs is based on the permanence of the calcareous shell as a record of previous tissue biomass. In a review of molluscan degrowth studies, Russell-Hunter (1985) emphasizes an important *caveat*, that ratio measurements of tissue-shell relationships and, hence, predicted values of tissue biomass should be obtained only from those species that demonstrably show no shell resorption. *Helisoma trivolvis* has been well studied in this respect, and its shell does not change in mass or in composition (Russell-Hunter and Eversole, 1976; Russell-Hunter *et al.*, 1983, 1984).

A more immediate difficulty is that, with experimental groups set up as in the present series, it is empirically impossible to provide polar trophic conditions. Under our experimental conditions, "fed" snails are not satiated, while "unfed" snails are not totally starved (microorganisms are present in 7-day-old water and on shells). Our controls represent unstressed snails, the fed snails represent some nutritional stress, and the unfeds greater stress. In similar experiments, which assessed the control of differential catabolism (by measuring oxygen consumption and nitrogenous excretion) during degrowth (Russell-Hunter *et al.*, 1983), highly stressed snails established an effective regime of metabolic compensation (by reducing the proportion of protein catabolism) more rapidly than less stressed snails. Unlike shell mass, tissue biomass is not a static value (see Russell-Hunter and Buckley, 1983, for discussion of this in the actuarial bioenergetics of molluscan productivity). While any individual organism remains alive, its tissue biomass continues to be in turnover. Thus, growth represents a positive value (and degrowth a negative value) for a combined net rate that involves both inputs and outputs as rate functions (Russell-Hunter and Buckley, 1983; Russell-Hunter *et al.*, 1983).

Tissue degrowth in our experiments was paralleled by abnormal patterns of radular secretion. This was manifest in several ways. Smaller lateral, marginal, and rachidian teeth; irregular (malformed) lateral, marginal, and rachidian teeth; and missing marginals were readily apparent (Fig. 1c). Most consistently, tissue degrowth was correlated with an increase in the number of radular rows per unit ribbon length. At 40 days it was apparent that either (1) production of subradular membrane by the membranoblasts and transport by the inferior epithelium had slowed, or (2) the production of radular teeth by the odontoblasts had hastened. Regardless of the relative contributions of these alternative processes, the result is the same. An obvious zone (Figs. 1, 4) of denser row-packing has been created. These observations, after confirmation from field analysis, suggest that activity of membranoblast and odontoblast cell lines is differentially impaired during periods of food deprivation. The nature of the control mechanism regulating these cells is still uncertain so it is not possible to determine how food deprivation influences the results documented here. However, membranoblast activity is reduced to a greater extent than that of the odontoblasts during periods of sustained stress, and this differential secretory response produces the characteristically packed rows. The fact that there are no observable ecophenotypic effects on tooth shape (thought to be under rigid genetic control in

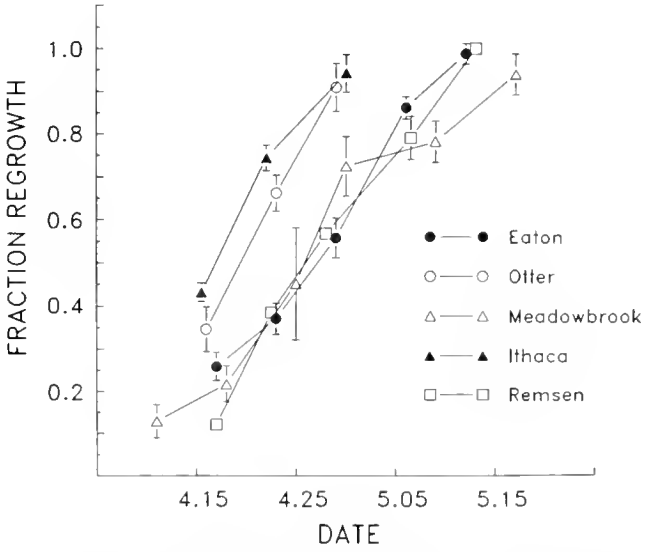

Figure 3. Return to normal radular secretion in spring in five natural populations of *Helisoma*, demonstrating recovery from radular row-packing overwinter (and from presumptive overwinter tissue degrowth). Vertical bars are 95% confidence limits of each mean.

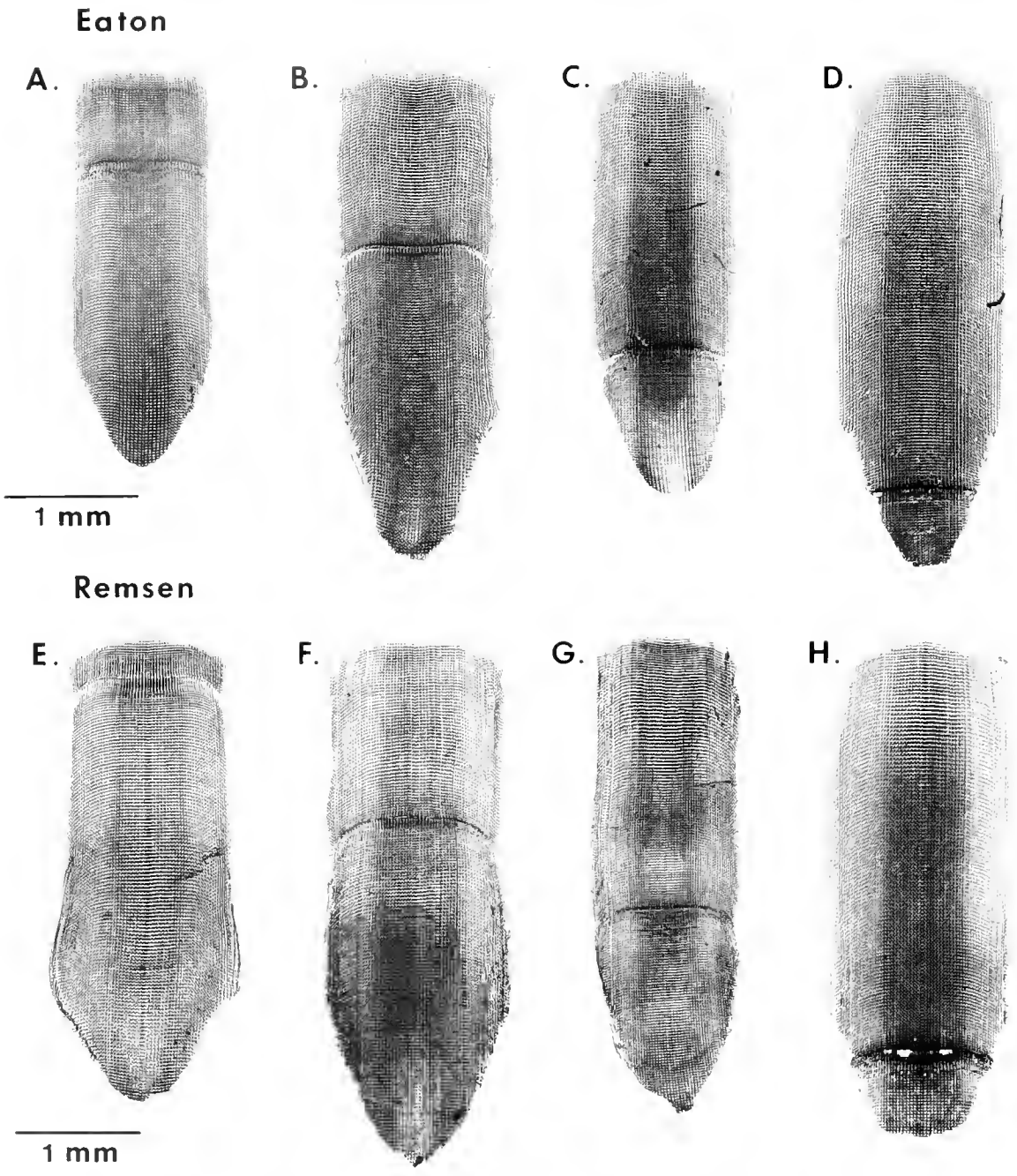

Figure 4. Untouched photographs showing patterns of return to normal radular secretion in two natural stocks of *Helisoma trivolvis*. Note that the most recently secreted radular rows are at the top of each photograph. Radulae from Eaton Reservoir (top, A–D, left to right) represent 29%, 40%, 61%, and 80% regrowth (as fraction new rows of total rows). Radulae from Silver Lake, Remsen (bottom, E–H, left to right) represent 17%, 36%, 53% and 76% regrowth. Samples from both sites were taken at weekly intervals beginning 4.22.85. Actual sizes are; Eaton (top, left to right), 3.1, 3.7, 3.2, and 3.8 mm, Remsen (bottom, left to right), 3.7, 4.3, 3.8, 3.9 mm.

each stock or population; Smith, 1987, 1989) emphasizes the unique significance of row-packing as a predictable response to environmental stress.

In one respect, that of the time sequence of return to normal tissue growth after stress, the radular record of row-packing can be more useful than any assessments based on shell-tissue ratios. In field studies of tissue degrowth (Russell-Hunter *et al.*, 1984), one pond stock of *Helisoma* recovered from 41.3% average degrowth to only 32.8% over three months in spring. In another stock

(from a highly eutrophic lake), overwinter degrowth was eliminated (47.1% net growth) in two spring months. The data on radular recovery (corresponding to regrowth) from the five sites sampled during this study not only show that the process was complete within 25–43 days, but also indicated its temporal sequence in stages.

As noted above, there are two significant aspects to the concurrence of abnormal radular secretion and of tissue degrowth as consequences of starvation stress. The first concerns a matter of fundamental biology in attempting to deduce the control mechanisms involved and, ultimately, the sequence of causality. All patterns of response to environmental stress have evolved to increase the fitness of individuals, and all basically require (i) receptors monitoring changes in the rate of abiotic and physiological parameters, (ii) some system capable of integrating such inputs, and (iii) effector tissues that carry out the response. In the case of the response to starvation in gastropods, we have quantified for (iii) several kinds of effects, we can deduce something of (ii), but we are almost completely ignorant of (i) in specific terms. At the very least we know that the simultaneous effects include both abnormal radular secretion and general tissue degrowth. The former involves both absolute and relative reductions of the secretory activity of membranoblasts. The latter involves not only highly reduced levels of general catabolic activity but also a metabolic shift towards relatively higher turnover of nonprotein carbon. As has been noted (Russell-Hunter, 1985), such controlled differential catabolism can be considered an appropriate parsimony in the net flow through of amino acids (rather than as the defense of a static protein biomass).

There are obvious elements of adaptive conservation in the fact that odontoblast activity is less reduced than membranoblast activity, and in the preservation (relatively) of structural proteins in the tissues. Both differential processes are adaptive in their potential to accelerate return to normal secretion and tissue regrowth when the period of stress has ended. Parenthetically, it should be noted that this capacity for controlled tissue degrowth [increasing individual survivorship under certain environmental conditions by a decrease in individual energy content (Russell-Hunter, 1985; and references therein)] compels reconsideration of certain fitness predictions from simple models of age structure and energy partitioning between growth and reproduction (see for example, Williams, 1966; Tinkle and Hadley, 1975; Browne and Russell-Hunter, 1978).

It seems likely that the ganglia of the snail's central nervous system are involved in integration after the onset of starvation stress. It is unlikely that the integrating system is linked neurally to the rate-controlling cells for membranoblast secretion and those of differential protein catabolism, and barely possible that a specialized endocrine tissue is involved. It can be postulated that the most likely link is through neurosecretory cells. Other systems of integrated control in molluscs involve neurosecretion. For example, sex change in *Crepidula* (Russell-Hunter *et al.*, 1971), and cyclic reproductive behavior in high littoral snails (Price, 1979) involve neurosecretion. Despite the degree of integration of the response to overwinter starvation, it may not be appropriate to term this a diapause, since it is less obligate and more plastic in these snails than in those nematodes and insect larvae from similar habitats for which an innate and essential seasonal diapause has been described. However, there is integration of responses (probably involving neurosecretion), and there can be no question either of abnormal radular secretion (row-packing) *causing* tissue degrowth or even of tissue degrowth *causing* row-packing directly. Although the common cause of both sets of responses appears to be the stress of starvation, these statements belong within David Hume's (1748) regularity theory of causation, which remains appropriate for the logical description of such biological sequences, despite being currently unfashionable among many professional philosophers.

Conclusions from these experimental data have a second significance to applied biology: the possibility of a retrospective detection, in the field, of earlier periods of stress affecting natural populations. Just as the trunks of long-lived forest trees can record in their rings the historical sequence of drought years and of minor forest fires, so the shells of long-lived bivalve molluscs (Clark, 1976; Mallet *et al.*, 1987; Peterson *et al.*, 1985) can record, in their growth rings, a history of severe winters. Radular records of degrowth periods as zones of modified toothrow secretion may provide a history of more recent environmental stress. This may be of applied value in some gastropod stocks by using comparative spring samples of radulae from known populations to assess relative levels of overwinter starvation, and thence to predict productivity for the rest of the year. In addition, similar radular records could be useful in assessing the metabolic stress of a transient period of pollution (such as an oil spill) on populations of freshwater or marine littoral gastropods, even if no records had been obtained *before* the populations were stressed.

Acknowledgments

Work was supported by grants from the Senate Research Committee of Syracuse University (D.A.S. and W.D.R-H.) and the Theodore Roosevelt Memorial Fund (D.A.S.). Preparation of this manuscript was supported by the Treves and Carscallen Funds of Wabash College. This is contribution #102 of the Upstate Freshwater Institute.

Literature Cited

Berrie, A. D. 1959. Variation in the radula of the freshwater snail *Lymnaea peregra* (Muller) from northwestern Europe. *Ark Zool* **12:** 391–404.

Browne, R. A., and W. D. Russell-Hunter. 1978. Reproductive effort in molluscs. *Oecologia (Berlin)* **37:** 23–27.

Clark, G. R., II. 1976. Shell growth in the marine environment: approaches to the problem of marginal calcification. *Am. Zool* **16:** 617–626.

Fujioka, Y. 1985. Seasonal aberrant radular formation in *Thais bronni* (Dunker) and *T. clavigera* (Küster) (Gastropoda: Muricidae). *J. Exp. Mar. Biol. Ecol.* **90:** 43–54.

Hume, D. 1748. *An Inquiry Concerning Human Understanding.* (Original title: *Philosophical Essays Concerning Human Understanding*). London. [republished in 1888, Oxford University Press (Clarendon), London and New York].

Hunter, R. D. 1975. Variation in populations of *Lymnaea palustris* in upstate New York. *Am. Midl. Nat.* **94:** 401–420.

Isarankura, K., and N. W. Runham. 1968. Studies on the replacement of the gastropod radula. *Malacologia* **7:** 71–91.

Kerth, K. 1971. Radula-ersatz und zahnchenmuster der weinbergschnecke im winterhalbjahr. *Zool. Jb. Anat. Bd.* **88:** 47–62.

Mackenstedt, U., and K. Märkel. 1987. Experimental and comparative morphology of radula renewal in pulmonates (Mollusca, Gastropoda). *Zoomorphology* **107:** 209–239.

Mallet, A. L., C. E. A. Carver, S. S. Coffen, and K. R. Freeman. 1987. Winter growth of the blue mussel Mytilus edulis L.: importance of stock and site. *J. Exp. Mar. Biol. Ecol.* **108:** 217–228.

Mischor, B., and A. Markel. 1984. Histology and regeneration of the radula of *Pomacea bridgesi* (Gastropoda, Prosobranchia). *Zoomorphology* **104:** 42–66.

Peterson, C. H., P. B. Duncan, H. C. Summerson, and B. F. Beal. 1985. Annual band deposition within shells of the hard clam, *Mercenaria mercenaria*, consistency across habitat near Cape Lookout, North Carolina. *Fishery Bull. N.O.A.A. (U.S.)* **83:** 257–260.

Price, C. H. 1979. Physical factors and neurosecretion in the control of reproduction in *Melampus* (Mollusca: Pulmonata). *J. Exp. Zool.* **207:** 269–282.

Runham, N. W. 1963. A study of the replacement mechanism of the pulmonate radula. *Q. J. Microsc. Sci.* **104:** 271–277.

Russell-Hunter, W. D. 1985. Physiological, ecological and evolutionary aspects of molluscan tissue degrowth. *Am. Malac. Bull.* **3:** 213–221.

Russell-Hunter, W. D., and D. E. Buckley. 1983. Actuarial bioenergetics of nonmarine molluscan productivity. Pp. 464–503 in *The Mollusca*, Vol. 6, K. M. Wilbur, ed. Academic Press, Orlando, New York, and London.

Russell-Hunter, W. D., and A. G. Eversole. 1976. Evidence for tissue degrowth in starved freshwater pulmonate snails (*Helisoma trivolvis*) from tissue, carbon and nitrogen analysis. *Comp. Biochem. Physiol.* **54A:** 447–453.

Russell-Hunter, W. D., M. L. Apley, and J. L. Banner III. 1971. Preliminary studies on brain implants and sex change in *Crepidula fornicata* (L.). *Biol. Bull.* **141:** 400.

Russell-Hunter, W. D., D. W. Aldridge, J. S. Tashiro, and B. S. Payne. 1983. Oxygen uptake and nitrogenous excretion rates during overwinter degrowth conditions in the pulmonate snail, *Helisoma trivolvis*. *Comp. Biochem. Physiol.* **74A:** 491–497.

Russell-Hunter, W. D., R. A. Browne, and D. W. Aldridge. 1984. Overwinter tissue degrowth in natural populations of freshwater pulmonate snails (*Helisoma trivolvis* and *Lymnaea palustris*). *Ecology* **65:** 223–229.

Smith, D. A. 1987. Functional adaptation and intrinsic biometry in the radula of *Helisoma trivolvis*. Ph.D. Dissertation, Syracuse University, Syracuse, New York (Entire dissertation available from *Dissertation Abstracts* **49:** 26B, Order #88-05183; or protocols can be supplied by D. A. S.).

Smith, D. A. 1988. Radular kinetics during grazing in *Helisoma trivolvis* (Gastropoda: Pulmonata). *J. Exp. Biol.* **136:** 89–102.

Smith, D. A. 1989. Radula-tooth biometry in *Helisoma trivolvis* (Gastropoda, Pulmonata): interpopulation variation and the question of adaptive significance. *Can. J. Zool* **67:** 1960–1965.

Tinkle, D. W., and N. F. Hadley. 1975. Lizard reproductive effort: calorific estimates and comments on its evolution. *Ecology* **56:** 427–434.

Williams, G. C. 1966. Natural selection, the costs of reproduction, and a refinement of Lack's principle. *Am. Nat.* **100:** 687–692.

Reference: *Biol. Bull.* **178**: 33–45. (February, 1990)

A Decapod Hemocyte Classification Scheme Integrating Morphology, Cytochemistry, and Function

JO ELLEN HOSE, GARY G. MARTIN, AND ALISON SUE GERARD

Department of Biology, Occidental College, Los Angeles, California 90041

Abstract. We have examined the hemocytes of three decapod crustaceans (*Homarus americanus, Panulirus interruptus,* and *Loxorhynchus grandis*) and propose a classification of these cells based on morphology, cytochemistry, and studies of cell functions. In all species, hyaline cells and granulocytes were identified. Although we have retained the widely used names for these cells, we show that traditional morphological features alone do not accurately differentiate between these categories. Historically, the term hyaline cell refers to hemocytes that contain no or only a few cytoplasmic granules, whereas granulocytes contain abundant granules. However, the size and number of granules in hyaline cells vary greatly between species and therefore are not useful criteria for identifying these cells. Since morphological identification alone is inadequate and misleading, especially with regard to hyaline cells, a combination of morphological, cytochemical and functional methods is necessary to identify decapod hemocytes. Features of hyaline cells include: a higher nucleocytoplasmic ratio than that of granulocytes, the presence of abundant small (~50 nm), round, electron-dense deposits in the cytoplasm, and their accumulation of trypan blue dye prior to cytolysis. Granulocytes do not take up trypan blue or lyse during a 5-min incubation, and they contain prophenoloxidase and hydrolases. Hyaline cells are involved in the initiation of hemolymph coagulation whereas granulocytes are involved in defense against foreign material by phagocytosis and encapsulation. We propose that these criteria be applied to other crustacean species and expect that they will facilitate our understanding of the physiological roles of their hemocytes.

Introduction

In crustaceans, circulating hemocytes are thought to be involved in hardening of the exoskeleton, prevention of blood loss and the confinement of invasive organisms by clot formation, recognition of non-self, phagocytosis, and encapsulation (Bauchau, 1981; Ratner and Vinson, 1983). Although recent research has expanded the various physiological roles played by crustacean hemocytes, extention of this information from one species to another is difficult because of the lack of a unified classification scheme for the hemocytes of all crustacea. Prior hemocyte classification systems rely on tinctorial properties of the cells, which are often subtle or subjective, and seldom apply to other species (Martin and Graves, 1985).

Using the penaeid shrimp *Sicyonia ingentis* as a prototype for decapod crustaceans, a hemocyte classification system was developed, which relates cellular morphology at the light and electron microscope levels, cytochemistry, and three essential functions: clotting, phagocytosis, and encapsulation (Martin *et al.*, 1987; Hose *et al.*, 1987; Omori *et al.*, 1989; Hose and Martin, 1989). The choice of this species proved serendipitous because the three types of hemocytes are morphologically distinct and clotting occurs by explosive cytolysis (Tait's type C coagulation; Tait, 1911), making identification of the clotting cell type relatively easy. At the electron microscope level, the cells that initiate clotting are readily identified by several features typical of hyaline cells (small size, a high nucleocytoplasmic ratio, and scarcity of cytoplasmic granules) and by the presence of numerous, small (~50 nm diameter), electron-dense deposits in the cytoplasm. In addition, the hyaline cells selectively stain with Sudan black B, as does coagulogen extracted from cell-free hemolymph of *Panulirus interruptus* and *Astacus leptodactylus* (Durliat, 1985). During lysis of these cells, the deposits appear to extend through breaks in the plasma membrane and hydrate to produce the clot (Omori *et al.*, 1989). The granulocytes are larger cells with a lower nucleocytoplasmic ratio and contain numerous small (0.4 μm diam.) or large (0.8 μm diam.) granules. Granulocytes (small and large granule hemocytes) show no

Received 3 April 1989; accepted 30 November 1989.

morphological changes during coagulation and are capable of phagocytosis of bacteria and encapsulation of fungal hyphae. Phagocytosis is accomplished primarily by small granule hemocytes (Hose and Martin, 1989); they contain many vesicles and occasional granules that stain for acid hydrolases (acid phosphatase, β-glucuronidase, and nonspecific esterase) (Hose *et al.*, 1987). Encapsulation is initiated by large granule hemocytes and, to a lesser extent, by small granule hemocytes (Hose and Martin, 1989). Prophenoloxidase (PPO), an enzyme involved with melanization of encapsulated material and possibly the recognition of non-self items (Söderhäll, 1982), is most abundant in large granule hemocytes and to a lesser degree in some small granule cells. In contrast, hyaline cells, which do not phagocytize bacteria or assist in capsule formation, do not contain PPO and only rarely acid phosphatase (Hose *et al.*, 1987). Thus the division of shrimp hemocytes into two functional groups, hyaline (or clotting) cells and granulocytes, is supported by morphology, cytochemistry, and function.

This paper extends the results of the shrimp studies to other decapods and attempts to develop a unified hemocyte classification system for the diverse assemblage of crustaceans. This diversity is exemplified by the existence of multiple coagulation mechanisms. In contrast to clotting via explosive cytolysis as in the shrimp (type C according to Tait, 1911), other decapods exhibit type-A coagulation which is distinguished by the formation of a dense hemocyte network which seals off the injury and plasma coagulation is not apparent or type-B coagulation in which hemocyte aggregation is followed by plasma coagulation (Tait, 1911). In the present study, we examined the hemocytes in one species with type-A coagulation (a crab, *Loxorhynchus grandis*), one species with type-B coagulation (the Maine lobster, *Homarus americanus*), and one species with type-C coagulation (the spiny lobster, *Panulirus interruptus*). Light and electron microscopic features of hemocytes from these three decapods are compared to those identified in the shrimp and correlated with a suite of cytochemical characteristics (Sudan black B, acid phosphatase, and PPO) and a group of essential physiological functions (clotting, phagocytosis, and encapsulation). The methods presented here should facilitate study of decapod hemocytes by providing a framework for practical hemocyte classification.

Materials and Methods

Animals

Spiny lobsters (*P. interruptus*) and sheep crabs (*L. grandis*) were collected in less than 10 m of water at King Harbor Marina, Los Angeles, California. Maine lobsters (*H. americanus*) were purchased commercially. Crustaceans were maintained in flow-through aquaria at 18°C and only intermolt animals were studied.

Microscopic examination of hemocytes

Freshly fixed hemocytes were examined by light microscopy (LM) (brightfield and phase contrast optics) to determine cell size, cell shape, granule size, and differential hemocyte counts. An aliquot of hemolymph (usually 0.2 cc) was withdrawn from the ventral sinus or heart into a 1 cc syringe containing 0.4 cc of fixative (2.5% glutaraldehyde in 0.1 *M* sodium cacodylate pH 7.8 containing 12% glucose).

Excess fixative was added to a second 0.2 cc hemolymph aliquot, and the cells were processed for examination by electron microscopy. The cells were fixed for 2 h at room temperature and pelleted (10,000 × *g* for 1.5 min). Following a 10-min wash in 0.1 *M* sodium cacodylate (pH 7.8) containing 24% sucrose, the cells were post-fixed in 1% OsO_4 in 0.1 *M* sodium cacodylate for 1 h at room temperature. Each sample was stained en bloc for 1 h with 3% uranyl acetate in 0.1 *M* sodium acetate, dehydrated in a graded series of ethanol, and infiltrated and embedded in Spurr's (1969) low viscosity plastic. Thin sections (90 nm) were cut on a Porter Blum MT2B ultramicrotome, stained with lead citrate and examined in a Hitachi HU 11A transmission electron microscope (TEM).

Nucleocytoplasmic ratios were determined by dividing the area of the nucleus by the area of the cell. For hyaline and small granule hemocytes, both areas were clearly identified in light micrographs of immediately fixed cells and measured using a digitizing tablet and Sigma-Scan® computer software (Jandel Scientific). Because the nucleus is difficult to visualize in phase contrast images of large granule hemocytes, measurements were made from thick plastic sections. To ensure that cells were sectioned through their greatest axis, only large granule hemocytes showing typical length and width measurements were used. There was no difference in size measurements of fixed cells examined in wet mounts by phase optics and cells embedded in plastic and sectioned.

Identification of cell-type initiating coagulation

Two previously used approaches helped to identify the type of hemocyte initiating coagulation of the hemolymph: (1) visual examination of hemocyte types accumulating trypan blue, an event we have previously shown to be a direct precursor to cytolysis and ensuing clot formation and (2) ultrastructural examination of hemocytes fixed at stages during clot formation (Omori *et al.*, 1989). For the first technique, 0.1 cc of freshly drawn hemolymph was gently mixed on a glass slide with 0.1 cc of a 1.2% solution of trypan blue in seawater. Within 1–2 min, certain hemocytes accumulate the blue color in

both the cytoplasm and nucleus. By 5 min these cells lyse and the cytoplasm is lost, but the blue staining nuclei remain. Individual cells may be identified and observed as they accumulate the dye and lyse. After 5 min, the number of blue stained nuclei and the cells remaining intact and colorless were counted. Six hundred cells were evaluated for each species.

The second method provided ultrastructural information on the type of hemocyte that initiates coagulation as well as changes in these cells during cytolysis. Aliquots of hemolymph (0.1 cc) and seawater (0.1 ml) were mixed for times ranging from 15 s to 5 min and then fixed by the addition of an excess amount of gluaraldehyde fixative and prepared for TEM examination as described above.

Phagocytosis of bacteria by hemocytes

In vitro phagocytosis experiments were performed as described by Hose and Martin (1989). A glass microscope coverslip was placed into each of two sterile plastic Petri dishes and each covered with 20 ml of shrimp culture medium (SCM, Brody and Chang, in press). Approximately 0.3 cc of hemolymph was added over each coverslip, and hemocytes were allowed to settle and attach to the coverslips for 15 min. Approximately 100,000 cells of a Gram-negative marine bacterium (*Cytophaga* sp.; Occidental College Isolate 1) were added to one of the dishes. Cultures were incubated at 12°C for 3 h. Coverslips were fixed in methanol for 5 min and stained with May Grunwald-Giemsa. Differential counts of approximately 200 hemocytes were performed and the numbers of phagocytic cells (hemocytes containing at least 1 bacterium within a vacuole) were recorded. Dead hemocytes were differentiated from viable cells by the presence of nuclear degeneration (karyolysis, pycnosis).

Fungal encapsulation

The method of Hose and Martin (1989) was used to determine the types of hemocyte that attached to fungal hyphae and initiated capsule formation. Approximately 1 ml of hemolymph was added to 12 ml SCM in a 15 ml plastic centrifuge tube. Small cubes (0.5 mm^3) of Sabouraud-dextrose agar containing primarily hyphae of *Fusarium solani* (University of Arizona strain 1623C) were added to the tube; the culture was incubated at 12°C. After 1, 2, and 5 min, a cube was removed and washed gently in SCM to remove nonadherent hemocytes. The cell types attached to the fungus were identified using phase contrast microscopy (total of 200 cells for each species).

Hemocyte cytochemistry

Hemolymph (0.2 cc) was withdrawn into 0.2 cc of 12.5% unbuffered citrate anticoagulant (which prevents lysis of hyaline cells), spread on three glass microscope slides, and allowed to air dry. Constituents of hemocyte granules and cytoplasm were visualized using methods given in Hose *et al.* (1987). Smears were prepared from six individuals of each species. Where possible, 200 cells per slide were evaluated using brightfield microscopy (1000×); each hemocyte was categorized and individual cellular reactions were recorded.

Lipids and lipoproteins were demonstrated using a commercial Sudan Black B kit (Sigma Chemical Co. Kit #380). Glutaraldehyde-fixed hemocytes were processed according to provided directions except that the nuclear counterstain was not used. Cytoplasmic staining was differentiated from staining of granule or plasma membranes and was termed a positive reaction (Hose *et al.*, 1987). Occasionally entire granules were stained by Sudan Black B; these are noted in the results.

Prophenoloxidase (PPO) activity was evaluated in smears fixed in 2.5% glutaraldehyde in 0.1 *M* phosphate buffer (pH 7.4) for 1 h at 4°C. The smears were rinsed three times in phosphate buffer (15 min each), then incubated in 0.1% L-DOPA in phosphate buffer for 16 h at room temperature. Black staining of the granules was interpreted as a positive reaction (Hose *et al.*, 1987).

Acid phosphatase in glutaraldehyde-fixed hemocytes was visualized using a commercial research kit (Sigma Chemical Co. Kit #386). Naphthol AS-Bl phosphate was used as the substrate, yielding a red-violet reaction product (naphthol AS-Bl-fast garnet GBC complex). Although the location and abundance of acid phosphatase was species-specific, the rating system previously used for the shrimp (Hose *et al.*, 1987) was acceptable for use with the lobsters. In the shrimp we recognized the following categories: rare (0 to 3 positive foci per cell), few (4 to 10 foci per cell), intermediate (11 to 30 foci per cell), and many (>30 foci per cell). Because *L. grandis* contained more acid phosphatase foci than the shrimp, the rating system was slightly modified for evaluation of crab hemocytes. A distribution of the number of positive foci per cell was constructed and the limit for the "rare" category placed between the groups containing rare and few foci. Thus while the rare category consisted of less than four foci for shrimp and the lobsters, it was enlarged to include less than six foci for the crab. A rare response was interpreted as negative. Remaining limits were identical for all four species. Two hundred cells were evaluated for each test; each hemocyte was identified and individual cellular reactions were recorded.

Results

Description of hemocyte types

Using morphological criteria previously developed for the shrimp (Martin *et al.*, 1987), three basic cell types were observed in each of the decapods studied; one type

Table I

Comparative hemocyte morphology

	Large granule cells	Small granule cells	Hyaline cells
Homarus americanus			
Cell size (length × width)	23.4 ± 2.2 × 12.3 ± 1.3 (11)	20.9 ± 0.6 × 13.9 ± 0.3 (18)	14.1 ± 0.8 × 11.2 ± 0.6 (16)
Granule diameter	1.3 ± 0.1 (30)	0.9 ± 0.1 (30)	0.9 ± 0.1 (30)
Number of granules	72.7 ± 4.6 (30)	27.3 ± 5.6 (30)	13.9 ± 3.0 (30)
Nucleocytoplasmic ratio	20.3 ± 1.8 (10)	27.5 ± 2.4 (10)	40.0 ± 2.5 (13)
Panulirus interruptus			
Cell size (length · width)	22.6 ± 1.3 · 14.1 ± 0.5 (12)	19.7 ± 0.9 × 10.0 ± 0.3 (18)	14.2 ± 0.5 × 10.6 ± 0.2 (18)
Granule diameter	1.4 ± 0.1 (30)	0.8 ± 0.1 (33)	1.2 ± 0.1 (30)
Number of granules	34.0 ± 2.4 (30)	10.8 ± 4.3 (30)	5.6 ± 0.8 (30)
Nucleocytoplasmic ratio	18.3 ± 1.3 (8)	24.6 ± 2.1 (16)	40.2 ± 1.5 (16)
Loxorhynchus grandis			
Cell size (length × width)	20.4 ± 0.5 · 13.7 ± 0.6 (19)	17.9 ± 0.5 × 10.6 ± 0.4 (15)	14.5 ± 1.0 × 9.1 ± 0.3 (12)
Granule diameter	1.4 ± 0.1 (30)	1.0 ± 0.1 (30)	1.0 ± 0.1 (30)
Number of granules	28.0 ± 4.1 (30)	8.0 ± 1.6 (30)	38.3 ± 5.6 (30)
Nucleocytoplasmic ratio	17.5 ± 1.5 (11)	23.5 ± 1.0 (11)	36.0 ± 1.5 (16)

Measurements are mean ± standard error (number of measurements). Cell sizes are presented in length × width. Cell and granule sizes are in μm. Number of granules is the number per sectioned cell. Nucleocytoplasmic ratios are percentages.

T-tests showed significantly smaller hyaline hemocyte size for all three species compared to either small or large granule hemocytes ($P < 0.05$). Nucleocytoplasmic ratios for hyaline hemocytes of all three species were significantly larger than those of small or large granule hemocytes ($P < 0.05$).

of hyaline cell and two subgroups of granulocytes (small and large granule hemocytes) (Table I).

Hyaline Cells (Figs. 1A–6A). Hyaline cells were the most morphologically diverse type of hemocyte. When examined by phase contrast microscopy, they were generally ovoid in shape, smaller than granulocytes and with a higher nucleocytoplasmic ratio (Table I), and either contained few large granules (*P. interruptus*) or numerous smaller granules (*H. americanus* and *L. grandis*). Most hyaline cells of *H. americanus* measured 21 × 11 μm although smaller hemocytes (from 12 μm in the largest dimension) were occasionally observed. The smaller cells may represent immature hyaline cells because they were continuous in size with the hyaline cell and probably correspond to the prohyalocyte category recognized by Cornick and Stewart (1978). Hyaline hemocytes of *H. americanus* had numerous (14/section) small, ovoid granules, 0.9 μm long, the contents of which appeared homogeneous and electron dense at the EM level. The cytoplasm contained Golgi bodies, abundant rough endoplasmic reticulum (RER), a circumferential band of microtubules, a few vesicles, mitochondria, and small (~50 nm diam.), round, electron-dense deposits (Fig. 7). Hyaline cells of the crab (*L. grandis*) resembled those of the *Homarus*, except they contained more granules (40/section) that, at the EM level, were ovoid, homogeneous, and electron dense. Hyaline hemocytes of the spiny lobster (*P. interruptus*) were distinctive in that only a few (6/section) large (1.2 μm diam.) granules were present. Ultrastructurally the granules had a punctate pattern. Otherwise, features of the cytoplasm were similar to those described for the other species.

Granulocytes. Granulocytes could be easily differentiated into two groups using phase contrast microscopy: small (Figs. 1B–6B) and large (Figs. 1C–6C) granule hemocytes. Small granule hemocytes contained few to many, round, dark, small (usually ≤1.0 μm diam.) granules and a relatively small, centrally located nucleus, whereas the cytoplasm of large granule hemocytes was packed with larger (1.3–2.0 μm diameter), refractile granules that obscured the eccentrically placed nucleus (Table I). However, it was sometimes difficult using TEM to distinguish between small granule hemocytes containing numerous granules and large granule hemocytes because the sectioned granules appeared similar in size. These cells may be part of a single line of maturation in which the number and size of granules in small granule hemocytes increase until the cell is recognized as a large granule hemocyte. To distinguish between small and large granule hemocytes, we relied on (1) the location of the nucleus (centrally or eccentrically placed) and (2) the presence of only large granules (>1.2 μm diam.) in large granule hemocytes while small granule hemocytes may contain both large and small granules. Both types of granules were often surrounded by a clear (artifactual?) space (see Figs. 6B and C), and in *P. interruptus*, granules in the large granule hemocytes often did not section cleanly but appeared fractured (see Fig. 4C), unlike those present in small granule cells. The cytoplasm of granulocytes, both small and large granule hemocytes, contained

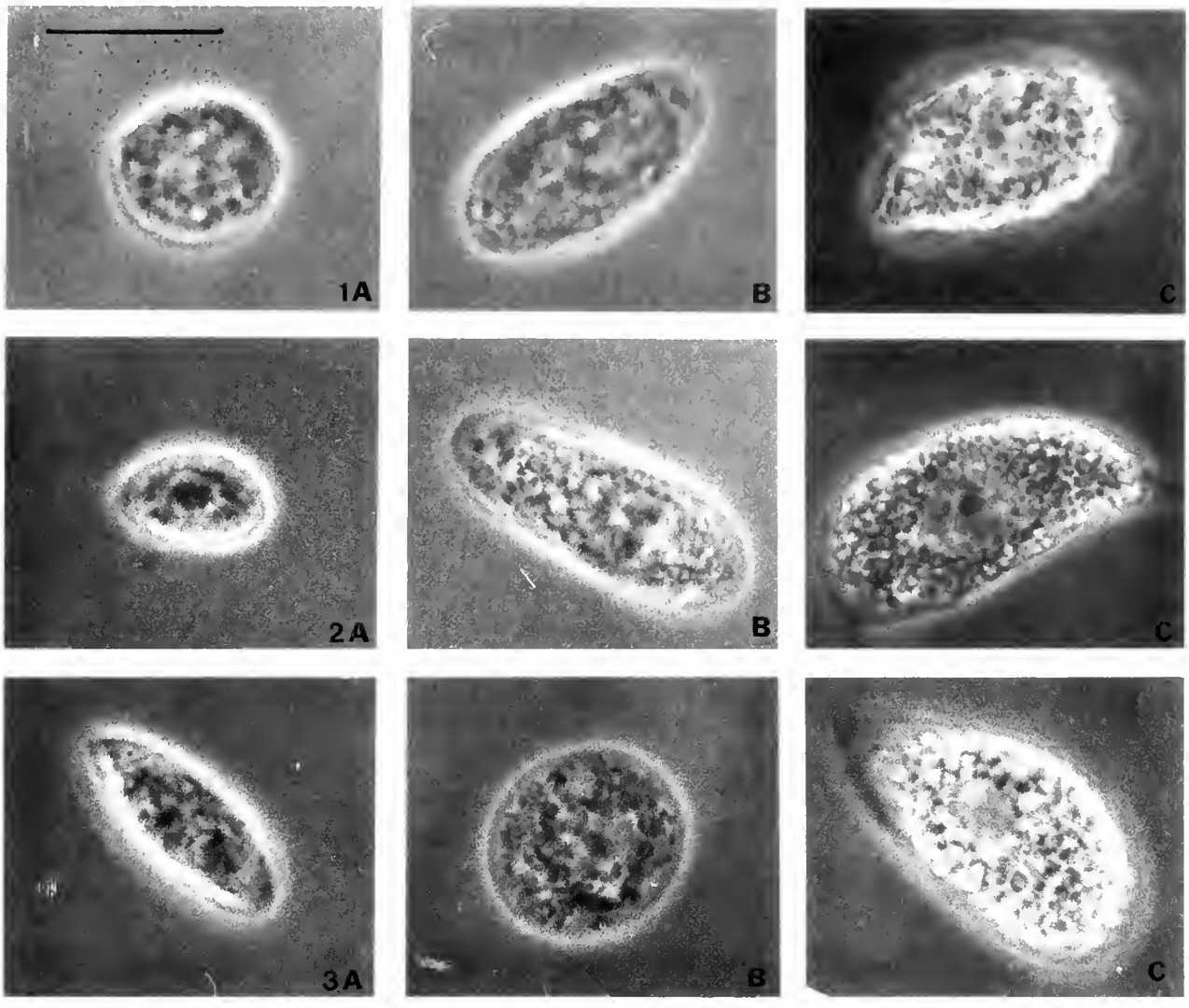

Figures 1–3. Light micrographs of hemocytes from *Panulirus interruptus* (Fig. 1), *Homarus americanus* (Fig. 2), and *Loxorhynchus grandis* (Fig. 3) showing hyaline cells (column A), small granule (column B), and large granule (column C) types. Note the small size of the hyaline cells compared to the granulocytes. The large granule cells are highly refractile and it is difficult to observe the nucleus. All figures at 2600×; scale bar = 10 μm.

Golgi bodies, RER, vesicles, mitochondria, ribosomes, and microfilaments scattered between the granules (see Fig. 7). Microtubules, typically in a band adjacent to the plasma membrane, were commonly seen.

Hemocyte differential counts

Differential counts were performed using phase contrast LM and TEM (Table II). Although individual paired counts are similar, we consider the TEM counts more accurate for comparison because of the inherent greater resolution. *P. interruptus* had the highest percentage of hyaline cells at 56%, whereas *L. grandis* and *H. americanus* were considerably lower at 21% and 27%, respectively. Large granule granulocytes constituted between 10% and 13% of the total with small granulocytes comprising about 65% in *H. americanus* and *L. grandis* and 31% in *P. interruptus*.

Clotting

Patterns of coagulation. The species studied represent the three coagulation patterns described by Tait (1911). In *L. grandis* (Tait category A), the bulk of the clot consisted of long cellular aggregations linked by strands of clot material. The clot produced by *H. americanus* (Tait category B) contained isolated islands of coagulated hemolymph with intervening areas of packed hemocytes, whereas in *P. interruptus* (Tait category C), cell ag-

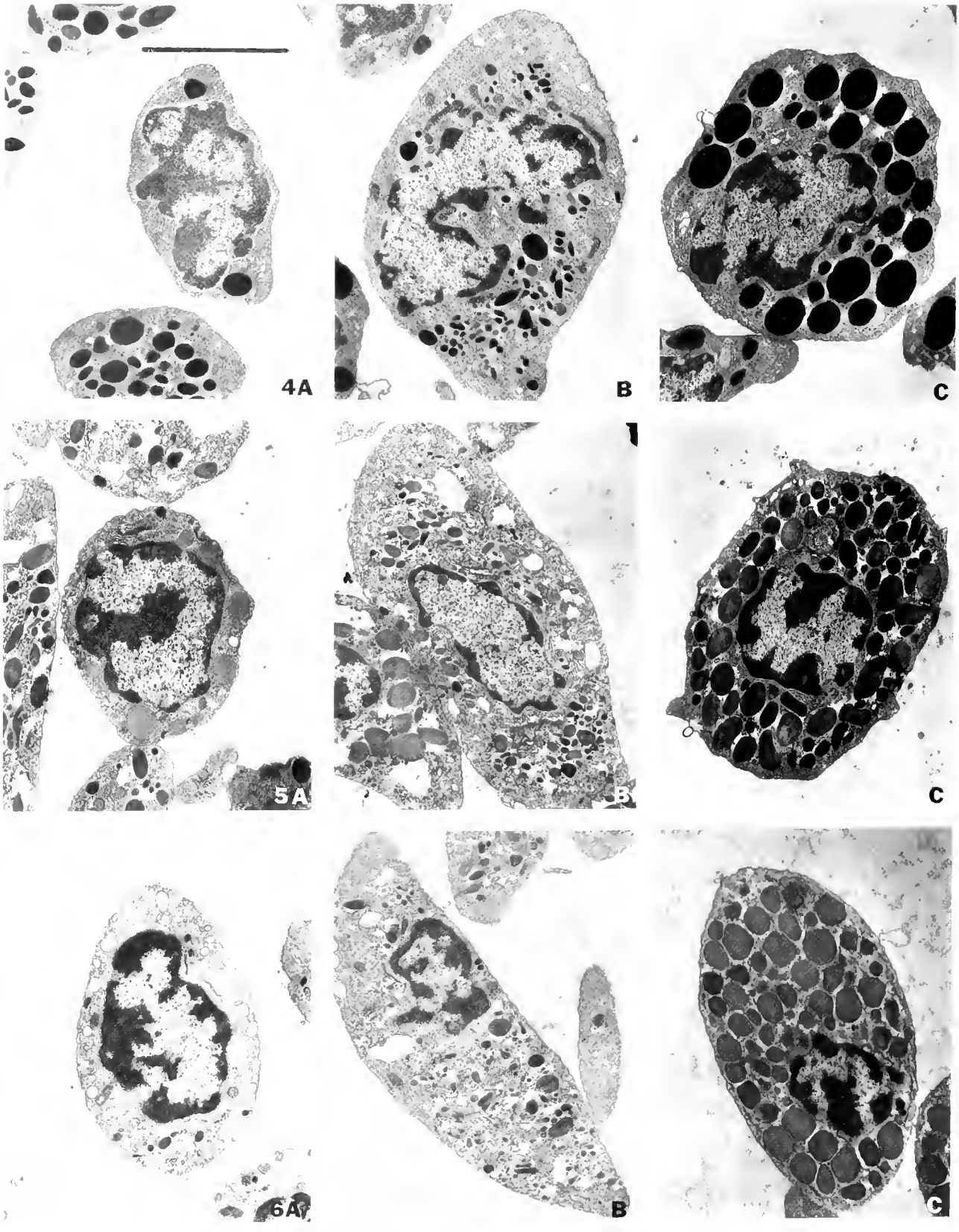

Figures 4–6. Transmission electron micrographs of hemocytes from *Panulirus interruptus* (Fig. 4), *Homarus americanus* (Fig. 5), and *Loxorhynchus grandis* (Fig. 6) showing hyaline (column A), small granule (column B) and large granule (column C) types. Granules are present in hyaline cells although not abundant. Small granule hemocytes are characterized by small granules in a relatively large amount of cytoplasm and in large granule hemocytes the granules fill much of the cytoplasm. All figures at 5500×; scale bar = 5 μm.

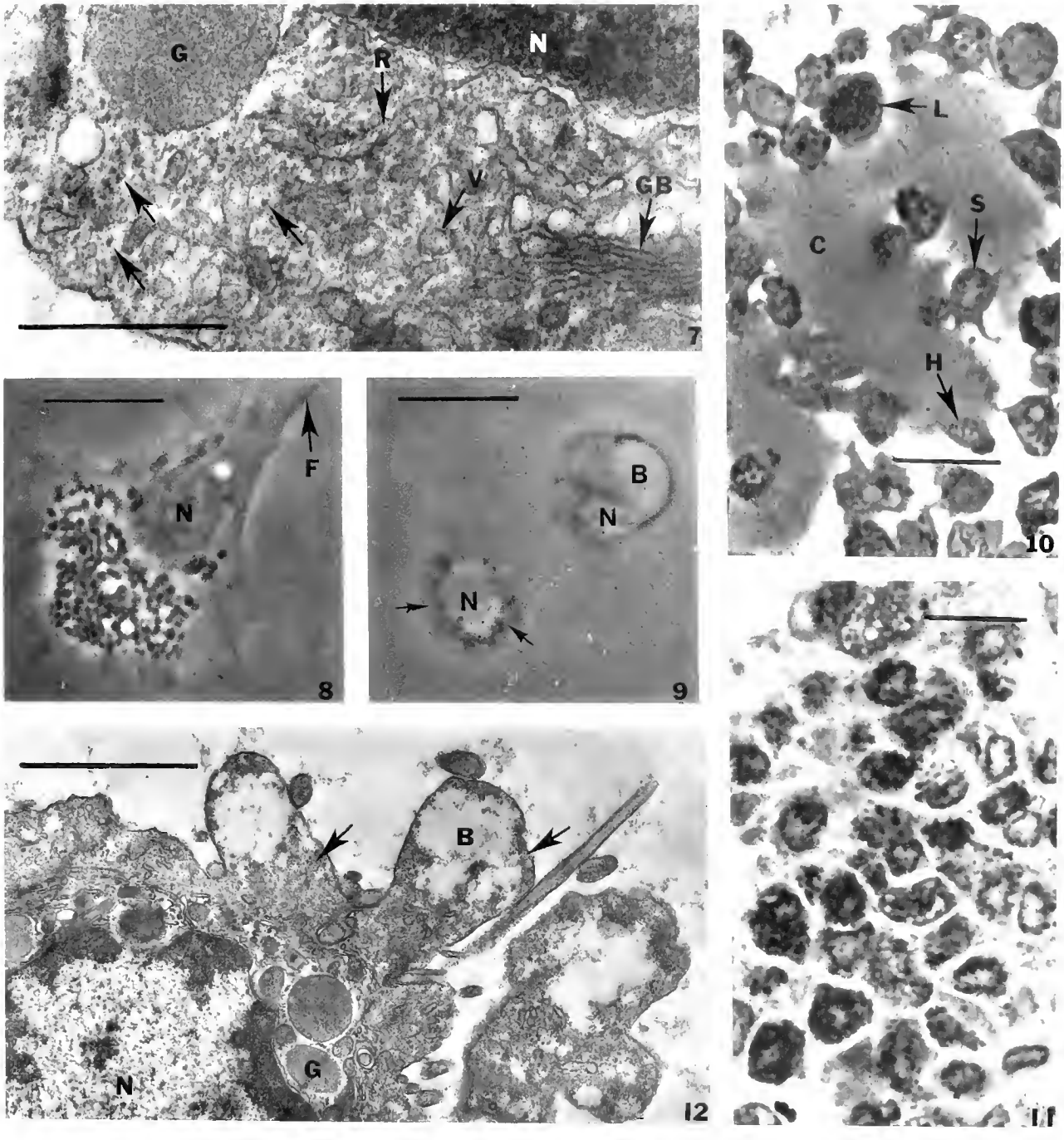

Figure 7. Transmission electron micrograph of a hyaline hemocyte from *Homarus americanus* showing cytoplasmic deposits (arrows), RER (R), a granule (G), vesicles (V), nucleus (N), and edge of Golgi body (GB). 70,000 ×; scale bar = 0.5 μm.

Figure 8. Light micrograph of a large granule hemocyte from *Panulirus interruptus* 2 min after mixing equal volumes of hemolymph and seawater containing trypan blue. Note the cell is intact and has spread on the glass substrate. Nucleus (N); filopodia (F). 2000 ×; scale bar = 10 μm.

Figure 9. Light micrograph of two hyaline cells from *P. interruptus* from the same preparation as cells in Figure 8. These cells have not attached to the substrate and they have lysed, leaving a light (blue-stained) nucleus (N), blebs (B), and thin rim of residual cytoplasm (arrows). 2000 ×; scale bar = 10 μm.

Figure 10. Light micrograph of hemocytes from *P. interruptus* during early clot formation (2 min after mixing with seawater). Note the clusters of hemocytes between the large circular areas of coagulated hemolymph (C). Large granule hemocytes (L); small granule hemocytes (S); and hyaline cell (H). 700 ×; scale bar = 25 μm.

Figure 11. Light micrograph of hemocytes from *Loxorhynchus grandis* during early clot formation (2 min after mixing with seawater). Note the large aggregation of hemocytes. Obvious areas of coagulated hemolymph are not present. 700 ×; scale bar = 25 μm.

Table II

Comparative hemocyte differential counts using light and transmission electron microscopy

	Large granule cells (%)	Small granule cells (%)	Hyaline cells (%)
Homarus americanus			
Light microscopy	16.4 ± 2.7 (10.0–26.5; 9)	60.2 ± 3.6 (41.5–76.2; 9)	22.4 ± 2.4 (11.9–34.2; 9)
Electron microscopy	10.3 ± 1.6 (7.8–19.5; 7)	62.4 ± 2.1 (53.8–71.3; 7)	27.3 ± 2.8 (15.2–35.9; 7)
Panulirus interruptus			
Light microscopy	9.8 ± 2.6 (4.0 + 21.0; 6)	29.2 ± 3.6 (22.0–45.5; 6)	61.0 ± 3.4 (50.0–72.0; 6)
Electron microscopy	12.6 ± 1.7 (6.3–18.7; 8)	31.1 ± 1.7 (26.6–40.2; 8)	56.3 ± 1.7 (48.5–62.8; 8)
Loxorhynchus grandis			
Light microscopy	14.1 ± 2.3 (6.0–21.0; 6)	67.8 ± 5.3 (49.0–79.0; 6)	18.1 ± 3.8 (11.0–35.0; 6)
Electron microscopy	10.4 ± 0.7 (8.0–13.0; 6)	68.8 ± 1.6 (62.2–72.0; 6)	20.8 ± 1.6 (15.4–25.6; 6)

Values are mean ± standard error (range; number of measurements).

gregates were small and widely separated by clotted hemolymph.

Trypan blue experiments. Previous work with decapods has shown hemocyte lysis to be the initiating step in hemolymph coagulation. The method used here to identify lysing hemocytes simulates coagulation resulting from a seawater influx such as a break in the exoskeleton. The addition of trypan blue (which does not alter the process of coagulation) facilitates early identification of lysing hemocytes. Cell categorization at the LM level is impossible following lysis; thus TEM was used to describe successive steps in coagulation (see next section). When hemolymph was mixed with seawater containing trypan blue, two populations of cells were observed. In one group, the cells contained distinct granules, spread on the glass slide, extended filopodia (Fig. 8), and did not accumulate trypan blue during the observation period. This group was composed of small and large granule hemocytes. The second group of cells remained ovoid and did not attach to or spread on glass slides; the cytoplasm and nucleus of these cells appeared blue. By 1 min, multiple blebs were apparent beneath the plasma membrane. Cytolysis occurred by 2 min in *L. grandis* and by 5 min for the lobsters, leaving a blue-staining nucleus and fragments of cytoplasm (Fig. 9). Visual observations of individual cells confirmed that the lysing cells were hyaline cells in all three species (Table III). In addition, the percentage of lysing cells in each species corresponded to the percentage of hyaline cells obtained from differential counts. Using the trypan blue method, the smallest proportion of clotting cells was found in *L. grandis* (19%), with *H. americanus* intermediate (34%) and *P. interruptus* highest (50–70%). We suggest that the coagulation patterns reported by Tait (1911) are not three distinct categories but rather represent a continuum relating to the percentage of hyaline cells. Species with the highest hyaline cell percentage exhibit type C coagulation; lysis of these cells results in large expanses of coagulated hemolymph with small intervening clusters of granulocytes. As the percentage of hyaline cells decreases, so does the amount of coagulated hemolymph. Therefore, in animals with type A coagulation, like the crab, the predominant feature is the aggregated granulocytes which are, in fact, connected by strands of coagulated hemolymph.

The trypan blue method was particularly useful with the crab because the hyaline cells are not abundant, lyse faster than in the other species, and the granulocytes rapidly attach to one another to produce large aggregations. Thus lysed cells in unstained preparations were difficult to identify within the mass of cells (primarily granulocytes) that appear unaffected and intact.

Morphology of coagulation. When equal volumes of hemolymph and seawater were mixed, coagulation began immediately and produced a strong clot within a few minutes. Clots produced in *P. interruptus* were composed primarily of coagulated hemolymph with hemocytes scattered throughout the matrix (Fig. 10). In *H. americanus*, less coagulated hemolymph was present and tightly compacted clusters of granulocytes were conspicuous. In *L. grandis*, the bulk of the clot was produced by aggregated cells (Fig. 11) and only strands of coagulated hemolymph.

In all three species, changes in cell morphology occurred primarily in the hyaline cells. Early changes involving loss of plasma membrane integrity were identical to those observed in the preceding trypan blue experiments. Electron microscopy revealed that the centers of the hyaline cell blebs appeared empty and were surrounded by round, electron-dense deposits (Fig. 12). Granules in these cells, which were homogeneous in sectioned material and dispersed throughout the cytoplasm,

Figure 12. Transmission electron micrograph of a hyaline cell from *L. grandis* 2 min after mixing with seawater showing the formation of blebs (B). Note the homogeneous granules (G) aggregated around the nucleus (N) and the small electron-dense deposits (arrows) throughout the cytoplasm. 12,000×; scale bar = 2.5 μm.

Table III

Comparative hemocyte functions

	Large granule cells (% positive)	Small granule cells (% positive)	Hyaline cells (% positive)
Homarus americanus			
Clotting:			
% accumulate trypan blue	0.0	1.2	100.0
Phagocytosis:			
% phagocytic	39.3	93.1	0.0
% dead (+ bacteria)	9.3	11.5	83.0
% dead (− bacteria)	0.0	0.0	29.7
Encapsulation:			
% of adherent cells	63.3	21.2	0.0
Panulirus interruptus			
Clotting:			
% accumulate trypan blue	0.0	0.0	100.0
Phagocytosis:			
% phagocytic	32.0	83.1	0.0
% dead (+ bacteria)	0.0	16.2	31.6
% dead (− bacteria)	0.0	0.0	1.6
Encapsulation:			
% of adherent cells	68.4	25.3	6.3
Loxorhynchus grandis			
Clotting:			
% accumulate trypan blue	0.3	0.7	100.0
Phagocytosis:			
% phagocytic	70.0	95.9	0.0
% dead (+ bacteria)	4.8	6.1	95.0
% dead (− bacteria)	16.7	1.7	24.3
Encapsulation:			
% of adherent cells	67.2	28.7	4.1

Mean percentage of each category which accumulates trypan blue, is phagocytic, or initiates encapsulation by adhering to fungal hyphae. In the clotting experiments, ≥100 hemocytes in each category were evaluated from each of 5 animals. In the phagocytosis experiments, ≥100 hemocytes in each category were evaluated from a single animal. Percentages of dead hemocytes were compared in the presence (+) and absence (−) of bacteria. In the encapsulation experiments, ≥100 hemocytes in each category were evaluated from each of 5 animals.

became concentrated around the nuclear envelope. As the plasma membrane over the blebs ruptured, cytoplasm containing the deposits and disrupted organelles was released. Surrounding the degenerating hyaline cell, long strands were formed in the hemolymph, which apparently hydrated into typical clot material. Concurrently, granules developed a scalloped margin, their contents became grainy, and adjacent granules sometimes fused. Granules released their constituents either by exocytosis or lysis into the cytoplasm.

As hyaline cells of *P. interruptus* lysed, spheres of coagulated hemolymph developed around each cell (Fig. 10). The spheres expanded and fused with adjacent spheres to produce a continuous hemolymph clot with clusters of granulocytes scattered between roughly spherical areas of coagulated hemolymph. Hemolymph clots of *Homarus* contained fewer areas of coagulated hemolymph and larger intervening granulocyte clusters. In contrast, the clotted hemolymph of *L. grandis* was composed of masses of aggregated granulocytes (Fig. 11) often adhering to long strands of clot material. The granulocytes in all three species did not lyse during the 1-h time period examined in this study, although they extended filopodia. Large and small granule hemocytes rarely displayed exocytosis of granules.

Phagocytosis of bacteria

Phagocytosis of the Gram-negative bacterium *Cytophaga* sp. was performed by most small granule hemocytes, some large granule hemocytes, and none of the hyaline hemocytes (Table III). The percentage of phagocytic small granule hemocytes ranged from 83% to 96%, whereas only 30% to 67% of the large granule cells were phagocytic. In contrast to incubation in seawater, where cytolysis of hyaline cells was observed, most hyaline cells and granulocytes remained viable when incubated in SCM (shrimp culture medium) for the 2-h duration of the phagocytosis experiments. However, enhanced autolysis was observed when hyaline cells and granulocytes were cultured in the presence of bacteria (Table III). Hyaline cells that did not lyse during the experiments did not

Table IV

Comparative hemocyte cytochemistry

	Large granule cells	Small granule cells	Hyaline cells
Homarus americanus			
Acid phosphatase	48.3 ± 8.5 (25.0–80.0)	23.6 ± 8.0 (6.7–59.5)	0.5 ± 0.5 (0.0–2.9)
Prophenoloxidase	86.6 ± 5.2 (71.4–100.0)	10.8 ± 1.3 (5.0–14.3)	0.0 ± 0.0 (0.0–0.0)
Sudan Black B	0.0 ± 0.0 (0.0–0.0)	0.4 ± 0.4 (0.0–2.5)	99.4 ± 0.6 (96.1–100.0)
Panulirus interruptus			
Acid phosphatase	72.1 ± 6.4 (44.4–90.0)	69.4 ± 7.2 (41.0–91.5)	4.9 ± 1.7 (0.0–11.1)
Prophenoloxidase	96.8 ± 3.4 (91.7–100.0)	35.2 ± 4.9 (20.7–55.7)	0.2 ± 0.2 (0.0–1.0)
Sudan Black B	0.0 ± 0.0 (0.0)	0.0 ± 0.0 (0.0)	99.6 ± 0.2 (98.8–100.0)
Loxorhynchus grandis			
Acid phosphatase	88.7 ± 5.8 (61.5–100.0)	76.6 ± 7.7 (51.9–96.5)	11.4 ± 2.8 (1.9–22.6)
Prophenoloxidase	100.0 ± 0.0 (100.0)	53.4 ± 4.2 (41.8–66.7)	1.0 ± 1.0 (0.0–5.9)
Sudan Black B	0.0 ± 0.0 (0.0)	0.4 ± 0.2 (0.0–1.3)	100.0 ± 0.0 (100.0)

Percentage of positive hemocytes ± standard error. Minimum and maximum values are in parenthesis. Twenty large granule, 50 small granule, and 50 hyaline hemocytes were examined from each of 6 animals.

attach to the glass and spread as did the granulocytes, but often adhered to the granulocytes and remained ovoid. Total phagocytosis rates (defined as the number of phagocytic cells divided by the total number of surviving hemocytes) were 79% and 88%, respectively, for *H. americanus* and *L. grandis* (the two species with no survival of hyaline hemocytes) and 54% for *P. interruptus* which had higher hyaline cell survival.

Encapsulation of fungal hyphae

LM observations of initial hemocyte contact with fungal hyphae showed that approximately two-thirds of adherent cells were large granule hemocytes, between 20% and 30% were small granule hemocytes and only small percentages were hyaline hemocytes (Table III). For all three species, percentages of adherent large granule cells were enriched 7 to 15 times over those found in hemolymph.

Hemocyte cytochemistry

Hemocyte smears were stained to identify sites of lipid (with Sudan black B), or acid phosphatase, or PPO activity (Table IV). Sudan black B, which stains lipids and lipoproteins, produced diffuse cytoplasmic staining in all hyaline cells of each species. However, the staining intensity was less than that previously reported for deposit-containing hyaline cells of the penaeid shrimp in which the entire cytoplasm is darkly stained in a clumpy pattern (Hose *et al.*, 1987). In the present species, the light grey, homogeneous staining of the cytoplasm was difficult to detect without prior experience with the stain. The most distinctive feature in Sudan black-stained cells was that the nucleus in hyaline cells was obscurred by the stain, similar to that observed in the shrimp (Hose *et al.*, 1987). Granules in the hyaline cells of all three species did not accumulate the stain, although membranes around the larger granules in some hyaline hemocytes of *H. americanus* displayed intense staining. The cytoplasm of the granulocytes remained unstained by Sudan black B and the nucleus was always visible. Except for intense staining of granule membranes in large granule hemocytes of *H. americanus*, staining reactions of granulocytes were identical to those reported for shrimp hemocytes.

Reaction sites demonstrating acid phosphatase were rare in hyaline cells and more abundant in granulocytes (Table IV). For each species, ranges of the percentages of positive cells did not overlap between the two categories. Most small granule hemocytes had few to an intermediate number of foci. As observed in the shrimp (Hose *et al.*, 1987), not all large granule hemocytes contained reaction sites, but positive cells had numerous foci. In *L. grandis*, acid phosphatase was primarily located in the granules, although some vesicles and tubules (most likely RER) stained positive as well. In the lobsters, only a few granules contained acid phosphatase and most of the reaction sites were located in vesicles and tubules of RER.

PPO activity was restricted to granulocytes (only one out of approximately 300 hyaline hemocytes of the crab and spiny lobster appeared positive). From 11% (*H. americanus*) to 53% (*L. grandis*) of small granule hemocytes had positively stained granules, whereas most (>87%) large granule hemocytes contained numerous dark-staining granules. The cytoplasm of large granule cells also contained PPO while staining in small granule hemocytes was confined to the granules.

Discussion

Our results suggest that hemocytes of decapod crustaceans are composed of two major groups, hyaline cells and granulocytes, which have distinct functional and cytochemical differences. Most investigators have historically recognized these two categories and separated them using morphological criteria (see Martin and Graves, 1985, for review). However, our work demonstrates that the morphological features traditionally used to identify these categories do not reliably correlate with cellular

functions. Although granulocytes of the three species studied in this paper, the penaeid shrimp (*Sicyonia ingentis*) used to develop the system, and several other species described in the literature (Bauchau, 1981) are morphologically almost indistinguishable, hyaline hemocytes constitute a heterogeneous group. Our observations may explain much of the confusion in the literature regarding hemocyte morphology and function. Such discrepancies have prevented information obtained on a particular species to be readily interpreted with regard to other decapods. In some cases, functional studies have not identified cell types involved in hemolymph coagulation and phagocytosis. For example, both Schapiro *et al.* (1977) and Goldenberg *et al.* (1986) presented quantitative data on phagocytosis of bacteria by *H. americanus* hemocytes, but neither group could identify the phagocytic hemocytes. In other cases, morphological identification did not correspond to functional roles. For instance, Söderhäll *et al.* (1986) refer to the hyaline cell as the main phagocytic hemocyte in the crab *Carcinus maenus* whereas in the crayfish *Pacifastacus leniusculus* phagocytosis is performed by both hyaline cells and semigranular cells. Such lack of consistency in ascribing similar functions to apparently similar hemocyte types stems from difficulties of using a classification system based on traditional morphological interpretations of hyaline and granular hemocytes (*i.e.*, granule number and size). Our data show that, for the four species investigated thus far, function is correlated with other morphological features such as cell size, nucleocytoplasmic ratio, and the presence of cytoplasmic deposits.

Historically, a second area of confusion is the identity of the type of hemocyte that initiates coagulation. Responsible cells have been described as either "explosive corpuscles" and "hyaline cells" (Wood and Visentin, 1967; Wood *et al.*, 1971; Ravindranath, 1980) or granulocytes (Toney, 1958; Hearing and Vernick, 1967; Mengeot *et al.*, 1977; Madaras *et al.*, 1981). Our studies provide an answer for the apparent confusion regarding the identity of clotting hemocytes. Hyaline cells lyse and initiate coagulation in all species; however in different species, these cells exhibit variations in the abundance and size of granules. For example, the granules of *Loxorhynchus grandis* are so abundant that the hyaline cells are easily confused with granulocytes while in *Panulirus interruptus*, the granules in large granule and hyaline hemocytes are approximately the same size. Hyaline hemocytes do have in common numerous, 50-nm diameter cytoplasmic deposits. These deposits can be detected using TEM, a technique rarely included in previous classification schemes, and by their propensity to stain with Sudan Black B.

We avoided the use of the term "hyaline cell" in our previous publications (Martin and Graves, 1985; Martin *et al.*, 1987; Hose *et al.*, 1987; Hose and Martin, 1989; Omori *et al.*, 1989) in an attempt to avoid bias in developing a classification scheme and instead referred to deposit cells (with and without granules), small granule and large granule hemocytes. We now consider that shrimp deposit cells are equivalent to hyaline cells. Therefore, in an attempt to simplify the classification of crustacean hemocytes, we suggest the following categories of hemocytes: hyaline, small and large granule hemocytes. It is very important to recognize that morphology alone is insufficient for assigning any cell to one of these categories; instead the following criteria for hemocyte identification are suggested.

Hyaline cells have a nucleocytoplasmic ratios of >0.35 and lyse during clot formation. Because lysis is rapid, identification of these cells, especially in species with relatively low numbers of hyaline cells, is facilitated by mixing a trypan blue-seawater solution with hemolymph. Hyaline cells turn blue prior to lysis, thereby allowing morphological identification of the cell and observation of changes in cell morphology during coagulation. At the TEM level, these cells contain tiny cytoplasmic deposits that appear to be involved with the clotting process because they are only present in the hyaline cells and their release from the lysing cell precedes hemolymph coagulation. In addition, hyaline cells in the species we have studied (this paper and Hose *et al.*, 1987), selectively stain with Sudan Black B. Although this is a general stain for lipid, it has also been shown to stain coagulogen isolated electrophoretically (Durliat, 1985). Coagulogen may be contained within hyaline hemocytes or perhaps produced but not stored in high levels by these hemocytes. In crustacean hyaline cells, the cytoplasmic deposits are sudanophilic, with the most intense staining observed from the clustered deposits present in shrimp (Hose *et al.*, 1987). Although the test is useful, interspecific variations in the intensity of Sudan Black B staining are subtle and require careful interpretation. The less subjective criterion for a positive reaction is the obscurance of the nucleus by the stain.

Our results suggest that coagulation in decapods involves a common mechanism; the release of cytoplasmic material through breaks in the plasma membrane, possibly including the granules. The identity of the materials released is not clear. It has been suggested that (1) coagulogen, the clotting protein, is found in the plasma and activated by chemicals released from hemocytes and (2) coagulogen and its activators are released from cells (see Omori *et al.*, 1989). Ghidalia *et al.* (1981) reviewed this topic and demonstrated the presence of coagulogen in the plasma of decapods representing Tait's (1911) three patterns of coagulation. Although the presence of coagulogen in plasma could result from lysis of hyaline hemocytes during cell separation, these investigators used an anticoagulant (1:9, hemolymph:10% sodium citrate, v:v) which we have shown to be effective in preventing hya-

line cell lysis. They conclude that differences between the three coagulation patterns are probably due to the manner in which the clot-initiating materials are released. From the present study we show that decapods placed in Tait's category C (characterized by rapid gelation of the plasma) have twice the percentage of hyaline cells as in species where hemocyte aggregation occurs followed by slight gelation of the plasma (Tait's category A). What remains unclear is the localization of the clotting protein coagulogen (in cells, plasma, or both) and an identification of the material released from the hyaline cells that initiates coagulation. The most abundant cytoplasmic material released during coagulation is the electron-dense deposits. These deposits were identified in the hyaline cells of all decapods we examined using TEM and appear similar to published micrographs of coagulocytes in some insects (Ratcliffe and Rowley, 1979). Clearly a specific labelling technique for these deposits and coagulogen is needed, as in Bohn *et al.*'s (1981) immunocytochemical study of insect coagulogen.

Granulocytes, the second major category of decapod hemocytes, have a nucleocytoplasmic ratio of <0.35 and they do not accumulate trypan blue or lyse rapidly in culture. They are identified by the presence of numerous cytoplasmic granules, positive staining reactions for acid phosphatase and PPO, and *in vitro* phagocytosis of bacteria and attachment to fungal hyphae. The two subdivisions of granulocytes may be distinguished by (1) central location of nuclei in small granule hemocytes and eccentric location of nuclei in large granule hemocytes, (2) the presence of only large granules in large granule hemocytes whereas in small granule hemocytes there is a mixture of granules with varying sizes, and (3) the refractile nature of granules only in large granule hemocytes when examined by phase contrast microscopy.

The functional roles of granulocytes correlate well with observed cytochemical features. Granulocytes are the primary defensive cells of the hemolymph and the two subtypes perform overlapping functions. Small granule hemocytes are the main cells involved in phagocytosis and contain many lysosomes, while large granule cells, which most frequently initiate encapsulation of fungi, show more intense staining for PPO (Hose and Martin, 1989).

The functional and cytochemical criteria for recognizing two categories of hemocytes (hyaline cells and granulocytes) are further supported by observations of hemocyte maturation within the hematopoietic tissue of the shrimp (Martin *et al.*, 1987). In this species, we observed mitosis only in agranular hyaline cells and small granule hemocytes. Clusters of hyaline cells and granulocytes were segregated within the hematopoietic tissue (Martin *et al.*, 1987). We propose that the two hemocyte categories represent two cell lines. Cell size is significantly smaller in hyaline cells and is discontinuous between hyaline cells and small granule hemocytes. The nucleocytoplasmic ratios of hyaline cells of shrimp and the three species considered here are significantly higher than those of granulocytes. The ratios of two granulocyte categories overlap and decrease in large granule hemocytes coincident with increases in granule number and size (Table I). Granulocytes thus appear as a continuum of differentiation from the less mature small granule hemocytes to the large granule hemocytes.

To summarize, a combination of morphological, cytochemical and functional methods must be used to identify decapod hemocytes, because traditional morphological features are inadequate and misleading, especially with regard to hyaline cells. Further studies by investigators utilizing other decapods are necessary to test the usefulness of this classification scheme and to offer improvements by developing more specific criteria.

Acknowledgments

We want to thank Heidi Parker and Laura Targgart for collecting and maintaining the crustaceans; Sidne Omori, Cathy Corazine, Celeste Chong, and Erin Campbell for technical support; and Dr. Don Lightner and Leona Mohney for supplying the cultures of *Fusarium solani*. The project was supported by NSF grant DCB-8502150 to GM and JEH.

Literature Cited

Bauchau, A. G. 1981. Crustaceans. Pp 386–420 in *Invertebrate Blood Cells*, Vol. 2. Academic Press, New York.

Bohn, H., B. Barwig, and B. Bohn. 1981. Immunochemical analysis of hemolymph clotting in the insect *Leucophaea medarae* (Blattaria). *J Comp Physiol* **143B:** 169–184.

Brody, M., and E. Chang. (In press). Ecdysteroid effects on primary cell cultures. *Int J Invertebr Repro. Dev*

Cornick, J. W., and J. E. Stewart. 1978. Lobster (*Homarus americanus*) hemocytes: classification, differential counts and associated agglutinin activity. *J Invertebr Pathol.* **31:** 194–203.

Durliat, M. 1985. Clotting processes in Crustacea Decapoda. *Biol. Rev.* **60:** 473–498.

Ghidalia, W., R. Vendrely, C. Montmory, Y. Coirault, and M. O. Brouard. 1981. Coagulation in decapod crustacea. *J Comp. Physiol.* **142:** 473–478.

Goldenberg, P. Z., A. H. Greenberg, and J. M. Gerrard. 1986. Activation of lobster hemocytes: cytoarchitectural aspects. *J Invertebr Pathol* **47:** 143–154.

Hearing, V. J., and S. H. Vernick. 1967. Fine structure of the blood cells of the lobster, *Homarus americanus*. *Ches. Sci.* **8:** 170–186.

Hose, J. E., G. G. Martin, V. A. Nguyen, J. Lucus, and T. Rosenstein. 1987. Cytochemical features of shrimp hemocytes. *Biol Bull.* **173:** 178–187.

Hose, J. E., and G. G. Martin. 1989. Defense functions of granulocytes in the ridgeback prawn *Sicyonia ingentis* Burkenroad 1938. *J Invertebr Pathol* **53:** 335–346.

Madaras, F., M. Y. Chew, and J. D. Parkin. 1981. Purification and characterization of the sand crab (*Ovalipes bipustulatus*) coagulogen (fibrinogen). *Thromb. Haemost.* **45:** 77–81.

Martin, G. G., and B. L. Graves. 1985. Fine structure and classification of shrimp hemocytes. *J Morphol* **185:** 339–348.

Martin, G. G., J. E. Hose, and J. J. Kim. 1987. Structure of hematopoietic nodules in the ridgeback prawn *Sicyonia ingentis* light and electron microscopic observations. *J. Morphol.* **192:** 193–204.

Mengeot, J. C., A. G. Bauchau, M. B. DeBrouwer, and E. Passelecq-Gérin. 1977. Isolément des granules des hémocytes de *Homarus vulgaris* Examens électrophorètiques du contenu protéique des granules. *Comp. Biochem. Physiol.* **58(A):** 393–403.

Omori, S. A., G. G. Martin, and J. E. Hose. 1989. Morphology of hemocyte lysis and clotting in the ridgeback prawn, *Sicyonia ingentis*. *Cell Tissue Res.* **255:** 117–123.

Ratcliffe, N. A., and A. F. Rowley. 1979. Role of hemocytes in defense against biological agents. Pp 332–414 in *Insect Hemocytes. Development, Form, Functions and Techniques*, A. P. Gupta, ed. Cambridge University Press, Cambridge.

Ratner, S., and S. B. Vinson. 1983. Phagocytosis and encapsulation: cellular immune responses in Arthropoda. *Am. Zool.* **23:** 185–194.

Ravindranath, M. H. 1980. Haemocytes in haemolymph coagulation of arthropods. *Biol. Rev.* **55:** 139–170.

Shapiro, H. C., J. F. Steenbergen, and Z. A. Fitzgerald. 1977. Hemocytes and phagocytosis in the american lobster, *Homarus americanus* Pp 126–134 in *Comparative Pathology*, Vol. 3. Plenum Press, New York.

Söderhäll, K. 1982. Prophenoloxidase activating system and melanization—a recognition mechanism of arthropods? A review. *Dev. Comp. Immunol.* **6:** 601–611.

Söderhäll, K., V. J. Smith, and M. W. Johansson. 1986. Exocytosis and uptake of bacteria by isolated haemocyte populations of two crustaceans evidence for cellular co-operation in the defense reactions of arthropods. *Cell Tissue Res.* **245:** 43–49.

Spurrs, A. 1969. A low viscosity epoxy embedding medium for electron microscopy. *J. Ultrastruct. Res.* **26:** 31–43.

Tait, J. 1911. Types of crustacean blood coagulation. *J. Mar. Biol. Assoc. U. K.* **9:** 191–198.

Toney, M. E. 1958. Morphology of the blood cells of some crustacea. *Growth* **22:** 35–50.

Wood, P. J., and L. P. Visentin. 1967. Histological and histochemical observations of the hemolymph cells in the crayfish, *Orconectes virilis*. *J. Morphol.* **123:** 559–568.

Wood, P. J., J. Podlewski, and T. E. Shenk. 1971. Cytochemical observations of hemolymph cells during coagulation in the crayfish, *Orconectes virilis*. *J. Morphol.* **134:** 479–488.

Reference: *Biol. Bull.* **178:** 46–54. (February, 1990)

Respiratory Responses of the Blue Crab *Callinectes sapidus* to Long-Term Hypoxia

PETER L. DEFUR[1]*, CHARLOTTE P. MANGUM[2], AND JOHN E. REESE[2]

[1]*Department of Biology, George Mason University, Fairfax, Virginia 22030 and* [2]*Department of Biology, College of William and Mary, Williamsburg, Virginia 23185*

Abstract. Blue crabs (*Callinectes sapidus*) were held in hypoxic (50–55 mm Hg) water for 7–25 days. Postbranchial blood PO_2 fell by about 80% within 24 h and then remained unchanged. Postbranchial blood total CO_2 increased within 24 h and remained elevated for the duration of the experiment. There was no change in postbranchial blood pH, osmolality, or Cl. Lactate, urate, and Ca^{+2} all raise the O_2 affinity of blue crab hemocyanin; by 25 days, blood lactate and urate had risen slightly, but Ca^{+2} had increased dramatically. Hemocyanin concentration had also increased by 25 days. At both 7 and 25 days there was an intrinsic increase in hemocyanin-O_2 affinity and a change in subunit composition. The highly adaptive homotropic change is believed to be due to an attendant shift in the proportions of two of the three variable monomeric hemocyanin subunits. Thus, both heterotropic and homotropic adaptations enhance blood oxygenation at the gill during long-term hypoxia.

Introduction

The respiratory response to long term hypoxia, defined here as exposure for three or more days, has been examined in six species of aquatic crustaceans: three crayfish (McMahon *et al.*, 1974; Dejours and Armand, 1980; Wilkes and McMahon, 1982a, b), a lobster (McMahon *et al.*, 1978), a crab (Burnett and Johansen, 1981), and a prawn (Hagerman and Uglow, 1985). In all cases, the initial response was hyperventilation, which resulted in a respiratory alkalosis. Subsequently, however, the response in different species became diverse. Blood pH either returned in full (Wilkes and McMahon, 1982a) or in large part (Butler *et al.*, 1978; McMahon *et al.*, 1978) to the normoxic level, or remained decidedly alkalotic for as long as 3–8 days (Dejours and Armand, 1980; Burnett and Johansen, 1981).

Crustacean hemocyanins (Hcs) typically have very large normal Bohr shifts; the quantity $\Delta \log P_{50}/\Delta pH$ is commonly near −1 (Mangum, 1980). Thus, the alkalosis, which had also been observed during acute hypoxia (Truchot, 1975; Burnett, 1979), would have the important respiratory consequence of raising blood O_2 affinity. The increases were observed, but were attributed by previous workers to the rise in blood pH. We now know that at least three other allosteric effectors, *viz.*, L-lactate (Truchot, 1980; Booth *et al.*, 1982), Ca^{+2} (Mangum, 1985) and urate (Morris *et al.*, 1985; Lallier *et al.*, 1987), also may increase HcO_2 affinity during acute hypoxia. The levels of these effectors in the blood during prolonged exposure, however, are not known.

Intrinsic changes in O_2 affinity of Hc in response to prolonged changes in environmental factors have recently been observed in both crayfish (Rutledge, 1981) and crabs (Mauro and Mangum, 1982; Mason *et al.*, 1983; Mangum and Rainer, 1988). In the blue crab, *Callinectes sapidus* Rathbun, salinity-induced changes are accompanied by shifts in the concentrations of two of the 5–6 subunits of the Hc polymers (Mason *et al.*, 1983). The changes in one of the two subunits fully explains the attendant shift in O_2 affinity (Mangum and Rainer, 1988).

Although an intrinsic molecular change would not be expected to occur during acute hypoxia, it might occur during long-term hypoxia. In the shrimp *Crangon crangon*, Hc levels increase sharply during prolonged hypoxia

Received 1 November 1988; accepted 30 November 1989.

* Present address: Environmental Defense Fund, 1108 E. Main St., Richmond, VA 23219.

(Hagerman, 1986); a similar increase in the blue crab appears to hasten intrinsic molecular adaptation to a salinity change (Mason *et al.*, 1983). Therefore, we have examined the possibility that a change in net synthesis or degradation during hypoxia produces additional or replacement molecules that differ from those in normoxic animals.

The blue crab inhabits many bodies of water that are not invariably normoxic (Carpenter and Cargo, 1957; May, 1973; Garlo, 1979; Harper *et al.*, 1981; Turner and Allen, 1982). Lethal levels (PO_2 < about 50 mmHg) often kill animals that cannot escape from pots (Carpenter and Cargo, 1957). Free-ranging animals may even emerge into air (Loesch, 1960; Officer *et al.*, 1984), despite limited tolerance of it. In the Chesapeake Bay system, sublethal O_2 levels, still well below normoxia, are so widespread that crabs must encounter them for long periods. Water PO_2 in the range 50–100 mmHg is characteristic of the Chesapeake Bay for several months during the spring and fall (Officer *et al.*, 1984; Seliger *et al.*, 1985). In the summer, cyclical destratification in the channels produces sublethal hypoxia throughout the water column for several weeks at a time (Webb and D'Elia, 1980). Processes ranging from tidal flushing of the marshes, to seiching of the water in the channels, produce sublethal hypoxia in extensive areas of shallow water as well (Carpenter and Cargo, 1957; Axelrad *et al.*, 1976; Kemp and Boynton, 1980; Taft *et al.*, 1980; Malone *et al.*, 1986; MacKiernan, 1987).

We have determined the response of blood respiratory and osmotic variables of the blue crab *Callinectes sapidus* Rathbun to sublethal hypoxia. The treatments include acute exposure, more prolonged exposures similar to those employed in previous studies, and still more prolonged exposures designed to elicit intrinsic changes in the Hc molecule. We have measured all of the known physiological effectors of HcO_2 binding, both hetero- and homotropic.

Materials and Methods

Animals

Large (*ca.* 120–220 gm wet wt.), male, intermolt crabs were obtained from commercial watermen or collected by the first author near the Rhode River or the mouth of the Patuxent River in Maryland. They were returned to Fairfax, Virginia, and maintained in open containers (100–200 l) of natural, aerated water (500–530 mOsM, 21–23°C) for 4–7 days prior to the experimental hypoxia. Water osmolality was monitored frequently and distilled water added as needed; water pH was also monitored and kept above 7.9 by the addition of $NaHCO_3$. Crabs were fed thawed smelt twice a week throughout the control and experimental periods, but not within 24 h of sampling.

Design

The experimental protocol consisted of taking blood from the same crabs before, during, and following exposure to hypoxia. Insofar as possible, the design of paired observations on the same individuals was maintained, and the data were analyzed accordingly. The significance of changes in blood pH, PO_2, total CO_2, lactate, Cl, and osmolality was tested according to Student's *t*-test for ungrouped (paired) data as the mean of the differences of each value from the control for the same individual, the null hypothesis being that there was none. Because the same individuals were sampled repetitively, the blood samples were necessarily small (0.5 ml), thus insufficient volumes of many samples remained for the other measurements. The paired observations design could not be maintained for the analysis of Ca^{+2}, urate, and Hc concentrations; these values were analyzed by Student's *t*-test for grouped data (two samples). For measurements such as O_2 binding, which require a total of more than 0.5 ml of material, samples were pooled; the results were analyzed by regression. In these measurements, pooled samples for −1 and 7-day exposure were made up of blood from the same individuals, whereas that for 25-day exposure was composed of blood from different animals.

Hypoxia

Nitrogen gas was bubbled into the water to reduce the PO_2 from 140–155 to approximately 55 mm Hg in 3–4 h, and then the bubbling was stopped. Thereafter a slow, steady air flow was maintained, and N_2 was bubbled into the water only as needed to offset the air.

N_2 flow was regulated by a metering system that balanced N_2 against rising O_2. The system consisted of an O_2 electrode and meter (Instrumentation Laboratories Models 1703B and 113, respectively), the output of which provided the signal for a logic circuit that controlled an electric gas valve. The circuit was set to evaluate the output of the meter every 5 min and to open the valve if the PO_2 had increased above the set point of 50 mmHg. Thus, once the initial PO_2 of 50 mmHg was reached, further changes were confined to the ranges 50–55 mmHg and occurred slowly. The continuous airflow stirred the water and ensured that O_2 uptake by the crabs did not reduce water PO_2 below 50 mmHg.

Blood sampling

Postbranchial hemolymph samples for the determination of *in vivo* respiratory variables were withdrawn through holes in the carapace dorsolateral to the heart.

The holes had been drilled four or more days prior to the control period, and covered with latex rubber affixed with cyanoacrylate cement. On occasion, prebranchial hemolymph was also withdrawn from the base of one of the legs for the measurement of Cl, osmolality, and lactate.

Blood samples were withdrawn into iced syringes and immediately placed on ice to slow clotting. After determination of blood gas and acid-base variables, these samples were frozen for the remaining analyses. The samples for HcO_2 binding were kept cool and, with the exception noted below, unfrozen; O_2 binding measurements on blood from normoxic and hypoxic animals were made within a few days.

In vivo *variables*

Hemolymph pH was measured with a thermostatted glass capillary electrode (Radiometer G299A) and meter (Radiometer PHM 84). PO_2 was measured with a polarographic electrode (Radiometer E5046) and acid-base analyzer (PHM 72). Total CO_2 was determined in 50 μl samples with a Corning Model 965 CO_2 analyzer. Lactate was measured enzymatically (Sigma Procedure No. 826), with the modifications for Hc-containing blood developed by Graham *et al.* (1983). Osmolality was determined with a vapor pressure osmometer (Wescor Model 5100C).

Ca^{+2} activity was determined with a Radiometer electrode and PHM 84 meter, following 1:99 dilution with 0.05 Tris Maleate buffer, pH 7.6 (Mangum and Lykkeboe, 1979). Chloride was measured by electrometric titration (Corning Model 920).

We determined urate as the quinoneimine produced by digestion with uricase (Sigma Procedure No. 685), after first verifying that 100% of the urate added to test samples of blood could be recovered. Because Hc absorbs at 685 nm, the absorbance was measured in replicate, once with and once without the analytical reagents, and the interference of Hc was subtracted.

HcO_2 binding and Hc concentration

Hemolymph was declotted with a tissue grinder, centrifuged, and then dialyzed at 4°C for 24–28 h against a saline made up according to Mason *et al.* (1983). HcO_2 binding was determined by the cell respiration method, in which the deviation from a constant rate of O_2 depletion is used to estimate fractional oxygenation at the measured PO_2 (Mangum and Lykkeboe, 1979).

Before determining Hc concentration in the blood, we eliminated the effect of light scattering, dissociating the native polymers to monomeric subunits by dilution (1:39) with Tris HCl containing 50 m*M* EDTA. Absorbance of Hc was measured at 338 n*M* with a Milton Roy Spectronic 501 spectrophotometer; the concentration was calculated using the extinction coefficient for portunid Hc reported by Nickerson and Van Holde (1971).

Electrophoresis

Alkaline dissociation electrophoresis (Hames and Rickwood, 1981) of Hc monomers on polyacrylamide gel slabs was performed as described by Mangum and Rainer (1988). In the present case, aliquots of the three pools of blood used to compare O_2 binding in normoxic and hypoxic animals were run on the same gels, which were scanned with a Gelman Instruments Model 3372 integrating densitometer (modified for transparent media). Changes were estimated by comparing peaks of the variable subunits with that of an invariant subunit.

Results

The experiment was performed three times. The first hypoxic exposure period was 7 days, and samples were taken at −1 (control), 1, 4, and 7 days. The second and third exposure periods were 25 and 23 days, and samples were taken at −1, 7, 9, or 16, and 23 or 25 days. In the first experiment, the crabs were also sampled one day after the return to normoxic water.

Behavior and mortality

When ambient PO_2 fell to 50 mm Hg, most of the crabs became active and moved slowly around the aquarium, as reported by Lowery and Tate (1986); some crabs tried to climb out of the water. Elevated activity ceased within a few hours, and the animals became quiescent for the duration of the hypoxic exposure. They frequently buried in the sand lining the bottom of the aquarium.

Mortality was low. There was none during the first experiment and only 20% during the longer exposures. In our experience, this level would be low under normoxic conditions.

Hemolymph variables

Many of the data for normoxic animals are unexceptional (Table I, day −1), but pH and PO_2 are high relative to those in the literature for this species (*e.g.*, Weiland and Mangum, 1975; Mangum *et al.*, 1985). Our value for blood urate in normoxic animals is also considerably lower than that reported by Morris *et al.* (1986) for the crayfish *Austropotamobius pallipes* (0.35 m*M*), but it is similar to the figure (0.08 m*M*) found in the portunid crab *Carcinus maenas* (Lallier *et al.*, 1987). The low urate levels in the portunid bloods may explain the absence (Mangum, 1983) or small size (Truchot, 1975) of

Table I

Respiratory variables[1] in the hemolymph of blue crabs exposed to moderate hypoxia[2] for 7–25 days[3] (day −1 = control)

Duration[4] (days)	No. animals		PaO_2 (mm Hg)		pHa		$CaCO_2$ (mM)		Lactate (mM)		Ca^{+2} (mM)	Urate (mM)	[Hc] (g/100 ml)
	7	23–25	7	23–25	7	23–25	7	23–25	7	23–25	23–25	23–25	23–25
Day −1 (control)	8	9–11	98 ± 3	70 ± 8	7.81 ± 0.03	7.71 ± 0.03	2.3 ± 0.2	2.3 ± 0.4	0.01 ± 0.01	0.94 ± 0.09	6.73 ± 0.75	0.05 ± 0.02	3.11 ± 0.41
1	8		18 ± 4		7.79 ± 0.02		5.4 ± 0.3		0.08 ± 0.05				
4	8		15 ± 4		7.80 ± 0.04		5.1 ± 0.3		0.08 ± 0.06				
7	8	4–8	13 ± 2	22 ± 2	7.83 ± 0.03		4.6 ± 0.4	3.6 ± 0.2	0.09 ± 0.05		4.73 ± 0.75	0.03 ± 0.00	1.26 ± 0.11
Recovery	8		87 ± 10		7.77 ± 0.02		3.3 ± 0.2		0.00 ± 0.00				
9		6		19 ± 3		7.81 ± 0.06		2.6 ± 0.2		0.80 ± 0.09			
16		4		21 ± 3									
23–25		5–11		21 ± 4		7.76 ± 0.04		3.2 ± 0.3		1.79 ± 0.50	10.1 ± 0.5	0.14 ± 0.02	4.40 ± 0.19

[1] Top no. = mean, bottom no. = S.E.
[2] ~50–55 mm Hg, 21–23°C, 500–530 mOsM.
[3] Symbols: PaO_2 = postbranchial blood PO_2, pH = postbranchial blood pH, $CaCO_2$ = postbranchial blood total CO_2.
[4] Two columns under the first five headings represent different exposure periods, as indicated.

changes in HcO_2 affinity following dialysis of normoxic serum against a physiological saline.

Within 24 h of the onset of the 7-day hypoxic exposure in the first experiment, postbranchial blood PO_2 (PaO_2) fell by 80% and total CO_2 ($CaCO_2$) more than doubled while pH remained unchanged (Table I). The subsequent changes in these three variables are not significant ($P > .05$). The apparent increase in lactate is not significant ($P > .05$) if the difference at each sampling period is tested against zero. If the particular sampling period is disregarded and the maximum increase for each individual is tested against the null hypothesis, however, then the mean increase (0.18 ± .06 m*M*) is significantly greater than zero ($P < .01$). More important, this change is very small, indicating a highly aerobic condition. Within 24 h of return to normoxic water, control levels of postbranchial PO_2 were restored, although total CO_2 remained slightly elevated ($P < .02$).

In the second and third experiments, the same and longer periods of exposure (23–25 days) to hypoxia resulted in similar patterns of PO_2, pH, and total CO_2 (Table I). Once again blood lactate increased slightly, although in this case significantly ($P = .05$), regardless of how the data are grouped. At 25 but not 7 days, blood Ca^{+2} rose by a large amount ($P = 0.025$), blood urate rose significantly ($P < .001$), and Hc concentration increased by almost half ($P < .05$).

In none of the three experiments, did blood Cl or osmolality change, nor were there any coherent trends in these variables. The mean values (±S.E., n = 61) for all periods are 355 (±4) m*M* Cl and 756 (±5) mOsm.

HcO_2 binding and subunit composition

At the end of the 7-day period, a change in HcO_2 affinity had clearly occurred (Fig. 1, upper panel). The 95% confidence intervals around the regression lines describing the data for −1 and 7 days in Figure 1 do not overlap at any point (Table II). The slopes of regression lines (−0.97 ± 0.21 95% C.I. for normoxic and −1.11 ± 0.11 for 7 days, hypoxic animals), and thus the Bohr shifts, do not differ significantly.

The relationship between cooperativity (n) and pH of the decapod Hcs is usually quite complex, often reaching a maximum in the middle of the physiological pH range and showing lower values at the extremes. No very sensi-

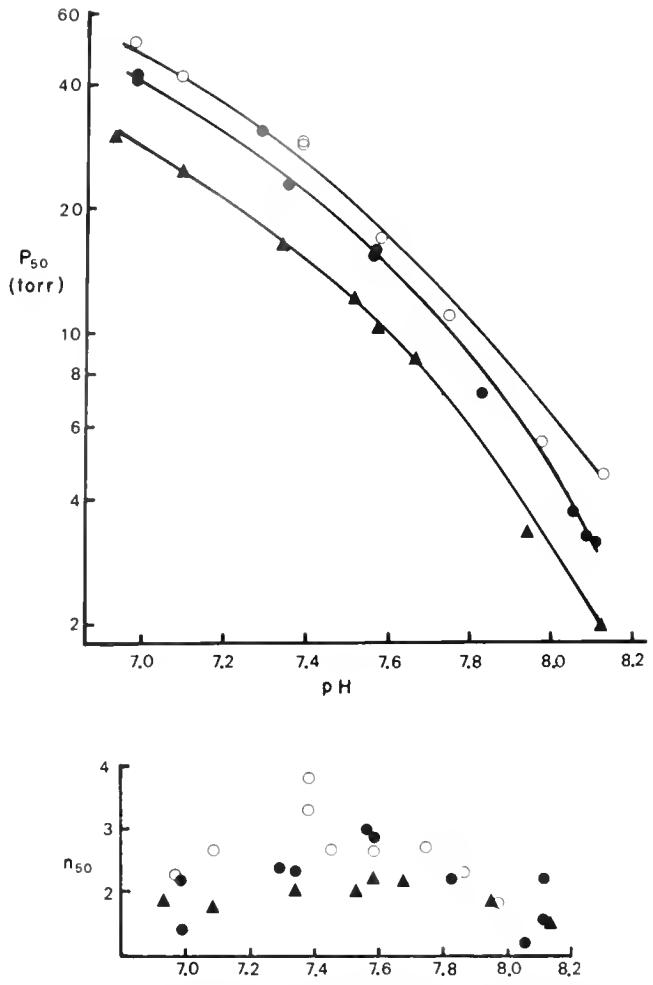

Figure 1. Oxygen binding by stripped Hc of normoxic (○), 7 days hypoxic (●), and 25 day hypoxic (▲) blue crabs. 25°C, 0.05 *M* Tris maleate buffered saline containing 494 m*M* NaCl, 16 m*M* KCl, 23 m*M* $CaCl_2$, 23 m*M* $MgCl_2$ 25 m*M* $(Na)_2SO_4$ and 2 m*M* $NaHCO_3$. Upper panel shows oxygen affinity (P_{50}), and lower panel shows the cooperativity at $PO_2 = P_{50}$ (n_{50}).

tive procedure for data analysis is available. In the lower panel of Figure 1, cooperativity seems to decrease at 7 days, but the mean values are not significantly different ($P = .10$). A Mann-Whitney U test also did not distinguish a significant change.

There was a clear change in the subunit composition of the Hcs (Fig. 2). Specifically, subunits 3, 5, and 6 decreased in concentration relative to subunit 4, which has remained invariant in samples taken, by now, from more than 500 individuals (Mangum, unpubl. obs.; Rainer, 1988).

After 25 days of hypoxia, HcO_2 affinity increased further (Fig. 1). The 95% confidence interval around a regression line describing O_2 affinity does not overlap those for control or 7-day hypoxic animals in any part of the pH range (Table II). The slope of the regression line describing the 25 day data (−1.00 ± 0.17 95% C.I.) does not differ from the other two. In this case, the mean value for cooperativity (1.95 ± 0.06 S.E.) of the Hc from 25 day hypoxic animals (Fig. 1) differs significantly ($P = .02$) from that for control and 7 day hypoxic animals (2.41 ± 0.14).

All three variable subunits decreased further in concentration relative to subunit 4 (Fig. 2). Indeed the presence of subunit 3, which is sometimes completely absent (Mason *et al.*, 1983), is dubious. By the end of 25 days of hypoxia, the concentration of subunit 6 had dropped from the highest in the control period to rank fourth; no. 5 had dropped from second to third; and no. 3 had dropped from clearly present to undetectable, or nearly so. The two weak bands appearing between peaks 1 and 2 of the Hc from hypoxic crabs (Fig. 2B, C) are usually not present: they are not copper containing and have no influence on oxygen binding (Mangum and Rainer, 1988).

Although the effects of elevated Ca^{+2} (and L-lactate) on *C. sapidus* Hc are well known (*e.g.*, Booth *et al.*, 1982; Mangum, 1983; Mason *et al.*, 1983; Johnson *et al.*, 1984), those of urate are not. Therefore we used the small amount of (frozen) blood remaining after the measurement of extrinsic co-factors to examine urate sensitivity. Figure 3 shows that small quantities of urate clearly raise O_2 affinity of the Hc of animals exposed to hypoxia for 25 days, with its altered subunit composition. The positions (but not slopes) of regression lines describing the data for 0, 0.55, and 2.35 m*M* urate all differ at $P = 0.05$. Although the data suggest little further difference beyond 1.17 m*M*, the small number of observations permitted by the volume of material available mandates some caution on this point.

We emphasize that, unlike the measurements in Figure 1, those in Figure 3 were made on Hcs that had been frozen for several months. As mentioned earlier (Mangum, 1983), freezing does not usually influence P_{50} (see also Morris, 1988), at least if the Hc retains its native

Table II

Ninety-five percent confidence intervals around semilogarithmic (log Y) regression lines fit to P_{50} data in Figure 1

pH	Control ($r^2 = 0.946$)	7-day hypoxia ($r^2 = 0.994$)	25-day hypoxia ($r^2 = 0.965$)
7.0	57.2–60.5	49.7–53.5	31.0–33.7
7.2	36.6–38.6	30.5–32.7	19.6–21.2
7.4	23.4–24.6	18.7–20.0	12.4–13.4
7.6	15.0–15.7	11.6–12.2	7.86–8.46
7.8	9.54–10.1	7.01–7.48	4.96–5.35
8.0	6.09–6.44	4.29–4.59	3.13–3.39
8.2	3.88–4.12	2.62–2.81	1.97–2.15

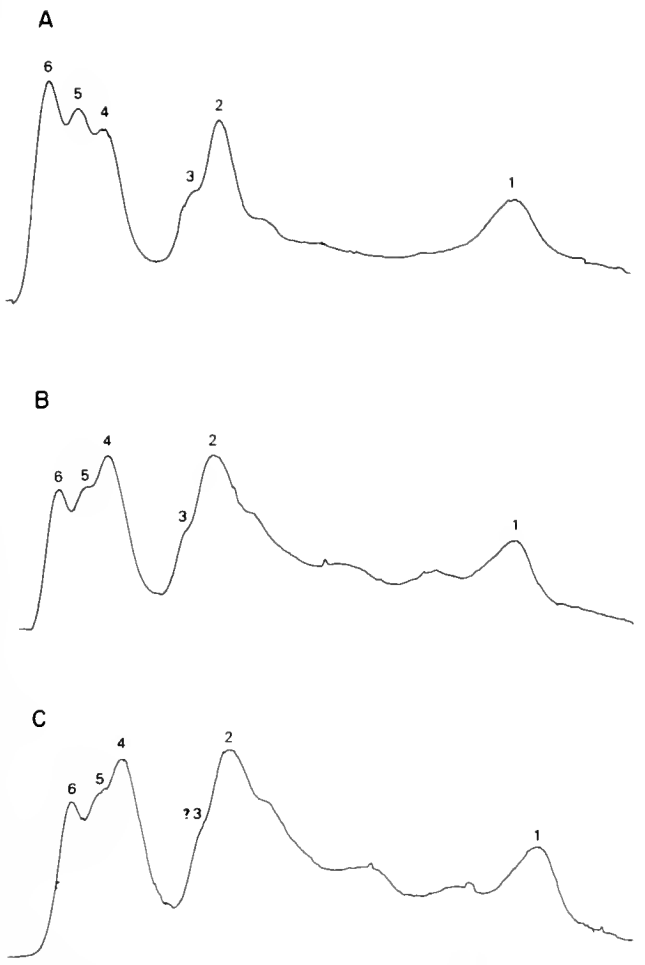

Figure 2. Densitometer scan of slab gels, showing native subunits (numbered peaks) of blue crab Hc separated by charge (subunit 1 is at the anodal end). The Hc applied to the gels was from the same samples from which data were collected for Figure 1. A. Normoxic. B. 7-day hypoxic. C. 25-day hypoxic. Subunit 3 in C is dubious.

optical properties. The control values in the two figures are essentially identical (95% confidence intervals around regression lines broadly overlap). Because freezing frequently influences cooperativity, however (Mangum, 1983; S. Morris, pers. comm.), we did not analyze the cooperativity of the thawed samples. Morris *et al.* (1986) found no effect of urate on cooperativity.

Discussion

Blood pH, PO_2, and CO_2

In view of the unanimity of previous reports of blood alkalosis accompanying hypoxia of virtually any duration in crustaceans, we were surprised to find none in the present experiments. Hyperventilation and alkalosis are not always precisely correlated; in the crayfish *O. rusticus*, ventilation returns to control levels while blood pH is still elevated (Wilkes and McMahon, 1982a). But all reports agree that blood pH rises at some point. In fact, in severely hypoxic *C. maenas*, Lallier *et al.* (1987) reported a pH increase of more than 0.3 units accompanying an increase in lactate of 25 m*M*, despite no change in base. In other investigations of *C. sapidus*, we have either found (Pease *et al.*, 1986), or not found (Mangum and Weiland, 1975, and unpubl. obs.), a hypoxic alkalosis. The response in this species is apparently highly labile, for reasons that are presently unclear. The increases in lactate observed here seem too small to offset a respiratory alkalosis brought about by vigorous hyperventilation (Pease and deFur, 1987). Further increases in pH and PO_2 might have been precluded because ventilation was already high. Elevated ventilation during the control period could have arisen from sensory stimulation (McDonald *et al.*, 1977) and been unrelated to ambient PO_2.

Extrinsic modulation of HcO_2 affinity

In many crustaceans L-lactate is a physiologically important modulator of HcO_2 affinity, both during exercise and hypoxia (Booth *et al.*, 1982; Graham *et al.*, 1983) and very severe environmental hypoxia (Lowery and Tate, 1986; Lallier *et al.*, 1987). The small increases observed here would raise HcO_2 affinity at physiological pH by less than 1 mmHg. The increase in urate would raise HcO_2 affinity by a similarly small amount. In contrast, Ca^{+2} may be an important effector after 23–25 (but not 7) days, by which time the increase in Ca^{+2} would raise HcO_2 affinity by more than 5 mmHg.

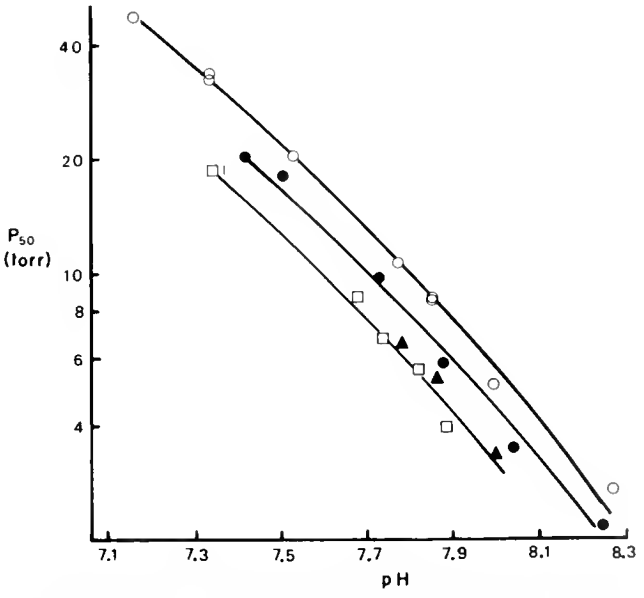

Figure 3. Effect of urate on O_2 affinity of stripped Hc from hypoxic animals. Conditions as in Figure 1. (○) no urate; (●) 0.57 m*M*; (▲) 1.15 mM; and (□) 2.35 m*M*.

These conclusions, inferred from the data in Figure 3 and those of Mason *et al.* (1983) and Johnson *et al.* (1984), assume that the two organic effectors act completely independently and cumulatively, which is not entirely true (S. Morris, pers. comm.). The interaction of Ca^{+2} with the organic effectors is included in the present data for HeO_2 affinity because the actions of urate and lactate were determined in the presence of Ca^{+2}. The interaction of urate and lactate would further diminish their effects, albeit by a small amount.

Intrinsic adaptation of HeO_2 affinity

Estuarine (and also normoxic) blue crabs transferred to high salinity in the laboratory show a rapid decrease in He concentrations. Concomitantly, HeO_2 affinity increases and the levels of subunits 3 and 5 decrease, closely resembling the He in animals freshly caught at a seaside location. Subunit 6 remains unchanged. In seaside (and normoxic) animals transferred to low salinity, the He concentration rapidly increases while the HeO_2 affinity decreases (Mason *et al.*, 1983). The intrinsic change opposes the effects of salinity-induced changes in extrinsic co-factors.

In initial samples freshly taken at the estuarine and seaside localities, the vast majority of animals exhibited the molecular phenotype associated with the comparable acclimation salinity in the laboratory (C. P. Mangum and G. Godette, unpubl. obs.; Rainer *et al.*, 1985). However, subunit 6 was variable in both samples, implicating another environmental or physiological effector unrelated to salinity *per se*. Moreover, when the field study was enlarged, no clinal variation of the three subunits was obvious along a salinity gradient between the two localities (Rainer, 1988); these findings also suggest a confounding variable.

Under the same ionic conditions, the O_2 affinities of blue crab Hcs composed of different combinations of the variable chains indicate that the levels of subunits 3 and 6 both influence oxygen binding; the effects of variation in subunit 5 are not entirely clear (Mangum and Rainer, 1988). Changes in subunit 3 (alone) can fully explain the difference between seaside and estuarine animals. However, changes in subunit 6 (alone), smaller than those observed here, significantly alter HeO_2 affinity by almost 20% at physiological pH. Although there is no difference between an He with low levels of only subunit 3, and one with low levels of both 3 and 5, an He with low levels of 5 alone has not been examined.

The present results suggest that blue crab He is intrinsically adaptable to prolonged hypoxia as well as to salinity. The adaptation may be expedited by an increase in He concentration, which is clear at 25 days, and it is accompanied by changes in the same three subunits already known to be variable. A decrease in concentration of subunits 3 and 6 during hypoxia has the same effect as that of decreasing either alone or in combination; *i.e.*, increasing O_2 affinity (Mangum and Rainer, 1988). The present findings suggest that, while subunits 3 and 5 respond to a change in both salinity and oxygen, subunit 6 responds only to oxygen. The changes in subunits 3 and 5 as a result of hypoxia were much smaller than the salinity-induced changes, but the changes in P_{50} were about the same in the two groups, at physiological pH. The smaller changes in the amounts of subunits 3 and 5 in hypoxia may be due to lower levels at the onset of hypoxia (for comparison see fig. 1 in Mangum and Rainer, 1988). The oxygen-induced change in subunit 6, however, was much larger than observed by Mangum and Rainer (1988). A greater change in subunit 6 may offset a smaller change in subunit 3, and the intrinsic adaptation of HeO_2 affinity to hypoxia may involve the change in subunit composition. Moreover, we suggest that the variation of subunit 6 in nature is related to hypoxia, which does not vary along a salinity gradient in a simple fashion.

Finally, the increase observed here in He concentration occurs widely in hypoxic crustaceans. In different species its magnitude may be much greater, it may occur in a far shorter period, and it may occur at a much lower temperature (Hagerman and Oksama, 1985; Hagerman and Uglow, 1985; Hagerman, 1986). It will be interesting to learn whether intrinsic molecular adaptability is similarly widespread.

Acknowledgments

Supported by NSF Grant DCB 84-14856 (Regulatory Biology) to CPM. This work is a result of research sponsored in part by NOAA Office of Sea Grant, U. S. Department of Commerce, under Grant No. NA85AA-D-SG016 to the Virginia Graduate Marine Science Consortium and Virginia Sea Grant College Program. The U. S. Government is authorized to produce and distribute reprints for governmental purposes notwithstanding any copyright notation that may appear hereon.

Literature Cited

Axelrad, D. M., K. A. Moore, and M. E. Bender. 1976. Nitrogen, phosphorous and carbon flux in Chesapeake Bay marshes. *Bull.* **79,** Water Resources Research Center, Virginia Polytechnic Institute, Blacksburg, VA. 182 pp.

Booth, C. E., B. R. McMahon, and A. W. Pinder. 1982. Oxygen uptake and the potentiating effects of increased hemolymph lactate on oxygen transport during exercise in the blue crab *Callinectes sapidus*. *J. Comp. Physiol.* **148:** 111–121.

Burnett, L. E. 1979. The effects of environmental oxygen levels on

the respiratory function of hemocyanin in the spider crab, *Libinia emarginata* and the ghost crab, *Ocypode quadrata*. *J. Exp. Zool.* **210:** 289–299.

Burnett, L. E., and K. Johansen. 1981. The role of branchial ventilation in hemolymph acid-base changes in the shore crab *Carcinus maenas* during hypoxia. *J. Comp. Physiol.* **141:** 489–494.

Butler, P. J., E. W. Taylor, and B. R. McMahon. 1978. Respiratory and circulatory changes in the lobster (*Homarus vulgaris*) during long term exposure to moderate hypoxia. *J. Exp. Biol* **73:** 131–146.

Carpenter, J. H., and D. G. Cargo. 1957. Oxygen requirement and mortality of the blue crab in the Chesapeake Bay. *Ches. Bay Inst. Tech. Rept* **13:** 1–22.

Dejours, P., and J. Armand. 1980. Hemolymph acid-base balance of the crayfish *Astacus leptodactylus* as a function of the oxygenation and the acid-base balance of the ambient water. *Resp. Physiol* **41:** 1–11.

Garlo, E. V. 1979. Impact of hypoxic conditions in the vicinity of Little Egg Inlet, New Jersey in summer 1976. *Estuar. Coast. Mar. Sci.* **8:** 421–432.

Graham, R. A., C. P. Mangum, R. C. Terwilliger, and N. B. Terwilliger. 1983. The effect of organic acids on oxygen binding of hemocyanin from the crab *Cancer magister*. *Comp. Biochem. Physiol.* **74A:** 45–50.

Hagerman, L. 1986. Haemocyanin concentration in the shrimp *Crangon crangon* (L.) after exposure to moderate hypoxia. *Comp. Biochem. Physiol.* **85A:** 721–724.

Hagerman, L. and M. Oksama. 1985. Haemocyanin concentration, carrying capacity and haemolymph pH under hypoxia in *Mesidothea entomon* (L.) (Isopoda, Crustacea). *Ophelia* **24:** 47–52.

Hagerman, L., and R. F. Uglow. 1985. Effects of hypoxia on the respiratory and circulatory regulation in *Nephrops norvegicus*. *Mar. Biol.* **87:** 273–278.

Hames, B. D., and D. Rickwood. 1981. *Gel Electrophoresis of Proteins*. IRL Press, Oxford. 290 pp.

Harper, D. E., L. D. McKinney, R. R. Salzer, and R. J. Case. 1981. The occurrence of hypoxic bottom water off the upper Texas coast and its effect on the benthic biota. *Contr. Mar. Sci.* **24:** 53–79.

Johnson, B. A., C. Bonaventura, and J. Bonaventura. 1984. Allosteric modulation of *Callinectes sapidus* hemocyanin by binding of L-lactate. *Biochemistry* **23:** 872–878.

Kemp, W. M., and W. R. Boynton. 1980. Influence of biological and physical processes on dissolved oxygen dynamics in an estuarine system: implications for measurement of community metabolism. *Estuar. Coast. Mar. Sci.* **11:** 407–431.

Lallier, Fl., F. Boitel, and J-P. Truchot. 1987. The effect of ambient oxygen and temperature on haemolymph L-lactate and urate concentrations in the shore crab *Carcinus maenas*. *Comp. Biochem. Physiol.* **86A:** 255–260.

Loesch, H. 1960. Sporadic mass shoreward migrations of demersal fish and crustaceans in Mobile Bay, Alabama. *Ecology* **41:** 292–298.

Lowery, T. A., and L. G. Tate. 1986. Effect of hypoxia on hemolymph lactate and behavior of the blue crab *Callinectes sapidus* Rathbun in the laboratory and field. *Comp. Biochem. Physiol.* **85A:** 689–692.

Mackiernan, G. B. 1987. Dissolved oxygen in the Chesapeake Bay: processes and effects. Maryland Sea Grant Publ. No. UM-SG-TS-87-03. 177 pp.

Malone, T. C., W. M. Kemp, H. W. Ducklow, W. R. Boynton, J. H. Tuttle, and R. B. Jonas. 1986. Lateral variation in the production and fate of phytoplankton in a partially stratified estuary. *Mar. Ecol. Prog. Ser.* **32:** 149–160.

Mangum, C. P. 1980. Respiratory function of the hemocyanins. *Am. Zool.* **20:** 19–38.

Mangum, C. P. 1983. On the distribution of lactate sensitivity among the hemocyanins. *Mar. Biol. Lettr* **4:** 139–149.

Mangum, C. P. 1985. Oxygen transport in the invertebrates. *Am. J. Physiol.* **248:** R505–514.

Mangum, C. P., and G. Lykkehoe. 1979. The influence of inorganic ions and pH on the oxygenation properties of the blood in the gastropod mollusc *Busycon canaliculatum*. *J. Exp. Zool.* **207:** 417–430.

Mangum, C. P., B. R. McMahon, P. L. deFur, and M. I. Wheatly. 1985. Gas exchange, acid-base balance and the oxygen supply to the tissues during a molt of the blue crab *Callinectes sapidus*. *J Crust. Biol.* **5:** 188–206.

Mangum, C. P., and J. S. Rainer. 1988. The relationship between subunit composition and oxygen binding of blue crab hemocyanin. *Biol. Bull.* **174:** 77–82.

Mangum, C. P., and A. L. Weiland. 1975. The quantitative function of hemocyanin in respiration of the blue crab *Callinectes sapidus*. *J. Exp. Zool.* **193:** 257–264.

Mason, R. P., C. P. Mangum, and G. Godette. 1983. The influence of inorganic ions and acclimation salinity of hemocyanin-oxygen binding in the blue crab *Callinectes sapidus*. *Biol. Bull.* **164:** 104–123.

Mauro, N. A., and C. P. Mangum. 1982. The role of the blood in the temperature dependence of oxidative metabolism in decapod crustaceans. I. Intraspecific responses to seasonal differences in temperature. *J. Exp. Zool.* **219:** 179–188.

May, E. 1973. Extensive oxygen depletion in Mobile Bay, Alabama. *Limnol. Oceanogr.* **18:** 353–366.

McDonald, D. G., B. R. McMahon, and C. M. Wood. 1977. Patterns of heart and scaphognathite activity in the crab, *Cancer magister*. *J. Exp. Zool.* **202:** 33–44.

McMahon, B. R., W. W. Burggren, and J. L. Wilkens. 1974. Respiratory responses to long term hypoxic stress in the crayfish *Orconectes virilis*. *J. Exp. Biol.* **60:** 195–206.

McMahon, B. R., P. J. Butler, and E. W. Taylor. 1978. Acid-base changes during recovery from disturbance and during long term hypoxic exposure in the lobster *Homarus vulgaris*. *J. Exp. Zool.* **205:** 361–370.

Morris, S. 1988. Effects of freezing on the function and association state of crustacean haemocyanins. *J. Exp. Zool.* **138:** 535–540.

Morris, S., C. R. Bridges, and M. K. Grieshaber. 1985. A new role for uric acid: modulator of haemocyanin oxygen affinity in crustaceans. *J. Exp. Zool.* **235:** 135–139.

Morris, S., C. R. Bridges, and M. K. Grieshaber. 1986. The potentiating effect of purine bases and some of their derivatives on the oxygen affinity of haemocyanin from the crayfish *Austropotamobius pallipes*. *J. Comp. Physiol.* **156:** 431–440.

Nickerson, K. W., and K. E. Van Holde. 1971. A comparison of molluscan and arthropod hemocyanin. I. Circular dichroism and absorption spectra. *Comp. Biochem. Physiol.* **39B:** 855–872.

Officer, C. B., R. B. Biggs, J. L. Taft, L. E. Cronin, M. A. Tyler, and W. R. Boynton. 1984. Chesapeake Bay anoxia: origin, development and significance. *Science* **223:** 22–27.

Pease, A. L., P. L. deFur, and C. Chase. 1986. Physiological compensation to long term hypoxia in the blue crab, *Callinectes sapidus*. *Am. Zool.* **26:** 122A.

Pease, A. L., and P. L. deFur. 1987. Effect of long term hypoxia on respiratory and circulatory function of blue crabs. *Callinectes sapidus*. *Am. Zool.* **27:** 109A.

Rainer, J. S., C. P. Mangum, and G. Godette. 1985. Subunit heterogeneity of the blue crab (*Callinectes sapidus*) hemocyanin along a salinity gradient. *Am. Zool.* **25:** 47A.

Rainer, J. S. 1988. The large-scale distribution of the heterogeneous hemocyanin subunits of *Callinectes sapidus* (Rathbun) along a salinity gradient. *Am Zool* **28:** 47A.

Rutledge, P. S. 1981. Effects of temperature acclimation on crayfish hemocyanin oxygen binding. *Am. J. Physiol.* **240:** R93–R98.

Seliger, H. H., J. A. Boggs, and W. H. Biggley. 1985. Catastrophic anoxia in the Chesapeake Bay in 1984. *Science* **228:** 70–73.

Taft, J. L., W. R. Taylor, E. D. Hartwig, and E. D. Loftus. 1980. Seasonal oxygen depletion in Chesapeake Bay. *Estuaries* **3:** 242–247.

Truchot, J-P. 1975. Changements de l'etat acid-base du sang en fonction de l'oxygenation de l'eau chez le crabe, *Carcinus maenas* (L.). *J Physiol* **70:** 583–592.

Truchot, J-P. 1980. Lactate increases the oxygen affinity of crab hemocyanin. *J Exp Zool* **214:** 205–208.

Turner, R. E., and R. L. Allen. 1982. Bottom water oxygen concentration in the Mississippi River Delta Bight. *Contr. Mar. Sci.* **25:** 161–172.

Webb, K. L., and C. F. D'Elia. 1980. Nutrient and oxygen redistribution during a spring neap tidal cycle in a temperate estuary. *Science* **207:** 983–985.

Weiland, A. L., and C. P. Mangum. 1975. The influence of environmental salinity on hemocyanin function in the blue crab, *Callinectes sapidus*. *J Exp Zool.* **193:** 265–274.

Wilkes, P. R. H., and B. R. McMahon. 1982a. Effect of maintained hypoxic exposure on the crayfish *Orconectes rusticus*. I. Ventilatory, acid-base and cardiovascular adjustments. *J Exp. Biol.* **98:** 119–137.

Wilkes, P. R. H., and B. R. McMahon. 1982b. Effect of maintained hypoxic exposure on the crayfish *Orconectes rusticus*. II. Modulation of haemocyanin oxygen affinity. *J. Exp. Biol.* **98:** 139–149.

Reference: *Biol. Bull.* **178:** 55–64. (February, 1990)

The Horseshoe Crab *Tachypleus tridentatus* has Two Kinds of Hemocytes: Granulocytes and Plasmatocytes

PER PLOUG JAKOBSEN AND PETER SUHR-JESSEN

Department of Anatomy & Cytology, University of Odense, Campusvej 55, 5230 Odense M, Denmark

Abstract. For the first time, the fine structure of the hemocytes from the horseshoe crab *Tachypleus tridentatus* is investigated by transmission electron microscopy and light microscopy serial sectioning. Two morphologically distinct, ellipsoidal, and mononucleate hemocytes—granulocytes (amebocytes) and plasmatocytes—are revealed. Granulocytes constitute about 97% of the hemocytes. They have a marginal band of microtubules, a heterochromatic nucleus, distended but poorly developed RER, few free ribosomes, few mitochondria, and many large secretory granules. The majority of these granules have a uniform content and are mature. Structured granules located in the proximity of Golgi complexes may be immature transitional stages leading to the mature uniform granules. Upon stimulation with endotoxin from gram negative bacteria, the mature granules become transitory structured before exocytosis. In contrast, the immature granules are not exocytosed. Plasmatocytes constitute about 3% of the hemocytes. They differ from granulocytes by having an euchromatic nucleus, a well-developed RER of flattened or tubular cisternae, many free ribosomes, many mitochondria, but only few, if any, large secretory granules. Apparently, plasmatocytes are not affected by endotoxin. The relationship and possible functions of granulocytes and plasmatocytes are discussed and compared with those of the horseshoe crab, *Limulus polyphemus*.

Introduction

Horseshoe crabs are "living fossils," which have undergone little morphological evolution during the last 360 million years; they can be traced back more than 500 million years (Sekiguchi and Sugita, 1980; Shishikura *et al.*, 1982; Mikkelsen, 1988). If this stability is reflected in their physiology, studies of their immune defense system may shed light on when and how the different parts of it evolved in horseshoe crabs and possibly also in higher and more recent phyla.

Inoculation of gram negative bacteria or their endotoxins into the hemolymph of horseshoe crabs cause fatal intravascular coagulation (Bang, 1956). This involves exocytosis of the large secretory granules from the hemocytes. These granules contain coagulogen and all other proteins necessary for the coagulation (Levin and Bang, 1964; Ornberg and Reese, 1981; Iwanaga *et al.*, 1986; Suhr-Jessen *et al.*, 1989). Hemocyte (amebocyte) lysates can be made from all four extant species of horseshoe crabs, and are now extensively used to detect minute quantities of endotoxin (Shishikura *et al.*, 1983; Watson *et al.*, 1987).

The horseshoe crab best characterized is *Limulus polyphemus*. Until recently, only one hemocyte, the granulocyte, had been identified in this species (Dumont *et al.*, 1966; Levin and Bang, 1968; Copeland and Levin, 1985; Tablin and Levin, 1988). However, a second hemocyte, the plasmatocyte, has been identified independently by light microscopical observations of live cells, by light microscopical serial sectioning of fixed cells, and by transmission electron microscopy alone and combined with immuno-gold labeling (Suhr-Jessen *et al.*, 1989). In addition, cyanocytes and cyanoblasts have been reported to be present in the sinusoids around the compound eyes (Fahrenbach, 1970). Early light microscopical studies suggested that *Tachypleus tridentatus* had two kinds of granulocytes (Shishikura *et al.*, 1977; Shishikura and Sekiguchi, 1979).

The aim of the present study is to characterize the fine structure of *T. tridentatus* hemocytes—the cellular part of the immune defense system—in the pres-

Received 14 June 1989; accepted 28 November 1989.

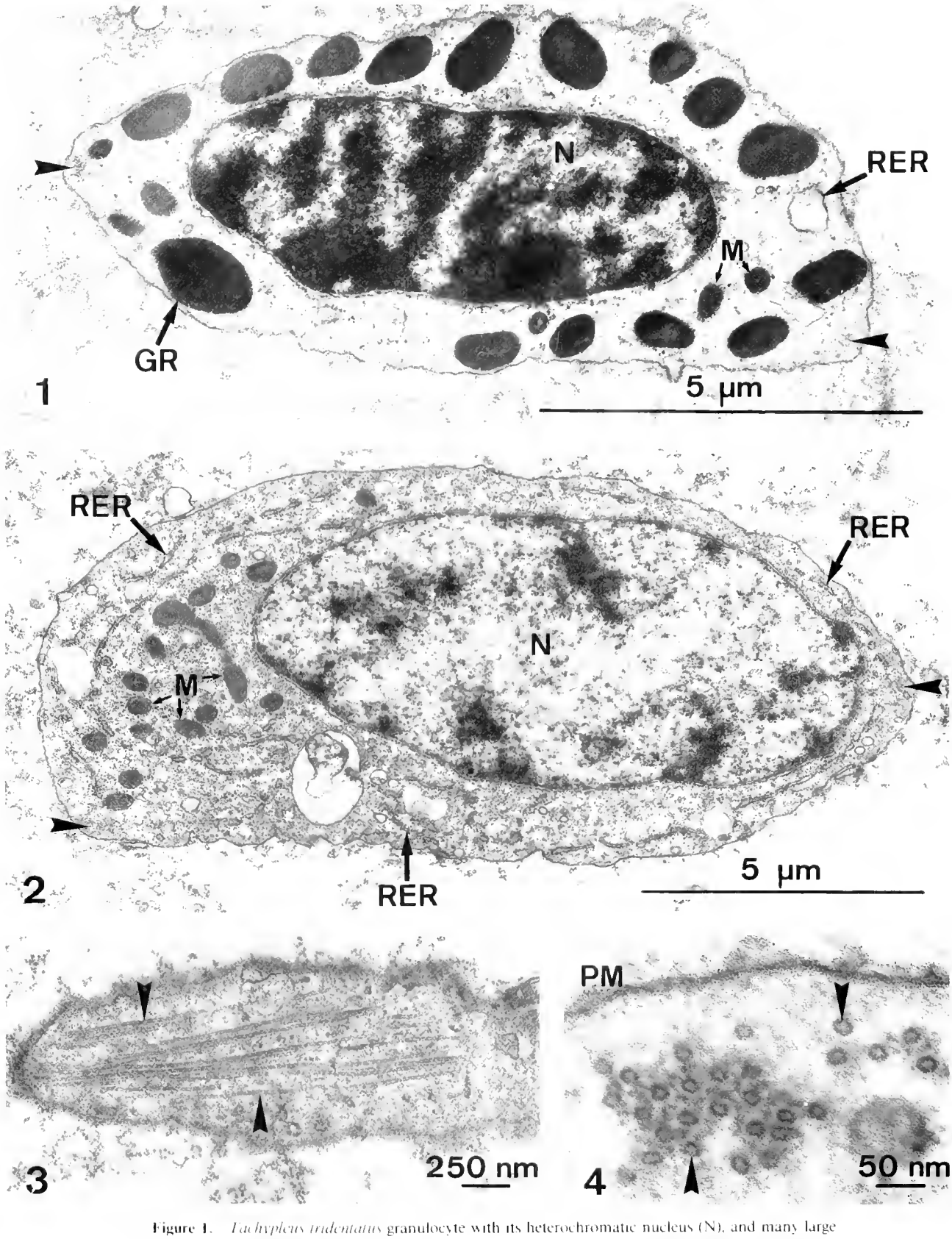

Figure 1. *Tachypleus tridentatus* granulocyte with its heterochromatic nucleus (N), and many large secretory granules (GR). Mitochondria (M). Rough endoplasmic reticulum (RER). Marginal band (arrowheads).

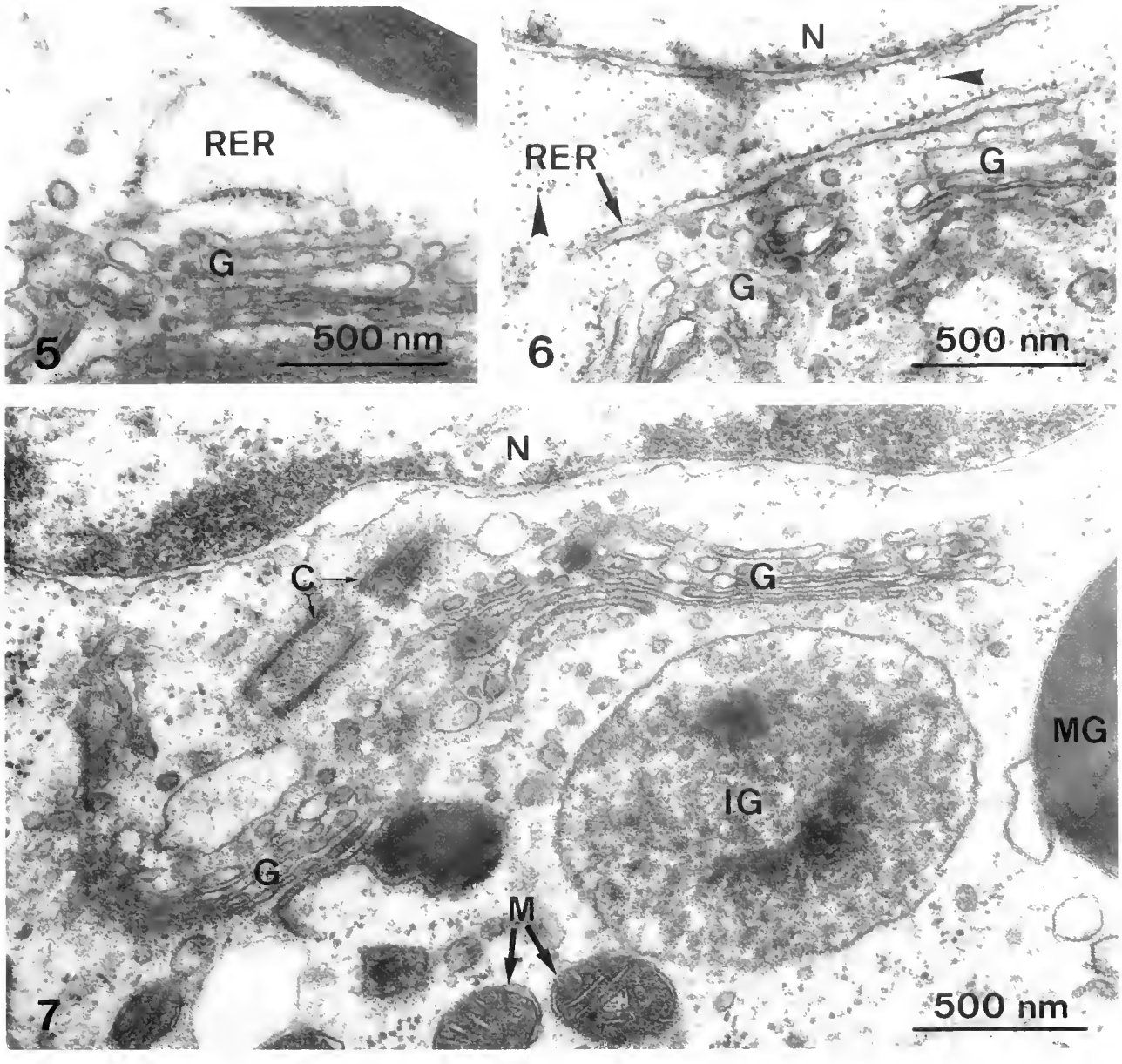

Figure 5. The distended rough endoplasmic reticulum (RER) from a *Tachypleus tridentatus* granulocyte. Golgi complex (G).

Figure 6. The flattened or tubular RER from a *T. tridentatus* plasmatocyte. Many free ribosomes are present (arrowheads). Golgi complex (G); nucleus (N).

Figure 7. *T. tridentatus* granulocyte with a structured (immature) large granule (IG) located in close proximity to a Golgi complex (G). Centrioles (C); mitochondria (M); uniform (mature) granule (MG); nucleus (N).

ence and absence of endotoxin. We show that the general circulation of *T. tridentatus* contains plasmatocytes and a single class of granulocytes. Furthermore, a temporal relationship is described for the formation to final secretion of the large secretory granules in the granulocytes.

Figure 2. *T. tridentatus* plasmatocyte with its euchromatic nucleus (N), well-developed RER, and many mitochondria (M). Marginal band (arrowheads).

Figures 3, 4. Longitudinal and transverse sections of marginal bands of microtubules (arrowheads) in *T. tridentatus* hemocytes. Plasma membrane (PM).

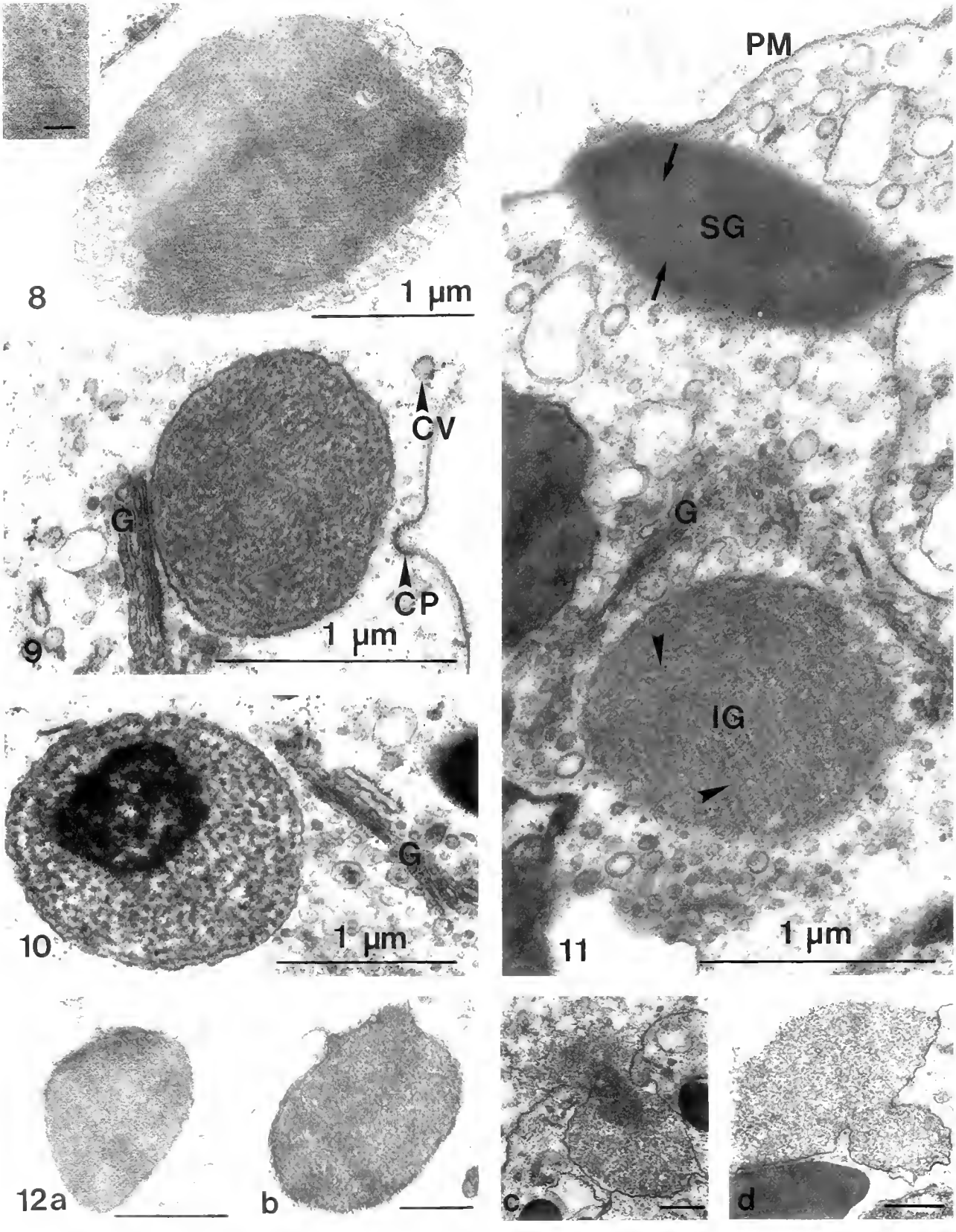

Figures 8–10. Differently structured immature large granules from *Tachypleus tridentatus* granulocytes. Insert: close-up of the about 17-nm tubular structures in transverse and longitudinal section (bar equals 100 nm). Apparently, a coated pit (CP) and a coated vesicle (CV) are present. Golgi complexes (G).

Materials and Methods

Six adult *T. tridentatus* females (males were not available) (prosomal width: 30–33 cm) were collected in the Tonkin Gulf, China, and kept in seawater (3.0% NaCl) at 15°C at The Danish Aquaculture Institute, Hørsholm, for up to nine months. Throughout this period, hemolymph samplings from all animals gave similar results. Hemolymph was drawn by cardiac puncture at the ethanol-cleaned prosoma-opistosoma junction. Access to the heart was made by a 19-gauge needle alone or combined with a 5-ml syringe containing fixative or, as part of a total bleed of the animal, through a large cut by a sterile (LPS-free) scalpel. The three methods gave similar results. Hemolymph was floating directly into 5% glutaraldehyde in 0.1 *M* sodium cacodylate buffer, pH 7.4, to give a final glutaraldehyde percentage of no less than 4. Samples were also incubated for 5 to 300 s with 10^{-4}–10^{-13} g *E. coli* endotoxin (Sigma no. L 3755)/ml hemolymph prior to fixation. The fixed samples were processed as described (Willumsen *et al.*, 1987). Transmission electron microscopy sections (about 50 nm) were mounted on pioloform F-50 coated Cu- or Ni-grids, contrasted with lead citrate, examined in a Jeol JEM-100CX electron microscope at 80 kV, and photographed using Agfa-Gevaert 23D56 film. Light microscopy serial sections (about 1.0 μm) were stained with toluidin blue, examined in a Zeiss microscope (numerical aparture: 1.30) at 400× using immersion oil, and photographed using Kodak panatomic X film. To eliminate inaccuracies due to minor differences in the thickness of the sections, a plasmatocyte was always compared with a nearby granulocyte starting and ending at almost the same section numbers. In the two cells, the number of cuts through mitochondria rather than the actual number of mitochondria was determined. Assuming that the mitochondria are randomly oriented and approximately of the same size in the two cells, any consistent deviation from 1 in the PL/GR ratio reflects differences in numbers of mitochondria.

Results

General morphology of the hemocytes

T. tridentatus hemocytes are spheroid, and about 15–20 μm at their longest axis (Figs. 1, 2, 15). A marginal band of microtubules run parallel to the longitudinal axis of the cells at least one microtubule diameter beneath the plasma membrane (Figs. 1–4). The almost parallel arrangement of the microtubules, combined with the electron-dense material seen between them, suggest that they are connected (Figs. 3, 4). Each hemocyte has a single, non-lobated nucleus containing one or a few nucleoli. The cells also contain rough endoplasmic reticulum (RER), free ribosomes, mitochondria with lamellar cristae, and Golgi complexes with 3–6 layers of cisternae—the cis-ones being more distended than the trans-ones (Figs. 1–2, 5–7). The paired centrioles form an obtuse angle to each other (Fig. 7). No sign of mitosis was seen in any of the examined hemocytes. Digestive vacuoles and apparently coated pits and coated vesicles are also present (Figs. 9, 14). No cytoplasmic crystals were observed.

Granulocytes

About 97% of the hemocytes are granulocytes. They have a heterochromatic nucleus, a poorly developed but distended RER, few free ribosomes, and few mitochondria (Figs. 1, 5). However, their most prominent feature is the many large secretory granules with diameters around 1–2 μm (see below).

Large secretory granules

The majority of the large secretory granules in granulocytes have a uniform content (Fig. 1). However, one class of granules, with structures ranging from amorphous to highly organized tubules with diameters around 17 nm, are seen in close proximity to Golgi complexes (Figs. 7–10). When hemocytes are stimulated with endotoxin a second class of structured granules containing tubules with diameters around 10 nm become transitorily present (Fig. 11). A reverse relationship seems to exist between the numbers of structured granules of the second class and the uniform granules. After this, exocytosis occurs (Fig. 12). In contrast, structured granules of the first class are usually not exocytosed following stimulation with endotoxin (Figs. 13, 14). Following exocytosis, the granulocytes gain numerous pseudopodia, and the organelles collect in the center of the cell surrounded by microtubules (Figs. 13, 14).

Plasmatocytes

Plasmatocytes constitute about 3% of the hemocytes. This conclusion is reached by examining duplicate sam-

Figure 11. Granulocyte from *T. tridentatus* incubated with 10^{-4} g endotoxin per ml hemolymph for 30 s. A stimulated large secretory granule (SG) is in close connection with the plasma membrane (PM). Its tubular structures (arrows) have a diameter around 10 nm, while 17-nm tubular structures (arrowheads) are present in the immature granule (IG) located in close proximity to a Golgi complex (G).

Figure 12. Successive stages in exocytosis of the large secretory granules from *T. tridentatus* granulocytes. Bar length: 500 nm.

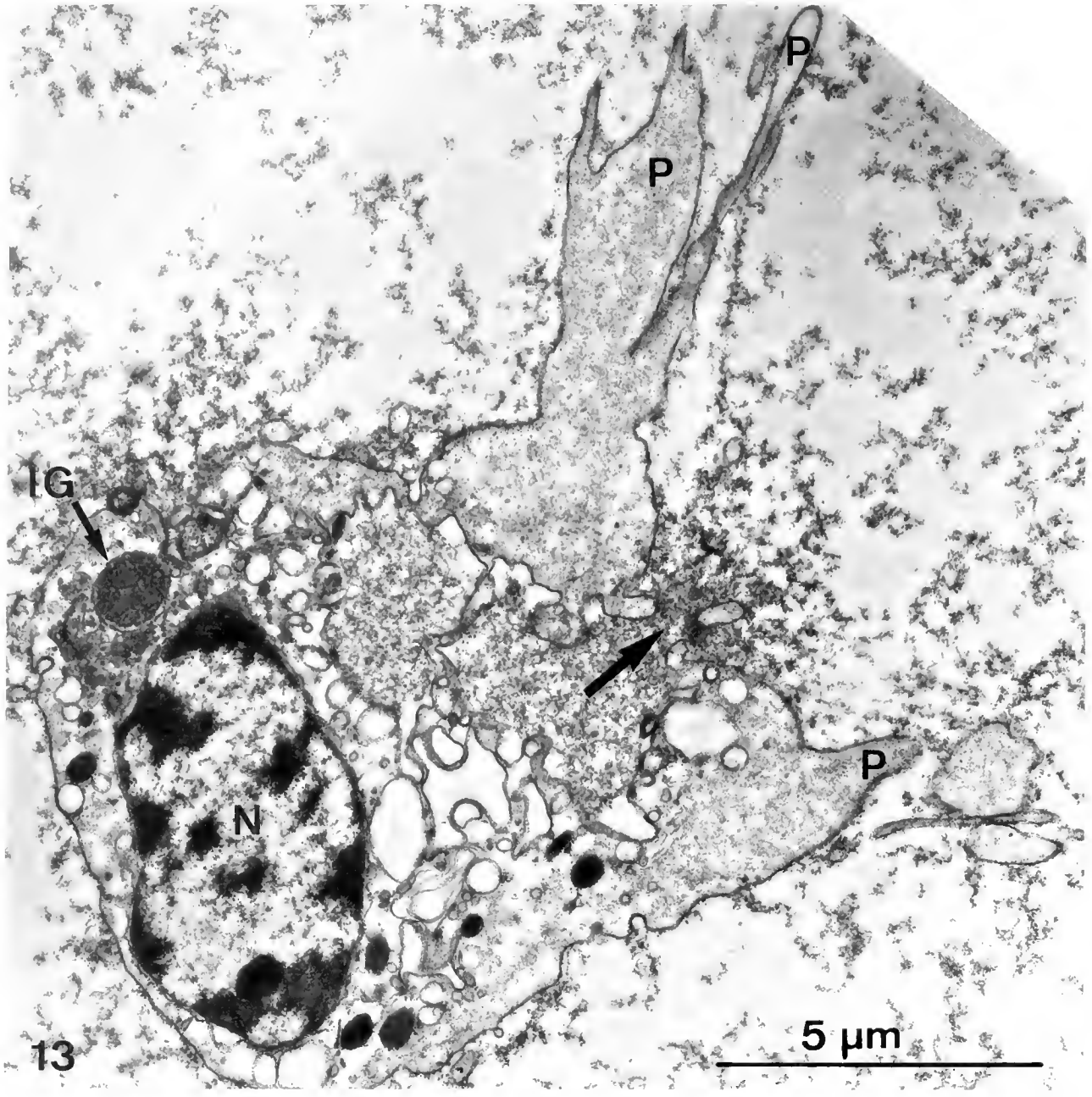

Figure 13. Granulocyte from *Tachypleus tridentatus* incubated with 10^{-4} g endotoxin per ml hemolymph for 300 s. The large secretory granules are exocytosed (arrow), except the immature ones (IG), and pseudopodia (P) are projected. Nucleus (N).

ples from each of six animals. From all samples, at least 10 sections, each containing more than 100 hemocytes, were examined by light microscopy; at least 10 sections were examined by transmission electron microscopy. The plasmatocyte has an euchromatic nucleus, a well-developed system of flattened or tubular cisternae of RER, and many free ribosomes (Figs. 2, 6). Mitochondria are approximately three times as frequent as in granulocytes (Table I). Plasmatocytes contain few, if any, large secretory granules. These observations are confirmed by LM serial sections of 12 different plasmatocytes (Fig. 15): two plasmatocytes contained zero, five contained one, three contained two, and two contained three large granules. Plasmatocytes are not affected by endotoxin stimulation.

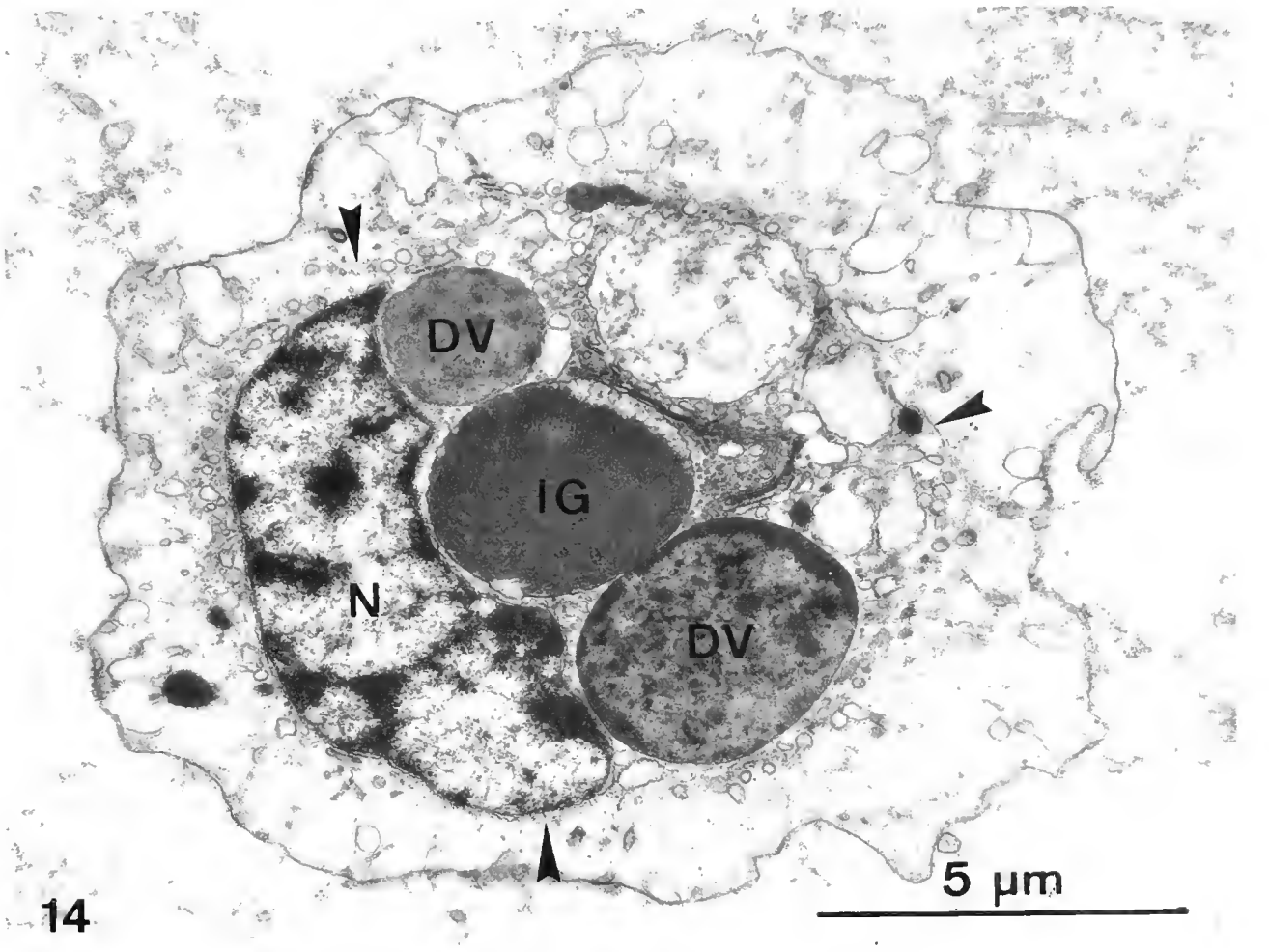

Figure 14. Granulocyte from *Tachypleus tridentatus* incubated with 10^{-4} g endotoxin per ml hemolymph for 300 s. After exocytosis, the remaining organelles collect in the middle of the cell surrounded by microtubules (arrowheads) as observed also in *Limulus polyphemus* (Tablin and Levin, 1988). Digestive vacuoles (DV). Immature granule (IG); nucleus (N).

Discussion

Two major groups of hemocytes

We reveal one granular and one almost agranular type of hemocyte in the general circulation of *T. tridentatus* (Figs. 1, 2, 15). In agreement with the terminology from other arthropods, including other chelicerates, these hemocytes are named granulocytes and plasmatocytes, respectively (Gupta, 1979; Sherman, 1981; Gupta, 1985; Suhr-Jessen *et al.*, 1989). Their main differences are summarized in Table II. The plasmatocyte has not previously been observed in *T. tridentatus*, but it makes up about 3% of the hemocytes in all samples from the six animals studied.

The plasmatocyte is not a cyanoblast or a cyanocyte (Fahrenbach, 1970), because plasmatocytes have the same size, are present in the general circulation of all animals studied at all times, and do not contain cytoplasmic crystals.

The plasmatocyte is not a granulocyte that exocytosed during sampling, because the two cells differ in amounts of hetrochromatin, RER, free ribosomes, and mitochondria (Table II). In other systems, such dramatic changes usually takes hours. Furthermore, the plasmatocyte has the smooth ellipsoidal shape with a marginal band characteristic of the unstimulated granulocyte in contrast to the pseudopodial form following exocytosis (Figs. 1, 13; Dumont *et al.*, 1966; Armstrong, 1980; Armstrong and Rickles, 1982; Armstrong, 1985; Tablin and Levin, 1988). However, it cannot be excluded that plasmatocytes are granulocytes, which have undergone spontaneous exocytosis so early prior to hemolymph sampling that the marginal band of microtubules have reformed. Because the production of gran-

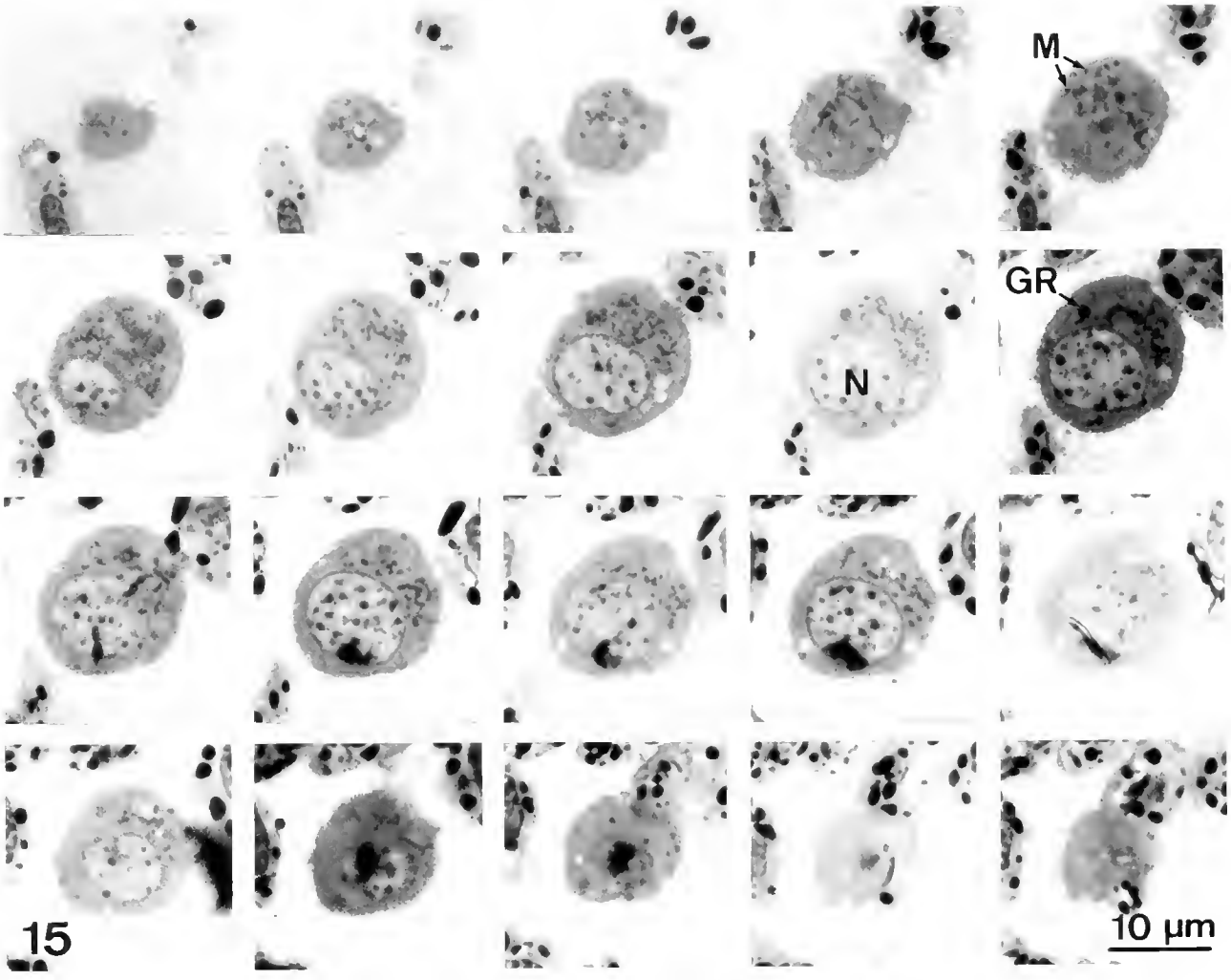

Figure 15. Serial sections of a plasmatocyte from *Tachypleus tridentatus*. The nucleus (N) is uniformly euchromatic; a single large granule (GR) and many mitochondria (M) are present. The neighboring granulocytes contain many large secretory granules, but few mitochondria.

ulocytes is not continuous (Cohen, 1985), this latter interpretation implies either: (1) that approximately 3% of the hemocytes in all *T. tridentatus* examined are constantly recovering from spontaneous exocytosis, and that the transition from plasmatocyte to granulocyte is so fast that intermediate stages are at least one order of magnitude less frequent than plasmatocytes; or (2) that approximately 3% of the hemocytes in each animal recover from a single burst of exocytosis long before the first sampling, and that this recycling is blocked at the plasmatocyte stage. In *L. polyphemus*, the independence of granulocytes and plasmatocytes is further supported by the detection of coagulogen only in granulocytes (Suhr-Jessen *et al.*, 1989).

Large secretory granules

The large structured granules seen in the proximity of Golgi complexes in granulocytes are apparently not affected by endotoxin (Figs. 7–10, 13, 14). This supports the interpretation that this class of structured granules is an immature stage leading to the mature uniform secre-

Table I

A comparison of the abundance of mitochondria in plasmatocytes (PL) and granulocytes (GR) of Tachypleus tridentatus

Serial section	Number of mitochondria in		Ratio PL/GR
	Plasmatocyte	Granulocyte	
#1	154	48	3.25
#2	276	86	3.21
#3	138	51	2.71
Total	568	185	≈3

Each serial section number refers to one plasmatocyte and one granulocyte. Eighteen to 23 serial sections were required to completely section a cell.

Table II

A comparison of the main differences between plasmatocytes and granulocytes in Tachypleus tridentatus

	Plasmatocyte	Granulocyte
Nucleus	Euchromatic	Heterochromatic
RER	Flattened and well developed	Distended but poorly developed
Free ribosomes	Many	Few
Large secretory granules	Few—if any	Many
Mitochondria	Many	Few
Frequency	3%	97%

tory granules, as suggested for *L. polyphemus* (Copeland and Levin, 1985; Suhr-Jessen *et al.*, 1989). Following endotoxin stimulation, the content of the mature uniform granules become transitorily structured before exocytosis (Fig. 11). This resembles the situation in rat mast cells and human platelets (Bloom, 1974; Morgenstern *et al.*, 1987). The different responses to endotoxin suggest that immature and mature secretory granules contain different membrane proteins.

Immune defense

Granulocytes and plasmatocytes from the Asian *T. tridentatus* are cytologically indistinguishable from those in the American *L. polyphemus* (Dumont *et al.*, 1966; Shishikura *et al.*, 1977; Gupta, 1979; Nemhauser *et al.*, 1980; Ornberg and Reese, 1981; Shishikura *et al.*, 1982; Armstrong, 1985; Copeland and Levin, 1985; Tablin and Levin, 1988; Suhr-Jessen *et al.*, 1989). This suggests that the cellular part of their immune defense systems has remained unchanged for more than 140 million years (Shishikura *et al.*, 1982).

Do granulocytes also participate in the endocytic part of the immune defense system, as debated by Armstrong and Levin (1979)? Although digestive vacuoles are present (Fig. 14), we have not observed the formation of large endocytic vacuoles, neither in plasmatocytes nor in granulocytes, but both cells form micropinocytotic (coated) vesicles (Fig. 9). It is tempting to speculate that granulocytes and plasmatocytes may operate together, and with the humoral part of the immune defense system, to recognize and destroy invading microorganisms.

Although the cellular part of the immune defense system in horseshoe crabs has been studied extensively, neither the hemocyte stem cell nor its location, regulation of maturation, differentiation, or proliferation is elucidated (Cohen, 1985). The fate of the granulocytes after exocytosis is also unknown. The gathering of the organelles in the middle of the granulocyte after exocytosis might be the first step in a recovery process (Fig. 14).

The present study describes a hitherto overlooked hemocyte, the plasmatocyte, in the general circulation of *T. tridentatus*. It also extends previous studies of the temporal relationship between maturation and structure of the large secretory granules in granulocytes. Both results prompt several questions pertinent to the molecular biology, structure, and function of hemocytes in horseshoe crabs in particular, and to the evolution and cell biology of the immune defense system in animals in general.

Acknowledgments

We thank Tom Mikkelsen for providing the horseshoe crabs and Ulla Hauschildt for technical assistence with the transmission electron microscopy and light microscopy preparations. Support from Knud Højgaards Foundation (to PPJ) and a student fellowship from the Carlsberg Foundation (to PPJ) is gratefully acknowledged.

Literature Cited

Armstrong, P. B., and J. Levin. 1979. *In vitro* phagocytosis by *Limulus* blood cells. *J. Invert. Pathol.* **34:** 145–151.

Armstrong, P. B. 1980. Adhesion and spreading of *Limulus* blood cells on artificial surfaces. *J. Cell Sci.* **44:** 243–262.

Armstrong, P. B., and F. R. Rickles. 1982. Endotoxin-induced degranulation of the *Limulus* amebocyte. *Exp. Cell Res.* **140:** 15–24.

Armstrong, P. B. 1985. Adhesion and motility of the blood cells of *Limulus*. Pp. 77–124 in *Blood Cells of Marine Invertebrates: Experimental Systems in Cell Biology and Comparative Physiology*, W. D. Cohen, ed. Alan R. Liss, Inc., New York.

Bang, F. B. 1956. A bacterial disease of *Limulus polyphemus*. *Bull. Johns Hopkins Hosp.* **98:** 325–351.

Bloom, G. D. 1974. Structural and biochemical characteristics of mast cells. Pp. 545–599 in *The Inflammatory Process*. Zweifach, B. W., L. Grants and R. T. McCluskey, eds. Academic Press, New York.

Cohen, W. D., ed. 1985. *Blood Cells of Marine Invertebrates. Experimental Systems in Cell Biology and Comparative Physiology*. Alan R. Liss, Inc., New York.

Copeland, D. E., and J. Levin. 1985. The fine structure of the amebocyte in the blood of *Limulus polyphemus*. I. Morphology of the normal cell. *Biol. Bull.* **169:** 449–457.

Dumont, J. N., E. Anderson, and G. Winner. 1966. Some cytologic characteristics of the hemocytes of *Limulus* during clotting. *J. Morphol.* **119:** 181–208.

Fahrenbach, W. H. 1970. The cyanoblast: hemocyanin formation in *Limulus polyphemus*. *J. Cell Biol.* **44:** 445–453.

Gupta, A. P. 1979. Arthropod hemocytes and phylogeny. Pp. 669–735 in *Arthropod Phylogeny*, A. P. Gupta, ed. Van Nostrand Reinhold Company, New York.

Gupta, A. P. 1985. Cellular Elements in the Hemolymph. Pp. 401–451 in *Comprehensive Insect Physiology Biochemistry and Pharmacology*, Vol. 3, G. A. Kerkut and L. I. Gilbert, eds. Pergamon Press, New York.

Iwanaga, S., T. Morita, T. Miyata, T. Nakamura, and J. Aketagawa, 1986. The hemolymph coagulation system in invertebrate animals. *J. Prot. Chem.* **5:** 255–268.

Levin, J., and F. B. Bang. 1964. The role of endotoxin in the extracellular coagulation of *Limulus* blood. *Bull. Johns Hopkins Hosp.* **115:** 265–274.

Levin, J., and F. B. Bang. 1968. Clottable protein in *Limulus*: its localization and kinetics of its coagulation by endotoxin. *Thromb. Diathes. Haemorrh.* **19:** 186–197.

Mikkelsen, T. 1988. *The Secret in the Blue Blood.* Science Press, Beijing, China.

Morgenstern, E., K. Neumann, and H. Patscheke. 1987. The exocytosis of human blood platelets. A fast freezing and freeze-substitution analysis. *Eur. J. Cell Biol.* **43:** 273–282.

Nemhauser, I., R. Ornberg, and W. D. Cohen. 1980. Marginal bands in blood cells of invertebrates. *J. Ultrastruc. Res.* **70:** 308–317.

Ornberg, R. L., and T. S. Reese. 1981. Beginning of exocytosis captured by rapid-freezing of *Limulus* amebocytes. *J. Cell. Biol.* **90:** 40–54.

Sekiguchi, K., and H. Sugita. 1980. Systematics and hybridization in the four living species of horseshoe crabs. *Evolution* **34:** 712–718.

Sherman, R. G. 1981. Chelicerates. Pp. 355–384 in *Invertebrate Blood Cells*, Vol. 2, N. A. Ratcliffe and A. F. Rowley, eds. Academic Press, New York.

Shishikura, F., J. Chiba, and K. Sekiguchi. 1977. Two types of hemocytes in localization of clottable protein in Japanese horseshoe crab, *Tachypleus tridentatus*. *J. Exp. Zool.* **201:** 303–308.

Shishikura, F., and K. Sekiguchi. 1979. Comparative studies on hemocytes and coagulogen of the asian and the american horseshoe crabs. *Prog. Clin. Biol. Res.* **29:** 185–201.

Shishikura, F., S. Nakamura, K. Takahashi, and K. Sekiguchi. 1982. Horseshoe crab phylogeny based on amino acid sequences of the fibrino-peptide-like peptide C. *J. Exp. Zool.* **223:** 89–91.

Shishikura, F., S. Nakamura, K. Takahashi, and K. Sekiguchi. 1983. Coagulogens from four living species of horseshoe crabs (Limulidae): comparison of their biochemical and immunochemical properties. *J. Biochem.* **94:** 1279–1287.

Suhr-Jessen, P., L. Baek, and P. P. Jakobsen. 1989. Microscopical, biochemical and immunological studies of the immune defense system of the horseshoe crab, *Limulus polyphemus*. *Biol. Bull.* **176:** 290–300.

Tablin, F., and J. Levin. 1988. The fine structure of the amebocyte in the blood of *Limulus polyphemus* II. The amebocyte cytoskeleton: a morphological analysis of native, activated, and endotoxin-stimulated amebocytes. *Biol. Bull.* **175:** 417–429.

Watson, S. W., J. Levin, and T. J. Novitsky, eds. 1987. *Detection of Bacterial Endotoxins with the* Limulus *Amebocyte Lysate Test. Prog. Clin. Biol. Res.* **231,** Alan R. Liss, Inc., New York.

Willumsen, N. B. S., F. Siemensma, and P. Suhr-Jessen. 1987. A multinucleate amoeba, *Parachaos zoochlorellae* (Willumsen, 1982) comb. nov., and a proposed division of the genus *Chaos* into the genera *Chaos* and *Parachaos* (Gymnamoebia, amoebidae). *Arch. Protistenkd.* **134:** 303–313.

Reference: *Biol. Bull.* **178:** 65–73. (February, 1990)

A_1 Adenosine Receptor Modulation of Adenylyl Cyclase of a Deep-living Teleost Fish, *Antimora rostrata*

JOSEPH F. SIEBENALLER[1] AND THOMAS F. MURRAY[2]

[1]*Department of Zoology and Physiology, Louisiana State University, Baton Rouge, Louisiana 70803, and* [2]*College of Pharmacy, Oregon State University, Corvallis, Oregon 97331*

Abstract. Low temperatures and high hydrostatic pressures are typical of the deep sea. The effects of these parameters on transmembrane signal transduction were determined through a study of the A_1 adenosine receptor-inhibitory guanine nucleotide binding protein-adenylyl cyclase system in brain membranes of the bathyal teleost fish, *Antimora rostrata* (Moridae). The components of this system were analyzed at 5°C and 1 atm, and the role of the A_1 receptor in the modulation of adenylyl cyclase was determined. The A_1 selective radioligand N^6-[^{3}H]cyclohexyladenosine bound saturably, reversibly, and with high affinity. The K_d of N^6-[^{3}H]cyclohexyladenosine estimated from kinetic measurements was 1.11 n*M;* the K_d determined from equilibrium binding was 4.86 n*M*. [^{32}P]ADP-ribosylation of brain membranes by pertussis toxin labeled substrates with apparent molecular masses of 39,000 to 41,000 Da. Basal adenylyl cyclase activity was inhibited in a concentration-dependent manner by the A_1 adenosine receptor agonist N^6-cyclopentyladenosine (IC_{50} = 5.08 μM). The inhibition of adenylyl cyclase activity was dependent upon GTP. Basal adenylyl cyclase activity was unaffected by 272 atm of pressure. The efficacy of 100 μM N^6-cyclopentyladenosine as an inhibitor of adenylyl cyclase was the same at atmospheric pressure and at 272 atm. The inhibition of adenylyl cyclase by the agonist 5′-N-ethylcarboxamidoadenosine (100 μM) at 272 atm was twice that observed at atmospheric pressure. Although consideration of the effects of low temperature and high hydrostatic pressure on acyl chain order suggest that deep-sea conditions will perturb membrane function, signal transduction by the A_1 receptor system of the bathyal fish *A. rostrata* is not disrupted by deep-sea conditions.

Received 1 September 1989; accepted 30 November 1989.

Abbreviations: ATP, adenosine triphosphate; cAMP, cyclic adenosine monophosphate; [^{3}H]CHA, N^6-[^{3}H]cyclohexyladenosine; CPA, N^6-cyclopentyladenosine; G protein, guanine nucleotide binding protein; GTP, guanosine triphosphate; NAD, nicotinamide adenine dinucleotide, NECA, 5′-N-ethylcarboxamidoadenosine; R-PIA, N^6-phenylisopropyladenosine, R(−) isomer; S-PIA, N^6-phenylisopropyladenosine, S(+) isomer.

Introduction

The low temperatures and high hydrostatic pressures of the deep ocean may disrupt the biochemical and physiological functions of organisms colonizing this habitat (Siebenaller and Somero, 1978, 1989). Membrane-associated systems are likely to be particularly sensitive because of the ordering effects of these environmental variables on the organization of acyl chains of lipids (Chong and Cossins, 1983; Hochachka and Somero, 1984). Comparisons of homologous cytoplasmic proteins from deep- and shallow-living teleost fishes have established the importance of adaptation to deep-sea temperatures and pressures (Siebenaller and Somero, 1989). Studies of membranes and associated systems in deep-sea organisms indicate that these systems also adapt (*e.g.*, Cossins and Macdonald, 1984, 1986; DeLong and Yayanos, 1985, 1987; Gibbs and Somero, 1989).

To further understand the effects of deep-sea conditions, and to identify potential adaptations of transmembrane signal transduction, we studied the A_1 adenosine receptor and its associated effector elements in brain tissue of a deep-living cold-adapted marine teleost fish, *Antimora rostrata*. The objectives of this study were: (1) to determine whether the A_1 receptor of a typical deep-sea species is coupled to adenylyl cyclase, and (2) to ascertain whether this coupling is functional under the conditions of low temperatures (0–6°C) and high hydrostatic pressures (85–250 atm) experienced by *A. rostrata*. To this end, we undertook a molecular dissection of this

signal transduction system, characterized ligand binding to the A_1 receptor, identified the associated GTP-binding proteins, and determined basal adenylyl cyclase activity and the role of A_1 receptor agonists and GTP-binding proteins in modulation of cAMP accumulation.

A. rostrata is a benthopelagic morid commonly found in the Atlantic and South Pacific Oceans at bathyal depths of 850 to 2500 m (Iwamoto, 1975; Wenner and Musick, 1977). [Pressure increases 1 atm (=101.3 kPa) for every 10 m of depth in the ocean.] *A. rostrata* is replaced by the congener *A. microlepis* in the North Pacific (Small, 1981). Many adaptations to hydrostatic pressure and low temperature have been documented for these species (*e.g.*, Hochachka, 1975; Siebenaller and Somero, 1979; Somero and Siebenaller, 1979; Cossins and Macdonald, 1984, 1986; Avrova, 1984; Yancey and Siebenaller, 1987; Hennessey and Siebenaller, 1987; Gibbs and Somero, 1989).

A_1 adenosine receptor modulation of adenylyl cyclase was selected for two reasons as a model with which to examine pressure and temperature effects on transmembrane signal transduction. First, our previous studies had documented the widespread distribution of this receptor among the classes of chordates, including deep-occurring teleosts (Siebenaller and Murray, 1986, 1988), and we had also identified potentially adaptive differences in ligand binding among species (Murray and Siebenaller, 1987; Siebenaller and Murray, 1988). Agonist occupation of the A_1 adenosine receptor inhibits cAMP accumulation in mammalian central nervous tissue preparations (reviews by Wolff *et al.*, 1981; Londos *et al.*, 1983; Snyder, 1985; Williams, 1987). The A_1 adenosine receptor is coupled to adenylyl cyclase [ATP pyrophosphate-lyase (cyclizing); EC 4.6.1.1] by an inhibitory guanine nucleotide binding protein (G_i protein). Agonist occupation of the other subclass of adenosine receptor coupled to adenylyl cyclase, the A_2 receptor, stimulates adenylyl cyclase activity. These receptors are further distinguished on the basis of the rank order potencies of adenosine analogs (Daly, 1983a, b; Stone, 1985; Williams, 1987).

At a measurement temperature of 22°C, the binding affinities, specificities, and pharmacological profiles of the A_1 adenosine receptors in teleost fishes are similar to those of mammals (Siebenaller and Murray, 1986; Murray and Siebenaller, 1987). The binding of agonists to the high affinity state of mammalian A_1 receptors is disrupted by the low temperatures typical of body temperatures of many cold-adapted fishes (*e.g.*, Bruns *et al.*, 1980; Trost and Schwabe, 1981; Murphy and Snyder, 1982; Lohse *et al.*, 1984; Siebenaller and Murray, 1988). However, agonist recognition and binding properties of the A_1 adenosine receptors are retained in evolutionary adaptation to different body temperatures. For instance, for eight vertebrate species with body temperatures of 1–40°C, K_d values for the agonist N^6-[^{3}H]cyclohexyladenosine ([^{3}H]CHA) measured at 5°C varied 30-fold; however, the binding affinities vary only four-fold when compared at temperatures similar to the species' body temperatures (Siebenaller and Murray, 1988).

Materials and Methods

Specimens

Demersal adult *Antimora rostrata* (Moridae) were collected by otter trawl at their depths of typical abundance (850–2500 m) off the coast of Newfoundland, Canada, on a cruise of the R/V *Gyre* in May 1986. Brain tissue was dissected, frozen in liquid nitrogen at sea, and transported to the laboratory where tissues were maintained at −80°C until used. For the [^{32}P]ADP-ribosylation experiments described below, brain tissue from the macrourids, *Macrourus berglax*, *Coryphaenoides rupestris*, and *C. armatus*, taken off the coast of Newfoundland, the scorpaenids, *Sebastolobus alascanus* and *S. altivelis*, taken on a cruise of the R/V *Wecoma* off the coast of Oregon, and the salmonid, *Oncorhynchus mykiss* (*Salmo gairdneri*), raised at the Food Toxicology and Nutrition Laboratory of Oregon State University, were also used. The macrourid species were chosen because they represent a primarily deep-sea family. The *Sebastolobus* species have been employed in a variety of pressure adaptation studies (Siebenaller and Somero, 1989), and *O. mykiss* is a pelagic freshwater species.

Reagents

[Adenylate-^{32}P]-nicotinamide adenine dinucleotide ([^{32}P]NAD, 31.31 Ci/mmol), [^{3}H]CHA (34.4 Ci/mmol), [α-^{32}P]ATP (800 Ci/mmol) and [^{3}H]cAMP (30.5 Ci/mol) were from DuPont NEN (Wilmington, Delaware). The R- and S-diastereomers of N^6-phenylisopropyladenosine (PIA), 5′-N-ethylcarboxamidoadenosine (NECA), and papaverine were obtained from Research Biochemicals, Inc. (Wayland, Massachusetts). Pertussis toxin was from List Biological Laboratories (Campbell, California). Electrophoresis reagents and molecular weight standards were from Bio-Rad (Richmond, California). Adenosine deaminase (Sigma, Type VI), N^6-cyclopentyladenosine (CPA), 2-chloroadenosine, and all other chemicals used were from Sigma Chemical Co. (St. Louis, Missouri). Water was processed through a four-bowl Milli-Q purification system (Millipore, Bedford, Massachusetts).

Preparation of brain membranes

Antimora rostrata brain membranes for assays of ligand binding were prepared following the procedures described by Murray and Siebenaller (1987).

For adenylyl cyclase assays, brain tissue was disrupted with a Dounce (pestle A) in 100 volumes of 10 m*M* HEPES, pH 7.6 at 5°C, and centrifuged at 27,000 × *g* (0–4°C) for 10 min. The pellet was resuspended in buffer, centrifuged at 27,000 × *g* for 10 min, resuspended in buffer, and 7.5 units/ml of adenosine deaminase were added. The homogenate was incubated at 18°C for 30 min, chilled on ice, centrifuged at 27,000 × *g*, and the pellet resuspended in buffer and 7.5 units/ml adenosine deaminase. Fifty microliters of this homogenate were used in the adenylyl cyclase assays.

For ADP-ribosylation experiments, membranes were homogenized with a Dounce (pestle A) in 40 volumes of 50 m*M* Tris-HCl, pH 7.6 at 5°C. The homogenate was centrifuged at 27,000 × *g* for 10 min. The pellet was resuspended in 40 volumes of Tris-HCl buffer. Fifty microliters of this were used for the ribosylation experiments.

Protein was determined by the method of Lowry *et al.* (1951) following solubilization of the samples in 0.5 *M* NaOH. Bovine serum albumin (Sigma Chemical Co.) was used as the standard.

Time course of agonist association and dissociation

Aliquots of brain membranes were incubated with 2.85 n*M* [^{3}H]CHA in 50 m*M* Tris-HCl, pH 7.6 at the incubation temperature of 5°C. Nonspecific binding was determined simultaneously in the presence of 60 μM R-PIA. For the dissociation experiments, samples were first incubated at 5°C with 2.85 n*M* [^{3}H]CHA for 240 min to allow binding to reach equilibrium. R-PIA (60 μM) was added in a negligible volume (1% of the total) to initiate the dissociation reaction. Samples were started at timed intervals, and all incubations were terminated simultaneously by filtration over No. 32 glass fiber filter strips (Schleicher and Schuell Inc., Keene, New Hampshire) using a cell harvester (Brandel Instruments, Gaithersburg, Maryland). The data were analyzed as described below.

Equilibrium binding assay for membrane bound A_1 adenosine receptors

The rapid filtration assay described by Bruns *et al.* (1980) and Murray and Cheney (1982) was used with minor modifications to determine the specific binding of the A_1-selective agonist [^{3}H]CHA to *A. rostrata* brain membranes. Assays were conducted in Tris-HCl, pH 7.6, at the incubation temperature of 5°C. The procedures described in Siebenaller and Murray (1988) were followed. Brain membrane protein (0.4–1.2 mg) was added to each assay tube.

[^{32}P]ADP-ribosylation

Pertussis toxin-catalyzed [^{32}P]ADP-ribosylation of GTP binding proteins followed the procedures described in Ribeiro-Neto *et al.* (1985) and Greenberg *et al.* (1987). The 100-μl incubation mixture contained 100 m*M* Tris-HCl, pH 7.5, at the incubation temperature of 5°C, 25 m*M* dithiothreitol, 2 m*M* ATP, 0.1 m*M* GTP, 5 μCi [^{32}P]-NAD, 1.5 μg soybean trypsin inhibitor, 15 μg bacitracin, 2 μg pertussis toxin, and 37–92 μg membrane protein. After 3 h, the reaction was stopped by adding 50 μl of stop solution (3% sodium dodecyl sulfate, 42% glycerol, 15% 2-mercaptoethanol, 200 m*M* Tris-HCl, pH 6.8, at 20°C) and boiled for 5 min. The denatured samples were subjected to sodium dodecyl sulfate polyacrylamide electrophoresis in a 1.5-mm thick 12.5% acrylamide gel following Laemmli (1970). The gel was stained with 0.25% Serva Blue R (Serva Fine Biochemicals, Westbury, New York) in 25% 2-propanol, 10% acetic acid, destained and dried. The dried gels were exposed to Kodak (Rochester, New York) X-Omat AR film. DuPont Cronex Lightning Plus intensifying screens were used.

Adenylyl cyclase assays

The standard adenylyl cyclase assay contained in a total volume of 150 μl, 10 to 20 μg of *A. rostrata* brain membrane protein, 50 m*M* HEPES, pH 7.6 at the assay temperature of 5°C, 50 μM 2-deoxy-ATP, approximately 1 to 1.5 × 10^6 cpm [α-^{32}P]ATP, 10 μM GTP, 6.25 m*M* Mg acetate, 100 m*M* NaCl, 7.5 units creatine kinase, 5 m*M* phosphocreatine, 1.5 μg soybean trypsin inhibitor, 15 μg bacitracin, and other constituents as indicated below. Assays were conducted in triplicate in a refrigerated water bath for 2 h. The reaction was stopped by adding 250 μl of 2% sodium dodecyl sulfate, 45 m*M* ATP, and 1.3 m*M* cAMP. The samples were boiled for 3 min and 600 μl of water were added. [^{32}P]cAMP generated in the assays was determined according to Salomon *et al.* (1974).

For assays of the effects of hydrostatic pressure on adenylyl cyclase activity and inhibition, samples were transferred to polyethylene tubing. The tubing was trimmed to exclude air bubbles and sealed using a pipet heat sealer. [^{3}H]cAMP (approximately 20,000 cpm) was used as an internal standard to monitor the recovery of sample through the sealing and incubation, and through the subsequent column chromatography steps isolating the [^{32}P]cAMP from the [^{32}P]ATP following Salomon *et al.* (1974). The pK_a of HEPES, the buffer used in these experiments, is relatively insensitive to pressure (Bernhardt *et al.*, 1988). Samples were incubated in high pressure vessels maintained at 5°C in a refrigerated circulating water bath. The high pressure apparatus is described in Hennessey and Siebenaller (1985). Samples were incubated for 120 min. The time required to seal and pressurize a group of four samples and the time required to re-

move the samples was less than 6% of the incubation time at elevated pressure. Samples sealed and incubated at atmospheric pressure have adenylyl cyclase activities identical to samples that are incubated in test tubes.

Data analysis

The kinetic parameters for the time course of association and dissociation of specific [^{3}H]CHA binding were estimated using the equations of Weiland and Molinoff (1981). Rate constants were calculated by least squares linear regression.

The association data were analyzed as a pseudo-first order reaction described by the equation:

$$\ln \frac{[B_{eq}]}{([B_{eq}] - [B])} = ([L]k_{+1} + k_{-1})t = k_{obs}t$$

where $[B_{eq}]$ is the amount of [^{3}H]CHA bound at equilibrium, [B] is the amount bound at time t, [L] is the concentration of [^{3}H]CHA. The pseudo-first order rate constant, k_{obs} is determined from the slope of plots of ln $[B_{eq}]/([B_{eq}] - [B])$ *versus* time (Weiland and Molinoff, 1981; Kitabgi *et al.*, 1977).

The first order dissociation constant (k_{-1}) was determined from a plot of the equation:

$$\ln [B]/[B_o] = k_{-1}t$$

where $[B_o]$ is the concentration of bound [^{3}H]CHA at time 0. The ratio of the rate constants (k_{-1}/k_{+1}) provides an estimate of the equilibrium dissociation constant (K_d) for [^{3}H]CHA binding.

Saturation isotherms were analyzed using LUNDON-1 (Lundon Software, Inc., Cleveland, Ohio) iterative curve fitting routines (Lundeen and Gordon, 1985).

Concentration-response data for inhibition of adenylyl cyclase were analyzed by fitting a three parameter logistic equation to the data. The equation used was:

$$Y = \frac{E - I}{1 + \frac{X}{(IC_{50})}} + I$$

where Y is the rate of adenylyl cyclase activity (pmol cAMP min^{-1} mg protein^{-1}) in the presence of a given concentration of adenosine analog (X); E is the activity of adenylyl cyclase in the absence of adenosine analog; I is the activity in the presence of a maximally inhibiting concentration of adenosine analog; and IC_{50} is the concentration of adenosine analog that produces a half-maximal inhibition of the adenylyl cyclase activity. The concentration-response data were analyzed with an unweighted nonlinear regression analysis program using FITFUN, a computer modeling program on the PROPHET II Computer System.

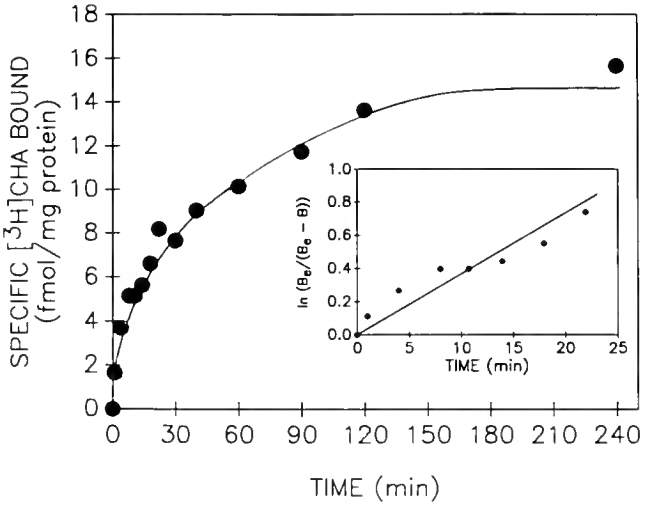

Figure 1. Time course of association of specific [^{3}H]CHA binding to *Antimora rostrata* brain membranes at 5°C. [^{3}H]CHA (2.85 n*M*) was incubated at 5°C with 0.52 mg membrane protein per tube prepared as described in Materials and Methods. Nonspecific binding was measured in the presence of 60 μM R-PIA and was constant throughout the association reaction. Inset shows the pseudo-first order replot of [^{3}H]CHA association data. A single representative experiment is shown.

Results

Time course of association and dissociation

At 5°C, the agonist [^{3}H]CHA bound specifically and reversibly to the *A. rostrata* brain membranes. By 120 min, the specific binding of [^{3}H]CHA was 87% of that observed at 240 min (Fig. 1). Nonspecific binding was constant throughout the association reaction. The k_{obs} calculated from the plot of ln $[B_{eq}]/([B_{eq}] - [B])$ against time was 0.0484 ± 0.00719 min^{-1} (Fig. 1, inset). Examination of the data in the inset suggest that a multiple parameter fit might provide a better fit. However, we approximated k_{obs} by a single parameter because we did not have sufficient data to fit a multiple parameter model. The dissociation rate constant (k_{-1}) was determined directly by following the dissociation of specifically bound [^{3}H]CHA by the addition of 60 μM R-PIA. The [^{3}H]-CHA was readily dissociated on addition of excess R-PIA (Fig. 2). The k_{-1} calculated from the plot of ln $[B]/[B_o]$ *versus* time was 0.0136 ± 0.0006 min^{-1} (Fig. 2, inset). K_d of [^{3}H]CHA was estimated from the ratio of k_{-1}/k_{+1}. This kinetically derived estimate of the equilibrium dissociation constant, K_d, was 1.11 n*M*.

Equilibrium saturation analysis

The specific binding of [^{3}H]CHA at 5°C to *A. rostrata* brain membranes was saturable (Fig. 3). Specific binding, defined as total binding minus nonspecific binding

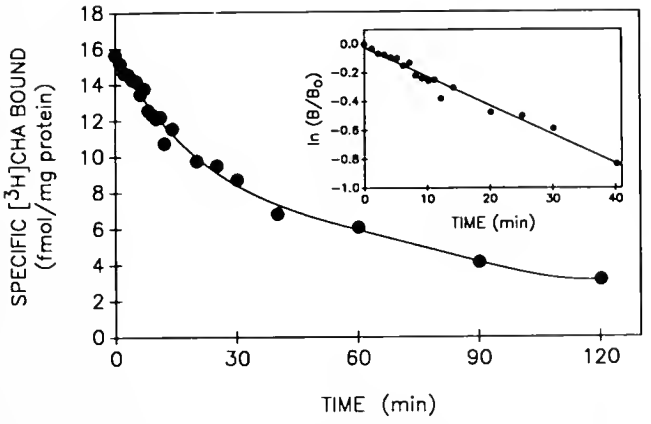

Figure 2. Time course of R-PIA-induced dissociation of specific [^{3}H]CHA binding in *Antimora rostrata* brain membranes. Membranes (0.52 mg protein) were first incubated at 5°C with 2.85 n*M* [^{3}H]CHA for 240 min to allow binding to reach equilibrium. Sixty μM R-PIA was added in a negligible volume (1% of the total incubation volume) to initiate the dissociation reaction. The nonspecific binding, which has been subtracted from each experimental point, was determined in the presence of 60 μM R-PIA. Inset depicts the first-order replot of dissociation data and represents the best least-squares regression line. Data shown are from a single experiment.

determined in the presence of 30 μM R-PIA, saturated over the range of 0.096 to approximately 16 n*M*. Nonspecific binding increased linearly as a function of [^{3}H]-CHA concentration. Analysis of the [^{3}H]CHA saturation isotherm, using equations based on mass action principles, indicated that the data were adequately described by interaction with a single high affinity state of the receptor. Computer modeling of replicate experiments

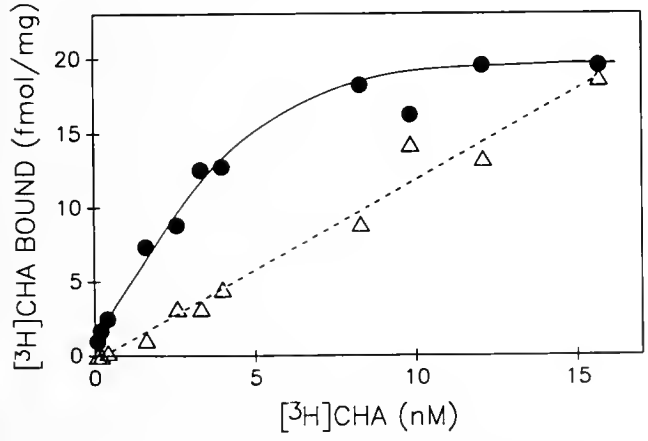

Figure 3. Equilibrium saturation binding of [^{3}H]CHA to *Antimora rostrata* brain membranes at 5°C. Membranes were incubated 150 min with 11 concentrations of free [^{3}H]CHA ranging from 0.096 to 15.7 n*M* in this experiment. Specific binding is indicated by the filled circles. Nonspecific binding, shown by the open triangles, was determined in the presence of 30 μM R-PIA.

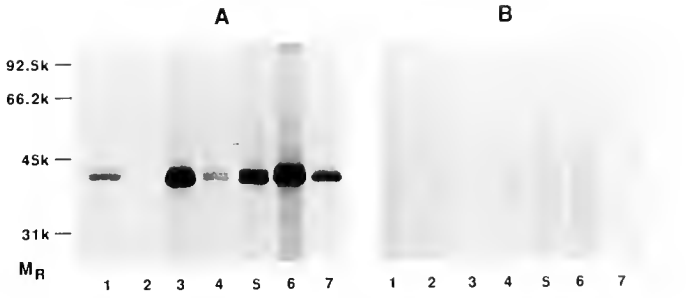

Figure 4. Autoradiogram of teleost fish brain membrane preparations [^{32}P]ADP-ribosylated by pertussis toxin at 5°C. Preparations were incubated for 2 h with [^{32}P]NAD with (A) or without (B) pertussis toxin. The samples were denatured and subjected to sodium dodecyl sulfate polyacrylamide electrophoresis in 12.5% acrylamide gels following Laemmli (1970). The gels were dried and exposed to x-ray film. 1. *Antimora rostrata*, 2. *Sebastolobus alascanus*, 3. *S. altivelis*, 4. *Macrurus berglax*, 5. *Coryphaenoides rupestris*, 6. *C. armatus*, 7. *Oncorhynchus mykiss*.

yielded an average K_d value of 4.86 ± 0.95 n*M* with a density of 25.6 ± 2.02 fmol mg membrane protein^{-1}. The K_d value obtained from the saturation isotherm is in relatively good agreement with the kinetically derived K_d value of 1.11 n*M*.

[^{32}P]*ADP-ribosylation*

Figure 4 shows an autoradiogram of a sodium dodecyl sulfate Laemmli gel used to resolve brain membrane preparations incubated with [^{32}P]NAD in the presence and absence of activated pertussis toxin. [^{32}P]ADP-ribosylation did not occur in the absence of pertussis toxin. Substrates of approximately 39,000 to 41,000 Da apparent molecular mass were specifically labeled in the brain membrane preparations from each of the seven teleost species surveyed. In the autoradiogram some preparations clearly have two labeled substrates, *e.g.*, *Macrourus berglax* and *Coryphaenoides rupestris* (Fig. 4). The ribosylation reaction was performed at 5°C to maintain membrane viscosity close to the body temperatures of these species. At this temperature, pertussis toxin-catalyzed ribosylation of membranes from cold-adapted deep- and shallow-living marine teleosts and the freshwater species, *O. mykiss*, results in labeling of components similar to those of warm-adapted species. The relative molecular masses of the components ribosylated are in the range corresponding to the molecular masses reported for the alpha subunits of the GTP-binding proteins G_i and G_o, an "other" G protein of unknown function, in other species (41,000 Da and 39,000 Da, respectively; Gilman, 1987; Pfeuffer and Helmreich, 1988).

Adenylyl cyclase

The time courses for basal and 0.1 μM forskolin-stimulated adenylyl cyclase activity in *A. rostrata* brain mem-

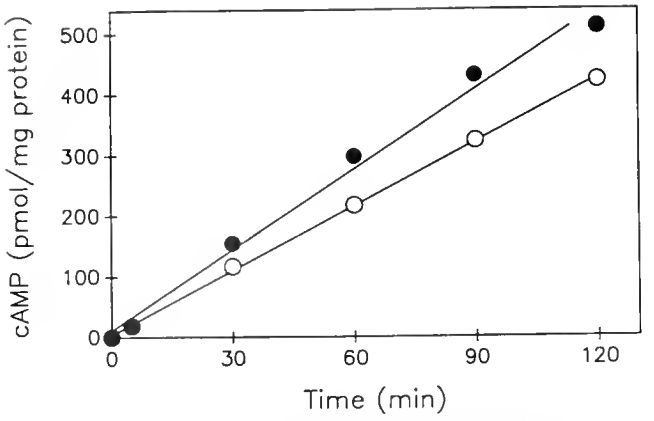

Figure 5. Time course of the adenylyl cyclase reaction at 5°C in brain membranes from *Antimora rostrata*. Open circles: basal adenylyl cyclase activity. Filled circles: forskolin (0.1 μM) stimulated activity. Reaction mixture contained 50 mM HEPES, pH 7.6, at 5°C, 4 mM magnesium acetate, 50 μM 2-deoxy ATP, 100 μM cAMP, 200 μM papaverine, 6.3 mg creatine phosphate, 2 mg creatine phosphokinase, 100 mM NaCl, 10 μM GTP, and 2.5 units/ml adenosine deaminase.

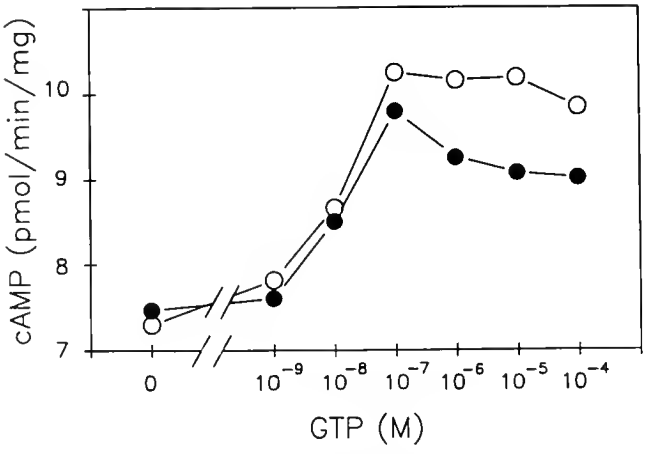

Figure 6. Effect of GTP concentration on *Antimora rostrata* brain membrane basal adenylyl cyclase activity in the absence (open circles) and presence (filled circles) of 100 μM CPA at 5°C.

branes are shown in Figure 5. At 5°C, both the basal and forskolin-stimulated rates were linear for at least 120 min. An incubation time of 120 min was used for all subsequent experiments.

The inhibition of basal adenylyl cyclase activity by N^6-cyclopentyladenosine (CPA) was used as a biochemical measure of the extent of coupling of A_1 receptors to adenylyl cyclase via a guanine nucleotide regulatory protein. CPA is a highly selective A_1 adenosine receptor agonist and was used to eliminate potential interactions with the A_2 adenosine receptor (Bruns *et al.*, 1986; Williams *et al.*, 1986) or with the P-site on the catalytic subunit of adenylyl cyclase (Londos *et al.*, 1983; Blair *et al.*, 1989; Johnson *et al.*, 1989). The dependence of CPA-induced inhibition of adenylyl cyclase activity on GTP concentration is depicted in Figure 6. Basal adenylyl cyclase activity in the absence and presence of 100 μM CPA is shown. CPA had little effect on adenylyl cyclase activity in the absence of added GTP; however, at GTP concentrations of 1 to 100 μM, the A_1 selective agonist inhibited activity. A representative concentration response curve in Figure 7 depicts the inhibition of basal adenylyl cyclase activity in *A. rostrata* brain membranes by various concentrations of CPA. The IC_{50} value for inhibition of adenylyl cyclase was 5.08 ± 2.65 μM. The maximal inhibition of basal activity by CPA ranged from 7 to 17%. Other adenosine analog agonists, such as R-PIA, 2-chloroadenosine, and NECA displayed similar efficacies as inhibitors of adenylyl cyclase activity (data not shown). The concentration-dependent inhibition of adenylyl cyclase activity is consistent with the involvement of A_1 receptors in the inhibitory modulation of the enzyme.

As shown in Figure 8, the basal adenylyl cyclase activity of the deep-living fish *A. rostrata* was unaffected by 272 atm of pressure, which is comparable to the pressures experienced by the species at the lower end of its depth range. At atmospheric pressure, basal adenylyl cyclase activity is 3.3 ± 0.07 pmol min^{-1} mg membrane $protein^{-1}$. Basal activity is unchanged at 272 atm (3.3 ± 0.11 pmol min^{-1} mg^{-1}). The efficacy of the adenosine receptor agonists CPA (100 μM) and NECA (100 μM) as inhibitors of adenylyl cyclase were compared at atmospheric pressure and 272 atm. As shown in Figure 8, the increased pressure doubled the mean percentage inhibition of basal activity by NECA over that observed at 1 atm (14 ± 8% at atmospheric pressure, 29 ± 2% at 272 atm) but had no effect on the inhibition by CPA (9 ± 5% at atmospheric pressure and 8 ± 5% at 272 atm).

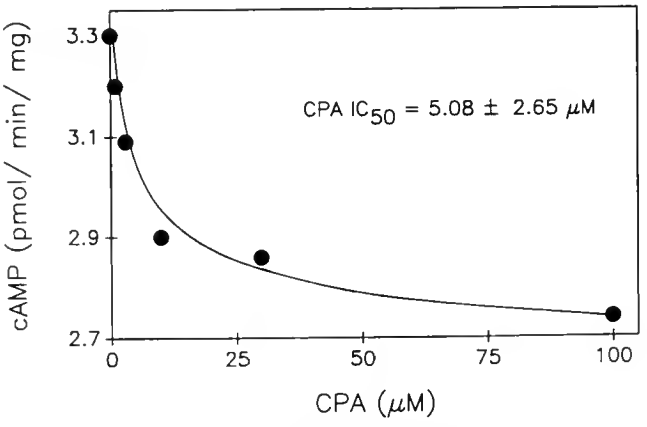

Figure 7. Inhibition of *Antimora rostrata* brain membrane basal adenylyl cyclase activity by the A_1 adenosine receptor agonist CPA at 5°C.

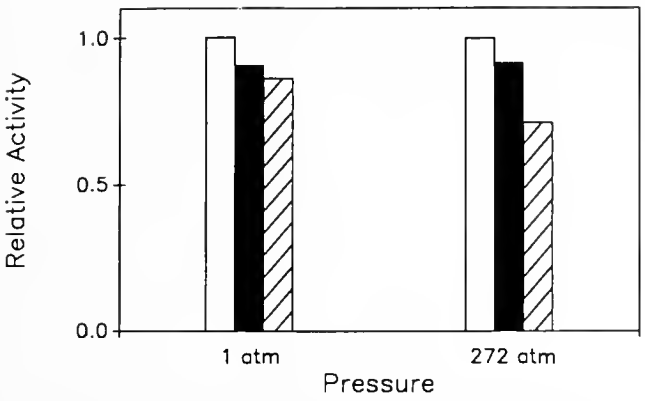

Figure 8. The effects of hydrostatic pressure on *Antimora rostrata* basal adenylyl cyclase activity (open bar) and inhibition of basal adenylyl cyclase activity by the adenosine analogs CPA (100 μM; filled bar) and NECA (100 μM; hatched bar). Membranes were incubated at atmospheric pressure or 272 atm pressure for 2 h at 5°C. All values are standardized to the 1 atm basal adenylyl cyclase activity. The 1 atm and 272 atm basal activities were 3.3 pmol min^{-1} mg $protein^{-1}$. The 1 atm data are the mean of three replicates; the 272 atm values are the mean of six replicates. The average standard errors are 11.7% of the values of the mean.

Discussion

Binding of the agonist [^{3}H]CHA to the A_1 receptor in *A. rostrata* brain membranes at 5°C is saturable and readily reversible (Figs. 1, 2, 3). At 5°C, the rate constants determined for *A. rostrata* from association-dissociation experiments are lower than those reported for two scorpaenid fishes, *Sebastolobus alascanus* and *S. altivelis*, at a measurement temperature of 22°C (Murray and Siebenaller, 1987). The k_{obs} for the *A. rostrata* binding reaction is only 21 to 25% of the values obtained for the *Sebastolobus* species at 22°C. The k_{-1} value for *A. rostrata* is only 40 to 65% of the 22°C values. At 22°C the binding reaction in *Sebastolobus* membranes is complete in 30 min. In contrast, at 5°C, the reaction in *A. rostrata* membranes takes more than four times as long to reach equilibrium (Fig. 1). At 5°C, which approximates the body temperatures of these three species, the K_d values are similar (Siebenaller and Murray, 1988).

At 5°C, the rank order potencies of agonists is compatible with that expected for the A_1 receptor (Fig. 9; Siebenaller and Murray, 1988). The K_i values indicate discrimination of the R- and S-diastereomers of PIA (4.5 and 115.9 nM, respectively). The rank order potency series expected for A_1 receptors is R-PIA ≥ 2-chloroadenosine ≥ NECA > S-PIA, and for A_2 receptors NECA > 2-chloroadenosine > R-PIA ≥ S-PIA (Daly, 1983 a, b; Stone, 1985; Williams, 1987). The rank order potencies, the discrimination between R-PIA and S-PIA, and the K_d of [^{3}H]CHA values are characteristic of an A_1 adenosine receptor.

The substrates specifically [^{32}P]ADP-ribosylated by pertussis toxin in *A. rostrata* and six other teleost species (Fig. 4) have apparent molecular masses characteristic of the class of alpha subunits from the guanine nucleotide binding regulatory proteins G_i and G_o (Gilman, 1987; Pfeuffer and Helmreich, 1988). The GTP-dependence of CPA-induced inhibition of cAMP accumulation (Fig. 6) demonstrates a role for these G proteins in the coupling of the A_1 receptor to negative modulation of adenylyl cyclase activity in *A. rostrata* brain membranes. In the presence of GTP, CPA inhibited basal adenylyl cyclase activity with an IC_{50} of 5.08 ± 2.65 μM (Fig. 7). The maximal inhibition ranged from 7 to 17%. This degree of inhibition is similar to the maximal inhibition of adenylyl cyclase by CPA in embryonic chick heart membranes (Blair *et al.*, 1989).

The A_1 adenosine receptor of the deep-living teleost, *Antimora rostrata*, is capable of modulating the activity of adenylyl cyclase under the conditions of low temperature and high hydrostatic pressure, which characterize the bathyal habitat (Fig. 8). Experiments currently underway, using brain tissues from other species, indicate that the A_1 adenosine receptor-G_i-adenylate cyclase system can be markedly perturbed by hydrostatic pressures less than the 272 atm used in the present study. For instance, in shallower-occurring fishes, basal adenylyl cyclase activity is inhibited 11 to 25% by 136 atm pressure (Siebenaller and Murray, work in progress). In contrast, *A. rostrata* brain tissue adenylyl cyclase is unaffected by 272 atm pressure, the highest pressure tested. The efficacy of agonists at the A_1 adenosine receptor is not lessened by increased pressure (Fig. 8). CPA-induced inhibition of adenylyl cyclase was unaltered, and the efficacy of NECA increased. Thus, basal adenylyl cyclase activity, as well as signal transduction by the A_1 receptor sys-

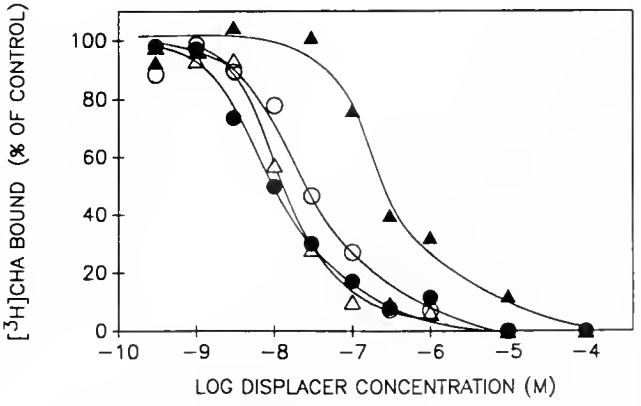

Figure 9. Inhibition of specific [^{3}H]CHA binding in *Antimora rostrata* brain membranes by adenosine analogs: R-PIA (open circle), NECA (open triangle), 2-chloroadenosine (filled circle), S-PIA (filled triangle). Eleven concentrations of each analog were incubated with membranes and 7.9 nM [^{3}H]CHA for 150 min at 5°C.

tem, are functional under the conditions of pressure and temperature at which *A. rostrata* occurs.

Consideration of the effects of low temperature and high hydrostatic pressure on membrane viscosity (Cossins and Macdonald, 1989) suggests that any of the components of the A_1 receptor-G_i protein-adenylyl cyclase complex may be susceptible to perturbation in organisms colonizing the deep sea. For *A. rostrata*, the function of this transmembrane signaling complex is maintained at low temperature and high hydrostatic pressure. The pressure insensitivity of this membrane-associated system in *A. rostrata* is analogous to the pressure adaptations observed for cytoplasmic proteins (Siebenaller and Somero, 1989). The K_m values of NAD-dependent dehydrogenases of deep-living species are relatively insensitive to perturbation by pressure. In contrast, homologous enzymes from shallow-living, cold-adapted species are perturbed by pressures as low as 68 atm. By having pressure-resistant enzymes, function is preserved over the range of depths that may be experienced by an individual during ontogeny or diel vertical migrations, or by a species maintaining populations over a broad depth gradient (Siebenaller, 1987).

Gibbs and Somero (1989) hypothesized, based on their study of Na^+/K^+-ATPase in teleost gill tissue, that clear adaptations of membrane-associated systems to pressure may only be apparent in species occurring at depths greater than 2000 m. Although our data do not directly test this hypothesis, the pressure insensitivity of the A_1 receptor and effector system in *A. rostrata*, which commonly occurs to depths of 2500 m, are compatible with their suggestion. This pressure resistance in *A. rostrata* is a standard with which to compare the effects of environmental parameters on transmembrane signal transduction in other deep- and shallow-occurring species.

Acknowledgments

This research was supported by NSF grant DCB-8710155, and ONR contracts N00014-88-K-0426, N0014-88-K-0432, and ONR grants N00014-89-J-1865 and N00014-89-J-1869. Shiptime on the R/V *Wecoma* off the coast of Oregon was supported by NSF grant DCB-8710155. Shiptime on the R/V *Gyre* off the coast of Newfoundland was supported by NSF grant DMB-8502857 to Dr. A. F. Riggs. We thank Drs. A. Riggs and R. Noble for their help in obtaining specimens and Drs. P. Franklin and M. Leid for their help with the ADP-ribosylation experiments.

Literature Cited

Avrova, N. F. 1984. The effect of natural adaptations of fishes to environmental temperature of brain ganglioside fatty acid and long chain base compositions. *Comp. Biochem. Physiol.* **78B:** 903–909.

Bernhardt, G., A. Distèche, R. Jaenicke, B. Koch, H.-D. Ludemann, and K.-O. Stetter. 1988. Effect of carbon dioxide and hydrostatic pressure on the pH of culture media and the growth of methanogens at elevated temperature. *Appl. Microbiol. Biotechnol.* **28:** 176–181.

Blair, T. A., M. Parenti, and T. F. Murray. 1989. Development of pharmacological sensitivity to adenosine analogs in embryonic chick heart: role of A_1 adenosine receptors and adenylyl cyclase inhibition. *Mol. Pharmacol.* **35:** 661–670.

Bruns, R. F., J. W. Daly, and S. H. Snyder. 1980. Adenosine receptors in brain membranes: binding of N^6-cyclohexyl[^{3}H]adenosine and 1,3-diethyl-8-[^{3}H]phenylxanthine. *Proc. Natl. Acad. Sci. USA* **77:** 5547–5551.

Bruns, R. F., G. H. Lu, and T. A. Pugsley. 1986. Characterization of the A_2 adenosine receptor labeled by [^{3}H]NECA in rat striatal membranes. *Mol. Pharmacol.* **29:** 331–346.

Chong, P. L.-G., and A. R. Cossins. 1983. A differential polarized phase fluorometric study of the effects of high hydrostatic pressure upon the fluidity of cellular membranes. *Biochemistry* **22:** 409–415.

Cossins, A. R., and A. G. Macdonald. 1984. Homeoviscous theory under pressure. II. The molecular order of membranes from deep-sea fish. *Biochim. Biophys. Acta* **776:** 144–150.

Cossins, A. R., and A. G. Macdonald. 1986. Homeoviscous adaptation under pressure. III. The fatty acid composition of liver mitochondrial phospholipids of deep-sea fish. *Biochim. Biophys. Acta* **860:** 325–335.

Cossins, A. R., and A. G. Macdonald. 1989. The adaptations of biological membranes to temperature and pressure: fish from the deep and cold. *J. Bioenergetics Biomembranes* **21:** 115–135.

Daly, J. W. 1983a. Adenosine receptors: characterization with radioactive ligands. Pp. 59–69 in *Physiology and Pharmacology of Adenosine Derivatives*, J. W. Daly, Y. Kuroda, J. W. Phillis, H. Shimizu, and M. Ui, eds. Raven, New York.

Daly, J. W. 1983b. Role of ATP and adenosine receptors in physiological processes: summary and prospectus. Pp. 275–290 in *Physiology and Pharmacology of Adenosine Derivatives*, J. W. Daly, Y. Kuroda, J. W. Phillis, H. Shimizu, and M. Ui, eds. Raven, New York.

DeLong, E. F., and A. A. Yayanos. 1985. Adaptation of the membrane lipids of a deep-sea bacterium to changes in hydrostatic pressure. *Science* **228:** 1101–1103.

DeLong, E. F., and A. A. Yayanos. 1987. Properties of the glucose transport system in some deep-sea bacteria. *Appl. Environ. Microbiol.* **53:** 527–532.

Gibbs, A., and G. N. Somero. 1989. Pressure adaptation of Na^+/K^+-ATPase in gills of marine teleosts. *J. Exp. Biol.* **143:** 475–492.

Gilman, A. G. 1987. G proteins: transducers of receptor-generated signals. *Ann. Rev. Biochem.* **56:** 615–649.

Greenberg, A. S., S. I. Taylor, and C. Londos. 1987. Presence of a functional inhibitory GTP-binding regulatory component, G_i, linked to adenylate cyclase in adipocytes of ob/ob mice. *J. Biol. Chem.* **262:** 4564–4568.

Hennessey, J. P., Jr., and J. F. Siebenaller. 1985. Pressure inactivation of tetrameric lactate dehydrogenase homologues of confamilial deep-living fishes. *J. Comp. Physiol. B* **155:** 647–652.

Hennessey, J. P., Jr., and J. F. Siebenaller. 1987. Pressure-adaptive differences in proteolytic inactivation of M_4-lactate dehydrogenase homologues from marine fishes. *J. Exp. Zool.* **241:** 9–15.

Hochachka, P. W., and G. N. Somero. 1984. *Biochemical Adaptation* Princeton University Press, Princeton, NJ.

Hochachka, P. W., ed. 1975. Pressure effects on biochemical systems of abyssal and midwater organisms: the 1973 Kona Expedition of the Alpha Helix. *Comp. Biochem. Physiol.* **52B:** 1–199.

Iwamoto, T. 1975. The abyssal fish *Antimora rostrata* (Günther). *Comp. Biochem. Physiol.* **52B:** 7–11.

Johnson, R. A., S.-M. H. Yeung, D. Stübner, M. Bushfield, and I. Shoshani. 1989. Cation and structural requirements for P site-mediated inhibition of adenylate cyclase. *Mol. Pharmacol* **35:** 681–688.

Kitabgi, P., R. Carraway, J. Van Rietschoten, C. Granier, J. L. Morgat, A. Menez, S. Leeman, and P. Freychet. 1977. Neurotensin: specific binding to synaptic membranes from rat brain. *Proc. Natl Acad. Sci. USA* **74:** 1846–1850.

Laemmli, U. K. 1970. Cleavage of structural proteins during the assembly of the head of bacteriophage T4. *Nature* **227:** 680–685.

Lohse, M. J., U. Lenschow, and U. Schwabe. 1984. Two affinity states of R_i adenosine receptors in brain membranes. Analysis of guanine nucleotide and temperature effects on radioligand binding. *Mol. Pharmacol.* **26:** 1–9.

Londos, C., J. Wolff, and D. M. F. Cooper. 1983. Adenosine receptors and adenylate cyclase interactions. Pp. 17–32 in *Regulatory Function of Adenosine*, R. M. Berne, T. W. Rall, and R. Rubio, eds. Martinus Nijhoff Publishers, The Hague, Boston, London.

Lowry, O. H., N. J. Rosebrough, A. L. Farr, and R. J. Randall. 1951. Protein measurement with the Folin phenol reagent. *J Biol. Chem.* **193:** 265–275.

Lundeen, J. E., and J. H. Gordon. 1985. Computer analysis of binding data. Pp. 31–49 in *Receptor Binding in Drug Research*, B. O'Brien, ed. Marcel Dekker, New York.

Murphy, K. M. M., and S. H. Snyder. 1982. Heterogeneity of adenosine A_1 receptor binding in tissue. *Mol. Pharmacol.* **22:** 250–257.

Murray, T. F., and D. L. Cheney. 1982. Localization of N^6-cyclohexyl[^{3}H]adenosine binding sites in rat and guinea pig brain. *Neuropharmacology* **21:** 575–580.

Murray, T. F., and J. F. Siebenaller. 1987. Comparison of the binding properties of A_1 adenosine receptors in brain membranes of two congeneric marine fishes living at different depths. *J. Comp. Physiol. B* **157:** 267–277.

Pfeuffer, T., and E. J. M. Helmreich. 1988. Structural and functional relationships of guanosine triphosphate binding proteins. *Current Topics in Cellular Regulation* **29:** 129–216.

Ribeiro-Neto, F. A. P., R. Mattera, J. D. Hildebrandt, J. Codina, J. B. Field, L. Birnbaumer, and R. D. Sekura. 1985. ADP-ribosylation of membrane components by pertussis and cholera toxin. *Methods Enzymol.* **109:** 566–572.

Salomon, Y., C. Londos, and M. Rodbell. 1974. A highly sensitive adenylate cyclase assay. *Analyt. Biochem.* **58:** 541–548.

Siebenaller, J. F. 1987. Biochemical adaptation in deep-sea animals. Pp. 33–48 in *Current Perspectives in High Pressure Biology*, H. W. Jannasch, A. M. Zimmerman, and R. E. Marquis, ed. Academic Press, London.

Siebenaller, J. F., and T. F. Murray. 1986. Phylogenetic distribution of [^{3}H]cyclohexyladenosine binding sites in nervous tissue. *Biochem. Biophys. Res. Commun.* **137:** 182–189.

Siebenaller, J. F., and T. F. Murray. 1988. Evolutionary temperature adaptation of agonist binding to the A_1 adenosine receptor. *Biol Bull* **175:** 410–416.

Siebenaller, J. F., and G. N. Somero. 1978. Pressure-adaptive differences in lactate dehydrogenases of congeneric fishes living at different depths. *Science* **201:** 255–257.

Siebenaller, J. F., and G. N. Somero. 1979. Pressure-adaptive differences in the binding and catalytic properties of muscle-type (M_4) lactate dehydrogenase of shallow- and deep-living marine fishes. *J Comp. Phys.* **129:** 295–300.

Siebenaller, J. F., and G. N. Somero. 1989. Biochemical adaptation to the deep sea. *Rev. Aquatic Sci.* **1:** 1–25.

Small, G. J. 1981. A review of the bathyal fish genus *Antimora* (Moridae: Gadiformes). *Proc. California Academy Sci.* **42:** 341–348.

Snyder, S. H. 1985. Adenosine as a neuromodulator. *Ann. Rev. Neurosci.* **8:** 103–124.

Somero, G. N., and J. F. Siebenaller. 1979. Inefficient lactate dehydrogenases of deep-sea fishes. *Nature* **282:** 100–102.

Stone, T. W. 1985. Summary of a symposium on purine receptor nomenclature. Pp. 1–5 in *Purines: Pharmacology and Physiological Roles*, T. W. Stone, ed. UCH Publishers, Deerfield Beach, Florida.

Trost, T., and U. Schwabe. 1981. Adenosine receptors in fat cells. Identification by (−)-N^6-[^{3}H]phenylisopropyladenosine binding. *Mol. Pharmacol.* **19:** 228–235.

Weiland, G. A., and P. B. Molinoff. 1981. Quantitative analysis of drug-receptor interactions: I. Determination of kinetic and equilibrium properties. *Life Sci.* **29:** 313–330.

Wenner, C. A., and J. A. Musick. 1977. Biology of the morid fish, *Antimora rostrata*, in the western North Atlantic. *J. Fish. Res. Board Can.* **34:** 2362–2368.

Williams, M. 1987. Purine receptors in mammalian tissues: pharmacology and functional significance. *Ann Rev. Pharmacol. Toxicol.* **27:** 315–345.

Williams, M., A. Braunwalder, and T. E. Erickson. 1986. Evaluation of the binding of the A-1 selective adenosine radioligand, cyclopentyladenosine (CPA), to rat brain tissue. *Naunyn-Schmiedeberg's Arch. Pharmacol.* **332:** 179–183.

Wolff, J., C. Londos, and D. M. F. Cooper. 1981. Adenosine receptors and the regulation of adenylate cyclase. *Adv Cyclic Nucleotide Res.* **14:** 199–214.

Yancey, P. H., and J. F. Siebenaller. 1987. Coenzyme binding ability of homologs of M_4 lactate dehydrogenases. *Biochim. Biophys. Acta* **924:** 483–491.

Reference: *Biol. Bull.* **178:** 74–83. (February, 1990)

Control of Cnida Discharge: III. Spirocysts are Regulated by Three Classes of Chemoreceptors

GLYNE U. THORINGTON AND DAVID A. HESSINGER[1]

Department of Physiology and Pharmacology, School of Medicine, Loma Linda University, Loma Linda, California 92350

Abstract. Spirocysts are two to three times more abundant than nematocysts in the feeding tentacles of acontiate sea anemones. Despite their prevalence, little experimental work has been done on the discharge of spirocysts because of the difficulty in detecting and counting them after they have discharged. To circumvent this problem, we have developed a simple, reliable, enzyme-linked lectin sorbent assay (ELLSA) for quantifying discharged spirocysts. With this method, we have shown that the discharge of spirocysts, like that of mastigophore nematocysts, is chemosensitized in a dose-dependent manner by three classes of low molecular weight substances, typified by N-acetylneuraminic acid (NANA), glycine, and certain heterocyclic amino compounds, such as proline and histamine. We also show that spirocysts exhibit considerable agonist-specific variation in the dose-responses of discharge, suggesting the existence of multiple populations of spirocyst-bearing cnidocyte/supporting cell complexes (CSCCs). Our findings call into question commonly held views regarding the respective roles of spirocysts and mastigophore nematocysts in the retention of captured prey.

Introduction

The cnidom of the feeding tentacles of acontiate sea anemones, including *Aiptasia pallida*, consists of three types of cnidae: spirocysts; microbasic p-mastigophore nematocysts, and basitrichous isorhiza nematocysts (Hand, 1955) in approximate ratios of 3:1:0.3, respectively (Bigger, 1982; Watson and Mariscal, 1983). Cnidae function primarily in the capture of prey (Ewer, 1947), in aggression (Purcell, 1977; Bigger, 1982), in defense (Francis, 1973), and in the attachment to appropriate substrates (Mariscal, 1972).

Spirocysts are adherent cnidae found only in zoantharian anthozoans (Mariscal *et al.*, 1978; Mariscal, 1984). An undischarged spirocyst consists of a single-layered capsule containing a long, spirally coiled, inverted tubule of uniform diameter (Mariscal, 1974). The tubule lacks spines, but bears hollow rods that dissociate upon discharge to form a web of fine, adhesive microfibrillae (Mariscal *et al.*, 1977).

Unlike nematocysts, discharged spirocysts are difficult to see under the light microscope due to their non-refractile, transparent capsules (Weill, 1934). Because the tubules of discharged spirocysts entangle extensively (Stephenson, 1929; Skaer and Picken, 1965; Picken and Skaer, 1966; Mariscal, 1974; Mariscal *et al.*, 1977), it is difficult to visually distinguish individual tubules. Thus, it is tedious and time-consuming to visually count spirocysts discharged onto test probes.

To circumvent this difficulty, we developed a simple, sensitive, and reproducible assay to quantify spirocysts discharged onto test probes. The method is based on the recent discovery that the everted tubules of spirocysts have a high affinity for free and conjugated N-acetylated sugars such as occur on mucins, asialomucins, and mucopolysaccharides (Watson and Hessinger, in prep.). The terminal sugars of the unbranched oligosaccharide chains of bovine submaxillary asialomucin are N-acetylgalactosamine. This saccharide binds specifically to the lectin from *Vicia villosa*. Subsequent to binding asialomucin to discharged spirocysts, we determine the number of discharged spirocysts adhering to gelatin-coated test probes by measuring the amount of asialomucin bound to probes using a peroxidase conjugate to the *Vicia* lectin.

We describe a relatively rapid enzyme-linked, lectin

Received 17 July 1989; accepted 30 November 1989.

[1] To whom all correspondence should be addressed.

sorbent assay (ELLSA) to determine the number of spirocysts discharged onto test probes. Using the ELLSA, we show that three classes of agonists sensitize spirocytes to discharge their spirocysts in response to triggering mechanical stimuli. The dose-response curves of spirocyst discharge to the agonists indicate that multiple populations of discharging spirocysts exist, each characterized by different sensitivities to the agonists.

Materials and Methods

Sea anemone maintenance

Monoclonal sea anemones (*Aiptasia pallida*, Carolina strain) were fed and maintained individually in glass finger bowls containing natural seawater at 24 ± 1°C as previously described (Thorington and Hessinger, 1988a).

Experimental animals and test solutions

Prior to each experiment, animals of the same size were starved for 72 h and kept under defined conditions and lighting (Thorington and Hessinger, 1988a). Test solutions of chemosensitizing agonists (N-acetylneuraminic acid, glycine, proline and histamine; Sigma, St. Louis, Missouri) were prepared in natural, filtered (Type 1, Whatman) seawater adjusted to pH 7.6 with 1 *N* HCl or NaOH. Animals were permitted to adapt to changes of medium for 10 min before cnidocyte responsiveness was measured.

Assays of cnidocyte responsiveness

Three methods were used to measure the discharge of cnidae: (1) cnida-mediated adhesive force; (2) microscopic enumeration of discharged microbasic p-mastigophores and spirocysts; and (3) an indirect, solid-state enzyme-linked lectin sorbent assay (ELLSA) of discharged spirocysts.

Cnida-mediated adhesive force. Cnida-mediated adhesive force was measured as previously described (Thorington and Hessinger, 1988a). In principle, this technique involves using a small, gelatin-coated nylon bead attached to a strain gauge via a stainless steal wire shaft. The gel-coated bead is made to contact the tip of a tentacle on an anemone in a finger bowl containing a solution of chemosensitizing agent in seawater. The discharge of cnidae initiated by contact of the probe with the tentacle results in the tubules of the everting cnidae either adhering to or penetrating the gelatin surface. Withdrawing the probe from the tentacle causes the discharged cnidae to exert an opposite and downward force on the probe, which is measured from a gravimetrically calibrated force-transducer connected to a strip-chart recorder. The adhesive force, measured in hybrid units of mg-force (mgf), is the force required to break the cnida-mediated attachment between the probe and the tentacle. It is an aggregate measure of several contributions, including the different kinds of discharged cnidae and the inherent "stickiness" of the tentacle surface, and is proportional to the total number of cnidae discharged onto the probe (Geibel *et al.*, 1988).

Enumeration of discharged mastigophores and spirocysts. Following the measurement of adhesive force, the same gel-coated probes were used to visually count the number of adhering mastigophore nematocysts by methods previously described (Geibel *et al.*, 1988).

Discharged spirocysts were visually counted by the same procedures used for discharge mastigophores. Even with phase contrast optics, however, fully discharged spirocysts were extremely difficult to see and time-consuming to count. To expedite counting of discharged spirocysts adhering to test probes, we developed a fast and reliable micro-assay termed an ELLSA.

Indirect, solid-state enzyme-linked lectin sorbant assay (ELLSA)

This assay for quantifying discharged spirocysts is based upon the observation that the everted tubules of discharged spirocysts bind conjugated N-acetylated sugars with high affinity (Watson and Hessinger, in prep.). In brief, the assay involves first dipping the gel-coated tips of spirocyst-bearing probes into a solution of asialomucin, then into a solution of *Vicia villosa* lectin/peroxidase conjugate, followed by colorimetric measurement of bound peroxidase activity. Some of the N-acetylgalactosaminyl residues on the asialomucin molecule bind to the adhesive "glue" of the everted tubules while the remaining terminal sugars bind the lectin/peroxidase.

Buffers. The following buffers were prepared: Buffer A (0.69 *M* NaCl and 0.25 *M* phosphate, pH 7.6); Buffer B (0.15 *M* NaCl and 0.01 *M* phosphate, pH 6.0 containing 0.02% Tween 20); Buffer C (0.15 *M* NaCl and 0.01 *M* phosphate, pH 6.0); and Buffer D (0.5 M sodium citrate-HCl pH 5.3).

Asialomucin solution. Asialomucin (12 μg/ml; A-0789, Sigma) in filtered seawater was divided into 10 ml aliquots and stored frozen. For assays, a solution of asialomucin (10.8 μg/ml) was prepared by adding nine parts of the stock solution to one part of Buffer D.

Lectin/enzyme conjugate. Horseradish peroxidase conjugated to *Vicia villosa* lectin (E-Y Laboratories, San Mateo, California) was diluted to a final concentration of 1.5 μg/ml in Buffer A. Aliquots of lectin/enzyme conjugate were protected from light and frozen (−20°C) until used. Mannose (50 m*M*) was added immediately prior to using the lectin conjugate to minimize nonspecific interactions between the lectin and the gelatin on test probes.

Enzyme substrate. Hydrogen peroxide (30%; Sigma)

was daily diluted to 3% (v/v) with distilled water and then to 0.3% with Buffer C. The final substrate solution was prepared immediately before use by adding 6 ml of 0.3% H_2O_2 to 0.05 ml of 1% *o*-dianisidine (Sigma) in methanol.

Assay procedure. The wells of flat-bottomed, 96-well microtiter plates (Dynatech) were each rinsed with 200 μl of Buffer B, emptied, and then air dried for 30 min. Test probes were secured to a plastic holder that permitted individual probes to be immersed in the contents of separate wells without coming into contact with the sides or bottom of the wells. All incubations were performed at room temperature. Probes were incubated in the asialomucin solution for 30 min, then rinsed by immersing in individual wells containing Buffer C for 2 min, and finally air-dried for 5 min.

Mucin-treated probes were incubated in separate wells containing 200 μl of lectin/enzyme conjugate for 60 min in the dark. Following a 2-min rinse in Buffer C, they were transferred to wells containing 200 μl of enzyme substrate where they were incubated for 60 min. Following the incubation, the probes were removed and 50 μl 40% sodium azide in Buffer C was added to each of the wells to stop peroxidase activity.

The absorbance of each well was measured at 492 nm using a microtiter well spectrophotometer (Model EL 308, Biotek Instruments, Cambridge, Massachusetts). The mean values of controls, consisting of gel-coated probes, which had not been touched to sea anemone tentacles, were subtracted from the values of individual experimental probes. Probes sputter-coated with gold for 4 min at 15 μA using a Polaron E 5100 sputter coater and then dipped into asialomucin (10.8 μg/ml) in Buffer D were used as external standards to assess reactivity of reagents and to normalize data from test probes to the standard curve, when necessary. The "gold" standard gave absorbances of 0.07 (±0.003 S.E.M.) O.D. at 492 nm. For experimental probes, the absorbance at 492 nm is linearly and directly proportional to the number of discharged spirocysts. Measurements of absorbance are directly converted to the number of discharged adherent spirocysts on a probe by extrapolation from the standard curve.

Results

Optimal dilution of ELLSA reagents

Checkerboard titrations of asialomucin and of lectin peroxidase were performed in microtiter plate wells. The dilutions ranged from 1:3 to 1:81 for asialomucin and 1:8 to 1:5832 for lectin peroxidase. Test probes were gold-coated insect pins (See Materials and Methods) with heads of 0.8 mm diameter. Negative controls were probes treated with 0.01 *M* phosphate buffered saline, pH 6.0. The dilutions chosen were those giving the greatest difference between controls and experimentals. The optimal dilution for asialomucin was 1:27, which is equivalent to 10.8 μg/ml; and for the lectin peroxidase it was 1.5 μg/ml.

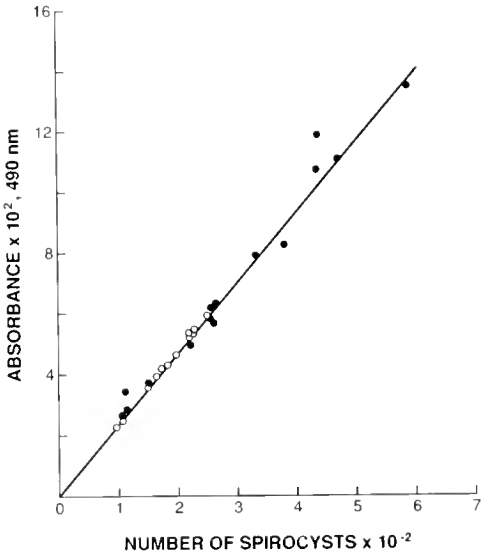

Figure 1. Standard curve for ELLSA determination of discharged spirocysts. The number of discharged spirocysts counted on test probes is plotted against absorbance at 490 nm. Solid circles represent mean values obtained from tentacles chemosensitized by N-acetylneuraminic acid and open circles from histamine-sensitized animals. Each point is the mean of separate absorbancy readings (n = 24) and direct countings (n = 11) (R = 0.99).

Standard curve

A standard curve was constructed by plotting visually counted spirocysts per probe as a function of absorbance at 490 nm. Visual counts of spirocysts discharged onto probes from animals that were chemosensitized by various concentrations of either NANA or histamine were performed under phase contrast optics. Direct counts and absorbancy readings were obtained using replicate probes from the same animals. For absorbancy readings, a total of four separate experiments were performed and averaged. Each experiment consisted of six replicate probes. A linear and direct relationship existed between the absorbance and the visually counted discharged spirocysts (Fig. 1).

Adhesive force measurements

Dose-response curves, expressing the mean adhesive force for all tested chemosensitizers, are biphasic. The curves for glycine, histamine, proline, and NANA exhibit a sigmoidal region of sensitization at low concentrations of sensitizer, a maximum response or effect (E_{max}) at higher concentrations (EC_{100}), and a region of apparent desensitization occurring at still higher concentra-

Table I

Dose-response parameters of agonist-sensitized cnida discharge and adhesive force measurements from Aiptasia pallida *tentacles*

	Spirocysts			Mastigophores			Adhesive force		
Agonists	E_{max} (no.)	EC_{100}	$K_{0.5}$ (M)	E_{max} (no.)	EC_{100}	$K_{0.5}$ (M)	E_{max} (mgf)	EC_{100}	$K_{0.5}$ (M)
Glycine	107 ± 15	5×10^{-11}	$5.4 \times 10^{-12} \pm 0$	160 ± 24	10^{-6}	$1.2 \times 10^{-8} \pm 0.23$	8.7 ± 0.7	10^{-6}	$2.0 \times 10^{-8} \pm 0.2$
Histamine							12.0 ± 0.9	2.7×10^{-7}	$1.4 \times 10^{-8} \pm 0.1$
Peak 1	138 ± 18	2.7×10^{-9}	$9.7 \times 10^{-10} \pm 1.0$	110 ± 23	10^{-9}	$1.6 \times 10^{-10} \pm 0$			
Peak 2	159 ± 23	2.7×10^{-6}	$1.0 \times 10^{-7} \pm 0.3$	201 ± 40	10^{-7}	$1.9 \times 10^{-9} \pm 0.3$			
Proline							10.7 ± 1.0	10^{-6}	$3.6 \times 10^{-8} \pm 0.4$
Peak 1	128 ± 6	2.7×10^{-8}	$3.2 \times 10^{-9} \pm 0.2$	70 ± 15	10^{-8}	$5.4 \times 10^{-9} \pm 0.3$			
Peak 2	93 ± 7	2.7×10^{-6}	$1.7 \times 10^{-7} \pm 0.3$	86 ± 4	10^{-6}	$5.0 \times 10^{-7} \pm 0$			
NANA				157 ± 9	10^{-5}	$8.1 \times 10^{-9} \pm 0.5$	14.0 ± 1.0	1.8×10^{-5}	$3.6 \times 10^{-7} \pm 0.5$
Peak 1	233 ± 15	10^{-8}	$5.0 \times 10^{-9} \pm 0$						
Peak 2	396 ± 9	10^{-7}	$8.0 \times 10^{-8} \pm 0.4$						
Peak 3	172 ± 46	10^{-5}	$3.2 \times 10^{-6} \pm 1.0$						

E_{max} (no.) represents the maximal number of cnidae discharged onto single test probes at optimal sensitization. EC_{100} is the molar concentration of agonist producing a maximal effect. This value was obtained by visual inspection of dose-response curves. $K_{0.5}$ (M) represents the molar concentration of agonist producing the half-maximal effects. E_{max} (mgf) represents the maximal cnida-mediated adhesive force at optimal sensitization. Both E_{max} and $K_{0.5}$ values are determined from least-square double reciprocal plot of the sensitized region of the dose-response curve. Values represent the response to agonists alone (*i.e.*, controls subtracted) and are means ± standard error of the mean.

tions (Figs. 2A, 3A, 4A, and 5A, respectively). The dose-response curves differ with regard to the specific dose-response parameters (Table I): E_{max}, the maximum effect; $K_{0.5}$, the dose at which a half-maximum effect occurs; and EC_{100}, the dose at which the maximum effect occurs.

Dose-responses of mastigophore and spirocyst discharge

Glycine. The dose-response curves representing the discharge of mastigophores (Fig. 2B) and spirocysts (Fig. 2C) to glycine are biphasic. The dose-response of the discharge of spirocysts to glycine consists of a single modal dose-response similar to that obtained from adhesive force measurements and from the discharge of mastigophores (Fig. 2A, B). However, there are significant differences in the dose-responses of these two types of cnidae. The response of spirocysts sensitized by glycine is shifted significantly to the left of the glycine-sensitized mastigophore response, indicating that responding spirocytes are approximately 10,000 times more sensitive to glycine than are the responding mastigophore-bearing cnidocytes (Table I).

Before chemosensitization, the mean number of discharged spirocysts on control probes was 116; after sensitization, the number rose to 214. This is equivalent to an average increase of 86%. Because insignificant spirocyst discharge occurs at higher concentrations, and because the dose-response for adhesive force and for discharged mastigophores coincide, it appears that the discharged mastigophores are the major contributors to glycine-induced adhesive force.

Histamine. The dose-responses of discharging spirocysts and mastigophores sensitized by histamine are bimodal, each displaying two biphasic peaks (Fig. 3) that are complementary and non-overlapping. The two peaks of discharging mastigophores each appear to be about ten times more sensitive to histamine than the corresponding two peaks of discharging spirocysts.

Proline. The dose-response curves of cnida discharge to proline (Fig. 4) are similar to those obtained for histamine. Both the mastigophore and spirocyst response profiles are bimodal, but unlike histamine, they are complementary and coincidental, rather than non-overlapping. The discharge of spirocysts is less sensitive to proline than to histamine (Table I).

N-acetylneuraminic acid (NANA). The pattern of discharge elicited by NANA for spirocysts is trimodal, but for mastigophores it is modal. This is in contrast to the responses elicited by the tested "amino" agonists in which agonist-induced patterns were similar for both spirocysts and mastigophores. Each of the three biphasic spirocyst responses is fairly narrow (Fig. 5C), in comparison to the mastigophore response (Fig. 5B), which spans a range of NANA concentrations of five to six orders of magnitude.

Effect of target hardness on retention of cnidae

To determine whether the hardness of the target contributes to the number of cnidae retained on target probes, we varied the concentrations of the gelatin used (5–50%; w/v) to coat target probes. We sensitized all anemones at 10^{-5} M NANA to assure that the number of discharging cnidae remained constant. Thus, the number of discharged cnidae retained on probes mea-

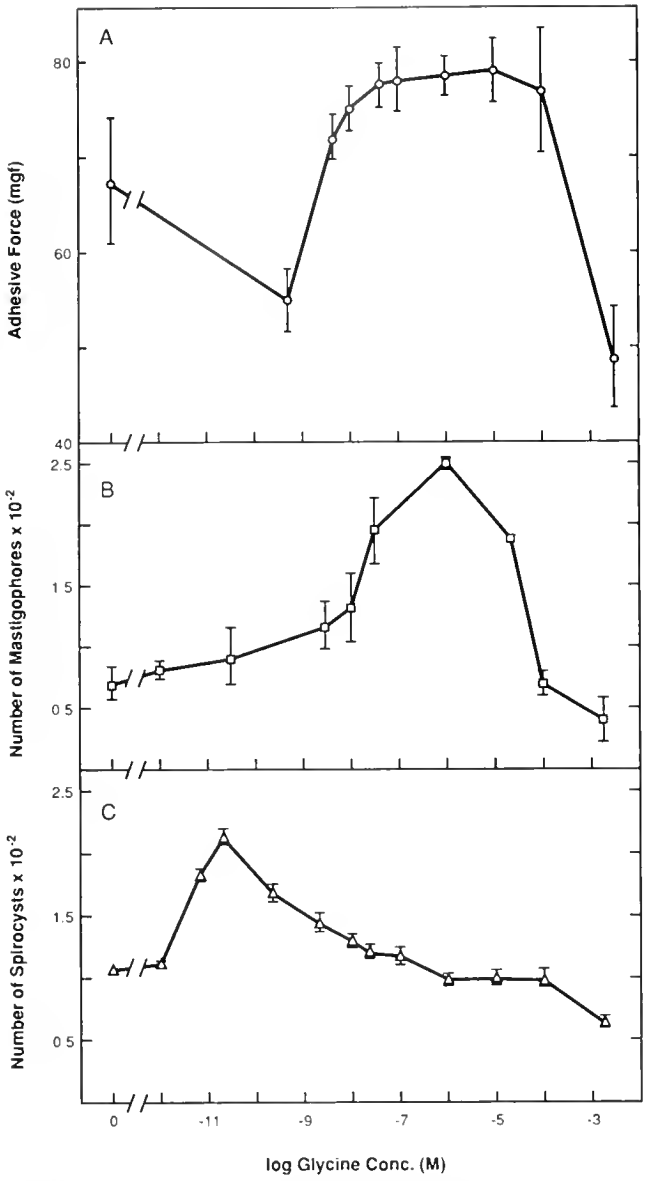

Figure 2. Dose-responses of glycine on discharge of cnidae. A. Effect of glycine on cnida-mediated adhesive force. Values express the mean of four separate experiments. Each experiment consists of eight replicate probes for each concentration; each probe and each tentacle is used only once (n = 32). B. Effect of glycine on the number of discharged mastigophores (n = 8). C. Effect of glycine on the number of discharged spirocysts (n = 24). The number of spirocysts was determined by the ELLSA assay. Vertical bars represent the standard error of the mean at 95% confidence limit.

sured the adhesion of the discharging cnidae to target surfaces of differing degrees of hardness.

We find that the retention of discharged mastigophores and spirocysts onto test probes of differing degrees of hardness is minimal at soft gelatin coatings of 5% (Fig. 6A, B). The adhesion curves with respect to gelatin concentration for retained mastigophores (Fig. 6A) and for adhesive force measurements (Fig. 6C) are biphasic, showing maxima at 40% and steep declines at 50%. The adhesion curve for spirocysts (Fig. 6B), on the other hand, is sigmoidal, reaching a maximum at 30% and then plateauing at harder coatings of gelatin.

At concentrations of gelatin below 20% the numbers of retained mastigophores predominated by as much as 2.5-fold (Fig. 6A, D). Approximately equal numbers of mastigophores and spirocysts were retained on probes

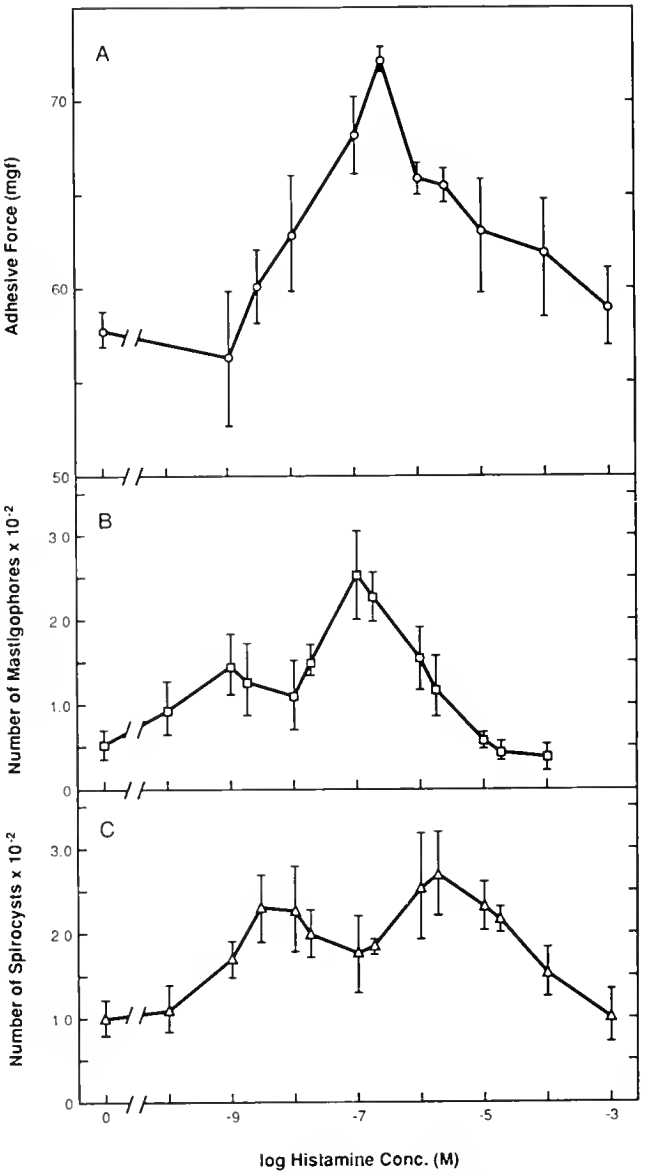

Figure 3. Dose-responses of histamine on discharge of cnidae. A. Effect of histamine on cnida-mediated adhesive force. Values express the mean of four experiments. Each experiment consists of eight replicate probes for each concentration; each probe and each tentacle is used only once (n = 32). B. Effect of histamine on the number of discharged mastigophores (n = 8). C. Effect of histamine on the number of discharged spirocysts (n = 24). The number of spirocysts was determined by the ELLSA assay on Figure 2C. Vertical bars represent the standard error of the mean at 95% confidence limit.

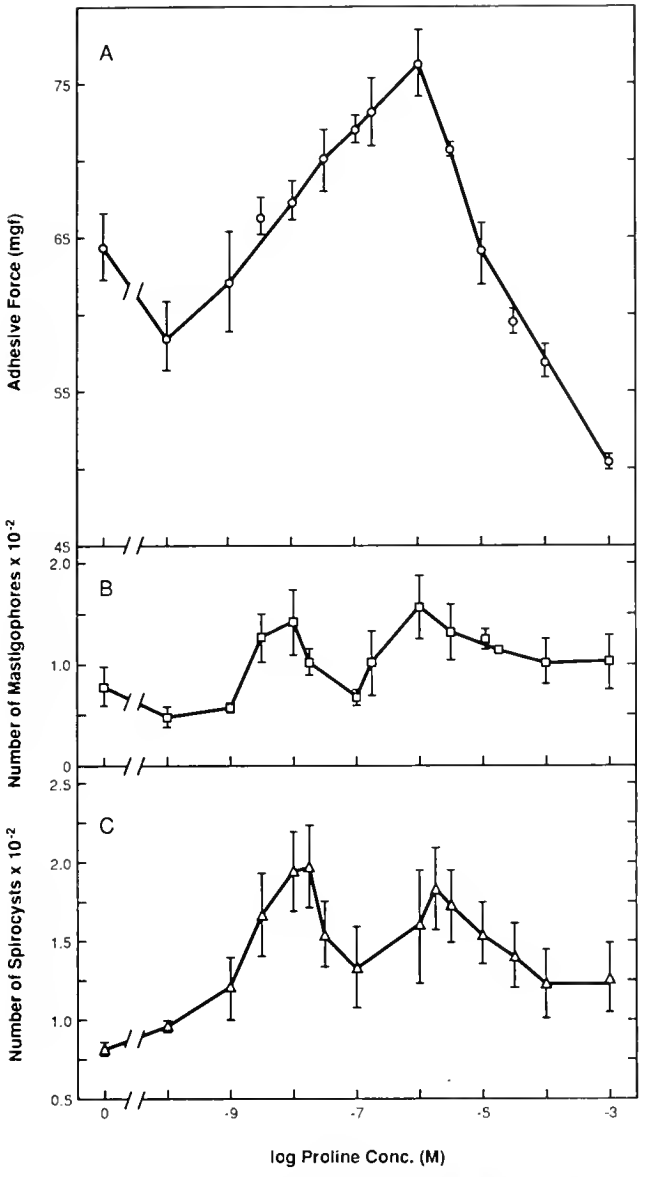

Figure 4. Dose-responses of proline on discharge of cnidae. A. Effect of proline on cnida-mediated adhesive force. Values express the mean of four experiments. Each experiment consists of eight replicate probes for each concentration; each probe and each tentacle is used only once (n = 32). B. Effect of proline on the number of discharged mastigophores (n = 7). C. Effect of proline on the number of discharged spirocysts (n = 24). The number of spirocysts was determined as in preceding figures. Vertical bars represent the standard error of the mean at 95% confidence limit.

coated with 20, 30 and 40% gelatin (Fig. 6D). However, the spirocysts predominated by about 3-fold at 50% gelatin (Fig. 6B, D).

Discussion

In the feeding tentacles of the sea anemone *Aiptasia pallida*, as in all acontiate anemones, three types of cnidae occur: the spirocysts, the microbasic p-mastigophores, and the basitrichous isorhizas (Hand, 1955). Recently, using cnida-mediated measurements of adhesive force in *A. pallida*, three different classes of chemoreceptors were identified that sensitize cnidocytes to discharge their cnidae in response to triggering mechanical stimuli (Thorington and Hessinger, 1988a, b). Although the discharge of the microbasic p-mastigophores is under the

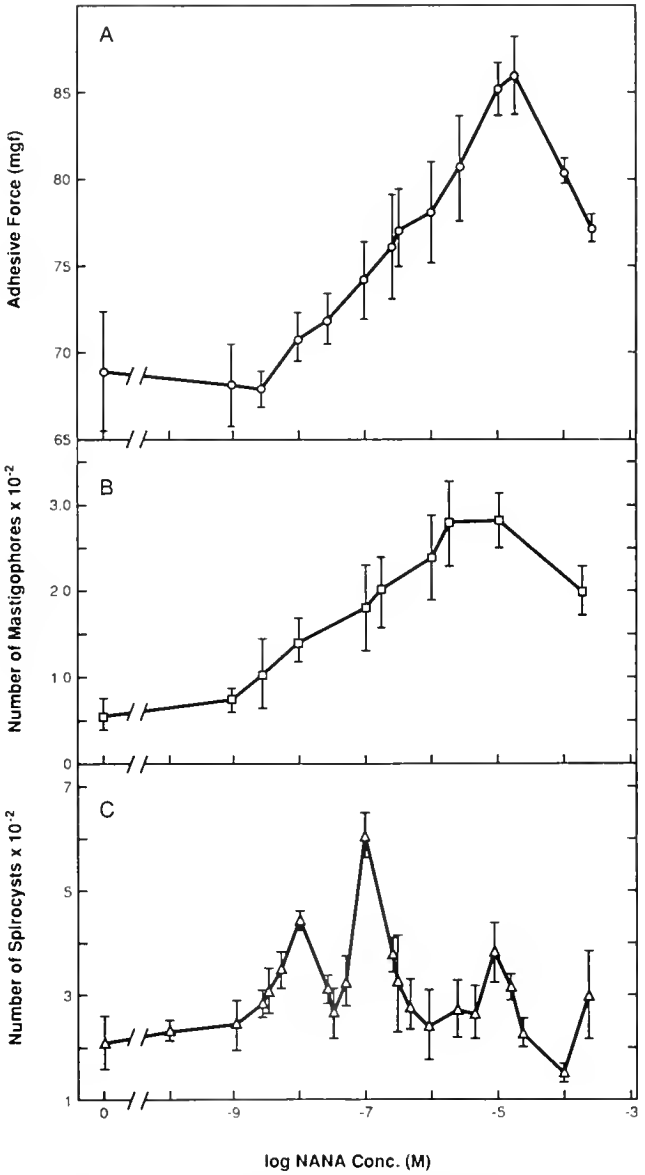

Figure 5. Dose-responses of N-acetylneuraminic acid (NANA) on discharge of cnidae. A. Effect of NANA on cnida-mediated adhesive force. Values express the mean of four experiments. Each experiment consists of eight replicate probes for each concentration; each probe and each tentacle is used only once (n = 32). B. Effect of NANA on the number of discharged mastigophores (n = 11). C. Effect of NANA on the number of discharged spirocysts (n = 24). The number of spirocysts was determined as in preceding figures. Vertical bars represent the standard error of the mean at 95% confidence limit.

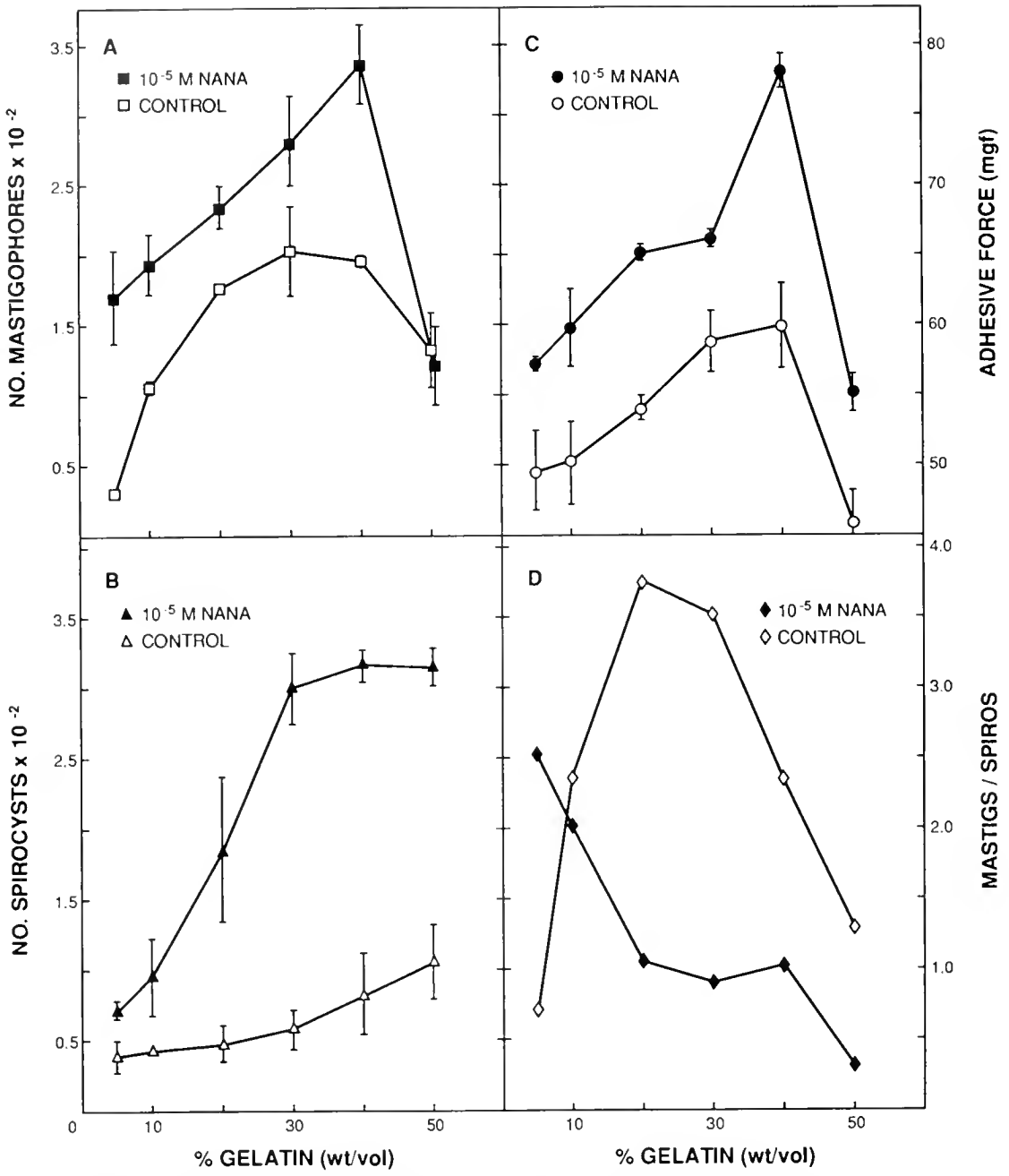

Figure 6. Dose-responses of retained discharged cnidae and of measured adhesive force using targets coated with varying concentrations of gelatin. A. Effect of target hardness on the number of mastigophores retained onto probes (n = 5). B. Effect of target hardness on the number of spirocysts retained onto probes (n = 5). C. Effect of target hardness on the measured adhesive force (n = 5). D. Ratio of retained mastigophores to retained spirocysts. All experiments were carried out either in 10^{-5} *M* N-acetylneuraminic acid or in seawater (controls). Data points are the mean ± standard error of the mean.

influence of at least two classes of sensitizing agonists, namely glycine and N-acetylated sugars (Geibel *et al.*, 1988), it is unknown whether such chemosensitizers, along with a third class of sensitizers, typified by heterocyclic amino compounds, also elicit similar responses from spirocytes.

Spirocysts have been described ultrastructurally (Mariscal and McLean, 1976; Mariscal *et al.*, 1976, 1977), but few experimental studies have been performed on spirocytes. The qualitative effects of remote mechanical stimuli (Conklin and Mariscal, 1976) and of food extracts (Williams, 1968) on the discharge of spiro-

cysts have been reported. Until now, the local, chemical control of spirocyst discharge and the purported primary role of spirocysts in retaining captured prey has not been quantitatively or experimentally verified. This lack of information is due in large part to the difficulty of detecting discharged spirocysts because they possess a highly transparent and non-refractile capsule. The counting of discharged spirocysts by optical methods is further complicated by the fact that the everted tubules entangle extensively. While the visibility of the capsules of discharged spirocysts is enhanced with phase contrast optics, the counting of these cnida is, nonetheless, tedious and time-consuming.

A rapid and sensitive assay of discharged spirocysts

To circumvent these problems, we developed a sensitive indirect, solid-state, enzyme-linked lectin sorbant assay (ELLSA) to detect discharged spirocysts. The assay is highly reproducible and is significantly faster than visually counting discharged spirocysts using phase contrast optics. The potential applications of this procedure include enumerating discharged spirocysts on experimental targets as well as detecting and characterizing the adhesive substance of spirocysts. In the present report we use this assay to study the effects on spirocyst discharge of two classes of substances known to sensitize the discharge of mastigophores (Geibel *et al.*, 1988), in addition to a third class of sensitizer known to sensitize cnida-mediated adhesive force (Thorington and Hessinger, 1988b).

Sensitization of spirocytes to discharge spirocysts

We have found that the three known classes of sensitizers as typified by glycine, NANA, and the heterocyclic amino compounds, histamine and proline, all sensitize spirocyst- and mastigophore-bearing CSCCs, albeit in very different and specific ways. In spite of the variability in sensitivity, magnitude, and pattern of spirocyte responsiveness induced by these agonists, each of the dose-response profiles consists of one or more biphasic peaks. Each biphasic peak reveals a region of sensitization reaching a maximal effect (E_{max}), followed by a region of desensitization at higher concentrations. The dose-response parameters (Table I) indicate that the discharge of spirocysts is most sensitive to glycine, followed by histamine, proline, and then NANA, while the discharge of mastigophores is most sensitive to histamine, followed by proline, NANA, and glycine. The differences in the sensitivity of spirocytes and nematocytes to glycine were the most pronounced.

In addition to differences in sensitivity to agonists, the dose-response patterns also exhibited differences. In contrast to the modal (*i.e.* biphasic) dose-responses exhibited by measurements of adhesive force (Thorington and Hessinger, 1988a, b; Geibel *et al.*, 1988; Figs. 2A, 3A, 4A, 5A), we observe that dose-responses of the discharge of spirocysts to glycine is modal, while the dose-responses to proline and histamine are both bimodal, and the response to NANA is trimodal. These contrast to the dose-responses of discharging mastigophores, which for glycine and NANA are modal, while for proline and histamine are bimodal. Although the dose-responses of mastigophore and spirocyst discharge are not coincidental for any of the tested agonists, except possibly proline, the fact that all of the adhesive force dose-response curves are coincidental with those of the mastigophores implies that discharging mastigophores contribute significantly more to adhesive force than do discharging spirocysts.

Are all of the receptors effecting multimodal responses (*i.e.*, NANA) associated directly with the cnidocytes or possibly located on remote sites where they exert indirect control over cnidocyte responsiveness, such as via the nervous system or by initiating changes in behavior that affect the availability of cnidae to discharge? By using mucin-labelled colloidal gold, we find that 99.4% of the labelled gold binds to supporting cells adjacent to spirocytes and nematocytes (Watson and Hessinger, 1988), while no label binds to tentacle sensory cells. We conclude that the receptors to the multimodal agonist, NANA, are entirely located on supporting cells of CSCCs and not on remote sensory sites.

A salient feature of modal dose-responses is that the response is "turned off" at concentrations of agonist exceeding those needed to evoke a maximum response. Where multimodal responses are exhibited, high concentrations of agonist turn off the response of CSCCs having dose-response maxima below that concentration. The existence of bimodal and, particularly, trimodal dose-responses provides for discharge of cnidae over a wide range of agonist concentrations while ensuring that only a portion of the available CSCCs are sensitized at any one time and dose. Thus, the total number of discharging cnidae never reaches the total number present. This effectively conserves cnidae by preventing both excessive discharge against living prey and nonproductive discharge against killed prey.

Multiple populations of cnidocyte/supporting cell complexes (CSCCs)

The display of bimodal and trimodal dose-responses implies the existence of multiple populations of spirocytes distinguished by different sensitivities (*i.e.*, $K_{0.5}$ values) to a given agonist. That multiple populations of CSCCs exist is indicated by the fact that there are CSCCs, termed type C CSCCs, that discharge their cnidae in response to tactile stimuli in the absence of added agonist (Figs. 2, 3, 4, 5), in addition to CSCCs, termed type B

CSCCs, that require chemosensitization by agonists before they can be triggered to discharge by static (*i.e.*, non-vibrating) targets. Furthermore, mastigophore-bearing CSCCs triggered by targets vibrating at specific frequencies (Watson and Hessinger, 1989) are termed type A CSCCs. Although we do not yet know if vibration-sensitive, spirocyst-bearing type A CSCCs exist, there obviously exist different populations of spirocyst- and nematocyst-containing CSCCs distinguished by differences in their sensitivities and specificities to agonists and by the ways they are triggered by mechanical stimuli to discharge their cnidae.

Roles of discharged mastigophores and spirocysts in the capture of prey

In the light of our current findings, the commonly accepted roles of the spirocysts and the mastigophores in the capture and adherence of prey must be re-evaluated and modified. We consider these matters from the perspectives of two questions addressed by this report: (i) which of the two kinds of discharged cnida contribute most to cnida-mediated adhesive force; and (ii) which physical types of target retain the two kinds of cnida.

To adequately address the first question, we must recognize that the cnida-mediated components of adhesive force measurements reflect both the number and the kinds of cnidae discharging onto targets. A quantitative analysis of the contributions and magnitudes of these individual factors to adhesive force is beyond the scope of the present discussion, but we can make preliminary qualitative assessments based upon the findings presented here. We have seen for several agonists that the dose-responses for adhesive force measurements and for the number of discharged mastigophores coincide and more closely resemble each other than do the dose-responses for discharging spirocysts (Figs. 2–5). This is also seen by comparing EC_{100} values for the discharge of cnidae with those for adhesive force (Table 1). To assess the second question, we performed measurements of adhesive force and cnidae discharge in which the hardness of the gelatin-coating on the target probes was varied. With gelatin coatings below 20%, the number of discharged mastigophores retained on the target probes predominated over spirocysts (Fig. 6A, D), presumably because proportionally fewer discharging spirocysts can adhere to the "softer" targets. Equal and maximal numbers of mastigophores and spirocysts are retained on probes coated with 20, 30, and 40% gelatin (Fig. 6D). Above 40% gelatin, however, the spirocysts predominate (Fig. 6B, D), presumably because mastigophores are incapable of penetrating these "harder" targets. Thus, when the targets are too soft for the discharging spirocysts to adhere, the penetrant nematocysts predominate as the kind of cnida retained on the target and, collectively, they are the primary contributors to measured adhesive force. On the other hand, when targets are too hard for the discharging mastigophores to penetrate, then the spirocysts predominate as the retained cnida and, collectively, they provide the major contribution to adhesive force. Thus, the correlation between measured adhesive force and the number of discharging mastigophores on both dose-responsive curves and on adhesion curves suggests that discharged mastigophores contribute significantly more to adhesive force than do discharged spirocysts under conditions in which the target is penetrable to discharging mastigophores.

Conclusions

In this paper, we show that the discharge of spirocysts is chemosensitized by the same agonists that sensitize the discharge of mastigophores. That is not to say that there may not also exist agonists that sensitize only the discharge of mastigophores or of spirocysts. However, the dose-responses of these two kinds of cnidae differ both qualitatively and quantitatively.

The dose-responses of discharging mastigophores are either modal (*e.g.*, to glycine and NANA) or bimodal (*e.g.*, to proline and histamine), and are coincidental to dose-responses obtained from measuring adhesive force under the same conditions. We have presented strong evidence that the similarity between the dose-response curves of adhesive force measurements and the discharge of mastigophores is due to the discharged mastigophores contributing significantly more to cnida-mediated adherence onto 30% gelatin-coated targets than the discharged spirocysts.

It seems appropriate, therefore, to modify the purported roles of penetrant microbasic p-mastigophores and adhesive spirocysts in the capture of prey. Spirocysts have been generally regarded as the primary means by which adhesion of prey to the tentacle occurs (Williams, 1968; Doumenc, 1971; McFarlane and Shelton, 1975; Mariscal, 1984). Mastigophores have been regarded as primarily penetrating and envenomating prey while, by implication, not contributing significantly to prey adhesion unless the tubules wrap around bristles or projections on prey (Mariscal, 1984). Our findings, however, indicate that mastigophores play a significant, and sometimes primary, role in the adhesion of prey, depending most likely upon the hardness of the prey surface. Indeed, it appears that mastigophores and spirocysts may be complimentary in their relative contributions to prey adhesion so that the contribution of mastigophores to adhesive force predominates with soft-surfaced targets, which they can penetrate. The contribution of spirocysts to adhesive force predominates when the target surface is hard enough for the spirocysts to adhere and too hard for the mastigophores to penetrate. Thus, in addition to

penetrating and immobilizing prey, discharging mastigophores contribute significantly, even predominantly, to the adhesion of prey, provided they are able to penetrate the surface of the prey.

Acknowledgments

Funded in part by NSF grant DCB-8609859 to D.A.H.

Literature Cited

Bigger, C. H. 1982. The cellular basis of the aggressive acrorhagial response of sea anemones. *J. Morphol.* **173:** 259–278.

Conklin, E. J., and R. N. Mariscal. 1976. Increase in nematocyst and spirocyst discharge in a sea anemone in response to mechanical stimulation. Pp. 549–558 in *Coelentrate Ecology and Behaviour,* G. O. Mackie, ed. Plenum Press, New York.

Doumenc, D. 1971. Aspects morphologiques de la dévagination du spirocyste chez *Actinia equina. L. J. Microsc.* **12:** 263–270.

Ewer, R. F. 1947. On the functions and mode of action of the nematocysts of hydra. *Proc. Zool. Soc. Lond.* **117:** 365–376.

Francis, L. 1973. Intraspecific aggression and its effect on the distribution of *Anthopleura elegantissima* and some related sea anemones. *Biol. Bull.* **144:** 73–92.

Geibel, G., G. Thorington, R. Y. Lim, and D. A. Hessinger. 1988. Control of cnida discharge: II. Microbasic p-mastigophore nematocysts are regulated by two classes of chemoreceptors. *Biol Bull.* **175:** 132–136.

Hand, C. 1955. The sea anemones of central California. Part III. The acontiarian anemones. *Wasmann J. Biol.* **13:** 189–251.

Mariscal, R. N. 1972. The nature of adhesion to shells of the symbiotic sea anemone *Calliactis tricolor.* (Leseur). *J Exp. Mar. Bio. Ecol.* **8:** 217–224.

Mariscal, R. N. 1974. Nematocysts. Pp. 129–178 in *Coelenterate Biology: Reviews and New Perspectives,* L. Muscatine and H. M. Lenhoff, eds. Academic Press, New York.

Mariscal, R. N. 1984. Cnidaria: Cnidae. Pp. 57–68 in *Biology of the Integument,* Vol. I. Invertebrates, J. Bereiter-Hahn, A. G. Maltolsy, and K. S. Richards, eds. Springer-Verlag, Berlin.

Mariscal, R. N., and R. B. McLean. 1976. The form and function of cnidarian spirocysts. II. Ultrastructure of the tip and wall and mechanism of discharge. *Cell Tissue Res.* **169:** 313–321.

Mariscal, R. N., C. H. Bigger, and R. B. McLean. 1976. The form and function of cnidarian spirocysts. I. Ultrastructure of the capsule exterior and relationship to the tentacles sensory surface. *Cell Tissue Res.* **168:** 465–474.

Mariscal, R. N., R. B. McLean, and C. Hand. 1977. The form and function of cnidarian spirocysts. III. Ultrastructure of the thread and the function of spirocysts. *Cell Tissue Res.* **178:** 427–433.

Mariscal, R. N., E. J. Conklin, and C. H. Bigger. 1978. The putative sensory receptors associated with the cnidae of cnidarians. *Scanning Electron Microsc.* **2:** 959–966.

McFarlane, I. D., and G. A. B. Shelton. 1975. The nature of the adhesion of tentacles to shells during shell-climbing in the sea anemone *Calliactis parasitica* (Couch). *J. Exp. Mar. Biol. Ecol.* **17:** 177–186.

Picken, L. E. R., and R. J. Skaer. 1966. A review of researches on nematocysts. In *The Cnidarians and Their Evolution,* W. J. Rees, ed. *Symp. Zool. Soc. Lond.* **16:** 15–50.

Purcell, J. E. 1977. Aggressive function and induced development of catch tentacles in the sea anemone *Metridium senile* (Coelenterata, Actiniaria). *Biol Bull* **153:** 355–368.

Skaer, R. J., and L. E. R. Picken. 1965. The structure of the nematocyst thread and the geometry of discharge in *Corynactis viridis.* (Allman). *Phil Trans. Roy. Soc. Lond* **250:** 131–164.

Stephenson, T. A. 1929. On the nematocysts of sea anemones. *J Mar Biol. Assoc. U.K.* **16:** 173–200.

Thorington, G. U., and D. A. Hessinger. 1988a. Control of cnida discharge: I. Evidence for two classes of chemoreceptors. *Biol. Bull.* **174:** 163–171.

Thorington, G., and D. A. Hessinger. 1988b. Control of discharge: factors affecting discharge of cnidae. Pp. 233–253 in *Biology of Nematocysts,* D. A. Hessinger and H. M. Lenhoff, eds. Academic Press, San Diego.

Watson, G., and R. Mariscal. 1983. The development of a sea anemone tentacle specialized for aggression: morphogenesis and regression of the catch tentacle of *Haliplanella luciae* (Cnidaria, Anthozoa). *Biol. Bull.* **164:** 507–517.

Watson, G., and D. A. Hessinger. 1988. Localization of a purported chemoreceptor involved in triggering cnida discharge in sea anemones. Pp. 255–272 in *Biology of Nematocysts,* D. A. Hessinger and H. M. Lenhoff, eds. Academic Press, San Diego.

Watson, G., and D. A. Hessinger. 1989. Cnidocyte mechanoreceptors are tuned to the movements of swimming prey by chemoreceptors. *Science* **243:** 1589–1591.

Weill, R. 1934. Contribution a l'étude des cnidaires et de leurs nématocysts. I. Réchérches sur les nématocystes. *Trav. Sta. Zool. Wimereux* **10:** 1–347.

Williams, R. B. 1968. Control of the discharge of cnidae in *Diadumene luciae* (Verill). *Nature* **219:** 959.

CONTENTS

Volume 178 Number 2

THE BIOLOGICAL BULLETIN

APRIL, 1990

Published by the Marine Biological Laboratory

THE
BIOLOGICAL BULLETIN

PUBLISHED BY
THE MARINE BIOLOGICAL LABORATORY

APRIL, 1990

Printed and Issued by
LANCASTER PRESS, Inc.
PRINCE & LEMON STS.
LANCASTER, PA

THE BIOLOGICAL BULLETIN

THE BIOLOGICAL BULLETIN is published six times a year by the Marine Biological Laboratory, MBL Street, Woods Hole, Massachusetts 02543.

Subscriptions and similar matter should be addressed to Subscription Manager, THE BIOLOGICAL BULLETIN, Marine Biological Laboratory, Woods Hole, Massachusetts 02543. Single numbers, $25.00. Subscription per volume (three issues), $57.50 ($115.00 per year for six issues).

Communications relative to manuscripts should be sent to Michael J. Greenberg, Editor-in-Chief, or Pamela L. Clapp, Managing Editor, at the Marine Biological Laboratory, Woods Hole, Massachusetts 02543. Telephone: (508) 548-3705, ext. 428. FAX: 508-540-6902.

POSTMASTER: Send address changes to THE BIOLOGICAL BULLETIN, Marine Biological Laboratory, Woods Hole, MA 02543.

Second-class postage paid at Woods Hole, MA, and additional mailing offices.
ISSN 0006-3185

INSTRUCTIONS TO AUTHORS

The Biological Bulletin accepts outstanding original research reports of general interest to biologists throughout the world. Papers are usually of intermediate length (10–40 manuscript pages). Very short papers (less than 9 manuscript pages including tables, figures, and bibliography) will be published in a separate section entitled "Notes." A limited number of solicited review papers may be accepted after formal review. A paper will usually appear within four months after its acceptance.

The Editorial Board requests that manuscripts conform to the requirements set below; those manuscripts that do not conform will be returned to authors for correction before review.

1. ***Manuscripts.*** Manuscripts, including figures, should be submitted in triplicate. (Xerox copies of photographs are not acceptable for review purposes.) The original manuscript must be typed in no smaller than 12 pitch, using double spacing (*including* figure legends, footnotes, bibliography, etc.) on one side of 16- or 20-lb. bond paper, 8½ by 11 inches. Please, no right justification. Manuscripts should be proofread carefully and errors corrected legibly in black ink. Pages should be numbered consecutively. Margins on all sides should be at least 1 inch (2.5 cm). Manuscripts should conform to the *Council of Biology Editors Style Manual*, 4th Edition (Council of Biology Editors, 1978) and to American spelling. Unusual abbreviations should be kept to a minimum and should be spelled out on first reference as well as defined in a footnote on the title page. Manuscripts should be divided into the following components: Title page, Abstract (of no more than 200 words), Introduction, Materials and Methods, Results, Discussion, Acknowledgments, Literature Cited, Tables, and Figure Legends. In addition, authors should supply a list of words and phrases under which the article should be indexed.

2. ***Title page.*** The title page consists of: a condensed title or running head of no more than 35 letters and spaces, the manuscript title, authors' names and appropriate addresses, and footnotes listing present addresses, acknowledgments or contribution numbers, and explanation of unusual abbreviations.

3. ***Figures.*** The dimensions of the printed page, 7 by 9 inches, should be kept in mind in preparing figures for publication. We recommend that figures be about 1½ times the linear dimensions of the final printing desired, and that the ratio of the largest to the smallest letter or number and of the thickest to the thinnest line not exceed 1:1.5. Explanatory matter generally should be included in legends, although axes should always be identified on the illustration itself. Figures should be prepared for reproduction as either line cuts or halftones. Figures to be reproduced as line cuts should be unmounted glossy photographic reproductions or drawn in black ink on white paper, good-quality tracing cloth or plastic, or blue-lined coordinate paper. Those to be reproduced as halftones should be mounted on board, with both designating numbers or letters and scale bars affixed directly to the figures. All figures should be numbered in consecutive order, with no distinction between text and plate figures. The author's name and an arrow indicating orientation should appear on the reverse side of all figures.

4. ***Tables, footnotes, figure legends, etc.*** Authors should follow the style in a recent issue of *The Biological Bulletin* in preparing table headings, figure legends, and the like. Because of the high cost of setting tabular material in type, authors are asked to limit such material as much as possible. Tables, with their headings and footnotes, should be typed on separate sheets, numbered with consecutive Roman numerals, and placed after the Literature Cited. Figure legends should contain enough information to make the figure intelligible separate from the text. Legends should be typed double spaced, with consecutive Arabic numbers, on a separate sheet at the end of the paper. Footnotes should be limited to authors' current addresses, acknowledgments or contribution numbers, and explanation of unusual abbreviations. All such footnotes should appear on the title page. Footnotes are not normally permitted in the body of the text.

5. ***Literature cited.*** In the text, literature should be cited by the Harvard system, with papers by more than two authors cited as Jones *et al.*, 1980. Personal communications and material in preparation or in press should be cited in the text only, with author's initials and institutions, unless the material has been formally accepted and a volume number can be supplied. The list of references following the text should be headed Literature Cited, and must be typed double spaced on separate

pages, conforming in punctuation and arrangement to the style of recent issues of *The Biological Bulletin*. Citations should include complete titles and inclusive pagination. Journal abbreviations should normally follow those of the U. S. A. Standards Institute (USASI), as adopted by BIOLOGICAL ABSTRACTS and CHEMICAL ABSTRACTS, with the minor differences set out below. The most generally useful list of biological journal titles is that published each year by BIOLOGICAL ABSTRACTS (BIOSIS List of Serials; the most recent issue). Foreign authors, and others who are accustomed to using THE WORLD LIST OF SCIENTIFIC PERIODICALS, may find a booklet published by the Biological Council of the U.K. (obtainable from the Institute of Biology, 41 Queen's Gate, London, S.W.7, England, U.K.) useful, since it sets out the WORLD LIST abbreviations for most biological journals with notes of the USASI abbreviations where these differ. CHEMICAL ABSTRACTS publishes quarterly supplements of additional abbreviations. The following points of reference style for THE BIOLOGICAL BULLETIN differ from USASI (or modified WORLD LIST) usage:

A. Journal abbreviations, and book titles, all underlined (for *italics*)

B. All components of abbreviations with initial capitals (not as European usage in WORLD LIST *e.g. J. Cell. Comp. Physiol.* NOT *J. cell. comp. Physiol.*)

C. *All* abbreviated components must be followed by a period, whole word components *must not* (*i.e. J. Cancer Res.*)

D. Space between all components (*e.g. J Cell. Comp. Physiol.*, not *J.Cell.Comp.Physiol.*)

E. Unusual words in journal titles should be spelled out in full, rather than employing new abbreviations invented by the author. For example, use *Rit Fisindafjélags Islendinga* without abbreviation.

F. All single word journal titles in full (*e.g. Veliger, Ecology, Brain*).

G. The order of abbreviated components should be the same as the word order of the complete title (*i.e. Proc.* and *Trans.* placed where they appear, not transposed as in some BIOLOGICAL ABSTRACTS listings).

H. A few well-known international journals in their preferred forms rather than WORLD LIST or USASI usage (*e.g. Nature, Science, Evolution* NOT *Nature, Lond., Science, N.Y.; Evolution, Lancaster, Pa.*)

6. ***Reprints, page proofs, and charges.*** Authors receive their first 100 reprints (without covers) free of charge. Additional reprints may be ordered at time of publication and normally will be delivered about two to three months after the issue date. Authors (or delegates for foreign authors) will receive page proofs of articles shortly before publication. They will be charged the current cost of printers' time for corrections to these (other than corrections of printers' or editors' errors). Other than these charges for authors' alterations, *The Biological Bulletin* does not have page charges.

Reference: *Biol. Bull.* **178**: 85–93. (April, 1990)

The Sperm Transfer System in *Kinbergonuphis simoni* (Polychaeta:Onuphidae)

HWEY-LIAN HSIEH[1] AND JOSEPH L. SIMON

Department of Biology, University of South Florida, Tampa, Florida 33620

Abstract. Tube dwelling *Kinbergonuphis simoni* (Santos, Day and Rice) achieves a 98.9% fertilization efficiency by means of a sperm transfer system involving spermatophores and seminal receptacles. The spermatophores are mushroom-shaped structures released as clumps. The seminal receptacles are paired sac-like organs embedded in the dorsal epidermis of female genital segments. Males release spermatophores into the environment, and females pick them up with their ventral palps and first pair of parapodia. Stored sperm remain viable for fertilization for at least one month. Spermatophore release and egg laying are independent of the presence of the opposite sex. Advantages associated with this system are discussed, and include asynchronous reproduction, a long breeding season, reduced sperm loss, and reduced exposure to risks. This sperm transfer mode is the first reported in the family Onuphidae and is proposed for other small, tube-dwelling onuphids.

Introduction

Sperm transfer in polychaetes occurs in two main modes: non-aggregate transfer, in which sperm are free swimming and not packed together before reaching eggs; and aggregate transfer, in which sperm are packed together by varying complex structures before reaching eggs.

Of the non-aggregate transfer modes, three different types have been recorded: broadcast spawning (Clark, 1961; Schroeder and Hermans, 1975), copulation (Just, 1914; Gray, 1969; Schroeder and Hermans, 1975; Westheide, 1984), and pseudocopulation (Reish, 1957; Pettibone, 1963; Daly, 1973). Three types of aggregate transfer have been recognized: indirect hypodermic impregnation, free transfer of spermatophores, and free transfer of spermatozeugmata. Among these three types, spermatozeugmata transfer (Austin, 1963; Eckelbarger, 1974) has not been elucidated with certainty, and will not be discussed further here.

In hypodermic impregnation, males actively place spermatophores on the body surface of females. Sperm may then be collected into seminal receptacles, or may penetrate through the epidermis into the coelom of females (Ax, 1968; Jouin, 1970; Westheide, 1984). In free transfer, the spermatophores are released into the environment and later picked up by females. Seminal receptacles are often noted. Free spermatophore transfer has been well demonstrated in members of the spionid genus *Polydora* (Rice, 1978a, 1987a), and has been strongly suggested to occur in serpulids and sabellids (Daly and Golding, 1977; Picard, 1980). The members of these three Families are tube dwellers.

Life history characteristics and habitat choice have been considered strong selective forces for the mode of sperm transfer (Rice, 1978a; Clark, 1981; Mann, 1984; Westheide, 1984). For example, sessile or tube dwelling life styles limit direct bodily contact, or decrease the mobility of individuals so that encounters between sexes are infrequent or impossible; thus, neither copulation, pseudocopulation, nor indirect hypodermic impregnation would be favored. Broadcast spawning or free transfer of spermatophores may be the only alternative for such species. However, broadcast spawning requires large numbers of gametes and synchronous reproduction in the population. The disadvantages of broadcast spawning have been reported (*e.g.*, in corals, Harrison *et al.*, 1984; Shlesinger and Loya, 1985; and in sea urchins, Pennington, 1985). In contrast, free spermatophore transfer with sperm storage, as found in the spionid *Poly-*

Received 17 October 1989; accepted 29 January 1990.

[1] Present address: Institute of Zoology, Academia Sinica, Taipei, Taiwan, 11529 R. O. C.

dora, has been proposed as an efficient low risk mode of sexual reproduction (Rice, 1978a). Liberation of spermatophores into the sea also has been considered as an adaptive character in sessile tubicolous pogonophorans (Flügel, 1977) and vermetid gastropods (Hadfield and Hopper, 1980). Recently, a high efficiency of fertilization has been recorded in bivalves with similar free spermatophore transfer (Ó Foighil, 1985).

Reproduction in the Onuphidae has been reviewed in general, and developmental patterns have been studied in a few species (Blake, 1975; Fauchald, 1983; Paxton, 1986; Hsieh and Simon, 1987). However, no studies have been done on sperm transfer modes in this group. The characteristics of life style and life history of *Kinbergonuphis simoni* are similar to those of many *Polydora* species. Both are dioecious tube dwellers and are small in size. Females produce few, large yolky eggs, brood their young in the tubes, and have an extended breeding season (Rice, 1978a, b; Hsieh and Simon, 1987; Hsieh and Simon, unpub. data).

The goals of this study are to address: (1) the mode of sperm transfer in *Kinbergonuphis simoni;* (2) the fertilization efficiency of this mode; and (3) the possibility that the mode represents convergent evolution between spionids and onuphids.

Materials and Methods

Seminal receptacles

Worms were collected from an intertidal sandy flat in Upper Tampa Bay, Florida, and brought alive into the laboratory in January 1985. The presence of seminal receptacles was determined as follows: Two treatments—control and isolation—were set up. Five replicates were used as controls. In each replicate, a pair of male and female worms were reared in a plastic dish surrounded by mesh cloth to keep adults and juveniles from escaping. In the isolation experiment, seven females were separately incubated in the same way. Three of the seven females were brooding when experiments began. The females were tapped out of their tubes and thus separated from their young. These young were at embryonic or segmented stages. Seawater, which had been sealed in jars for four months, was filtered through Whatman No. 1 filter paper before being added to the aquaria. Salinity and temperature were maintained at 22‰ and 20°C, respectively. The presence of larvae and juveniles was noted at one- or two-week intervals. This study was conducted for three months.

Spermatophores

Mature worms were collected in March 1988 to determine the occurrence of spermatophores. In the laboratory, males were reared in mesh-enclosed dishes with and without females. Salinity was kept at 22–24‰, and temperature at 20–22°C. Observations on behavior and spermatophore production were made at intervals of 2 to 3 h during daylight hours for three weeks. In all laboratory experiments, the worms were fed ground alfafa.

Seminal receptacles and spermatophores: morphology

Mature females collected in May 1985, were prepared for paraffin sections after being fixed in Bouin's fixative. Subsequently, they were cut into 7- to 10-μm sections and stained in Ehrlich's hematoxylin and eosin (Knudsen, 1966). Spermatophores were prepared for SEM studies following the procedures of Hsieh and Simon (1987).

Fertilization efficiency

Worms were collected at the study site monthly in 1982, and from June to October in 1985, to determine the fertilization efficiency. Worms were relaxed in 0.15% propylene phenoxytol and fixed in 10% formalin in the field. Broods were examined in the laboratory. Unfertilized eggs could be recognized by a white coloration and a clear space appearing at one end (Fig. 1). Only the broods at early developmental stages (blastula to 5-setiger stages) were used to avoid underestimating the number of unfertilized eggs due to disintegration. Fertilization efficiency was expressed as the percentage of eggs fertilized of all eggs spawned.

Results

Seminal receptacles

Table I shows that, over three months, paired females produced one to three normally developing broods. Isolated females also laid eggs, suggesting that spawning was not induced by the presence of males. In some isolated females (No. 3, 4, and 6), eggs were present in maternal tubes, but no development was observed. In four of the seven isolated females, each produced only one viable brood, indicating that females did store sperm, but that the amount was insufficient for subsequent broods. In isolated females, 0 to 7 juveniles were produced, while in control pairs 9 to 64 offspring were produced (Table I).

Spermatophores

Spermatophores were released from male tube openings as clumps, which stuck to the bottom of the culture dishes or to pieces of debris. Occasionally, in clean dishes where no food particles were present, spermatophores were trapped in the water surface film. Freshly released spermatophores were white, almost transparent, very

Table I

Comparison of breeding success between isolated females and paired males and females of Kinbergonuphis simoni *reared in the laboratory from January to March, 1985*

	Date (1985)								
Treatment	Jan 27	Feb 3	10	17	24	Mar 3	9	Number of viable broods produced	Number of juveniles produced
Control pairs									
1	*	J, 3		*	*	*	J, 6, *	2	9
2	J, 27	*	*	J, 9	*	*	J, 28	3	64
3	*	*	*	*	J, 17			1	17
4	J, 18	*	*	J, 16, *	*	*	J, 8	3	42
5	J, 5	*	*	*	J, 7			2	12
Isolated females									
1	*	J, 2						1	2
2		*	*	*	J, 4			1	4
3		*	*	*	*			0	0
4		*	*	*	*			0	0
5 brooder	*	J, 3						1	3
6 brooder		*	*	*	*			0	0
7 brooder	*	J, 7						1	7

* Larvae or eggs present in maternal tubes; J = juveniles present in dishes; numerals following J = brood sizes.

sticky, and easily broken when handled. Motile sperm were observed inside the intact spermatophores. The thin mucous sheets to which the spermatophores were attached were quickly broken down by ciliates or rotifers; however, the spermatophores themselves remained intact for more than 48 h.

Spermatophores produced at one time by individual males could form more than one clump. The number of spermatophores in each clump varied, ranging from 33 to 160 (mean ± 1 S.E. = 84.90 ± 12.66, n = 10). The average number of spermatophores produced by an individual male at one time was 80.25 ± 18.26 (n = 4). Spermatophores were present in all of the culture dishes, with or without females, indicating that production of spermatophores was not influenced by the presence of females or other males.

Seminal receptacles and spermatophores: morphology

Seminal receptacles are found in the genital segments of females, which run roughly from the 80th segment to the 100th segment. They are located dorsal and posterior to the nephridiopores, near the intersegmental junctions (Figs. 2, 3). Seminal receptacles are paired, blind, sac-like organs embedded in the body wall (Fig. 4). Each sac is about 40 μm long, and possesses a single 6 μm wide opening to the exterior. The wall of the sac is composed of columnar cells, except at the blind end where cuboidal cells predominate (Fig. 5). Some sacs are branched into two to four lobes (Fig. 6), and the number of lobes varies among and within females.

Each spermatophore is mushroom shaped, with a stalk and a spherical portion (Figs. 7, 8) containing sperm. Heads of individual spermatophores are about 40 μm in diameter, with the stalk about 135 μm in length. The spherical heads are covered by two layers, the outer characterized by a granular appearance, and the inner one with symmetrically arranged bands (Fig. 9a–c). Not every spermatophore produced is equipped with both layers, some occasionally lacking the outer layer (see arrows in Fig. 7). The sperm from broken spermatophores are morphologically identical to mature sperm seen in the coeloms of males (Fig. 10; also see Fig. 20c in Hsieh, 1984).

Transfer of spermatophores

Although the direct release of spermatophores from male gonoducts was not observed, expulsion of spermatophores from the tube openings of males was observed several times. When spermatophores were placed around the tube openings of female worms, these females—usually within one minute—would extend their anterior body portions out of the tubes, searching. Upon locating the spermatophores, they would pick them up with their first pair of parapodia and ventral palps, and then immediately withdraw to their tubes. In one instance, some spermatophores were literally carried out of a female's tube by larvae when the female and larvae were disturbed by routine observations. Upon examination under SEM, these spermatophores did not contain the outer granular layer (see Fig. 9c), suggesting that fe-

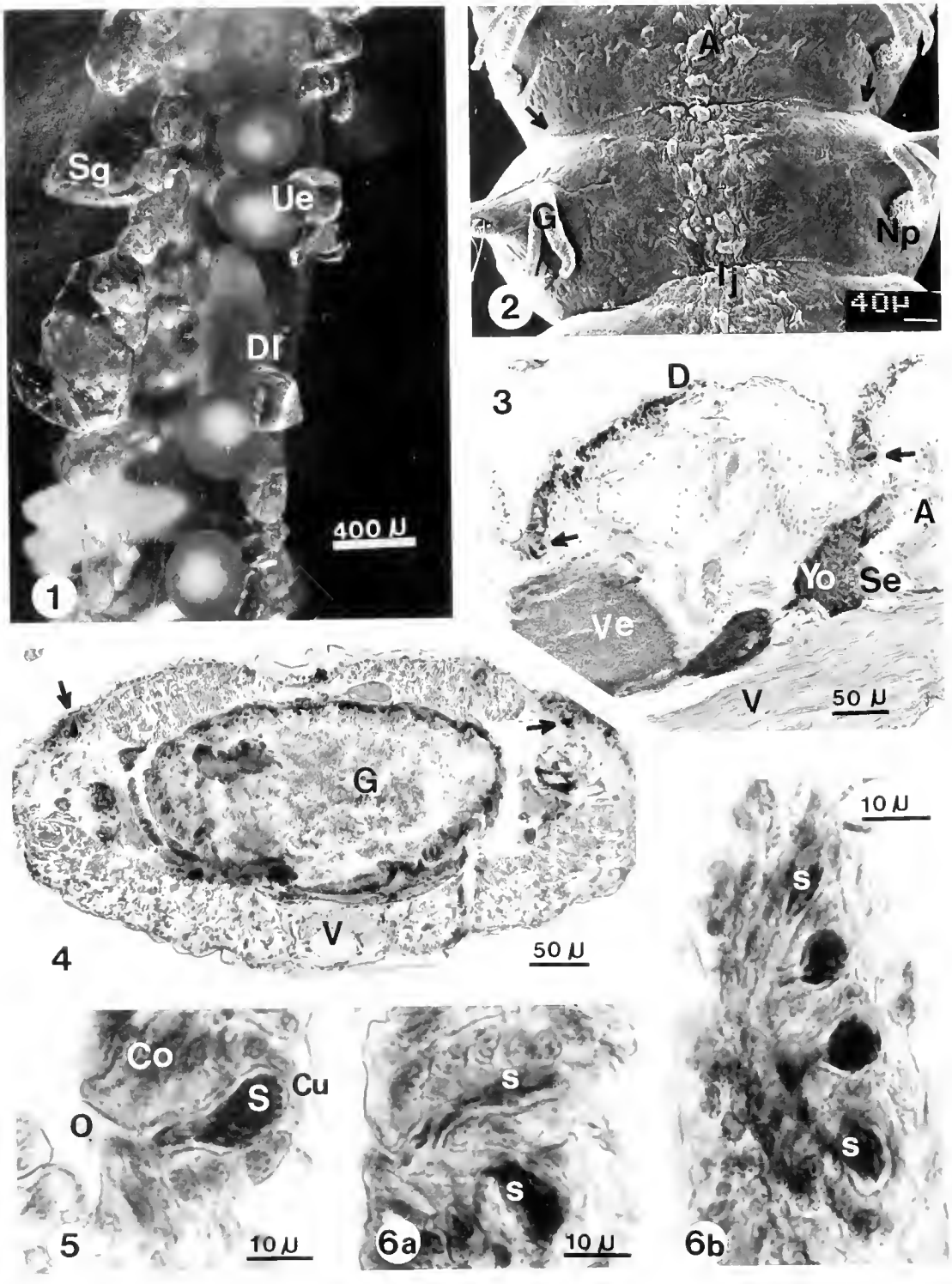

Figure 1. Unfertilized eggs and a developing embryo within a tube of *Kinbergonuphis simoni*. Dl = developing larva with 5 setigers; Ue = unfertilized eggs; Sg = sand grains.

Figure 2. Dorsal view (SEM) of a female *Kinbergonuphis simoni* showing the relative positions of seminal receptacles (arrows), nephridiopores (Np) and intersegmental junctions (Ij). A = anterior end of the worm; G = gill.

males might manipulate spermatophores and mechanically break down the layers.

Fertilization efficiency

Fifty-one broods and 982 spawned eggs were examined. Out of 982 eggs, only 11 were unfertilized; this represents a fertilization efficiency of 98.9%.

Discussion

Sperm transfer in *Kinbergonuphis simoni* involves spermatophores and seminal receptacles. The seminal receptacles are embedded in the dorsal body wall, with external openings close to the nephridiopores. The nephridiopores serve as gonopores, while the adults' tubes serve as brood chambers. A similar spatial arrangement has also been found in the spionids (Söderström, 1920; Simon, 1967; Rice, 1987a), in the serpulids *Spirorbis spirorbis* (L.) (Daly, 1978), and in the capitellids (Eckelbarger and Grassle, 1987). A comparable situation also occurs in the galeommatacean bivalve *Mysella tumida*, where eggs are spawned, sperm are stored, and young are brooded in the same place: the suprabranchial chamber (Ó Foighil, 1985). The close proximity between openings of the sperm storage organs, gonoducts and brood chambers leads to a high fertilization efficiency. Efficiency has been shown to be 98.9% in *K. simoni* (this study), 98.8% in *S. spirorbis* (Daly, 1978), 100% in *Capitella* (Eckelbarger and Grassle, 1987), and 99.9% in a galeommatacean bivalve (Ó Foighil, 1985).

In *Kinbergonuphis simoni* the production of spermatophores can occur in the absence of females, and the release of eggs also can occur without the presence of males. Such phenomena have also been observed in spionids (S. Rice, University of Tampa, pers. comm.). Moreover, in *K. simoni*, *Polydora ligni*, and *Pseudopolydora paucibranchiata* (Myohara, 1980), females isolated from males can continuously produce viable offspring until the stored sperm are depleted. Two cases in *K. simoni* (Hsieh, unpub. data) also showed that, after their male mates had died, each remaining female (isolated from other males) continued to produce 4 more viable broods over periods of 30 to 40 days. These features reveal that sperm release and egg laying can take place separately, and that sperm are stored alive until needed. Thus, the pressure of breeding synchrony required in broadcast spawning is relieved. Consequently, asynchronous, prolonged, or even continuous reproduction can take place in the population over time. This prediction is consistent with the breeding pattern found in the field (Hsieh and Simon, unpub. data). Asynchrony and extended breeding may have advantages since the risk of reproductive failure can be spread over several reproductive events, and the chance that at least some offspring survive is higher (Stearns, 1976).

Sperm loss due to dilution by seawater has been assessed experimentally in broadcast spawning sea urchins (Pennington, 1985). With successful spermatophore transfer, females are provided with sperm packed in such a localized dense form that sperm dilution does not occur. Furthermore, in *Kinbergonuphis simoni*, spermatophores can remain intact for one to two days after being released into seawater. The reduction of sperm loss may be one of the advantages of having spermatophores.

The morphology of spermatophores in polychaetes is varied and species specific (*e.g.*, in the spionids, Richards, 1970; Greve, 1974; Rice, 1978a; and in an onuphid, this study). Despite the morphological differences, the method of spermatophore transfer in polychaetes appears similar. Spermatophores are released from the male tubes and subsequently are picked up by females. As proposed by Rice (1978a), this demonstrates that individuals do not have to leave their tubes or burrows for sperm transfer, and implies that the risks of being exposed to predation or disturbance are minimized when compared to other alternatives (*e.g.*, copulation, pseudocopulation, or indirect hypodermic impregnation).

Table II summarizes the modes of sperm transfer known in polychaetes. Both the spionids and the onuphid have seminal receptacles in females, and spermatophores in males, for free transfer. In both families, worms are tube dwellers, tend to aggregate, and have similar life histories, suggesting similar selective pressures. In the Onuphidae, the predominant developmental pattern is lecithotrophic. Small-sized onuphids brood

Figure 3. Sagittal section of a female *Kinbergonuphis simoni* showing the position of seminal receptacles (arrows). A = anterior end of the worm; D = dorsal; V = ventral; Ve = vitellogenic egg; Se = septa; Yo = young oocytes.

Figure 4. Cross section of a female *Kinbergonuphis simoni* showing paired seminal receptacles (arrows). G = gut; V = ventral nerve cord.

Figure 5. Individual seminal receptacle in female *Kinbergonuphis simoni* showing stored sperm (S). Co = columnar cell; Cu = cuboidal cell; O = opening of seminal receptacle.

Figure 6. Branched seminal receptacles in female *Kinbergonuphis simoni*. (a) Bi-lobed. (b) Four-lobed. S = stored sperm.

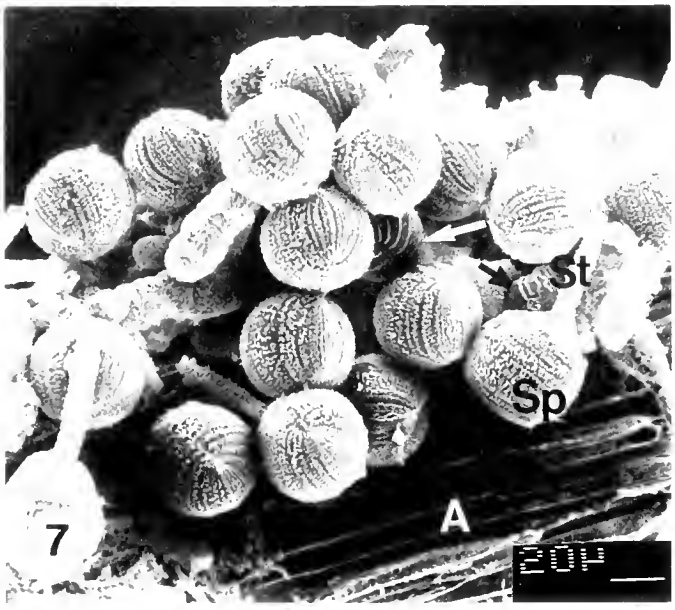

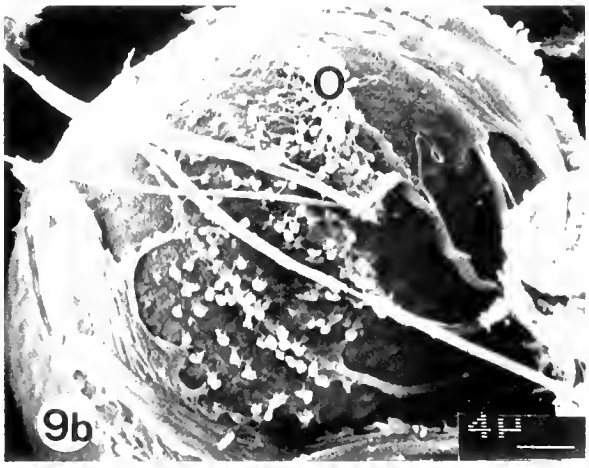

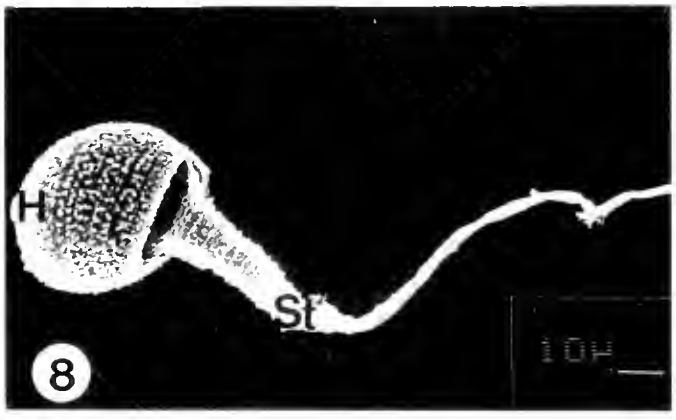

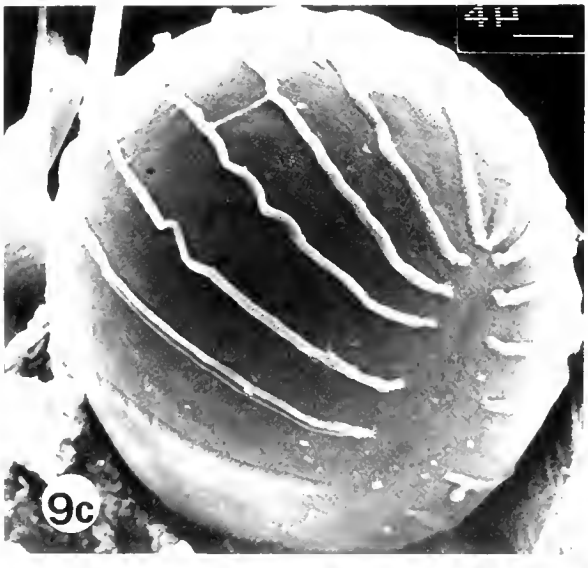

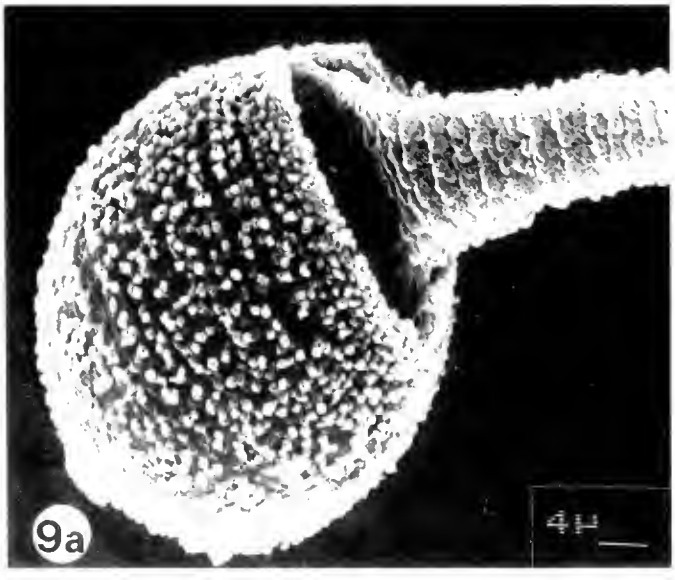

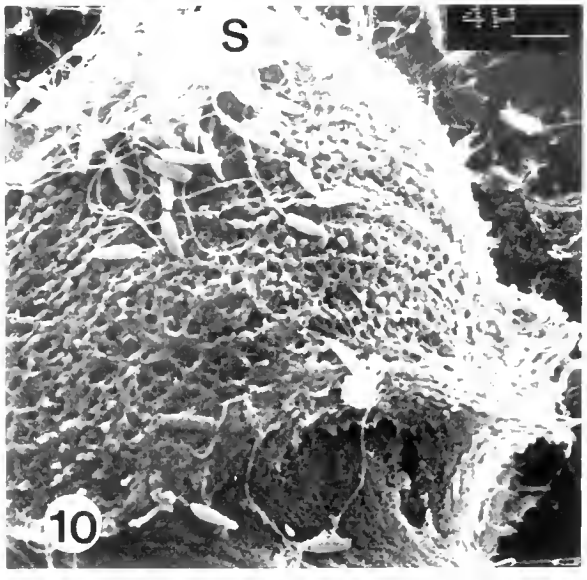

Figure 7. A clump of spermatophores produced by a male *Kinbergonuphis simoni*. A = a piece of ground alfalfa. Sp = individual spermatophore. St = stalk of spermatophore. Arrows = spermatophores without outer layers.

Table II

Summary of sperm transfer modes in polychaete Families

Family	Adult life	Mode of sperm transfer	Reference
A) Non-aggregate transfer			
Nereidae Eunicidae Syllidae	Benthic motile forms	Broadcast spawning, mature individuals undergo swarming spawning with epitoke or stolon formation	Clark, 1961; Schroeder and Hermans, 1975
Pisonidae Saccocirridae	Interstitial forms	Copulation, females have seminal receptacles, males have copulatory organs	Gray, 1969; Westheide, 1984
Nereidae Polynoidae Phyllodocidae	Benthic motile forms	Pseudocopulation with pair formation or aggregations	Reish, 1957; Daly, 1973; Pettibone, 1963
B) Aggregate transfer			
Dinophilidae Protodrilidae Hesionidae	Interstitial forms	Hypodermic impregnation associated with spermatophores, seminal receptacles are present	Ax, 1968; Jouin, 1970; Westheide, 1984, 1988
Arenicolidae	Benthic burrowers	Free spermatophore transfer, the presence of seminal receptacles is unknown	Okuda, 1946
Spionidae	Benthic tube dwellers	Free spermatophore transfer, seminal receptacles are present	Söderström, 1920; Simon, 1967; Rice, 1978a, 1987a
Onuphidae	Benthic tube dwellers	Free spermatophore transfer, seminal receptacles are present	This study
C) Sperm transfer modes uncertain			
Alciopidae	Pelagic forms	Copulation or hypodermic impregnation has been suggested; naked sperm masses are embedded in epidermis; seminal receptacles are present	Pettibone, 1963; Rice, 1987b; Rice and Eckelbarger, 1989
Syllidae	Benthic motile forms	Copulation has been suggested; spermatophore-like structures are present in seminal receptacles	Goodrich, 1930
Terebellidae	Benthic tube dwellers	Pseudocopulation with pair formation or free transfer of aggregated sperm has been suggested; males become errant during spawning period; sperm morulae and free sperm are produced; the presence of seminal receptacles is unknown	Eckelbarger, 1974
Pectinariidae	Benthic tube dwellers	Free transfer of aggregated sperm has been suggested; sperm packets (spermatozeugmata) are produced; the presence of seminal receptacles is unknown	Austin, 1963, 1965
Capitellidae	Benthic burrowers or tube dwellers	Copulation, pseudocopulation or free spermatophore transfer has been suggested; seminal receptacles are present	Hartman, 1947; Reish, 1974; Eckelbarger and Grassle, 1987
Serpulidae Sabellidae	Benthic tube dwellers	Free spermatophore transfer has been suggested; seminal receptacles are present	Daly and Golding, 1977; Picard, 1980

larvae in maternal tubes (Fauchald, 1983; Hsieh and Simon, 1987). These reproductive characteristics lead us to predict that the sperm transfer mode seen in *Kinbergonuphis simoni* and spionids may commonly operate in other small onuphids as well. This proposal may also extend to other tube dwelling or burrowing polychaetes, if they share similar characters with onuphids and spionids in their life histories. Certainly, extensive studies covering tube dwellers and burrowers from different taxa are needed to test this hypothesis.

Most spionid spermatophores are morphologically adapted for flotation or enhanced suspension in the water (Rice, 1978a). In contrast, spermatophores of *Kinbergonuphis simoni* are sticky and often deposited on the bottom of culture dishes, or tangled with objects such as detritus or food particles, suggesting that the dispersal

Figure 8. Individual spermatophore of *Kinbergonuphis simoni*. H = head portion; St = stalk.

Figure 9. Covering layers of spermatophores in *Kinbergonuphis simoni*. (a) Outer layer with granular appearance. (b) Inner layer exposed after the outer layer being partially eroded. O = outer layer. (c) Inner layer showing symmetrical bands.

Figure 10. A broken spermatophore of *Kinbergonuphis simoni* showing escaped sperm (S).

ability of spermatophores is low. As a result, the exchange of spermatophores between individuals in distant populations is greatly reduced. Any changes in the timing of release, quantity and quality of spermatophores, or in the processes of spermatophore transfer and sperm storage, may alter the efficiency of fertilization. In turn, different methods of fertilization can serve as a barrier between populations and act as a reproductive isolation mechanism. In *K. simoni*, preliminary analyses of isoenzymes and morphometric measurements of populations from Tampa Bay, Ft. Myers, and the Indian River indicate that these populations differ (K. Fauchald, Smithsonian Institution, pers. comm.), suggesting that some form of divergence has taken place. Comparative studies of sperm transfer modes and sperm storage mechanisms among distantly distributed populations would be useful.

Acknowledgments

We thank Drs. B. Cowell, E. McCoy, S. Bell, and F. Friedl for their advice during this study. We also thank Drs. S. Rice, K. Fauchald, C.-P. Chen, and two anonymous reviewers for their discussions and comments. Special thanks are due C.-P. Chen for his help in preparing histological sections.

Literature Cited

Austin, C. R. 1963. Fertilization in *Pectinaria (Cistenides) gouldii*. *Biol. Bull* **124:** 115–124.

Austin, C. R. 1965. *Fertilization* Prentice-Hall Inc., Englewood Cliffs, New Jersey. 59 pp.

Ax, P. 1968. Das fortpflanzungs verhalten von *Trilobodrilus* (Archiannelida, Dinophilidae). *Mar. Biol.* **1:** 330–335.

Blake, J. A. 1975. The larval development of polychaeta from the northern California coast. II. *Nothria elegans* (Family Onuphidae). *Ophelia* **13:** 43–61.

Clark, R. B. 1961. The origin and formation of the heteronereis. *Biol. Rev.* **36:** 199–236.

Clark, W. C. 1981. Sperm transfer mechanisms: some correlates and consequences. *N. Z. J. Zool* **8:** 49–65.

Daly, J. M. 1973. Some relationships between the process of pair formation and gamete maturation in *Harmothoe imbricata* (L.) (Annelida: Polychaeta). *Mar. Behav. Physiol.* **1:** 277–284.

Daly, J. M. 1978. Growth and fecundity in a Northumberland population of *Spirorbis spirorbis* (Polychaeta: Serpulidae). *J. Mar. Biol. Assoc. U. K.* **58:** 177–190.

Daly, J. M. and D. W. Golding. 1977. A description of the spermatheca of *Spirorbis spirorbis* (L.) (Polychaeta: Serpulidae) and evidence for a novel mode of sperm transmission. *J. Mar. Biol. Assoc. U. K.* **57:** 219–227.

Eckelbarger, K. J. 1974. Population biology and larval development of the terebellid polychaete *Nicolea zostericola*. *Mar. Biol.* **27:** 101–113.

Eckelbarger, K. J., and J. P. Grassle. 1987. Spermatogenesis, sperm storage and comparative sperm morphology in nine species of *Capitella*, *Capitomastus* and *Capitellides* (Polychaeta: Capitellidae). *Mar. Biol.* **95:** 415–429.

Fauchald, K. 1983. Life diagram patterns in benthic polychaetes. *Proc. Biol. Soc. Wash.* **96**(1): 160–177.

Flügel, H. 1977. Ultrastructure of the spermatophores of *Siboglinum ekmani* Jagersten (Pogonophora). *Nature* **269:** 800–801.

Goodrich, E. S. 1930. On a new hermaphrodite syllid. *Q. J. Microsc. Sci.* **73**(4): 651–666.

Gray, J. S. 1969. A new species of *Saccocirrus* (Archiannelida) from the west coast of North America. *Pac. Sci.* **23:** 238–251.

Greve, W. 1974. Planktonic spermatophores found in a culture device with spionid polychaetes. *Helgolander. Wiss. Meeresunters.* **26:** 370–374.

Hadfield, M. G., and C. N. Hopper. 1980. Ecological and evolutionary significance of pelagic spermatophores of a vermetid gastropod. *Mar. Biol* **57:** 315–325.

Harrison, P. L., R. C. Babcock, G. D. Bull, J. K. Oliver, C. C. Wallace, and B. L. Willis. 1984. Mass spawning in tropical reef corals. *Science* **223:** 1186–1189.

Hartman, O. 1947. *Polychaetous Annelids. Part 7 Capitellidae.* Allan Hancock Pacific Expeditions vol. 10. The University of Southern California Press, Los Angeles, California. Pp. 391–481.

Hsieh, H. L. 1984. Morophological studies on reproduction and larval development of *Kinbergonuphis simoni* (Polychaeta: Onuphidae). M. Sc. Thesis. Department of Biology, University of South Florida, Tampa, FL. 120 pp.

Hsieh, H. L., and J. L. Simon. 1987. Larval development of *Kinbergonuphis simoni*, with a summary of developmental patterns in the Family Onuphidae (Polychaeta). *Biol. Soc. Wash. Bull.* **7:** 194–210.

Jouin, C. 1970. Recherches sur les Protodrilidae (Archiannelides): I. Etude morphologique et systematique du Genre *Protodrilus*. *Cah. Biol. Mar.* **11:** 367–434.

Just, E. E. 1914. Breeding habits of the heteronereis form of *Platynereis megalops* at Woods Hole, Mass. *Biol. Bull* **27:** 201–212.

Knudsen, J. W. 1966. *Biological Techniques.* Harper and Row, Publishers, New York. 525 pp.

Mann, T. 1984. Spermatophores. In *Zoophysiology*, Vol. 15 D. S. Farner, ed. Springer-Verlag, Berlin. 217 pp.

Myohara, M. 1980. Reproduction and development of *Pseudopolydora paucibranchiata* (Polychaeta: Spionidae) under laboratory conditions, with special regard to the polar lobe formation. *J. Fac. Sci. Hokkaido Univ. (Ser 6).* **22**(2): 145–155.

Ó Foighil, D. 1985. Sperm transfer and storage in the brooding bivalve *Mysella tumida*. *Biol. Bull.* **169:** 602–614.

Okuda, S. 1946. Studies on the development of Annelida Polychaeta I. *J. Fac. Sci. Hokkaido Imp. Univ. (Ser 6)* **9:** 115–219.

Paxton, H. 1986. Generic revision and relationships of the family Onuphidae (Annelida: Polychaeta). *Rec. Aust. Mus.* **38:** 1–74.

Pennington, J. T. 1985. The ecology of fertilization of echinoid eggs: the consequences of sperm dilution, adult aggregation, and synchronous spawning. *Biol. Bull.* **169:** 417–430.

Pettibone, M. H. 1963. *Marine Polychaete Worms of the New England Region* Museum of Natural History, Smithsonian Institution, Washington. 356 pp.

Picard, A. 1980. Spermatogenesis and sperm-spermatheca relations in *Spirorbis spirorbis* (L.). *Inter. J. Invertebr. Reprod.* **2:** 73–83.

Reish, D. J. 1957. The life history of the polychaetous annelid, *Neanthes caudata* (delle Chiaje) including a summary of development in the Family Nereidae. *Pac. Sci.* **11:** 216–228.

Reish, D. J. 1974. The establishment of laboratory colonies of polychaetous annelids. *Thalassia Jugosl.* **10**(1/2): 181–195.

Rice, S. A. 1978a. Spermatophores and sperm transfer in spionid polychaetes. *Trans. Am. Micros. Soc.* **97**(2): 160–170.

Rice, S. A. 1978b. Intraspecific variation in the opportunistic polychaete *Polydora ligni* (Spionidae). Ph. D. Dissertation. Department of Biology, University of South Florida, Tampa, FL. 203 pp.

Rice, S. A. 1987a. Sperm storage organs in spionid polychaetes, implications for speciation and systematics. *Am. Zool.* **27**(4): 59A.

Rice, S. A. 1987b. Reproductive biology, systematics and evolution in the polychaete family Alciopidae. *Biol. Soc. Wash. Bull.* **7:** 114–127.

Rice, S. A., and K. J. Eckelbarger. 1989. An ultrastructural investigation of spermatogenesis in the holopelagic polychaetes *Vanadis formosa* and *Krohnia lepidota* (Polychaeta:Alciopidae). *Biol. Bull.* **176:** 123–134.

Richards, S. L. 1970. Spawning and reproductive morphology of *Scoloplos squamata* (Spionidae, Polychaeta). *Can. J. Zool.* **48:** 1369–1379.

Schroeder, P. C., and C. O. Hermans. 1975. Annelida: Polychaeta. Pp. 1–213 in *Reproduction of Marine Invertebrates, vol. 3 Annelids and Echiurans*, A. C. Giese and J. S. Pearse, eds. Academic Press, New York.

Shlesinger, Y., and Y. Loya. 1985. Coral community reproductive patterns: Red Sea versus the Great Barrier Reef. *Science* **228:** 1333–1335.

Simon, J. L. 1967. Reproduction and larval development of *Spio setosa* (Spionidae: Polychaeta). *Bull. Mar. Sci.* **17:** 398–431.

Söderström, A. 1920. Studien uber die polychaetenfamilie Spionidae. *Inaug. Diss. Uppsala, Almqvist and Wiksell.* 286 pp.

Stearns, S. C. 1976. Life-history tactics: a review of the ideas. *Q. Rev. Biol.* **51**(1): 3–47.

Westheide, W. 1984. The concept of reproduction in polychaetes with small body size: adaptations in interstitial species. In *Polychaete Reproduction*, A. Fischer and H-D. Pfannenstiel, eds. *Fortschr. Zool.* **29:** 267–287.

Westheide, W. 1988. The ultrastructure of Polychaeta. Pp. 263–279 in *Microfauna Marina*, vol. 4, W. Westheide and C. O. Hermans, eds. Gustav Fischer Verlag, Stuttgart, New York.

Reference: *Biol. Bull.* **178**: 94–100. (April, 1990)

Structure and Function of a Special Tissue in the Female Genital Ducts of the Chinese Freshwater Crab *Eriocheir sinensis*

TAI-HUNG LEE* AND FUMIO YAMAZAKI

Laboratory of Embryology and Genetics, Faculty of Fisheries, Hokkaido University, Hakodate, Hokkaido 041, Japan

Abstract. The histological anatomy of the genital ducts of adult females of *Eriocheir sinensis* was studied before and after copulation, and during and after egg-laying. A strongly basophilic valve-like tissue was discovered at the junction of the spermatheca and the oviduct. This tissue prevents communication between the spermatheca and the oviduct except during oviposition. At this time, it functions as a valve, allowing ripe eggs out of the oviduct and preventing sperm from entering the oviduct during and after egg-laying. These findings suggest that the actual site of gamete contact in *E. sinensis* is within the spermatheca, instead of in the lumen of the ovary or in the oviduct. The presence of the valve-like tissue assures that the ripe eggs collected from the ovary during egg-laying are unfertilized. This observation is of great importance for obtaining unfertilized ripe eggs in studies of artificial fertilization (*in vitro*) and hybridization. The valve-like tissue has not been described in other brachyurans, and this genital duct should be classified as new for the Brachyura.

Introduction

The goal of this study was to define the actual site of fertilization in the Chinese freshwater crab, *Eriocheir sinensis*, in preparation for artificial fertilization (*in vitro*). This crab is widely distributed in fresh and brackish waters in southeastern China and has great economic value in the country.

The female reproductive system of the Brachyura, with the exception of two superfamilies, consists of a series of ducts leading from the ovary to the exterior of the animal. These ducts are composed of four regions: oviduct, spermatheca, vagina, and vulva (Hartnoll, 1968). During copulation, the male transfers its spermatophores into the spermatheca of the female; therefore, fertilization in the Brachyura is generally accepted as being internal. But what is the actual site of this fertilization? And what is meant by "internal fertilization" in the Brachyura? These two questions have not yet been answered conclusively.

Early reports were contradictory. Binford (1913) suggested that in *Menippe mercenaria*, fertilization occurred in the lumen of the ovary, because spermatozoa were found on the surface of the ripe eggs, and many could develop into embryos. Spalding (1942), Cheung (1966), and Goudeau (1982) reported that fertilization of *Carcinus maenas* occurs in the lumen of the ovary or within the oviduct. On the other hand, studies of *Portunus sanguinolentus* (by Ryan, 1967) and *Libinia emarginata* (by Hinsch, 1971) suggested that the spermatozoan contacts the membrane of the ripe egg internally, and that the remaining processes in fertilization occur outside the body of the female. This suggestion agrees with that of Yonge (1937).

In *E. sinensis*, we found a valve-like tissue within the spermathecal wall which is connected to the oviduct. Except during oviposition, this valve-like tissue prevents communication between the oviduct and the spermatheca. During egg-laying, the tissue functions as a valve, freeing eggs and preventing spermatozoa from entering the oviduct. Thus, we will comment on the expression "internal fertilization" as it pertains to *E. sinensis* and other brachyurans.

Materials and Methods

Specimens of the Chinese freshwater crab, *Eriocheir sinensis*, were obtained from Yang Qin Lake in Jiangsu

Received 15 May 1989; accepted 19 January 1990.

* To whom all correspondence should be addressed.

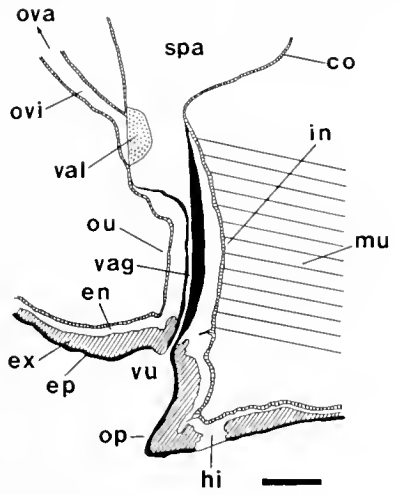

Figure 1. Schematic illustration of the longitudinal section of the genital ducts of the female *Eriocheir sinensis*. Abbreviations: (co) columnar epithelium; (en) endocuticle; (ex) exocuticle; (ep) epicuticle; (hi) hinge; (in) inner wall; (mu) muscles; (op) operculum; (ou) outer wall; (ova) ovary; (ovi) oviduct; (spa) spermatheca; (vag) vagina; (val) valve-like tissue; (vu) vulva. Bar = 1 mm.

Province, China, in November 1986 during the crab's spawning migration season. The maximum carapace widths of the specimens used in this study were 7–8 cm. Some specimens were used immediately after they arrived at the laboratory (Faculty of Fisheries, Hokkaido University, Hakodate, Japan); these were at the germinal vesicle stage. The remaining specimens were maintained for about two months in individual compartments of a well-aerated, closed circulating seawater system (28‰ S, 20°C). Female genital ducts, in various stages—before and after copulation, during egg-laying, and one day and four days after egg-laying—were excised carefully and fixed in Bouin's solution for histological observations. Sections (8–10 μm) were made by the standard paraffin method and stained with Delafield's haematoxylin and eosin.

Results

Structure of the female genital ducts and the valve-like tissue

In adults of *Eriocheir sinensis*, we found that the female genital ducts have four regions: oviduct, spermatheca, vagina, and vulva (Fig. 1).

The oviduct, a short, tube-like passage connecting the ovary and the spermatheca, is about 4.1 mm long. The opening of the oviduct leading to the spermatheca is on the epithelium of the spermatheca, just above the outer wall of the vagina. The undulant wall of the oviduct is composed of a columnar epithelium. The cavity of the oviduct is full of basophilic material in colloidal form.

The spermatheca is ovoid, about 19 mm high and 8 mm wide. It consists of a single crumpled layer of columnar epithelium; its cavity is filled with a basophilic colloidal substance. The portion of the spermathecal cavity nearest the vagina sharply tapers downward, its narrow end continuous with the cavity of the vagina. The vagina, about 3 mm long, is formed by two cuticular walls; one face (inner wall) is invaginated into a concavity of the other (outer wall) (Fig. 2). Muscles run diagonally from the inner wall to the sternum. The opening of the vagina (*i.e.*, the vulva) is on the sternite of the sixth thoracic segment. The vulva is characterized by the presence of an operculum—the continuation of the inner wall of the vagina. The operculum can be opened and closed by contracting and relaxing the muscles of the inner wall during copulation or egg-laying.

A strongly basophilic tissue (hereafter referred to as the valve-like tissue) can be found at the opening of the spermatheca leading to the oviduct (Fig. 1; Fig. 3A); it is about 1.1 mm high and 0.4 mm wide. Because the border of the valve-like tissue is connected to the epithelium of the opening, it prevents communication between the oviduct and the spermatheca. The tissue is composed of a mass of cells in which no nuclear division is observed; thus, it appears to originate from epithelial cells somewhere nearby.

Under light microscopy, the tissue appeared to be a syncytium because no cell membranes were observed. Most of the nuclei are nearly oval, with a long axis of about 5.6 μm and a short axis of about 3.5 μm; the directions of the long axes are random (Fig. 3B). In contrast, the nuclei in the middle of this tissue are somewhat condensed and spindle-shaped, with a long axis of about 7.3 μm and a short axis of about 2.0 μm; all the long axes of these nuclei point toward the cavity of the spermatheca (Fig. 3C). The nuclei within the middle part of that surface of the tissue facing the spermathecal cavity appeared to be pycnotic (Fig. 3D). This observation suggests that old nuclei are displaced through the middle part of the tissue into the cavity of the spermatheca.

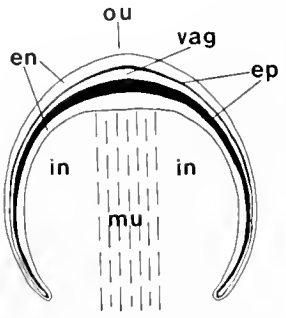

Figure 2. Schematic illustration of a transverse section of the vagina showing its concave shape. Abbreviations: (en) endocuticle; (ep) epicuticle; (in) inner wall; (mu) muscles; (ou) outer wall; (vag) vagina.

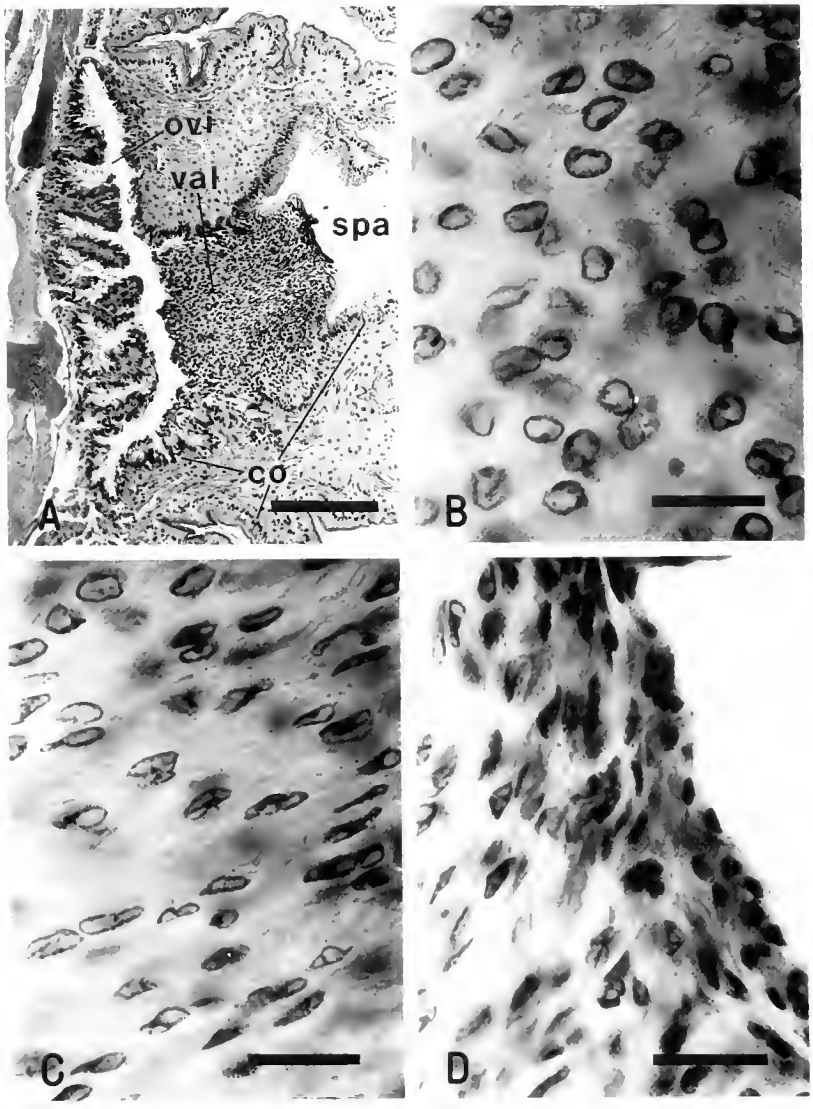

Figure 3. Transverse sections from the middle of the valve-like tissue and oviduct before copulation. A: Whole figure of the valve-like tissue. B: Most of the nuclei of the tissue are oval and the directions of long axes are at random. C: The nuclei in the middle of the tissue are somewhat condensed and spindle-shaped, all the long axes of these nuclei point toward the cavity of the spermatheca. D: The nuclei within the middle part of that surface of the tissue facing the spermathecal cavity appear to be pycnotic. Abbreviations: (co) columnar epithelium; (ovi) oviduct; (spa) spermatheca; (val) valve-like tissue. Bar (A) = 200 μm. Bar (B, C, D) = 20 μm.

Structural changes in the valve-like tissue and the oviduct

Five hours after copulation. Spermatophores and free spermatozoa introduced during copulation swell the spermatheca to about three times its pre-copulatory size. The valve-like tissue is a bit flattened due to the pressure of the seminal fluid (Fig. 4A). Besides these, no other changes in the oviduct were observed.

During egg-laying. Changes occur in both the oviduct and the valve-like tissue. The undulant surface of the oviduct straightens, and its circumference expands to some degree. The valve-like tissue is perforated by the extruded eggs in the middle with its broken parts prolonged toward the cavity of the spermatheca (Fig. 4B, C, Fig. 5A). Figures 4D and E and 5B show that near the end of egg-laying, eggs are extruded continually. The split parts of the tissue are closely attached to each other when there are no eggs passing through.

One day after egg-laying. A new thin layer of valve-like tissue appears on the border that is connected to the epithelium of the spermatheca. The split parts of the valve-like tissue have already fused together. However, no nuclear-division is observed in this tissue. The old tis-

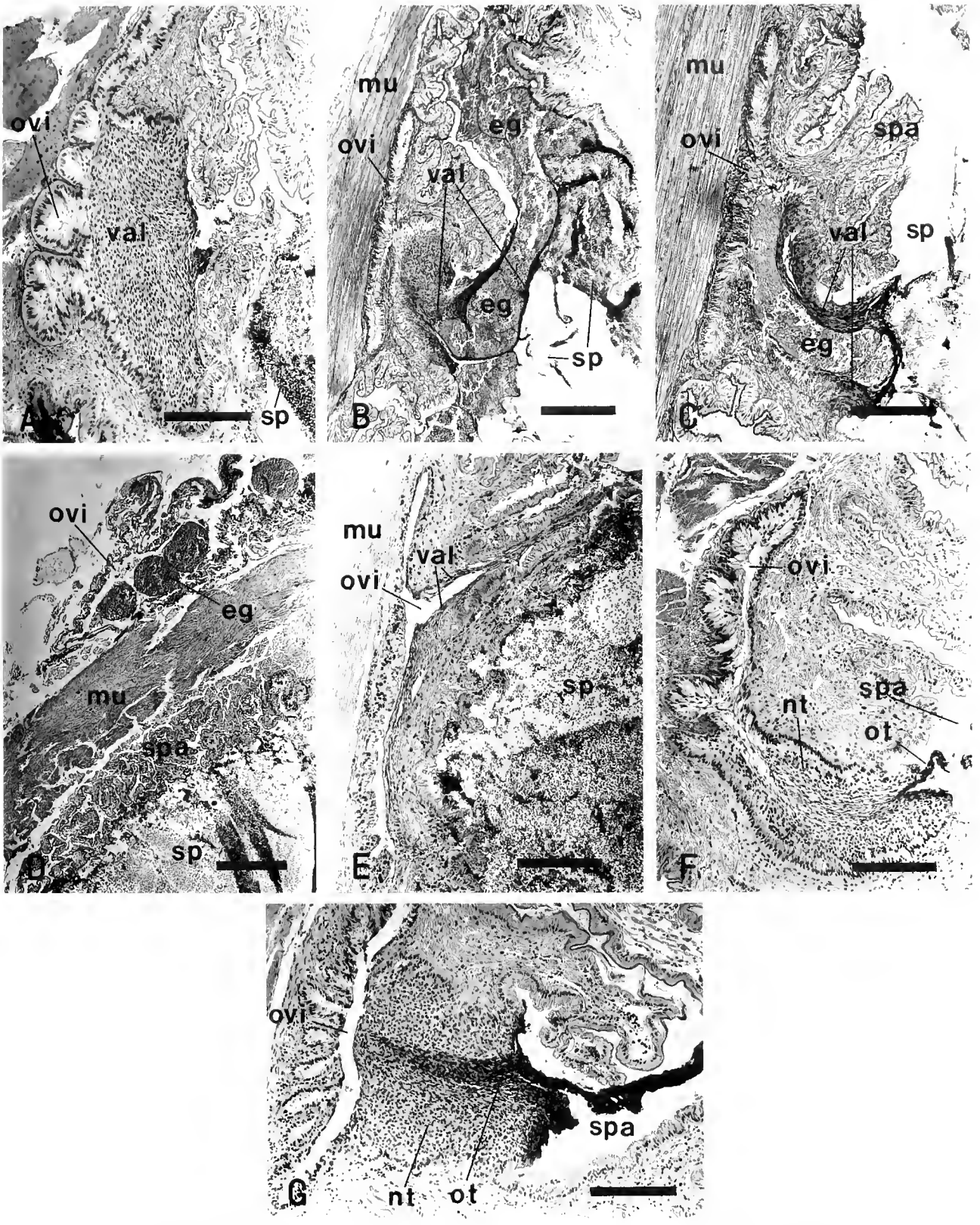

Figure 4. Transverse sections from the valve-like tissue and oviduct showing the structural changes in different stages. A: Five hours after copulation. B and C: During egg-laying (from the same spermatheca). D and E: Near the end of egg-laying (from the same spermatheca). F: One day after egg-laying. G: Four days after egg-laying. Abbreviations: (eg) egg; (mu) muscles; (nt) new valve-like tissue; (ot) old valve-like tissue; (ovi) oviduct; (sp) spermatozoa; (spa) spermatheca; (val) valve-like tissue. Bar (A, C, E, F, G) = 200 μm. Bar (B, D) = 400 μm.

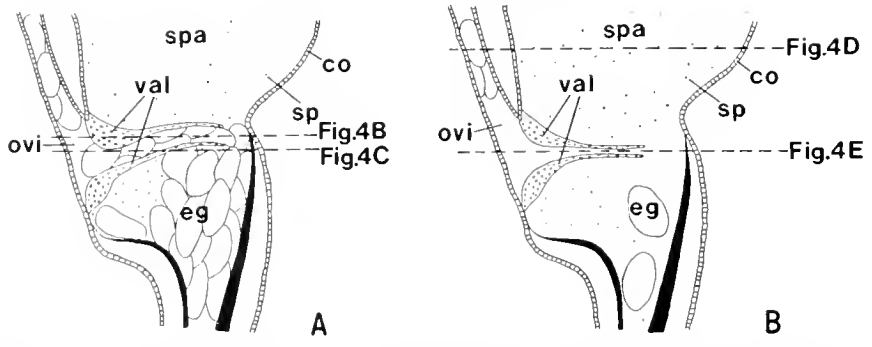

Figure 5. Schematic illustration of the longitudinal sections of the valve-like tissue. A: Based on observation of continuous transverse sections of the same spermatheca as shown in Figure 4B and C. B: Based on observation of continuous transverse sections of the same spermatheca as shown in Figure 4D and E. Abbreviations: (co) columnar epithelium; (eg) egg; (ovi) oviduct; (sp) spermatozoa; (spa) spermatheca; (val) valve-like tissue.

sue is being discharged into the cavity of the spermatheca. The surface of the oviduct changes again from being straight to undulant (Fig. 4F).

Four days after egg-laying. The old valve-like tissue is almost discharged and a new valve-like tissue is formed (Fig. 4G).

No spermatozoa were found inside the oviduct or the ovary during the different stages discussed above. Moreover, none of the ripe eggs removed from the egg-laying ovary developed into embryos.

Discussion

In the present study, no spermatozoa were found in either the oviduct or the ovary in *Eriocheir sinensis* before, during, or after egg-laying. Moreover, the ripe eggs removed from the egg-laying ovary did not develop into embryos. Therefore, the spermatozoa in the spermatheca never entered the oviduct or ovary. This phenomenon can be explained by the presence of the valve-like tissue. This tissue not only prevents the sperm from entering the oviduct or the ovary before egg-laying, but it also functions as a valve. It allows ripe eggs out of the oviduct during egg-laying and prevents the sperm from entering the oviduct, both near the end of egg-laying and after egg-laying, by closing once the positive pressure of the seminal fluid acts upon it (Fig. 6). Therefore, the only site where the eggs and sperm come into contact is in the spermatheca.

In *E. sinensis*, egg-laying continues for approximately 15–30 min. About 300,000–500,000 eggs or more can be found in one brood. The capacity of the spermatheca is no more than 100 eggs, and the opening of the vagina will only allow the passage of two or three eggs at one time. Thus, we estimate that the time an egg takes from entering the spermatheca to release from the vagina is no more than 1 s (unpub. data). Accordingly, there is only enough time for the sperm to attach to or penetrate the surface of the outer membrane of the ripe egg in the spermatheca, so the remaining events of fertilization must then occur externally. This conclusion is similar to the suggestions made by Yonge (1937), Ryan (1967), and Hinsch (1971).

Because fertilization is a series of phenomena that generally involves the contact of sperm and egg, penetration, and karyogamy, the term "internal fertilization" is apparently not appropriate for *E. sinensis*. However, in this study, we could not determine whether any interaction (*e.g.*, acrosome reaction) occurred between the sperm and the egg within the spermatheca. If such an interaction does occur, then fertilization in this crab cannot be external. On the other hand, if the sperm simply attaches to the egg membrane and has no further interaction with it within the spermatheca, then the term "external fertilization" is applicable. Hence, further research is required to determine whether this crab performs "external fertilization."

In early studies of the brachyurans by Binford (1913; *Menippe mercenaria*), Ryan (1967; *Portunus sanguinolentus*), and Hartnoll (1968; *Carcinus maenas, Hyas coarctatus* and *Hyas araneus*), the structure of the oviduct and its opening into the spermatheca were described as being similar to one another. Unlike *E. sinensis*, the oviducts of these crabs do not function as a passage from the ovary into the cavity of the spermatheca; rather, they are simply a convoluted cord of cells with a blind end extended toward the stratified epithelium of the spermatheca, except during ovulation (Fig. 7A). Some time before either ovulation or egg-laying, this cord of cells forms a passage between the ovary and the cavity of the spermatheca; but no valve-like tissue preventing the sperm from entering the oviduct was observed (Fig. 7B).

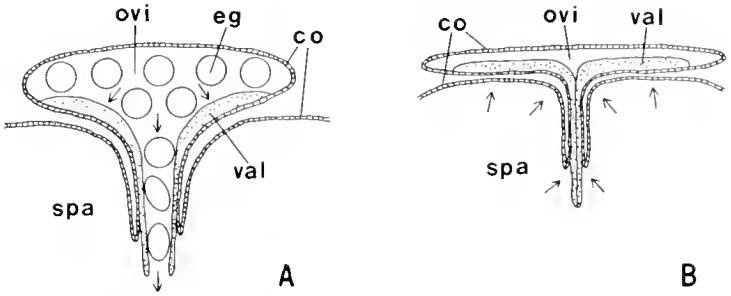

Figure 6. Schematic illustration of the transverse sections of the valve-like tissue showing the function of freeing eggs and preventing sperm from entering the oviduct. A: Valve-like tissue opens when the eggs are extruded. B: Valve-like tissue closes when the positive pressure of the seminal fluid acts upon it. Abbreviations: (co) columnar epithelium; (eg) egg; (ovi) oviduct; (spa) spermatheca; (val) valve-like tissue. Arrows indicate the directions of positive pressure.

Our view of the relation between the structural changes in the oviduct and the site of fertilization differs from those of previous investigators. Ryan (1967) found a small amount of sperm in the open oviduct of *P. sanguinolentus*. With no further explanation, he concluded that the spermatheca was the site of sperm-egg contact, and that the rest of the fertilization process occurred externally. He thought that there was insufficient time for the sperm to penetrate the egg within the body of the female crab. Diesel (1989) also reported sperm-egg contact within the spermatheca of *I. phalangium*, but did not report whether any sperm were present in the oviduct or ovary immediately before or after spawning. In studies of *M. mercenaria* (by Binford, 1913), and *C. maenas* (by Spalding, 1942; Cheung, 1966; Goudeau, 1982), the authors believed that fertilization occurred in the lumen of the ovary or within the oviduct because: (1) sperm were found in the lumen of the ovary; and (2) some of the eggs removed from that ovary could develop into embryos. We cannot deny that sperm might be naturally pressed into the oviduct and the lumen of the ovary when the blind-ended oviduct opens. However, the evidence cited by Binford (1913) and other investigators is too weak to support their conclusions. During their dissection and removal, the genital organs may have experienced negative pressure inside the ovary, drawing the sperm into the oviduct or the ovary. This artificial phenomenon might have misled investigators. This may also account for the presence of the sperm in the oviduct of *P. sanguinolentus* (by Ryan, 1967). Further experiments are needed to clarify the site of fertilization in the crabs that have no apparatus to prevent sperm from entering the oviduct.

There are two known types of oviducal openings into spermatheca: one is that reported by Binford (1913), Ryan (1967), and Hartnoll (1968), and the other is the one we describe in the present study. Besides *E. sinensis*, we also found the same valve-like tissue and patent oviduct in *Eriocheir japonicus* and *Hemigrapsus sanguineus* (unpub. data). In *Pachygrapsus crassipes*, Chiba and Honma (1971) discovered an oviduct of the same structure; unfortunately, they did not mention whether there was a valve-like tissue. What does the distribution of these two types of openings in the Brachyura mean? What is their taxonomic significance? Does the valve-like tissue have functions other than preventing sperm from entering the oviduct? From where are the cells that rebuild the split valve-like tissue?

The presence of the valve-like tissue in crabs helps ensure that the ripe eggs removed from the egg-laying ovary are all unfertilized. This finding is of importance for obtaining unfertilized ripe eggs in studies of artificial fertilization (*in vitro*) (Lee and Yamazaki, 1989) in *E. sinensis*. Furthermore, crabs with this valve-like tissue would be good laboratory animals for studies on fertilization, hybridization, and embryology in the Brachyura.

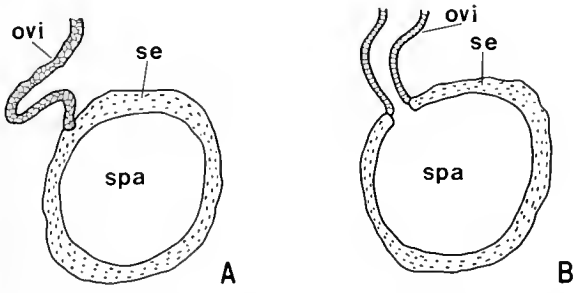

Figure 7. Schematic illustration of the transverse sections of the oviduct and spermatheca described in early studies by Binford (1913), Ryan (1967), and Hartnoll (1968). A: Non-spawning stage. B: Some time before or during ovulation and egg-laying. Abbreviations: (ovi) oviduct; (se) stratified epithelium; (spa) spermatheca.

Acknowledgments

The authors thank Dr. Akira Goto of Laboratory of Embryology and Genetics, Faculty of Fisheries at Hok-

kaido University, for his constructive criticism, and John Goodier for reading the manuscript. We also thank our friends Chun-Min Liu and Yaichiro Kamataki for their assistance in collecting the specimens, and Paul Endo for his helpful suggestions. Finally we wish to express our hearty thanks to Mrs. Enid Mok Lee for her continuous assistance.

Literature Cited

Binford, R. 1913. The germ-cells and the process of fertilization in the crab, *Menippe mercenaria*. *J. Morph.* **24:** 147–201.

Cheung, T. S. 1966. The development of egg-membranes and egg attachment in the shore crab, *Carcinus maenas*, and some related decapods. *J. Mar. Biol. Assoc. U. K.* **46:** 373–400.

Chiba, A., and Y. Honma. 1971. Studies on gonad maturity in some marine invertebrates—II. Structure of the reproductive organ of the lined shore crab. *Nippon Suisan Gakkaishi* **37:** 699–706. (in Japanese, with English abstract)

Diesel, R. 1989. Structure and function of the reproductive system of the symbiotic spider crab *Inachus phalangium* (Decapoda: Majidae): observations on sperm transfer, sperm storage, and spawning. *J. Crust. Biol.* **9:** 266–277.

Goudeau, M. 1982. Fertilization in a crab: I. Early event in the ovary, and cytological aspects of the acrosome reaction and gamete contacts. *Tissue Cell* **14:** 97–111.

Hartnoll, R. G. 1968. Morphology of the genital ducts in female crabs. *J. Linn. Soc. (Zool).* **47:** 279–300.

Hinsch, G. W. 1971. Penetration of the oocyte envelope by spermatozoa in the spider crab. *J. Ultrastruct. Res.* **35:** 86–97.

Lee, T. H., and F. Yamazaki. 1989. Cytological observations on the fertilization in the Chinese freshwater crab *Eriocheir sinensis* by artificial insemination (*in vitro*) and incubation. *Aquaculture* **76:** 347–360.

Ryan, E. P. 1967. The structure and function of the reproductive system of the crab, *Portunus sanguinolentus* (Herbst) (Brachyura: Portunidae). II. The female system. *Proc. Symp. Crustacea, Mar. Biol. Assoc., India, Jan. 12–15, 1965, Ernakulam.* Pt II: 522–544.

Spalding, J. F. 1942. The nature and formation of the spermatophore and sperm plug in *Carcinus maenas*. *Q. J. Microsc. Sci.* **83:** 399–422.

Yonge, C. M. 1937. The nature and significance of the membranes surrounding the developing eggs *Homarus vulgaris* and other Decapoda. *Proc. Zool. Soc. Lond. A* **107:** 499–517.

Reference: *Biol. Bull.* **178**: 101–110. (April, 1990)

Sperm Attachment and Acrosome Reaction on the Egg Surface of the Polychaete, *Tylorrhynchus heterochaetus*[1]

MASANORI SATO[2] AND KENZI OSANAI

Marine Biological Station, Tohoku University, Asamushi, Aomori, 039-34, Japan

Abstract. Sperm binding to the egg envelope (chorion) was examined in fixed eggs and isolated chorions of the polychaete, *Tylorrhynchus heterochaetus*. Sperm binding included two successive steps: attachment (acrosomal outer surface-chorion binding) before the acrosome reaction and adhesion (acrosomal process-chorion binding) after the acrosome reaction. The attachment between sperm head-tip and the outermost layer of the chorion was observed in Ca-free seawater, in which the acrosome reaction did not occur. The surface of the chorion was stained with phosphotungstic acid (PTA). Sperm did not attach to pronase-treated eggs, in which the PTA-positive layer disappeared. When isolated chorions were soaked in distilled water for several hours, they lost the capacity for sperm attachment, and the PTA-positive layer thinned. The acrosome reaction was induced by material that was dissolved from the chorions into distilled water. This suggests that both the receptor for sperm attachment and the inducer of the acrosome reaction are involved in the PTA-positive layer.

Introduction

In many animals, ripe unfertilized eggs have one or more extracellular coats (envelopes). During fertilization, egg envelopes play a key role in sperm binding, in the induction of the sperm acrosome reaction, and in the exclusion of supernumerary sperm (see Epel and Vacquier, 1978; Lopo, 1983; Monroy and Rosati, 1983; Jaffe and Gould, 1985).

Previous studies on sperm-egg binding have suggested that two types of binding exist (see Epel and Vacquier, 1978): (1) binding between the outer surface of unreacted sperm heads and egg envelopes before the acrosome reaction (referred to as attachment in the present paper) in mice (Saling and Storey, 1979; Bleil and Wassarman, 1983; Wassarman *et al.*, 1985; Soldani and Rosati, 1987), ascidians (DeSantis *et al.*, 1980; Rosati, 1985), a horseshoe crab (Brown, 1976; Barnum and Brown, 1983), polychaetes (Anderson and Eckberg, 1983; Osanai, 1983; Sato and Osanai, 1983, 1986), an abalone (Lewis *et al.*, 1982) and a sea urchin (Aketa, 1973, 1975); and (2) binding between acrosomal processes of reacted sperm and egg envelopes after the acrosome reaction (referred to as adhesion in the present paper) in ascidians (DeSantis *et al.*, 1980; Rosati, 1985), a horseshoe crab (Brown, 1976), polychaetes (Osanai, 1983; Sato and Osanai, 1983, 1986), sea urchins (Summers and Hylander, 1975; Vacquier, 1980), a sand dollar (Summers and Hylander, 1974), bivalves (Hylander and Summers, 1977; Brandriff *et al.*, 1978), and a crustacean (Clark *et al.*, 1981). Studying sperm-egg binding can be difficult because, during normal fertilization in most organisms, the acrosome reaction usually follows sperm attachment too quickly to be examined. Using phase-contrast microscopy, Osanai (1983) observed that sperm remained attached to isolated egg envelopes (chorions) without the acrosome reaction in Ca-free solution, and that sperm adhered to the chorion with its acrosome reacted in Ca-containing solution in the polychaete *Tylorrhynchus heterochaetus*.

In the present study, we use electron microscopy to

Received 16 December 1988; accepted 18 December 1989.

[1] Contribution No. 558 from the Marine Biological Station, Tohoku University.

[2] Present address: Department of Biology, Faculty of Science, Kagoshima University, Korimoto, Kagoshima 890, Japan.

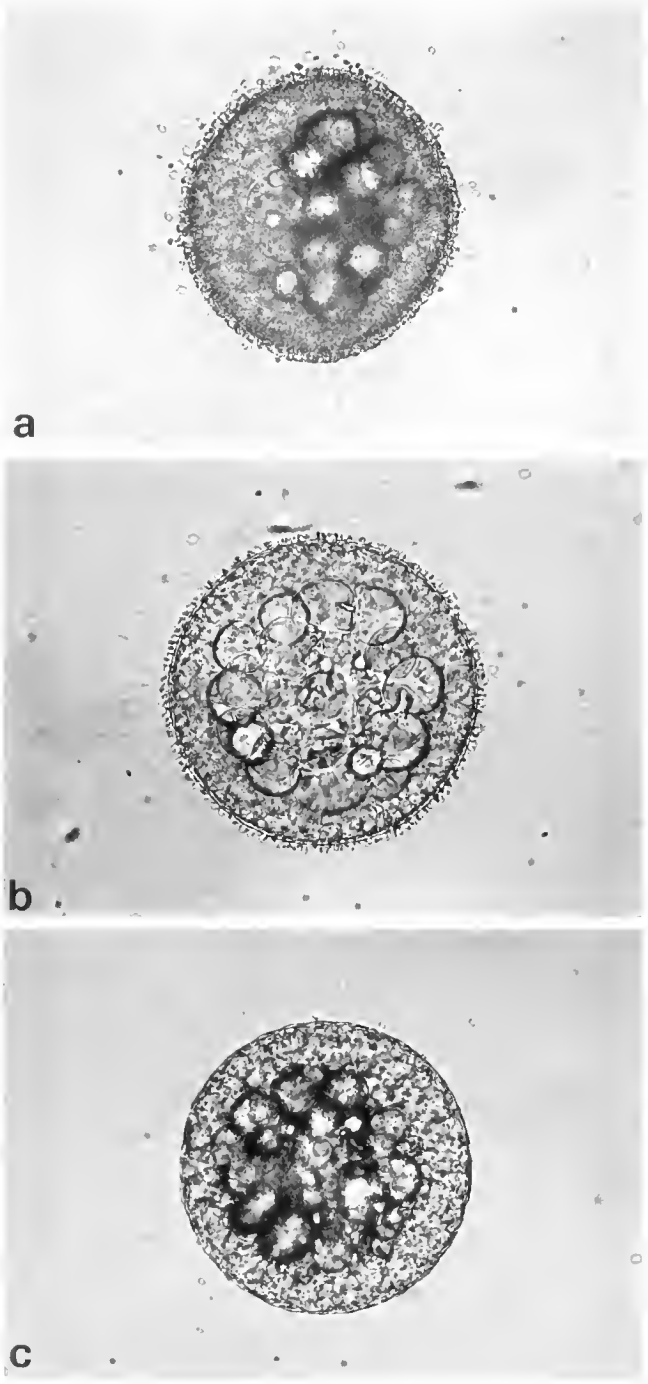

Figure 1. Sperm binding to the fixed *Tylorrhynchus* eggs. Two hours after insemination. ×260. (a) *Tylorrhynchus* sperm were bound to the egg in artificial ordinary seawater. (b) *Tylorrhynchus* sperm were bound to the egg in artificial Ca-free seawater. (c) Sperm of the sea star *Asterina pectinifera* were not bound to the egg in artificial ordinary seawater.

confirm these sperm bindings, and demonstrate that factors for the reception of initial sperm attachment and for the induction of sperm acrosome reaction are distributed in the outermost layer of the egg envelope all over the egg surface.

Materials and Methods

Preparation of gametes

Mature worms of the nereidid polychaete *Tylorrhynchus heterochaetus* were collected in Natori, Miyagi Prefecture, Japan. They were placed in 30% seawater (salinity: about 10), and refrigerated at 0–5°C. Gametes were obtained by compressing or cutting the body with forceps. Unfertilized eggs were washed several times in 30% seawater; sperm were diluted in ordinary seawater (*cf.* Osanai, 1978).

Experimental media

Natural seawater filtered with a paper filter (Toyoroshi No. 2) or Herbst's artificial seawater (ordinary and Ca-free seawater) modified by Motomura (1938) were used. Ca-free seawater was prepared by substituting NaCl for $CaCl_2$.

Isolation of chorion from eggs

Egg envelopes (chorions) were isolated from unfertilized eggs as described by Osanai (1976, 1983). The unfertilized eggs were suspended in 30% seawater and then gently homogenized with a teflon homogenizer. The homogenate was centrifuged at $300 \times g$ for 5 min. After removing the supernatant, the sedimented chorions were resuspended in fresh 30% seawater and centrifuged again. Transparent chorions were obtained by repeating this procedure several times.

Preparation of fixed eggs

The sperm-egg binding process was examined using fixed unfertilized eggs as described in sea urchins by Kato and Sugiyama (1978). The eggs were prefixed in 1% glutaraldehyde in 30% seawater for 0.5–2 h. After rinsing in 30% seawater several times, the eggs were inseminated. In other cases, unfertilized eggs were pretreated with 0.1% pronase (Kaken Chemical Co.) in 30% seawater for 20 min prior to prefixation.

Insemination

Tylorrhynchus eggs are fertilizable in media over a wide range of salinity. In this study, sperm were added to isolated chorions and fixed eggs in 30% or 100% seawater. When insemination occurred in Ca-free seawater, the chorions and eggs had been rinsed several times in Ca-free seawater, so that the concentration of contaminating Ca at insemination might be less than 1/1000 of that in ordinary seawater. Egg or chorion suspensions ($1–5 \times 10^2$/ml) were inseminated with sperm suspension (final concentration: 10^{-4} dilution of dry sperm, 5×10^6–1×10^7/ml) at room temperature (10–20°C).

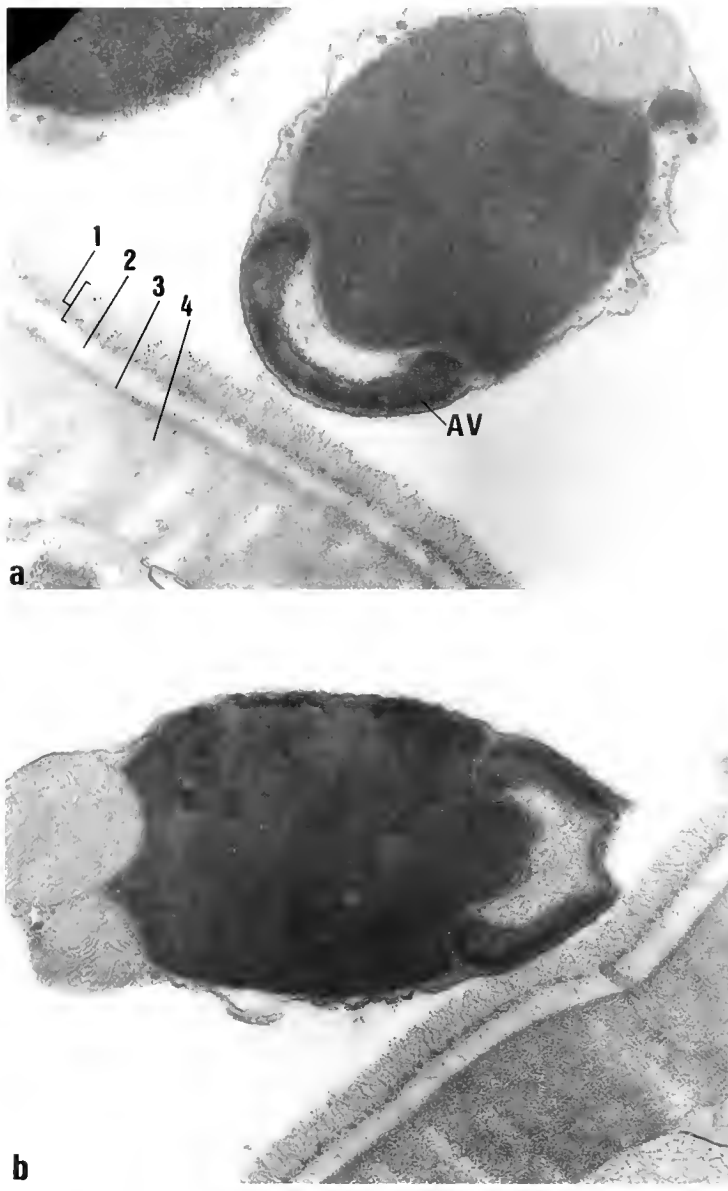

Figure 2. Attachment of unreacted sperm to the fixed eggs in artificial Ca-free seawater. One minute after insemination. ×31,500. (a) A spermatozoon attached to the first layer (1) of chorion by its head-tip without any acrosomal change. (2, 3, 4) The second, third, and fourth layer of the chorion, respectively. AV: acrosomal vesicle. (b) A spermatozoon with its acrosomal vesicle open at the head-tip. The outer membrane of sperm head was attached to the first layer of chorion.

Test of acrosome reaction-inducing activity in material dissolving from chorions

Isolated chorions were placed in distilled water (DW) (2% V/V) for 0.5–5 h. The chorion suspension was filtered through filter paper. The filtrate was diluted with ordinary seawater to 30% seawater and used as chorion extract.

Sperm suspension was added to the chorion extract (final sperm concentration: $1–5 \times 10^7$/ml). The test solution was fixed with 1–2% glutaraldehyde 15–40 min later. Sperm acrosome reaction was checked by phase-contrast microscopy (×1000).

Electron microscopy

Specimens were fixed in 2% glutaraldehyde in 70–90% seawater for several days at 0–4°C. After rinsing, they were postfixed in 1% OsO_4 in 70–90% seawater for 1 h at 0–4°C. The specimens were dehydrated in ethanol and embedded in Epon 812. Thin sections were stained with uranyl acetate and lead citrate or with 10% phosphotung-

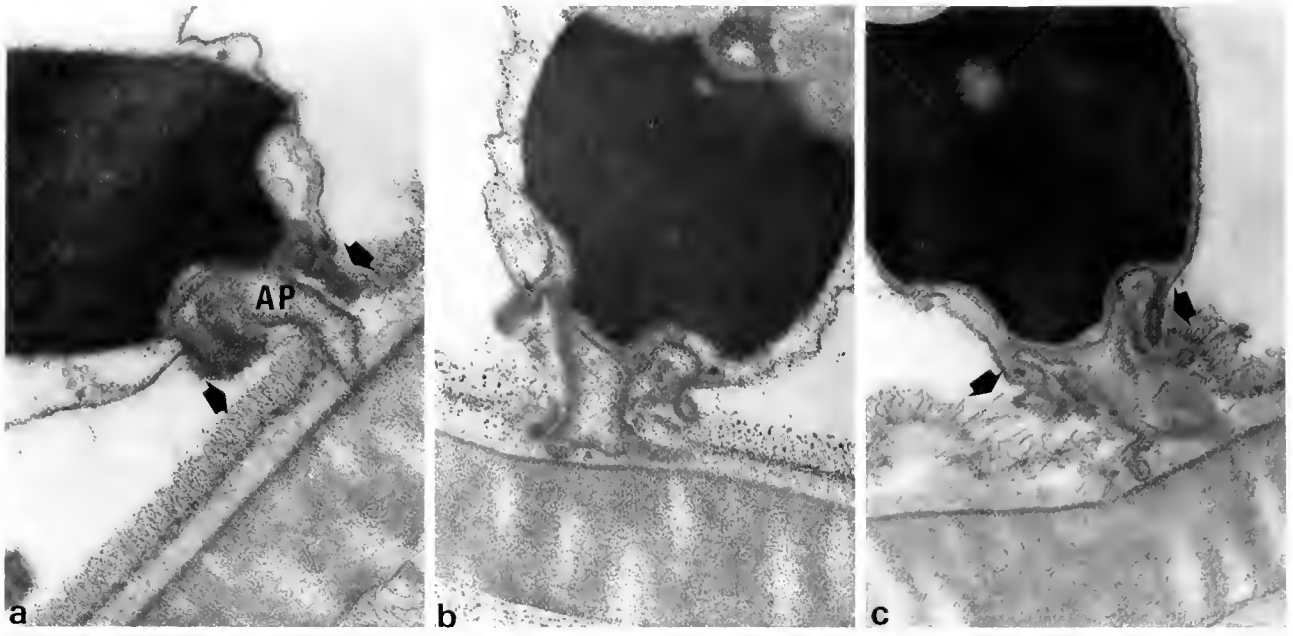

Figure 3. Adhesion of reacted sperm to the fixed eggs in artificial ordinary seawater (a, b, c). One minute after insemination. The acrosomal process (AP) penetrated the first and second layers of chorion and adhered to the third layer. The outer membrane of acrosome was in contact with the fibrous component of the first layer of chorion (arrows). ×35,000.

stic acid (PTA), and then examined with a transmission electron microscope.

Results

Sperm binding to fixed eggs

In both ordinary seawater and Ca-free seawater, *Tylorrhynchus* sperm were bound to the surface of fixed eggs at their head-tip (Fig. 1a, b). When the fixed eggs were inseminated with sperm of the sea star *Asterina pectinifera* and the sea urchin *Strongylocentrotus nudus*, the sperm were not bound to the eggs (Fig. 1c).

The chorion (1–1.5 μm thick) consists of four layers (Fig. 2; see also Sato and Osanai, 1983). The first (outermost) layer is composed of a row of small packed spheres wrapped in fibrous matter. The second layer is composed of less electron-dense material. The third layer is a thin electron-dense layer. The fourth layer (innermost and thickest) is composed of densely packed material with many cavities opening toward the inner surface.

The ultrastructure of the sperm-egg binding was examined with specimens fixed 1 min after insemination. In Ca-free seawater, most sperm were attached to the first layer of chorion by their head-tip without any acrosomal change, though the acrosomal vesicle had opened in a few sperm (Fig. 2). The opening of the acrosomal vesicle was sometimes observed in free sperm suspended in seawater, and the usual morphological change associated with a true acrosome reaction did not occur. Thus, opening of the vesicle may be either a spontaneous phenomenon or an artifact of fixation. In any case, the outer surface of the sperm head-tip made contact with the fibrous component of the first layer.

When live eggs were inseminated in Ca-free seawater, sperm temporarily attached to the egg surface, but soon detached. The sperm-egg attachment without a sperm acrosome reaction seems to be less stable in live eggs than in fixed eggs.

In ordinary seawater, most sperm bound to the chorion underwent the acrosome reaction and formed a lobular acrosomal process (Fig. 3). The acrosomal process penetrated the first and second layers of the chorion and adhered to the third layer. At the same time, the outer membrane of the acrosome (the lateral side of the opened acrosomal vesicle) continued to contact the fibrous component of the first layer of the chorion. Some sperm that had not undergone the acrosome reaction were attached to the first layer of the chorion.

Sperm binding to isolated chorions

In intact unfertilized eggs, the first layer of the chorion was stained by PTA (Fig. 4a, see also, Sato and Osanai, 1983). The outer surface of the isolated chorion (morphologically similar to the third layer) was stained with PTA (Fig. 4b), suggesting that the first and second layers had been deformed or had collapsed onto the third layer.

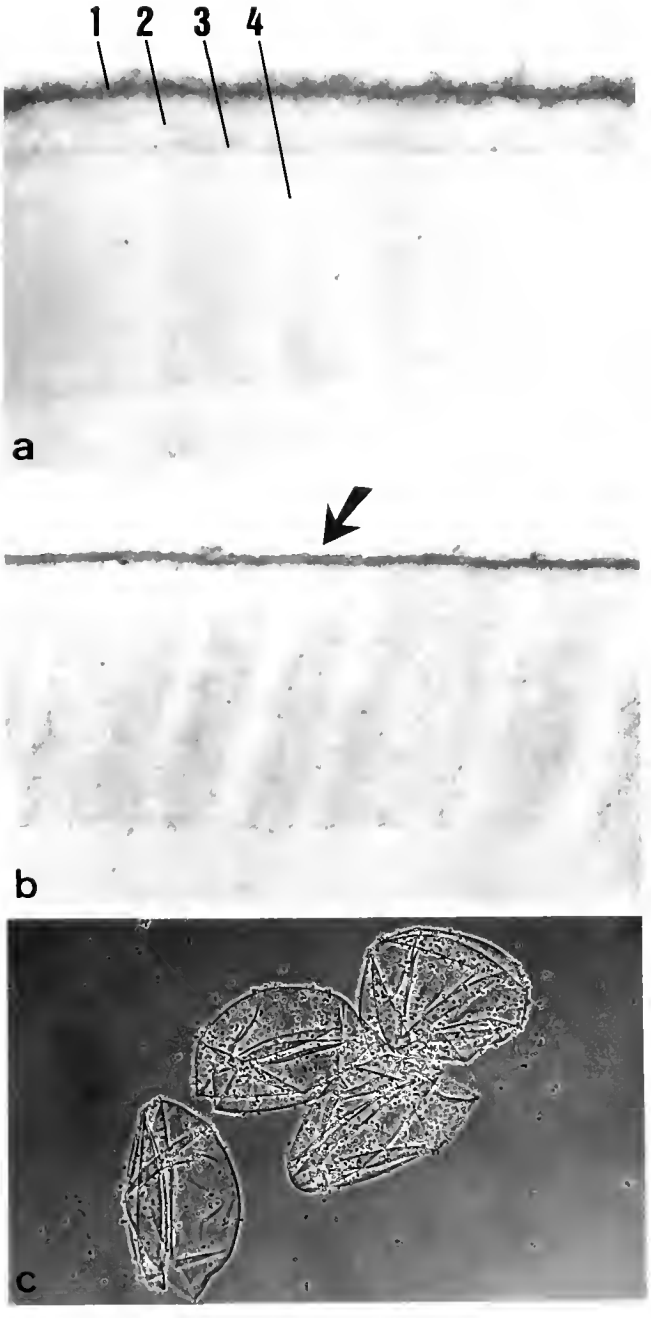

Figure 4. (a) Ultrastructure of the surface of an intact unfertilized egg. A section stained with phosphotungustic acid (PTA). The first layer (1) of the chorion was stained intensively. (2, 3, 4) The second, third, and fourth layer of the chorion, respectively. ×40,800. (b) Ultrastructure of the isolated chorion. A section stained with PTA. The outer surface (arrow), which was morphologically similar to the third layer, was stained. ×45,600. (c) Sperm binding to the isolated chorions in artificial ordinary seawater. Two minutes after insemination. ×140.

Sperm were bound to the isolated chorion in both ordinary and Ca-free seawater, and the bindings of sperm were kept for a long time (Fig. 4c). Because the isolated chorion was transparent, the acrosome reaction of the attached sperm could be checked by phase-contrast microscopy. In ordinary seawater, many sperm underwent the acrosome reaction (Table I, Fig. 5). These sperm were also examined by electron microscopy. The lobular acrosomal process adhered to the outer surface of the chorion and did not penetrate it (Fig. 6a). In Ca-free seawater, the

Table I

Percentage of occurrence of acrosome reaction in sperm bound to isolated chorion in presence or absence of Ca^{2+}

Expt. No.	Percentage of acrosome reaction	
	Ordinary seawater	Ca-free seawater
1	83.0	0.4
2	64.4	0
3	61.3	0.2
4	11.6	0

Isolated chorions were fixed 1–10 min after insemination. Occurrence of acrosome reaction was checked by phase contrast microscopy in 200–300 spermatozoa on 3–6 chorions.

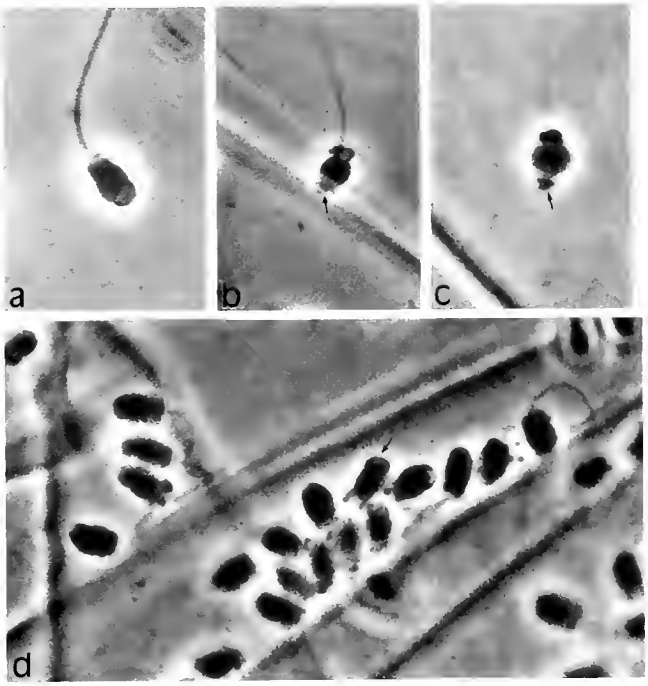

Figure 5. Phase contrast micrographs of sperm binding to the transparent isolated chorions. × 1900. (a) Control. An intact free-swimming spermatozoon. (b, c) Spermatozoa undergoing acrosome reaction and adhering to the chorion in artificial ordinary seawater. Ten minutes after insemination. Arrows indicate the development of acrosomal process. (d) Spermatozoa attached to the chorion without acrosome reaction in artificial Ca-free seawater. An arrow indicates an intact acrosomal vesicle. Ten minutes after insemination.

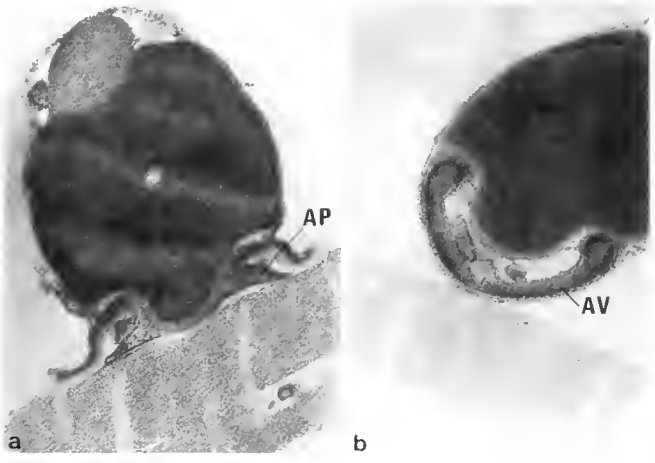

Figure 6. Electron micrographs of sperm binding to the isolated chorion. One minute after insemination. × 24,800. (a) A spermatozoon adhering to the outer surface of chorion with the spread acrosomal process (AP) in artificial ordinary seawater. (b) A spermatozoon attached to the outer surface of the chorion without acrosome reaction in artificial Ca-free seawater. AV: Acrosomal vesicle.

sperm bound to the isolated chorion did not undergo the acrosome reaction (Table I, Fig. 6b). The outer acrosomal membrane of sperm head-tip was attached to the chorion surface. No spermatozoon was bound to the inner surface of the chorion (the fourth layer) in both ordinary and Ca-free seawater.

Effect of pronase treatment of eggs on sperm-egg binding

We tried to remove the egg-surface component that binds sperm and induces the acrosome reaction. Unfertilized eggs were pretreated with pronase and then fixed. After rinsing, the eggs were inseminated in 30% seawater. Sperm attachment was blocked or greatly reduced (Table II, Fig. 7).

The pronase-treated eggs were examined by electron microscopy. The first and the second layers were removed from the chorion in the pronase-treated eggs (Fig. 8). The outer surface of the chorion did not stain with PTA.

Acrosome reaction-inducing activity in chorion extract

Chorion extracts were prepared by soaking chorions in DW. Sperm were added to the chorion extract diluted with natural seawater. Many of the free swimming sperm underwent acrosome reaction (Fig. 9, Table III). The sperm did not undergo acrosome reactions in control media (30% seawater).

After isolated chorions were treated with DW, they were mixed with sperm in 30% seawater. Few sperm were bound to the chorions (Fig. 10). These chorions were examined by electron microscopy. The PTA-positive layer at the outer surface of the chorions became thinner after the DW-treatment (Fig. 11). No morphological change was observed in other parts of chorion.

Discussion

Osanai (1983) used light microscopy to examine sperm binding to the isolated chorion in *Tylorrhynchus heterochaetus*. He showed that sperm binding includes two steps: sperm attachment before the acrosome reaction and sperm adhesion after the acrosome reaction. He also showed that the progression from sperm attachment to adhesion requires external calcium ions. We used electron and light microscopy to observe sperm-chorion binding using fixed eggs and isolated chorions. Our results confirm the validity of Osanai's (1983) report.

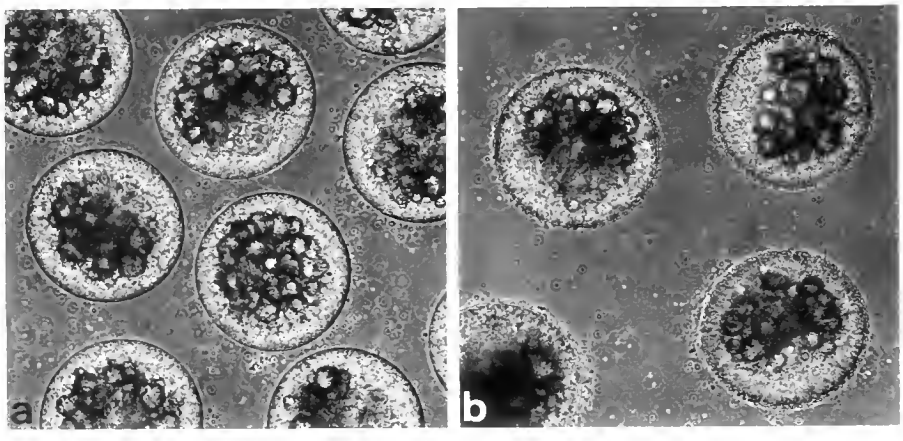

Figure 7. Inhibition of sperm binding by pronase-pretreatment of eggs. The eggs were inseminated in 30% natural seawater after glutaraldehyde-fixation, and observed 10 min after insemination. × 140. (a) The eggs pretreated with pronase for 20 min. Sperm did not bind to the eggs. (b) The eggs without pronase-pretreatment. Many sperm bound to the eggs.

Table II

Decrease of sperm binding by pronase-pretreatment of eggs

Eggs	No. of sperm bound on the egg contour*
Pronase-treated	3.2 ± 0.7 (n = 20)
Untreated	66.5 ± 3.6 (n = 12)

* Average ± SD (No. of eggs examined).

Sperm attachment and adhesion were demonstrated ultrastructually in Ca-free seawater and ordinary seawater, respectively. Both were also photographed 1 min after insemination during normal fertilization (Sato and Osanai, 1983). However, in normal fertilization, the sperm attachment step is rather inseparable, because it is followed quickly by the acrosome reaction. We could separate the sperm attachment step in Ca-free medium, in which the acrosome reaction was prevented.

Sperm attachment occurred at only the head-tip of conspecific sperm. This appears to be a species-specific and site-specific reaction for the first sperm-egg recognition. Specific attachment between sperm and egg envelope before the acrosome reaction is also known in an ascidian (Rosati and De Santis, 1978) and in mammals (Wassarman *et al.*, 1985). Sperm attachment was inde-

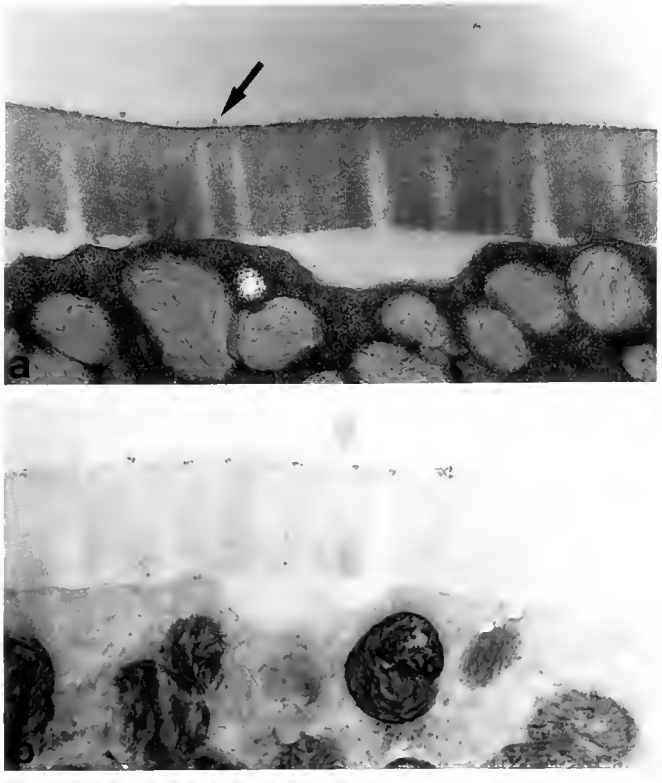

Figure 8. Ultrastructure of the pronase-treated eggs. The eggs were treated with pronase for 20 min. ×24,000. (a) A section stained with uranyl acetate and lead citrate. Most parts of the first and second layers of the chorion disappeared with a few spherical components of the first layer remaining on the surface (arrow). (b) A section stained with phosphotungstic acid. The outer surface of the chorion was not stained as compared with the untreated egg and the isolated chorion (Fig. 4).

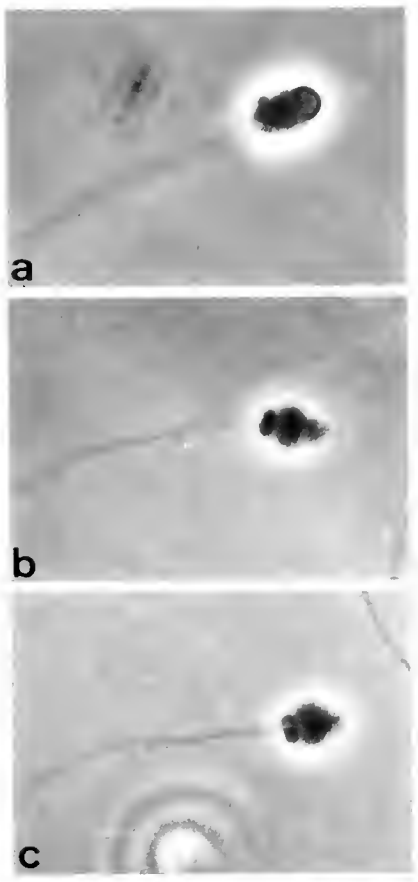

Figure 9. Induction of acrosome reaction by the chorion extract. ×2,100. (a) Unreacted sperm in control medium (30% seawater). (b, c) Sperm undergoing acrosome reaction in the chorion extract.

Table III

Acrosome reaction-inducing activity of the chorion extract

Expt. No.	Duration of incubation in distilled water (h)	Percentage of acrosome reaction*	
		Extract	Control**
1	0.5	82.4	0
2	1.5	3.7	2.7
3	5	77.4	1.9
4	5	19.1	7.6

* Occurrence of acrosome reaction was checked in 100–150 spermatozoa by phase contrast microscopy.

** 30% natural seawater.

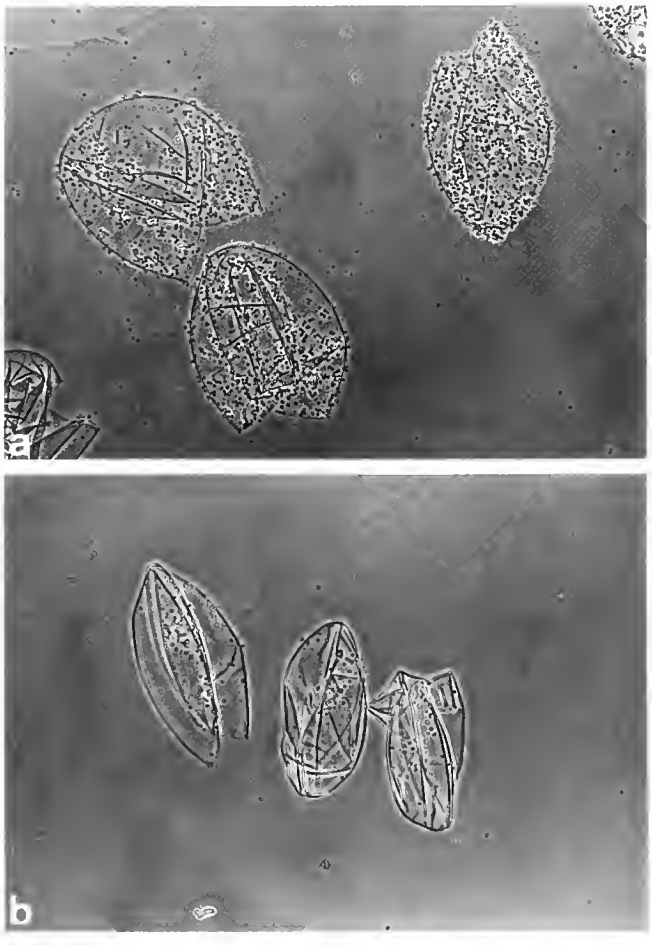

Figure 10. Decrease of sperm binding by soaking of the isolated chorions in distilled water. The isolated chorions were inseminated in 30% natural seawater just after preparation (a) or after distilled water-treatment of the chorions for 90 min (3 times). Many sperm bound to the chorion in the former (a), but not in the latter (b) 30 min after insemination. · 130.

pendent of external calcium ions in *Tylorrhynchus heterochaetus*, while it was calcium-dependent in mouse eggs (Saling *et al.*, 1978; Saling and Storey, 1979; Soldani and Rosati, 1987). Why sperm attachment to live *Tylorrhynchus* eggs is less stable than to fixed eggs or isolated chorions, in Ca-free seawater, is unknown. The outermost layer of the chorion of live eggs may be less tightly fastened to the chorion proper. Alternatively, attached sperm may be detached by a factor secreted from live eggs, as in normally fertilized eggs (Osanai, 1976). However, it is unknown whether unfertilized eggs secrete the sperm-detaching factor in Ca-free solution.

The acrosome reaction in *Tylorrhynchus heterochaetus* evidently requires external calcium ions as in sea urchins (Dan, 1954; Collins and Epel, 1977). The jelly, the outermost layer of the sea urchin egg envelope, induces the acrosome reaction and sperm aggregation behavior (see Epel, 1978). Sperm aggregation can be induced even in a medium of low Ca^{2+} concentration, in which the acrosome reaction is prevented (Dan, 1954). Aggregation-inducing and acrosome reaction-inducing factors were separated from jelly of a starfish (Uno and Hoshi, 1978). Uno and Hoshi (1978) considered that sperm aggregation might reflect the initial sperm-egg interaction, *i.e.*, the sperm attachment to the jelly surface.

In intact *Tylorrhynchus* eggs, the PTA-positive fibrous substance coats the outer surface of chorion. Our results show that both the receptor for sperm attachment and the inducer for the acrosome reaction are associated with the PTA-positive layer. It is unknown whether the components of the PTA-positive layer function differently or whether a single factor has both functions. Because the PTA-positive layer corresponds to a periodic acid-Schiff (PAS)-positive one observed by light microscopy (Sato and Osanai, 1983) and is digested by pronase, it seems to contain polysaccharide and protein. The glycoprotein ZP3 of mouse zona pellucida is responsible for both sperm attachment and the induction of the acrosome reaction (Bleil and Wassarman, 1983). Other reports

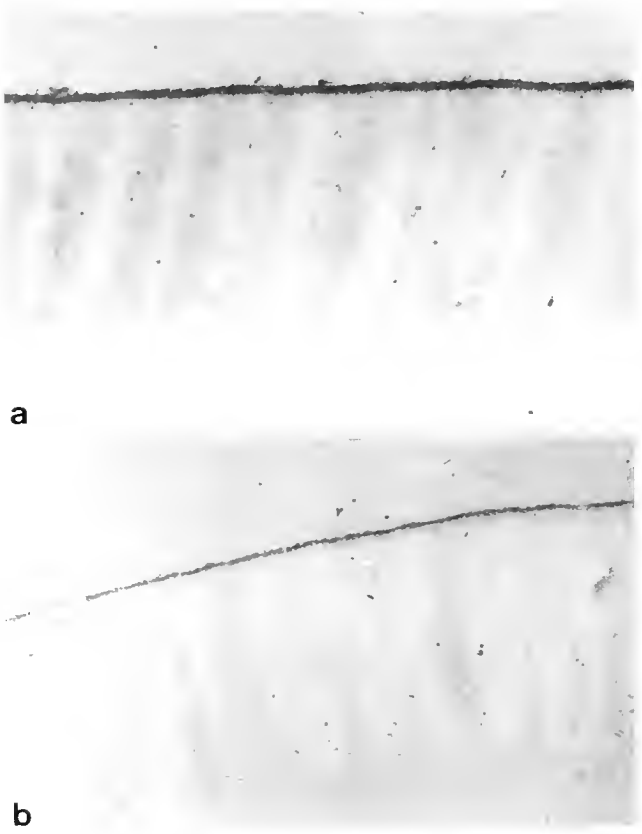

Figure 11. Ultrastructural alteration of the isolated chorion by the distilled-water treatment. Sections were stained with phosphotungstic acid (PTA). · 36,700. (a) An isolated chorion just after preparation. (b) An isolated chorion after distilled-water treatment for 60 min. The PTA-positive layer at the outer surface of the chorion became thinner.

showed that a sugar or glycoprotein on an egg envelope plays an important role in sperm attachment or induction of the acrosome reaction in the eggs of a mouse (Shur and Hall, 1982a, b), an ascidian (Rosati and De-Santis, 1980; Pinto *et al.*, 1981), a horseshoe crab (Barnum and Brown, 1983), a sea urchin (Segall and Lennarz, 1979; Yoshida and Aketa, 1983), a seastar (Uno and Hoshi, 1978), and a bivalve (Tumboh-Oeri and Koide, 1982).

The acrosomal process of the fertilizing spermatozoon fuses with a microvillus projecting from the egg through the chorion in *T. heterochaetus* (Sato and Osanai, 1983). However, no morphological difference of the PTA-positive layer was observed between regions around microvilli and the other regions. In contrast with *T. heterochaetus*, the acrosome reaction-inducing activity was localized to a limited number of specialized sites above egg microvilli in the nereidid polychaete *Neanthes japonica* (Sato and Osanai, 1986).

Sperm seem to initiate the acrosome reaction just after attaching to the chorion in the presence of Ca. Their acrosomal processes usually penetrate the first and second layers of the chorion and adhere to the third layer. Such sperm can fuse with an egg microvillus to fertilize the egg (Sato and Osanai, 1983). The initial attachment between the sperm head-tip and the outermost layer of chorion may be important for keeping the sperm oriented for successful fertilization during the acrosome reaction. Holding the sperm erect on the chorion surface should lead to proper penetration and adhesion of the acrosomal process.

Literature Cited

Aketa, K. 1973. Physiological studies on the sperm surface component responsible for sperm-egg bonding in sea urchin fertilization. I. Effect of sperm-binding protein on the fertilizing capacity of sperm. *Exp. Cell Res.* **80:** 439–441.

Aketa, K. 1975. Physiological studies on the sperm surface component responsible for sperm-egg bonding in sea urchin fertilization. II. Effect of Concanavalin A on the fertilization capacity of sperm. *Exp. Cell. Res.* **90:** 56–62.

Anderson, W. A., and W. R. Eckberg. 1983. A cytological analysis of fertilization in *Chaetopterus pergamentaceus*. *Biol. Bull.* **165:** 110–118.

Barnum, S. R., and G. G. Brown. 1983. Effect of lectins and sugars on primary sperm attachment in the horseshoe crab, *Limulus polyphemus* L. *Dev. Biol* **95:** 352–359.

Bleil, J. D., and P. M. Wassarman. 1983. Sperm-egg interactions in the mouse: sequence of events and induction of the acrosome reaction by a zona pellucida glycoprotein. *Dev. Biol.* **95:** 317–324.

Brandriff, B., G. W. Moy, and V. D. Vacquier. 1978. Isolation of sperm binding from the oyster (*Crassostrea gigas*). *Gamete Res.* **1:** 89–99.

Brown, G. G. 1976. Scanning electron-microscopical and other observations of sperm fertilization reaction in *Limulus polyphemus* L. *J. Cell Sci* **22:** 547–562.

Clark, Jr., W. H., M. G. Kleve, and A. I. Yudin. 1981. An acrosome reaction in natantian sperm. *J. Exp. Zool.* **218:** 279–291.

Collins, F., and D. Epel. 1977. The role of calcium ions in the acrosome reaction of sea urchin sperm: regulation of exocytosis. *Exp. Cell Res.* **106:** 211–222.

Dan, J. C. 1954. Studies on the acrosome. III. Effect of calcium deficiency. *Biol. Bull.* **107:** 335–349.

De Santis, R., G. Jamunno, and F. Rosati. 1980. A study of the chorion and the follicle cells in relation to the sperm-egg interaction in the ascidian, *Ciona intestinalis*. *Dev. Biol.* **74:** 490–499.

Epel, D. 1978. Mechanisms of activation of sperm and egg during fertilization of sea urchin gametes. Pp. 185–246 in *Current Topics in Developmental Biology*, Vol. 12, A. A. Moscona and A. Monroy, eds. Academic Press, New York.

Epel, D., and V. D. Vacquier. 1978. Membrane fusion events during invertebrate fertilization. Pp. 1–63 in *Membrane Fusion*, G. Poste and G. L. Nicolson, eds. Elsevier/North-Holland Biomedical Press, Amsterdam.

Hylander, B. L., and R. G. Summers. 1977. An ultrastructural analysis of the gametes and early fertilization in two bivalve molluscs, *Chama macerophylla* and *Spisula solidissima* with special reference to gamete binding. *Cell Tiss. Res.* **182:** 469–489.

Jaffe, L. A., and M. Gould. 1985. Polyspermy-preventing mechanisms. Pp. 223–250 in *Biology of Fertilization*, Vol. 3, C. B. Metz and A. Monroy, eds. Academic Press, New York.

Kato, K. H., and M. Sugiyama. 1978. Species-specific adhesion of spermatozoa to the surface of fixed eggs in sea urchins. *Dev. Growth Differ.* **20:** 337–347.

Lewis, C. A., C. F. Talbot, and V. D. Vacquier. 1982. A protein from abalone sperm dissolves the egg vitelline layer by a nonenzymatic mechanism. *Dev. Biol.* **92:** 227–239.

Lopo, A. C. 1983. Sperm-egg interactions in invertebrates. Pp. 269–324 in *Mechanism and Control of Animal Fertilization*, J. F. Hartmann, ed. Academic Press, New York.

Monroy, A., and F. Rosati. 1983. A comparative analysis of sperm-egg interaction. *Gamete Res.* **7:** 85–102.

Motomura, I. 1938. Effect of some salt solutions on the parthenogenetic membrane formation of sea urchin eggs. *Sci. Rep. Tohoku Univ. Ser. IV (Biol.)* **13:** 85–88.

Osanai, K. 1976. Egg membrane-sperm binding in the Japanese palolo eggs. *Bull. Mar. Biol. Stn. Asamushi, Tohoku Univ.* **15:** 147–155.

Osanai, K. 1978. Early development of the Japanese palolo, *Tylorrhynchus heterochaetus*. *Bull. Mar. Biol. Stn. Asamushi, Tohoku Univ.* **16:** 59–69.

Osanai, K. 1983. Induction of Acrosome reaction with the isolated chorion in polychaete spermatozoa. *Bull. Mar. Biol. Stn. Asamushi, Tohoku Univ* **17:** 159–164.

Pinto, M. R., R. De Santis, G. D'Alessio, and F. Rosati. 1981. Studies on fertilization in the ascidians. Fucosyl sites on vitelline coat of *Ciona intestinalis*. *Exp. Cell Res.* **132:** 289–295.

Rosati, F. 1985. Sperm-egg interaction in ascidians. Pp. 361–388 in *Biology of Fertilization*, Vol. 2, C. B. Metz and A. Monroy, eds. Academic Press, New York.

Rosati, F., and R. De Santis. 1978. Studies on fertilization in the ascidians. I. Self-sterility and specific recognition between gametes of *Ciona intestinalis*. *Exp. Cell Res* **112:** 111–119.

Rosati, F., and R. De Santis. 1980. Role of the surface carbohydrates in sperm-egg interaction in *Ciona intestinalis*. *Nature* **283:** 762–764.

Saling, P. M., and B. T. Storey. 1979. Mouse gamete interactions during fertilization in vitro. Chlortetracycline as a fluorescent probe for the mouse sperm acrosome reaction. *J. Cell Biol.* **83:** 544–555.

Saling, P. M., B. T. Storey, and D. P. Wolf. 1978. Calcium dependent binding of mouse epididymal spermatozoa to the zona pellucida. *Dev. Biol.* **65:** 515–525.

Sato, M., and K. Osanai. 1983. Sperm reception by an egg microvillus in the polychaete, *Tylorrhynchus heterochaetus*. *J. Exp. Zool.* **227:** 459–469.

Sato, M., and K. Osanai. 1986. Morphological identification of sperm receptors above egg microvilli in the polychaete, *Neanthes japonica*. *Dev. Biol.* **113:** 263–270.

SeGall, G. K., and W. J. Lennarz. 1979. Chemical characterization of the component of the jelly coat from sea urchin eggs responsible for induction of the acrosome reaction. *Dev. Biol.* **71:** 33–48.

Shur, B. D., and N. G. Hall. 1982a. Sperm surface galactosyltransferase activities during *in vitro* capacitation. *J. Cell Biol.* **95:** 567–573.

Shur, B. D., and N. G. Hall. 1982b. A role of mouse sperm surface galactosyltransferase in sperm binding to the egg zona pellucida. *J. Cell Biol.* **95:** 574–579.

Soldani, P., and F. Rosati. 1987. Sperm-egg interaction in the mouse using live and glutaraldehyde-fixed eggs. *Gamete Res.* **18:** 225–235.

Summers, R. G., and B. L. Hylander. 1974. An ultrastructural analysis of early fertilization in the sand dollar, *Echinarachnius parma*. *Cell Tiss. Res.* **150:** 343–368.

Summers, R. G., and B. L. Hylander. 1975. Species-specificity of acrosome reaction and primary gamete binding in echinoids. *Exp. Cell Res.* **96:** 63–68.

Tumboh-Oeri, A. G., and S. S. Koide. 1982. Mechanism of sperm-oocyte interaction during fertilization in the surf clam *Spisula solidissima*. *Biol. Bull.* **162:** 124–134.

Uno, Y., and M. Hoshi. 1978. Separation of the sperm agglutinin and the acrosome reaction-inducing substance in egg jelly of starfish. *Science* **200:** 58–59.

Vacquier, V. D. 1980. The adhesion of sperm to sea urchin eggs. Pp. 151–168 in *The Cell Surface: Mediator of Developmental Processes*, S. Subtelny and N. K. Wessells, eds. Academic Press, New York.

Wassarman, P. M., H. M. Florman, and J. M. Greve. 1985. Receptor-mediated sperm-egg interactions in mammals. Pp. 341–360 in *Biology of Fertilization*, Vol. 2, C. B. Metz and A. Monroy, eds. Academic Press, New York.

Yoshida, M., and K. Aketa. 1983. A 225 K dalton glycoprotein is the active core structure of the sperm-binding factor of the sea urchin, *Anthocidaris crassispina*. *Exp. Cell Res.* **148:** 243–248.

Reference: *Biol. Bull.* **178**: 111–117. (April, 1990)

A Photoperiod Determined Life-Cycle in an Oligochaete Worm

BERND SCHIERWATER[1] AND CARL HAUENSCHILD

Zoologisches Institut der Technischen Universitaet, Pockelsstr. 10a, 3300 Braunschweig, West Germany

Abstract. For one common cosmopolitan naidid worm, *Stylaria lacustris*, we studied the effects of different environmental factors upon (1) the alternation of reproductive modes, (2) the rates of population increase, and (3) the combination of each of (1) and (2). While age, temperature, population density, or rate of feeding did not affect the mode of reproduction, photoperiod had a dominant effect. Under long-day conditions (LD > 12:12), all worms reproduced exclusively by paratomic fission, theoretically *ad infinitum*. When transferred to short-day conditions (LD ≤ 12:12) the worms ceased vegetative reproduction, and within 2 to 4 weeks developed the hermaphroditic genital apparatus and a clitellum. After an additional two weeks, the first cocoons were produced. The switch to the bisexual mode of reproduction was *cum grano salis* irreversible. These findings are consistent with observations of field samplings, and allow one to predict the annual life-cycle strategy of *S. lacustris*. This is the first example of a photoperiod determined life-cycle within the oligochaete worms.

The vegetative mode of reproduction led to extremely high rates of population increase, whereas with the bisexual mode of reproduction the number of individuals was roughly stable. However, because *S. lacustris* could not withstand temperatures of 5°C or lower, the switch to sexual reproduction and the formation of diapausing cocoons appear to be the only mechanism of overwintering. Nevertheless, some 'asexual' clones never switch to sexual reproduction, whereas a loss of the asexual vegetative mode of reproduction did not occur. In contrast to some general predictions from life-history theories, the reproductive strategy of *S. lacustris* is highly preprogrammed and cannot respond to sudden and unexpected environmental changes.

Received 13 November 1989; accepted 2 January 1990.

[1] Present address: Yale University, Department of Biology, P.O. Box 6666, New Haven, CT 06511.

Introduction

With the pollution of our environment, present day ecology demands investigation of the biological mechanisms that regulate the distribution and dynamics of populations in a given environment (*e.g.*, Brinkhurst and Jamieson, 1971; McElhone, 1978; Brinkhurst and Cook, 1980; Tauber *et al.*, 1986; Zaslwaski, 1988; Klerks and Levington, 1989). The rapid increase in theories on the evolution of life histories demands extended experimental work and empirical data (*cf.* Stearns, 1976, 1980; Reznick, 1985; Hoekstra, 1987; Michod and Levin, 1988; Hauenschild, 1989; Nunney, 1989).

The study of particular oligochaete worms can be highly fruitful to our understanding of both the ecological and the evolutionary implications of animal life-cycles for two reasons: (1) the oligochaete worms in general are regarded as perhaps the most important group concerned with the retrieval of organic matter in freshwaters (*e.g.*, Brinkhurst and Jamieson, 1971; Dumnicka and Pasternak, 1978; Brinkhurst and Cook, 1980). (2) Those oligochaete worms that are capable of reproducing both by a bisexual and by a vegetative mode of reproduction, in particular the Aeolosomatidae and Naididae, allow intraspecific comparisons of the consequences of sexual *vs.* asexual life-history tactics; such systems allowing experimental work are badly needed but are difficult to find (*cf.* Bell, 1980; Townsend and Calow, 1981; Calow, 1983; Reznick, 1985; Hoekstra, 1987; Abugov, 1988; Schierwater, 1989; Hadrys *et al.*, 1990). Unfortunately, the number of well understood life-cycles that include an 'alternation of reproductive modes,' is surprisingly low (*cf.*, Giese, 1959; Giese and Pearse, 1959; Kinne, 1970; Brinkhurst and Cook, 1980; Townsend and Calow, 1981; Holm, 1988).

Records of the reproductive ecology of most oligochaetes are limited to notes on the presence of sexually mature specimens in field populations, but almost no conclusions can be drawn from these scattered notes; thus, little is known about the mechanisms affecting the mode of reproduction and hence their annual life-cycles (*e.g.,* Vershinin and Semernoi, 1977; McElhone, 1978, 1982; Mill, 1978; Brinkhurst and Cook, 1980; Pascar-Gluzman, 1981; Wetzel, 1982).

In this study we will present the annual life-cycle model as well as quantitative data on the consequences of sexual *vs.* asexual reproduction for the cosmopolitan naidid *Stylaria lacustris* Linnaeus 1758. Its life-cycle has not been described, though growth rates of vegetative worms have been studied (Streit, 1978; McElhone, 1982; Finogenova, 1984) and several brief notes about sexual worms are available (Kamlyuck and Kovaltchuk, 1972; McElhone, 1978, 1982; Wetzel, 1982). McElhone (1982) suggested that food supply, food quality, and water quality may affect the 'alternation of reproductive modes' in *S. lacustris.* In this study we will demonstrate that the life cycle of *S. lacustris* is strictly and exclusively determined by the photoperiod (day-length). We shall discuss this first finding of a photoperiod-determined life-cycle in an oligochaete worm in an ecological context regarding the evolution of the life-history strategy.

Materials and Methods

Animals

Stylaria lacustris is one of the most common and widely distributed oligochaete species, found in Europe, Asia, Africa, and North America (*e.g.,* Brinkhurst and Jamieson, 1971; Vershinin and Semernoi, 1977; McElhone, 1978; Pascar-Gluzman, 1981; Wetzel, 1982). In *S. lacustris,* the vegetative mode of reproduction follows the type of paratomic fission of animal chains of between two to three individuals (Stephenson, 1930). The biology of sexual reproduction has not been described.

Worms were counted as 'sexual' if either gonads and/or a clitellum were visible. All other worms were called 'vegetative' independent of the formation of tomits.

Field samples

All animal material of *Stylaria lacustris* was collected from the field at different times and transferred into the laboratory for culturing under defined laboratory conditions. Worms were collected in W. Germany from a pond at Weddel, Braunschweig, in July 1985, Sept. and Oct. 1987, June and July 1988, and from the river Ilmenau at Uelzen in August 1986, '87, '88. Right after sampling, as many worms as possible were isolated and checked within 24 h for their reproductive status (*i.e.,* presence or absence of a clitellum, gonads, tomits) by means of a dissection microscope at 20×.

Laboratory studies

Under defined laboratory conditions, we investigated whether the following environmental factors influence the 'alternation of reproductive modes': temperature, feeding, population density, and photoperiod.

Culturing. Culture dishes (400 cm^3 'deep freeze' plastic containers) were kept in thermoregulated rooms or in chambers providing temperature constancy to ±1°C, as controlled by mini-max-thermometers; normal photoperiod setting was LD = 16:8, unless otherwise stated. *S. lacustris* was cultured either in filtered and heated (2 h at 80°C) water of its natural environment, or in carbonic-acid-free natural mineral water ('Vittel' or 'Volvic'). Worms were fed on the green algae *Haematococcus lacustris* and *Gonium sociale ad lib.* The air bubbled culture dishes were washed, and water and food were renewed twice a week.

Acclimation time to any new experimental condition was 24 h. The highest changes in temperature were 5°C per day. Temperature changes of 10°C were done stepwise within 4 days. For long-period observations on the reproductive activity under different feeding, temperature, and photoperiod conditions, acclimation time was 14 days, unless otherwise stated.

Animals were observed through a binocular microscope ('Zeiss' 475052-9901) with variable magnifications from 8× to 50×. One ocular was equipped with a μm-scale for *in vivo* measurements of one-dimensional distances.

Photoperiod settings. Experiments on the effects of photoperiod on the mode of reproduction were run at 20 ± 1°C, unless otherwise stated. The following LD settings were used: LD = 6:18, 12:12, 16:8, 18:6, and 24:0. Light intensities were 500–2000 lx during light periods and ≈0.05 lx in the dark, respectively. The light intensities were measured with a lightmeter (Gossen, Mavolux 6C 18493), and because of the use of fluorescent lights (Osram L40W/22-1), the light intensity values have to be taken with care. During all experiments and observations on the effects of temperature, feeding rate, population density and age, light-dark rhythm was held constant at LD = 16:8.

Mean doubling times. For observations on mean doubling times (mdt), 30 worms each were placed in plastic chambers of ≈400 cm^3, and the number of worms per chamber was counted once a week. After each counting, the total number of worms was reduced to a maximum of 50 worms per chamber. Two populations (one from Weddel pond and one from the river Ilmenau) were followed over 8 weeks (2 weeks acclimation plus 6 weeks of registration) at 10, 15, 20, and 25°C. The mdt's were

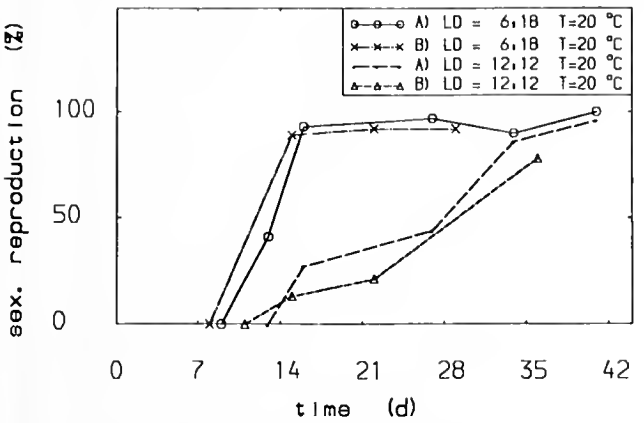

Figure 1. Examples for the time course of switching from the vegetative to the bisexual mode of reproduction induced by the photoperiod in *Stylaria lacustris*. Vegetatively reproducing worms from the field were exposed to short-day conditions of either LD = 12:12 or LD = 6:18 at day 0 in the figure; A = Weddel 1985, B = Ilmenau 1986 population; the points for LD = 16:8 are not shown, for all of them would lie along the abscissa (= 0% sexual reproduction); N > 1000 for each population.

calculated from the initial population size (N1), the final population size (N2) and the time (t) in days between the countings: mdt = log 2 t/(log N2 − log N1).

Statistics. The non-parametric Mann-Whitney-U test (two-tailed) was used to compare the means of two independent samples, and the Jonckheere test was used to look for monotonous trends in three or more independent samples (Lienert, 1976). The number of statistical replicates (*i.e.*, number of cultures tested under the same experimental conditions) is given as n in the text, whereas N means the total number of worms checked for their reproductive mode during one experiment.

Results

Photoperiod

The mode of reproduction was strictly determined by the photoperiod. Under long-day conditions (LD > 12:12) the worms reproduced exclusively vegetatively by paratomic fission. Exposure to short-day conditions (LD ≤ 12) induced a quantitative switch from paratomic fission to sexual reproduction within 10 to 30 days (Fig. 1), *i.e.*, the hermaphroditic genital apparatus has been developed. The formation of the clitellum always occurred after the gonads became visible (in some cases up to 25 days later). The reaction time to the short-day condition, *i.e.*, for the switch in the mode of reproduction, was affected by the temperature. One population was divided into three portions and each portion cultured at either 15, 20, or 25°C. With increasing temperature the time for switching from the vegetative to the sexual mode of reproduction was significantly shortened ($P \leq 0.001$, Jonckheere, N = 3 × 38; see Fig. 2).

The alternation of reproductive mode worked only in one direction, *i.e.*, only vegetative worms switched to sexual reproduction. Once this switch had occurred, it was *cum grano salis* irreversible. Ninety-one clitellate worms had been transferred back from LD = 6:18 to LD = 16:8 (T = 20°C) and watched for 42 continuous days. Only three worms reverted to vegetative asexual reproduction by forming tomits; in these three worms the clitellum of the parent individual was retained, whereas the daughter individuals showed normal asexual shape.

Bisexual reproduction excluded fission, *i.e.*, clitellate worms never formed tomits. Therefore, once a population became sexual, the number of worms per chamber became constant or even declined slightly, because some worms always died after changing the photoperiod. Under laboratory conditions, the number of cocoons produced per sexual worm was low at all tested temperatures. Rates of cocoon production ranged from 0.25 to 2.0 cocoons per sexual worm until death. The highest rates of cocoons produced per sexual worm, within 3 weeks after the clitellum became visible, were 0.5 (T = 15°C), 0.7 (T = 20°C), and 0.8 (T = 25°C). Generally the first cocoons were produced at 16.3 ± 5.61 days (range 7–31 days; N = 650, n = 13) after clitellum formation. Bisexual reproduction thus led to a very limited rate of production of reproductive units. Cocoons were lemon-shaped and preferably placed in the corners of the culture dishes. Mean ± SD cocoon length was 0.8 ± 0.07 mm (n = 78), and each cocoon contained a maximum of three embryos.

Asexual clones. Two culture populations of *S. lacustris* that came from the Weddel pond and had been cultured exclusively vegetatively (T = 20°, LD = 16:8) over 14 or 23 months, respectively, failed to show a photoperiodic

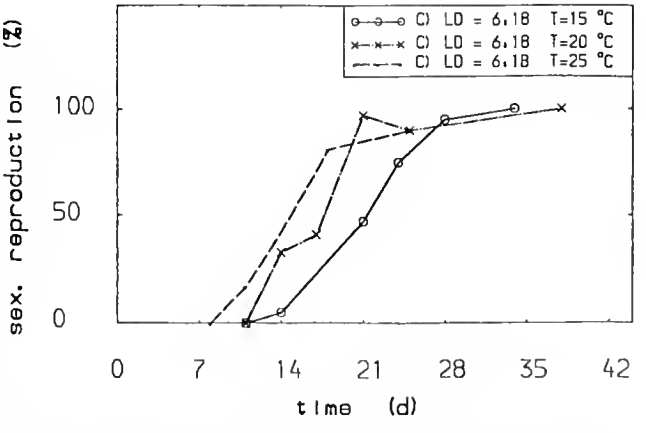

Figure 2. Example of the effect of temperature on the time course of switching from the vegetative to the bisexual mode of reproduction in *Stylaria lacustris;* one vegetative population (C = Weddel 1988) of 114 worms was divided into 3 portions, and each group of 38 worms was exposed to one of three different temperatures under short-day conditions (LD = 6:18) at day 0.

Table I

The mean doubling times (mdt) of vegetatively reproducing Stylaria lacustris *at different experimental temperatures*

T [°C]	N	n	mdt [d]	range min	range max
10	277	7	11.1 ± 4.04	9.3	16.9
15	657	12	6.9 ± 2.47	4.8	10.9
20	733	12	5.1 ± 2.83	2.7	13.2
25	854	12	5.0 ± 3.49	2.5	14.4

The means ± SD and the ranges over a 6-week observation period of each two cultures are given. At 10°C, one culture died after the first week of observation period, hence here n = 7.

reaction. Samples of each population were tested at both LD = 12:12 and LD = 6:18 each at 15°C and 20°C over 13 weeks. From 238 worms, only 8 worms, *i.e.*, ≈3%, became sexually mature.

Mean doubling times for vegetative populations. The differences in mdt between the Weddel and the Ilmenau populations were not significant (U-test) and hence the groups were pooled in Table I. The mdt decreased significantly with increasing temperature ($P \leq 0.05$, Jonckheere). However, the differences between 20°C and 25°C were not significant (U-test).

Other environmental factors

No *S. lacustris* worm reproduced sexually when the light period was ≥12 h per day. Thus, the mode of reproduction was independent of temperature, feeding and population density, and age (see Table II).

Temperature. Different populations of *S. lacustris* were exposed to temperatures between 5 and 30°C for 14 weeks. Temperatures of 5°C and 30°C were not tolerated, and all experimental animals died within 6 days (N = 2 × 63, n = 2 × 3). In the zone of thermal-tolerance, not one sexually reproducing individual was found (N > 1000) during 14 weeks of observation. One culture at 10°C was cultured for another 9 weeks and checked 3 times per week. On 10 October 1988 (after 21 weeks in controlled conditions), two worms were found that had a well developed genital apparatus and a clitellum. Neither worm was found after two weeks; their fate is unknown. Cocoons were not found.

Feeding. Feeding rates reduced to 3 days feeding per week over 10 weeks never led to a sexual worm. All worms kept reproducing vegetatively (N > 600, n = 3). Starvation experiments, resulting in LD_{50} values of 18 ± 3.75 days (range for total population extinction: 20–31 days), also never led to sexually reproducing worms (N = 100, n = 3; T = 20°C, LD = 16:8).

Population density. Different population densities of 0.1–1.5 worms cm^{-2} bottom area of culture dish were tested over 10 weeks at T = 20°C. No sexual worms were found (N > 1000, n = 3).

Field samples

Field samples of *S. lacustris* were taken at different times of the year. Only in one sample, collected in October 1987, were both vegetative as well as sexual worms found. In all other samples collected between June and September exclusively aclitellate worms were found (see Table III). The only exception was observed on 19 August 1988. Two clitellate worms were detected in a field sample from the Weddel pond collected on 17 July 1988. The sample (including plant material) had been stored in a plastic beaker in our laboratory for four weeks at natural daylight. Other worms found in the sample were aclitellate (N = 108) on 19–21 August.

Discussion

Although studies of the seasonal development of organisms have always occupied an important place in experimental biology, the leading role of the signaling factors in determining seasonal phenomena have been largely unknown. For *S. lacustris*, the results of this study unmistakably demonstrate that the life-cycle is strictly determined by the photoperiod as the relevant external signaling factor. Since the outstanding discoveries of Garner and Allard (1920) and Rowan (1926) on photoperiodic phenomena in plants and animals, many important contributions have derived from studies in particular on polychaetes and insects (for overview see Giese, 1959; Kinne, 1970; Segal, 1970; Hauenschild, 1975; Tauber *et al.*, 1986; Zaslawski, 1988), but none from the phylogenetically closely related oligochaetes.

The alternation of reproductive modes

Stylaria lacustris apparently measures the day-length (proximate factor) to prepare for the sharp temperature decline (ultimate factor) during winter. Under long-day (summer) conditions, the worms reproduced exclusively asexually by paratomic fission, theoretically *ad infinitum*. In the 1960's, Hauenschild (unpubl.) cultured a population of *S. lacustris* for more than six continuous years in the laboratory at LD = 16:8 and T = 20°C, and he did not find a single sexually mature worm during this period. In the short-day (autumn conditions), *S. lacustris* reproduces only once and then the worms die. Hence, *S. lacustris* can best be termed as a 'continuous asexual and monotelic bisexual breeder' (using the terminology as reviewed by Mill, 1978).

The two findings of sexual worms of unknown origin under long-day conditions can hardly weaken the results. However, the two observed asexual populations that al-

Table II

The effects of age and different environmental factors on the switch from vegetative to bisexual reproduction in Stylaria lacustris

	Age	Temperature	Pop. dens.	Feeding rate	Short-day
N_{veg} (n)	>1000 (5)	>1000 (5)	>1000 (3)	>600 (3)	>1000 (5)
time [d]	98	98	70	70	21–36
sexual [%]	0	0	0	0	>95

N_{veg} = initial number of vegetative worms exposed to the conditions listed.
(n) = Number of different populations tested.
time = Observation time.
Short-day = LD ≤ 12:12. The photoperiod (short-day) is the only factor found to determine the switch from the vegetative to the bisexual mode of reproduction. Under long-day conditions the worms never became sexually mature (as followed continuously over more than 20 generations), independent of temperature, population density (pop. dens.) and feeding rate.

most did not switch to sexual reproduction under short-day conditions are noteworthy. It is unknown whether an irreversible genetically based loss of sexuality or some kind of 'permanent modification' had occurred in these populations. The latter was first observed by Hauenschild (1956, 1957) in the anthomedusae of *Eleutheria dichotoma* from the Mediterranean. Here, a small percentage of primary medusae directly budded off from the polyp was regularly found to be asexual. In the field a loss of the sexual mode of reproduction is known from the sedentary polychaete *Ctenodrilus serratus*. In the North Sea, *C. serratus* reproduces exclusively asexually by paratomic fission, whereas in the Mediterranean Sea sexually mature (hermaphroditic) worms are known. In *S. lacustris*, asexual clones were only found in populations that had been cultured vegetatively for a long time in the laboratory (here, more than 14 or 23 months, respectively). Whether field samples also include a small percentage of asexual clones cannot be answered, because some worms always died when changing the photoperiod from long- to short-day. In the field, the asexual clones would go extinct whenever the temperature dropped below 5°C, *i.e.*, normally during the winter in the Palaearctic area. Only the 'normal' clones showing the photoperiodic reaction can survive. However, in biotopes showing annual temperature fluctuations between only 10°C and 25°C, a loss of the bisexual mode of reproduction in field populations of *S. lacustris* seems likely, analogous to the polychaete *C. serratus*. If those habitats are found this can be easily tested by exposing population samples to short-day conditions.

The annual life-cycle

From the findings of this study, the life-cycle of *S. lacustris* can be roughly described as shown in Figure 3. The prediction is rough in the sense that the tested LD scalings were broad and the within-population genetic variation is unknown. The predicted life-cycle from this study allows *S. lacustris* to start sexual reproduction and hence production of diapausing cocoons prior to, and in anticipation of, the cold winter period, which is critical for the worms' survival (*cf.* Denlinger *et al.*, 1978; Ingrisch, 1984; Zaslawski, 1988). At 52°N. lat. this would be from October to November, corresponding to the natural habitats in north Germany, where ponds usually do

Table III

Proportions of reproductive modes in field samples of Stylaria lacustris

Date	Place	N	Sex [N]	Veg [N]	{ } [N]	Clit [%]	Aclit [%]
14 July 1985	pond Weddel	26	0	11	15	0	100
10 Aug. 1986	river Ilmenau	161	0	68	93	0	100
30 Aug. 1987	river Ilmenau	107	0	57	50	0	100
20 Sept. 1987	pond Weddel	4	0	1	3	0	100
16 Oct. 1987	pond Weddel	48	41	0	7	85	15
12 June 1988	pond Weddel	96	0	53	43	0	100

Samples were taken from different plants (*e.g.*, of the genera *Ceratophyllum, Chara, Elodea, Nasturbium*) from a pond at Weddel (near Braunschweig) or from the river Ilmenau near Uelzen (Niedersachsen, W. Germany); Oct. 16, 1987 is the only sample collected under natural short-day conditions; { } refers to individuals in which no kind of actual reproduction was obvious; Clit and Aclit refer to clitellate and aclitellate individuals, respectively.

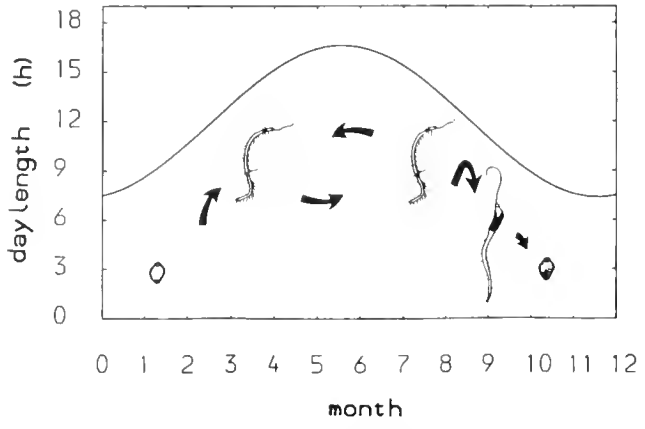

Figure 3. The annual life-cycle of *Stylaria lacustris*. The external signaling factor daylength is given for 52°N. lat. The laboratory studies and field samples suggest that the switch from asexual paratomic fission to bisexual reproduction occures in mid September at this latitude. About three weeks later the first worms become sexually mature, and the first diapausing cocoons are produced during October. Further explanations are given in the text.

not freeze before December. The genetic variation within and between populations would be the predicted basis for adapting *S. lacustris* to different annual cycles with respect to temperature and photoperiod (*e.g.*, Sauer, 1977; Sauer *et al.*, 1986; Groeters and Dingle, 1987). This could be tested by collecting *S. lacustris* at different latitudes with similar annual temperature cycles, or at different altitudes with similar annual photoperiod cycles, and measuring the threshold for the photoperiodic reaction (*cf.* Hairston and Olds, 1984, 1986).

'All or nothing' life-history strategy

By using the vegetative mode of reproduction, *S. lacustris* can double its number at least every 5 days at 20 to 25°C (Table 1). Data on the rates of population increase by vegetatively reproducing populations of *S. lacustris* given in the literature range from mean doubling times of 3.6 to 12 days between 15°C and 20°C (Streit, 1978; McElhone, 1982; Finogenova, 1984). The data agree with Streit (1978), who calculated mdt of 3.6 (T = 19°C) and McElhone (1982), who estimated values of 4–6 days (T = 20°C). In the latter case it is not clear whether these are mean values or maximal values. During summer all efforts are invested in vegetative reproduction, leading to the most rapid population increases, regardless of the actual physical environmental conditions (r-strategy); during one season (April through September) one single worm can theoretically give rise to a population of 3.4 billion worms. During autumn all effort is invested in sexual reproduction, *i.e.*, the number of cocoons produced for overwintering is maximized, regardless of whether the winter temperatures go below 5°C or not. An unexpected and abnormal temperature decline to ≤5°C during summer or early autumn would lead to the total extinction of populations. Furthermore, the reproductive strategy cannot respond to unexpected changes in other environmental factors, like food supply and population density. Therefore, the life-cycle strategy of *S. lacustris* is an 'all or nothing' strategy maximizing reproductive output as far as possible (*cf.* Hirshfield and Tinkle, 1975; Pianka, 1976; Stearns, 1976). This is consistent with a high degree of adaptation to predictable annual cycles of environmental conditions; thus the life history strategy of *S. lacustris* does not fulfill some predictions from life history theories. In a fluctuating and unpredictable environment (such as small freshwater ponds), we would expect *S. lacustris* (a) to reach early sexual maturity, instead of postponing it as far as possible to the end of the season or (b) to show reproductive flexibility in order to minimize the risk of total failure in a bad year (*cf.* Stearns, 1976, 1980; Glesener and Tilman, 1978; Mill, 1978; Sauer, 1984; Groetersand Dingle, 1987).

The high abundances and the wide distribution of *S. lacustris*, however, indicate that the photoperiodic life-cycle strategy can also be very successful in oligochaetes. It seems unlikely that *S. lacustris* should be the only oligochaete worm that has been found to synchronize its life-cycle with the seasons of the year by measuring daylength, and it might be reasonable to look for photoperiodic reactions in other oligochaete worms that perform an alternation of reproductive modes.

Acknowledgments

We thank Hansi Fauter, Heike Fee Hadrys, and Dr. D. Teschner (all Braunschweig). We are indebted to Prof. L. W. Buss, Dr. N. W. Blackstone, and Matt Dick (all Yale) for their critical comments and corrections on earlier versions of the manuscript. The work was supported by a grant from 'GradFoeg des Landes Niedersachsen,' W. Germany.

Literature Cited

Abugov, R. 1988. A sex-specific quantitative genetic theory for life-history and development. *J. Theor. Biol.* **132:** 437–442.

Bell, G. 1980. The costs of reproduction and their consequences. *Am. Nat.* **116:** 45–76.

Brinkhurst, R. O., and B. G. M. Jamieson. 1971. *Aquatic Oligichaeta of the World.* Oliver & Boyd, Edingburgh. 860 pp.

Brinkhurst, R. O., and D. G. Cook, eds. 1980. *Aquatic Oligichaete Biology.* Plenum Press, New York. 530 pp.

Calow, P. 1983. Energetics of reproduction and its evolutionary implications. *Biol. J. Linn. Soc.* **20:** 153–165.

Denlinger, D. L., C. P. Chen, and S. Tanaka. 1978. The impact of diapause on the evolution of other life-history traits in flesh flies. *Oecologia* **77:** 350–356.

Dumnicka E., and K. Pasternak. 1978. The influence of physico-chemical properties of water and bottom sediments in the river

Nida (Poland) on the distribution and number of oligochaeta. *Acta Hydrobiol.* **20:** 215–232.

Finogenova, N. P. 1984. Growth of *Stylaria lacustris* (L.) (Oligochaeta, Naididae). *Hydrobiol.* **115:** 105–107.

Garner, N. H., and A. H. Allard. 1920. Effect of the relative length of day and night and other factors of the environment on growth and reproduction in plants. *J. Agricult. Res.* **18:** 553–606.

Giese, A. C. 1959. Comparative physiology: annual reproductive cycles of marine invertebrates. *Ann. Rev. Physiol.* **21:** 547–576.

Giese, A. C., and J. S. Pearse, eds. 1959. *Reproduction of Marine Invertebrates.* Vol. 1. Academic Press, New York.

Glesener, R. R., and D. Tilman. 1978. Sexuality and the components of environmental uncertainty: clues from geographic parthenogenesis in terrestrial animals. *Am. Nat.* **112:** 659–673.

Groeters, F. R., and H. Dingle. 1987. Genetic and maternal influences on life history plasticity in response to photoperiod by milkweed bugs (*Oncopeltus fasciatus*). *Am. Nat.* **129:** 332–346.

Hadrys, H., B. Schierwater, and W. Mrowka. 1990. The feeding behaviour of a semi-sessile hydromedusa and how it is affected by the mode of reproduction. *Anim. Behav.* (in press)

Hairston, N. G., Jr., and E. J. Olds. 1984. Population differences in the timing of diapause: adaptation in a spatially heterogeneous environment. *Oecologia* **61:** 42–48.

Hairston, N. G., Jr., and E. J. Olds. 1986. Partial photoperiodic control of diapause in three populations of the freshwater copepod *Diaptomus sanguineus*. *Biol. Bull.* **171:** 135–142.

Hauenschild, C. 1956. Experimentelle Untersuchungen ueber die Entstehung asexueller Klone bei der Hydromeduse *Eleutheria dichotoma*. *Z. Naturf.* **11b:** 394–402.

Hauenschild, C. 1957. Ergaenzende Mitteilung ueber die asexuellen Medusenklone bei *Eleutheria dichotoma*. *Z. Naturf.* **12b:** 412–413.

Hauenschild, C. 1975. Die Beteiligung endokriner Mechanismen an der geschlechtlichen Entwicklung und Fortpflanzung von Polychaeten. *Verh. Deutsch. Zool. Ges.* **67:** 292–308.

Hauenschild, C. 1989. Book review: Stearns, S. C., ed. 1987. *The Evolution of Sex and its Consequences.* Birkhaeuser, Basel. *Ethology* **88:** 335–336.

Hirshfield, M. F., and D. Tinkle. 1975. Natural selection and the evolution of reproductive effort. *Proc. Nat. Acad. Sci. USA* **72:** 2227–2231.

Hoekstra, R. F. 1987. The evolution of sexes. Pp 59–91 in *The Evolution of Sex and its Consequences*, Stearns S. C., ed. Birkhaeuser, Basel.

Holm, E. 1988. Environmental restraints and life strategies: a habitat templex matrix. *Oecologia* **75:** 141–145.

Ingrisch, S. 1984. The influence of environmental factors on dormancy and duration of egg development in *Metrioptera roeseli* (Orthoptera: Tettigoniidae). *Oecologia* **61:** 254–258.

Kamlyuck, L. V., and M. M. Kovaltchuk. 1972. Some data about number, growth and production of oligochaete *Stylaria lacustris* (Naididae, Oligochaeta) in littoral lake Narotch. Pp. 148–151 in *Aquatic Oligochaeta*. All Union Symposium, Borok 27–30 June 1972, Jaroslawl, (Russ.).

Kinne, O., ed. 1970. *Marine Ecology.* Vol I, part I. Wiley, New York. 681 pp.

Klerks, P. L., and J. S. Levington. 1989. Rapid evolution of metal resistance in a benthic oligochaete inhabiting a metal-polluted site. *Biol. Bull.* **176:** 135–141.

Krehan, J. 1970. Die Steuerung von Jahresrhytmik und Diapause bei Larval- und Imaginalueberwinterern der Gattung *Pterostichus* (Col., Carab.) *Oecologia* **6:** 58–105.

Lienert, G. A. 1976. *Verteilungsfreie Methoden in der Biostatistik.* Bd. I. Anton Hain, Meisenheim a.Gl.

McElhone, M. J. 1978. A population study of littoral dwelling Naididae (Oligochaeta) in shallow mesotrophic lakes in North Wales. *J. Anim. Ecol.* **47:** 615–626.

McElhone, M. J. 1982. The distribution of Naididae (Oligochaeta) in the littoral zone of selected lakes in North Wales and Shropshire. *Freshwater Biol.* **12:** 421–425.

Michod R. E., and B. R. Levin, eds. 1988. *The Evolution of Sex. An Examination of Current Ideas.* Blackwell Scientific, Oxford. 342 pp.

Mill, P. J., ed. 1978. *Physiology of Annelids.* Academic Press, New York

Nunney, L. 1989. The maintenance of sex by group selection. *Evolution* **43:** 245–257.

Pascar-Gluzman, C. 1981. A preliminary list of aquatic oligochaeta from Israel naididae and tubificidae. *Isr. J. Zool.* **30:** 230–232.

Pianka, E. R. 1976. Natural selection of optimal reproductive tactics. *Am. Zool.* **16:** 775–784.

Precht, H., J. Christophersen, H. Hensel, and W. Larcher. 1973. *Temperature and Life.* Springer, New York. 779 pp.

Reznick, D. 1985. Cost of reproduction: an evaluation of the empirical evidence. *Oikos* **44:** 257–267.

Rowan, W. 1926. On photoperiodism, reproductive periodicity and the annual migration of birds and certain fishes. *Proc. Boston Soc. Nat. Hist.* **38:** 141–189.

Sauer, K. P. 1977. Die adaptive Bedeutung der genetischen Variabilitaet der photoperiodischen Reaktion von *Panorpa vulgaris* (Mecoptera, Panorpidae). *Zool. Jahrb. Syst.* **104:** 489–538.

Sauer, K. P. 1984. The evolution of reproductive strategies as an adaptation to fluctuating environments. *Adv. Inv. Reprod.* **3:** 317–326.

Sauer, K. P., H. Speith, and C. Gruener. 1986. Adaptive significance of genetic variability of photoperiodism in Mecoptera and Lepidoptera. Pp. 153–172 in *The Evolution of Insect Life Cycles*, F. Taylor and R. Karban, eds. Springer, New York.

Schierwater, B. 1989. Allometric changes during growth and reproduction in *Eleutheria dichotoma* (Athecata, Hydrozoa) and the problem of estimating body size in a microscopic animal. *J. Morphol.* **200:** 255–267.

Segal, E. 1970. Light. Animals. Invertebrates. Pp. 159–211 *Marine Ecology*, Vol I, part I, O. Kinne, ed. Wiley, New York.

Stearns, S. C. 1976. Life-history tactics: a review of ideas. *Q. Rev. Biol.* **51:** 3–47.

Stearns, S. C. 1980. A new view of life-history evolution. *Oikos* **35:** 266–281.

Stephenson, J. 1930. *The Oligochaeta.* Oxford University Press, Oxford.

Streit, B. 1978. A note on the nutrition of *Stylaria lacustris* (Naididae, Oligichaeta). *Hydrobiol.* **61:** 273–276.

Tauber, M. J., C. A. Tauber, and S. Masaki. 1986. *Seasonal Adaptation in Insects.* Oxford University Press, Oxford. 411 pp.

Townsend, C. R., and P. Calow, eds. 1981. *Physiological Ecology. An Evolutionary Approach to Resource Use.* Blackwell Scientific, Oxford. 393 pp.

Vershinin, N. V., and V. P. Semernoi. 1977. Qualitative and quantitative characteristics of oligochaetes of the Krasnoyarsk reservoir. *Ekologiya* **1:** 105–107.

Wetzel, M. J. 1982. Aquatic oligochaeta in Kansas, USA, with notes on their distribution and ecology. *Tech. Publ. State. Biol. Surv. Kans.* **12:** 112–130.

Zaslawski, V. A. 1988. *Insect Development. Photoperiodic and Temperature Control.* Springer, Berlin. 187 pp.

Reference: *Biol. Bull.* **178:** 118–125. (April, 1990)

Visualization of the Transparent, Gelatinous House of the Pelagic Tunicate *Oikopleura vanhoeffeni* Using *Sepia* Ink

PER R. FLOOD[1], DON DEIBEL[2], AND CLAUDE C. MORRIS[2]

[1] *Institute of Anatomy, University of Bergen, Arstadveien 19, 5009 Bergen, Norway and*
[2] *Marine Science Research Laboratory, Ocean Sciences Centre, Memorial University of Newfoundland, St. John's, Newfoundland, Canada, A1C 5S7*

Abstract. Appendicularian tunicates of the genus *Oikopleura* feed using an external, acellular, transparent structure known as the house. Previously, dilute particulate dyes have been used to visualize the internal structure of this house. However, because of toxicity, large particle size, and flocculation, many of these dyes have been of limited practical and scientific use. We report on a new marker, the ink from the cephalopod *Sepia officinalis*, that solves many of these problems.

Specimens of *Oikopleura vanhoeffeni* relished *Sepia* ink, having dark black stomachs and producing many dark fecal pellets over several days. When *O. vanhoeffeni* expanded houses in dilute ink, the internal walls, septae, and filters were shown in great detail, whereas high concentrations of ink showed delicate patterns of lines on the internal walls.

We present documentary photographs of previously unillustrated or undescribed morphologies: the escape slot; the incurrent funnels; two dimples caused by insertion of suspensory filaments on the upper wall of the posterior chamber, a large, posterior keel; both the open and closed positions of the exit valve; and the complex pattern of lines on the inner walls. However, the external walls of the house had no affinity for the dye and could only be seen by dark field illumination.

We believe that *Sepia* ink can be used to visualize functionally important transparent structures of other gelatinous zooplankton and can be a colloidal marker in feeding experiments of a wide range of filter feeders.

Received 25 September 1989; accepted 30 January 1990.

Introduction

Oikopleurid appendicularians are suspension feeding zooplankters that are surrounded by a transparent, acellular, gelatinous "house," which they secrete. The house contains a complex system of fine filters that are used by the animals to concentrate and remove food particles from suspension. Using its muscular tail as a pump, the animal draws water into the house through a pair of coarse, bilateral, incurrent filters. The water is then pumped through the tail chamber into bilateral passageways leading to the lateral edge of expansive food-concentrating filters. Here much of the water is pushed through a mesh with 0.22 μm pore size (Deibel *et al.*, 1985). Particles are retained between the food concentrating filter screens, resulting in a concentrated food suspension that is drawn into a medial food-collecting tube leading to the animal's mouth. This food suspension is 100 to 1000 times more concentrated than are particles in the environment surrounding the animal (Jörgensen, 1984; Flood, in prep.). A third filter inside the pharynx of the animal traps the food particles for ingestion. The filtered water exiting the food concentrating filter leaves the house through a narrow exit spout and valve, producing a jet that propels the house and animal slowly through the sea.

The existence of the house has been known since the work of Fol (1872) and Lohmann (1899). However, many details of its structure remained unknown until recent improvements in microscopical techniques and special staining procedures made further progress possible. Dilute particulate dyes have been used to visualize the internal walls, chambers, and filters of the house (Alldredge, 1977; Flood, 1978, 1983; Deibel *et al.*, 1985;

Deibel, 1986; Fenaux, 1986). When added to seawater, dye particles are retained by the filters within the house in the same way as are naturally occurring particles. Lohmann (1899) and Alldredge (1977) used dilute suspensions of carmine particles to visualize both the incurrent and food-concentrating filters of many oikopleurids. However, the animals may not feed normally when carmine is present (Alldredge, 1977). We have found that freshly prepared dilutions of carmine and extreme care are required to prevent the animals from leaving their houses. In addition, carmine particles settle rapidly and stain only the incurrent and food-concentrating filters.

Fenaux (1986) used dilute India ink to stain the incurrent and food concentrating filters, and the internal walls and septae of houses of *Oikopleura dioica*. One of us (P.R.F.) has used a similar technique since 1978. If India ink is added to seawater before the animal expands a new house, all internal walls and septae of the house are stained (Flood, in prep.). However, if the ink is added after the house has been expanded, only the food-concentrating filter is stained. This approach requires freshly prepared ink solutions and great care to prevent the animal from leaving its house. The carbon particles that make up India ink tend to aggregate in seawater and settle rapidly as do particles in carmine suspensions.

Deibel (1986) used several types of particles to mark specific parts of the house of *Oikopleura vanhoeffeni* differentially. These particles included finely ground charcoal, starch, latex beads, and the unicellular green alga *Isochrysis galbana*. Charcoal particles adhered specifically to an intermediate, coarse screen between the two walls of the food-concentrating filter. The alga, on the other hand, stuck to the upper and lower walls of the food-concentrating filter. Starch granules did not adhere to any of the filters of the house, but stained the pharyngeal filter within the trunk of the animal. This suggests that physical and chemical properties of both the marker and the house structures in question affect the staining result.

We recently found another marker that may be used to visualize structural details of oikopleurid houses that, in the past, have been difficult or impossible to document. Information about these structures is needed to understand the behavioral and functional details of the feeding process on which the ecology of these animals depends. The new marker may be used not only to visualize feeding structures and quantify particle clearance rates of pelagic tunicates, but also to observe transparent structures of other marine plankton.

Materials and Methods

Individuals of *Oikopleura vanhoeffeni*, in their houses, were collected in 500-ml glass jars by SCUBA diving in Logy Bay, Newfoundland, during May and June 1989. Animals were maintained in these jars for up to 10 days in laboratory tanks containing circulating seawater at 1 to 5°C, about 1°C above ambient sea surface temperature.

Ink was collected from freshly dead specimens of the cuttlefish *Sepia officinalis* at the Plymouth Marine Laboratory, Devon, U.K. The ink duct of each animal was clamped with a hemostat while the ink sac was removed. Once excised, a loop of the duct was placed in a collection vial and the duct cut to allow the ink to drain into the vial. This ink was diluted immediately with 10 parts of distilled water and 10,000 units of pennicillin G added per ml of solution to help prevent bacterial decomposition. Diluted ink remains liquid for several years, but undiluted ink coagulates after several weeks at room temperature. The ink was dispersed with gentle agitation in seawater to a dilution of *ca.* 10^{-5} just before use.

Solid *Sepia* ink is available commercially, but must be ground before use. It also contains phenol or other chemical preservatives that may be noxious or toxic to marine animals, and therefore it was not used in these experiments.

Houses were examined using a Wild M420 macroscope with bright or dark-field illumination. The light source used for routine observation was a 100W halogen lamp, whereas two modified Sunpak GX14 electronic flashes and a Wild MPS 55/-51 photoautomat were used for still photography. We used Kodak Ektachrome 100 and 400 ASA film for slides, and Kodak Tmax at 100 to 3200 ASA for prints. By using 0.5- and 2.0-times accessory lenses on the macroscope, final magnification of the photographs ranged from 1.25- to 25-times.

Results and Comments

Liquid *Sepia* ink was easily miscible in seawater, and, contrary to other dyes that have been used to visualize the house of Appendicularia, it stayed evenly dispersed in solution for up to 14 days.

Transmission electron microscopy (TEM) revealed that this ink consists of uniformly spherical melanin granules with diameters ranging between 56 and 161 nm (arithmetic mean = 102 nm, Standard deviation = 21 nm, Flood, pers. obs. by TEM).

In spite of this low particle size, some of the ink particles were easily concentrated and ingested by *Oikoploeura vanhoeffeni*. In fact, these animals seemed to relish the *Sepia* ink, having full stomachs and producing abundant opaque, black fecal pellets (Fig. 1) that appeared to be composed entirely of ink.

However, much of the ink passed through the house of *Oikopleura vanhoeffeni*, without being witheld by the food-concentrating filters. Some of these particles ad-

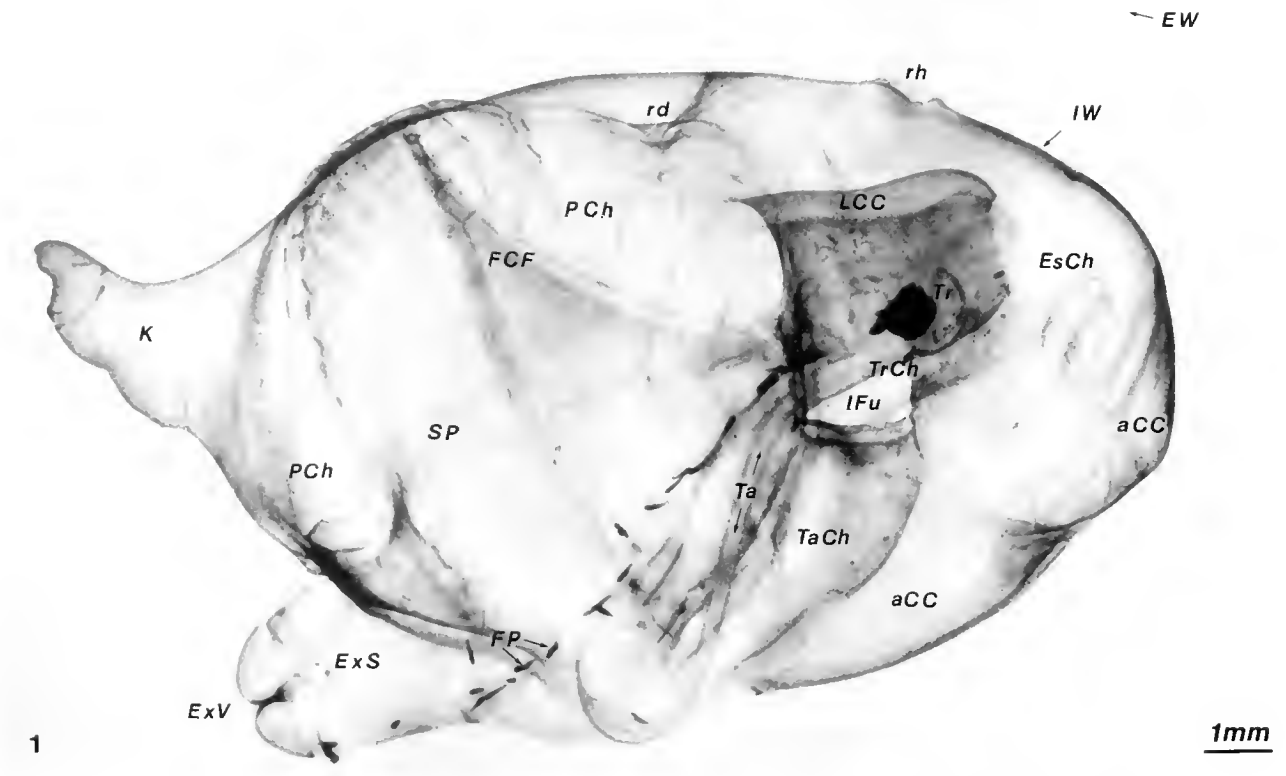

Figure 1. Lateral view of a live *Oikopleura vanhoeffeni* beating its tail inside a house faintly stained by *Sepia* ink. Bright field macrograph at seven times magnification. [The nomenclature used is adopted from Flood (1983) and is largely a direct translation of Lohmann's German names (Lohmann, 1956).]

In addition to numerous details of the inside walls (*IW*) of the house, like the prominent exit spout (*ExS*) and valve (*ExV*), a keel (*K*), cushion chambers lateral (*LCC*) and antero-medial (*aCC*) to the inlet openings, inlet funnels (*IFu*), roof dimples (*rd*), and a roof hump (*rh*), numerous internal details can be seen. The animals trunk (*Tr*), tail (*Ta*), and escape chamber (*EsCh*) as well as the trunk chamber (*TrCh*), tail chamber (*TaCh*), supply passage (*SP*), and suspension of the food-concentrating filters (*FCF*) in the posterior chamber (*PCh*) are faintly outlined. Numerous fecal pellets (*FP*) stained completely black by *Sepia* ink are seen along the floor of the posterior chamber. The external wall (*EW*) is only visible above the hump in the inside roof.

hered to the internal walls and septae of the house and made them easily visible.

By varying the concentration of *Sepia* ink from experiment to experiment, the intensity of staining could be controlled to reveal different features of the house. When a specimen of *Oikopleura vanhoeffeni* expanded its house in seawater containing very dilute *Sepia* ink, the internal walls, septae, and filters were shown in great detail (Fig. 1), whereas heavy staining made the house less transparent and revealed delicate patterns of lines and fields on the internal walls and septae throughout the house (Figs. 2, 3).

The outer wall of the house, however, had no affinity for the ink and was rarely seen at all in bright field illumination (Fig. 1). However, in most cases its presence was revealed by adhering detritus particles. This was particularly true for the prominent bow of the house (Fig. 2). In dark field illumination, on the other hand, the external walls and their variable thickness in distinct parts of the house became more evident (Fig. 3).

The difference in volume between the internal water-filled spaces and the total house could be estimated from such pictures. If the internal transverse diameter of the house was considered to be unity, the external transverse diameter was generally close to 1.2, the internal longitudinal diameter about 1.3, and the outside longitudinal diameter about 1.7. Considering the house to be an elliptical rotatory body, this makes the total volume approximately 1.5 times as large as the internal water-filled spaces. We do not know if the spaces between the inside and outside walls are filled with a compact (gel-like) substance or if they are water-filled chambers unaccessible to the *Sepia* particles.

By varying the staining intensity of the house, we dis-

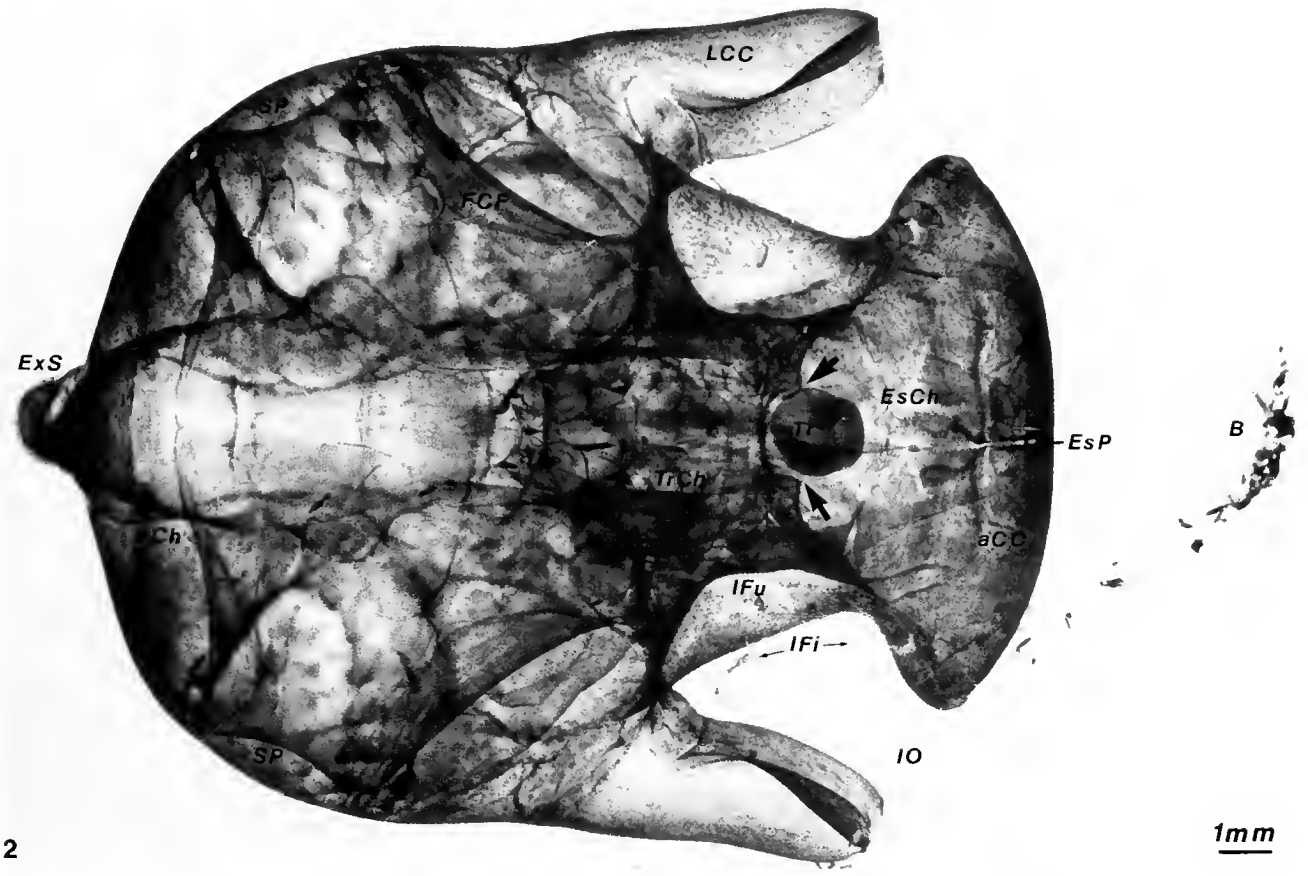

Figure 2. Top view of live *Oikopleura vanhoeffeni* inside its house. Bright field macrograph at seven times magnification after strong staining with *Sepia* ink.

Intricate patterns of *Sepia* ink are seen on many walls, as for example near the escape passage (*EsP*) and supply passages (*SP*). Note also the attachment (*arrows*) of the animal trunk (*Tr*) to the walls separating the trunk chamber (*TrCh*) from the escape chamber (*EsCh*). The inlet openings (*IO*), inlet filters (*IFi*), and the inlet funnels (*IFu*) are visible on both sides of the house. Note the prominent bow (*B*) made visible only by adhering detritus particles. Otherwise, same labeling as in Figure 1.

covered many structural details of which we were previously unaware or had insufficient knowledge. Here we will only describe some of the most prominent features and comment briefly on their functional significance.

(1) *The escape port in the anterior chamber (Figs. 2, 5B).* The animal forces its way through this preformed weak part when it leaves the house, thereby tearing it open to a wide escape slot. This escape port is covered by the massive bow of the house (Fig. 2), and somehow a preformed channel must exist through this bow material towards the external house wall. Otherwise the animal could not force its way out of the house as easily, frequently, and uniformly as it does (*cp.* Fenaux, 1985).

(2) *The incurrent funnels leading into the house (Figs. 1–3).* In the only existing description of the house of *Oikopleura vanhoeffeni* (Deibel, 1986, Fig. 1), these have been given quite a different shape from what we have been able to photograph.

(3) *The attachment of the anterior walls of the incurrent funnels to the lateral part of the trunk (Fig. 2).* These walls seem to meet the trunk exactly where the Langerhans bristle is located. Through this sensory organ the animal may monitor accordingly the inflation and condition of the house (Bone and Ryan, 1979). Perhaps the entire house in this context may be regarded as a tactile sensory structure.

A rather rigid suspension of the trunk of the animal within the house is needed for the tail to perform its pumping action. This prevents the "tail from wagging the dog" as may be observed just before the animal leaves its house, when the trunk has detached from some of its anchoring points. Stimulation of the Langerhans receptor may then initiate the vigorous jerk and swimming movement that enables the animal to detach completely from the house and force its way through the escape slot.

(4) *The shape of prominent chambers and lateral flaps*

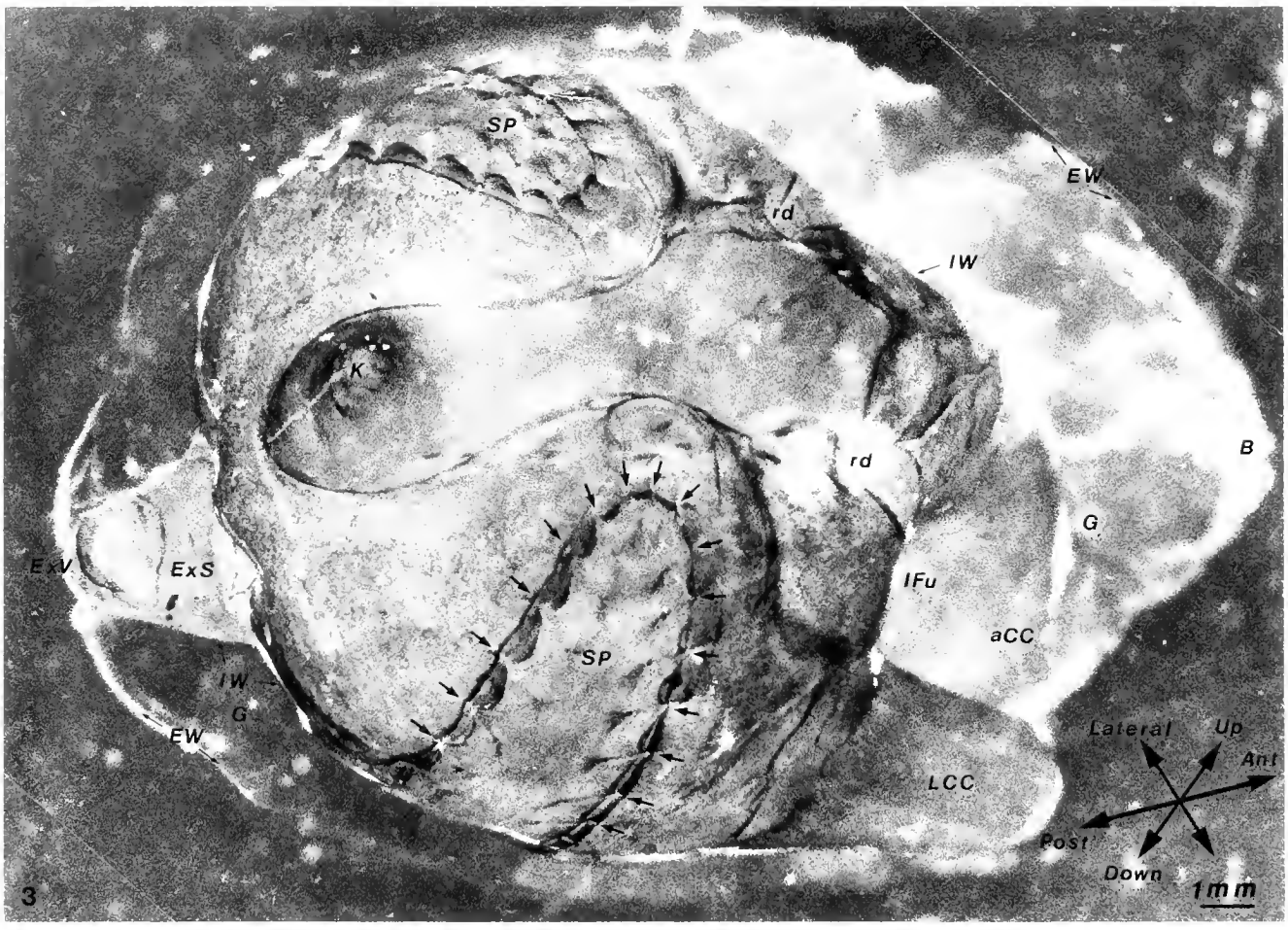

Figure 3. Inhabitated house of *Oikopleura vanhoeffeni* as seen in dark field illumination from a point above, behind, and to the side of the house. (The axes of the house as it normally moves through the sea are indicated in the lower right hand corner.) Magnified seven times.

Note the prominent patterning of the internal walls (*IW*) corresponding to the attachment sites of the filter ridges of the food-concentrating filters (*arrows*) along the periphery of the supply passages (*SP*), and the presence of a prominent semitransparent jelly-like substance (*G*) covering the posterior side and the anterior bow-like pole (*B*) of the house. The outer limit of this jelly-like substance represent the true external walls (*EW*) of the house. The orientation of the house as it moves through the water is indicated by axes in the lower right hand corner of the figure. For other abbreviations refer to Figure 1.

in the anterior part of the house, medial and lateral to the incurrent openings (Figs. 1–3). These chambers are probably filled by water flowing from the tail chamber through a hole in its distal floor (Flood, in prep.). It is also possible that the anterior chambers communicate with the upper compartment of the posterior chamber and may be filled by water via this route, as suggested by Fenaux (1986). A positive pressure in the anterior chambers surrounding the incurrent funnels is needed to resist the collapsing force generated by the negative pressure within these passageways as water is drawn into the house. The lateral flaps may serve as vertical stabilizers to control the orientation of the house as it moves through the sea or as flaps to prevent the immediate reclogging of the incurrent filters after they have been backwashed (Flood, in press).

(5) *Two large dimples in the inner house wall of the upper compartment of the posterior chamber (Figs. 1, 3).* These probably represent the anchoring sites of suspensory filaments originating somewhere along the anterior edge of the food-concentrating filters.

(6) *A medial hump in the inner house wall above the trunk of the animal (Fig. 1).* The external house wall had its highest optical density and could be faintly seen even in bright field illumination above this hump. Although of unknown functional significance, this hump is also found in houses of *Oikopleura dioica* and *O. labradoriensis* (Flood, pers. obs.).

(7) *A large "keel" at the back of the house just above the exit valve (Figs. 1, 3).* This keel may serve as a rudder to inhibit rolling and to facilitate looping motions as the house is propelled through the water. A looping motion, which has been described for other oikopleurans by Alldredge (1976), allows the animal to stay within and exploit a patch of nanoplankton more efficiently than by a linear motion. This keel was discovered by Deibel (1986), but due to poor visibility, even in dark field illumination, his description is incomplete (Compare his Fig. 1 to our Fig. 1).

(8) *A posterior exit spout and valve below the longitudinal midline of the house (Figs. 1, 3).* Strong staining by *Sepia* ink allowed us to observe the opening and closing action of this pressure sensitive valve. In its closed position its upper and lower lips were inverted (Fig. 4A). One to five seconds after the pumping action of the tail started and increased the pressure inside the posterior chamber and exit spout, the lips everted and exposed a medial oval opening with a strongly birefringent and elastic rim (Fig. 4B). This central exit opening was evident even when the animal pumped slowly. However, when the tail pumped at maximum efficiency, the exit spout became much longer, and four additional exit openings were exposed peripheral to the central one. The tissue surrounding the exit valves was then stretched to such a degree that it left very little contrast in our photographs (Fig. 4C). Fenaux (1986), studying *Oikopleura dioica* houses, found the four peripheral openings to open before the central one.

The propulsive thrust generated by the jet of water leaving the house was directed somewhat below the center of the house, resulting in a tendency to turn the front of the house upward. When combined with the slightly upward-pointing bow and the directional control of the keel and lateral flaps (see above), this thrust will result in a slow upward movement of the house, or even a vertical looping motion as sometimes seen in the field (*cp.* Alldredge, 1976).

The more intense staining resulting from higher concentrations of *Sepia* ink revealed delicate patterns of lines and fields on most internal walls of the house (Figs. 2, 5). In some areas, complex patterns of straight or curved lines were visible (Fig. 5A). These may correspond to decorated filaments, corrugated surfaces, or small pockets. In other areas, faint patterns of polygonal fields were apparent (Fig. 5B). Although each polygon was quite large, their pattern reminded us of the oikoplast cell pattern on the trunk of the animal. These cells are responsible for the production of the house (Lohmann, 1933/1956); perhaps *Sepia* ink might be used to map the areas of the house made by individual cells. This represents a major problem yet to be properly elucidated for all appendicularians.

Discussion

The usefulness of the *Sepia* ink for visualizing distinct parts of *Oikopleura* houses probably depends on three or four factors: (1) *Sepia* ink forms stable solutions in seawater and does not aggregate and sediment like most other particulate dyes. Such flocculent particles seem to interfere with the house expansion process of animals kept in captivity. (2) The particle size of *Sepia* ink is small enough to allow a significant proportion of particles to pass the food-concentrating filters to stain the walls of the posterior chamber, the exit spout, and possibly the anterior chambers of the house. (3) The animals seem to relish the *Sepia* ink as a food source and do not find it noxious or toxic like many other dyes. (4) The physico-chemical properties of the *Sepia* ink particles may be particularly favorable to stain the internal walls and septae of the house.

These excellent properties of *Sepia* ink may make it useful in the study of other gelatinous zooplankters.

The reason why *Sepia* ink, like all other particulate dyes we have used, failed to stain the external walls of the house remains obscure. It may depend on special physico-chemical properties of this layer, but a more likely explanation may be that the dye particles are prevented from having direct physical contact with it. The walls surrounding the water-filled spaces inside the house are probably not entirely waterproof. Due to the higher hydrostatic pressure inside the house, water will seep slowly out through the walls, leaving its particles behind as a decoration on the internal walls, and producing a thin halo of particle-free water just outside the house. Such a halo may be enough to prevent the proper staining of the external walls.

The pore size of the food-concentrating filters of *Oikopleura vanhoeffeni*—1.0×0.22 μm according to Deibel *et al.* (1985)—was significantly larger than was the particle size of *Sepia* ink (0.1 ± 0.02 μm according to Flood, unpub. res.). In spite of this, the animals used in this study easily concentrated and ingested the dye, and incorporated it into fecal pellets. This may depend on a selection of the largest particles in the ink, on a selection of aggregated particles, or on an ability to retain smaller particles than hitherto believed. In fact, the carbon budgets of oikopleurans seem to be such that ingested particles > 0.2 μm in diameter rarely account for more than 30% of the energy expenditure for growth, respiration, and house production (Paffenhofer, 1976; Gorsky, 1980; King, 1981). It seems likely that the animals may obtain much of their nurishment from particles < 0.2 μm in diameter, or from dissolved organic matter. We foresee the use of monodisperse *Sepia* ink particles in future feeding experiments on appendicularians and other filter feeding marine animals.

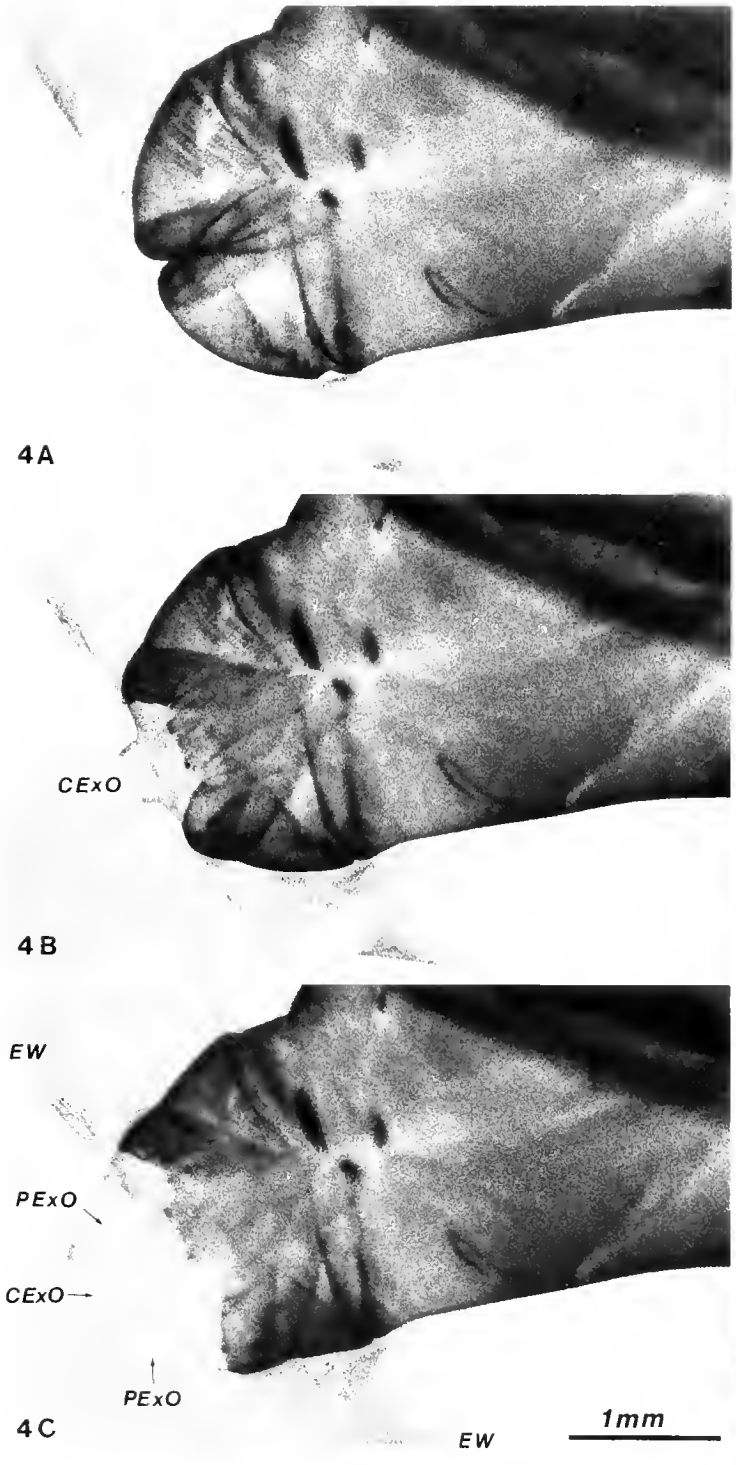

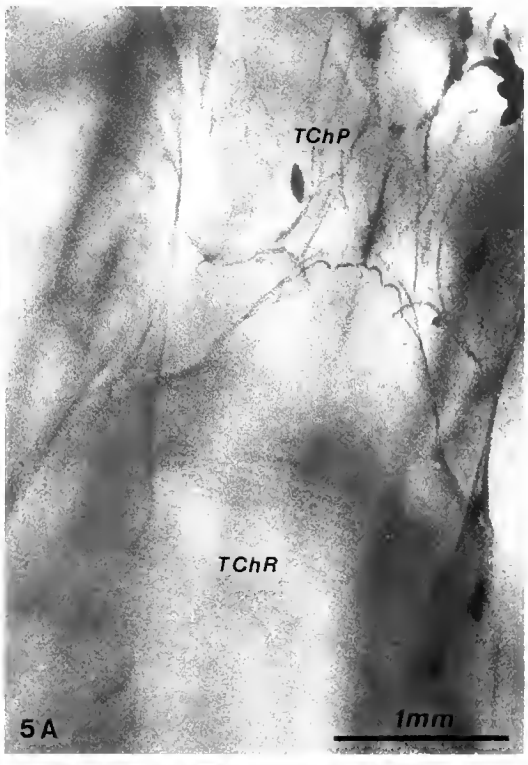

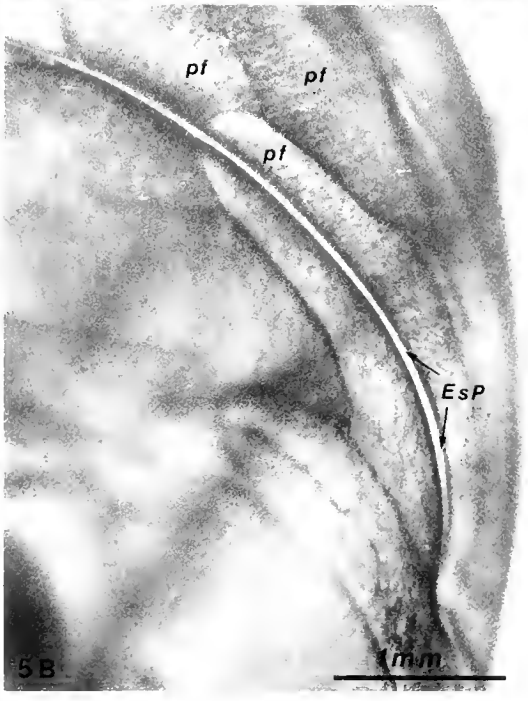

Figure 4. Bright field macrographic details of the exit spout and valve of a heavily *Sepia*-ink stained house of *Otkopleura vanhoeffeni* at 20 times magnification.

(A) In its closed state, (B) in its half open state, and (C) in its full open position. Unfortunately the exit openings themselves [one central (*CExO*) and four peripheral (*PExO*)] didn't give sufficient contrast to be seen in picture C. The external wall (*EW*) of the house is seen next to the exit spout.

Figure 5. Bright field macrographic details of an *Otkopleura vanhoeffeni* house heavily stained by *Sepia* ink at 23 times magnification.

In (A), parallel ruffles (*TChR*) and numerous pockets (*TChP*) are seen in the roof of the tail chamber. In (B), polygonal fields (*pf*) resembling cell outlines are seen next to the escape passage (*EsP*) of the house.

Acknowledgments

Many thanks to the members of the Diving Unit (G. Chaisson, Divemaster) of the Ocean Sciences Centre, Memorial University, for assisting D.D. with the collection of *Oikopleura vanhoeffeni*, and to Mr. Edward Downton for designing and fabricating laboratory equipment. This work is a result of a Bergen-Memorial Universities Exchange Fellowship to P.R.F., and we thank Drs. Bodil Larsen and R. L. Haedrich, Memorial University, for making this visit possible. This work was supported by a grant from the Norwegian Research Council for Science and the Humanities to P.R.F., and by Operating and Equipment Grants from the Natural Sciences and Engineering Research Council of Canada to D.D. This is Ocean Sciences Centre contribution number 61.

Note added in proof: We have used commercial ink from *Sepia* recently available from Sigma Chemical Co. (St. Louis, Missouri). *Oikopleura vanhoeffeni* took up this ink similarly to that we collected from *Sepia* ourselves.

Literature Cited

Alldredge, A. L. 1976. Field behavior and adaptive strategies of appendicularians (Chordata: Tunicata). *Mar. Biol.* **38:** 29–39.

Alldredge, A. L. 1977. House morphology and mechanisms of feeding in the Oikopleuridae (Tunicata, Appendicularia). *J. Zool. (Lond.)* **181:** 175–178.

Bone, Q., and K. P. Ryan. 1979. The Langerhans receptor of *Oikopleura* (Tunicata: Larvacea). *J. Mar. Biol. Assoc. U. K.* **59:** 69–75.

Deibel, D. 1986. Feeding mechanism and house of the appendicularian *Oikopleura vanhoeffeni*. *Mar. Biol.* **93:** 429–436.

Deibel, D., M.-L. Dickson, and C. V. L. Powell. 1985. Ultrastructure of the mucous feeding filter of the house of the appendicularian *Oikopleura vanhoeffeni*. *Mar. Ecol. Progr. Ser.* **27:** 79–86.

Fenaux, R. 1985. Rythm of secretion of oikopleurid's houses. *Bull. Mar. Sci.* **37:** 498–503.

Fenaux, R. 1986. The house of *Oikopleura dioica* (Tunicata, Appendicularia): structure and functions. *Zoomorphology* **106:** 224–231.

Flood, P. R. 1978. Filter characteristics of appendicularian food catching nets. *Experientia* **34:** 173–175.

Flood, P. R. 1983. The gelationous house of *Oikopleura dioica* (Appendicularia, Tunicata): its architecture and water filtration mechanism. Ann. Meet. Western Soc. Naturalists, Burnaby, B. C. Canada, Dec. 1983 (Abstract).

Fol, H. 1872. Etudes sur des Appendiculaires de Detroit de Messine. *Mem. Soc. Phys. Hist. Nat. Geneve* **21**(2): 445–499.

Gorsky, G. 1980. Optimisation des cultures d'appendiculaires. Approche du metabolisme de *O. dioica*. Ph. D. thesis, Univ. P. & M. Curie, Paris VI. 110 pp.

Jorgensen, C. B. 1984. Effect of grazing: metazoan suspension feeders. Pp. 445–464 in *Heterotrophic Activity in the Sea*, J. E. Hobbie and P. J. leB. Williams, eds. New York, Plenum Press.

King, K. R. 1981. The quantitative natural history of *Oikopleura dioica* (Urochordata, Larvacea) in the laboratory and in enclosed water collumns. Ph. D. thesis, Univ. Washington, Seattle.

Lohmann, H. 1899. Das Gehause der Appendicularien, sein Bau, seine Funktion und seine Entstehung. *Schr. Naturwiss. Ver. Schleswig-Holstein* **11:** 347–407.

Lohmann, H. 1933/1956. Appendiculariae. *Handb. Zool.* **5,II:** 15–202.

Paffenhofer, G. A. 1976. On the biology of the Appendicularia of the southeastern North Sea. *10th Eur. Symp. Mar. Biol., Ostend, Belgium, Sept. 1975.* **2:** 437–455.

Reference: *Biol. Bull.* **178**: 126–136. (April, 1990)

The Morphology and Mechanics of Octopus Suckers

WILLIAM M. KIER AND ANDREW M. SMITH*

Department of Biology, Coker Hall, CB# 3280, The University of North Carolina, Chapel Hill, North Carolina 27599-3280

Abstract. The functional morphology of the suckers of several benthic octopus species was studied using histology and cinematography. The suckers consist of a tightly packed three-dimensional array of musculature. Three major muscle orientations are found in the wall of the sucker: (1) radial muscles that traverse the wall; (2) circular muscles that are oriented circumferentially around the sucker, including a major and minor sphincter muscle; and (3) meridional muscles that are oriented perpendicular to the circular and radial muscles. The connective tissue of the sucker includes inner and outer fibrous connective tissue layers and an array of crossed connective tissue fibers embedded in the musculature of the sucker.

Attachment is achieved by reducing the pressure inside the sucker cavity. We propose the following mechanism to explain this pressure reduction. Contraction of the radial muscles thins the wall and thus increases the enclosed volume of the sucker. If the sucker is sealed to the substratum, however, the cohesiveness of water resists this expansion. Thus, contractile activity of the radial muscles reduces the pressure of the enclosed water. The radial muscles are antagonized by the circular and meridional muscles so that the three-dimensional array of muscle functions as a muscular-hydrostat. The crossed connective tissue fibers of the sucker may store elastic energy, providing a mechanism for maintaining attachment over extended periods.

Introduction

Octopus suckers perform a remarkable variety of functions. Packard (1988) listed six distinct roles of the suckers of benthic octopuses including: (1) locomotion; (2) anchoring the body and holding prey; (3) sampling, collecting, and manipulating small objects; (4) chemotactile recognition; (5) displays; and (6) cleaning maneuvers. These diverse roles demand that the suckers be flexible and dexterous yet capable of generating large forces (see Dilly *et al.*, 1964). Previous research has focussed on the chemotactile ability of the suckers (see Wells, 1978), on the sensory receptors of the suckers (Graziadei, 1962; Graziadei and Gagne, 1976a, b), and on their morphology (see below). Our understanding of how the sucker generates the movements that allow it to manipulate and forcefully grip objects is incomplete.

The morphology of octopus suckers has been described previously. Nixon and Dilly (1977) described the surface features of octopus and squid suckers from different genera. The sucker musculature has been described by Girod (1884), Guérin (1908), Nachtigall (1974), Niemiec (1885), and Tittel (1961, 1964), but the proposed mechanisms of action are incorrect both in their analysis of the function of the musculature and in understanding the ability of water to sustain sub-ambient pressures. Previous studies also overlooked important features of the connective tissue.

The suckers are muscular-hydrostats as defined by Kier and Smith (1985) (see also Smith and Kier, 1989). The musculature is arranged in a tightly packed, three-dimensional array that provides the skeletal support and the force for movement. This type of system produces movements that are localized and remarkably complex, allowing precise changes in shape by bending, contracting, or stretching at any point. In this paper we describe the muscle arrangements in the suckers of several octopus species and discuss the function of these arrangements.

Materials and Methods

Experimental animals

Specimens of *Eledone cirrosa* were supplied by The Laboratory of the Marine Biological Association of the

Received 16 October 1989; accepted 30 January 1990.

* Order of authorship is merely alphabetical.

United Kingdom, Plymouth. Specimens of *Octopus joubini* and *Octopus maya* were supplied by The Marine Biomedical Institute of the University of Texas Medical Branch at Galveston, Texas. Specimens of the *Octopus bimaculoides/bimaculatus* complex (see Pickford and McConnaughey, 1949) were supplied by Pacific Bio-Marine, Venice, California, and Chuck Winkler Enterprises, San Pedro, California. Observations of sucker behavior and kinematics were made primarily on *O. bimaculoides/bimaculatus* and *O. maya*. A detailed morphological analysis of the suckers was performed on specimens of *E. cirrosa*, *O. joubini*, and *O. bimaculatus/bimaculoides*.

Histology

Blocks of arm tissue that included several suckers were obtained from freshly killed animals that were anesthetized in 1% ethanol in seawater. The tissue was fixed in Bouin-Dubosq fixative (Humason, 1979) or in 10% formalin in seawater for 24–48 h. In some cases, blocks of tissue were obtained from specimens that had been fixed whole in 10% formalin in seawater after anesthesia. The tissue was dehydrated in ethanol and embedded in paraffin (MP 56°C). The blocks were sectioned serially at 5–10 μm on a rotary microtome. Serial sections were made in three mutually perpendicular planes. The sections were stained using one of the following techniques: (1) Mallory's triple stain as outlined by Pantin (1946); (2) Milligan trichrome stain; (3) Picro-Ponceau with iron hematoxylin; or (4) Mowry's colloidal iron method. The procedures followed for stains 2–4 above are outlined by Humason (1979). Sections were examined with bright-field, phase contrast, and polarized light microscopy.

Computer-assisted three-dimensional reconstruction

The extrinsic musculature of the suckers of one specimen of *E. cirrosa* was examined using a computer program for three-dimensional reconstruction (PC3D Three-Dimensional Reconstruction Software, Jandel Scientific, Corte Madera, California). Serial frontal sections (see description of section planes below) 10 μm thick were used for the reconstructions. The outlines of the major muscle groups of every fourth section were traced using a camera lucida on a compound microscope. Alignment of the series of tracings was performed according to the visual best-fit method (Gaunt and Gaunt, 1978; Young *et al.*, 1985). The tracings were then digitized with a Numonics 2210 digitizing tablet. The PC3D software, running on a CompuAdd 286/12 AT microcomputer, stacked the outlines of specified muscle bundles from each section, producing a three-dimensional representation of the muscular morphology that could be viewed in any orientation. The reconstructions shown in Figure 8 were plotted on a Hewlett-Packard HP 7475A plotter.

Cinematography

A specimen of *O. maya* was filmed walking on a glass aquarium wall with a Canon Scoopic 16mm movie camera filming at 48 frames/s using Eastman Ektachrome Video News Film. The film was viewed frame by frame on an L-W International film analyzer, and calipers were used to measure the diameter of the sucker and the diameter of the opening to the acetabulum. The measurement error was <5%. Measurements were made from one 100-ft roll of film, choosing every sucker (total of 26 suckers) that attached or released and whose outlines were distinct enough to measure. Suckers attached to the glass could be distinguished because they remained stationary relative to the movement of the arm.

Results

Gross morphology of the suckers

The gross morphology of the suckers of different octopus species has been described previously (Girod, 1884; Guérin, 1908; Niemiec, 1885; Nixon and Dilly, 1977; Packard, 1988), and a brief summary of observations on the species we examined is provided here. The sucker consists of two general regions: the acetabulum and infundibulum (Girod, 1884) (Fig. 1). The infundibulum is the exposed portion of the sucker that is applied to the substratum during attachment. The acetabulum is a more or less spherical cavity that opens to the infundibulum through a constricted orifice (Fig. 1). The surface of the infundibulum bears a series of radial grooves and ridges while the surface of the acetabulum is smooth. The sucker is covered by a chitinous cuticle or sucker lining (see below) that is particularly well-developed on the infundibulum. The sucker lining is shed periodically and renewed continuously (Girod, 1884; Naef, 1921–1923; Nixon and Dilly, 1977; Packard, 1988). The infundibulum is encircled by a rim covered with a deeply folded, loose epithelium. The suckers are attached to the arms by a short muscular base that is covered by a continuation of the dermis and epidermis of the arms. A single row of suckers is present on the arms of *E. cirrosa* and two rows of suckers are present on the arms of the *Octopus* species.

Sucker microanatomy

For the purposes of this discussion, we refer to transverse and frontal sectional planes. Transverse sectional planes are defined as sections perpendicular to the long axis of the arm. Frontal sections are parallel to the plane defined by the opening of the sucker.

Intrinsic sucker musculature. Although we did not

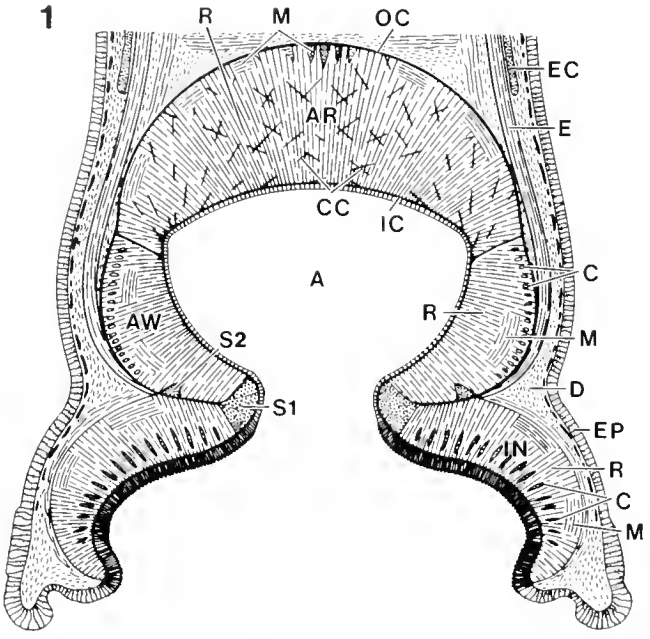

Figure 1. Schematic diagram of the microanatomy of the sucker of *Octopus* in transverse section. A, acetabulum; AR, acetabular roof; AW, acetabular wall; C, circular muscle; CC, crossed connective tissue fibers; D, dermis; E, extrinsic muscle; EC, extrinsic circular muscle; EP, epithelium; IN, infundibulum; IC, inner connective tissue layer; M, meridional muscle; OC, outer connective tissue layer; R, radial muscle; S1, primary sphincter muscle; S2, secondary sphincter muscle.

make a systematic study of a wide range of sucker sizes and sucker locations on the arms, the general arrangement of the muscle and connective tissue of the suckers is the same for the different species and sucker sizes we examined. Several minor differences between genera were observed and are noted below. The acetabular and infundibular portions of the sucker consist primarily of a tightly packed, three-dimensional array of muscle fibers. The muscle fibers can be categorized by orientation into three major groups: radial muscle fibers that extend across the wall of the sucker more or less perpendicular to the inner surface; circular muscle fibers that are oriented circumferentially around the sucker and parallel to the frontal plane; and meridional muscle fibers that are oriented perpendicular to the radial and circular muscle fibers (Fig. 1).

The acetabular portion consists of a wall region and a domed roof. The acetabular wall includes radial, circular, and meridional muscle fibers. The acetabular roof includes radial and meridional muscle fibers but lacks circular muscle fibers. Radial muscle fibers extend between their origins and insertions on an inner fibrous connective tissue layer lining the acetabulum and an outer fibrous connective tissue layer encapsulating the sucker (Figs. 1–3). As the radial fibers project toward the outer surface, they interdigitate with bundles of meridional muscle fibers. In the acetabular wall, the radial muscle fibers also interdigitate with circular muscle bundles (Fig. 2). The circular muscle bundles extend around the perimeter of the acetabular wall.

The location of the circular and meridional muscle bundles in the acetabular wall of the suckers of *Eledone cirrosa* is different from that of the *Octopus* species examined in this study. In *E. cirrosa*, the meridional muscle bundles are located peripheral to the circular muscle bundles. In the *Octopus* species, however, the arrangement is reversed; a distinct series of circular muscle bundles are located peripheral to the meridional muscle bundles (Compare Figs. 1 and 2).

In addition to the circular muscle bundles of the acetabular wall, a mass of circular muscle forms a sphincter located adjacent to the inner surface at the level of the narrow orifice that connects the infundibulum to the acetabulum (Figs. 1, 2). A secondary sphincter is also evident near the junction between the outer surfaces of the walls of the acetabulum and infundibulum and has a cross-sectional area that is approximately 10% of the area of the primary sphincter.

The meridional muscle fibers project from a point near the apex of the acetabular roof toward the sphincter muscles as an array of flat bundles that lie between the radial muscle fibers. When the outer surface of the acetabular roof is viewed in a grazing frontal section, the meridional muscle fiber bundles appear to be arranged in a stellate pattern (Fig. 4). Many of the meridional muscle fibers insert on the outer connective tissue layer at the level of the sphincter muscles. Some meridional muscle fibers extend into the wall of the infundibulum.

The arrangement of muscle fibers in the wall of the infundibulum is similar to that of the acetabular wall described above. Radial muscle fibers extend across the wall from their origins and insertions on the inner and outer connective tissue layers of the infundibulum. The radial muscles pass between a series of flat bundles of circular muscle fibers located adjacent to the inner surface of the infundibular wall (Fig. 5). Meridional muscle fibers are also present in the infundibular wall (Fig. 1, Fig. 5). Many originate on the outer connective tissue layer at the level of the sphincter muscles and extend toward their insertion at the margin of the infundibulum while others appear to be extensions of the meridional fibers of the acetabular wall. The bundles of meridional fibers are flat and are interwoven between the radial muscle fibers.

Sucker connective tissue. The two major components of the connective tissues of the sucker are an array of crossed connective tissue fibers embedded in the musculature of the acetabular roof, and the inner and outer connective tissue capsules. Thin layers of connective tissue also surround the circular and meridional muscle bundles of the sucker. It is likely that the connective tissue fibers observed in the sucker are collagenous because

they appear birefringent when viewed with polarized light microscopy and show staining characteristics typical of collagen.

The inner and outer connective tissue capsules are compact layers of fibers that enclose the sucker musculature. The layers appear to be arranged as a crossed-fiber array when viewed in transverse sections that graze the inner or outer surface of the wall (Fig. 6). At the level of the sphincter muscles, fibers of the outer connective tissue layer penetrate into the musculature of the sucker wall (Fig. 5). These fibers branch repeatedly and extend to the primary sphincter muscle, dividing it into fascicles. The extension of the outer connective tissue capsule that encloses the infundibulum is thinner than that of the acetabulum. The inner connective tissue capsule extends from the acetabulum to the infundibulum without any appreciable change in thickness.

In addition to the connective tissue layers encasing the sucker, crossed connective tissue fibers are present in the musculature of the roof of the acetabulum (Figs. 1, 3). These fibers extend between the inner and outer connective tissue capsule at oblique angles to the radial muscle fibers. They are reminiscent of the "intermuscular" connective tissue fibers described by Gosline and Shadwick (1983a, b) and Bone *et al.* (1981) in the mantle of squid and cuttlefish and those described by Kier (1989) and Kier *et al.* (1989) in the fins of squid and cuttlefish. However, the angle they make with the radial fibers is not constant (Fig. 3). These connective tissue fibers do not occur in the acetabular wall. The boundary between the acetabular roof and the acetabular walls includes a particularly robust band of intermuscular connective tissue fibers, and the wall is thinner at this point (Fig. 1).

Sucker epithelium. Several distinct zones of epithelium are present on the sucker (see also Girod, 1884; Guérin, 1908; Nixon and Dilly, 1977; Packard, 1988). The epithelium lining the infundibulum consists of tall columnar cells resting on a basal lamina and the inner connective tissue capsule. These cells secrete a tough, chitinous cuticle (Hunt and Nixon, 1981). The surface of the cuticle bears numerous tiny denticles or pegs, each secreted by a single columnar epithelial cell (see Nixon and Dilly, 1977). The epithelial cells lining the radial grooves of the infundibulum are cuboidal, and the cuticle lining the grooves lacks denticles. The cells of the epithelium lining the acetabulum are cuboidal. In addition, the denticles are rudimentary or absent from the cuticle lining the acetabulum. The transition between the epithelial surfaces of the infundibulum and acetabulum occurs at the level of the primary sphincter muscle (Figs. 1, 2, 5). Another transition is observed in the groove that separates the rim and the infundibulum. The epithelial cells in the groove are cuboidal and the cuticle is thin and lacks denticles. The epithelium covering the pillows and folds of the rim is columnar and the underlying dermis is loose and folded. An additional differentiation of the epithelium was observed in a zone surrounding the sucker rim. Cells in this zone showed intense staining by Mowry's colloidal iron stain (Humason, 1979) for acid mucopolysaccharides (Fig. 7).

Girod (1884) described the infundibulum of the suckers of *Octopus vulgaris* as being covered by numerous small "hillocks" of tall columnar epithelial cells and cuticle with denticles. He describes the epithelium between the hillocks as being flattened. Although small hillocks are visible on the surface of the infundibulum or on shed sucker linings of the species we examined, no differentiation of the epithelium was observed between the hillocks. A flattened epithelium was only observed in the radial grooves.

Extrinsic sucker musculature. The suckers are attached to the arms by a series of extrinsic muscle bundles (see also Guérin, 1908). A group of major extrinsic muscle bundles is associated with each sucker and originates on the connective tissue sheath surrounding the arm musculature (Kier, 1988) and extends orally to converge on the sucker (Fig. 8). These bundles insert on the outer connective tissue capsule of the sucker at the level of the sphincter muscle (Figs. 1, 2). The extrinsic muscle bundles are, in turn, surrounded along much of their length by a sheet of circumferential muscle fibers (Fig. 8). In addition to the major extrinsic muscle bundles illustrated in Figure 8, a medial group of smaller diameter extrinsic muscle bundles was observed in the region enclosed by the major extrinsic bundles. Although many are oriented parallel to the major bundles, some follow oblique courses, crossing from one side to the other.

Kinematics

Octopus suckers are capable of a wide range of movements. The animals explore their environment with their arms, holding their suckers extended and splayed out. The muscular base that attaches the sucker to the arm can elongate to twice its resting length, extending the suckers away from the arm. Sometimes individual suckers were observed to probe through small openings such as a screen, then extend fully and tilt up and down or side to side. If the sucker is stimulated lightly, it either extends to attach to the stimulus or withdraws, always orienting so that the infundibulum faces the object. When the octopus is active, the infundibuli of the suckers are flattened. Sucker "footprints" in wax show that the entire infundibulum is pressed firmly against the substratum during attachment. When the animal is at rest, the infundibuli are cone-shaped.

An octopus can grip nearly any size object with its suckers. They seem to prefer large flat surfaces but can easily grip irregular objects and objects smaller than their suckers. When manipulating threads or thin sheets, the

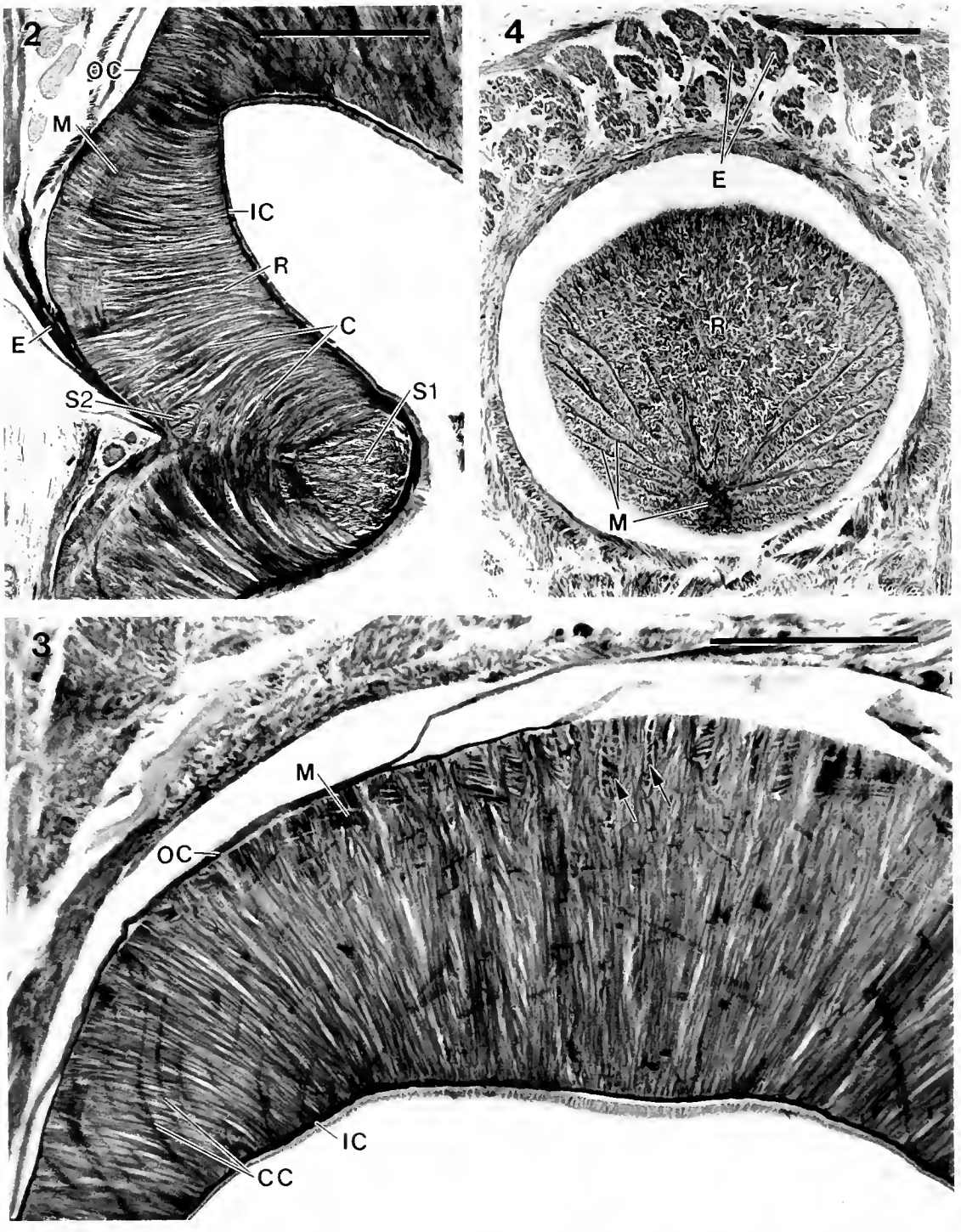

Figure 2. Photomicrograph of a transverse section of a sucker from *Eledone cirrosa* in the region of the primary and secondary sphincter muscles (S1, S2) and the acetabular wall. The radial muscles (R) extend from the inner connective tissue capsule (IC) to the outer connective tissue capsule (OC). Interwoven between the radial muscle fibers are meridional muscles (M) and circular muscles (C). An extrinsic muscle (E) inserts on the outer connective tissue capsule adjacent to the secondary sphincter muscle. The photomicrograph was made using brightfield microscopy of a 15 μm-thick paraffin section stained with Milligan trichrome. The scale bar equals 0.5 mm.

Figure 3. Photomicrograph of a transverse section of a sucker of *Octopus bimaculoides/bimaculatus* in the region of the acetabular roof. The crossed connective tissue fibers (CC) extend across the roof from the inner (IC) to the outer (OC) connective tissue capsule at oblique angles to the radial muscle fibers. Meridional muscle fibers (M) are also visible adjacent to the outer surface of the acetabular roof. The intersection of the meridional bundles at the axis of radial symmetry is apparent in the top of the micro-

suckers sometimes fold so that the two halves of the infundibulum grasp the object like a mittened hand (see also Packard, 1988). A sucker can grip a strand of fishing line and pull on it with surprising force. When it does this, the crease of the fold is usually parallel to the long axis of the arm. Suckers are often observed to fold over the corner of an object without noticeably weakening the force of attachment. A striking example of this occurs when a sucker is attached to the end of a cylinder with a smaller diameter than that of the sucker. Here the perimeter of the infundibulum folds around the side of the cylinder while the remainder of the infundibulum presses flat against the end.

The movies allowed us to distinguish and quantify changes in the sucker's dimensions during suction, particularly the diameter of the large sphincter. We considered the diameter of the orifice leading to the acetabulum to be the same as the diameter of the inner surface of the sphincter. We measured the diameter of the rim and the diameter of the orifice when the sucker was attached (x) and when it was relaxed (x_0). When gripping, the rim diameter increased from its resting state ($x = 1.26x_0^{0.94}$; $r = 0.82$) as does the orifice diameter ($x = 1.48x_0^{0.87}$; $r = 0.80$). The movies also showed that the roof of the acetabulum does not press against the substratum during attachment, contrary to the mechanism reported by Packard (1988).

Discussion

Principles of forming a suction attachment

Suckers attach to the substratum by forming a seal at the rim and reducing the pressure in the acetabular cavity. This decrease in pressure has been measured and can account for all of the attachment force of octopus suckers (A. M. Smith, in prep). The acetabular cavity is filled with water, and the ability of water to withstand this decrease in pressure is critical to sucker function. The distinction between water-filled and air-filled suckers has not been emphasized in previous studies of sucker function (see Denny, 1988).

A sucker filled with air has different mechanical requirements from one that is filled with water. An air-filled sucker must significantly increase its enclosed volume to decrease the pressure in the cavity. Starting from 0.1 MPa ambient pressure (1 atm), doubling the volume would halve the pressure to 0.05 MPa, increasing the volume ten times would only reduce the pressure to 0.01 MPa. To create a vacuum, the cavity must be reduced to a negligible volume before attachment. The lowest possible pressure inside such a sucker would be a vacuum (0 MPa). At normal ambient pressure (0.1 MPa), the force holding this sucker and the substratum together would be 0.1 MPa multiplied by the area exposed to the vacuum.

Octopus suckers operate in water rather than air, which leads to two important functional consequences: first, the sucker can decrease pressure without detectably expanding, and second, the pressures generated will not necessarily be limited to a vacuum. Water is essentially inexpansible at physiological stresses because of its cohesive strength. Therefore, water resists the activity of the muscles that expand the enclosed volume. Thus, if more water does not leak into the sucker, the muscles involved in generating suction contract isometrically, reducing the water's pressure. As long as the water adheres to all surfaces, the sub-ambient pressure in the water pulls the substratum tightly to the sucker. Also, as long as the water adheres to all surfaces, the sub-ambient pressure is only limited by the strength of the water-water bonds. Water columns have sustained pressures as low as −27.0 MPa in the laboratory without breaking (cavitating) (Briggs, 1950). Pressures of this magnitude are extremely difficult to achieve in practice because water does not adhere perfectly to all solid/liquid interfaces. Nevertheless, unlike the situation in air, suckers filled entirely with water have the potential to generate pressures well below 0 MPa. In fact, pressures below 0 MPa have been measured inside octopus suckers (A. M. Smith, in prep).

The difference between air and water has been overlooked in previous work in which octopus suckers were assumed to operate by creating a vacuum (Girod, 1884; Guérin, 1908), or where the pressure was assumed to be limited to a vacuum (Nixon and Dilly, 1977). Parker (1921) measured the suction force from one sucker, but apparently performed this experiment in air, which would explain why he did not measure pressures lower than 0.028 MPa.

The failure to make a distinction between air and water may have led to errors in the literature dealing with such diverse groups as limpets and torrential stream-dwelling vertebrates. Hora (1930) claimed that certain

graph (arrows). The photomicrograph was made using brightfield microscopy of a 10 μm-thick paraffin section stained with Milligan trichrome. The scale bar equals 0.25 mm.

Figure 4. Photomicrograph of a grazing frontal section of the acetabular roof of a sucker from *O. bimaculoides/bimaculatus*. The stellate arrangement of the meridional muscles (M) is visible. The radial muscle fibers (R) and extrinsic muscles (E) appear in cross section in this micrograph. The photomicrograph was made using brightfield microscopy of a 10 μm-thick paraffin section stained with Mallory's triple stain. The scale bar equals 0.25 mm.

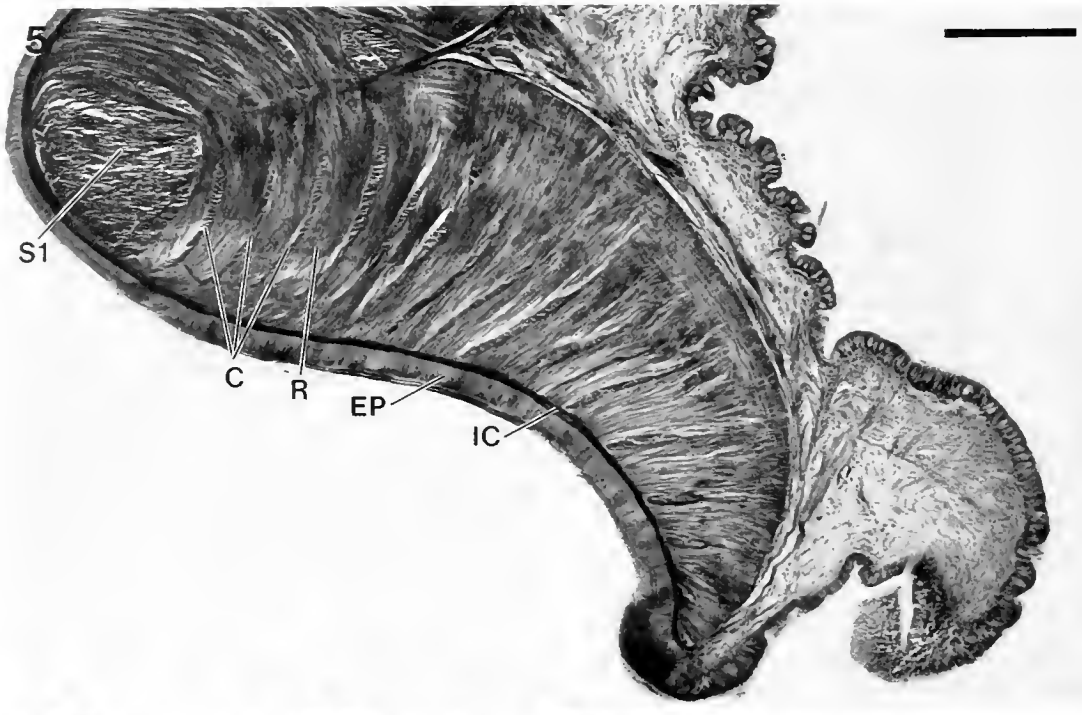

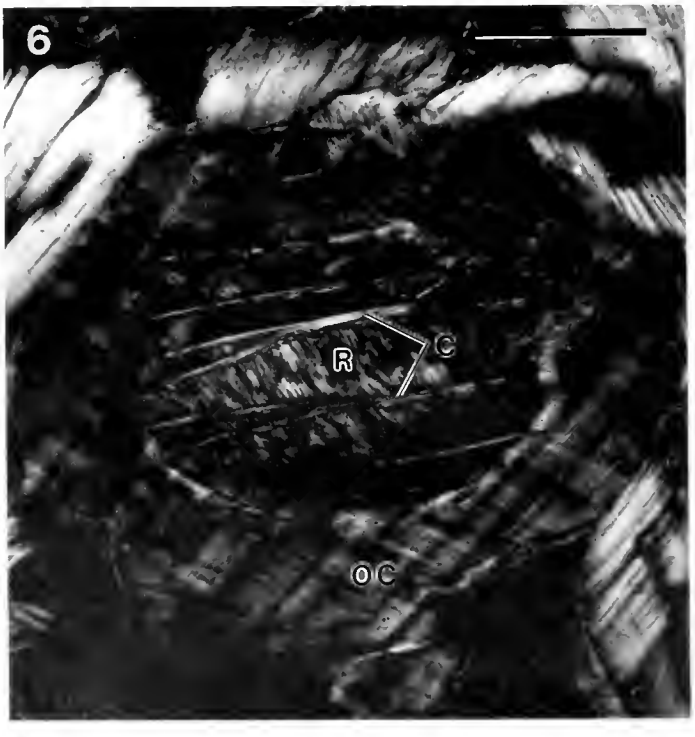

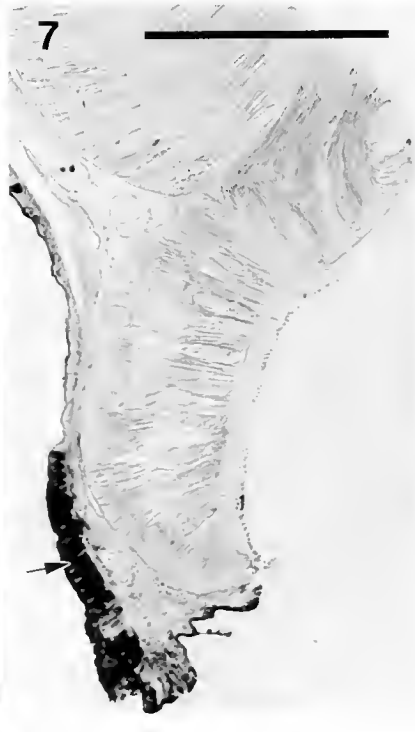

Figure 5. Photomicrograph of a transverse section of a sucker from *Eledone cirrosa* in the region of the infundibulum. The layers of circular muscle bundles (C) are interwoven between the radial muscle bundles (R). The inner connective capsule (IC) underlies the tall columnar epithelium (EP) of the infundibulum. The primary sphincter muscle (S1) is also visible. The photomicrograph was made using brightfield microscopy of a 15 μm-thick paraffin section stained with Milligan trichrome. The scale bar equals 0.25 μm.

Figure 6. Photomicrograph of a grazing transverse section of a sucker from *Octopus bimaculoides/bimaculatus* in the region of the acetabular wall. The connective tissue fibers of the outer connective tissue capsule (OC) are oriented in a crossed-fiber array. Radial (R) and circular (C) muscle fibers of the acetabular wall are also visible. The photomicrograph was made using polarized light microscopy of a 10 μm-thick paraffin section stained with Picro-Ponceau and iron hematoxylin. The scale bar equals 100 μm.

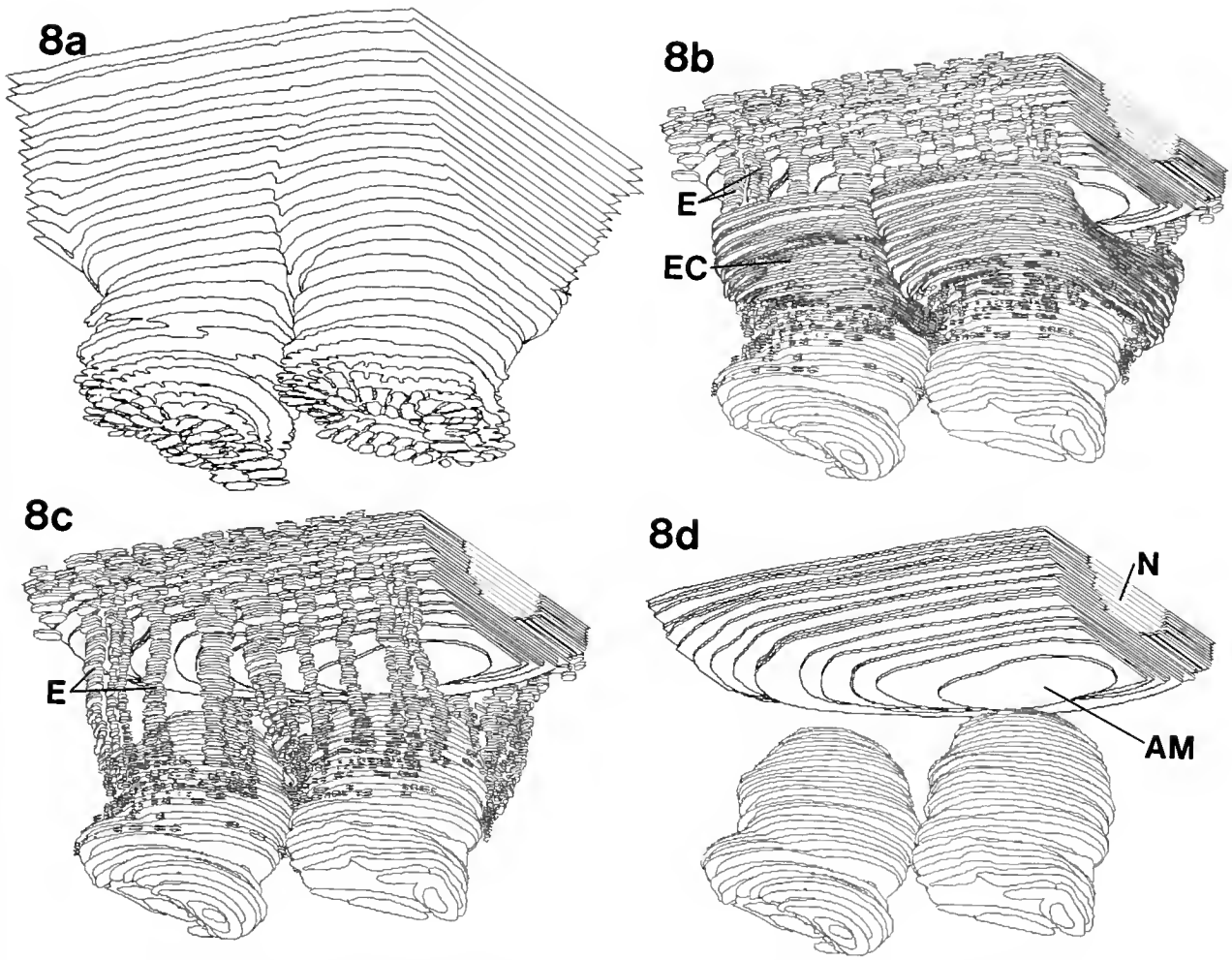

Figure 8. Computer-assisted three-dimensional reconstruction of a portion of an arm of *Eledone cirrosa* showing the extrinsic musculature associated with two suckers. In (a), the outer surface of the arm and suckers is visible. In (b), the epithelium and dermis have been removed to reveal the extrinsic muscles (E) that are surrounded by the extrinsic circular muscles (EC). In (c), the extrinsic circular muscles have been removed to reveal the course of the regularly arrayed extrinsic muscles (E). In (d) the extrinsic muscles have been removed to reveal the arm muscle (AM) and the musculature of the two suckers. The axial nerve cord (N) is also visible.

fish are not using suction because the center of the adhesive disc is not elevated during attachment, as it must be to create a partial vacuum in air. But these suckers are water-filled and therefore there would be no detectable expansion of the cavity while generating sub-ambient pressure. The attachment of limpets has also been attributed to mechanisms other than suction because their tenacity exceeds that which can be explained if one assumes that water cavitates at 0 MPa (Branch and Marsh, 1978; Grenon and Walker, 1981). Seawater can, in fact, endure pressures lower than 0 MPa without cavitating (A. M. Smith, in prep). Thus, suction attachment mechanisms may be used in both groups.

Another important factor that may have been overlooked is the depth-dependence of the attachment force. The depth at which an octopus lives will have an effect on the relative pressure difference that can be created in the sucker. Just below the surface, the maximum pressure differential is determined by the ambient pressure (approximately 0.1 MPa) outside the sucker and the absolute pressure at which seawater cavitates inside the sucker. With an increase in depth, the ambient pressure

Figure 7. Photomicrograph of a transverse section of a sucker from *O. joubini*. The epithelium surrounding the sucker rim (arrow) shows intense staining of acid mucopolysaccharides. The remaining tissues of the sucker are unstained in this micrograph. The photomicrograph was made using brightfield microscopy of a 10 μm-thick paraffin section stained with Mowry's colloidal iron stain. The scale bar equals 0.25 mm.

outside of the sucker increases while the absolute pressure at which seawater cavitates is unaffected. The potential relative pressure difference increases by 0.1 MPa with every 10 m of depth, rather than doubling as stated by Denny (1988) in his discussion of gas-filled suckers. Since the attachment force of a sucker is the pressure differential multiplied by the area of attachment, the greater pressure differential at depth might allow deep-sea octopuses to create the same attachment force with smaller suckers, assuming that sufficient force can be produced by the sucker musculature. It is of interest in this regard that Voight (1990) has observed an inverse correlation between sucker diameter and depth of occurrence for a variety of octopus species.

Proposed function of octopus suckers

In the following discussion, we propose hypotheses of sucker function, based on the principles of suction attachment outlined above and a biomechanical analysis of the musculature and connective tissue. Further experimental work is required to test these proposals.

Initial contact: forming and maintaining a seal. The first step in generating suction is forming a tight seal to prevent water from leaking in and equalizing the pressure. This implies that the infundibulum must be flexible and dexterous enough to mold itself to a wide range of surface shapes and textures. The infundibulum is composed of a tightly packed three-dimensional array of muscles that allow precise bending. Kier and Smith (1985) outlined the basic principles of this type of system, termed a muscular-hydrostat, and described the wide variety of movements of which it is capable. Since the muscular system itself has a constant volume, contraction in one dimension must be compensated by expansion in at least one other. Contraction of the radial muscles of the infundibulum will thin the infundibulum and thereby extend the rim, increasing the circumference and the surface area facing the substratum. More importantly, the radial muscles can hold the rim extended by resisting the increase in thickness that must accompany retraction of the rim. If the distance from the rim to the primary sphincter cannot decrease when the meridional muscles of the infundibulum contract, the infundibulum will bend toward the arm, flattening the face of the sucker. The circumferential muscles of the infundibulum may function as antagonists to the meridional muscles by constricting the infundibulum to a conical shape. One major advantage the sucker gains by using a muscular-hydrostatic mechanism rather than hard skeletal elements is the local control of movement that is possible. The effect of muscle contraction in the infundibulum is localized such that it can bend at any point. This allows it to match exactly the contours of the substratum. Once matched to the substratum, the mucus and loose epithelium of the rim may provide the seal.

The denticles on the chitinous lining of the infundibulum probably play an important role in maintaining a seal at the rim margin rather than close to the orifice. If the ends of the denticles are resting on the substratum, then an interconnected, water-filled network of spaces will be formed between them. This network may provide a means of transmitting the subambient pressure of the acetabular cavity underneath the entire infundibulum, thereby pulling it tightly against the substratum. The wax impressions of attached suckers demonstrate that the entire infundibulum is forcefully applied to the substratum during attachment. Without such a provision for transmitting pressure, the seal would probably be formed at the orifice and no force would be available to hold the infundibulum against the substratum. This would dramatically decrease the shear resistance of the sucker.

To form an effective attachment, suckers must be able to resist not only forces that lift the sucker away from the substratum but also shearing forces that slide the sucker along the substratum (see Denny, 1988). This is particularly important since the animals appear to prefer holding objects so that the arms are aligned parallel to the force and most of the suckers are thus being sheared rather than being pulled normal to the surface. The friction between the rim and the substratum resists shearing forces and also prevents the rim from sliding towards the center as the pressure in the cavity drops. The denticles on the infundibulum may enhance the friction between the rim and the substratum. As long as the sub-ambient pressure presses the infundibulum against the substratum, the denticles provide a substantial frictional force. In shear, this force determines the tenacity of the attachment. The constant wear from friction may require the sucker linings to be shed periodically.

Some form of denticles or roughened pads often occur on the suckers of other animals. Green and Barber (1988) reported numerous discrete papillae on the marginal region of the sucker of the clingfish. These are covered with a keratin-like cuticle. The authors suggest that these may provide frictional resistance to shear. It is also possible that they allow transmission of the sub-ambient pressure to the rim, as we suggest above for octopus suckers. Denticles or projections are also observed on the surfaces of suckers of other aquatic vertebrates (Hora, 1930; Nachtigall, 1974), lumpsuckers (Arita, 1967), and tadpoles (Gradwell, 1973; Inger, 1966).

Nixon and Dilly (1977) proposed an adhesive function for the denticles on the infundibulum, but they are unclear whether the proposed force comes from capillarity or suction. There is no evidence that the denticles alone are adhesive. Our analysis suggests that only the musculature and connective tissue of the acetabulum are needed to generate the attachment force (see below).

Also important for initial contact are the extrinsic muscles that move and orient the entire sucker. Our me-

chanical analyses predict the following functions for these muscle groups. The major extrinsic muscles link the sucker to the arm, transmitting the force of attachment. They also retract the sucker. The band of extrinsic circular muscles surrounding these dorsoventral muscles will extend the entire sucker away from the arm by thinning the base that connects the sucker to the arm. Simultaneous contraction of both sets of muscles will tilt the sucker, depending on the location of the active dorsoventral extrinsic muscles relative to the axis of rotation. If the circumferential muscles did not provide resistance, the major extrinsic muscles would only retract the sucker.

The primary sphincter muscle probably serves an important function in maintaining suction. As previously suggested, the extrinsic muscles transmit the force of attachment to the arm. These muscles converge from their origin on the arm to insert adjacent to the sphincter. Thus, in transmitting force to the arm, the extrinsic muscles also tend to increase the diameter of the sphincter. During attachment, the diameter of the orifice was observed to increase. Contraction of the sphincter restricts the extent of this increase. If the sphincter could not resist the increase, then the sucker would deform and probably lose its grip. Interestingly, Guérin (1908) stated that pelagic octopuses in the family Alloposidae lack a primary sphincter. His figure illustrating a histological section of an allopsid sucker does not show any large extrinsic muscles, only diffuse connective tissue. Another pelagic octopus, *Japatella diaphana,* appears also to lack both primary sphincter muscles and large extrinsic muscles (Nixon and Dilly, 1977). The coincident lack of a primary sphincter and large extrinsic muscles would be predicted if the sphincter serves to resist deformation from the stress of muscles that connect the sucker to the arm.

Sub-ambient pressure generation. Although the infundibulum is critical for making the initial contact, it is the muscles of the acetabulum that probably create the sub-ambient pressure required for attachment. The radial muscles are arranged such that their contraction would increase the enclosed volume, were it not for the resistance of the water. Contraction of the radial muscles of the acetabulum generates a force that tends to thin the wall. Because the wall has a constant volume, a decrease in thickness must increase the internal surface area, or overall size, of the hemisphere and cause the cavity to expand. The cavity cannot expand, however, because of the resistance of the enclosed water. In resisting this expansion, the water is put in tension. The muscular-hydrostat mechanism of the sucker allows suction attachment to occur even if no force is being transmitted from the arm to the sucker. Indeed, the suckers of amputated arms can still attach strongly (Rowell, 1963) as can isolated suckers (Parker, 1921).

The circumferential muscles and meridional muscles of the acetabulum probably function as antagonists to the radial muscles. Contraction of the circumferential muscles alone would decrease the circumference and increase the height of the acetabulum. Contraction of the meridional muscles alone would decrease the height of the acetabulum. When the sucker is not attached, their simultaneous contraction evenly decreases the hemisphere volume and thereby thickens the cavity wall. The arrangement of radial, meridional, and circumferential muscles in the wall of the acetabulum appears typical of most of the suckers from a variety of phyla as described by Niemiec (1885).

An important aspect of sucker morphology that has been overlooked previously is the array of crossed connective tissue fibers in the musculature of the acetabular roof. Gosline and Shadwick (1983a, b) described an array of crossed connective tissue fibers in the mantle of squid and showed that it could serve as an elastic energy storage mechanism during locomotion and mantle ventilation. Perhaps the connective tissue fibers in octopus suckers also store energy. This elastic energy could maintain sub-ambient pressure in the sucker over extended periods of time, which might account for the observation that octopuses often hold onto objects for several hours. Prior to attachment, the connective tissue fibers of the acetabular roof could be prestrained by the thickening of the acetabular muscle mass that is created by the activity of the meridional and circumferential muscles. Then, upon attachment, the stored strain energy might exert a force analogous to that created by the radial muscles. Thus, rather than expending energy by contracting the radial muscles to maintain suction, suction could be maintained by virtue of the elastic properties of the connective tissue fibers. Nevertheless, several aspects of the arrangement of the connective tissue fibers are perplexing in the context of this mechanism. For example, it is unclear why the acetabular wall lacks these fibers and why the fiber angle is not more regular. Further work is needed to clarify the function of the crossed connective tissue fibers.

Acknowledgments

We thank S. F. Huggins for help with histology and O. Moe for help with the kinematics. We are grateful to K. K. Smith, J. R. Voight, S. A. Wainwright, and anonymous reviewers for comments on the manuscript. H. Crenshaw and the Duke University Department of Zoology biomechanics lab group provided valuable discussion. The Marine Biomedical Institute of the University of Texas Medical Branch at Galveston provided assistance with animal maintenance and supply. We thank A. K. Harris for the use of a 16mm cine film analyzer and S. A. Wainwright for the use of a 16mm cine camera. This material is based upon work supported under a National Science Foundation Presidential Young Investiga-

tor Award (DCB-8658069) to W.M.K. and a National Science Foundation Predoctoral Fellowship to A.M.S. A National Science Foundation Research Experiences for Undergraduates Supplement to W.M.K.'s Presidential Young Investigator Award provided support for the participation of S. F. Huggins in the preliminary histological study.

Literature Cited

Arita, G. S. 1967. A comparative study of the structure and function of the adhesive apparatus of the Cyclopteridae and Gobiesocidae. M. Sc. thesis, University of British Columbia, Vancouver.

Bone, Q., A. Pulsford, and A. D. Chubb. 1981. Squid mantle muscle. *J. Mar. Biol. Assoc. U. K.* **61:** 327–342.

Briggs, L. J. 1950. Limiting negative pressure of water. *J. Appl. Physics* **21:** 721–722.

Branch, G. M., and A. C. Marsh. 1978. Tenacity and shell shape in six *Patella* species: adaptive features. *J. Exp. Mar. Biol. Ecol.* **34:** 111–130.

Denny, M. 1988. *Biology and the Mechanics of the Wave-Swept Environment.* Princeton University Press, Princeton. 329 pp.

Dilly, N., M. Nixon, and A. Packard. 1964. Forces exerted by *Octopus vulgaris*. *Pubbl. Staz. Zool. Napoli* **34:** 86–97.

Gaunt, P. N., and W. A. Gaunt. 1978. *Three Dimensional Reconstruction in Biology.* University Park Press, Baltimore. 174 pp.

Girod, P. 1884. Recherches sur la peau des céphalopodes. La ventouse. *Arch. Zool. Exp. Gen.* **2:** 379–401.

Gosline, J. M., and R. E. Shadwick. 1983a. The role of elastic energy storage mechanisms in swimming: an analysis of mantle elasticity in escape jetting in the squid, *Loligo opalescens*. *Can. J. Zool.* **61:** 1421–1431.

Gosline, J. M., and R. E. Shadwick. 1983b. Molluscan collagen and its mechanical organization in squid mantle. Pp. 371–398 in *The Mollusca, Metabolic Biochemistry and Molecular Biomechanics*, Vol. 1, P. W. Hochachka, ed. Academic Press, New York.

Gradwell, N. 1973. On the functional morphology of suction and gill irrigation in the tadpole of *Ascaphus* and notes on hibernation. *Herpetologica* **29:** 84–93.

Graziadei, P. 1962. Receptors in the suckers of *Octopus*. *Nature* **195:** 57–59.

Graziadei, P. P. C., and H. T. Gagne. 1976a. Sensory innervation in the rim of the octopus sucker. *J. Morphol.* **150:** 639–679.

Graziadei, P. P. C., and H. T. Gagne. 1976b. An unusual receptor in the octopus. *Tissue & Cell* **8:** 229–240.

Green, D. M., and D. L. Barber. 1988. The ventral adhesive disc of the clingfish *Gobiesox maeandricus*: integumental structure and adhesive mechanisms. *Can. J. Zool.* **66:** 1610–1619.

Grenon, J. F., and G. Walker. 1981. The tenacity of the limpet, *Patella vulgata L.*: an experimental approach. *J. Exp. Mar. Biol. Ecol.* **54:** 277–308.

Guérin, J. 1908. Contribution à l'étude des systèmes cutané, musculaire et nerveux de l'appareil tentaculaire des céphalopodes. *Arch. Zool. Exp. Gen.* **38:** 1–178.

Hora, S. L. 1930. Ecology, bionomics and evolution of the torrential fauna, with special reference to the organs of attachment. *Philos. Trans. R. Soc. Lond. B* **218:** 171–282.

Humason, G. L. 1979. *Animal Tissue Techniques.* W. H. Freeman and Co., San Francisco. 661 pp.

Hunt, S., and M. Nixon. 1981. A comparative study of protein composition in the chitin-protein complexes of the beak, pen, sucker disc, radula and oesophageal cuticle of cephalopods. *Comp. Biochem. Physiol. B* **68:** 535–546.

Inger, R. F. 1966. The systematics and zoogeography of the Amphibia of Borneo. *Fieldiana Zool.* **52:** 1–402.

Kier, W. M. 1988. The arrangement and function of molluscan muscle. Pp. 211–252 in The *Mollusca, Form and Function*, Vol. 11, E. R. Trueman and M. R. Clarke, eds. Academic Press, New York.

Kier, W. M. 1989. The fin musculature of cuttlefish and squid (Mollusca, Cephalopoda): morphology and mechanics. *J. Zool.* **217:** 23–38.

Kier, W. M., and K. K. Smith. 1985. Tongues, tentacles and trunks: the biomechanics of movement in muscular-hydrostats. *Zool. J. Linn. Soc. Lond.* **83:** 307–324.

Kier, W. M., K. K. Smith, and J. A. Miyan. 1989. Electromyography of the fin musculature of the cuttlefish *Sepia officinalis*. *J. Exp. Biol.* **143:** 17–31.

Nachtigall, W. 1974. *Biological Mechanisms of Attachment. The Comparative Morphology and Bioengineering of Organs for Linkage, Suction, and Adhesion.* Springer-Verlag, New York. 194 pp.

Naef, A. 1921–1923. Cephalopoda. Pp. 1–917 in *Fauna and Flora of the Bay of Naples*, No. 35, Israel program for scientific translations, Jerusalem.

Niemiec, J. 1885. Recherches mophologiques sur les ventouses dans la regne animal. *Recueil Zool. Suisse* **2:** 1–147.

Nixon, M., and P. N. Dilly. 1977. Sucker surfaces and prey capture. *Symp. Zool. Soc. Lond.* **38:** 447–511.

Packard, A. 1988. The skin of cephalopods (coleoids): general and special adaptations. Pp. 37–67 in *The Mollusca, Form and Function*, Vol. 11, E. R. Trueman and M. R. Clarke, eds. Academic Press, San Diego.

Pantin, C. F. A. 1946. *Notes on Microscopical Technique for Zoologists.* Cambridge University Press, Cambridge. 73 pp.

Parker, G. H. 1921. The power of adhesion in the suckers of *Octopus bimaculatus* Verrill. *J. Exp. Zool.* **33:** 391–394.

Pickford, G. E., and B. H. McConnaughey. 1949. The *Octopus bimaculatus* problem: a study in sibling species. *Bull. Bingham Oceanogr. Collect. Yale Univ.* **12:** 1–66.

Rowell, C. H. 1963. Excitatory and inhibitory pathways in the arm of *Octopus*. *J. Exp. Biol.* **40:** 257–270.

Smith, K. K., and W. M. Kier. 1989. Trunks, tongues and tentacles: moving with skeletons of muscle. *Am. Sci.* **77:** 28–35.

Tittel, K. 1961. Der functionelle Aufbau des Tintenfischarmes im Vergleich mit dem Muskelkörper der Säugerzungen. *Verh. Anat. Ges.* **57:** 264–275.

Tittel, K. 1964. Saugnapf-, epi- und hypofasciale Armmuskulatur der Kephalopoden—ein Beitrag zur funktionellen Anatomie freibeweglicher Skelettmuskelkörper. *Gegenbaurs Morphol. Jahrb.* **106:** 90–115.

Voight, J. R. 1990. Population biology of *Octopus digueti* and the morphology of American tropical octopods. Ph.D. Dissertation, University of Arizona, Tucson.

Wells, M. J. 1978. *Octopus: Physiology and Behaviour of an Advanced Invertebrate.* Chapman and Hall, London. 417 pp.

Young, S. L., E. K. Fram, and B. L. Craig. 1985. Three-dimensional reconstruction and quantitative analysis of rat lung type II cells: a computer-based study. *Am. J. Anat.* **174:** 1–14.

Reference: *Biol. Bull.* **178:** 137–143. (April, 1990)

The *Limulus* Blood Cell Secretes α_2-Macroglobulin When Activated

PETER B. ARMSTRONG[1], JAMES P. QUIGLEY[2], AND FREDERICK R. RICKLES[3]

Marine Biological Laboratory, Woods Hole, Massachusetts 02543

Abstract. Alpha$_2$-macroglobulin, a protease-binding protein that is reactive with almost all endopeptidases, is present in high concentrations in the plasma of the horseshoe crab, *Limulus*. Alpha$_2$-macroglobulin was demonstrated by its ability to protect the active site of trypsin from inactivation by the macromolecular active site inhibitor, soybean trypsin inhibitor, and by reaction with an antiserum prepared against purified *Limulus* α_2-macroglobulin. The blood cells also contain α_2-macroglobulin in a form that is released when washed cells are stimulated to undergo exocytosis by treatment with the ionophore, A23187. Alpha$_2$-macroglobulin is detected in the materials released from the cells during degranulation both by activity in the soybean trypsin inhibitor-protection assay and by immunochemical staining of Western blots. The subunit molecular weight of the cell-associated form of α_2-macroglobulin, 185 kDa, is identical to that of the plasma form. The amount of α_2-macroglobulin contained within the cells of a given volume of blood is 0.5–2% of the quantity in solution in that volume of plasma. The distilled water lysates of N-ethylmaleimide-stabilized amebocytes used to detect endotoxin (*e.g.*, *Limulus* amebocyte lysate or LAL) contain relatively large quantities of active α_2-macroglobulin. These preparations are essentially free of the principal plasma protein, hemocyanin, indicating that the cells had been well washed prior to lysis.

Received 20 September 1989; accepted 18 January 1990.

[1] Department of Zoology, University of California, Davis, California 95616.

[2] Department of Pathology, Health Sciences Center, State University of New York, Stony Brook, New York 11794-8691.

[3] Medical Research Service, Veterans Administration Medical Center, Newington, Connecticut 06111 and the Division of Hematology-Oncology, Department of Medicine, School of Medicine, University of Connecticut Health Center, Farmington, Connecticut 06032.

Introduction

Higher animals deploy a variety of defense systems to cope with invading pathogens that are based on components in solution in the blood or associated with the blood cells. These systems operate to restrict the growth and invasion of pathogens and to disable their toxic products. The protein, α_2-macroglobulin, is an element in the system of humoral defenses that binds proteases of all of the major classes and from diverse sources, including proteases of microbes (Barrett, 1981; Feinman, 1983; Sottrup-Jensen, 1987, 1989). This breadth of reactivity contrasts with the relatively narrow range of proteases recognized by individual active-site protease inhibitors (Laskowski and Kato, 1980; Travis and Salvesen, 1983). Proteases bound to α_2-macroglobulin are rendered incapable of hydrolyzing protein substrates and, at least in mammals, are removed from the circulation when the α_2-macroglobulin-protease complex is internalized into secondary lysosomes following receptor-mediated endocytosis (Van Leuven, 1984). Alpha$_2$-macroglobulin is apparently of considerable evolutionary antiquity, because it has been demonstrated in vertebrates (Starkey and Barrett, 1982), arthropods (Armstrong and Quigley, in prep.; Quigley and Armstrong, 1983, 1985; Armstrong *et al.*, 1985; Hergenhahn and Söderhäll, 1985; Spycher *et al.*, 1987; Hergenhahn *et al.*, 1988), and molluscs (Armstrong, unpub. data)—forms whose evolutionary lineages diverged approximately 0.5–0.6 billion years ago. In the arthropod, *Limulus* (the American horseshoe crab), α_2-macroglobulin is present in the plasma at concentrations of approximately 0.3–3 μM (unpub. data), which is similar to the levels reported for humans (3.5 μM: Coan and Roberts, 1989; Harpel, 1987).

The blood of *Limulus* contains a single type of cellular element, the granular amebocyte (Armstrong, 1985a),

which functions as a thrombocyte. Blood clotting involves formation of a cellular plug of adherent amebocytes at sites of injury (Loeb, 1920; Bursey, 1977) and the release of the extracellular clotting system from exocytotic vesicles contained within the amebocyte (Bang, 1979; Mürer *et al.*, 1975; Armstrong and Rickles, 1982). This latter system consists of the structural protein of the clot and a system of proteases that act on the apo form of the clottable protein to convert it into the form that polymerizes into the fibrils of the extracellular clot (Levin, 1985). The present report documents the presence of α_2-macroglobulin in the granular amebocyte in a form that is released from the cell during exocytosis.

Materials and Methods

Limulus *blood cells*

One hundred ml of blood obtained under sterile, endotoxin-free conditions from pre-chilled animals by cardiac puncture (Armstrong, 1985b) was collected into sterile chilled 50 ml plastic centrifuge tubes (Falcon Plastics, Lincoln Park, New Jersey) and centrifuged at 150 $\times g$. The plasma was discarded and the cells were resuspended in 20 ml of ice-cold anti-coagulant buffer [0.5 *M* sterile, endotoxin-free NaCl (Travenol Laboratories, Deerfield, Illinois), 0.01 *M* ethylenediaminetetraacetate, 0.1 *M* glucose, 0.056 *M* citrate buffer, final pH 4.6 (Söderhäll and Smith, 1983)]. The amount of cells in a preparation is presented as the volume of the cell pellet present at this stage. The cells were then washed 3 times with 20 ml/wash ice-cold endotoxin-free 0.5 *M* NaCl and resuspended in 15 ml endotoxin-free 0.5 *M* NaCl, 0.01 *M* $CaCl_2$. Exocytosis was initiated by adding the ionophore, A23187 (Sigma Chemicals, St. Louis, Missouri), to a final concentration of 10 μM. The preparation was incubated at 22°C for 3 h to allow the blood cells to degranulate, aggregate, and for the cell aggregate to contract. Approximately 13–14 ml of cell-free fluid was collected. This fluid contains the contents of the exocytotic granules, apparently uncontaminated by cytoplasmic constituents, because the cytoplasmic marker enzyme (lactate dehydrogenase) is present in the cells and can be released by detergent extraction of the cell pellet, but is absent from the materials released by the A23187-treated cells (Armstrong and Quigley, 1985).

SDS-polyacrylamide gel electrophoresis

Standard techniques were used for SDS-polyacrylamide gel electrophoresis (Laemmli, 1970). Soluble samples were dissolved in reducing sample buffer and were not boiled, to prevent heat fragmentation of the α_2-macroglobulin (Armstrong and Quigley, 1987), and electrophoresed at constant current on 7.5% polyacrylamide gels. We have found the coagulin clot of *Limulus* to dissolve only sparingly in reducing sample buffer (Rickles, unpub. data); not surprisingly, live blood cells and the cell clot produced following A23187-stimulated degranulation of blood cells failed to dissolve completely. Coagulin is the most abundant protein of both preparations. However, soluble proteins from the cells, including α_2-macroglobulin, are dissolved under these conditions.

Anti-α_2-macroglobulin antiserum

A purified preparation of the plasma form of *Limulus* α_2-macroglobulin (Quigley and Armstrong, 1985) was subjected to SDS-polyacrylamide gel electrophoresis (Laemmli, 1970; reducing conditions, 12% polyacrylamide gel) and transferred to nitrocellulose paper by electrophoretic blotting (Towbin *et al.*, 1979). The position of the protein was determined by Ponceau S staining. The band at 185 kDa was cut out, and the paper minced with scissors, suspended in water, and then fragmented by ultrasonication. Approximately 200 μg of nitrocellulose-bound α_2-macroglobulin was injected with Freund's complete adjuvant subcutaneously in multiple sites into female New Zealand white rabbits. A booster dose of 200 μg was given in incomplete adjuvant after 4 weeks, and antiserum was collected at 2-week intervals thereafter (Daino *et al.*, 1987).

Assay for α_2-macroglobulin activity

The functional assay for α_2-macroglobulin is essentially that of Armstrong *et al.* (1985). Briefly, bovine pancreatic trypsin (Sigma) was prepared as a stock solution at 1 mg/ml in 1 m*M* HCl and stored frozen until used. Protease activity was measured by the hydrolysis of the low molecular mass amide substrate, Nα-benzoyl-DL-arginine p-nitroanilide (BAPNA) (Sigma). The assay for α_2-macroglobulin activity depends on the ability of α_2-macroglobulin to bind trypsin without inactivating the active site of the enzyme. Alpha$_2$-macroglobulin-bound trypsin can hydrolyze BAPNA with equal efficiency to that of free trypsin (Quigley and Armstrong, 1983, Fig. 1). The ability of α_2-macroglobulin to suppress the proteolytic activity of proteases apparently depends on its ability to form a molecular cage around the protease molecule that establishes a steric barrier that prevents contact between protease and target proteins. This molecular cage also prevents the inactivation of the active site of the protease by high molecular mass active site protease inhibitors. Specifically, trypsin bound to *Limulus* α_2-macroglobulin is protected from inactivation by the active site inhibitor, soybean trypsin inhibitor (M_r = 21,000). This property is unique to the α_2-macroglobulin family of protease inhibitors and is the basis for an assay for α_2-macroglobulin activity (Ganrot, 1966) that

has been used to detect α_2-macroglobulin in the plasma of molluscs (Armstrong, unpub. data), *Limulus*, and crustaceans (Armstrong *et al.*, 1985). The sample suspected of containing α_2-macroglobulin is incubated with trypsin, and then saturating amounts of soybean trypsin inhibitor are added to inactivate all unbound trypsin. The determination of the rate of hydrolysis of BAPNA allows quantitation of the fraction of trypsin that is protected from inactivation by virtue of its binding to the α_2-macroglobulin in the sample. As far as we know, the assay is specific for the α_2-macroglobulin family of protease inhibitors.

Preparation of Limulus *amebocyte lysate (LAL)*

Lysates of *Limulus* amebocytes were prepared by hypotonic disruption of washed amebocytes at room temperature with sterile, pyrogen-free distilled water, essentially as described by Levin and Bang (1968). All glassware was siliconized, sterilized, and then rendered endotoxin-free by heating at 180°C in a dry oven. Adult female horseshoe crabs were bled directly into an equal volume of warm (40°C) 0.5 *M* NaCl, 0.005 m*M* N-ethyl maleimide (NEM, Sigma). Following sedimentation, the blood cells were resuspended in warm, NEM-containing saline, and then washed twice in warm saline without NEM. Hypotonic lysis of the cell button was accomplished by incubation in pyrogen-free distilled water (3/1 v/v of cells) at room temperature. The cell suspension was vortexed daily for 2 days and the resultant lysate (primary extract) was collected following centrifugation. The pellet was re-extracted by further incubation with distilled water (secondary extract). Lysate was stored at 4°C. Reactivity was determined by incubation with a standard preparation of endotoxin (*E. coli*, 026:B6, Difco Laboratories, Detroit, Michigan). In general, *Limulus* amebocyte lysate prepared in this manner has a protein concentration of 1.5–3.0 mg/ml and forms a gel in the presence of 10–100 pg/ml of endotoxin (Rickles *et al.*, 1979).

Results

Anti-α_2-macroglobulin antiserum

The antiserum recognized specifically the 185 kDa band of α_2-macroglobulin on immunoblots of purified α_2-macroglobulin (Fig. 1, lanes A.2 and B.1), whole *Limulus* plasma (Fig. 1, lanes A.3 and B.2), and *Limulus* plasma depleted of hemocyanin by ultracentrifugation (not shown). The antiserum did not cross react with α_2-macroglobulin from *Homarus* (the American lobster) or with human α_2-macroglobulin (not shown).

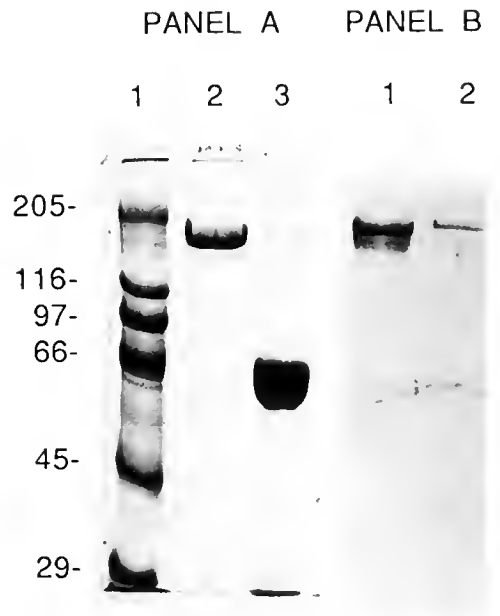

Figure 1. Characterization of the anti-*Limulus* α_2-macroglobulin antiserum by immunoblotting. The antiserum reacts specifically with a band at an apparent molecular mass of 185 kDa with purified α_2-macroglobulin (lanes A.2 and B.1) and with whole plasma (lanes A.3 and B.2). The arc-like density at about 40–60 kDa on panel B is due to a scratch on the nitrocellulose, and does not represent specific deposits of HRP reaction product. Lane A.2 contained 2.2 μg of protein; lane B.1 contained 0.55 μg of protein; and lanes A.3 and B.2 contained 0.25 μl of plasma. In Figures 1, 2, and 4, panel A is a SDS-polyacrylamide gel (7.5% polyacrylamide) run under reducing conditions and stained with Coomassie blue, and panel B is a Western blot of a parallel gel stained with the anti-*Limulus* α_2-macroglobulin antiserum.

Immunological demonstration of α_2-macroglobulin

The materials released from washed *Limulus* blood cells that had been stimulated to undergo exocytosis by exposure to A23187 were subjected to SDS-polyacrylamide gel electrophoresis under reducing conditions and then electrophoretically transferred to nitrocellulose paper. Alpha$_2$-macroglobulin was demonstrated by probing the transfers with the anti-α_2-macroglobulin antiserum. A single band at an apparent molecular weight of 185 kDa was recognized by the antibody (Fig. 2, lanes A.5 and B.6). The penultimate cell wash buffer contained no immunoreactive material (Fig. 2, lanes A.4 and B.5), indicating that the presence of α_2-macroglobulin in the material released during exocytosis of washed blood cells was not a result of contamination by plasma. Alpha$_2$-macroglobulin could likewise be demonstrated in blots of protein from whole, washed blood cells (Fig. 2, lanes A.3, B.3 and B.4). Attempts to demonstrate α_2-macroglobulin by immunoblotting of the proteins extracted from the residual pellet of cells that had undergone exocytosis were unsuccessful (Fig. 2, lanes A.6 and

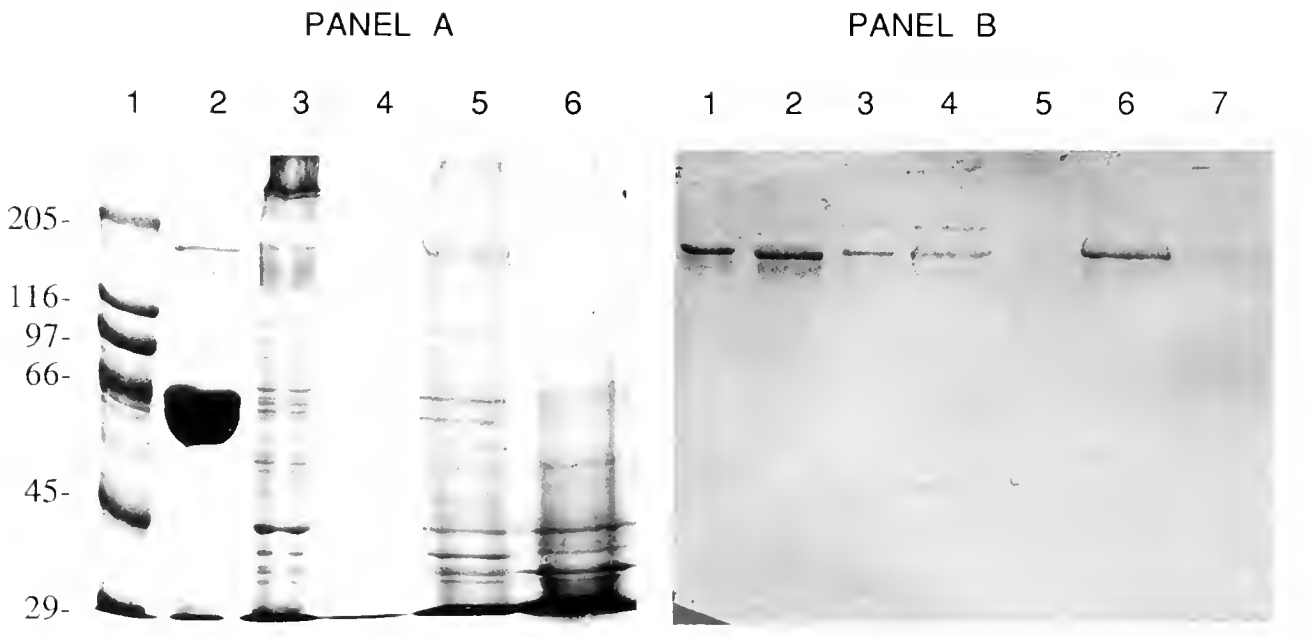

Figure 2. Immunologic demonstration of α_2-macroglobulin in *Limulus* blood cells and in the materials released during degranulation of the cells. Alpha$_2$-macroglobulin is evident in the plasma (lanes A.2 and B.2) and whole, undegranulated cells (lanes A.3, B.3 and B.4) but is not demonstrable in the penultimate wash of the cells (lanes A.4 and B.5). Alpha$_2$-macroglobulin is also demonstrable in the materials released from the cells during degranulation (lanes A.5 and B.6) but not in the degranulated cells (lanes A.6 and B.7). Lane B.1 was loaded with 1.1 μg of purified *Limulus* α_2-macroglobulin. Lanes A.2 and B.2 contained 0.25 μl of plasma; lane A.3 contained 2 μl of pelleted live, whole blood cells; lane B.3 contained 1 μl of pelleted whole, live blood cells; lanes A.4 and B 5 contained 10 μl of buffer from the penultimate cell wash; and lanes A.5 and B.6 contained 10 μl of releasate.

B.7), indicating that most or all of the cell-associated α_2-macroglobulin had been released during exocytosis. The apparent molecular weight of the subunit of cell-associated α_2-macroglobulin was identical to that of the plasma form of α_2-macroglobulin. The relative amounts of protein in different bands of Coomassie blue-stained gels were estimated spectrophotometrically with the curve integration function of a Bio Rad Model 620 scanning densitometer. Estimations of the relative amounts of α_2-macroglobulin by the optical density of the 185 kDa band on Coomassie blue-stained gels of whole cells and plasma indicate that the cells contained in a given volume of whole blood contain approximately 0.5–2% of the α_2-macroglobulin contained in the same volume of plasma.

Measurement of α_2-macroglobulin activity

The ability to protect trypsin from inactivation by soybean trypsin inhibitor was used to estimate the amounts of active α_2-macroglobulin in samples of plasma and the materials released by blood cells stimulated to undergo exocytosis. Comparable results to the immunological studies were obtained: plasma contained large quantities of α_2-macroglobulin, the cells of a given volume of blood contained about 0.5–2% of that amount of α_2-macroglobulin, and the penultimate wash buffer was negative (Fig. 3).

Alpha$_2$-macroglobulin in Limulus *amebocyte lysate (LAL)*

Limulus amebocyte lysate (LAL) is the soluble materials recovered by distilled water lysis of N-ethyl maleimide-stabilized *Limulus* amebocytes and is used for the detection of lipopolysaccharides from Gram-negative bacteria (Levin, 1979). Both immunostaining of protein blots (Fig. 4) and activity measurements (data not shown) indicated the presence of large amounts of α_2-macroglobulin in preparations of LAL. Primary extracts (Fig. 4, lanes A.2 and B.2) contained significantly more α_2-macroglobulin than secondary extracts (Fig. 4, lanes A.1 and B.1), on a per mg of total protein basis. The amounts of α_2-macroglobulin in primary extracts is significantly larger than would be expected from the amounts present in washed, live cells. Preparation of LAL involves exposing whole blood to a warm solution of n-ethyl maleimide, followed by extensive washing of

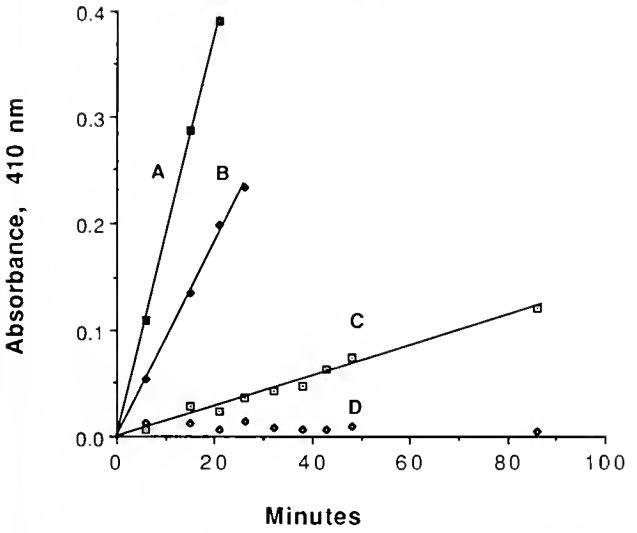

Figure 3. Demonstration of α_2-macroglobulin in materials released by saline-washed *Limulus* blood cells stimulated to degranulate by exposure to the ionophore, A23187, and in plasma from the same animal. The released materials protect trypsin from inactivation by the high molecular mass active site inhibitor, soybean trypsin inhibitor. Ten μg samples of trypsin were preincubated with 20 μl of plasma (curve B), the materials released from 12 μl of packed cells, which was the amount of cells contained in 530 μl of whole blood (curve C), or 160 μl of the penultimate saline wash (curve D) for 10 min and then 20 μg of soybean trypsin inhibitor was added. The remaining active trypsin (*e.g.*, the trypsin bound to the α_2-macroglobulin in the sample, and thereby protected from inactivation by soybean trypsin inhibitor) was assayed by its ability to hydrolyze the low molecular mass amide substrate, BAPNA. This was followed by the increase in optical absorbance at 410 nm. In the absence of added α_2-macroglobulin, the hydrolysis of BAPNA is zero (not shown). Curve A is the activity of 10 μg of trypsin in the absence of soybean trypsin inhibitor or α_2-macroglobulin. In this sample, the cells from a given volume of blood (curve C) contained 0.6% as much α_2-macroglobulin as the plasma from the same volume of blood (curve B). In other trials, the cells have contained as much as 2% of the total α_2-macroglobulin in a given volume of blood.

the cells and then their lysis in distilled water. The efficiency of washing is indicated by the minimal contamination of the LAL preparations with hemocyanin (compare the relative intensities of the hemocyanin band at 67 kDa and the α_2-macroglobulin band at 185 kDa in plasma (Fig. 2, lanes A.2 and B.2) with that in LAL (Fig. 4, lanes A.2 and B.2).

We speculate that α_2-macroglobulin in the plasma specifically becomes associated with the cells during the exposure of blood to n-ethyl maleimide and is released during the distilled water lysis step. The amounts of α_2-macroglobulin in the NEM-containing plasma phase that is the by-product of the preparation of cells for production of LAL were low or undetectable (Armstrong, unpub. data), consistent with the possibility that significant quantities of plasma α_2-macroglobulin become associated with the cells during treatment of blood with NEM.

Discussion

The blood is the principal organ involved in the defense against pathogens that have entered the body. In most animals, both plasma- and blood cell-mediated systems participate in immunity. The α_2-macroglobulin system of protease-binding proteins is a well-studied example of a humoral system of immunity, both in vertebrates (Sottrup-Jensen, 1987, 1989) and arthropods (Quigley and Armstrong, 1983, 1985; Armstrong *et al.*, 1985; Hergenhahn and Söderhäll, 1985; Spycher *et al.*, 1987; Hergenhahn *et al.*, 1988; Armstrong and Quigley, in prep.). The present report documents that the sole blood cell type of *Limulus*, the granular amebocyte, also contains α_2-macroglobulin in a form that is released during degranulation. The cell-associated form of α_2-macroglobulin is immunologically reactive with an antiserum prepared against the plasma form of *Limulus* α_2-macroglobulin and has an identical subunit molecular weight. Although the plasma of a given volume of whole blood contains much more α_2-macroglobulin than do the blood cells of that same volume of blood, the cell-associated form may play an important role in suppression of proteases in the densely cellular clot formed by aggregated blood cells at sites of wound healing (Loeb, 1920; Bursey, 1977). In this situation, exocytosis into the confined spaces between cells would be expected to yield high local concentrations of α_2-macroglobulin that might be of importance specifically because diffusion of α_2-macroglobulin from the plasma into these spaces

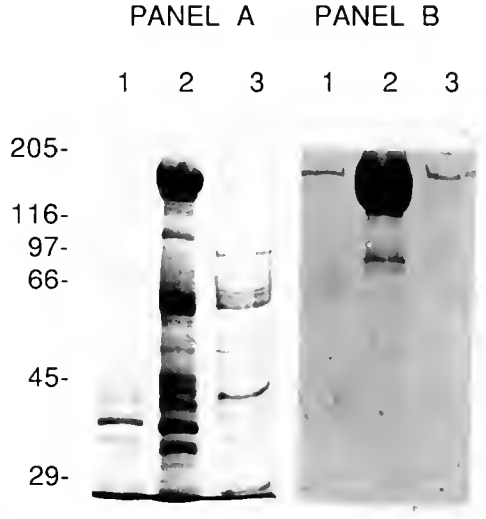

Figure 4. Demonstration of α_2-macroglobulin in preparations of *Limulus* amebocyte lysate. Lanes A.1 and B.1 show a secondary extract, lanes A.2 and B.2 show a primary extract, and lanes A.3 and B.3 show the materials released from live cells exposed to A23187. Lanes A.1 and B.1 contain 18 μg of protein, lanes A.2 and B.2 contain 125 μg of protein, and lanes A.3 and B.3 contain 10 μl of released materials (45 μg of protein).

might be expected to be slow. By forming a temporary barrier between the septic external milieu and the internal tissues of the animal, the blood clot is a critical battleground between invading pathogens and the animal. The gradual release of α_2-macroglobulin as cells of the clot degranulate may play an important role in defense during the early stages of wound healing. The mammalian blood platelet—a cell with homologous function to the *Limulus* amebocyte—also contains α_2-macroglobulin and other protease inhibitors in forms that are released by exocytosis (Nachman and Harpel, 1976; Plow and Collen, 1981). Like the *Limulus* amebocyte, the concentrations of protease inhibitors in platelets are small fractions of the total concentrations in whole blood (Nachman and Harpel, 1976; Plow and Collen, 1981).

The *Limulus* blood cells also release both acid-stable and acid-labile active site inhibitors of serine proteases during degranulation (Armstrong and Quigley, 1985; Nakamura *et al.*, 1987). The importance of α_2-macroglobulin in this situation may derive from its ability to bind such a wide selection of proteases. Although the spectrum of proteases that is susceptible to the active site inhibitors of the blood cells has not been established, most active site inhibitors are reactive only to a defined subclass of proteases, in contrast to the near universal reactivity of α_2-macroglobulin. Interestingly, the only protease that we have found to be unreactive to *Limulus* α_2-macroglobulin is the terminal protease in the blood clotting cascade (Armstrong *et al.*, 1984). In *Limulus*, both the clottable protein and the proteases involved in clotting are localized in the secretory granules of the blood cells and are released by exocytosis. It can be suggested that the unique resistance of the clotting protease to inactivation by α_2-macroglobulin is a physiological adaptation to the requirement that blood clotting can proceed in a milieu containing an abundance of α_2-macroglobulin. The active site inhibitors of the blood cells do inhibit this protease.

Acknowledgments

This research was supported by NIH Grants No. GM 35185 and CA22202 and the Medical Research Service of the Veterans Administration (RDIS 7446).

Literature Cited

Armstrong, P. B. 1985a. Adhesion and motility of the blood cells of *Limulus*. Pp. 77–128 in *Blood Cells of Marine Invertebrates*, W. D. Cohen, ed. Alan R. Liss, New York.

Armstrong, P. B. 1985b. Amebocytes of the American "horseshoe crab," *Limulus*. Pp. 253–258 in *Blood Cells of Marine Invertebrates*, W. D. Cohen, ed. Alan R. Liss, New York.

Armstrong, P. B., and J. P. Quigley. 1985. Proteinase inhibitory activity released from the horseshoe crab blood cell during exocytosis. *Biochim. Biophys. Acta* **827:** 453–459.

Armstrong, P. B., and J. P. Quigley. 1987. *Limulus* α_2-macroglobulin. First evidence in an invertebrate for a protein containing an internal thiol ester bond. *Biochem. J.* **248:** 703–707.

Armstrong, P. B., and F. R. Rickles. 1982. Endotoxin-induced degranulation of the *Limulus* amebocyte. *Exp. Cell Res.* **140:** 15–24.

Armstrong, P. B., J. Levin, and J. P. Quigley. 1984. Role of endogenous proteinase inhibitors in the regulation of the blood clotting system of the horseshoe crab, *Limulus polyphemus*. *Thrombos. Haemostasis (Stuttgart)* **52:** 117–120.

Armstrong, P. B., M. T. Rossner, and J. P. Quigley. 1985. An α_2-macroglobulinlike activity in the blood of chelicerate and mandibulate arthropods. *J. Exp. Zool.* **236:** 1–9.

Bang, F. B. 1979. Ontogeny and phylogeny of response to Gram-negative endotoxins among the marine invertebrates. *Prog. Clin Biol. Res.* **29:** 109–123.

Barrett, A. J. 1981. α_2-Macroglobulin. *Meth. Enzymol.* **80:** 737–754.

Bursey, C. R. 1977. Histological response to injury in the horseshoe crab, *Limulus polyphemus*. *Can. J. Zool.* **55:** 1158–1165.

Coan, M. H., and R. C. Roberts. 1989. A redetermination of the concentration of α_2-macroglobulin in human plasma. *Biol. Chem. Hoppe-Seyler* **370:** 673–676.

Daino, M., A. Le Bivic, and M. Hirn. 1987. A method for the production of highly specific polyclonal antibodies. *Anal. Biochem.* **166:** 224–229.

Feinman, R. D. (ed.). 1983. *Chemistry and Biology of α_2-Macroglobulin.* Annals of the New York Academy of Sciences, vol. 421. New York Academy of Sciences, New York, NY.

Ganrot, P. O. 1966. Determination of α_2-macroglobulin as trypsin-protein esterase. *Clin. Chim. Acta* **14:** 493–501.

Harpel, P. C. 1987. Blood proteolytic enzyme inhibitors: their role in modulating blood coagulation and fibrinolytic enzyme pathways. Pp. 219–234 in *Hemostasis and Thrombosis. Basic Principles and Clinical Practice*, R. W. Colman, J. Hible, V. J. Marder, and E. W. Salz, eds. J. B., Lippincott Co., Philadelphia, PA.

Hergenhahn, H. -G., and K. Söderhäll. 1985. α_2-Macroglobulin-like activity in plasma of the crayfish *Pacifastacus lemusculus*. *Comp. Biochem. Physiol. B* **81:** 833–835.

Hergenhahn, H. -G., M. Hall, and K. Söderhäll. 1988. Purification and characterization of an α_2-macroglobulin-like proteinase inhibitor from plasma of the crayfish *Pacifastacus lemusculus*. *Biochem. J.* **255:** 801–806.

Laemmli, U. K. 1970. Cleavage of structural proteins during the assembly of the head of bacteriophage T4. *Nature* **227:** 680–685.

Laskowski, M., and I. Kato. 1980. Protein inhibitors of proteinases. *Ann. Rev. Biochem.* **49:** 593–626.

Levin, J. 1979. The reaction between bacterial endotoxin and amebocyte lysate. Pp. 131–146 in *Biomedical Applications of the Horseshoe Crab (Limulidae)*, E. Cohen, F. B. Bang, J. Levin, R. J. Marchalonis, T. G. Pistole, R. A. Prendergast, C. Schuster, and S. W. Watson, eds. A. R. Liss, New York.

Levin, J. 1985. The role of amebocytes in the blood coagulation mechanism of the horseshoe crab *Limulus polyphemus*. Pp. 145–163 in *Blood Cells of Marine Invertebrates*, W. D. Cohen, ed. Alan R. Liss, New York.

Levin, J., and F. B. Bang. 1968. Clottable protein in *Limulus*: its localization and kinetics of its coagulation by endotoxin. *Thrombos. Diathesis Haemorrh.* **19:** 186–197.

Loeb, L. 1920. The movements of the amoebocytes and the experimental production of amoebocyte (cell fibrin) tissue. *Wash. Univ. Studies* **8:** 3–79.

Mürer, E. H., J. Levin, and R. Holme. 1975. Isolation and studies of

the granules of the amebocytes of *Limulus polyphemus*, the horseshoe crab. *J. Cell. Physiol.* **86:** 533–542.

Nakamura, T., T. Hirai, F. Tokunaga, S. Kawabata, and L. Iwanaga. 1987. Purification and amino acid sequence of Kunitz-type protease inhibitor found in the hemocytes of the horseshoe crab (*Tachypleus tridentatus*). *J. Biochem.* **101:** 1297–1306.

Nachman, R. L., and P. C. Harpel. 1976. Platelet α_2-macroglobulin and α_1-antitrypsin. *J. Biol. Chem.* **251:** 4514–4521.

Plow, E. F., and D. Collen. 1981. The presence and release of α_2-antiplasmin from human platelets. *Blood* **58:** 1069–1074.

Quigley, J. P., and P. B. Armstrong. 1983. An endopeptidase inhibitor, similar to mammalian α_2-macroglobulin, detected in the hemolymph of an invertebrate, *Limulus polyphemus*. *J. Biol. Chem.* **258:** 7903–7906.

Quigley, J. P., and P. B. Armstrong. 1985. A homologue of α_2-macroglobulin purified from the hemolymph of the horseshoe crab *Limulus polyphemus*. *J. Biol. Chem.* **260:** 12,715–12,719.

Rickles, F. R., J. Levin, D. I. Rosenthal, and E. Atkins. 1979. Functional interaction of concanavalin A and bacterial endotoxin (lipopolysaccharide): effects on measurement of endogenous pyrogen release, human mononuclear cell tissue factor activation, lymphocyte DNA synthesis and gelation of *Limulus* amebocyte lysate. *J. Lab. Clin. Med.* **93:** 128–145.

Söderhäll, K., and V. J. Smith. 1983. Separation of the haemocyte populations of *Carcinus maenas* and other marine decapods, and prophenoloxidase distribution. *Dev. Comp. Immunol.* **7:** 229–239.

Sottrup-Jensen, L. 1987. α_2-Macroglobulin and related thiol ester plasma proteins. Pp. 191–291 in *The Plasma Proteins, Structure, Function, and Genetic Control*, 2nd ed., Vol. 5, F. W. Putnam, ed. Academic Press, Orlando, FL.

Sottrup-Jensen, L. 1989. α_2-Macroglobulins: structure, shape and mechanism of proteinase complex formation. *J. Biol. Chem.* **264:** 11,539–11,542.

Spycher, S. E., S. Arya, D. E. Isenman, and R. H. Painter. 1987. A functional, thioester-containing α_2-macroglobulin homologue isolated from the hemolymph of the American lobster (*Homarus americanus*). *J. Biol. Chem.* **262:** 14,606–14,611.

Starkey, P. M., and A. J. Barrett. 1982. Evolution of α_2-macroglobulin. The demonstration in a variety of vertebrate species of a protein resembling human α_2-macroglobulin. *Biochem. J.* **205:** 91–95.

Towbin, H., T. Staehelin, and J. Gordin. 1979. Electrophoretic transfer of proteins from polyacrylamide gels to nitrocellulose sheets: procedure and some application. *Proc. Nat. Acad. Sci., USA* **76:** 4350.

Travis, J., and G. S. Salvesen. 1983. Human plasma proteinase inhibitors. *Annu. Rev. Biochem.* **52:** 655–709.

Van Leuven, F. 1984. Human α_2-macroglobulin. Primary amines and the mechanisms of endoprotease inhibition and receptor-mediated endocytosis. *Mol. Cell. Biochem.* **58:** 121–128.

Reference: *Biol. Bull.* **178:** 144–159. (April, 1990)

Ontogenetic Change in Digestive Enzyme Activity of Larval and Postlarval White Shrimp *Penaeus setiferus* (Crustacea, Decapoda, Penaeidae)

DONALD L. LOVETT* AND DARRYL L. FELDER

Department of Biology and Center for Crustacean Research, University of Southwestern Louisiana, Lafayette, Louisiana 70504

Abstract. Whole specimens of developmental stages of *Penaeus setiferus* (Linnaeus, 1767) were homogenized and assayed for activities of digestive enzymes. In all developmental stages, activities were present for trypsin, carboxypeptidase A and B, amylase, and non-specific esterase; none for pepsin or lipase were detected. Activities assayed with substrates for chymotrypsin and aminopeptidase are not apparently due to the presence of these enzymes in the gut. Peak activities for all enzymes occurred during late zoeal or early mysis larval stages; low activities occurred at metamorphosis. During postlarval development, amylase activity increased steadily (by a tenfold increase over five weeks), whereas most other enzyme activities were relatively constant until the fifth week of postlarval development. Although it alters enzyme activity, diet does not appear to be the primary effector of ontogenetic change in digestive enzyme activity. Instead, ontogenetic change in digestive enzyme activity may reflect either a developmentally cued change in enzyme synthesis, or a secondary effect of change in the function and relative size of the midgut during its differentiation.

Introduction

Most previous studies of digestive enzymes in penaeid shrimp (Appendix 1) and other decapod crustaceans have been restricted to adult specimens; interactions between changes in gut morphology, diet, and digestive enzyme activity during early stages of the life cycle are incompletely understood. Penaeid shrimp are ideal crustacean models with which to examine sequential changes in gut structure and function during ontogeny. This is because the ontogeny of these animals is unique among decapod crustaceans: all larval stages are free swimming, rather than embryonated, and transformations to adult morphology and habit are protracted over several weeks, rather than occurring as abrupt transformations in the decapodid stage (PL_1) or in the stages that immediately precede or follow it (Pérez-Pérez and Ros, 1975; Wickins, 1976; Felder *et al.*, 1985; Lovett and Felder, 1989).

After hatching, penaeid larvae pass through five nonfeeding naupliar stages (N_1–N_5), three protozoeal stages (Z_1–Z_3), and three mysis stages (M_1–M_3) before they metamorphose into the decapodid. Within the first two weeks of post-metamorphic life, postlarvae migrate to inshore brackish nursery grounds, adopt a benthic existence, and exhibit a change in feeding habits (Flint, 1956; Pérez-Farfante, 1969; Sastrakusumah, 1970; Jones, 1973; Gleason and Zimmerman, 1984; Gleason, 1986). Experience from aquaculture has shown that this phase of development (PL_1–PL_{14}) represents a "critical period" during which high rates of mortality are encountered (Wickins, 1976; Bages and Sloane, 1981). We hypothesize that this critical period coincides with a change-over in digestive enzyme activity that accommodates the change in habit, so that the shrimp can efficiently digest and assimilate a new diet.

Changes in digestive enzyme activity during development have been studied in relatively few decapod species [*Palaemon serratus:* Van Wormhoudt (1973), Ceccaldi and Trellu (1975), and Van Wormhoudt and Sellos (1980); *Homarus americanus:* Biesiot (1986); and *Penaeus japonicus:* Laubier-Bonichon *et al.* (1977), Gal-

Received 15 May 1989; accepted 22 January 1990.

* Present address: Department of Biology, Lake Forest College, Lake Forest, Illinois 60045.

gani (1983), and Galgani and Benyamin (1985)]. In most of these cases, assays were conducted for only amylase and general protease activity, and studies were limited to early developmental stages through the decapodid. In the present study, activities for a spectrum of digestive enzymes in *Penaeus setiferus* from early larval stages through the fifth week of postmetamorphic development was measured. These data are evaluated to determine: (1) whether ontogenetic change in digestive enzyme activity is protracted into the postlarval stages (as would be predicted from protracted development of gut morphology); (2) whether ontogenetic change in digestive enzyme activity may reflect ontogenetic change in diet; and (3) whether change in digestive enzyme activity may in part explain occurrence of the "critical period" in development.

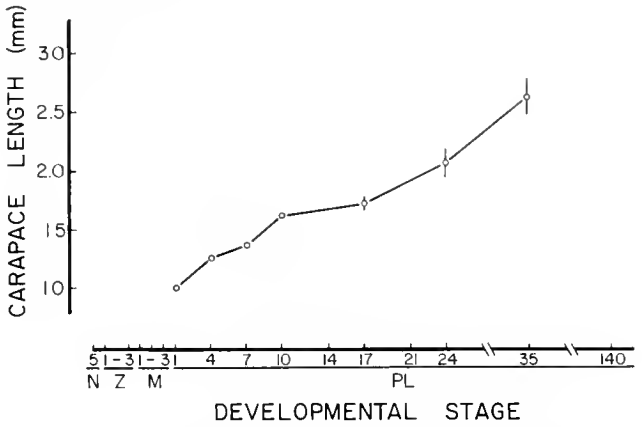

Figure 1. Average carapace length (excluding rostrum) for postlarval stages of *Penaeus setiferus* used in enzyme assays. Error bars indicate 95% confidence interval about mean carapace length of each developmental stage (n = 30). Average carapace length of PL_{140} was 3.42 ± 0.18 mm (n = 15). N, nauplis stage 5; Z, protozoeal stages 1–3; M, mysis stages 1–3; PL, age of postlarvae in days.

Materials and Methods

Specimens examined

Larvae of *Penaeus setiferus* (Linnaeus, 1767) were reared in the laboratory in cylindrical containers (120 l) of natural seawater at 28°C and maintained on a 12:12 light:dark cycle. At stage PL_5 (see Fig. 1 for corresponding carapace length of this and later stages), all shrimp were transferred to plastic tanks (diameter, 1.5 m) filled to 0.1 m depth with continuously aerated seawater. Sand or other natural substrate was not provided. Brood stock was obtained seaward of Freeport, Texas, during July 1986, and spawned within 48 h of capture. Larvae were reared on a diet of algae (*Isochrysis, Chaetocerus,* and *Tetraselmis*) and 24-h *Artemia* nauplii (Aquacop, 1983; McVey and Fox, 1983). Beginning with PL_5, the diet consisted entirely of *Artemia* nauplii (Great Salt Lake Brand®, Sanders Brine Shrimp Co., Ogden, Utah).

Larval stage was identified in accord with descriptions by McVey and Fox (1983). Postlarval stages were identified by postmetamorphic age, as is the practice in culture of penaeid shrimp. Specimens were isolated in a brass sieve of appropriate mesh size, blotted dry, weighed, and placed in −70°C ultracold freezer until assays were conducted. Fresh samples were also assayed to monitor the effect of freezing on enzyme activity. Two separate spawns were examined; results from each spawn were not combined. To compare enzyme activities of early postlarval stages with those of juveniles, one brood was reared to PL_{140}. Individual juvenile shrimp were assayed as single samples. Samples of *Artemia* (but not algae) were also assayed.

Because diel rhythmicity in enzyme activity has been reported for adults of *Penaeus* (Van Wormhoudt *et al.*, 1972; Van Wormhoudt, 1973; Ceccaldi, 1981; Cuzon *et al.*, 1982; Maugle *et al.*, 1982b), samples for assays of all postlarval specimens, beginning with stage PL_4, were collected in mid-morning when peak enzyme activities reportedly occur. However, because duration of each larval stage is relatively short, samples of larvae and PL_1 were collected when 80% of the population had attained the desired stage, irrespective of time of day. Temperature, photoperiod, salinity, and time of day that food was presented were held constant to reduce variability in enzyme activity. Because ecdysis is not entirely synchronous and because it would not have been feasible to sort by molt stage the large number of specimens required for each sample, it was not possible to control stage in molt cycle.

To determine whether activity assayed in whole-animal homogenates came primarily from gut tissues or instead from enzymes in other tissues of the shrimp, the entire gut was dissected from specimens of juvenile shrimp. The remaining carcass was rinsed and blotted dry. The gut and carcass were frozen at −70°C and assayed independently.

Assays

Whole-animal homogenates were used in all assays. Samples were homogenized in 9 volumes of 0.05 *M* Tris (hydroxymethyl) aminomethane hydrochloride buffer, pH 7.8, with 0.011 *M* $CaCl_2$ in a Wheaton ground-glass tissue grinder. Homogenates were centrifuged at 4800 × *g* for 60 min at 4°C in accord with Lee's (1984) method. The supernatant, exclusive of the lipid layer, was collected and stored at 4°C until assayed. All enzyme assays were conducted within 20 h of homogenization.

Duplicate assays were conducted for each sample, and the mean value was used in calculations. Total soluble protein was measured with the Peterson (1977) modification of the Lowry *et al.* (1951) method, but with human serum albumin as a standard (bovine serum albumin is subject to surface denaturation in dilute solutions).

Tryptic enzyme activity was assayed using two methods: 1.00 m*M* α-p-toluenesulphonyl-L-arginine methyl ester hydrochloride (TAME) at pH 8.1, 25°C by the method of Hummel (1959) as adapted by Rick (1974b), and 0.417 m*M* N-α-benzoyl-DL-arginine ρ-nitroanilide hydrochloride (BAPNA) at pH 8.2, 25°C, by the method of Erlanger *et al.* (1961). Because some inhibition of BAPNA hydrolysis was observed in early developmental stages, substrate concentration was reduced below that suggested by Erlanger *et al.*

Carboxypeptidase A was assayed with 0.35 m*M* hippuryl-L-phenylalanine at pH 7.6, 37°C, by the method of Folk and Schirmer (1963) as modified by Appel (1974). Carboxypeptidase B was assayed with 0.352 m*M* hippuryl-L-arginine at pH 7.6, 37°C, by the method of Folk *et al.* (1960) as modified by Appel (1974).

Chymotryptic-like esterase activity was assayed with 0.342 m*M* N-benzoyl-L-tyrosine ethyl ester (BTEE) at 25°C, pH 7.8, by the method of Rick (1974a). Assays of either fresh or frozen specimens with glutaryl-L-phenylalanine-ρ-nitroanilide (GPANA) by the method of Erlanger *et al.* (1964) did not yield activity that differed significantly from controls.

Arylamidase ("aminopeptidase") activity was assayed with 0.7 m*M* L-leucine-ρ-nitroanilide (LPNA) at pH 7.8, 25°C, by the method of Binkley and Torres (1960) as modified by Appel (1974). To determine whether this activity was membrane-associated in *P. setiferus*, both homogenate with buffer and homogenate with 1% Triton-X 100 were centrifuged at 100,000 × *g* for 1 h. Total activity was not significantly different in the two resulting supernatants or in the original homogenate. No activity was found in resuspended pellets. Assays with L-leucinamide hydrochloride, by the method of Binkley and Torres (1960), or with L-leucyl-β-naphthylamide hydrochloride, by the method of Burstone and Folk (1956), did not yield activities significantly different from controls.

Non-specific esterase and lipase activities were measured with three separate substrates at pH 7.4 by the method of Nachlas and Seligman (1949): 0.4603 m*M* β-naphthyl acetate (C_2) at 25°C for 20 min, 0.2625 m*M* β-naphthyl laurate (C_{12}) at 37°C for 60 min, and 0.2088 m*M* β-naphthyl stearate (C_{18}) at 37°C for 180 min. Cholinesterase activity was inhibited by addition of 10^{-5} *M* eserine to substrate solution. Activity was determined from a standard curve of β-naphthol absorbance. Although a titrimetric technique with tributyrin may be a preferred method for assay of lipase activity (Desnuelle, 1972), limited sample volume precluded application of such a method in the present study. Assay of lipase activity with the copper method of Schmidt *et al.* (1974) did not yield activity significantly different from controls.

Amylase activity was assayed with two separate substrates at pH 6.9 with 0.01 *M* NaCl, 25°C: 1.0% purified potato starch solution (4.634 mg/ml in reaction mixture) and 0.66% purified oyster glycogen (3.059 mg/ml) (obtained from Sigma Chemical Co., St. Louis, Missouri). Maltose released by hydrolysis of substrate was measured by reaction with dinitrosalicylic acid reagent by the method of Bernfeld (1955) as modified by Rick and Stegbauer (1974). Activity was determined from a standard curve of D (+) maltose absorbance. To exclude activity due to disaccharidases in the homogenate, a separate assay was conducted in which maltose was the substrate; this disaccharidase activity (which was very low) was subtracted from total activity measured in amylase assays.

Peptic activity was measured with N-acetyl-L-phenylalanine-L-3,5-di-iodotyrosine by the method of Rick and Fritsch (1974). Activity did not differ significantly from controls.

Amylase/protease ratio

The ratio of amylase activity to protease activity (A/P ratio), frequently used to characterize digestive capability (for example, Laubier-Bonichon *et al.*, 1977; Lee *et al.*, 1980; Van Wormhoudt *et al.*, 1980), was estimated from the ratio of amylase activity (starch as substrate) to trypsin activity (BAPNA as substrate). Because trypsin accounts for 40–50% of the proteolytic activity in adult penaeids (Galgani, 1983; Galgani *et al.*, 1984), we feel justified in substituting activity of this enzyme for total protease activity in the calculation.

Estimation of activity in hepatopancreas

While digestive enzyme activity is often determined as activity per mg soluble protein in the hepatopancreas, isolation of the hepatopancreas from larvae and small postlarvae is impractical. Therefore, the ratio of hepatopancreas volume to total body volume was used to estimate enzyme activity per gram wet weight of hepatopancreas. The ratio of hepatopancreas density to density of non-gut tissue, and the ratio of lipid content to protein content of tissues, were assumed to be similar in all developmental stages. For each developmental stage, the hepatopancreas and total body volume were estimated from reconstructed serial sections (8 μm) of formalin-fixed, paraffin-embedded specimens. The area of each section was measured, and the volume was calculated by

Table I

Effect of freezing on digestive enzyme activities in homogenates of Penaeus setiferus

Enzyme (Substrate)	Ratio of frozen to fresh activity (range)
Trypsin (BAPNA)	1.03 (0.91–1.18)
Carboxypeptidase A	0.63* (0.53–0.68)
Carboxypeptidase B	1.47* (1.10–1.54)
Esterase (β-naphthol acetate)	2.27* (1.67–3.57)
Esterase (β-naphthol laurate)	2.04* (1.67–2.17)
Amylase (starch)	0.81 (0.69–1.02)

Effect expressed as ratio of specific activity of enzyme in previously frozen samples to specific activity in fresh samples. Values reported are averages of ratio calculated for all developmental stages compared. Assays for trypsin (TAME), non-specific esterase (β-naphthol stearate), and amylase (glycogen) were not conducted for fresh specimens.

* = Indicates that difference in activity between frozen and fresh samples was significantly different ($P < 0.05$) within respective developmental stages.

summing frusta. The average ratio, of soluble protein content of hepatopancreas to soluble protein content of the carcass in juveniles (5.43), was used to estimate enzyme activity per mg protein in the hepatopancreas. Protein content of tissues was assumed to be constant across all developmental stages, and all measured activity was assumed to have come from the hepatopancreas.

Results

None of the enzymes were inactivated completely by freezing, although carboxypeptidase A activity was diminished significantly ($P < 0.05$) (Table I). Carboxypeptidase B and non-specific esterase activities were significantly higher ($P < 0.05$) in frozen than in fresh specimens. Ratio of the activity in frozen specimens to that in fresh specimens was similar for each enzyme for all larval and postlarval stages. Furthermore, enzyme activity in samples frozen for 48 hours was not significantly different ($P < 0.05$) from activity in samples frozen for 6 months.

Most chymotryptic-like esterase activity, and a substantial proportion of arylamidase activity, came from non-gut tissues (Table II). There also was a small amount of activity for trypsin (with BAPNA as substrate) and non-specific esterase (with β-naphthol acetate as substrate) in non-gut tissues. For all other enzyme assays (including the trypsin assay with TAME as substrate), activity measured in whole-animal homogenates can be attributed largely to gut tissue. In addition, enzyme activities in *Artemia* nauplii (Table III) were always sufficiently low to exclude the possibility that a substantial proportion of enzyme activity measured in *P. setiferus* originated from ingested *Artemia*.

Because total protein per gram wet weight influences specific enzyme activity, it was important to determine whether ontogenetic change in soluble protein content of whole-animal homogenates occurred. In fact, relative protein content remained essentially constant through all developmental stages, except in the first two larval stages examined (Fig. 2). These two larval stages are highly setose and dense setae may have precluded removal of adherent water when samples were blotted dry.

Three general patterns of ontogenetic change in enzyme activity were observed: (1) proteases (Fig. 3)—activities are low in N_5, increase to a peak at Z_3, decrease to a low around PL_1, remain somewhat low until about PL_{17}, and thereafter increase slightly through the remainder of postlarval development; (2) esterases (Fig. 4)—activities are low in N_5, increase to a peak at Z_1, decrease to a low at M_3, and thereafter increase slightly or stabilize during the remainder of postlarval development; and (3) amylase (Fig. 5)—activity is relatively low in N_5, increases to a peak at M_2, decreases to a low at PL_1–PL_4, and thereafter increases markedly through the remainder of postlarval development. The pattern for esterases is similar to that of proteases, except that changes in esterase activity precede changes in protease activity by one stage. The A/P ratio (Fig. 6) is high in N_5 and M_2, but low at Z_3. An increase in the A/P ratio begins at PL_7 and continues until PL_{24}.

Significant ontogenetic decrease in the ratio of hepatopancreas volume to volume of the whole body occurs during larval and early postlarval development (Fig. 7). By about PL_7, this ratio reaches a low value and remains unchanged during the remainder of postlarval development; postlarval body size increases at a relatively constant rate throughout postlarval development (Fig. 1).

In the three patterns described above, enzyme activity is expressed as activity per mg soluble protein in the whole shrimp. When activity of enzymes in *P. setiferus* is corrected to reflect developmental change in the ratio of hepatopancreas volume to total body volume (see Materials and Methods) and is expressed as a function of soluble protein in the hepatopancreas (Fig. 8), patterns for ontogenetic change in enzyme activity differ considerably from those described above. Activities of proteases are low at N_5, and increase slightly to peaks in the middle stages of larval development. However, activities of these enzymes remain relatively constant during postlarval development until PL_{21}–PL_{28} and then increase at PL_{35}. Amylase activity is essentially constant (and low) during larval development, but after PL_4, activity increases steadily through development. Only in esterolytic enzymes is there a peak in activity at N_5. Activity decreases dramatically during the mysis stages, and increases only slightly during postlarval development.

Table II

Enzyme activity assayed separately in gut and non-gut tissues of Penaeus setiferus *juveniles*

Enzyme (substrate)	Activity (IU/g wet weight)			Activity (IU/mg protein)		
	Gut	Carcass	Ratio	Gut	Carcass	Ratio
Trypsin (BAPNA)	0.207 (±0.094)	0.023 (±0.038)	9.0	0.0527 (±0.0235)	0.0010 (±0.0017)	52.3
Trypsin (TAME)	29.7 (±12.2)	1.17 (±1.43)	25.4	7.53 (±2.31)	0.05 (±0.07)	150.6
Carboxypeptidase A	3.08 (±0.67)	0.13 (±0.055)	23.7	0.787 (±0.258)	0.006 (±0.003)	131.2
Carboxypeptidase B	5.90 (±1.76)	0.27 (±0.25)	21.8	1.504 (±0.498)	0.013 (±0.011)	115.7
Chymotryptic-like esterase	0.27 (±0.10)	3.95 (±4.15)	0.1	0.067 (±0.022)	0.184 (±0.216)	0.4
Arylamidase	0.204 (±0.205)	0.136 (±0.204)	1.5	0.0517 (±0.0488)	0.0064 (±0.0093)	8.0
Esterase (β-naphthol acetate)	0.188 (±0.052)	0.018 (±0.016)	10.4	0.0478 (±0.0072)	0.0007 (±0.0006)	68.3
Amylase (starch)	21.5 (±3.7)	0.5 (±0.6)	43.0	5.47 (±1.01)	0.02 (±0.03)	273.5

Ratio of activity in gut tissues to activity in remaining carcass indicated. Activity expressed both as International Units of activity per gram wet weight and International Units of activity per mg protein. Mean activity (±95% confidence limit) is indicated (n = 3).

Discussion

The ontogenetic decrease in specific activities of digestive enzymes at metamorphosis coincides with degeneration of the gut (from M_1–PL_4) in *Penaeus setiferus*. The subsequent increase in enzyme activities during postlarval development coincides with differentiation of the gut into the adult form. This increase represents both an increase in enzyme activities in hepatopancreatic tissues, and an allometric increase in the relative size of the hepatopancreas. Observed changes in enzyme activities during postlarval development are not the result of change in diet because diet was held constant during this period. Thus, the ontogenetic change in activities represents some other change associated with development.

Table III

Specific activities for digestive enzymes for 24-h Artemia *nauplii, obtained from whole-animal homogenates*

Enzyme (Substrate)	Specific activity (IU/mg protein)
Trypsin (BAPNA)	0.0055 ± 0.0012
Trypsin (TAME)	0.27 ± 0.08
Carboxypeptidase A	0.034 ± 0.013
Carboxypeptidase B	0.20 ± 0.02
Non-specific esterase (β-naphthol acetate)	0.023 ± 0.005
Non-specific esterase (β-naphthol laurate)	0.0016 ± 0.0002
Non-specific esterase (β-naphthol stearate)	0.00014 ± 0.00002
Amylase (starch)	0.100 ± 0.004
Amylase (glycogen)	0.038 ± 0.018

Activities expressed as International Units of activity per mg protein. Mean activity ± 95% confidence limit is indicated for three replicates.

Ontogenetic change in digestive enzyme activity

The ontogenetic patterns of enzyme activity found in *Penaeus setiferus* are similar to those described for other decapod species (Van Wormhoudt, 1973; Laubier-Bonichon *et al.*, 1977; Van Wormhoudt and Sellos, 1980; Galgani and Benyamin, 1985; Biesiot, 1986). In *P. setiferus*, *P. japonicus*, *Palaemon serratus*, and *Homarus americanus*, specific activities of both amylase and protease are low in those developmental stages preceding the first

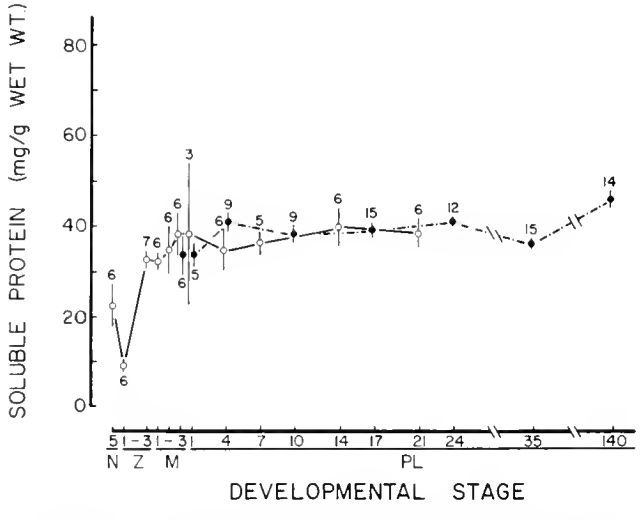

Figure 2. Soluble protein content in developmental stages of *Penaeus setiferus*, obtained from whole-animal homogenates. Solid *versus* broken lines indicate separate spawnings. Error bars indicate 95% confidence interval about mean value for each developmental stage. Sample size for each mean is indicated by numbers above or below bars. N, nauplis stage 5; Z, protozoeal stages 1–3; M, mysis stages 1–3; PL, age of postlarvae in days.

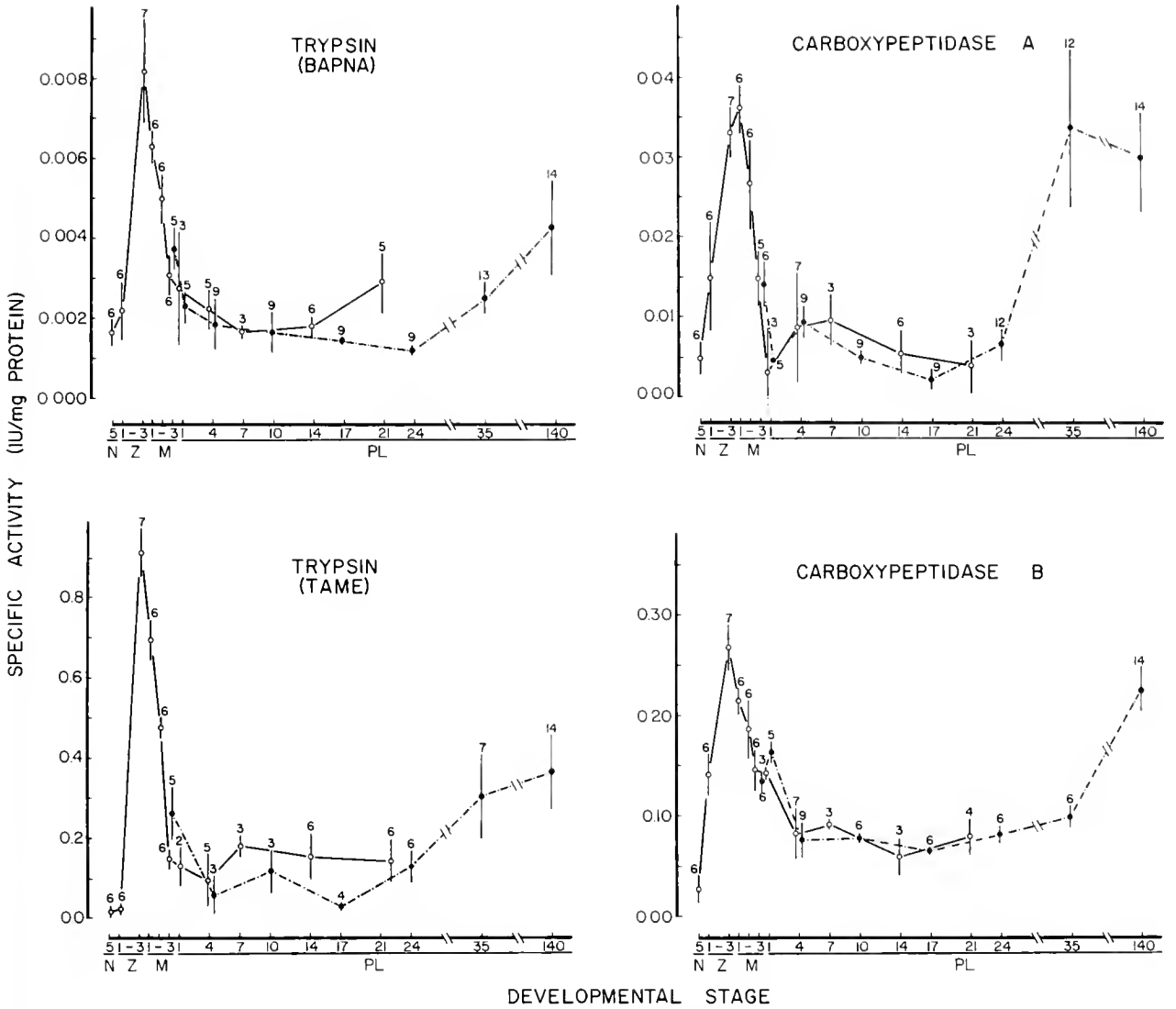

Figure 3. Specific activity of trypsin (with substrate indicated), carboxypeptidase A, and carboxypeptidase B for developmental stages of *Penaeus setiferus*, obtained from whole-animal homogenates. Activity expressed as International Units of activity per mg protein in entire animal. Solid *versus* broken lines indicate separate spawnings. Error bars indicate 95% confidence interval about mean activity for each developmental stage. Sample size for each mean is indicated by numbers above or below bars. N, nauplius stage 5; Z, protozoeal stages 1–3; M, mysis stages 1–3; PL, age of postlarvae in days.

feeding stage. Enzyme activities increase during early larval development in all four species. In *P. setiferus* and *P. japonicus*, amylase activity decreases to a low level by metamorphosis, but activity remains relatively constant in *P. serratus* and *H. americanus*. In all species, amylase activity increases during postlarval development. Protease activity in all four species decreases at metamorphosis. During early postlarval development, protease activity remains low in *Penaeus* spp., but increases in *P. serratus* and *H. americanus*. There is a peak in A/P ratio for *P. japonicus* at Z_3, but in *P. setiferus* the peak occurs at M_2; in both species the ratio declines to a low level at metamorphosis.

Ontogeny of gut. Increase in digestive enzyme activity has been correlated with differentiation of the gut in larvae of both teleosts (Buddington and Doroshov, 1986) and echinoderms (Vacquier *et al.*, 1971). In *P. setiferus*, the decrease in most enzyme activities immediately after metamorphosis coincides with degeneration of the anterior midgut caeca into the vestigial anterior midgut diverticulum (Lovett and Felder, 1989). Laubier-Bonichon *et al.* (1977) examined whole-animal concentra-

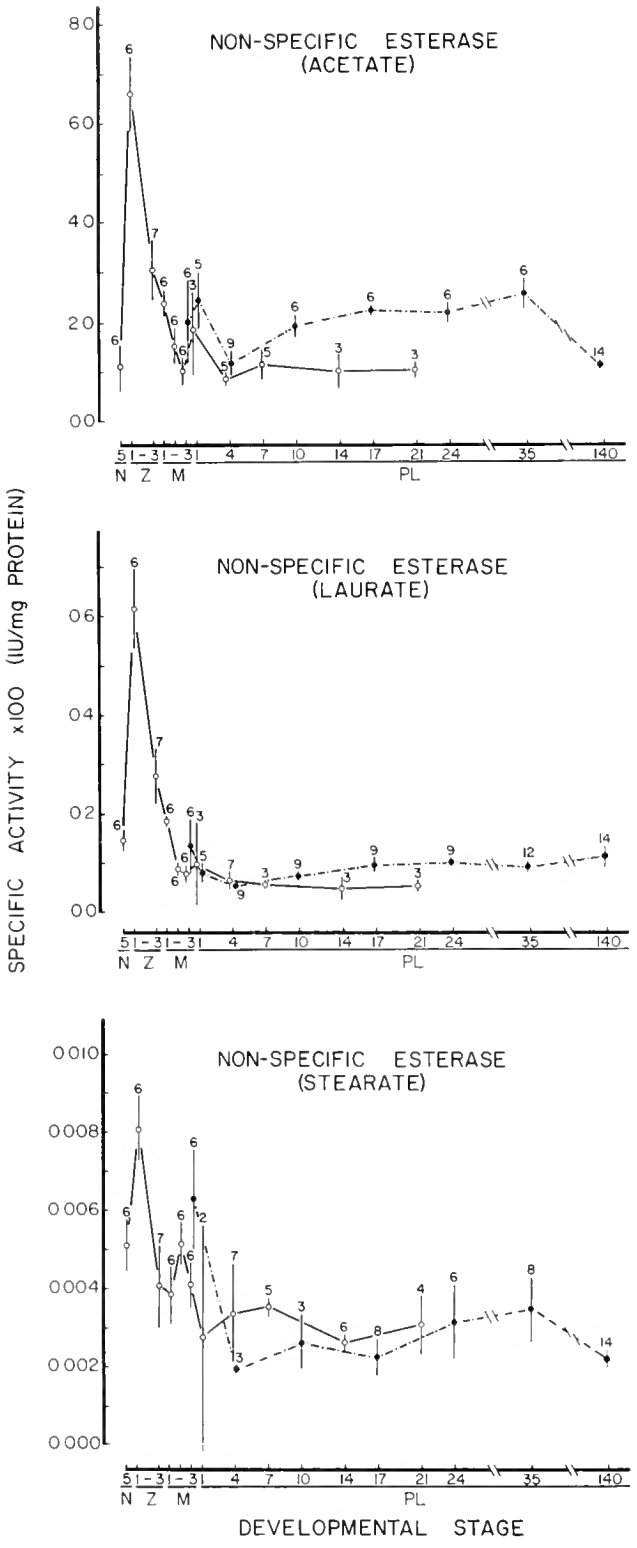

Figure 4. Specific activity of non-specific esterase (with fatty acid chain of β-naphthol substrate indicated) for developmental stages of *Penaeus setiferus*, obtained from whole-animal homogenates. Activity expressed as International Units of activity per mg protein in entire animal. Solid *versus* broken lines indicate separate spawnings. Error bars indicate 95% confidence interval about mean activity for each developmental stage. Sample size for each mean is indicated by numbers above or below bars. N, nauplius stage 5; Z, protozoeal stages 1–3; M, mysis stages 1–3; PL, age of postlarvae in days.

tions of RNA and DNA in *P. japonicus* and concluded that the rates of cell multiplication, cell hypertrophy, and cellular metabolic rate were at peak levels during larval development, but then dropped to low levels during the first week of postlarval life. Thus, reduced metabolic activity during the critical period may coincide with low digestive enzyme activity observed, and may reflect some accommodation to limited nutrient uptake during this transformational period of morphogenesis in the gut.

The increase in enzyme activities following the critical period in *P. setiferus* coincides with the ramification of lobes of the hepatopancreas into small-diameter tubules (Lovett and Felder, 1989). In *Palaemon serratus*, the increase in enzyme activity also coincides with an increase in the number of caeca in the hepatopancreas (Van Wormhoudt, 1973; Richard, 1974, thesis cited in Van Wormhoudt and Sellos, 1980), but unlike the situation in *P. setiferus*, the increase in number of caeca in *P. serratus* occurs during larval development. In *P. setiferus*, substantial increases in enzyme activities (particularly for trypsin, carboxypeptidase A, and amylase) occur during the fourth and fifth week of postlarval development and coincide with completion of differentiation by the hepatopancreas. Moreover, by this stage in development, the foregut has nearly attained the adult morphology and function, the posterior diverticulum has differentiated, and retention time of food in the gut has increased dramatically over that of early postlarval stages (Lovett and Felder, 1989, 1990). Thus, protraction in development of gut morphology of *P. setiferus* is reflected in the protraction of ontogenetic change in digestive enzyme activity.

Ontogeny of feeding habits. Ontogenetic change in enzyme activity can also be correlated with diet and feeding habit. In stage Z_1, larvae of *P. setiferus* begin to feed on algae; esterase activity is maximal. We provided *Artemia* nauplii beginning at stage M_1 (although larvae of *P. setiferus* will feed on *Artemia* beginning at stage Z_3); activities of trypsin and carboxypeptidase A and B in larvae are maximal at Z_3–M_1. Larvae shift from being primarily filter feeders to being primarily raptorial feeders at M_3, and filtering efficiency continues to decline during PL_1 (Emmerson, 1980, 1984); enzyme activities decline during M_3 and become very low at PL_1. The diet in wild populations is reported to change from predominately algae in early postlarval stages to include a more substantial portion of animal matter in later (PL_{28}–PL_{35}) postlarval stages (Flint, 1956; Fujinaga, 1969; Sastrakusu-

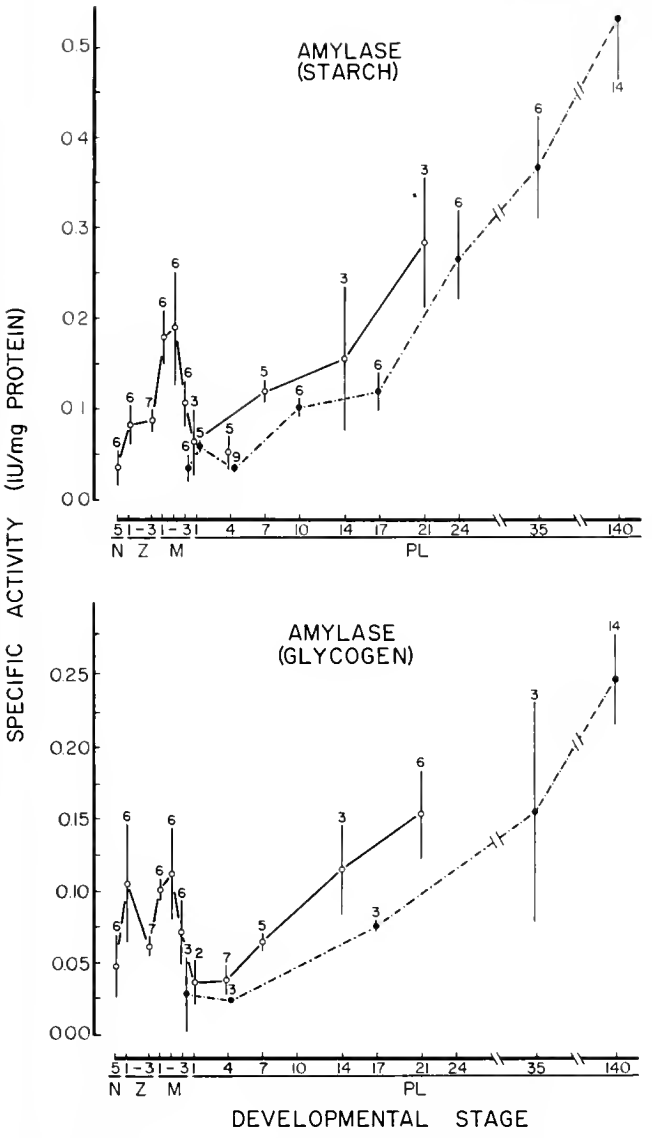

Figure 5. Specific activity of amylase (with substrate indicated) for developmental stages of *Penaeus setiferus*, obtained from whole-animal homogenates. Activity expressed as International Units of activity per mg protein in entire animal. Solid *versus* broken lines indicate separate spawnings. Error bars indicate 95% confidence interval about mean activity for each developmental stage. Sample size for each mean is indicated by numbers above or below bars. N, nauplius stage 5; Z, protozoeal stages 1–3; M, mysis stages 1–3; PL, age of postlarvae in days.

mah, 1970; Jones, 1973; Chong and Sasekumar, 1981; Nelson, 1981; Gleason and Zimmerman, 1984; but see also Kitting *et al.*, 1984; Gleason, 1986). In PL_{28}–PL_{35}, enzyme activity increases substantially.

Despite the correlation of ontogenetic change in enzyme activity with change in feeding habits, ontogenetic change in activity may be developmentally cued and may reflect temporal genetic regulation of enzyme synthesis, rather than a change in diet. For example, ontogenetic change of digestive enzyme activity in the first feeding stages of *Homarus* larvae occurs even in the absence of access to exogenous food substrates (Biesiot, 1986). In *Artemia*, ontogenetic change in enzyme synthesis is likely under genetic control, which then is modulated by diet and nutritional requirements (Samain *et al.*, 1980). Moreover, no consistent correlation of A/P ratio with composition of diet has been found within a single crustacean species (Hoyle, 1973; Boucher *et al.*, 1976; Samain *et al.*, 1980; Maugle *et al.*, 1982b; Båmstedt, 1984; Harris *et al.*, 1986). Because both amylase activity and the A/P ratio in *P. setiferus* increase during postlarval development, it might be inferred that postlarval shrimp become more herbivorous. However, beginning with PL_5, the diet consisted entirely of *Artemia*. Thus, change in enzyme activity in *P. setiferus* occurs without a change in diet.

Dietary implications

Even though we did not vary diet in the present study, we can infer that diet is not the only factor influencing enzyme activity. Attempts have been made to correlate digestive enzyme activity with diet and to use ontogenetic change in enzyme activity as an index of trophic state to estimate the phase in development where diet formulations for cultured shrimp need to be changed

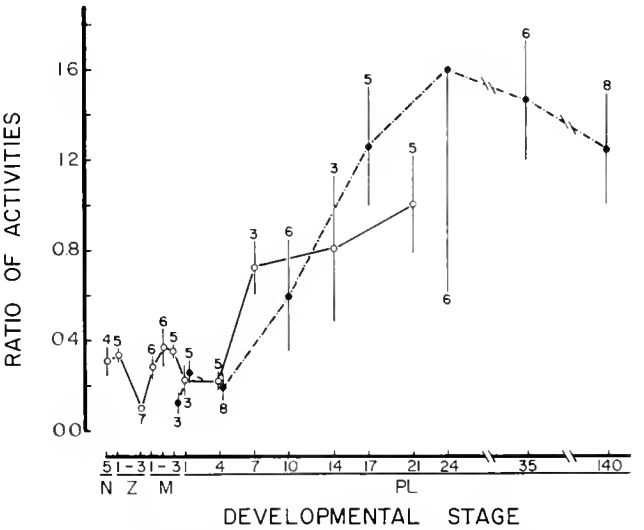

Figure 6. Ratio of amylase activity (starch used as substrate) to trypsin activity (BAPNA used as substrate), for developmental stages of *Penaeus setiferus*. Solid *versus* broken lines indicate separate spawnings. Error bars indicate 95% confidence interval about mean activity for each developmental stage. Sample size for each mean is indicated by numbers above or below bars. N, nauplius stage 5; Z, protozoeal stages 1–3; M, mysis stages 1–3; PL, age of postlarvae in days.

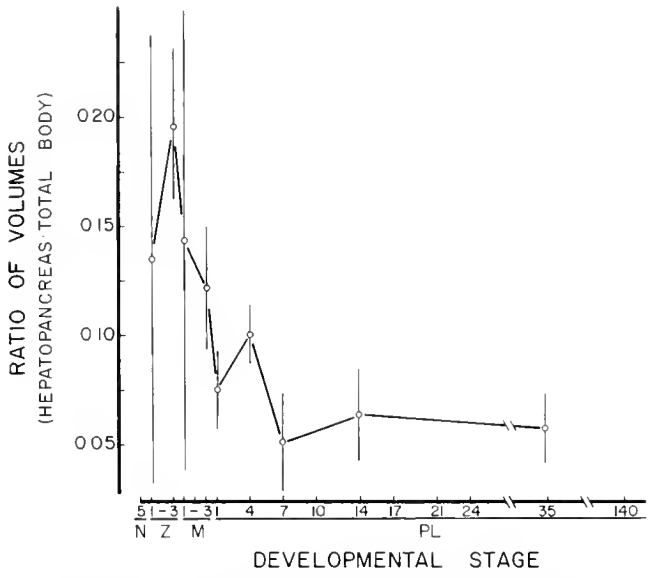

Figure 7. Ratio of volume of hepatopancreas (in early stages, volume of anterior midgut caeca plus lateral midgut caeca) to total body volume for developmental stages of *Penaeus setiferus*. Areas were measured on 8 μm serial sections of formalin-fixed, paraffin-embedded specimens. Volumes were calculated by summing frusta. Error bars indicate 95% confidence interval about mean ratio of volumes are indicated for each developmental stage (n = 3). N, nauplius stage 5; Z, protozoeal stages 1–3; M, mysis stages 1–3; PL, age of postlarvae in days.

(Hoyle, 1973; Van Wormhoudt, 1973; Laubier-Bonichon *et al.*, 1977; Cuzon *et al.*, 1980; Lee *et al.*, 1980, 1984; Van Wormhoudt *et al.*, 1980; Maugle *et al.*, 1982b; Galgani, 1983; Galgani *et al.*, 1984; Lee and Lawrence, 1985). Despite postlarval diet being held constant in the present study, a significant ontogenetic change occurred in digestive enzyme activity and in the A/P ratio. Therefore, we question the validity of using the A/P ratio to predict the degree to which an organism is carnivorous or herbivorous. In those larval stages of *Penaeus* with maximal amylase activity and A/P ratio, the diet is indeed composed of phytoplankton. However, the significance of high amylase activity here is not clear; very few groups of marine phytoplankton use starch as a storage product, and those storage products used most widely by marine phytoplankton are not hydrolyzed by amylase.

In contrast to the usual explanation for diet effects on enzyme activity, Harris *et al.* (1986) and Hofer (1982) propose that secretion of large amounts of enzyme may maximize the use of a scarce component in the diet. Such elevated enzyme activity could maximize hydrolysis and the resulting extraction of a dietary substrate that was present in small amounts. Thus, the substantial increase in amylase activity observed in *P. setiferus* during postlarval development may be a response to low levels of carbohydrate in the postlarval diet. A similar response to elimination of starch from the diet was observed by Hernandorena (1982) in *Artemia*. However, such a response is contrary to an assumption that is widely held among aquaculturists: *i.e.*, that enzyme activity is high for those substrates most common in the diet.

An additional problem associated with the use of enzyme activity to evaluate diet is that the stage of molt cycle, nutritional status of shrimp, season, sexual condition, and ontogenetic stage have been shown to affect size, histological condition, water content, and protein content of the hepatopancreas, (Cuzon *et al.*, 1980; Rosemark *et al.*, 1980; Van Wormhoudt *et al.*, 1980; Van Wormhoudt and Sellos, 1980; Storch *et al.*, 1982; Barclay *et al.*, 1983; Pascual *et al.*, 1983; Storch and Anger, 1983; Lee, 1984; Lee *et al.*, 1984; Storch *et al.*, 1984; Vogt *et al.*, 1985). Thus, the units selected to express enzyme activity (either activity per mg protein in hepatopancreas, activity per g wet weight of hepatopancreas, activity per mg protein in whole shrimp, or activity per g wet weight of shrimp) can affect whether significant change in digestive enzyme activity is reported (Cuzon *et al.*, 1980; Van Wormhoudt *et al.*, 1980; Barclay *et al.*, 1983; Lee, 1984; Lee *et al.*, 1984; present study). Little is known about the implications of using any one of these units to describe enzyme activity in shrimp.

Enzymes present in gut

Lack of specificity in assay substrates precludes conclusive identification of enzymes responsible for hydrolysis of substrates. For example, the substrates TAME and BAPNA are specific for trypsin only in the sense that they are not hydrolyzed by chymotrypsin (Hummel, 1959; Rick, 1974b). They can be hydrolyzed by both non-specific esterases and crustacean collagenase (Hess and Pearse, 1958; Pearse, 1972; Grant and Eisen, 1980; Grant *et al.*, 1983). The chymotrypsin-specific substrate BTEE also is subject to hydrolysis by both non-specific esterase and Type I crustacean collagenase, whereas GPANA is relatively resistant to hydrolysis by either of these enzymes (Eisen *et al.*, 1973; DeVillez, 1975). Chymoptryptic-like activity is not considered further in the present study because: (1) no activity was measured with GPANA, (2) most activity measured with BTEE occurred in non-gut tissues, and (3) conclusive evidence that crustaceans secrete chymotrypsin in quantities significant for digestion is lacking (DeVillez, 1975; Vonk and Western, 1984; Appendix 1). Both arylamidase and aminopeptidase are not considered further because: (1) no activity was found with either of the aminopeptidase substrates L-leucinamide or L-leucyl-β-naphthylamide as substrates, (2) activity measured with the substrate

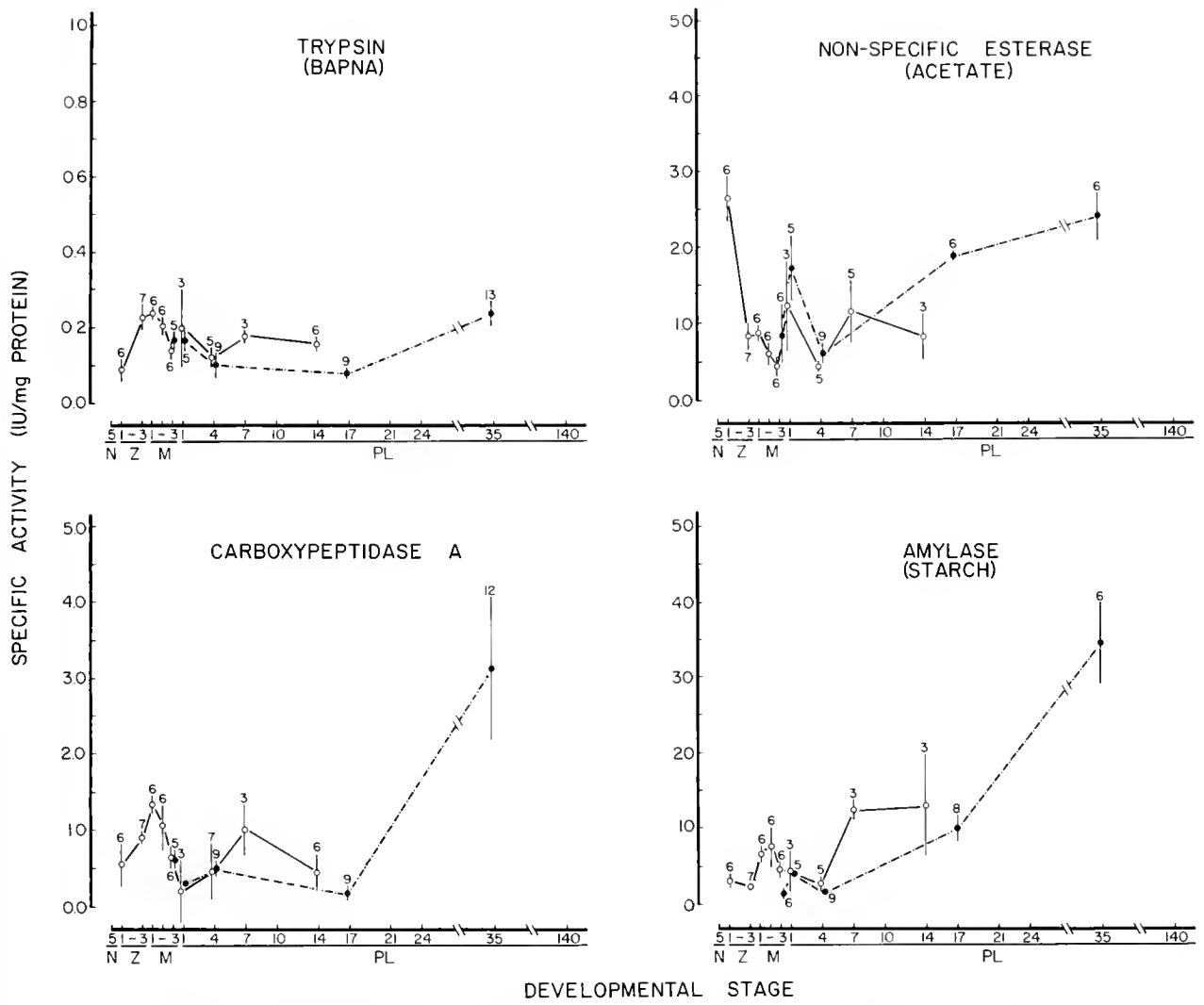

Figure 8. Specific activity of trypsin (BAPNA used as substrate), carboxypeptidase A, non-specific esterase (β-naphthyl acetate used as substrate) and amylase (starch used as substrate) corrected to International Units of activity per mg protein in hepatopancreas, for developmental stages of *Penaeus setiferus*. Concentration of soluble protein was determined for total body; correction to concentration of soluble protein in hepatopancreas was estimated from ratio of hepatopancreas volume to total body volume. Solid *versus* broken lines indicate separate spawnings. Error bars indicate 95% confidence interval about mean activity for each developmental stage. Sample size for each mean is indicated by numbers above or below bars. N, nauplius stage 5; Z, protozoeal stages 1–3; M, mysis stages 1–3; PL, age of postlarvae in days.

LPNA was not membrane-associated (as is aminopeptidase activity in other systems), and (3) substantial activity measured with LPNA came from non-gut tissue. Because there is considerable overlap in the substrates that each esterolytic enzyme can hydrolyze (Nachlas and Seligman, 1949), and because activity of homogenate in the present study decreased as chain length of fatty acid in the substrate increased, activity assayed with each of the three β-naphthol substrates appears to represent a single type of non-specific esterase; lipase activity appears to be absent.

Enzyme activity detected in tissue homogenates may not necessarily represent activity of enzymes that will be secreted into the digestive lumen. In crustaceans, activity for proteases, amylase, chitinase, chitobiase, and non-specific esterase has been found in tissues outside of the gut (Osuna *et al.*, 1977; Trellu and Ceccaldi, 1977; Mykles and Skinner, 1986; Mattson and Mykles, 1987; O'Brien and Skinner, 1987, 1988). Even though such enzymes would contribute to activity assayed in whole-animal homogenates, most enzyme activity detected in *Penaeus setiferus* was restricted to gut tissues. Some diges-

tive enzymes, particularly those associated with lysosomes, are involved in intracellular processes only (deDuve and Wattiaux, 1966). Furthermore, because there is no evidence to suggest that digestive enzymes in crustaceans are produced in a zymogen form (Gates and Travis, 1969; Zwilling *et al.*, 1969; Brockerhoff *et al.*, 1970; Eisen *et al.*, 1973; Zwilling and Neurath, 1981; Vonk and Western, 1984), enzymes that have been synthesized, but have not yet been secreted, also contribute to the enzyme activity measured in tissue homogenates. Nonetheless, intracellular concentration of digestive enzymes in *Palaemon* directly reflected luminal concentration of enzymes (Rodriguez *et al.*, 1976). Thus, activities assayed in the present study are probable indicators of relative enzyme activities in the lumen.

Acknowledgments

Thanks are extended to A. L. Lawrence and his staff, Texas A&M Shrimp Mariculture Project, for generous provision of *Penaeus setiferus* nauplii and algal cultures. S. C. Hand, University of Colorado, and E. J. DeVillez, Miami University of Ohio, provided valuable advice on enzyme assays. J. H. Spring, R. C. Brown, J. F. Jackson, B. E. Felgenhauer, K. R. Roberts, and J. L. Staton, University of Southwestern Louisiana, assisted our work in varied capacities. Primary funding was provided under research grant NA85AA-D-SG141 to D. L. Felder and D. L. Lovett from the Louisiana Sea Grant College Program. Additional funds were provided to D. L. Felder by research grants from the Louisiana Education Quality Support Fund, 86-USL(1)-126-07 and 86-LUM(1)-083-13, and from the Coypu Foundation. Louisiana Universities Marine Consortium (LUMCON) Marine Center and the USL Electron Microscopy Center provided valuable technical assistance to the project. This is contribution number 21 from the USL Center for Crustacean Research.

Literature Cited

Appel, W. 1974. Peptidases. Pp. 949–999 in *Methods in Enzymatic Analysis*, H. U. Bergmeyer, ed., Academic Press, New York.

Aquacop. 1983. Penaeid larval rearing in the Centre Océanologique du Pacifique. Pp. 123–127 in *CRC Handbook of Mariculture: Crustacean Aquaculture*, Vol. 1, J. P. McVey, ed. CRC Press, Inc., Boca Raton, Florida.

Bages, M., and L. Sloane. 1981. Effects of dietary protein and starch levels on growth and survival of *Penaeus monodon* (Fabricius) postlarvae. *Aquaculture* **25:** 117–128.

Båmstedt, U. 1984. Diel variations in the nutritional physiology of *Calanus glacialis* from latitude 78°N in the summer. *Mar. Biol.* **79:** 257–267.

Barclay, M. C., W. Dall, and D. M. Smith. 1983. Changes in lipid and protein during starvation and the moulting cycle in the tiger prawn, *Penaeus esculentus* Haswell. *J. Exp. Mar. Biol. Ecol.* **68:** 229–244.

Bernfeld, P. 1955. Amylases, A and B. Pp. 147–150 in *Methods in Enzymology*, Vol. 1, S. P. Colwick and N. O. Kaplan, eds. Academic Press, New York.

Biesiot, P. M. 1986. Changes in midgut gland morphology and digestive enzyme activities associated with development in early stages of the American Lobster. *Woods Hole Oceanogr. Inst. Publ.* WHOI-86-20:1–237.

Binkley, F., and C. Torres. 1960. Spectrophotometric assay of peptidase activity. *Arch. Biochem. Biophys.* **86:** 201–203.

Boucher, J., A. Laurec, J. F. Samain, and S. L. Smith. 1976. Étude de la nutrition, du régime et du rythme alimentaire du zooplancton dan les conditions naturelles, par la mesure des activités enzymatiques digestives. Pp. 85–110 in *Proceedings of the 10th Europ. Symposium on Marine Biology*, Vol. 2, G. Persoone and E. Japsers, eds. Universa Press, Wattern, Belgium.

Brockerhoff, H., R. J. Hoyle, and P. C. Hwang. 1970. Digestive enzymes of the American lobster (*Homarus americanus*). *J. Fish. Res. Board Can.* **27(8):** 1357–1370.

Buddington, R. K., and S. I. Doroshov. 1986. Development of digestive secretions in white sturgeon juveniles (*Acipenser transmontanus*). *Comp. Biochem. Physiol.* **83A:** 233–238.

Burstone, M. S., and J. E. Folk. 1956. Histochemical demonstration of aminopeptidase. *J. Histochem. Cytochem.* **4:** 217–226.

Ceccaldi, H. J. 1981. Problemes poses par les variations chronobiologiques de la physiologie des Crustacés. *Bull. Soc. Ecophysiol.* **6:** 87–95.

Ceccaldi, H. J., F. Galgani, Y. Benyamin, and A. Van Wormhoudt. 1983. Variations des activités digestives en fonction des facteurs du milieu chez les Crustacés. *Res. Comm. Bases Biol. Aquac. Montpellier* **83:** 30–31.

Ceccaldi, H. J., and J. Trellu. 1975. Apparation des activités enzymatiques digestives dans les oeufs de *Palaemon serratus* Pennant (Crustacé Decapodé) au cours de l'embryogenèse. *C. R. Soc. Biol. (Paris)* **169**(5): 1249–1255.

Chong, V. C., and A. Sasekumar. 1981. Food and feeding habits of the white prawn *Penaeus merguiensis*. *Mar. Ecol. Prog. Ser.* **5:** 185–191.

Cuzon, G., C. Cahu, J. F. Aldrin, J. L. Messager, G. Stephan, and M. Mevel. 1980. Starvation effect on metabolism of *Penaeus japonicus*. *Proc. World Maricult. Soc.* **11:** 410–423.

Cuzon, G., M. Hew, D. Cognie, and P. Soletchnick. 1982. Time lag effect of feeding on growth of juvenile shrimp, *Penaeus japonicus* Bate. *Aquaculture* **29:** 33–44.

deDuve, C., and R. Wattiaux. 1966. Functions of lysosomes. *Ann. Rev. Physiol.* **28:** 435–492.

Desnuelle, P. 1972. The Lipases. Pp. 575–616 in *The Enzymes*, Vol. 7, P. D. Boyer, ed. Academic Press, New York.

DeVillez, E. J. 1975. Current status concerning the properties of crustacean digestive proteinases. Pp. 195–201 in *Second International Symposium on Freshwater Crayfish*, J. W. Avault Jr. ed. Louisiana State University, Division of Continuing Education, Baton Rouge.

Eisen, A. Z., K. O. Henderson, J. J. Heffrey, and R. A. Bradshaw. 1973. A collagenolytic protease from the hepatopancreas of the fiddler crab, *Uca pugilator*. Purification and properties. *Biochemistry* **12:** 1814–1822.

Emmerson, W. D. 1980. Ingestion, growth and development of *Penaeus indicus* larvae as a function of *Thalassiosira weissflogii* cell concentration. *Mar. Biol.* **58(1):** 65–74.

Emmerson, W. D. 1984. Predation and energetics of *Penaeus indicus* (Decapoda: Penaeidae) larvae feeding on *Brachionus plicatilis* and *Artemia* nauplii. *Aquaculture* **38:** 201–209.

Erlanger, B. F., G. A. Cooper, and A. J. Bendich. 1964. On the heterogeneity of three-times-crystalized α-chymotrypsin. *Biochemistry* **3:** 1880–1883.

Erlanger, B. F., N. Kokowsky, and W. Cohen. 1961. The preparation

and properties of two new chromogenic substrates of trypsin. *Arch. Biochem. Biophys.* **95:** 271–278.

Felder, D. L., J. W. Martin, and J. W. Goy. 1985. Patterns in early postlarval development of decapods. Pp. 163–225 in *Crustacean Issues,* Vol. 2, *Larval Growth,* A. M. Wenner, ed. A. A. Balkema, Rotterdam.

Flint, L. H. 1956. Notes on the algal food of shrimp and oysters. *Proc. La. Acad. Sci.* **19:** 11–14.

Folk, J. E., K. A. Piez, W. R. Carroll, and J. A. Gladner. 1960. Carboxypeptidase B. IV. Purification and characterization of the porcine enzyme. *J. Biol. Chem.* **235:** 2272–2277.

Folk, J. E., and E. W. Schirmer. 1963. The porcine pancreatic carboxypeptidase A system. *J. Biol. Chem.* **238:** 3884–3894.

Fujinaga, M. 1969. Kuruma shrimp (*Penaeus japonicus*) cultivation in Japan. *FAO Fish. Rep.* **57:** 811–821.

Galgani, F. G. 1983. *Etude des Proteases Digestives de Crevettes Peneides (Crustacea, Decapoda)* These (3eme cycle. Oceanology). Fac. Sciences Luminy, Universite d'Aix-Marseille, Marseille, France. 125 pp.

Galgani, F. G., and Y. Benyamin. 1985. Radioimmunoassay of shrimp trypsin: application to the larval development of *Penaeus japonicus* Bate, 1888. *J. Exp. Mar. Biol. Ecol.* **87:** 145–151.

Galgani, F. G., Y. Benyamin, and H. J. Ceccaldi. 1984. Identification of digestive proteinases of *Penaeus kerathurus* (Forskål): a comparison with *Penaeus japonicus* Bate. *Comp. Biochem. Physiol.* **78B:** 355–361.

Galgani, F. G., Y. Benyamin, and A. Van Wormhoudt. 1985. Purification, properties, and immunoassay of trypsin from the shrimp *Penaeus japonicus. Comp. Biochem. Physiol.* **81B:** 447–452.

Gates, B. J. 1972. *Purification and Characterization of Carboxypeptidases from the Shrimp.* Ph.D. Thesis, University of Georgia. (Reference not seen; cited in Zwilling and Neurath, 1981).

Gates, B. J., and J. Travis. 1969. Isolation and comparative properties of shrimp trypsin. *Biochemistry* **8:** 4483–4489.

Gates, B. J., and J. Travis. 1973. Amino acid sequence in the vicinity of the reactive serine residue in shrimp trypsin. *Biochim. Biophys. Acta* **310:** 137–141.

Gleason, D. F. 1986. Utilization of salt marsh plants by postlarval brown shrimp: carbon assimilation rates and food preferences. *Mar. Ecol. Prog. Ser.* **31:** 151–158.

Gleason, D. F., and R. J. Zimmerman. 1984. Herbivory potential of postlarval brown shrimp associated with salt marshes. *J. Exp. Mar. Biol. Ecol.* **84:** 235–246.

Grant, G., and A. Eisen. 1980. Substrate specificity of the collagenolytic serine protease from *Uca pugilator.* Studies with noncollagenous substrates. *Biochemistry* **19:** 6089–6095.

Grant, G., J. Sacchettini, and H. Welgus. 1983. A collagenolytic serine protease with trypsin-like specificity from the fiddler crab, *Uca pugilator. Biochemistry* **22:** 354–358.

Harris, R. P., J. F. Samain, J. Moal, V. Martin-Jézéquel, and S. A. Poulet. 1986. Effects of algal diet on digestive enzyme activity in *Calanus helgolandicus. Mar. Biol.* **90:** 353–361.

Hernandorena, A. 1982. *Artemia* nutrition. Pp. 166–179 in *Proceedings of the Second International Conference on Aquaculture Nutrition: Biochemical and Physiological Approaches to Shellfish Nutrition,* G. D. Pruder, C. J. Langdon, and D. E. Conklin, eds. Louisiana State University, Division of Continuing Education, Baton Rouge.

Hess, R., and A. G. E. Pearse. 1958. The histochemistry of indoxylesterase of rat kidney with special reference to its cathepsin-like activity. *Br. J. Exp. Pathol.* **39:** 292–299.

Hofer, R. 1982. Protein digestion and proteolytic activity in the digestive tract of an omnivorous cyprinid. *Comp. Biochem. Physiol.* **72A:** 55–63.

Hoyle, R. J. 1973. Digestive enzyme secretion after dietary variation in the American lobster (*Homarus americanus*). *J. Fish. Res. Board Can.* **30:** 1647–1653.

Hummel, B. C. 1959. A modified spectrophotometric determination of chymotrypsin, trypsin, and thrombin. *Can. J. Biochem. Physiol.* **37(12):** 1393–1399.

Jones, R. R. Jr. 1973. *Utilization of Louisiana Estuarine Sediments as a Source of Nutrition for the Brown Shrimp* Penaeus aztecus. Ph.D. Dissertation. Louisiana State University, Baton Rouge. 130 pp.

Karunakaran, S. K., and K. P. Dhage. 1977. Amylase activity of the digestive tract of the prawns, *Penaeus indicus* and *Metapenaeus monoceros. Bull. Inst. Zool., Academia Sinica* **16:** 85–90.

Kitting, C. L., B. Fry, and M. D. Morgan. 1984. Detection of inconspicuous epiphytic algae supporting food webs in seagrass meadows. *Oecologia (Berlin)* **62:** 145–159.

Laubier-Bonichon, A., A. Van Wormhoudt, and D. Sellos. 1977. Croissance larvaire contrôleé de *Penaeus japonicus* Bate enzymes digestives et changements de régimes alimentaires. *Act. Coll. CNEXO* **4:** 131–145.

Lee, P. G. 1984. Digestive enzymes of penaeid shrimp: A descriptive and quantitative examination of the relationships of enzyme activity with growth, age and diet. Ph.D. Dissertation. Texas A&M University. 154 pp.

Lee, P. G., N. J. Blake, and G. E. Rodrick. 1980. A quantitative analysis of digestive enzymes for the freshwater prawn *Macrobrachium rosenbergii. Proc. World. Maricult. Soc.* **11:** 392–402.

Lee, P. G., and A. L. Lawrence. 1982. A quantitative analysis of digestive enzymes in penaeid shrimp, influences of diet, age and species. *Physiologist* **25:** 241.

Lee, P. G., and A. L. Lawrence. 1985. Effects of diet and size on growth, feed digestibility, and digestive enzyme activities of the marine shrimp, *Penaeus setiferus* Linnaeus. *J. World Maricult. Soc.* **16:** 275–287.

Lee, P. G., L. L. Smith, and A. L. Lawrence. 1984. Digestive proteases of *Penaeus vannamei* Boone: relationship between enzyme activity, size, and diet. *Aquaculture* **42:** 225–239.

Lovett, D. L., and D. L. Felder. 1989. Ontogeny of gut morphology in the white shrimp *Penaeus setiferus* (Decapoda, Penaeidae). *J. Morphol.* **201:** 253–272.

Lovett, D. L. and D. L. Felder. 1990. Ontogeny of kinematics in the gut of the white shrimp *Penaeus setiferus* (Decapoda, Penaeidae). *J. Crust. Biol.* **10:** 53–68.

Lowry, O. H., N. J. Rosenbrough, A. L. Farr, and R. J. Randall. 1951. Protein measurement with the Folin phenol reagent. *J. Biol. Chem.* **193:** 265–275.

Mattson, J., and D. L. Mykles. 1987. Degradation of myofibrillar proteins by calcium-dependent proteinases in lobster. *Am. Zool.* **27:** 81A.

Maugle, P. D., O. Deshimaru, T. Katayama, and K. L. Simpson. 1982a. Characteristics of amylase and protease of the shrimp *Penaeus japonicus. Bull. Jpn. Soc. Sci. Fish.* **48:** 1753–1757.

Maugle, P. D., O. Deshimaru, T. Katayama, and K. L. Simpson. 1982b. Effect of short necked clam diets on shrimp growth and digestive enzyme activities. *Bull. Jpn. Soc. Sci. Fish.* **48:** 1759–1764.

Maugle, P. D., O. Deshimaru, T. Katayama, and K. L. Simpson. 1983. The use of amylase supplements in shrimp diets. *J. World Maricult. Soc.* **14:** 25–37.

McVey, J. P., and J. M. Fox. 1983. Hatchery techniques for penaeid shrimp utilized by Texas A&M-NMFS Galveston Laboratory Pro-

gram. Pp. 129–154 in *CRC Handbook of Mariculture Crustacean Aquaculture*, Vol. 1, CRC Press, Inc., Boca Raton, Florida.

Mykles, D. L., and D. M. Skinner. 1986. Four Ca^{2+}-dependent proteinase activities isolated from crustacean muscle differ in size, net charge, and sensitivity to Ca^{2+} and inhibitors. *J. Biol. Chem.* **261:** 9865–9871.

Nachlas, M. M., and A. M. Seligman. 1949. Evidence for the specificity of esterase and lipase by the use of three chromogenic substrates. *J. Biol. Chem.* **181:** 343–355.

Nelson, W. G. 1981. Experimental studies of decapod and fish predation on seagrass macrobenthos. *Mar. Ecol. Prog. Ser.* **5:** 141–149.

O'Brien, J. J., and D. M. Skinner. 1987. Characterization of enzymes that degrade crab exoskeleton: I. Two alkaline cysteine proteinase activities. *J. Exp. Zool.* **243:** 389–400.

O'Brien, J. J., and D. M. Skinner. 1988. Characterization of enzymes that degrade crab exoskeleton: II. Two acid proteinase activities. *J. Exp. Zool.* **246:** 124–131.

Osuna, C., A. Olalla, A. Sillero, M. A. G. Sillero, and J. Sebastián. 1977. Induction of multiple proteases during the early larval development of *Artemia salina*. *Dev. Biol.* **61:** 94–103.

Pascual, F. P., R. M. Coloso, and C. T. Tamse. 1983. Survival and some histological changes in *Penaeus monodon* Fabricius juveniles fed various carbohydrates. *Aquaculture* **31:** 169–180.

Pearse, A. G. E. 1972. *Histochemistry Theoretical and Applied* Vol. 2. Williams and Wilkins Co., Baltimore. 1518 pp.

Pérez-Farfante, I. 1969. Western Atlantic shrimps of the genus *Penaeus*. *Fish. Bull.* **67:** 461–591.

Pérez Pérez, D., and R. M. Ros. 1975. Descripcion y desarrollo de los estadios postlarvales del camaron blanco *Penaeus schmitti* Burkenroad. *Ciencias, Serie 8, Centro de Investigaciones Marinas, Universidad de la Habana*. No. 21. 114 pp.

Peterson, G. L. 1977. A simplification of the protein assay method of Lowry *et al.* which is more generally applicable. *Anal. Biochem.* **83:** 346–356.

Richard, P. 1974. Contribution à l'étude du développement larvaire et de l'organogénèse chez *Palaemon serratus* et du métabolisme des acides aminés libres chez cette espèce et chez *Penaeus kerathurus*. Thèse 3c cycle, Océanogr. Biol., Aix-Marseille, 140 pp. (Reference not seen; cited in Van Wormhoudt and Sellos, 1980).

Rick, W. 1974a. Chymotrypsin. Pp. 1006–1012 in *Methods in Enzymatic Analysis*, H. U. Bergmeyer, ed. Academic Press, New York.

Rick, W. 1974b. Trypsin. Pp. 1013–1024 in *Methods in Enzymatic Analysis*, H. U. Bergmeyer, ed. Academic Press, New York.

Rick, W., and W. P. Fritsch. 1974. Pepsin. Pp. 1046–1055 in *Methods in Enzymatic Analysis*, H. U. Bergmeyer, ed. Academic Press, New York.

Rick, W., and H. P. Steghauer. 1974. Alpha-Amylase. Pp. 885–903 in *Methods in Enzymatic Analysis*, H. U. Bergmeyer, ed. Academic Press, New York.

Rodriguez, D., A. Van Wormhoudt, and Y. Le Gal. 1976. Separation, properties, localization, and nycthemeral variations of DNAse, a phosphodiesterase, a RNAse and an alkaline phosphatase from the hepatopancreas of *Palaemon serratus* (Crustacea Natantia). *Comp. Biochem. Physiol.* **54B:** 181–191.

Rosemark, R., P. R. Bowser, and N. Baum. 1980. Histological observations of the hepatopancreas in juvenile lobsters subjected to dietary stress. *Proc. World Mariculr. Soc.* **11:** 471–478.

Samain, J. F., J. Moal, J. Y. Daniel, J. R. Le Coz, and M. Jezequel. 1980. The digestive enzymes amylase and trypsin during the development of *Artemia*. Pp. 239–255 in *The Brine Shrimp Artemia*, Vol. 2. *Physiology, Biochemistry, and Molecular Biology*, G. Persoone, P. Sorgeloos, O. Roels, and E. Jaspers, eds. Universa Press, Wetteren, Belgium.

Sastrakusumah, S. 1970. A study of the food of juvenile migrating pink shrimp, *Penaeus duorarum* Burkenroad. *Fla. Sea Grant Tech. Bull.* **9:** 1–31.

Schmidt, F. H., H. Stork, K. von Dahl. 1974. Lipase. Pp. 819–823 in *Methods in Enzymatic Analysis*, H. U. Bergmeyer, ed. Academic Press, New York.

Storch, V., and K. Anger. 1983. Influence of starvation and feeding on the hepatopancreas of larval *Hyas araneus* (Decapoda, Majidae). *Helgol. Meeresunters.* **36:** 67–75.

Storch, V., H. H. Janssen, and E. Cases. 1982. The effects of starvation on the hepatopancreas of the coconut crab, *Birgus latro* (L.) (Crustacea, Decapoda). *Zool. Anz.* **208:** 115–123.

Storch, V., J. V. Juario, and F. P. Pascual. 1984. Early effects of nutritional stress on the liver of milkfish, *Chanos chanos* (Forskal), and on the hepatopancreas of the tiger prawn, *Penaeus monodon*. *Aquaculture* **36:** 229–236.

Trellu, J. 1978. Étude de diverses enzymes de Crustacés marins suivant le régime alimentaire, le développement, les chocs thermiques et l'éclairement: application à la'aquaculture et aux effets des rejets thermique en mer. Thèse de Doeteur Ingenier, Université d'Aux-Marseille, Marseille, France. 216 pp. (Reference not seen, cited in Lee et al., 1984).

Trellu, J., and H. J. Ceccaldi. 1977. Circadian variations of some enzymatic activities in *Palaemon squilla* Linné (Crustacea, Decapoda). *J. Interdiscp. Cycle Res.* **8:** 357–359.

Tsai, I. H., K. L. Chuang, and J. L. Chuang. 1986. Chymotrypsins in digestive tracts of crustacean decapods (shrimps). *Comp. Biochem. Physiol.* **85:** 235–240.

Vacquier, V. D., L. J. Korn, and D. Epel. 1971. The appearance of α-amylase activity during gut differentiation in sand dollar plutei. *Dev. Biol.* **26:** 393–399.

Van Wormhoudt, A. 1973. Variations des protéases, des amylases, et des protéines soluble au curs du développement larvaire chez *Palaemon serratus*. *Mar. Biol.* **19:** 245–248.

Van Wormhoudt, A., H. J. Ceccaldi, and Y. Le Gal. 1972. Activité des protéases et amylases chez *Penaeus kerathurus* existence d'un rythme circadien. *C. R. Acad. Sci. (Paris) Ser. D.* **74:** 1208–1211.

Van Wormhoudt, A., H. J. Ceccaldi, and B. Martin. 1980. Adaptation de la teneur en enzymes digestives de l'hepatopancreas de *Palaemon serratus* (Crustacea, Decapoda), a la composition d'aliments experimentaux. *Aquaculture* **21:** 63–78.

Van Wormhoudt, A., and D. Sellos. 1980. Aspects biochemiques de la croissance: acides nucléiques et enzymes digestives chez *Palaemon serratus* (Crustacea Natantia). *Oceanol. Acta* **3**(1): 97–105.

Vogt, G., V. Storch, E. T. Quinitio, and F. P. Pascual. 1985. Midgut gland as monitor organ for the nutritional value of diets in *Penaeus monodon* (Decapoda). *Aquaculture* **48:** 1–12.

Vonk, H. J., and J. R. H. Western. 1984. *Comparative Biochemistry and Physiology of Enzymatic Digestion*. Academic Press, New York. 501 pp.

Wickins, J. F. 1976. Prawn biology and culture. *Ann. Rev. Oceanogr. Mar. Biol.* **14:** 435–507.

Yokoe, Y., and I. Yasumasu. 1964. The distribution of cellulase in invertebrates. *Comp. Biochem. Physiol.* **13:** 323–338.

Zwilling, R. H., and H. Neurath. 1981. Invertebrate proteases. *Methods Enzymol.* **80:** 633–664.

Zwilling, R., G. Pfleiderer, H. H. Sonneborn, V. Kraft, and I. Stucky 1969. The evolution of endopeptidases—V. Common anc different traits of bovine and crayfish trypsin. *Comp. Biochem. Physiol.* **28:** 1275–1287.

Appendix 1

Digestive enzymes for which presence or absence (+/−) of activity has been reported in Penaeus *spp. (Activity of general protease is not included)*

Enzyme	Species	Substrate*	Activity	Reference
Trypsin				
	P. setiferus	BAEE	+	Gates and Travis, 1969
		BAPNA	+	Lee, 1984; Lee and Lawrence, 1982, 1985; Lovett and Felder, present paper
		TAME	+	Lovett and Felder, present paper
	P. aztecus	BAPNA	+	Lee, 1984; Lee and Lawrence, 1982
	P. japonicus	BAPNA	+	Cuzon *et al.*, 1980; Galgani, 1983; Galgani *et al.*, 1984, 1985; Tsai *et al.*, 1986; Laubier-Bonichon *et al.*, 1977; Trellu, 1978
		TAME	+	Galgani, 1983; Galgani and Benyamin, 1985; Galgani *et al.*, 1984, 1985; Trellu, 1978
	P. kerathurus	BAPNA	+	Ceccaldi *et al.*, 1983; Galgani, 1983; Galgani *et al.*, 1984
		TAME	+	Galgani, 1983; Galgani and Benyamin, 1985; Galgani *et al.*, 1984; Van Wormhoudt *et al.*, 1972
	P. monodon	BAPNA	+	Galgani, 1983; Tsai *et al.*, 1986
		TAME	+	Galgani, 1983
	P. merguiensis	BAPNA	+	Galgani, 1983
		TAME	+	Galgani, 1983; Galgani and Benyamin, 1985
	P. occidentalis	BAPNA	+	Lee and Lawrence, 1982
	P. penicillatus	BAPNA	+	Tsai *et al.*, 1986
	P. stylirostris	BAPNA	+	Galgani, 1983; Lee and Lawrence, 1982
		TAME	+	Galgani, 1983; Galgani and Benyamin, 1985
	P. vannamei	BAPNA	+	Galgani, 1983; Lee, 1984; Lee and Lawrence, 1982; Lee *et al.*, 1984
		TAME	+	Galgani, 1983; Galgani and Benyamin, 1985
Carboxypeptidase A				
	P. setiferus	BZGPA	+	Gates and Travis, 1973; Lee, 1984; Lee and Lawrence, 1982, 1985; Lovett and Felder, present paper
	P. aztecus	BZGPA	+	Lee, 1984; Lee and Lawrence, 1982
	P. japonicus	FALPP	+	Tsai *et al.*, 1986
		HPLA	+	Galgani, 1983; Galgani *et al.*, 1984
	P. kerathurus	HPLA	+	Ceccaldi *et al.*, 1983; Galgani, 1983; Galgani *et al.*, 1984
	P. merguiensis	HPLA	+	Galgani, 1983
	P. monodon	FALPP	+	Tsai *et al.*, 1986
		HPLA	+	Galgani, 1983
	P. occidentalis	BZGPA	+	Lee and Lawrence, 1982
	P. penicillatus	FALPP	+	Tsai *et al.*, 1986
	P. stylirostris	BZGPA	+	Lee and Lawrence, 1982
		HPLA	+	Galgani, 1983
	P. vannamei	BZGPA	+	Lee, 1984; Lee and Lawrence, 1982
		HPLA	+	Galgani, 1983
Carboxypeptidase B				
	P. setiferus	BZGA	+	Gates and Travis, 1973; Lee, 1984; Lee and Lawrence, 1982, 1985; Lovett and Felder, present paper
	P. aztecus	BZGA	+	Lee, 1984; Lee and Lawrence, 1982
	P. japonicus	BZGA	+	Galgani, 1983; Galgani *et al.*, 1984; Tsai *et al.*, 1986
	P. kerathurus	BZGA	+	Ceccaldi *et al.*, 1983; Galgani, 1983; Galgani *et al.*, 1984
	P. merguiensis	BZGA	+	Galgani, 1983
	P. monodon	BZGA	+	Galgani, 1983; Tsai *et al.*, 1986
	P. occidentalis	BZGA	+	Lee and Lawrence, 1982
	P. penicillatus	BZGA	+	Tsai *et al.*, 1986

Appendix I (*Continued*)

Enzyme	Species	Substrate*	Activity	Reference
Carboxypeptidase B (*Continued*)				
	P. stylirostris	BZGA	+	Galgani, 1983; Lee and Lawrence, 1982
	P. vannamei	BZGA	+	Galgani, 1983; Lee, 1984; Lee and Lawrence, 1982; Lee *et al.*, 1984
Arylamidase (Aminopeptidase)				
	P. setiferus	LA	+	Lee, 1984
			−	Lovett and Felder, present paper
		LNA	−	Lovett and Felder, present paper
		LPNA	+	Lovett and Felder, present paper
	P. japonicus	LPNA	+	Galgani, 1983; Galgani *et al.*, 1984; Trellu, 1978
	P. kerathurus	LPNA	+	Ceccaldi *et al.*, 1983; Galgani, 1983; Galgani *et al.*, 1984
	P. merguiensis	LPNA	+	Galgani, 1983
	P. monodon	LPNA	+	Galgani, 1983
	P. stylirostris	LPNA	+	Galgani, 1983
	P. vannamei	LPNA	+	Galgani, 1983
Collagenase				
	P. kerathurus	collagen	+	Ceccaldi *et al.*, 1983; Galgani, 1983; Galgani *et al.*, 1984
Elastase				
	P. kerathurus	elastin		Galgani, 1983; Galgani *et al.*, 1984
Pepsin				
	P. setiferus	APAIT		Lee, 1984; Lee and Lawrence, 1985; Lovett and Felder, present paper
	P. aztecus	APAIT		Lee, 1984
	P. japonicus	APAIT		Maugle *et al.*, 1982a
	P. kerathurus	APAIT	−	Galgani, 1983
	P. vannamei	APAIT	−	Lee, 1984; Lee *et al.*, 1984
Low molecular weight protease				
	P. setiferus	?	+	Gates, 1972
		hemoglobin	−	Lee, 1984
	P. kerathurus	gelatin	+	Ceccaldi *et al.*, 1983; Galgani, 1983; Galgani *et al.*, 1984
"Chymotrypsin"				
	P. setiferus	BTEE	+	Lovett and Felder, present paper
		GPANA	−	Lee, 1984; Lee and Lawrence, 1982, 1985; Lee *et al.*, 1984; Lovett and Felder, present paper
	P. aztecus	GPANA	−	Lee, 1984; Lee and Lawrence, 1982
	P. japonicus	BPANA	−	Trellu, 1978
		BTEE	+	Galgani, 1983; Galgani *et al.*, 1984
		SAAPPNA	+	Tsai *et al.*, 1986
		SPNA	−	Galgani, 1983; Galgani *et al.*, 1984
	P. kerathurus	BTEE	+	Galgani, 1983; Galgani *et al.*, 1984; Van Wormhoudt *et al.*, 1972
		SPNA	+	Galgani, 1983; Galgani *et al.*, 1984
	P. merguiensis	BTEE, SPNA	+	Galgani, 1983
	P. monodon	BTEE	+	Galgani, 1983; Tsai *et al.*, 1986
		SAAPPNA	+	Tsai *et al.*, 1986
		SPNA	+	Galgani, 1983
	P. occidentalis	GPANA	−	Lee and Lawrence, 1982
	P. penicillatus	SAAPPNA	+	Tsai *et al.*, 1986
	P. stylirostris	BTEE, SPNA	+	Galgani, 1983
		GPANA	−	Lee and Lawrence, 1982; Lee *et al.*, 1984
	P. vannamei	BTEE	+	Galgani, 1983
		GPANA	−	Lee and Lawrence, 1982; Lee *et al.*, 1984
		SPNA	−	Galgani, 1983

Appendix 1 (*Continued*)

Enzyme	Species	Substrate*	Activity	Reference
Non-specific esterase				
	P. setiferus	α-naphthol	+	Lee, 1984; Lee and Lawrence, 1982
		β-naphthol	+	Lovett and Felder, present paper
	P. aztecus	α-naphthol	+	Lee, 1984; Lee and Lawrence, 1982
	P. occidentalis	α-naphthol	+	Lee and Lawrence, 1982
	P. stylirostris	α-naphthol	+	Lee and Lawrence, 1982
	P. vannamei	α-naphthol	+	Lee, 1984; Lee and Lawrence, 1982
Lipase				
	P. setiferus	olive oil	−	Lovett and Felder, present paper
		tributyrin	+	Lee, 1984; Lee and Lawrence, 1982
	P. aztecus	tributyrin	+	Lee, 1984; Lee and Lawrence, 1982
	P. occidentalis	tributyrin	+	Lee and Lawrence, 1982
	P. stylirostris	tributyrin	+	Lee and Lawrence, 1982
	P. vannamei	tributyrin	+	Lee, 1984; Lee and Lawrence, 1982
Amylase				
	P. setiferus	glycogen	+	Lovett and Felder, present paper
		starch	+	Lee, 1984; Lee and Lawrence, 1982, 1985; Lovett and Felder, present paper
	P. aztecus	starch	+	Lee, 1984; Lee and Lawrence, 1982
	P. indicus	starch	+	Karunakaran and Dhage, 1977
	P. japonicus	glycogen	+	Maugle *et al.*, 1982b, 1983
		starch	+	Cuzon *et al.*, 1980; Laubier-Bonichon *et al.*, 1977; Maugle *et al.*, 1982a, b
	P. kerathurus	starch	+	Van Wormhoudt *et al.*, 1972
	P. occidentalis	starch	+	Lee and Lawrence, 1982
	P. stylirostris	starch	+	Lee and Lawrence, 1982
	P. vannamei	starch	+	Lee, 1984; Lee and Lawrence, 1982
Chitinase				
	P. setiferus	chitin	+	Lee, 1984; Lee and Lawrence, 1985
	P. aztecus	chitin	+	Lee, 1984
	P. vannamei	chitin	+	Lee, 1984
Cellulase				
	P. japonicus	CMC	+	Yokoe and Yasumasu, 1964
Maltase				
	P. japonicus	maltose	+	Maugle *et al.*, 1982b
Sucrase				
	P. japonicus	sucrose	+	Maugle *et al.*, 1982b

* —α-naphthol, α-naphthol acetate; β-naphthol, β-naphthol acetate, laurate, or stearate; APAIT, N-acetyl-L-phenylalanine-L-3,5-di-iodotyrosine; BAEE, N-α-benzoyl arginine ethyl ester; BAPNA, N-α-benzoyl-DL-arginine *p*-nitroanilide·HCl; BPANA, N-benzoyl-DL-phenylalanine-2-naphthylamide; BTEE, N-benzoyl-L-tyrosine ethyl ester; BZGA, hippuryl-L-arginine; BZGPA, hippuryl-L-phenylalanine; CMC, sodium carboxylmethyl cellulose; FALPP, N-(2-furylacryloyl)-L-phenylalanine-phenylalanine; GPANA, gluaryl-L-phenylalanine*p*-nitroanilide; HPLA, hippuryl-L-phenyllactate; LA, L-leucinamide hydrochloride; LNA, L-leucyl-β-naphthylamide hydrochloride; LPNA, L-leucine-*p*-nitroanilide; SAAPPNA, succinyl-L-alanine-L-alanine-L-phenylalanine-L-phenylalanine; SPNA, succinyl-L-phenylalanine nitroanilide; TAME, α-*p*-toluenesulphonyl-L-arginine methyl ester hydrochloride.

Reference: *Biol. Bull.* **178**: 160–174. (April, 1990)

Ontogenetic Changes in Enzyme Distribution and Midgut Function in Developmental Stages of *Penaeus setiferus* (Crustacea, Decapoda, Penaeidae)

DONALD L. LOVETT* AND DARRYL L. FELDER

Department of Biology and Center for Crustacean Research, University of Southwestern Louisiana, Lafayette, Louisiana 70504

Abstract. Ultrastructure and histochemical distribution of enzymes were examined in the midgut of larval and postlarval stages of *Penaeus setiferus*. Acid phosphatase and esterase activities were present in all gut tissues at all stages. Protease activity was present in the anterior and lateral midgut caeca, as well as in the anterior portion of the midgut trunk (MGT) of larvae and early postlarvae (PL_1–PL_4). Amylase activity could not be detected histochemically in larvae or early postlarvae, even though it was detected in assays of whole-animal homogenates. In later postlarvae, both protease and amylase activities were present in the hepatopancreas and anterior MGT, but were absent from the anterior midgut diverticulum.

In larvae, alkaline phosphatase activity is present throughout the midgut, suggesting that absorption is widespread. In juveniles, activity is restricted to the hepatopancreas and regions of the MGT within the cephalothorax. The abdominal MGT (or "intestine") is no longer absorptive by the time the hepatopancreas has attained its adult form. Although epithelial cells of the MGT synthesize protein and produce electron-dense secretory vesicles, they are substantially different in ultrastructure from those cells in the hepatopancreas responsible for digestive enzyme synthesis and secretion.

Epithelial cells of the larval anterior and lateral midgut caeca are structurally and functionally similar to cells of the postlarval hepatopancreas. However, the lateral midgut caeca retain these features as they transform into the hepatopancreas, while the anterior midgut caeca lose these functions as they degenerate into the anterior diverticulum and change in ultrastructure during early postlarval development. The anterior and posterior midgut diverticula of postlarvae are similar ultrastructurally even though they differ in ontogenetic history.

Introduction

In crustaceans, the foregut and hindgut are chitin-lined, while the intervening midgut is uncuticularized. The midgut is thus the region in which cells are in contact with the lumen of the alimentary canal. It comprises a tubular portion, which we call the "midgut trunk" (MGT)[1], and the various outpocketings (diverticula and caeca) of this MGT (Lovett and Felder, 1989).

In adult penaeids, such as *Penaeus setiferus* (Linnaeus, 1767), outpocketings of the MGT include the complex hepatopancreas (= digestive caeca or midgut gland, by some authors), a single anterior midgut diverticulum at the junction of the foregut with the MGT, and the posterior midgut diverticulum at the junction of the MGT with the hindgut (Dall, 1967a). These adult structures arise, during ontogeny, by the progressive transformation of several larval structures: a pair of anterior caeca located at the foregut-MGT junction, and a pair of lateral caeca that arise slightly posteriad to the foregut-MGT junction. During late larval and early postlarval development, the two anterior caeca decrease in relative and actual size, fuse medially, and begin to form the single ante-

Received 4 October 1989; accepted 22 January 1990.

* Present address: Department of Biology, Lake Forest College, Lake Forest, Illinois 60045.

[1] The term "intestine" has usually been used to refer to this tubular region of the midgut. But we and others consider this to be a misapplication of vertebrate terminology and a practice to be discouraged (Dall and Moriarty, 1983; Lovett and Felder, 1989).

rior midgut diverticulum of the adult. At about the same time, the adult hepatopancreas is derived by ramification of the larval lateral midgut caeca. Finally, and in contrast, the adult posterior midgut diverticulum first makes its appearance during the third week of postlarval development. The ontogeny of the penaeid gut is described in detail elsewhere (Lovett and Felder, 1989, 1990a).

The ultrastructure and function of the crustacean midgut is only partly known, and most work has been done with adult specimens only. The adult hepatopancreas has been well-studied in *Penaeus* (Al-Mohanna *et al.*, 1985a, b; Vogt, 1985; Vogt *et al.*, 1985, 1986; Al-Mohanna and Nott, 1986; Caceci *et al.*, 1988) and in other decapod crustaceans (see Gibson and Barker, 1979; Dall and Moriarty, 1983), but relatively little attention has been given to other regions of the midgut.

Functions previously attributed to the crustacean MGT include: (1) absorption of nutrients from digested food (Yonge, 1924; Reddy, 1937; Speck and Urich, 1970; Talbot *et al.*, 1972; Ahearn, 1974; Quaglia *et al.*, 1976; Ahearn and Maginniss, 1977; Barker and Gibson, 1977, 1978; Brick and Ahearn, 1978; Gemmel, 1979); (2) absorption of ions and control of net water flux between the midgut lumen and the hemolymph (Yonge, 1924; Croghan, 1958; Green *et al.*, 1959; Gifford, 1962; Dall, 1965, 1967b; Geddes, 1975; Malley, 1977; Ahearn *et al.*, 1978; Mykles and Ahearn, 1978; Mykles, 1979, 1980, 1981; Ahearn, 1980, 1982, 1984; Wyban *et al.*, 1980); (3) excretion of ions (Green *et al.*, 1959; Gifford, 1962; Dall, 1967b, 1970); and (4) secretion of the peritrophic membrane (Georgi, 1969; Mykles, 1979; Johnson, 1980; Dall and Moriarty, 1983). Some of these functions, in particular the absorption of nutrients, have been assigned on the basis of an assumed analogy between the MGT and the vertebrate intestine.

The functions of the anterior and posterior midgut caeca and diverticula remain obscure; yet some proposals have been made: (1) both may increase surface area of the midgut for absorption of either water at ecdysis (Holliday *et al.*, 1980) or nutrients during digestion (Yonge, 1924; Reddy, 1937); (2) both may secrete digestive enzymes (Holliday *et al.*, 1980); (3) both may function in excretion (Dall, 1967b); (4) both may function in ion and water balance (Young, 1959; Heeg and Cannone, 1966; Dall, 1967b; Mykles, 1977, 1979); (5) both may secrete the peritrophic membrane (Pugh, 1962; Dall, 1967a; Georgi, 1969; Mykles, 1979); (6) both serve as sources of replacement cells (sites of cell regeneration) for the hepatopancreas and MGT (Davis and Burnett, 1964; Johnson, 1980); (7) the anterior diverticulum may accommodate volume change during contraction of the foregut (Powell, 1974); and (8) the anterior diverticulum may contribute essential components of digestive fluid that function in activation of proteolytic enzymes or pH change (Dall and Moriarty, 1983).

In most decapod crustaceans, the adult form of the gut appears immediately following metamorphosis (Felder *et al.*, 1985). However, in *Penaeus setiferus*, transformation of the gut to the adult form is protracted, taking place over several weeks after metamorphosis (Lovett and Felder, 1989, 1990a). Thus, this shrimp has enabled us to correlate the development of digestive function with that of structure. Toward that end, we have investigated the ontogenetic changes in the distribution of digestive enzymes in *Penaeus setiferus* and have compared those changes with simultaneous ontogenetic transformations in midgut ultrastructure, gross morphology, and movement.

Materials and Methods

Specimens examined

Larvae of *Penaeus setiferus* were reared in the laboratory with natural seawater (for details, see Lovett and Felder, 1990b) on a diet of algae (*Isochrysis* sp., *Chaetoceros gracilis*, and *Tetraselmis chuii*) and 24-h *Artemia* nauplii, by the method of McVey and Fox (1983). Beginning with PL_5 (the fifth day of postmetamorphic life), the diet consisted entirely of *Artemia* nauplii. Larval stages (protozoea and mysis) were identified in accord with descriptions by McVey and Fox (1983). Postlarval (PL_n) stages are identified by postmetamorphic age (where n = days beyond metamorphosis), as is the practice in culture of penaeid shrimp. "Juveniles" examined were at postlarval stage PL_{140}.

Histochemical localization of enzymes

Sample preparation. Because diel rhythmicity in enzyme activity has been reported for adults of *Penaeus* (Van Wormhoudt *et al.*, 1972; Cuzon *et al.*, 1982), all specimens were collected in mid-morning when peak enzyme activities reportedly occur. Food was available continually and the guts of all specimens were filled with food. Specimens were embedded in Tissue-Tek O.C.T. Compound® (Miles Scientific, Naperville, Illinois), quench frozen in liquid nitrogen, and stored until use at −70°C in an ultracold freezer. Serial sections were cut at 8 μm thickness with a Miles Cryostat II. All slides used in this study were coated with a chrome alum-gelatin subbing solution (Pappas, 1971). Sections were placed on cold (−25°C) slides (but see amylase and protease tests below) and then melted by placing a thumb on the underside of the slide. Slides were allowed to dry at room temperature before incubation. Control sections for alkaline phosphatase, acid phosphatase, and esterase tests were immersed in 90°C water for 5 min before incuba-

tion. After incubation, sections were counterstained with Mayer's haemalum; color was developed by dipping sections in Scott's solution (2% $MgSO_4$ with 0.2% $NaHCO_3$). Sections were mounted in glycerol gel.

Reconstruction of serial sections. Distribution of sites of enzyme activity within the midgut was determined by reconstruction of serial sections. To determine the abdominal segment within which sites of activity occurred, the product of total number of sections multiplied by 8 μm was compared with average total length and length of each abdominal segment for the respective developmental stage.

Non-specific esterase. Sections were incubated for 30 min at room temperature in a 0.01% solution of Naphthol AS-LC acetate by a method adapted from Burstone (1962): substrate solution was made by dissolving 5.0 mg Naphthol AS-LC acetate in 1.0 ml N,N-dimethylformamide. After the substrate had dissolved, 10 ml of ethylene glycol monomethyl ether was added, followed by 10 ml of 0.2 *M* Tris (hydroxymethyl) aminomethane hydrochloride buffer at pH 7.1. Immediately before incubation, 40 mg of Fast Garnet GBC dissolved in 29 ml of distilled water were filtered into the substrate solution. Cholinesterase activity was inhibited by adding 10^{-5}*M* eserine to the final substrate solution. Sites of esterase activity were indicated by deep violet precipitate.

While esterase activity was detected successfully with Naphthol AS-LC acetate as the substrate, neither esterase nor lipase activity was detected when several other substrates were used. When other substrates were used to incubate frozen sections and paraffin sections of fresh, formalin-fixed, acetone-fixed, and freeze dried specimens, the following results were obtained: The 5-bromoindoxyl acetate substrate by the method of either Barrnett and Seligman (1951) or Holt and Withers (1952) yielded a highly diffuse, faint blue precipitate that was unsuitable for study. Incubation of sections with Tween 20, 40, 60, or 80 substrates by the method of Gomori (1945, 1949) and with Tween 85 by the method of Bokdawala and George (1964), followed by demonstration of calcium soaps with either yellow ammonium sulfide or Alizarin Red S, yielded a diffuse precipitate that could not be differentiated from that obtained in control sections heated at 90°C for 5 min prior to incubation.

Alkaline phosphatase. Sections were incubated for 25 min at room temperature in a 0.02% solution of Naphthol AS-MX phosphate free acid with 0.06% Fast Red Violet LB salt at pH 8.5 by the method of Burstone (1962). Sites of alkaline phosphatase activity were indicated by magenta precipitate.

Acid phosphatase. After sections had dried on the slide, they were fixed in 4°C 10% neutral formalin for 30 s and washed for 3 min to localize the reaction. Sections were incubated for 30 min at 37°C in a 0.02% solution of Naphthol AS-BI phosphate with 0.06% Fast Red Violet LB salt at pH 5.2 using Burstone's (1958, 1962) method. Sites of acid phosphatase activity were indicated by a magenta precipitate.

Amylase. By a technique modified from that of Tremblay and Charest (1968), slides coated with chrome alum-gelatin subbing were dipped in a solution of 4% purified potato starch in 20 m*M* phosphate buffer pH 6.9 with 10 m*M* NaCl and dried at room temperature. The solution had been boiled, filtered, and degassed under vacuum prior to use. Frozen sections were placed on the starch substrate film of slides that were prechilled to −25°C. Sections were melted and air-dried at room temperature. Slides were then incubated at 37°C for 1–2 h in covered petri dishes lined with water-soaked filter paper. Slides were thereafter air-dried, immersed in a solution of 5:1:5 methanol:acetic acid:distilled water for 15 min, treated with Periodic Acid-Schiff's (PAS) by the method of McManus (1948), and air-dried again. Sites of amylase activity were indicated by clear areas where the starch film (now stained magenta) had been digested away.

Protease. Sections were incubated on the gelatin emulsion of Kodachrome-25™ color transparency film that had been previously exposed to daylight and developed commercially. By a technique adapted from Fratello (1968), sections were placed on emulsion prechilled to −25°C. Sections were then melted, air-dried at room temperature, incubated at 37°C for 1–2 h in petri dishes lined with water-soaked filter paper, and then dried again at room temperature. No buffer was added to control pH. Sites of protease activity were indicated by light blue-green or white areas where the darkly colored emulsion had been digested away.

Activity of specific proteolytic enzymes were not detected successfully. Sections were incubated with N-(α-benzoyl-DL-arginine-β-naphthylamide) hydrochloride in the method of Glenner and Cohen (1960) to detect trypsin-like activity and with both L-leucyl-β-naphthylamide by the methods of Burstone and Folk (1956) and Loizzi and Peterson (1971) and L-leucyl-4-methoxynaphthylamide hydrochloride by the method of Nachlas *et al.* (1960) to detect arylamidase (aminopeptidase) activity. Regardless of the method used for fixation and embedment, all preparations yielded results not different from controls.

Transmission electron microscopy

Specimens were fixed in cold (4°C) 4% glutaraldehyde solution buffered to pH 7.2 with 0.2 *M* phosphate buffer and postfixed with 2% buffered osmium tetroxide. Specimens were dehydrated in acetone, infiltrated by centrifugation at 2500 rpm (after Millonig, 1976), and embedded in Spurr's low viscosity resin (obtained from Polysci-

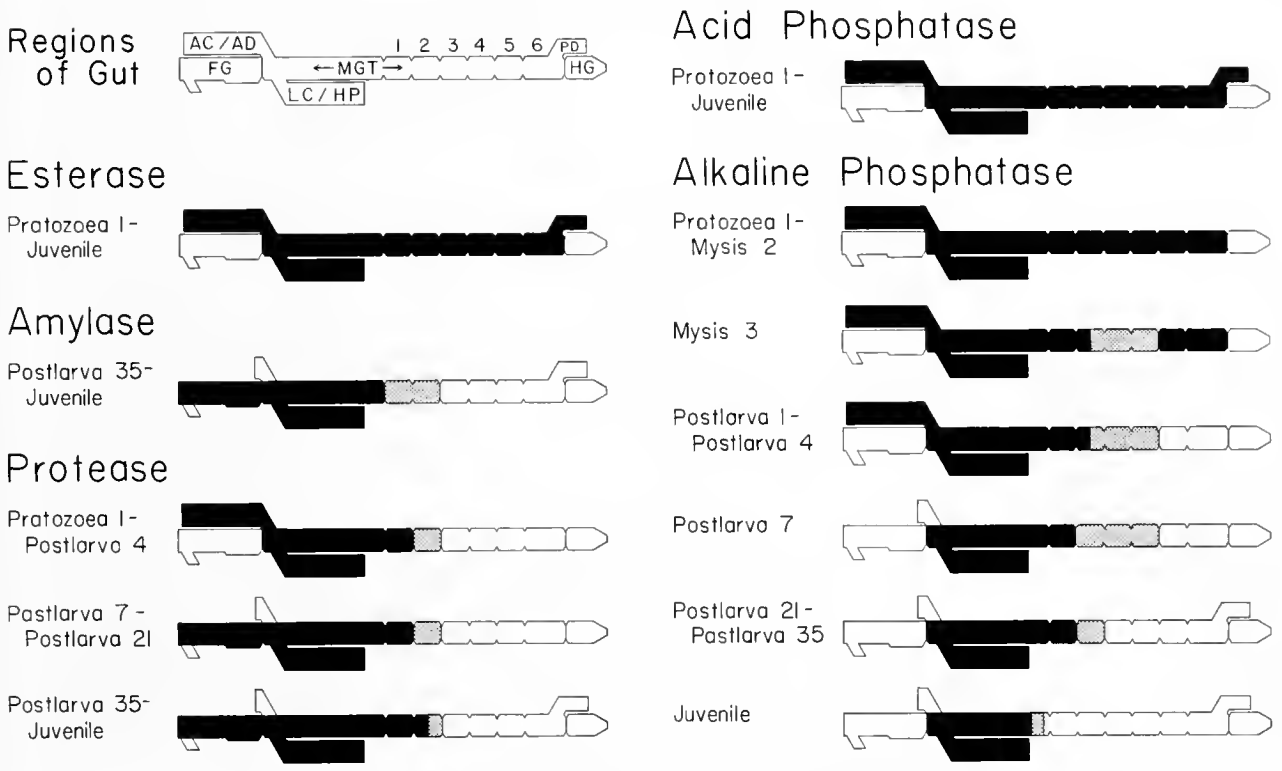

Figure 1. Diagrammatic representation of a lateral view of the gut in *Penaeus setiferus* illustrating distribution of enzymes during development. AC, anterior midgut caeca; AD, anterior midgut diverticulum; FG, foregut; HG, hindgut; HP, hepatopancreas; LC, lateral midgut caeca; MGT, midgut trunk (= "intestine"); PD, posterior midgut diverticulum. Abdominal segments 1–6 are numbered. Label to left indicates developmental stages included for each diagram. Solid black areas indicate regions of gut where presence of enzyme was detected in all specimens. Stippled areas indicate regions where enzyme was detected in some, but not all specimens.

ences, Inc., Warrington, Pennsylvania). Material was sectioned both with glass and diamond knives on a Sorval MT-5000. Ultrathin sections of 80–90 nm were stained with methanolic uranyl acetate and lead citrate and examined at 75 kV with an Hitachi H-600 transmission electron microscope.

Results

Ontogenetic change in enzyme distribution

Non-specific esterase. Esterase activity was found in all regions of the midgut in all stages examined (Figs. 1, 2b).

Amylase. No amylase activity was detected histochemically in developmental stages before PL_{35}. In late postlarval stages activity was found in the hepatopancreas, anterior portion of the MGT, and the lumen of the foregut (Fig. 1). Because of the nature of the test it could not be determined with certainty whether activity in the MGT was restricted to either the extraperitrophic or endoperitrophic lumen. No activity was found in the anterior diverticulum or in any areas of the gut posteriad to abdominal segment 2.

Protease. In all larval and postlarval stages, protease activity was found in the hepatopancreas and in the anterior region of the MGT (Fig. 1). Resolution was inadequate to differentiate intracellular activity from luminal activity. Furthermore, it could not be determined whether activity was restricted to either the extraperitrophic or the endoperitrophic lumen of the MGT. Activity was never found posteriad to abdominal segment 2. In larval and early postlarval stages (PL_1–PL_4), protease activity was found in the anterior midgut caeca, but not in the foregut. When the anterior caeca had degenerated into the anterior diverticulum, activity no longer was found in this caecal extension of the midgut, but activity then was found in the lumen of the foregut.

Acid phosphatase. Acid phosphatase activity was found in all regions of the midgut in all developmental stages (Figs. 1, 2d).

Alkaline phosphatase. Alkaline phosphatase activity was detected in the hepatopancreas and the anterior region of the MGT in all developmental stages (Figs. 1, 3d). However, distribution of alkaline phosphatase for the remaining regions of the midgut becomes limited during

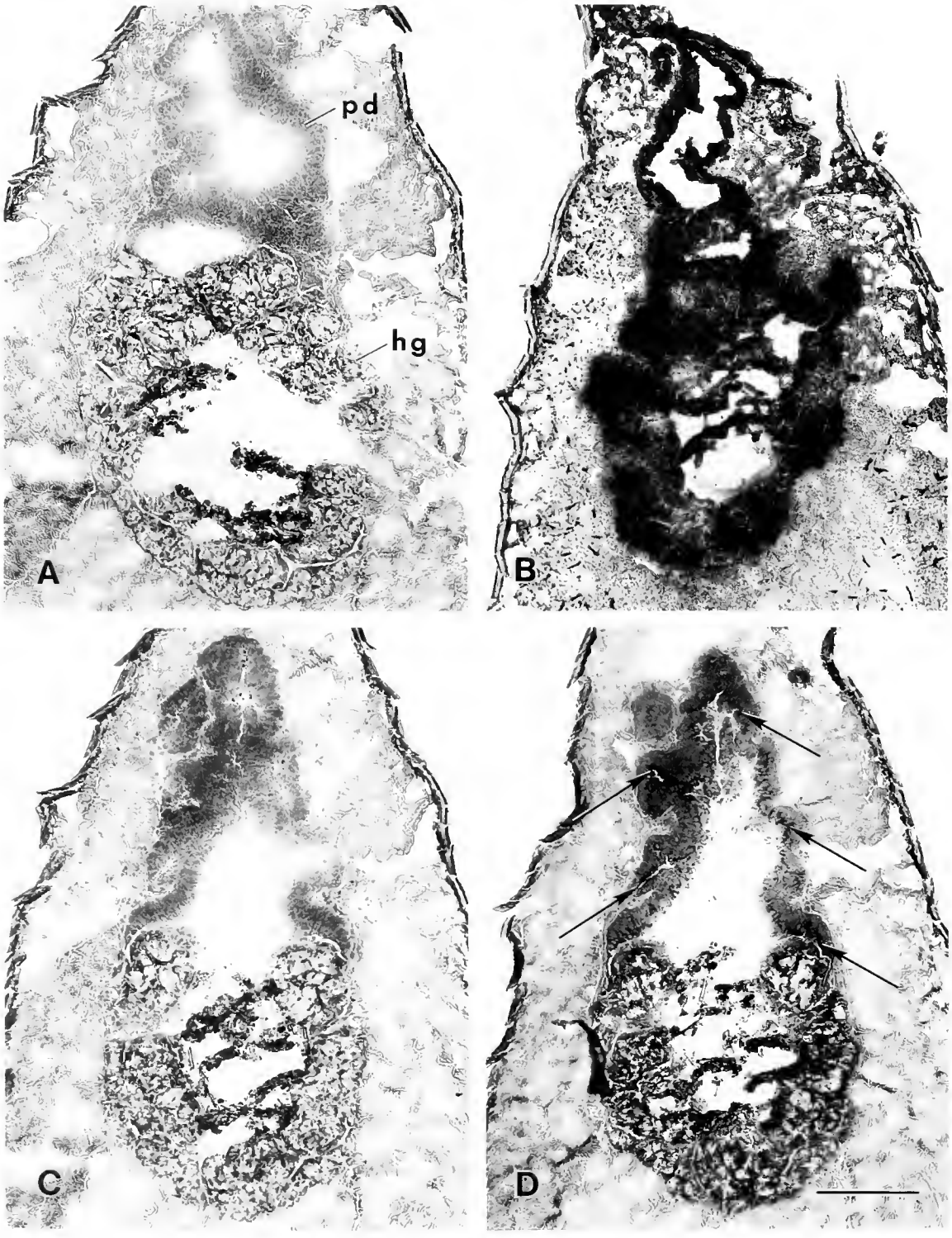

Figure 2. Histochemical localization of enzymes in fresh frozen transverse sections of posterior midgut diverticulum and hindgut in *Penaeus setiferus* juveniles (PL_{140}). A, control section. B, section incubated with Naphthol AS-LC acetate as substrate to indicate esterase activity. C, section incubated with Naphthol AS-BI as substrate to indicate alkaline phosphatase activity (no precipitate present). D, section incubated with Naphthol AS-MX phosphate as substrate to indicate acid phosphatase activity [in diverticulum, precipitate present (arrows) along apical surfaces of cells]. (hg, hindgut; pd, posterior midgut diverticulum). Scale bar indicates 150 μm for all figures.

development. For all larval and early postlarval stages, activity was found in the anterior midgut caeca (Fig. 3b). In PL_1 and PL_4, alkaline phosphatase activity was always more intense in the anterior caeca than in any other region of the midgut. However, no activity was detected in the anterior diverticulum of subsequent postlarval stages. Activity was found along the entire length of the MGT in larval stages Protozoea 1 through Mysis 2 (Fig. 3d, f). However, all specimens of Mysis 3 larvae had a short region in the MGT between the middle of abdominal segment 2 and the end of abdominal segment 4, in which no activity was found (Fig. 1); the exact location of this region varied from specimen to specimen. In PL_1 and PL_4, no activity could be demonstrated posteriad of abdominal segment 2 in some specimens, while in all specimens of these stages no activity was detected posteriad of abdominal segment 4. During development, the posterior limit of alkaline phosphatase activity progressed anteriad until, in the juvenile (PL_{140}), no activity was found in any portion of the abdominal MGT (Fig. 3h). Alkaline phosphatase activity was never demonstrated in the posterior midgut diverticulum (Fig. 2c).

Ontogenetic change in ultrastructure

In larval and early postlarval stages, the ultrastructure of cells of the anterior midgut caeca resembled that of cells of the lateral midgut caeca (Fig. 4a, b). However, the degeneration of the anterior caeca into the anterior diverticulum was accompanied by considerable change in the ultrastructure of the epithelial cells. The cells became elongate and no longer contained large vacuoles. In some cells, particularly in those ventral to the lumen of the diverticulum, the cytoplasm and all recognizable organelles became electron dense (Figs. 4c, 5a). Because adjacent cells varied in electron density (Fig. 5a, b), this density was not attributable to thick sections or overstaining.

Cells of the anterior diverticulum bore apical microvilli with a glycocalyx. Golgi bodies had swollen cisternae and produced secretory granules similar to those produced by the MGT. The lateral cell membranes were distinctly undulatory in nature. Where the epithelium of the anterior diverticulum tapered into the MGT, a mosaic of cell types was present (Fig. 5b). Epithelial cells of the posterior midgut diverticula (Fig. 5c) were similar in ultrastructure to those of the anterior diverticulum.

In all developmental stages of *Penaeus setiferus*, epithelial cells of the MGT had apical microvilli with a distinct glycocalyx (Fig. 6). Active Golgi produced electron-dense secretory vesicles, which accumulated in the apical cytoplasm. Cisternae of the smooth endoplasmic reticulum were often distended. Rough endoplasmic reticulum usually was dense and its membranes were arranged in parallel rows. Intracellular lipid droplets were found occasionally in cells of the MGT, within both the cephalothorax and first abdominal segment.

Discussion

In the early postlarval stages of *Penaeus setiferus*, both the anterior and lateral midgut caeca secrete digestive enzymes, and the entire midgut is absorptive. As the two anterior caeca degenerate into the single anterior diverticulum, there is tremendous change in both function and ultrastructure: the capacity for both secretion of digestive enzymes and absorption is lost; the epithelium changes from being ultrastructurally similar to that of the adult hepatopancreas to being ultrastructurally similar to that of the posterior midgut diverticulum, even though the latter has an independent ontogenetic origin. As the hepatopancreas differentiates and increases allometrically in size, the MGT loses its absorptive capacity. Contrary to some reports, the abdominal MGT (or "intestine") does not absorb digested food substrates once the gut has attained the adult form.

Enzyme distribution

With a few exceptions (notably Holliday *et al.*, 1980), the histochemical distribution of enzymes observed in *Penaeus setiferus* is consistent with that reported for other species of decapod crustaceans (Travis, 1955, 1957; Miyawaki *et al.*, 1961; Davis and Burnett, 1964; Loizzi, 1966; Van Herp, 1970; Loizzi and Peterson, 1971; Momin and Rangneker, 1974, 1975; Barker and Gibson, 1977, 1978). Although arylamidase activity was reported in hepatopancreatic cells of *Scylla* (Barker and Gibson, 1978), neither arylamidase nor aminopeptidase activity has been demonstrated unequivocally in histochemical studies of any other species of decapod. In tissue homogenates of *P. setiferus*, we measured significant amylase activity for all developmental stages, but activity remained low until late in postlarval development (Lovett and Felder, 1990b). Lack of histochemical evidence for amylase activity in larval and early postlarval stages of *P. setiferus* suggests that concentrations were below the limits of detection for the technique used.

Lateral midgut caeca and hepatopancreas

Both acid phosphatase and esterase activities within the hepatopancreas of decapods have been associated with the synthesis and secretion of digestive enzymes by this tissue, whereas alkaline phosphatase activity in the hepatopancreas has been associated with transmembrane transport of metabolites (Momin and Rangneker, 1974; Barker and Gibson, 1977, 1978; Lane, 1984). Although the exact function of alkaline phosphatase in ab-

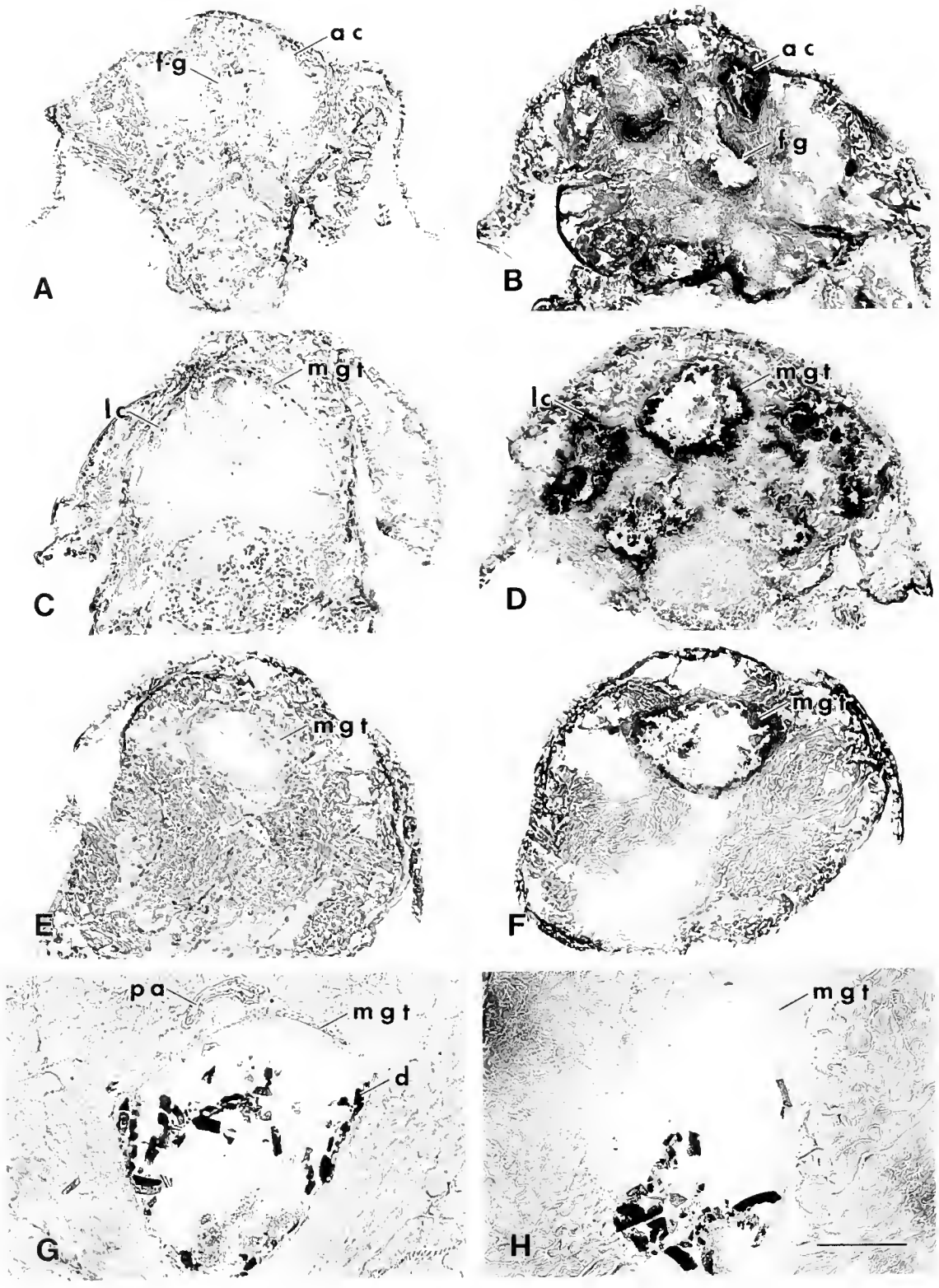

Figure 3. Histochemical localization of alkaline phosphatase activity in fresh frozen sections of *Penaeus setiferus*. A, C, E, G, control sections. B, D, F, H, sections incubated with Naphthol AS-BI phosphate as substrate. A, B, transverse section through foregut and anterior midgut caeca of larval stage Mysis 2. C, D, transverse section through lateral midgut caeca and midgut trunk of Mysis 2. E, F, transverse section through abdominal segment 2 of Mysis 2. G, H, transverse section through abdominal segment 2 of juvenile (PL_{140}). (ac, anterior midgut caecum; fg, foregut; d, debris in lumen; lc, lateral midgut caecum; mgt, midgut trunk; pa, posterior artery). Scale bar indicates 100 μm for A–F and 125 μm for G and H.

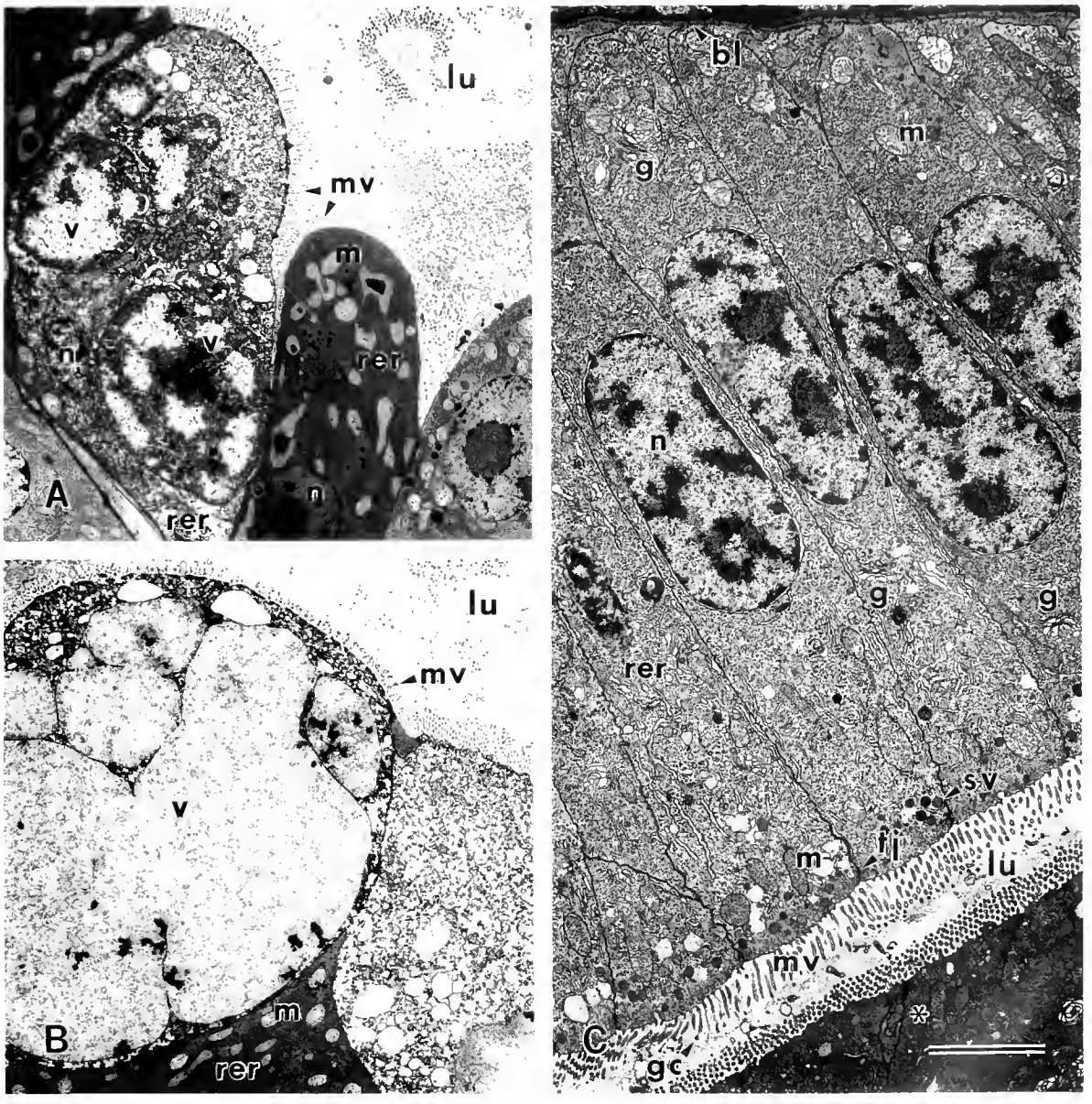

Figure 4. Epithelia of larval midgut caeca and postlarval anterior midgut diverticulum in *Penaeus setiferus*. A, lateral midgut caecum. B, anterior midgut caecum. C, anterior midgut diverticulum. (bl, basal lamina; g, Golgi bodies; gc, glycocalyx; lu, lumen; m, mitochondrion; mv, microvilli; n, nucleus; rer, rough endoplasmic reticulum; sv, secretory vesicle; tj, tight junction; v, vacuole; asterisk indicates electron dense epithelium ventral to lumen of anterior diverticulum; arrow indicates undulatory lateral membranes). A, B, larval stage Protozoea 3. C, postlarval stage PL_{35}. Scale bar indicates 6.8 μm for A and B and 4 μm for C.

sorption has yet to be demonstrated, tissues in which alkaline phosphatase activity is present are generally thought to function in absorption by active transport (see review by McComb *et al.*, 1979). Localization of amylase and protease activity within the hepatopancreas in the present study is consistent with previous detection of amylase and tryptic activity within B-cells of the hepatopancreas of other decapod species (Malcoste *et al.*, 1983; De-Villez and Fyler, 1986). Localization of alkaline phosphatase in the hepatopancreas of *P. setiferus* in the present study is consistent with the absorption usually attributed to this tissue (Gibson and Barker, 1979; Dall and Moriarty, 1983). Ultrastructure also has been used to infer that the hepatopancreas functions in protein synthesis, secretion, and absorption in *Penaeus* (Al-Mohanna *et al.*, 1985b; Vogt, 1985; Al-Mohanna and Nott,

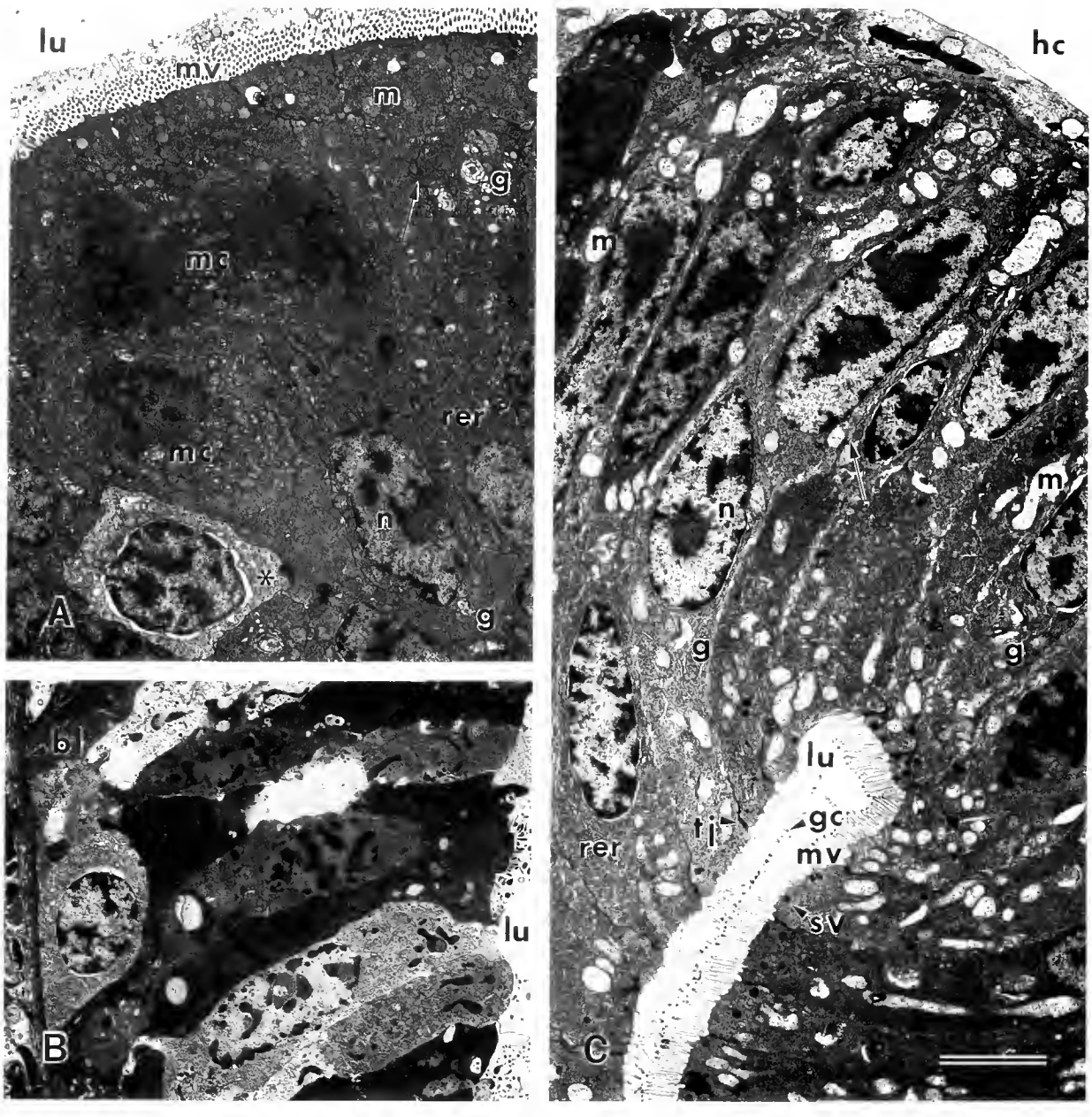

Figure 5. Epithelia of midgut diverticula in *Penaeus setiferus*, postlarval stage PL_{3-5}. A, anterior midgut diverticulum ventral to lumen (see Fig. 5c); these cells attach to hypodermis of dorsal pyloric valve of foregut, note "normal" cell (asterisk) surrounded by electron-dense cells. B, mosaic of cells where epithelium of anterior diverticulum tapers into midgut trunk. C, posterior diverticulum dorsal to lumen. (bl, basal lamina; g, Golgi bodies; gc, glycocalyx; hc, hemocoel; lu, lumen; m, mitochondrion; mc, cell undergoing mitosis; mv, microvilli; n, nucleus; rer, rough endoplasmic reticulum; sv, secretory vesicle; tj, tight junction; arrows indicate undulatory lateral membranes). Scale bar indicates 4 μm for A and C and 5.8 μm for B.

1986; Caceci *et al.*, 1988), and in other decapod crustaceans (Gibson and Barker, 1979).

In *P. setiferus*, substantial morphological change occurs when the lateral midgut caeca of larvae differentiate into the hepatopancreas during early postlarval development (see Lovett and Felder, 1989). However, except for a decrease in the number and size of lipid droplets within cells during the mysis stages of development, the epithelial cells of the larval lateral caeca and of the mature hepatopancreas are identical in ultrastructure. The amylase, protease, and alkaline phosphatase activities that are evident in the lateral caeca during early development

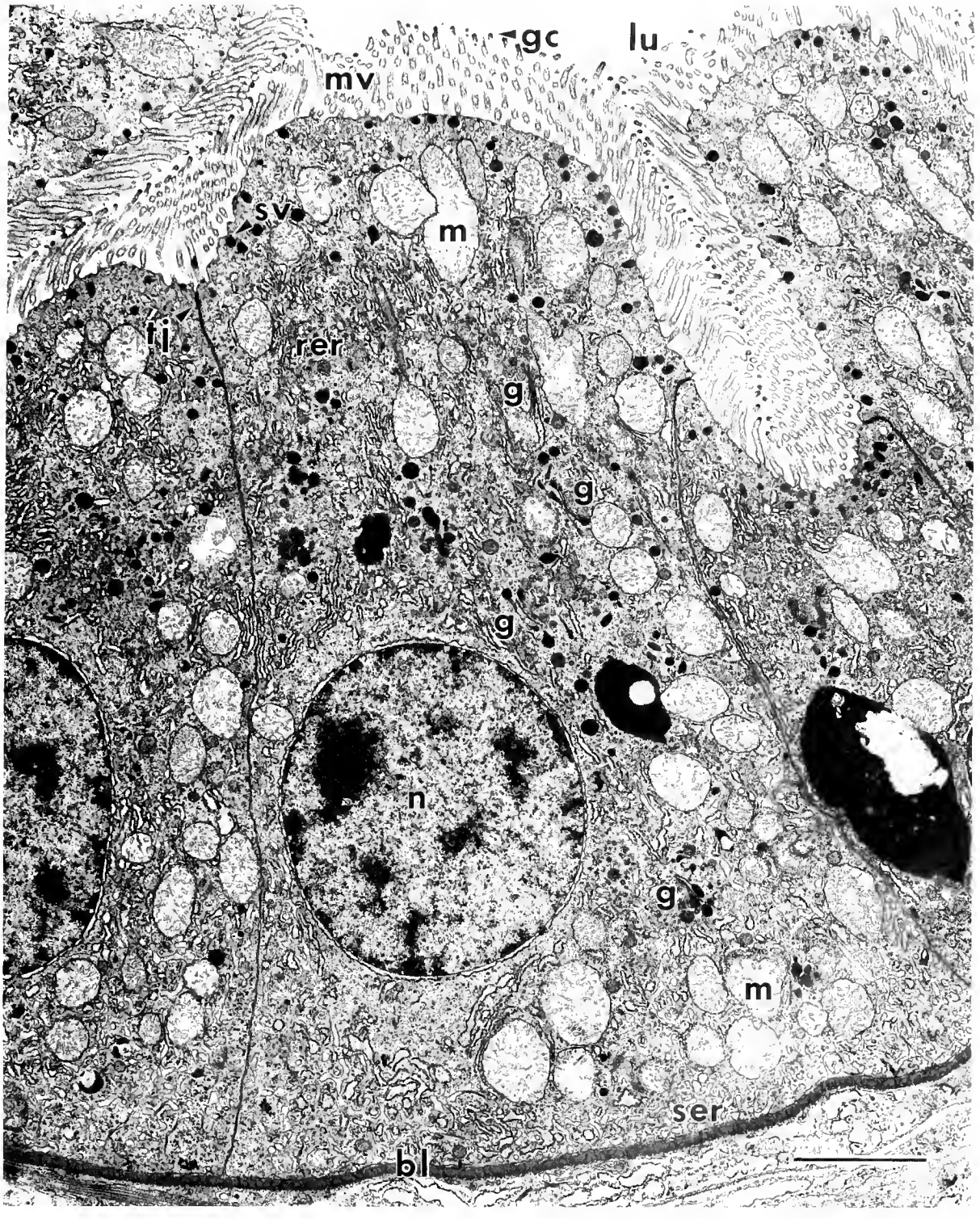

Figure 6. Typical epithelium of midgut trunk in *Penaeus setiferus* (bl, basal lamina; g, Golgi bodies; gc, glycocalyx; lu, lumen; m, mitochondrion; mv, microvilli; n, nucleus; rer, rough endoplasmic reticulum; ser, smooth endoplasmic reticulum; sv, secretory vesicle; tj, tight junction). Scale bar indicates 3 μm.

are also evident in the mature hepatopancreas. Thus, this region of the gut retains the functions of digestive enzyme synthesis, secretion, and absorption throughout development.

Anterior midgut caeca

In larvae of *P. setiferus*, chyme does not appear to flow from the lateral midgut caeca into the anterior midgut caeca (Lovett and Felder, 1990a). Therefore, protease activity in the anterior midgut caeca most likely represents enzyme that has been secreted by the anterior caeca. Ultrastructural similarity of the anterior midgut caeca with both the larval lateral midgut caeca and the mature hepatopancreas also suggests that the anterior caeca secrete digestive enzymes.

Although chyme does not flow into the anterior caeca from the lateral midgut caeca, it does flow into the anterior caeca from the foregut and the anterior-most portion of the MGT. Absorption in the anterior caeca, as inferred from both alkaline phosphatase activity and ultrastructure, is consistent with the observed movement of chyme into the caeca and secretion of digestive enzymes by the caeca.

Anterior and posterior midgut diverticula

The absence of alkaline phosphatase activity from the anterior diverticulum of postlarvae of *P. setiferus* suggests that this diverticulum is not absorptive, while the absence of amylase or protease activity suggests that it does not secrete digestive enzymes. The apparent postmetamorphic loss of both absorption and the capacity to secrete digestive enzymes in this portion of the midgut is reflected in (1) the complete absence of chyme from the lumen of the anterior diverticulum, and (2) the extensive change in ultrastructure that occurs when the anterior midgut caeca degenerate into the anterior diverticulum. Vacuolated F-cells and B-cells, usually associated with synthesis and secretion of digestive enzymes (Gibson and Barker, 1979), are not present in this portion of the midgut after metamorphosis.

Unlike the anterior midgut diverticulum, which develops from the larval anterior midgut caeca, the posterior midgut diverticulum first differentiates as a distinct structure about three weeks after metamorphosis (Lovett and Felder, 1989, 1990a). Absence of alkaline phosphatase and digestive enzyme activity and absence of chyme from the lumen of the posterior diverticulum suggest that this diverticulum, like the anterior midgut diverticulum, does not function in absorption or digestion. Also, while the anterior and posterior diverticula differ in ontogenetic histories, their epithelia are similar in ultrastructure.

Even though many functions have been proposed for the anterior and posterior diverticula (see Introduction), the precise function of the diverticula remains obscure. As mentioned, neither of these structures appear to function in either the secretion of digestive enzymes or absorption through active transport. However, because the epithelial cells of the diverticula in *P. setiferus* and the mucus-secreting cells in the intestine of mammals both have electron-dense cytoplasm (Ito, 1965), cells of the diverticula may function in secretion of a mucus-like substance. Such a mucous secretion could contribute to the formation of the peritrophic membrane, as proposed by other authors (Pugh, 1962; Dall, 1967a; Georgi, 1969; Mykles, 1979); Holliday *et al.* (1980) dispute this interpretation.

Midgut trunk

Because both absorption in postlarval stages (as inferred from alkaline phosphatase activity) and the presence of digestive enzymes in all developmental stages are restricted to the anterior portion of the MGT in *P. setiferus*, we initially predicted that epithelial cells in the anterior region of the MGT might be differentiated ultrastructurally from those in the posterior MGT. Furthermore, because there is significant ontogenetic change in the distribution of alkaline phosphatase in the MGT, we also predicted that there may be ontogenetic change in ultrastructure of the abdominal MGT during larval and early postlarval development. However, essentially no difference in ultrastructure was found along the length of the MGT and no ontogenetic change in ultrastructure occurred that could be correlated with presence or absence of alkaline phosphatase activity. We also could not distinguish the two types of MGT epithelial cells (light and dark) identified by Talbot *et al.* (1972).

The distribution of acid phosphatase in *P. setiferus* suggests that the entire MGT is involved in active protein synthesis and secretion, and this is consistent with the observed ultrastructure. However, ultrastructural evidence does not necessarily indicate that digestive enzymes present in the anterior MGT are being synthesized and secreted by the MGT. The F-cells and B-cells associated with secretion of digestive enzymes in the hepatopancreas are absent from the MGT. From our *in vivo* observations of flow of chyme within the gut of *P. setiferus*, the observed activity of amylase and protease in the anterior lumen of the MGT likely represents enzymes discharged into the MGT from either the larval midgut caeca or the hepatopancreas. We also observed in all postlarval stages that chyme within the MGT as far posteriad as abdominal segment 2, is regularly "regurgitated" anteriad into the hepatopancreas (Lovett and Felder, 1990a). Moreover, digestive enzymes also occur in the MGT as far posteriad as abdominal segment 2,

where they mix with chyme. These enzymes and the digesting chyme are periodically carried anteriad into the midgut caeca or the hepatopancreas where final digestion and absorption take place.

The presence of apical microvilli, a glycocalyx, tight junctions, and a well-developed basal lamina in epithelial cells along the length of the MGT in adult specimens of *Penaeus* and other decapod crustaceans has led some investigators to conclude that these cells are absorptive (Talbot *et al.*, 1972; Hootman and Conte, 1974; Kurata and Shigueno, 1976; Mykles, 1979). From the distribution of alkaline phosphatase in *P. setiferus*, it appears that the entire MGT is absorptive in the early larval stages. However, this apparent absorption is lost from the abdominal MGT during postlarval development. Other investigators also have concluded that the MGT in adults of *Penaeus* and other decapod crustaceans probably play a minimal role in absorption of organic nutrients, because only low rates of transport for amino acids, sugars, and vitamins could be measured across the MGT epithelium from the lumen (Ahearn, 1982, and citations therein; Chu, 1986). Even though small amounts of these solutes are transported from the lumen of the MGT into the cytoplasm of epithelial cells, intracellular metabolism of the solutes results in no net transepithelial flux into the hemolymph. From studies of carrier-mediated transmembrane transport systems for amino acids and glucose, it is also evident that relative rate of transepithelial solute transport in the adult decapod MGT by these carrier systems is almost two orders of magnitude lower than in the decapod hepatopancreas (Ahearn *et al.*, 1983, 1985, 1986; Ahearn and Clay, 1987a, b, 1988). These observations independently support the conclusion that the adult hepatopancreas is the primary area of absorption and that the MGT does not function significantly in this role. From histological and ultrastructural evidence, together with demonstration of *in vivo* uptake of radiolabeled solutes, it is usually inferred that the hepatopancreas is the primary site of nutrient absorption in adult crustaceans (Yonge, 1924; van Weel, 1955, 1970; Vonk, 1960; Speck and Urich, 1970; Dall, 1981).

The MGT in *Penaeus* is reported to function in ion transport and regulation of water flux from the midgut lumen to the hemolymph (Dall, 1967b; Talbot *et al.*, 1972; Ahearn *et al.*, 1978; Ahearn, 1982). Evidence for such a function is not surprising given the degree to which anal drinking and antiperistaltic water movements occur in some decapods (Fox, 1952; Pillai, 1960; Dall, 1965; Lovett and Felder, 1990a), and osmoregulatory function may, in part, account for observed ultrastructure of the MGT. Absence of alkaline phosphatase activity from the MGT is also consistent with an osmoregulatory function as alkaline phosphatase activity was not detected in either the gills or branchiostegites (primary osmoregulatory tissues) of *P. setiferus*.

Ontogeny of midgut function

Because the developing midgut tissue in embryos and nauplii of *Penaeus* functions in digestion and absorption of yolk, it is not unexpected that the entire midgut might retain similar functions during larval development. Even so, these functions are gradually lost from the abdominal MGT and from the anterior midgut caecum during larval and postlarval development. By the juvenile stage, only the hepatopancreas and that portion of the MGT within the cephalothorax are absorptive, while only the hepatopancreas functions in digestion. A similar ontogenetic change (from an undifferentiated and unspecialized larval gut to an adult gut in which functions are segregated) is also seen in teleost fish (Prakash, 1961; Blaxter, 1969) and may represent a general developmental phenomenon.

Dendrobranchiate shrimp such as *P. setiferus* may be unique among decapod crustaceans in their retention of both digestion and absorption in the anterior midgut caeca throughout larval development. In *Homarus*, after yolk material has been depleted during the first larval stage, the anterior caeca rapidly decrease in size. Similar to the change in the cells of the anterior caeca of *P. setiferus* after metamorphosis, there is a change in the epithelia of the anterior caeca in *Homarus* after the first larval stage: cuboidal, highly vacuolated cells are replaced by the highly columnar cells characteristic of the adult epithelium (Hinton and Corey, 1979).

Absorption in the abdominal MGT of larvae and early postlarvae may compensate for the small surface area in the anterior and lateral midgut caeca. In addition, because the gastric mill of the foregut is not functional during larval development, and because food has a relatively short retention time in the gut of larvae, retention of absorptive capacity along the entire length of the MGT could maximize assimilation of ingested food. As the simple lobes of the lateral midgut caeca ramify into the many tubules of the hepatopancreas, the relative surface area of this region of the gut increases substantially (Lovett and Felder, 1989). Thus, with loss of absorption in the anterior midgut caeca and the abdominal MGT, there is an increase in relative surface area (and hence absorptive capacity) of the hepatopancreas.

Acknowledgments

Special thanks are extended to A. L. Lawrence and his staff, Texas A&M Shrimp Mariculture Project, and to C. Howell and J. Benty, Continental Fisheries, Ltd., Panama City, Florida, for their generous provision of *Penaeus setiferus* larvae and postlarvae. B. E. Felgenhauer,

R. C. Brown, and J. F. Jackson, University of Southwestern Louisiana (USL), and S. C. Hand, University of Colorado, offered useful comments on the manuscript. E. J. DeVillez, Miami University of Ohio, provided extensive assistance in development of histochemical methodology. K. R. Roberts and J. L. Staton (USL) assisted in culture of algae and shrimp. Primary support for this study was provided under research grant NA85AA-D-SG141 to D. L. Felder and D. L. Lovett from the Louisiana Sea Grant College Program. Additional funds were provided to D. L. Felder by research grants from the Louisiana Education Quality Support Fund, projects 86-USL(1)-126-07 and 86-LUM(1)-083-13, and by a grant from the Coypu Foundation. Louisiana Universities Marine Consortium (LUMCON) Marine Center and the USL Electron Microscopy Center provided valuable technical assistance to the project. This is contribution number 22 from the USL Center for Crustacean Research.

Literature Cited

Ahearn, G. A. 1974. Kinetic characteristics of glycine transport by the isolated midgut of the marine shrimp, *Penaeus marginatus*. *J Exp Biol* **61:** 677–696.

Ahearn, G. A. 1980. Intestinal electrophysiology and transmural ion transport in freshwater prawns. *Am J Physiol.* **239:** C1–C10.

Ahearn, G. A. 1982. Water and solute transport by crustacean gastrointestinal tract. Pp. 261–339 in *Membrane Physiology of Invertebrates*, R. B. Podesta, ed. Marcel Dekker, Inc., New York.

Ahearn, G. A. 1984. Sigmoid kinetics of sodium chloride transport in crustacean intestine. Pp. 121–149 in *Chloride Transport Coupling in Biological Membranes and Epithelia*, G. A. Gereneser, ed. Elsevier Science Publishers B. V., Amsterdam.

Ahearn, G. A., and L. P. Clay. 1987a. Membrane-potential-sensitive, Na^+-independent lysine transport by lobster hepatopancreatic brush border membrane vesicles. *J Exp Biol* **127:** 373–387.

Ahearn, G. A., and L. P. Clay. 1987b. Na^+-Cl^--glutamate cotransport by lobster hepatopancreatic brush border membrane vesicles. *J Exp. Biol.* **130:** 175–191.

Ahearn, G. A., and L. P. Clay. 1988. Electroneutral, Na^+-2Cl^--leucine cotransport by lobster hepatopancreatic brush border membrane vesicles. *J Exp. Biol* **136:** 363–381.

Ahearn, G. A., M. L. Grover, and R. E. Dunn. 1985. Glucose transport by lobster hepatopancreatic brush-border membrane vesicles. *Am J Physiol* **248:** R133–R141.

Ahearn, G. A., M. L. Grover, and R. E. Dunn. 1986. Effects of Na^+, H^+, and Cl^- on alanine transport by lobster hepatopancreatic brush border membrane vesicles. *J Comp. Physiol* **156B:** 537–548.

Ahearn, G. A., O. Koosawad, and N. F. Hadley. 1978. Differential rectifying properties of three arthropod intestines to osmotic water flow. *Comp Biochem. Physiol.* **61A:** 183–186.

Ahearn, G. A., and L. A. Maginniss. 1977. Kinetics of glucose transport by the perfused midgut of the freshwater prawn, *Macrobrachium rosenbergii*. *J Physiol (London)* **271:** 319–336.

Ahearn, G. A., E. A. Monekton, A. E. Henry, and M. C. Botfield. 1983. Alanine transport by lobster hepatopancreatic cell suspensions. *Am J Physiol* **244:** R150–R162.

Al-Mohanna, S. Y., and J. A. Nott, 1986. B-cells and digestion in the hepatopancreas of *Penaeus semisulcatus* (Crustacea: Decapoda). *J Mar Biol Assoc. U. K.* **66:** 403–414.

Al-Mohanna, S. Y., J. A. Nott, and D. J. W. Lane. 1985a. M-'midget' cells in the hepatopancreas of the shrimp *Penaeus semisulcatus* de Haan, 1844 (Decapoda, Natantia). *Crustaceana* **48:** 260–268.

Al-Mohanna, S. Y., J. A. Nott, and D. J. W. Lane. 1985b. Mitotic E- and secretory F-cells in the hepatopancreas of the shrimp *Penaeus semisulcatus* (Crustacea: Decapoda). *J Mar. Biol. Assoc. U. K.* **65:** 901–910.

Barker, P. L., and R. Gibson. 1977. Observations on the feeding mechanism, structure of the gut, and digestive physiology of the European lobster *Homarus gammarus* (L.) (Decapoda: Nephropidae). *J. Exp Mar. Biol. Ecol.* **26:** 297–324.

Barker, P. L., and R. Gibson. 1978. Observations on the structure of the mouthparts, histology of the alimentary tract, and digestive physiology of the mud crab *Scylla serrata* (Forskal) (Decapoda: Portunidae). *J Exp. Mar. Biol. Ecol.* **32:** 177–196.

Barrnett, R. J., and A. M. Seligman. 1951. Histochemical demonstration of esterases by production of indigo. *Science* **114:** 579–582.

Blaxter, J. H. S. 1969. Development: eggs and larvae. Pp. 177–252 in *Fish Physiology*, Vol. 3, W. S. Hoar and D. J. Randall, eds. Academic Press, New York.

Bokdawala, F. D., and J. C. George. 1964. Histochemical demonstration of muscle lipase. *J Histochem. Cytochem.* **12:** 768–771.

Brick, R. W., and G. A. Ahearn. 1978. Lysine transport across the mucosal border of the perfused midgut in the freshwater shrimp, *Macrobrachium rosenbergii*. *J Comp Physiol.* **124:** 169–179.

Burstone, M. S. 1958. Histochemical comparison of naphthol AS-phosphates for the demonstration of phosphatases. *J Nat. Cancer Inst* **20:** 601–615.

Burstone, M. S. 1962. *Enzyme Histochemistry and its Application in the Study of Neoplasm* Academic Press, New York.

Burstone, M. S., and J. E. Folk. 1956. Histochemical demonstration of aminopeptidase. *J Histochem Cytochem.* **4:** 217–226.

Caceci, T., K. F. Neck, D. H. Lewis, and R. F. Sis. 1988. Ultrastructure of the hepatopancreas of the Pacific white shrimp, *Penaeus vannamei* (Crustacea: Decapoda). *J Mar Biol. Assoc. U. K* **68:** 323–337.

Chu, K. H. 1986. Glucose transport by the *in vitro* perfused midgut of the blue crab, *Callinectes sapidus*. *J Exp Biol* **123:** 325–344.

Croghan, P. C. 1958. The mechanism of osmotic regulation in *Artemia salina* (L.). The physiology of the gut. *J Exp. Biol.* **35:** 243–249.

Cuzon, G., M. Hew, D. Cognie, and P. Soletchnick. 1982. Time lag effect of feeding on growth of juvenile shrimp, *Penaeus japonicus* Bate. *Aquaculture* **29:** 33–44.

Dall, W. 1965. Studies on the physiology of a shrimp, *Metapenaeus* sp. (Crustacea: Decapoda: Penaeidae). V. Calcium metabolism. *Aust J Mar Freshw. Res* **16:** 181–203.

Dall, W. 1967a. Functional anatomy of the digestive tract of a shrimp *Metapenaeus bennettae* (Crustacea: Decapoda: Penaeidae). *Aust. J Zool* **15:** 699–715.

Dall, W. 1967b. Hypo-osmoregulation in Crustacea. *Comp. Biochem. Physiol* **21:** 653–678.

Dall, W. 1970. Osmoregulation in the lobster *Homarus americanus*. *J Fish. Res Board Can* **27:** 1123–1130.

Dall, W. 1981. Lipid absorption and utilization in the Norwegian lobster, *Nephrops longipes* (L.). *J Exp. Mar. Biol Ecol* **50:** 33–45.

Dall, W., and D. J. W. Moriarty. 1983. Functional aspects of nutrition and digestion. Pp. 215–261 in *The Biology of the Crustacea*, Vol. 5, *Internal Anatomy and Physiological Regulation*, L. H. Mantel, ed. Academic Press, New York.

Davis, L. E., and A. L. Burnett. 1964. A study of the growth and cell differentiation in the hepatopancreas of the crayfish. *Dev Biol.* **10:** 122–153.

DeVillez, E. J., and D. J. Fyler. 1986. Isolation of hepatopancreatic

cell types and enzymatic activities in B cells of the crayfish *Orconectes rusticus*. *Can. J. Zool.* **64:** 81–83.

Felder, D. L., J. W. Martin, and J. W. Goy. 1985. Patterns in early postlarval development of decapods. Pp. 163–225 in *Crustacean Issues*, Vol. 2, *Larval Growth*, A. M. Wenner, ed. A. A. Balkema, Rotterdam.

Fox, H. M. 1952. Anal and oral water intake by Crustacea. *J. Exp. Biol.* **29:** 583–599.

Fratello, B. 1968. Enhanced interpretation of tissue protease activity by use of photographic color film as a substrate. *Stain Technol.* **43:** 125–128.

Geddes, M. C. 1975. Studies on Australian brine shrimp, *Parartemia zietziana* Sayce (Crustacea: Anostraca)—III. The mechanisms of osmotic and ionic regulation. *Comp. Biochem. Physiol.* **51A:** 573–578.

Gemmel, P. 1979. Feeding habits and structure of the gut of the Australian freshwater prawn, *Paratya australiensis* Kemp (Crustacea, Caridea, Atyidae). *Proc. Linn. Soc. N. S. W.* **103:** 209–216.

Georgi, R. 1969. Bildung peritrophischer Membranen von Decapoden. *Z. Zellforsch.* **99:** 570–607.

Gibson, R., and P. L. Barker. 1979. The decapod hepatopancreas. *Oceanogr. Mar. Biol. Ann. Rev.* **17:** 285–346.

Gifford, C. A. 1962. Some aspects of osmotic and ionic regulation in the blue crab, *Callinectes sapidus*, and the ghost crab, *Ocypode albicans*. *Publ. Inst. Mar. Sci., Univ. Texas* **8:** 97–125.

Glenner, G. G., and L. A. Cohen. 1960. Histochemical demonstration of a species-specific trypsin-like enzyme in mast cells. *Nature* **185:** 846–847.

Gomori, G. 1945. The microtechnical demonstration of sites of lipase activity. *Proc. Soc. Exp. Biol. Med.* **58:** 362–364.

Gomori, G. 1949. Histochemical localization of true lipase. *Proc. Soc. Exp. Biol. Med.* **72:** 697–700.

Green, J. W., M. Hersch, L. Barr, and C. L. Prosser. 1959. The regulation of water and salt by the fiddler crabs, *Uca pugnax* and *Uca pugilator*. *Biol. Bull.* **116:** 76–87.

Heeg, J., and A. J. Cannone. 1966. Osmoregulation by means of a hitherto unsuspected organ in two grapsid crabs. *Zool. Afr.* **2:** 127–129.

Hinton, D. J., and S. Corey. 1979. The mouthparts and digestive tract in the larval stages of *Homarus americanus*. *Can. J. Zool.* **57:** 1413–1423.

Holliday, C. W., D. L. Mykles, R. C. Terwilliger, and L. J. Dangott. 1980. Fluid secretion by the midgut caeca of the crab, *Cancer magister*. *Comp. Biochem. Physiol.* **67A:** 259–263.

Holt, S. J., and R. F. J. Withers. 1952. Cytochemical localization of esterases using indoxyl derivatives. *Nature* **170:** 1012–1014.

Hootman, S. R., and F. P. Conte. 1974. Fine structure and function of the alimentary epithelium in *Artemia salina* nauplii. *Cell Tiss. Res.* **155:** 423–436.

Ito, S. 1965. The enteric surface coat on cat intestine. *J. Cell Biol.* **27:** 475–491.

Johnson, P. T. 1980. *Histology of the Blue Crab*, Callinectes sapidus. Praeger Publishers, New York. 440 pp.

Kurata, H., and K. Shigueno. 1976. Recent progress in the farming of Kuruma shrimp (*Penaeus japonicus*). Pp. 258–268 in *Advances in Aquaculture*, T. V. R. Pillay and W. A. Dill, eds. Fishing News Books, Ltd., Surrey, England.

Lane, R. L. 1984. Histochemical studies on the digestive system of *Porcellio scaber* (Crustacea: Isopoda). *Am. Zool.* **24:** 66A.

Loizzi, R. F. 1966. *Cellular and Physiological Changes During Secretion in Crayfish Hepatopancreas*. PhD. Dissertation. Iowa State University, Ames. 184 pp.

Loizzi, R. F., and D. R. Peterson. 1971. Lipolytic sites in crayfish hepatopancreas and correlation with fine structure. *Comp. Biochem. Physiol.* **39B:** 227–236.

Lovett, D. L., and D. L. Felder. 1989. Ontogeny of gut morphology in the white shrimp *Penaeus setiferus* (Decapoda, Penacidae). *J. Morphol.* **201:** 253–272.

Lovett, D. L., and D. L. Felder. 1990a. Ontogeny of kinematics in the gut of the white shrimp *Penaeus setiferus* (Decapoda, Penaeidae). *J. Crust. Biol.* **10:** 53–68.

Lovett, D. L., and D. L. Felder. 1990b. Ontogenetic change in digestive enzyme activity of larval and postlarval white shrimp *Penaeus setiferus* (Crustacea, Decapoda, Penaeidae). *Biol. Bull.* **178:** 144–159.

Malcoste, R., A. Van Wormhoudt, and C. Bellon-Humbert. 1983. La caractérisation de l'hépatopancréas de la crevette *Palaemon serratus* Pennant (Crustacé Décapode Natantia) en cultures organotypiques. *C. R. Seances Acad. Sci. Vie Acad.* **296:** 597–602.

Malley, D. F. 1977. Salt and water balance of the spiny lobster *Panulirus argus*: the role of the gut. *J. Exp. Biol.* **70:** 231–245.

McComb, R. B., G. N. Bowers Jr., and S. Posen. 1979. *Alkaline Phosphatase*. Plenum Press, New York. Pp. 865–902.

McManus, J. F. A. 1948. Histological and histochemical uses of periodic acid. *Stain Technol.* **23:** 99–108.

McVey, J. P., and J. M. Fox. 1983. Hatchery techniques for penaeid shrimp utilized by Texas A&M-NMFS Galveston Laboratory Program. Pp. 129–154 in *CRC Handbook of Mariculture: Crustacean Aquaculture*. Vol. 1, J. P. McVey, ed. CRC Press, Inc., Boca Raton, Florida.

Millonig, G. 1976. *Laboratory Manual of Biological Electron Microscopy*. Mario Saviolo, Vercilli, Italy.

Miyawaki, M., M. Matsuzaki, and N. Sasaki. 1961. Histochemical studies on the hepatopancreas of the crayfish, *Procambarus clarkii*. *Kumamoto J. Sci. B* **5:** 161–169.

Momin, M. A., and P. V. Rangneker. 1974. Histochemical localization of acid and alkaline phosphatases and glucose-6-phosphatase of the hepatopancreas of the crab, *Scylla serrata* (Forskal). *J. Exp. Mar. Biol. Ecol.* **4:** 1–16.

Momin, M. A., and P. V. Rangneker. 1975. Histochemical localization of oxidative enzymes in the hepatopancreas of *Scylla serrata* (Forskal) (Brachyura: Decapoda). *J. Exp. Mar. Biol. Ecol.* **20:** 249–264.

Mykles, D. L. 1977. The ultrastructure of the posterior midgut caecum of *Pachygrapsus crassipes* (Decapoda, Brachyura) adapted to low salinity. *Tissue Cell* **9:** 681–691.

Mykles, D. L. 1979. Ultrastructure of alimentary epithelia of lobsters, *Homarus americanus* and *H. gammarus*, and crab *Cancer magister*. *Zoomorphologie* **92:** 201–215.

Mykles, D. L. 1980. The mechanism of fluid absorption at ecdysis in the American lobster, *Homarus americanus*. *J. Exp. Biol.* **84:** 89–101.

Mykles, D. L. 1981. Ionic requirements of transepithelial potential difference and net water flux in the perfused midgut of the American lobster, *Homarus americanus*. *Comp. Biochem. Physiol.* **69A:** 317–320.

Mykles, D. L., and G. A. Ahearn. 1978. Changes in fluid transport across the perfused midgut of the freshwater prawn, *Macrobrachium rosenbergii*, during the molting cycle. *Comp. Biochem. Physiol.* **61A:** 643–645.

Nachlas, M. M., B. Monis, D. Rosenblatt, and A. M. Seligman. 1960. Improvement in the histochemical localization of leucine aminopeptidase with a new substrate L-leucyl-4-methoxy-2-naphthylamide. *J. Biophys. Biochem. Cytol.* **7(2):** 261–275.

Pappas, P. W. 1971. The use of chrome alum-gelatin (subbing) solution as a general adhesive for paraffin sections. *Stain. Technol.* **46:** 121–124.

Pillai, R. S. 1960. Studies on shrimp *Caridina laevis* (Heller). 1. The digestive system. *J. Mar. Biol. Assoc. (India)* **2:** 57–74.

Powell, R. R. 1974. The functional morphology of the fore-gut of the thalassinid crustaceans *Callianassa californiensis* and *Upogebia pugettensis*. *Univ. Calif. Publ. Zool.* **102:** 1–41.

Prakash, A. 1961. Distribution and differentiation of alkaline phosphatase in the gastro-intestinal tract of steelhead trout. *J. Exp. Zool.* **196:** 237–246.

Pugh, J. E. 1962. A contribution toward a knowledge of the hind-gut of fiddler crabs (Decapoda, Grapsidae). *Trans. Am. Micros. Sci.* **81:** 309–320.

Quaglia, A., B. Sabelli, and L. Villani. 1976. Studies on the intestine of Daphnidae (Crustacea, Cladocera). Ultrastructure of the midgut of *Daphnia magna* and *Daphnia obtusa*. *J. Morphol.* **150:** 711–726.

Reddy, A. R. 1937. The physiology of digestion and absorption in the crab *Paratelphusa* (*Oziotelphusa*) *hydrodromus* (Herbst). *Proc. Ind. Acad. Sci. B***6:** 170–193.

Speck, U., and K. Urich. 1970. Das Schicksal der Nahrstoffe bei dem Flusskrebs *Orconectes limosus*. II. Resorption U-^{14}C-markierter Nahrstoffe and ihre Verteilung auf die Organe. *Z. Verg. Physiol.* **68:** 318–333.

Talbot, P., W. H. Clark Jr., and A. L. Lawrence. 1972. Fine structure of the midgut epithelium in the developing brown shrimp, *Penaeus aztecus*. *J. Morphol.* **138:** 467–486.

Travis, D. F. 1955. The molting cycle of the spiny lobster, *Panulirus argus* Latreille. II. Pre-ecdysial histological and histochemical changes in the hepatopancreas and integumental tissues. *Biol. Bull.* **108:** 88–112.

Travis, D. F. 1957. The molting cycle of the spiny lobster, *Panulirus argus* Latreille. IV. Post-ecdysial histological and histochemical changes in the hepatopancreas and integumental tissues. *Biol. Bull.* **113:** 451–479.

Tremblay, G., and J. Charest. 1968. Modified starch film method for the histochemical localization of amylase activity. *J. Histochem. Cytochem.* **16:** 147–148.

Van Herp, F. 1970. Study of the influence of sinus gland extirpation on the alkaline phosphatase in the hepatopancreas of the crayfish, *Astacus leptodactylus*. *Comp. Biochem. Physiol.* **34:** 439–445.

van Weel, P. B. 1955. Processes of secretion, restitution, and resorption in gland of mid-gut (glandula media intestini) of *Atya spinipes* Newport (Decapoda-Brachyura). *Physiol. Zool.* **28:** 40–54.

van Weel, P. B. 1970. Digestion in Crustacea. Pp. 97–115 in *Chemical Zoology*, Vol. 5, *Arthropoda*, Part A, M. Florkin and B. T. Scheer, eds. Academic Press, New York.

Van Wormhoudt, A., H. J. Ceccaldi, and Y. Le Gal. 1972. Activité des protéases et amylases chez *Penaeus kerathurus*: existence d'un rythme circadien. *C. R. Acad. Sci. (Paris) Ser. D.* **74:** 1208–1211.

Vogt, G. 1985. Histologie und cytologie der Mitteldarmdrüse von *Penaeus monodon* (Decapoda). *Zool. Anz.* **215:** 61–80.

Vogt, G., V. Storch, E. T. Quinitio, and F. P. Pascual. 1985. Midgut gland as monitor organ for the nutritional value of diets in *Penaeus monodon* (Decapoda). *Aquaculture* **48:** 1–12.

Vogt, G., E. T. Quinitio, and F. P. Pascual. 1986. *Leucaena leucocephala* leaves in formulated feed for *Penaeus monodon*: a concrete example of the application of histology in nutrition research. *Aquaculture* **59:** 209–234.

Vonk, H. J. 1960. Digestion and Metabolism. Pp. 291–316 in *Physiology of the Crustacea*, Vol. 2, T. H. Waterman, ed. Academic Press, Inc. New York.

Wyban, J. A., G. A. Ahearn, and L. A. Maginniss. 1980. Effects of organic solutes on transmural PD and Na transport in freshwater prawn intestine. *Am. J. Physiol.* **239:** C11–C17.

Yonge, C. M. 1924. Studies on the comparative physiology of digestion. II. The mechanism of feeding digestion, and assimilation in *Nephrops norvegicus*. *Br. J. Exp. Biol.* **1:** 343–389.

Young, J. H. 1959. Morphology of the white shrimp *Penaeus setiferus* (Linnaeus 1758). *Fish. Bull.* **145:** 1–168.

Reference: *Biol. Bull.* **178:** 175–186. (April, 1990)

Host-Zooxanthella Interactions in Four Temperate Marine Invertebrate Symbioses: Assessment of Effect of Host Extracts on Symbionts

D. C. SUTTON[1] AND O. HOEGH-GULDBERG[2]*

[1]*Sir George Fisher Centre for Tropical Marine Studies, James Cook University, Townsville, Queensland 4811, Australia and* [2]*School of Biological Sciences, University of Sydney, Sydney, New South Wales 2006, Australia*

Abstract. Photosynthesis and translocation of photosynthetic products from symbiotic zooxanthellae in four species of temperate-latitude invertebrates were investigated *in vivo* and *in vitro*. *In vivo*, zooxanthellae fixed ^{14}C and translocated a substantial proportion of fixed products to host tissues. *In vitro*, the effect of host tissue extracts on isolated zooxanthellae varied. Extracts of the soft coral *Capnella gaboensis*, lysed zooxanthellae after a relatively short exposure. Those of the zoanthid *Zoanthus robustus* and the nudibranch *Pteraeolidia ianthina* had little effect on translocation of organic carbon from zooxanthellae. In contrast, host extract of the scleractinian coral *Plesiastrea versipora* stimulated the release of up to 42% of the total ^{14}C fixed, and the magnitude of release was positively correlated with the protein concentration of the extract. Host extracts had no effect on photosynthetic rates in algal symbionts.

The effect of *P. versipora* extract on isolated zooxanthellae was studied. This extract caused zooxanthellae to divert photosynthetic products from lipid synthesis to the production of neutral compounds, principally glycerol, and these compounds were the predominant form of carbon detected extracellularly after incubating zooxanthellae in this extract. Only organic compounds made during the period of exposure of zooxanthellae to host extract, and not pre-formed photosynthetic products, were translocated. The translocation-inducing activity of host extract was almost completely destroyed by heating (100°C), and a preliminary attempt to fractionate the tissue extract revealed that the active constituent did not pass through dialysis tubing of nominal pore size 10,000 D. These results are discussed in relation to host control of symbiotic partners, and to previous reports of "host-release factors" in other invertebrate symbioses.

Received 21 October 1986; accepted 8 January 1990.

* Present address: Department of Biological Sciences, University of Southern California, Los Angeles, California 90089-0371.

Introduction

Many marine invertebrates belonging to the phyla Mollusca, Platyhelminthes, Cnidaria, and Protozoa contain endosymbiotic dinoflagellates, collectively known as zooxanthellae. In nudibranch molluscs (Rudman, 1981a, 1982) and the majority of cnidarians (Trench, 1979), zooxanthellae are found within vacuoles in host cells derived from the endoderm. Zooxanthellae carry out photosynthesis within the confines of the host cell, and make significant contributions to host cell metabolism by translocation of organic compounds to the host (for review, see Trench, 1979). Muscatine and co-workers estimate that up to 95% of the carbon fixed during photosynthesis is translocated to coral hosts (Muscatine *et al.*, 1983, 1984), and at least some of the translocated carbon is used by the host for respiration and growth (Franzisket, 1970; Johannes, 1974; Kevin and Hudson, 1979; Kempf, 1984). Moreover, the animal provides organic and inorganic nutrients, some of them metabolic waste products, to the algae (Cook, 1971; Muscatine and Porter, 1977).

Most of the studies noted above concern tropical symbioses. In temperate latitudes, many marine symbiotic associations involve zooxanthellae, and a number of studies of these associations show that zooxanthellae contribute to metabolic processes in their hosts and to

calcification rates (Jacques and Pilson, 1980; Jacques *et al.*, 1983; Tytler and Davies, 1986). However, the extent and significance of *in vivo* translocation of photosynthetic products to host tissues in these interactions have rarely been studied.

Little is known about the control of translocation between the partners in symbiosis. Several *in vitro* studies have suggested that the host may contain compounds ("host factors") that cause carbon to be translocated from the alga (Muscatine, 1967; Trench, 1971c), but no chemical entity with this function has been identified, and no mechanism for host factor action has been demonstrated. In some associations, host factors have been reported only in extracts of symbiotic hosts and not in extracts from aposymbiotic individuals (Trench, 1971c). Host factors from some (Muscatine, 1967; Yu and Dietrich, 1977), but not all (Muscatine *et al.*, 1972) symbiotic invertebrates are heat-labile, and cross-reactivity experiments suggest that invertebrates having zooxanthellae have similar host factors. Thus, host extract from the symbiotic clam *Tridacna* stimulates the release of organic carbon from zooxanthellae from the coral, *Pocillopora damicornis*, and the coral extract has a similar effect on clam zooxanthellae (Muscatine, 1967). Host factors may also influence the photosynthetic rate of zooxanthellae (Trench, 1971c; Muscatine *et al.*, 1972), and their alanine uptake (Carroll and Blanquet, 1984b; Blanquet *et al.*, 1988). In summary, the distribution of host factors and their effects among invertebrates having zooxanthellae is obscure.

This study had three objectives: the first was to determine whether *in vivo* translocation in a range of temperate invertebrates occurs. To this end, four relatively abundant marine invertebrates from Latitude 34°S, New South Wales, Australia, having zooxanthellae as symbionts and representing diverse taxa, were chosen for experimentation: the soft coral *Capnella gaboensis*, the stony coral *Plesiastrea versipora*, the zoanthid *Zoanthus robustus*, and the aeolid nudibranch *Pteraeolidia ianthina*. The second objective was to determine whether there was evidence, in these temperate marine invertebrate symbioses, for host factor control of zooxanthellar processes, particularly of photosynthesis, metabolism, and translocation of photosynthetic products. The final objective was to characterize the active components of host extracts affecting zooxanthellar processes, should they be found.

Materials and Methods

Source and maintenance of animals

The invertebrates used in this study were collected from the Sydney region, New South Wales, Australia (Latitude 34° S), between May 1980 and May 1981. The nudibranch *Pteraeolidia ianthina* was collected at Ben Buckler Point at depths of 20 m. *Plesiastrea versipora*, *Capnella gaboensis*, and *Zoanthus robustus* were collected at 5-m depth at Port Jackson. Specimens were placed in seawater in plastic bags, transported to the laboratory, and kept in seawater aquaria illuminated by cool white fluorescent lighting (photoperiod 12 h light/12 h dark; 12 $\mu E \cdot m^{-2} \cdot s^{-1}$) in an air conditioned room (21 ± 2°C). Animals were used in experiments within three weeks of collection.

Isolation of zooxanthellae and preparation of host extracts

Unless otherwise stated, filtered (0.45 μm, Millipore) natural seawater was used in all experiments. Suspensions of zooxanthellae were prepared from each species as follows: the surfaces of small colonies (approximately 100 cm^2) of *P. versipora* were abraded with a stainless steel brush, flooded with seawater, and scraped with a nylon toothbrush into a glass dish. For *C. gaboensis*, several branch tips (up to 50 g wet weight) were macerated using a mortar and pestle. The resulting slurries from each animal were passed through one layer of Miracloth (Calbiochem) and made up to 10 ml total volume with seawater. Whole individuals of *Z. robustus* were split longitudinally with a scalpel, and the gastrodermis, containing the zooxanthellae, was scraped into 10 ml of seawater. The cerata of several individuals of *Pa. ianthina* were excised and homogenized in 5 ml of seawater, using a ground-glass homogenizer. Microscopic observations indicated that these techniques did not disrupt zooxanthellae.

The suspensions of zooxanthellae were centrifuged at 2000 rpm (490 × *g*) for 60 s (M.S.E. benchtop centrifuge). The supernatant ("host extract") was poured off. The zooxanthellae were then washed three times by resuspension in 10 ml of seawater followed by re-centrifugation. The pH of the host extract (pH = 7.5–7.9) was adjusted to that of seawater (pH = 8.1) with 0.1 *N* NaOH. The extract was stored at 5°C for not more than 20 min until used. The protein concentration of each extract was determined at the end of each experiment (Lowry *et al.*, 1951), from samples frozen (0°C) following extract preparation.

Electron microscopy

Isolated zooxanthellae and small pieces of intact tissue were fixed for 3–4 h in 3% glutaraldehyde in sodium cacodylate buffer (pH 7.3) and then washed for 10 min in each of three changes of 0.1 *M* sodium cacodylate buffer. Fixed sections of coral tissues were decalcified in a solution of 10% sucrose containing 3% EDTA (sodium ethylenediaminetetraacetic acid; Borowitzka and Vesk,

1978). Specimens were post-fixed for 1 h in 1.0% osmium tetroxide in sodium cacodylate buffer, dehydrated through an acetone series, and embedded in Spurr's (1969) resin. Sections were cut, stained with lead acetate and uranyl acetate, and examined with a Philips-300 transmission electron microscope.

Measurement of release of ^{14}C from zooxanthellae

In the intact association. Whole zoanthids, or 2 cm branch tips of *C. gaboensis*, were incubated in seawater containing 15 $\mu Ci^{14}C \cdot ml^{-1}$ (as $NaH^{14}CO_3$; Amersham) at 25°C under fluorescent light (78–80 $\mu E \cdot m^{-2} \cdot s^{-1}$). After 1 h, the zooxanthellae and host tissues were separated (see above), and the radioactivity of each fraction was measured using liquid scintillation counting. Supernatants were made up to a known volume, while zooxanthellae were resuspended in 20 ml of distilled water. Three 100-μl subsamples were taken from the supernatants and three 50-μl subsamples from the resuspended zooxanthellae. Each subsample was acidified with 100 μl of 0.1 *M* HCl and left in a fume hood for 4 h. Scintillation fluid (10 ml) was added to each subsample and the vial shaken to ensure mixing. The scintillation cocktail contained 0.2 g POPOP, 3.0 g PPO, and 0.5 l Teric-10 dissolved in toluene (1 l). *In vivo* experiments with *P. versipora* were not undertaken because the host tissues could not be completely extracted, nor all the zooxanthellae removed from the calcareous skeleton.

In vitro. Freshly isolated zooxanthellae ($10^6 \cdot ml^{-1}$) were incubated in 2 ml of host extract or seawater in 20 ml glass scintillation vials on a linear shaker (Grant SS40, 100 strokes $\cdot min^{-1}$) under fluorescent light (78–80 $\mu E \cdot m^{-2} \cdot s^{-1}$). At the beginning of each experiment, 10 $\mu Ci \cdot ml^{-1}$ $NaH^{14}CO_3$ was added and the vials shaken to ensure complete mixing. Triplicate 50-μl samples were taken immediately following mixing for the determination of specific activity. Each 50 μl was added to 10 ml of scintillation fluid (see above) made basic by the addition of 0.1 ml of 1.0 *M* NaOH. The radioactivity of each sample was counted for 5 min in a Packard Tri-Carb scintillation counter. Counts were corrected for quenching and background radioactivity and expressed as mg C using calculated specific activities. Calculation of specific activities was based on the total inorganic carbon content of seawater (2.52×10^{-2} mg $C \cdot ml^{-1}$, Skirrow, 1975).

Following incubation, triplicate 50-μl samples were removed from each treatment and filtered under vacuum (0.45 μm, Millipore). The filters were washed three times under vacuum with 0.65 ml of seawater to give a total filtrate volume of 2.0 ml. Three 100-μl subsamples from each filtrate were acidified with 100 μl 0.1 *M* HCl before adding 10 ml of scintillation fluid. The filters supporting zooxanthellae were dissolved in 1.0 ml 2′-methoxyethanol before adding 100 μl 0.1 *M* HCl and 10 ml of scintillation fluid. The samples were counted as described above.

The percentage of photosynthetic products released from the zooxanthellae during incubation was calculated from the ratio of the filtrate activity (^{14}C released by the algae) to the total activity (filtrate plus filter, total fixed ^{14}C).

Measurement of photosynthetic rates

Photosynthetic rates in zooxanthellae in each treatment were determined from the total ^{14}C fixed during the experiment (*i.e.*, the radioactivity of filter and filtrate combined), the specific activity and the total chlorophyll content (determined for each vial at the end of each experiment). Rates were calculated as ^{14}C-carbon fixed per mg total chlorophyll per hour. Total chlorophyll was measured using the methods of Jeffrey and Humphrey (1975).

Identification of labeled compounds

Zooxanthellae were incubated in 2 ml of seawater or host extract with 25 $\mu Ci \cdot ml^{-1}$ $NaH^{14}CO_3$. After 1 h, the zooxanthellae were removed from suspension by centrifugation, and resuspended in 3 ml of distilled water. Supernatants and suspensions of zooxanthellae were extracted by the methanol/formic acid/chloroform procedure of Barnes and Crossland (1978). The resulting chloroform phase (lipid fraction) was made up to 20 ml with chloroform, while the methanol/formic acid phase was dried at 65°C, and redissolved in 20 ml of distilled water. The radioactivity of each fraction was measured by scintillation counting as described above.

The methanol/formic acid extract was separated into neutral, acidic, and basic fractions by ion-exchange chromatography (on Sephadex SP and QAE) using Redgwell's (1980) method. The eluted fractions from the ion-exchange columns were dried and resuspended in 0.5 ml ethanol (neutral compounds and organic acids) or pyridine (amino acids and phosphate esters). Compounds in each ion-exchange fraction were separated by thin-layer chromatography on cellulose plates (Machery-Nagel Cel 300, 10 cm × 10 cm). Plates were spotted with 60 μl of sample and 20 μg of each of a set of nonradioactive standards. Basic fractions (amino acids) were chromatographed twice in the same direction in pyridine:dioxane: NH_4OH (25%):water (2:2:1:1, v/v; G.O. Kirst pers. com.). The acidic (organic acids) and neutral fractions were chromatographed twice in the same direction in EDTA:NH_4OH:water:n-propanol:isopropanol:n-butanol:isobutyric acid (0.25:20:190:70:15:15:500, w/v/v/v/v/v/v; Feige *et al.*, 1969). After drying, the compounds on each plate were visualized using a range of chemically

sensitive sprays. Ninhydrin spray reagent (Gelman catalog No. 72818) was used to detect amino acids, aniline/xylose was used for organic acids (Smith, 1960), and silver nitrate was used for monosaccharides, carbohydrates, and phosphate esters (Smith, 1960). Plates were also exposed to X-ray film (Kodak X-Omat S) for 8 weeks; the film was then developed to determine the distribution of radioactively labeled compounds. To measure the amount of ^{14}C incorporated into a given compound, the cellulose powder from each spot was scraped off and the radioactivity determined by liquid scintillation counting, as described above.

Effect of host extracts on zooxanthellae from other invertebrates

Experiments were undertaken to assess the effects of host extracts on zooxanthellae from other animals used in this study. *C. gaboensis* zooxanthellae and host extract were not included. Extracts and zooxanthellae were prepared as described above. At the beginning of the experiment, zooxanthellae from each host were resuspended in extracts of *P. versipora, Pa. ianthina, Z. robustus,* or seawater. Incubation conditions with ^{14}C, and subsequent analyses, were as described above for *in vitro* studies.

Effect of P. versipora *host extract on pre-formed products of photosynthesis*

To obtain additional information on the biochemical effects of host extracts on zooxanthellae, experiments were performed to determine if previously formed photosynthetic products are subsequently released during incubation in host extract. Zooxanthellae were incubated for one hour in seawater containing 5 $\mu Ci \cdot ml^{-1}$ $NaH^{14}CO_3$ then washed three times by centrifugation and resuspension. The zooxanthellae were then incubated for 1 h in host extract, at which time release of the "pre-formed" labeled products (formed prior to exposure to host extract) was determined. In a parallel experiment, zooxanthellae were first incubated for 1 h in seawater without ^{14}C, washed as above, then incubated in host extract, this time with $NaH^{14}CO_3$. After 1 h of incubation, release of labeled products (formed during incubation in host extract) was determined.

Effect of boiling and dialysis on P. versipora *host extracts*

To determine the heat-sensitivity of *P. versipora* extract, a freshly prepared sample was incubated in a water bath (100°C) for 10 min then cooled to room temperature. The ability of heated extract to stimulate the release of carbon from zooxanthellae was compared with that of unheated host extract.

To determine the effect of dialysis on host extract activity, a freshly prepared sample was first centrifuged for 3 min at 12,000 rpm (27,000 × *g*; 4°C; M.S.E. High Speed 18). The supernatant was filtered (0.45 μm; Millipore HA), then dialysed (Selby's, type 20, nominal pore size 10,000 D) for 6 h with rapid stirring at 4°C (two changes of 1 l buffered seawater). The ability of this treated extract to stimulate release of ^{14}C products from zooxanthellae was compared with that of undialysed extract stored at 4°C for 6 h. Dialysis tubing was boiled in deionized water for 2 h, and rinsed extensively in seawater prior to use.

Results

Photosynthesis and the release of organic ^{14}C from zooxanthellae

In the intact association (see Table I). Zooxanthellae in *C. gaboensis, Z. robustus,* and *Pa. ianthina* photosynthesized at rates ranging from 0.109 to 0.221 mg $C \cdot mg\ chlorophyll^{-1} \cdot h^{-1}$. Dark fixation rates varied from 2.7% to 6.4% of rates in the light. After one hour, a significant portion (up to 47%) of the fixed ^{14}C-carbon was found associated with host tissues. The percentage of total fixed ^{14}C-carbon detected in tissues of *Z. robustus* during July was significantly lower than at other times of the year. As noted previously, *in vivo* experiments with *P. versipora* were not conducted due to problems in complete extraction of host tissues from the calcarious skeleton.

In vitro *(see Tables IIa, IIb and III).* Zooxanthellae isolated from all the hosts photosynthesized in seawater at rates that ranged between 0.503 and 0.886 mg $C \cdot mg\ chlorophyll^{-1} \cdot h^{-1}$ (Table IIa). Dark fixation rates in seawater were 2.0–4.0% of those in light. Photosynthetic rates for zooxanthellae in host extracts were not significantly different from those in seawater ($P < 0.05$), except for *C. gaboensis.* In this case, rates in host extract were less than 1% of those in seawater, suggesting damage to algal cells or inhibition of photosynthesis. Subsequent microscopic examination revealed that all cells were lysed after incubation for one hour in this host extract (Fig. 1a). In view of this observation, zooxanthellae incubated in extracts of the other hosts were also examined microscopically (Fig. 1b, *P. versipora*), but they showed no signs of damage and were indistinguishable from those fixed in the host.

Zooxanthellae from all hosts retained approximately 95% of the organic ^{14}C fixed during incubation for 1 h in seawater. In host extracts, zooxanthellae released differing proportions of the organic ^{14}C fixed during 1 h of incubation (Table IIb). For *P. versipora,* the percentage of fixed carbon found outside zooxanthellae in host extract was significantly higher than that released in seawater ($P < 0.01$) and ranged from 10.9 to 42% of the total

Table I

Photosynthetic rates in, and percentage translocation of fixed ^{14}C-products from, zooxanthellae in vivo

Host	Experiment number[1]	% Fixed ^{14}C-products translocated[2]	Photosynthetic rate (light)[2,3]	Dark fixation rate[2,3]
Zoanthus robustus	1	35.2 ± 11.9	0.221 ± 0.092	0.006 ± 0.012
	2	42.2 ± 5.2	n.d.[4]	n.d.
	3	11.8 ± 6.2	0.126 ± 0.022	0.008 ± 0.009
Pteraeolidia ianthina[5]	1	23.8 ± 6.2	0.179 ± 0.080	0.007 ± 0.004
	2	47.5 ± 14.4	0.166 ± 0.026	0.006 ± 0.003
	3	25.1 ± 4.0	0.109 ± 0.027	0.007 ± 0.017
Capnella gaboensis	1	18.1 ± 3.5	0.185 ± 0.074	n.d.
	2	19.1 ± 3.1	0.135 ± 0.036	n.d.

[1] Experiment numbers represent investigations done in March (1), May (2), and July (3) 1981.
[2] Mean ± 95% confidence interval; n = 3 for all experiments.
[3] mg C · mg chlorophyll^{-1} · h^{-1}.
[4] n.d.—not determined.
[5] Data for *Pa. ianthina* from Hoegh-Guldberg and Hinde, 1986.

^{14}C fixed. The magnitude of release from *P. versipora* zooxanthellae was positively correlated with the protein content of the host extract (Fig. 2, *P. versipora*, $r^2 = 0.54$, $P < 0.05$). For *Z. robustus* and *Pa. ianthina*, zooxanthellae in host extracts released only a small proportion (less than 10%) of fixed ^{14}C-carbon. The proportion released was significantly ($P < 0.05$) but only slightly higher than that released in seawater, even at concentrations of host extract (as determined by protein concentration, Fig. 2) that caused in excess of 30% release in experiments with *P. versipora*. For *C. gaboensis*, between 60 and 90% of the organic ^{14}C fixed during 1 h in host extract was subsequently found outside the cells. However, as noted previously, this host extract caused lysis of zooxanthellae and inhibited photosynthesis.

The proportion of fixed ^{14}C-carbon released from *P. versipora* and *Pa. ianthina* zooxanthellae in seawater or host extracts was monitored over 4 h of incubation (Fig. 3), and did not change significantly during that period.

To investigate the possible similarities of host factors

Table II

Photosynthetic rates in, and percentage translocation of fixed ^{14}C-products from, isolated zooxanthellae in seawater and host extract[1]

a) Photosynthetic rate (mg C · mg chl^{-1} · h^{-1})

Host	Incubation medium		
	Host extract	Seawater, light	Seawater, dark
Zoanthus robustus	0.438 ± 0.231 (7)	0.503 ± 0.287 (7)	0.018 ± 0.009 (4)
Pteraeolidia ianthina	0.578 ± 0.301 (19)	0.520 ± 0.298 (19)	0.023 ± 0.003 (6)
Capnella gaboensis	0.002 (4)	0.886 ± 0.625 (3)	n.d.
Plesiastrea versipora	0.919 ± 0.612 (12)	0.877 ± 0.594 (12)	0.018 ± 0.001 (5)

b) Percentage of fixed ^{14}C-products translocated

Host	Incubation medium	
	Host extract	Seawater, light
Zoanthus robustus	7.88 ± 1.32 (7)	2.97 ± 0.88 (7)
Pteraeolidia ianthina	6.31 ± 3.15 (19)	2.42 ± 0.34 (19)
Capnella gaboensis	70.11 ± 15.40 (4)	3.45 ± 0.92 (4)
Plesiastrea versipora	26.76 ± 15.85 (12)	4.83 ± 0.51 (12)

[1] Mean ± 95% confidence interval; number of experiments conducted for each host is shown in brackets; 10^6 zooxanthellae · ml^{-1} incubation medium for each treatment; incubation time—1 h.

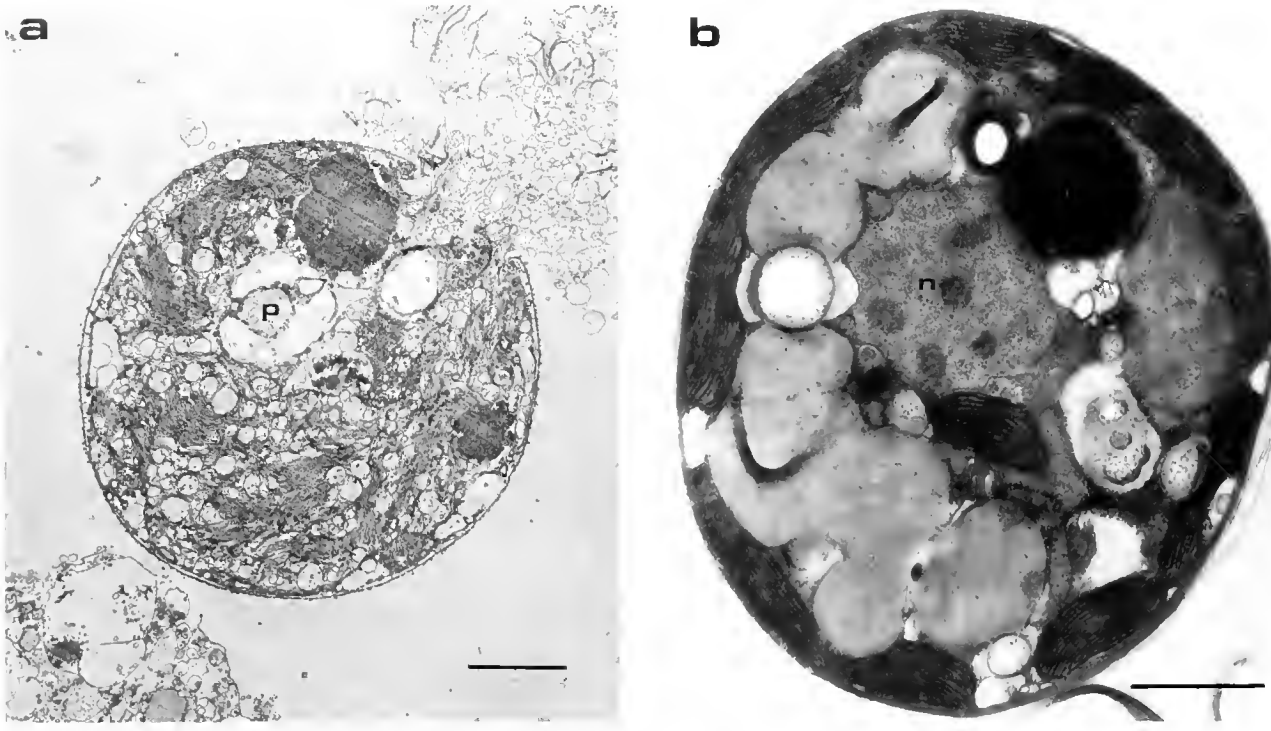

Figure 1. Ultrastructure of zooxanthellae: (a) Isolated from *Capnella gaboensis* and incubated for one hour in host extract. Note lysis and internal cellular disruption. (b) Isolated from *Plesiastrea versipora* and incubated for one hour in host extract. Transmission electron micrographs; scale bar is equivalent to 2 microns; nucleus (n), pyrenoid (p).

from different invertebrates, zooxanthellae were incubated in extracts of their own host and in extracts of hosts other than their own (Table III). *Z. robustus* and *Pa. ianthina* extracts had little effect (approximately 8% and 4–8%, respectively) on the release of ^{14}C products from both their own and other zooxanthellae. In contrast, *P. versipora* extract had no effect on *Pa. ianthina* zooxanthellae (approximately 3% release), but had a marked effect on *Z. robustus* zooxanthellae (approximately 30% release). In this latter case, the magnitude of release from *Z. robustus* zooxanthellae in host extract of *P. versipora* was about 12 times greater than in seawater, more than three times than that in *Z. robustus* extract of similar concentration, and the same as that of release by zooxanthellae from *P. versipora* in their own host extract ($P < 0.01$).

Labeled compounds detected in host extract incubations

Zooxanthellae incubated in host extract for 1 h incorporated less ^{14}C into lipid, and substantially more into neutral and organic acid fractions than they did in seawa-

Table III

Percentage of fixed ^{14}C-products released from zooxanthellae in host extract and extracts of non-host invertebrates[1]

Source of zooxanthellae	Source of host extract: *Plesiastrea versipora* (2.60)[2]	*Zoanthus robustus* (2.75)	*Pteracolidia ianthina* (2.30)	Seawater
P. versipora	27.18 ± 7.11	8.61 ± 1.00	6.49 ± 1.19	4.01 ± 0.62
Z. robustus	30.80 ± 5.62	8.52 ± 0.75	11.81 ± 3.52	2.61 ± 0.85
P. ianthina	3.97 ± 3.11	8.11 ± 4.02	7.28 ± 3.37	2.57 ± 0.41

[1] Mean ± 95% confidence interval; n = 3.

[2] Numbers in brackets refer to host extract protein concentration in mg(N)·ml^{-1}.

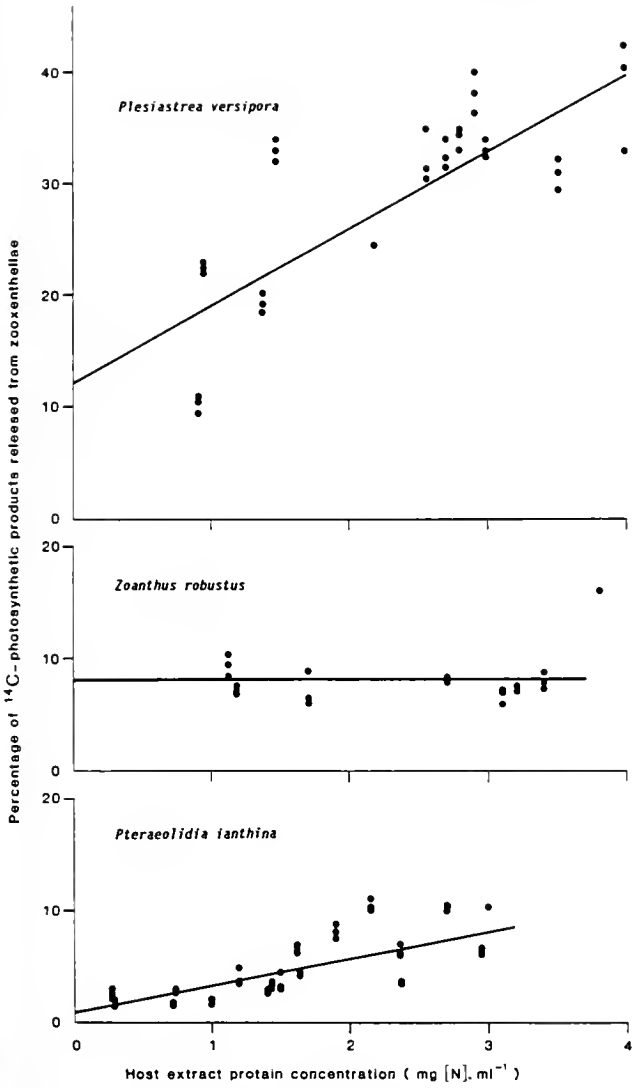

Figure 2. Release of photosynthetically fixed ^{14}C-organic carbon from zooxanthellae in host extract as a function of host extract protein content. *Plesiastrea versipora*, $r^2 = 0.54$, significant at $P < 0.01$, $y = 6.9(\times) + 12.1$. *Pteraeolidia ianthina*, $r^2 = 0.70$, significant at $P < 0.05$, $y = 2.36(\times) - 0.76$.

ter (Table IV). Neutral compounds, and to a lesser extent organic acids, were the dominant soluble labeled compounds detected outside the zooxanthellae in both seawater and host extract treatments. About 30% of the extracellular label in each treatment was in the form of glycerol (Table V), representing about 10% and 2% of the total ^{14}C fixed by zooxanthellae in host extract and seawater, respectively. There were 3–5 unidentified compounds detected extracellularly in each treatment, representing about 10% and 0.3% of the total ^{14}C fixed by zooxanthellae in host extract and seawater, respectively. In addition to neutral compounds, labeled glycollate, pyruvate, malate, and leucine were detected extracellularly in host extract but not seawater. Labeled fructose and aspartate were detected extracellularly in seawater but not host extract. Labeled alanine was found in both treatments, but was not the major labeled amino acid detailed extracellularly in either case. The major amino acid present was not identified.

Effect of P. versipora *host extract on pre-formed products of photosynthesis*

Zooxanthellae incorporating ^{14}C into photosynthetic products during an initial treatment of incubation for 1 h in seawater with label, retained most of those ("preformed") labeled products when subsequently incubated in host extract for 1 h. In contrast, zooxanthellae having an initial treatment in seawater without label but which incorporated ^{14}C into photosynthetic products during subsequent incubation for 1 h in host extract, released a significant proportion of labeled products formed during that incubation (Table VI).

Effect of boiling on host extract activity

Heating of *P. versipora* extract at 100°C for 10 min resulted in a significant loss of release-inducing activity (Table VIIa). However, zooxanthellae incubated in

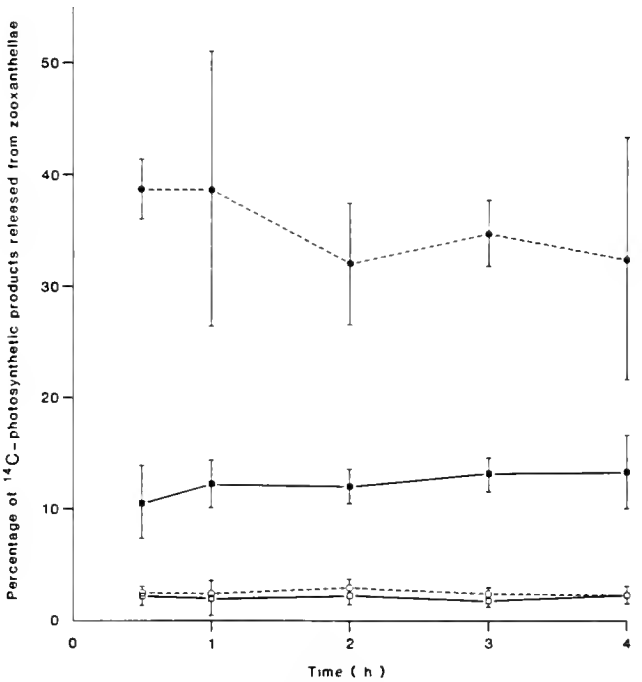

Figure 3. Release of photosynthetically fixed ^{14}C-organic carbon by zooxanthellae with time during extended exposure (4 h) to host extract. Zooxanthellae isolated from *Plesiastrea versipora* (○) and *Pteraeolidia ianthina* ([]) and incubated in seawater; zooxanthellae isolated from *P. versipora* (●) and *Pa. ianthina* (■) and incubated in host extract.

Table IV

Incorporation of ^{14}C into zooxanthellae lipid, amino acid, organic acid, and neutral compound classes, and percentage of each class detected extracellularly after incubation for one hour in seawater or Plesiastrea versipora *extract*

#	Class of compound	Zooxanthellae in seawater			Zooxanthellae in host extract		
		Intracellular	Extracellular[1]	Total	Intracellular	Extracellular[1]	Total
1	Lipid	75.4	0.2	75.6	22.5	0.5	23.0
	Amino acid	8.5	0.5	9.0	11.7	1.1	12.8
	Organic acid	3.9	0.1	4.0	11.7	9.6	21.3
	TOTAL	96.0	4.0	100.0	67.9	32.1	100.0
2	Lipid	54.1	0.6	54.7	9.0	5.3	14.3
	Amino acid	11.4	0.4	11.8	13.1	2.3	15.4
	Organic acid	9.1	1.0	10.1	13.5	18.6	32.1
	Neutral	20.5	2.9	23.4	27.0	11.2	38.2
	TOTAL	95.1	4.9	100.0	62.6	37.4	100.0
3	Lipid	53.3	0.8	54.1	24.7	0.4	25.1
	Amino acid	10.9	0.5	11.4	12.9	0.8	13.7
	Organic acid	9.1	1.3	10.4	12.8	7.7	20.5
	Neutral	20.4	3.7	24.1	24.2	16.5	40.0
	TOTAL	93.7	6.3	100.0	74.6	25.4	100.0

[#] Experiment number.
[1] "Total" extracellular for each experiment = percent ^{14}C released from zooxanthellae.

heated host extract still released slightly more ^{14}C-products than did cells incubated in seawater.

Effect of dialysis on host extract activity

The release-inducing activity of *P. versipora* extract did not decrease when the extract was dialyzed against seawater for 6 h at 4°C (Table VIIb).

Discussion

In this study, aspects of the interaction between four temperate marine invertebrates and their symbiotic zooxanthellae were examined. Extracts of the stony coral *P. versipora* may contain "host factors" that control translocation of photosynthetic products from symbiont to host. In the other invertebrates examined, no evidence of a "host factor" effect on translocation of photosynthates was found. Therefore, these observations extend to temperate symbioses the likelihood that host factors are not a universal property of symbiotic associations involving zooxanthellae. We also found that host extracts may affect zooxanthellae in previously unreported ways, apparently through their effect on metabolic pathways. Thus, in at least some symbioses, the host may have a much greater control over zooxanthellar processes then previously thought.

The transfer of fixed carbon *in vivo* from symbiont to animal tissues is significant in the nutrition of the host and has been investigated for a number of zooxanthellae/invertebrate symbioses. In tropical invertebrates, zooxanthellae release between 24 and 27% of total fixed carbon to the host in sea anemones (von Holt and von Holt, 1968a), 26–55% in corals (Muscatine and Cernichiari, 1969; Muscatine *et al.*, 1984), and 20–42% in zoanthids (von Holt and von Holt, 1968b; Trench, 1971a). Studies of translocation in temperate invertebrates are few, although significant translocation has been reported for the two temperate sea anemones, *Anthopleura elegantissima* (56%, Trench, 1971a) and *Anemonia sulcata* (60%, Taylor, 1969), respectively.

One objective of the present study, therefore, was to determine whether there was evidence for translocation of photosynthetic products from zooxanthellae to host in diverse temperate invertebrates. Results showed that zooxanthellae *in vivo* photosynthesized at rates comparable to those reported for zooxanthellae in tropical invertebrates (Porter, 1976; Scott and Jitts, 1977; Muscatine *et al.*, 1984), and that a variable but significant proportion of total fixed carbon was subsequently transferred to the host tissues. Thus, the proportion translocated ranged from 11.8% to 35.2% for *Z. robustus*, 23.8% to 47.5% for *Pa. ianthina*, and 18.0% to 19.1% for *C. gaboensis*. Difficulties encountered in achieving complete separation of tissues from the calcareous skeleton of *P. versipora* prevented any statement being made concerning photosynthesis and translocation in this association when it is intact. The possibility of seasonal variation in the translocation of fixed carbon to the host

Table V

Percentage of total extracellular fixed ^{14}C present as specific compounds after incubation of zooxanthellae for one hour in seawater or Plesiastrea versipora *extract*[1]

Compounds	Percentage of total ^{14}C released into seawater (%)	Percentage of total ^{14}C released into host extract (%)
LIPID	12.7	1.1
AMINO ACIDS		
Alanine	3.4	0.1
Aspartate	0.4	–
Leucine	–	2.3
Unidentified	4.1	1.0
ORGANIC ACIDS		
Lactate	2.1	8.5
Oxaloacetate	6.1	–
Pyruvate	–	2.9
Glycollate	–	5.4
Malate	–	3.8
Unidentified	12.4	9.7
NEUTRAL		
Glycerol	33.5	31.5
Glucose	14.4	1.7
Fructose	6.1	–
Unidentified	4.8	32.2
TOTAL	100.0	100.0

[1] % recovery of ^{14}C from incubation medium was 85% and 95% for seawater and host extract, respectively.

was suggested for *Z. robustus*, but was not demonstrated conclusively. Therefore, if the symbioses examined in this study are representative of temperate interactions involving zooxanthellae, it is apparent that they are similar to their tropical counterparts in terms of short-term movement of substantial amounts of fixed carbon from symbiont to host. The contribution of symbionts to the energy demands of the hosts in this study and in temperate invertebrates in general remains to be elucidated.

This study, and previous ones addressing the question of ways in which the host may exert control over zooxanthellae in symbiosis, relied on *in vitro* experimentation using host extracts and isolated zooxanthellae. Interpretation of results in studies of this nature is made difficult due to the possibility of experimental artifacts as a consequence of extraction or incubation procedures. Lytic effects of host extracts on isolated zooxanthellae have been reported previously (Steele and Goreau, 1977), and, in the present study, extracts of *C. gaboensis* caused both lysis of zooxanthellae and inhibition of photosynthesis. However, for *P. versipora*, *Pa. ianthina*, and *Z. robustus*, the microscopic and biochemical evidence suggests that isolation from these hosts and subsequent *in vitro* experimentation in host extracts had no detrimental effects on zooxanthellae. First, the photosynthetic rates of isolated zooxanthellae were equal to or higher than rates measured for zooxanthellae in the intact association, and were comparable to rates determined for isolated zooxanthellae from other marine invertebrates (Burris, 1977; Dunstan, 1982; Muller-Parker, 1984). Second, zooxanthellae in seawater retained more than 95% of the organic carbon fixed during four hours of incubation. Third, following incubation in host extract or seawater, zooxanthellae were microscopically indistinguishable from zooxanthellae *in vivo*.

Many studies, principally of tropical invertebrates, have suggested that the host may exert control over its symbiotic partner in at least two ways, namely by affecting the photosynthetic rate in zooxanthellae and by stimulating release of photosynthetic products. A second objective of this study was to seek evidence for similar host control of these processes in temperate invertebrates, and to determine whether there was evidence for host control of other zooxanthellar processes.

Table VI

Effect of Plesiastrea versipora *extract on release of pre-formed ^{14}C-photosynthetic products from zooxanthellae*

Initial treatment	Pre-formed ^{14}C-products present	Subsequent treatment	% Release of ^{14}C-products during 1 h in "subsequent treatment" Experiment 1	Experiment 2
SW	–	SW + ^{14}C	5.54 ± 2.83	5.95 ± 2.19
	–	HE + ^{14}C	22.43 ± 2.97	32.19 ± 2.12
SW + ^{14}C	+	SW	10.68 ± 2.71	4.60 ± 0.95
	+	HE	9.73 ± 2.53	3.92 ± 0.81

[1] Zooxanthellae (10^6/ml) incubated for 1 h in the listed treatments. SW = seawater; HE = host extract; $^{14}C = NaH^{14}CO_3$, 5 $\mu Ci \cdot ml^{-1}$.
[2] Zooxanthellae removed from "initial treatment" and incubated for 1 h in the listed "subsequent treatments."
[3] Mean ± 95% confidence interval, n = 3.

Table VII

Effect of 100°C and dialysis on ^{14}C release-inducing activity of Plesiastrea versipora *host extract*[1]

a) 100°C

	% Release of ^{14}C-products from zooxanthellae	
	Experiment 1	Experiment 2
Seawater	4.67 ± 1.14	4.70 ± 0.95
Host extract	30.37 ± 1.13	47.68 ± 1.13
100°C-treated host extract[2]	8.53 ± 1.11	12.68 ± 1.15

b) Dialysis

	% Release of ^{14}C-products from zooxanthellae
	Experiment 1
Seawater	6.40 ± 1.94
Fresh host extract	28.50 ± 3.78
Dialyzed (6 h, 4°C) extract[3]	37.40 ± 3.21
Undialyzed (6 h, 4°C) extract[3]	36.50 ± 1.59

[1] Mean ± 95% confidence interval; n = 3.

[2] Fresh host extract treated at 100°C for 10 min.

[3] Extract dialyzed at 4°C for 6 h against 2 changes of phosphate buffer, or held at 4°C for 6 h (undialyzed extract).

No evidence was found that any of the host invertebrates in this study stimulated enhanced photosynthetic rates in their symbionts. Zooxanthellae in the intact association had rates the same as, or lower than, those freshly isolated, and there was no difference in rates *in vitro* for isolated zooxanthellae in host extract or seawater. This result contrasts with two previous ones, the first for zooxanthellae from *A. elegantissima*, which were reported to fix ^{14}C in host extract at rates an order of magnitude higher than in seawater (Trench, 1971c), and the second by Muscatine *et al.* (1972) who observed an opposite trend in experiments with the hydrozoan *Millepora alcicornis*. One explanation for the different results in these three studies may be found in the experimental procedures involved. In the present study, the pH of host extracts was measured and adjusted to that of seawater at the beginning of each experiment. This may be significant, particularly considering the recent demonstration of a correlation between increased photosynthetic rate in zooxanthellae and high incubation pH (Hoegh-Guldberg, unpub. data). In the other studies noted above, the pH of the host extract was not reported, but it may have been sufficiently different from seawater controls to account for the observed differences in photosynthetic rates. A second explanation is that hosts' ability to influence photosynthetic rates in their symbiotic partners varies, and that the results of this and previous studies reflect that variability.

The second way in which hosts may exert control over zooxanthellae is through stimulation of release of photosynthetic products. Evidence that host tissues contain factors controlling release in invertebrates having zooxanthellae has been found in one temperate anemone [*A. elegantissima* (Trench, 1971c)] and in several tropical corals (Muscatine, 1967; Muscatine *et al.*, 1972). Only for *P. versipora* was strong evidence found for the presence of host release factors in this study. Relative to seawater controls, host extract of *P. versipora* stimulated release of a large proportion (up to 42%) of the carbon fixed during photosynthesis in that extract. The rate of release remained constant over four hours of incubation, and the magnitude of release was correlated with the total protein concentration of the extract. It is likely that the constant rate of release reflects the stability of the host extract factor during the incubation period. Unpublished data suggests that removal of zooxanthellae from host extract and subsequent incubation in seawater with ^{14}C causes an immediate reversion to levels of release characteristic of those in seawater. Therefore, host factor appears to cause only a temporary (during exposure) effect on release patterns.

Preliminary attempts to chemically characterize an active component from the host extract of *P. versipora* demonstrated that the release-inducing activity did not pass through dialysis tubing (nominal pore size 10,000 D) and was almost completely destroyed (approximately 80% reduction) by heating. The correlation of the magnitude of release with protein concentration, constant rate of release of fixed products, sensitivity to heat, and non-dialyzability are consistent with the host extract containing an active chemical constituent, possibly proteinaceous in nature and stimulating release of photosynthetic products from zooxanthellae. It is possible that "host factor" activity in this and previous studies is an artifact of the experimental procedure. However, the identification of a chemical having release-inducing activity *in vitro* will be a first major step in assessing the role of such chemicals in intact associations.

Results of experiments with *P. versipora* suggested the possibility of a third, and previously unreported, level of control by the host over zooxanthellar processes. Extracts of this host had a marked effect on the metabolism of zooxanthellae, resulting principally in the incorporation of photosynthetically fixed carbon into glycerol and other neutral compounds (predominantly monosaccharides). This contrasted with the incorporation of most of the photosynthetically fixed carbon into lipids in cells incubated in seawater. This is particularly interesting in view of the observation that only carbon fixed in the presence of host extract was released, while photosyn-

thetic products formed prior to exposure to extract were retained during incubation in extract. This latter result suggests that pre-formed products have entered pathways or pools where they are not affected by host extracts. Therefore, it may be that these results demonstrate a degree of host control over metabolic processes in the symbiont, whereby organic carbon, which is normally incorporated into lipids in free-living dinoflagellates, is diverted in symbiosis to pathways that result in the formation of products that may be more readily translocated to the host.

Glycerol constituted a large proportion of the algal photosynthetic products detected outside zooxanthellae after incubation in *P. versipora* extracts. It was not possible, using available methods, to demonstrate conclusively that the glycerol, or other labeled compounds detected extracellularly, was translocated, and not formed in the incubation medium as a result of heterotrophic fixation or the activity of host enzymes on unidentified compounds released from zooxanthellae. However, non-zooxanthellae (heterotrophic) fixation in host extracts of other marine invertebrates is negligible (Trench, 1971b), and glycerol is thought to be the major product translocated from zooxanthellae in marine invertebrates (Trench, 1979; Battey and Patton, 1984); up to 90% of the organic carbon translocated in short-term incubations has been reported to be in this form. Other compounds translocated include lipids (Patton *et al.*, 1977a; Kellog and Patton, 1983; Battey and Patton, 1984) and amino acids (Trench, 1971b, c). Glycerol is a lipid-soluble substance that moves easily through biological membranes (Davson and Danielli, 1952; Dainty and Ginzburg, 1964; Wright and Diamond, 1969). If the translocation of glycerol is not restricted by a membrane barrier, it seems unlikely that host factors act by affecting membrane permeability to glycerol at the interface between host and symbiont, as has been suggested (Trench, 1979) in previous studies. An alternative possibility is that host factors operate by influencing glycerol catabolism and anabolism, thereby determining the concentration gradient of glycerol between host and symbiont.

Experiments with the other invertebrates used in our study provided no strong evidence for the presence of host factors influencing translocation of photosynthetic products from zooxanthellae. This raises the question of whether temperate invertebrates in general possess host factor activity. *C. gaboensis* extract inhibited photosynthesis and lysed freshly isolated zooxanthellae. This result clearly demonstrates the possibility of artifacts in experiments of this nature, and points to the need for assessment of algal condition and physiology to detect such artifacts. Extracts prepared from *Z. robustus* and *Pa. ianthina* stimulated little release of carbon from their zooxanthellae. These latter results are in contrast with the results obtained for *P. versipora* and with the substantial release detected for *Z. robustus* and *Pa. ianthina* in the intact association. One explanation is that the active constituent or a required cofactor is destroyed during the isolation procedure for *Z. robustus* and *Pa. ianthina*. Indirect evidence that this may be the case for *Z. robustus* comes from the observation that zooxanthellae from this host released a significant proportion of photosynthetic products when exposed to *P. versipora* extract. This observation would also suggest a similarity in host factors in these two invertebrates, a phenomenon previously reported for two tropical invertebrates (Muscatine, 1967). A second explanation is that host factors are absent in *Z. robustus* and *Pa. ianthina*. Given the diversity of invertebrate hosts and different species of zooxanthellae (Blank and Trench, 1985), it is quite possible that nutrient exchange in some symbioses may be mediated, not through the activity of host factors, but through mechanisms that remain to be elucidated.

Acknowledgments

The authors gratefully acknowledge the input and guidance of Drs. R. Hinde and M. A. Borowitzka. They also thank Drs. L. Muscatine, R. K. Trench, G. J. Smith, P. V. Dunlap, M. McFall-Ngai, and M. D. Hauser for reviewing an earlier draft of this manuscript.

Literature Cited

Barnes, D. J., and C. J. Crossland. 1978. Diurnal productivity and apparent ^{14}C-calcification in the staghorn coral *Acropora acuminata*. *Comp. Biochem. Physiol.* **59:** 133–138.

Battey, J. F., and J. S. Patton. 1984. A re-evaluation of the role of glycerol in carbon-translocation in zooxanthellae-ceolenterate symbiosis. *Mar. Biol.* **79:** 27–38.

Blank, R. J., and R. K. Trench. 1985. Speciation and symbiotic dinoflagellates. *Science* **229:** 656–658.

Blanquet, R. S., D. Emanuel, and T. A. Murphy. 1988. Suppression of exogenous alanine uptake in isolated zooxanthellae by cnidarian host homogenate fractions: species and symbiosis specificity. *J. Exp. Mar. Biol. Ecol.* **117:** 1–8.

Borowitzka, M. A., and M. Vesk. 1978. Ultrastructure of the Corallinaceae: 1. The vegetative cells of *Corallina officialis* and *Corallina cuverii*. *Mar. Biol.* **46:** 295–304.

Burris, J. E. 1977. Photosynthesis, photorespiration and dark respiration in eight species of algae. *Mar. Biol.* **39:** 371–379.

Carroll, S., and R. S. Blanquet. 1984. Alanine uptake by isolated zooxanthellae of the mangrove jellyfish, *Cassiopea xamachana*. II. Inhibition by host homogenate fraction. *Biol. Bull.* **166:** 419–426.

Cook, C. B. 1971. Transfer of ^{35}S-labelled material from food ingested by *Aiptasia* sp. to its endosymbiotic zooxanthellae. In *Experimental Coelenterate Biology*, H. M. Lenhoff and L. Muscatine, eds. University of Hawaii Press, Honolulu.

Dainty, J., and B. Z. Ginzburg. 1964. The reflection coefficients of plant cell membranes for certain solutes. *Biochem. Biophys. Acta* **79:** 129–137.

Davson, H., and J. F. Danielli. 1952. *The Permeability of Natural Membranes*, 2nd ed. Cambridge University Press.

Dustan, P. 1982. Depth-dependent photoadaptation by zooxanthellae of the coral *Montastrea annularis*. *Mar. Biol.* **68:** 252–264.

Feige, B., H. Gimmler, W. D. Jeschke, and W. Simonis. 1969. Eine methode zur dunnschichtchromatographischen auftrennung von ^{14}C und ^{32}P-markierten stoffwechselprodukten. *J. Chromatog.* **41:** 80–90.

Franzisket, L. 1970. The atrophy of hermatypic reef corals maintained in darkness and their subsequent regeneration in the light. *Int. Rev. Ges. Hydrobiol.* **55:** 1–12.

Hoegh-Guldberg, O., and R. Hinde. 1986. Studies on a nudibranch that contains zooxanthellae. I. Photosynthesis, respiration and the translocation of newly fixed carbon by zooxanthellae in *Pteraeolidia ianthina*. *Proc. R. Soc. Lond. B.* **228:** 493–509.

von Holt, C., and M. von Holt. 1968a. Transfer of photosynthetic products from zooxanthellae to coelenterate hosts. *Comp. Biochem. Physiol.* **24:** 73–81.

von Holt, C., and M. von Holt. 1968b. The secretion of organic compounds by zooxanthellae isolated from various types of *Zoanthus*. *Comp. Biochem. Physiol.* **24:** 83–92.

Jacques, T. G., and M. E. Q. Pilson. 1980. Experimental ecology of the temperate scleractinian coral *Astrangia danae* I. Partition of respiration, photosynthesis and calcification between host and symbionts. *Mar. Biol.* **60:** 167–178.

Jacques, T. G., N. Marshall, and M. E. Q. Pilson. 1983. Experimental ecology of the temperate scleractinian coral *Astrangia danae* II. Effect of temperature, light intensity and symbiosis with zooxanthellae on metabolic rate and calcification. *Mar. Biol.* **76:** 135–148.

Jeffrey, S. W., and G. F. Humphrey. 1975. New spectrophotometric equations for determining chlorophylls *a*, *b*, *c* and *c* in higher plants, algae and natural phytoplankton. *Biochem. Physiol. Pflanzen* **167:** 191–194.

Johannes, R. E. 1974. Sources of nutritional energy for reef corals. *Proc. 2nd Int. Coral Reef Symp.* 133–137.

Kellog, R. B., and J. S. Patton. 1983. Lipid droplets: medium of energy exchange in the symbiotic anemone *Condylactis gigantea*: a model coral polyp. *Mar. Biol.* **75:** 137–150.

Kempf, S. C. 1984. Symbioses between the zooxanthella *Symbiodinium* (= *Gymnodinium*) *microadriaticum* (Freudenthal) and four species of nudibranch. *Biol. Bull.* **166:** 110–126.

Kevin, K. M., and R. C. L. Hudson. 1979. The role of zooxanthellae in the hermatypic coral *Plesiastrea urvillea* (Milne-Edwards & Haime) from cold waters. *J. Exp. Mar. Biol. Ecol.* **36:** 157–170.

Lowry, O. H., N. J. Rosenbrough, A. L. Farr, and R. J. Randall. 1951. Protein measurement with the Folin reagent. *J. Biol. Chem.* **193:** 265–275.

Muller-Parker, G. 1984. Photosynthesis-irradiance responses and photosynthetic periodicity in the sea anemone *Aiptasia pulchella* and its zooxanthellae. *Mar. Biol.* **82:** 225–232.

Muscatine, L. 1967. Glycerol excretion by symbiotic algae from corals and *Tridacna*, and its control by the host. *Science* **156:** 516–519.

Muscatine, L., and E. Cernichiari. 1969. Assimilation of photosynthetic products of zooxanthellae by a reef coral. *Biol. Bull.* **137:** 506–523.

Muscatine, L., R. R. Pool, and E. Cernichiari. 1972. Some factors influencing selective release of soluble organic material by zooxanthellae from reef corals. *Mar. Biol.* **13:** 298–308.

Muscatine, L., and J. W. Porter. 1977. Reef corals: mutualistic symbioses adapted to nutrient-poor environments. *Bioscience* **27:** 454–460.

Muscatine, L., P. G. Falkowski, and Z. Dubinsky. 1983. Carbon budgets in symbiotic associations. Pp. 649–658 in *Endocytobiology II Intracellular Space as Oligogenetic Ecosystem*, H. E. A. Schenk and W. Schwemmler, eds. Walter de Gruyter, Berlin and New York.

Muscatine, L., P. G. Falkowski, J. W. Porter, and Z. Dubinsky. 1984. Fate of photosynthetic carbon in light- and shade-adapted colonies of the symbiotic coral *Stylophora pistillata*. *Proc. R. Soc. Lond. B* **222:** 181–202.

Patton, J. S., S. Abraham, and A. A. Benson. 1977. Lipogenesis in the intact coral *Pocillopora capitata* and its isolated zooxanthellae: evidence for a light-driven cycle between symbiont and host. *Mar. Biol.* **44:** 235–247.

Porter, J. W. 1976. Autotrophy, heterotrophy and resource partitioning in Caribbean reef-building corals. *Am. Nat.* **110:** 731–742.

Redgewell, R. J. 1980. Fractionation of plant extracts using ion-exchange Sephadex. *Anal. Biochem.* **107:** 44–50.

Rudman, W. B. 1981. The anatomy and biology of alcyonarian-feeding aeolid opisthobranch molluscs and their development of symbiosis with zooxanthellae. *Zool. J. Linn. Soc.* **72:** 219–262.

Rudman, W. B. 1982. The taxonomy and biology of further aeolid and arminacean nudibranch molluscs with symbiotic zooxanthellae. *Zool. J. Linn. Soc.* **74:** 147–196.

Scott, B. D., and H. R. Jitts. 1977. Photosynthesis of phytoplankton and zooxanthellae on a coral reef. *Mar. Biol.* **41:** 307–315.

Skirrow, G. 1975. The dissolved gases—carbon dioxide. Pp. 1–192 in *Chemical Oceanography*, J. P. Riley and G. Skirrow, eds. Academic Press, New York and London.

Smith, I. 1960. *Chromatographic and Electrophoretic Techniques*, Heinemann, London. 617 pp.

Spurr, A. R. 1969. A low-viscosity epoxy resin embedding medium for electron microscopy. *J. Ultrastr. Res.* **26:** 31–43.

Steele, R. D., and N. I. Goreau. 1977. The breakdown of symbiotic zooxanthellae in the sea anemone *Phyllactis* (= Oulactus) *flosculifera* (Actiniara). *J. Zool. Lond.* **181:** 421–437.

Taylor, D. L. 1969. On the regulation and maintenance of algal numbers in zooxanthellae-coelenterate symbiosis, with a note on the nutritional relationship in *Anemonia sulcata*. *J. Mar. Biol. Assoc. U. K.* **49:** 1057–1065.

Trench, R. K. 1971a. The physiology and biochemistry of zooxanthellae symbiotic with marine coelenterates. I. The assimilation of photosynthetic products of zooxanthellae by two marine coelenterates. *Proc. R. Soc. Lond. B* **177:** 224–235.

Trench, R. K. 1971b. The physiology and biochemistry of zooxanthellae symbiotic with marine coelenterates. II. Liberation of fixed ^{14}C by zooxanthellae *in vitro*. *Proc. R. Soc. Lond. B* **177:** 235–250.

Trench, R. K. 1971c. The physiology and biochemistry of zooxanthellae symbiotic with marine coelenterates. III. The effect of homogenates of host tissues on the excretion of photosynthetic products *in vitro* by zooxanthellae from two marine coelenterates. *Proc. R. Soc. Lond. B* **177:** 251–264.

Trench, R. K. 1979. The cell biology of plant-animal symbiosis. *Ann. Rev. Pl. Physiol.* **30:** 485–531.

Tytler, E. M., and P. S. Davies. 1986. The budget of photosynthetically derived energy in the *Anemonia sulcata* (Pennant) symbiosis. *J. Exp. Mar. Biol. Ecol.* **99:** 257–269.

Wright, E. M., and J. M. Diamond. 1969. Patterns of non-electrolyte permeability. *Proc. R. Soc. Lond. B* **172:** 227–271.

Yu, S. L., and W. E. Dietrich. 1977. Effect of host homogenates on photosynthate excretion by zoochlorellae of *Hydra viridis*. *Proc. Pennsylvania Acad. Sci.* **51:** 137–138.

CONTENTS

Volume 178 Number 3

THE BIOLOGICAL BULLETIN

JUNE, 1990

Published by the Marine Biological Laboratory

THE BIOLOGICAL BULLETIN

PUBLISHED BY
THE MARINE BIOLOGICAL LABORATORY

JUNE, 1990

Printed and Issued by
LANCASTER PRESS, Inc.
PRINCE & LEMON STS.
LANCASTER, PA

THE BIOLOGICAL BULLETIN is published six times a year by the Marine Biological Laboratory, MBL Street, Woods Hole, Massachusetts 02543.

Subscriptions and similar matter should be addressed to Subscription Manager, THE BIOLOGICAL BULLETIN, Marine Biological Laboratory, Woods Hole, Massachusetts 02543. Single numbers, $25.00. Subscription per volume (three issues), $57.50 ($115.00 per year for six issues).

Communications relative to manuscripts should be sent to Michael J. Greenberg, Editor-in-Chief, or Pamela L. Clapp, Managing Editor, at the Marine Biological Laboratory, Woods Hole, Massachusetts 02543. Telephone: (508) 548-3705, ext. 428. FAX: 508-540-6902.

POSTMASTER: Send address changes to THE BIOLOGICAL BULLETIN, Marine Biological Laboratory, Woods Hole, MA 02543.

Second-class postage paid at Woods Hole, MA, and additional mailing offices.
ISSN 0006-3185

INSTRUCTIONS TO AUTHORS

The Biological Bulletin accepts outstanding original research reports of general interest to biologists throughout the world. Papers are usually of intermediate length (10–40 manuscript pages). Very short papers (less than 9 manuscript pages including tables, figures, and bibliography) will be published in a separate section entitled "Notes." A limited number of solicited review papers may be accepted after formal review. A paper will usually appear within four months after its acceptance.

The Editorial Board requests that manuscripts conform to the requirements set below; those manuscripts that do not conform will be returned to authors for correction before review.

1. ***Manuscripts.*** Manuscripts, including figures, should be submitted in triplicate. (Xerox copies of photographs are not acceptable for review purposes.) The original manuscript must be typed in no smaller than 12 pitch, using double spacing (*including* figure legends, footnotes, bibliography, etc.) on one side of 16- or 20-lb, bond paper, 8½ by 11 inches. Please, no right justification. Manuscripts should be proofread carefully and errors corrected legibly in black ink. Pages should be numbered consecutively. Margins on all sides should be at least 1 inch (2.5 cm). Manuscripts should conform to the *Council of Biology Editors Style Manual*, 4th Edition (Council of Biology Editors, 1978) and to American spelling. Unusual abbreviations should be kept to a minimum and should be spelled out on first reference as well as defined in a footnote on the title page. Manuscripts should be divided into the following components: Title page, Abstract (of no more than 200 words), Introduction, Materials and Methods, Results, Discussion, Acknowledgments, Literature Cited, Tables, and Figure Legends. In addition, authors should supply a list of words and phrases under which the article should be indexed.

2. ***Title page.*** The title page consists of: a condensed title or running head of no more than 35 letters and spaces, the manuscript title, authors' names and appropriate addresses, and footnotes listing present addresses, acknowledgments or contribution numbers, and explanation of unusual abbreviations.

3. ***Figures.*** The dimensions of the printed page, 7 by 9 inches, should be kept in mind in preparing figures for publication. We recommend that figures be about 1½ times the linear dimensions of the final printing desired, and that the ratio of the largest to the smallest letter or number and of the thickest to the thinnest line not exceed 1:1.5. Explanatory matter generally should be included in legends, although axes should always be identified on the illustration itself. Figures should be prepared for reproduction as either line cuts or halftones. Figures to be reproduced as line cuts should be unmounted glossy photographic reproductions or drawn in black ink on white paper, good-quality tracing cloth or plastic, or blue-lined coordinate paper. Those to be reproduced as halftones should be mounted on board, with both designating numbers or letters and scale bars affixed directly to the figures. All figures should be numbered in consecutive order, with no distinction between text and plate figures. The author's name and an arrow indicating orientation should appear on the reverse side of all figures.

4. ***Tables, footnotes, figure legends, etc.*** Authors should follow the style in a recent issue of *The Biological Bulletin* in preparing table headings, figure legends, and the like. Because of the high cost of setting tabular material in type, authors are asked to limit such material as much as possible. Tables, with their headings and footnotes, should be typed on separate sheets, numbered with consecutive Roman numerals, and placed after the Literature Cited. Figure legends should contain enough information to make the figure intelligible separate from the text. Legends should be typed double spaced, with consecutive Arabic numbers, on a separate sheet at the end of the paper. Footnotes should be limited to authors' current addresses, acknowledgments or contribution numbers, and explanation of unusual abbreviations. All such footnotes should appear on the title page. Footnotes are not normally permitted in the body of the text.

5. ***Literature cited.*** In the text, literature should be cited by the Harvard system, with papers by more than two authors cited as Jones *et al.*, 1980. Personal communications and material in preparation or in press should be cited in the text only, with author's initials and institutions, unless the material has been formally accepted and a volume number can be supplied. The list of references following the text should be headed Literature Cited, and must be typed double spaced on separate

pages, conforming in punctuation and arrangement to the style of recent issues of *The Biological Bulletin*. Citations should include complete titles and inclusive pagination. Journal abbreviations should normally follow those of the U. S. A. Standards Institute (USASI), as adopted by BIOLOGICAL ABSTRACTS and CHEMICAL ABSTRACTS, with the minor differences set out below. The most generally useful list of biological journal titles is that published each year by BIOLOGICAL ABSTRACTS (BIOSIS List of Serials; the most recent issue). Foreign authors, and others who are accustomed to using THE WORLD LIST OF SCIENTIFIC PERIODICALS, may find a booklet published by the Biological Council of the U.K. (obtainable from the Institute of Biology, 41 Queen's Gate, London, S.W.7, England, U.K.) useful, since it sets out the WORLD LIST abbreviations for most biological journals with notes of the USASI abbreviations where these differ. CHEMICAL ABSTRACTS publishes quarterly supplements of additional abbreviations. The following points of reference style for THE BIOLOGICAL BULLETIN differ from USASI (or modified WORLD LIST) usage:

A. Journal abbreviations, and book titles, all underlined (for *italics*)

B. All components of abbreviations with initial capitals (not as European usage in WORLD LIST *e.g. J. Cell. Comp. Physiol.* NOT *J. cell. comp. Physiol.*)

C. *All* abbreviated components must be followed by a period, whole word components *must not* (*i.e. J. Cancer Res.*)

D. Space between all components (*e.g. J. Cell. Comp. Physiol.*, not *J Cell Comp Physiol.*)

E. Unusual words in journal titles should be spelled out in full, rather than employing new abbreviations invented by the author. For example, use *Rit Visindafjélags Islendinga* without abbreviation.

F. All single word journal titles in full (*e.g. Veliger, Ecology, Brain*).

G. The order of abbreviated components should be the same as the word order of the complete title (*i.e. Proc.* and *Trans.* placed where they appear, not transposed as in some BIOLOGICAL ABSTRACTS listings).

H. A few well-known international journals in their preferred forms rather than WORLD LIST or USASI usage (*e.g. Nature, Science, Evolution* NOT *Nature, Lond., Science, N.Y., Evolution, Lancaster, Pa.*)

6. ***Reprints, page proofs, and charges.*** Authors receive their first 100 reprints (without covers) free of charge. Additional reprints may be ordered at time of publication and normally will be delivered about two to three months after the issue date. Authors (or delegates for foreign authors) will receive page proofs of articles shortly before publication. They will be charged the current cost of printers' time for corrections to these (other than corrections of printers' or editors' errors). Other than these charges for authors' alterations, *The Biological Bulletin* does not have page charges.

CONTENTS

No. 3, June 1990

BEHAVIOR

DEVELOPMENT AND REPRODUCTION

GENERAL BIOLOGY

PHYSIOLOGY

SHORT REPORTS

Reference: *Biol. Bull.* **178**: 187–194. (June, 1990)

Electromyographic Record of Classical Conditioning of Eye Withdrawal in the Crab

RICHARD D. FEINMAN, RAFAEL H. LLINAS, CHARLES I. ABRAMSON, AND ROBIN R. FORMAN[1]

Department of Biochemistry, State University of New York Health Science Center at Brooklyn, Brooklyn, New York 11203, [1]Department of Neurology, Medical College of Virginia, Richmond, Virginia 23298, and Marine Biological Laboratory, Woods Hole, Massachusetts 02543

Abstract. Classical (Pavlovian) conditioning of the eye withdrawal reflex of the green crab, *Carcinus maenas*, was studied by recording electromyograms (EMGs) from the main abductor muscle of the eye (19a). The EMG record was a reliable indicator of the response, and it was always correlated with physical movement of the eye, whether evoked by the unconditioned stimulus (a puff of air to the eye), or by the conditioned stimulus (a mild vibration of the carapace). The EMG was used to study the acquisition of conditioned responses in animals with an immobilized eye. Six of eight experimental animals developed responses to the conditioned stimulus in a manner similar to that for animals with freely moving eyes; unpaired controls showed few responses. The results indicate that eye movement is not required for learning. Behavioral tests after conditioning and after the eyes had been freed supported this conclusion. The results exclude theories of classical conditioning of eye withdrawal that invoke a role for stimuli due to eye movement (such as a change in visual field).

Introduction

The eye withdrawal reflex of the crab is one of the simple invertebrate behaviors in which learning can be demonstrated (Abramson and Feinman, 1987; Abramson *et al.*, 1988; Abramson and Feinman, 1988; Appleton and Wilkens, 1990). Classical (Pavlovian) conditioning of the response is brought about by pairing a previously neutral stimulus (vibration of the carapace) with an aversive stimulus (an air-puff to one of the eyes). The air-puff [unconditioned stimulus (US)] invariably causes eye retraction. After several pairings of the US with the vibration [conditioned stimulus (CS)], eye retraction begins to appear during CS presentations. The responses can be recorded in several ways. In addition to direct observation, movement can be recorded by optical or capacitive methods (Sandeman, 1968; Forman and Brumbley, 1980; Miall and Hereward, 1988), or by the force generated during retraction (Erber and Sandeman, 1989; Appleton and Wilkens, 1990). Electromyograms (EMGs) are also easily recorded (Burrows and Horridge, 1968) and, in this report, we describe the use of EMGs recorded from the main abductor muscle of the eye (muscle 19a) as an indicator of the response. The method allows us to record responses in the restrained eye, and we use it to show that physical movement of the eye is not required for learning.

One of the virtues of this system is that some of the physiology has already been characterized (Burrows, 1967; Sandeman, 1967, 1969b) and, therefore, the neuronal substrate of conditioning may be accessible. Several features of eye withdrawal make it desirable for such an analysis. Retraction is mediated by only two motor neurons, one of which is identified and has a giant axon (Burrows, 1967; Sandeman, 1967, 1969a; Burrows and Horridge, 1968); the activity of this unit is the signal of greatest amplitude in the EMG recorded from muscle 19a. Studies of eye withdrawal have shown that there is no requirement for proprioceptive feedback; whether this is true under conditions where learning occurs is unknown. Although less well characterized, the sensory

Received 18 January 1990; accepted 22 March 1990.

Abbreviations: Electromyogram (EMG); conditioned stimulus (CS); unconditioned stimulus (US); conditioned response (CR); and unconditioned response (UR).

afferents are also known and are believed to make largely monosynaptic contacts with the motor neuron (Sandeman, 1969a, 1969b).

The role of eye movement also bears on long-standing problems in the psychology of learning. The eye withdrawal reflex can be trained in a signalled avoidance procedure in which US presentation can be avoided, if the eye is retracted during the CS, which acts as a "warning signal" (Abramson *et al.*, 1988). Acquisition of conditioned eye withdrawal in avoidance followed a time course similar to that for classical conditioning, suggesting that animals might not benefit from being able to control the contingencies of reinforcement. In other words, the animal might effectively have been in a classical conditioning experiment in which some USs were omitted. The paradox is that controls that were subjected to the same sequence of USs and omissions did poorly, whereas, if the contingency between eye withdrawal and absence of US were not important, they should have done as well as the experimentals. A similar result has been observed for vertebrates in some learning procedures (Moore and Gormezano, 1961; Gormezano, 1965; Woodward and Bitterman, 1973). One theory that has been proposed to explain these results is that animals are receiving a compound CS composed of the vibration *plus* the change in sensory input (such as visual field) that occurs as a consequence of the eye movement. The results reported here suggest that the consequences of the eye movement do not play a necessary role in classical conditioning, and therefore, that the theory cannot explain the similarity of classical conditioning and avoidance, at least in the crab eye withdrawal reflex.

Materials and Methods

The general experimental setup for classical conditioning has been described (Abramson and Feinman, 1988). The CS was a low amplitude 200 Hz vibration administered to the carapace via a needle attached to a loudspeaker. The US was a low intensity puff of air delivered to the eye to be conditioned. In the experiments described here, a 1-s presentation of the CS was followed immediately by a 0.1-s presentation of the US. In general, the eye was re-elevated after the retraction; in cases where this did not occur, the animal was gently tipped or one of the legs was moved to cause the eye to come back up. For recording myograms, a single hole was made, with the tip of a hypodermic needle, in the cuticle surrounding the eye, and two 50-μ wires were inserted into muscle 19a and attached to the cuticle with cyanoacrylate glue. Placement of electrodes was confirmed by dissection of formaldehyde-fixed samples. The insertion of the EMG electrodes had a sensitizing effect, and animals would respond to a level of vibration that was normally without effect. Thirty minutes after implanting the electrodes, this sensitivity was sufficiently reduced so that there was no response to three or four successive stimuli. Scoring of conditioned responses in myographic records of animals with restrained eyes was done blind; a naive observer was instructed to score EMG patterns during the CS that resembled those seen during the US.

Results

Electromyographic measurement of acquisition

The first experiment demonstrated the feasibility of using the EMG record to follow conditioning. Four experimental animals and four controls had EMG electrodes implanted in muscle 19a of one eye; the eye moved freely after this manipulation. The experimentals were subjected to 50 paired presentations of stimuli as described in Materials and Methods; controls were given 50 presentations of unpaired stimuli. Panel A of Figure 1 shows EMG records of several trials for one of the experimental animals. The characteristic spiking pattern due to the activity of the fast retractor motor neuron of the optic nerve is reliably seen in response to presentation of the US. Slow tonic activity is also seen in some traces in panel A. These are due to the activity of a smaller neuron of the oculomotor nerve; the tonic firing of this unit correlates with the eye being held down (Sandeman, 1964; Burrows, 1967; Burrows and Horridge, 1968). Muscle 19a is more sparsely innervated by this neuron than by the larger retractor neuron, and the tonic activity is not seen in every preparation. After several trials, a pattern of spiking activity similar to that caused by the US is now evoked during the CS. This pattern in the CS or US was always correlated with observed retraction of the eye.

Two features of the EMG record were not obvious from simple observation of the gross behavior. First, as is evident in Figure 1, the conditioned responses (CRs), when they appear, are frequently more robust than the unconditioned response (UR). In addition, although not a feature of all sessions, the UR frequently showed habituation even as the CR developed (data not shown). This phenomenon has been studied more thoroughly by Appleton and Wilkens (1990). The pattern of acquisition seen in the present work is qualitatively similar to the acquisition of CRs as previously described (Abramson *et al.*, 1988; Abramson and Feinman, 1988). There were few, if any, spontaneous eye retractions (or bursts of phasic activity in the EMG record) during the intervals between stimuli presentation.

To assess the effect of the insertion of electrodes, the behavior was compared to that of a second group of four experimental and four unpaired control animals that had never had EMG wires implanted. Responses of the experimentals and the controls were tallied and the aver-

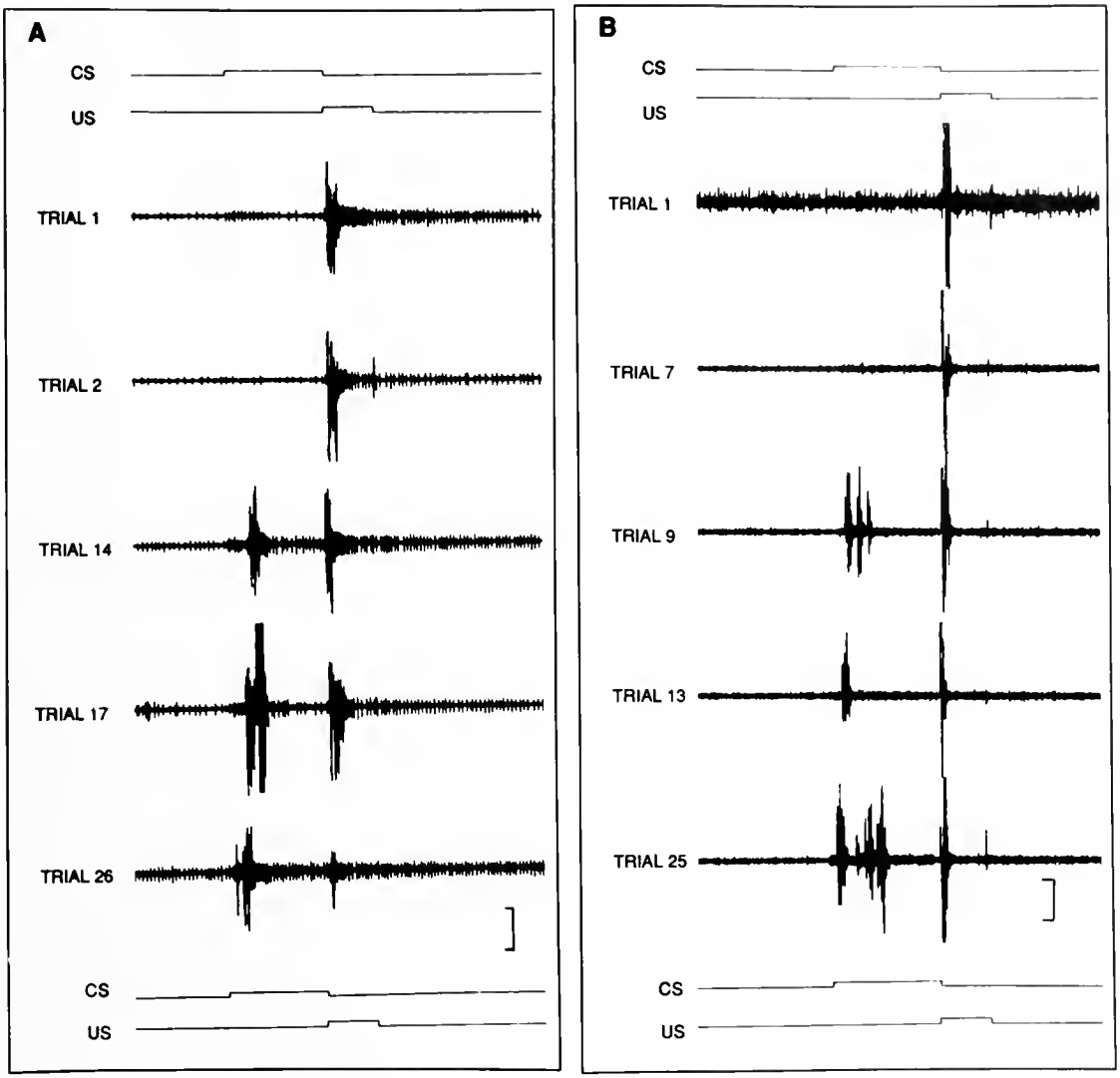

Figure 1. Electromyographic record of classical conditioning. EMGs were recorded from muscle 19a of the eye to be conditioned. A. Results for a typical animal with a freely moving eye. B. Results while the eye is physically restrained. Large amplitude spikes are due to activity of the fast phasic motor neuron of the optic nerve. Slow tonic activity evident in traces in panel A are due to a neuron of the oculomotor nerve which more sparsely innervates 19a and whose activity correlates with maintenance of the retracted state. The CS duration is 1 s. The vertical bar corresponds to 200 μV except in TRIAL 1 of panel B where it represents 100 μV. Animals were trained with paired presentation of CS and US (top and bottom traces). Animals in panel B had the eye temporarily immobilized with a rubber band.

age responses for each five-trial block were plotted (first panel of Fig. 2). The behavior of the two sets of animals, with and without EMG wires, is manifestly similar: the paired animals of each group showed an increase in the probability to respond reaching a plateau probability of 50–60%, whereas the corresponding unpaired groups showed a much lower tendency to respond (see below for statistical comparison). Thus, learning is fundamentally the same in animals with and without EMG electrodes; for qualitative comparisons to animals with restrained eyes, these two groups were pooled and considered as a population of eight animals trained with freely moving eyes. However, there were some differences. First, Figure 2 shows that the EMG animals were sensitized, as indicated by their higher probability to respond at the outset of training (first 5-trial block). The mean probability of response for EMG animals in this period was 0.35 (SD 0.25) compared to 0.05 (SD 0.10) for unoperated animals. A second difference is the somewhat greater variability in the EMG animals. To see this difference we plotted individual animal data as a cumulative record, or running total, in Figure 3 (panels A and B). Usually

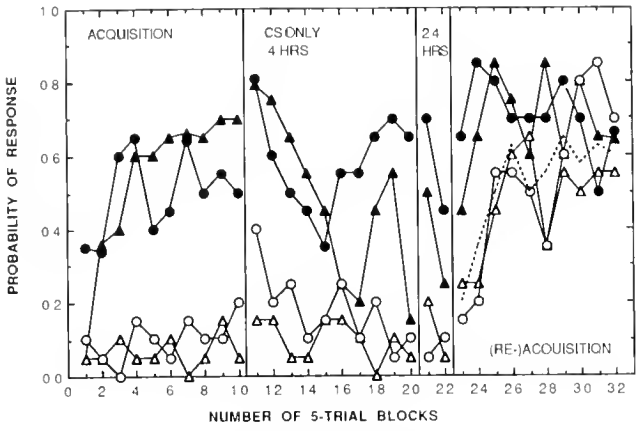

Figure 2. Effect of implanting EMG electrodes during acquisition on behavioral performance. Group data for behavior in ACQUISITION, RETENTION, and RE-ACQUISITION of classical conditioning. Data points are averages of four animals each. Filled symbols: animals receiving paired stimuli during ACQUISITION. Open symbols: animals receiving specifically unpaired stimuli during ACQUISITION. Two populations were used. Triangles: normal unoperated animals; Circles: animals with EMG wires implanted. In RE-ACQUISITION, dotted line is first day performance of the average of the (8) experimental animals and is included for comparison. Probability of response is calculated as the total number of responses per animal per five-trial block.

applied to operant conditioning experiments, a cumulative record is a good method for looking at trial-by-trial data. It is evident that, again, the groups are very similar, but inserting the EMG wires introduces variability in the pattern of response. In summary, the EMG record is a reliable method for following conditioning—the large differences between paired and unpaired groups are maintained—but the process of inserting electrodes may have a somewhat sensitizing effect on the CS responses.

Pattern of behavior after conditioning

As a second method of assessing the effect of training, we recorded a profile of behavioral responses after conditioning. For animals with EMG leads, wires were cut. All animals were returned to the home tank and then all (paired and unpaired controls) were tested for responses in three behavioral procedures. First, after 4 h, animals were given 50 CS-only presentations (second panel of Fig. 2). Then, after an additional 20 h, they were re-tested for responses to 10 CS-presentations (third panel of Fig. 2). Immediately after these 10 CS-only trials, animals were subjected to a second training session (last panel). During this second training period, the unpaired controls from the first day were given paired presentation of stimuli to determine whether this population was, in fact, capable of learning and whether there was an effect of the previous day's experience as controls. It is evident from Figure 2 that: the paired group showed substantial retention after 4 h as measured by the CS-only responses, and that extinction is fairly rapid; unpaired controls showed few CRs; and in both cases there was a considerable variation among animals. There is also a rebound of the experimentals' response to the conditioned stimulus after 24 h; the unpaired group, again, showed few responses. The last panel in Figure 2 indicates an enhanced re-acquisition of the task by the subjects that had been experimentals on the first day; this is consistent with earlier re-

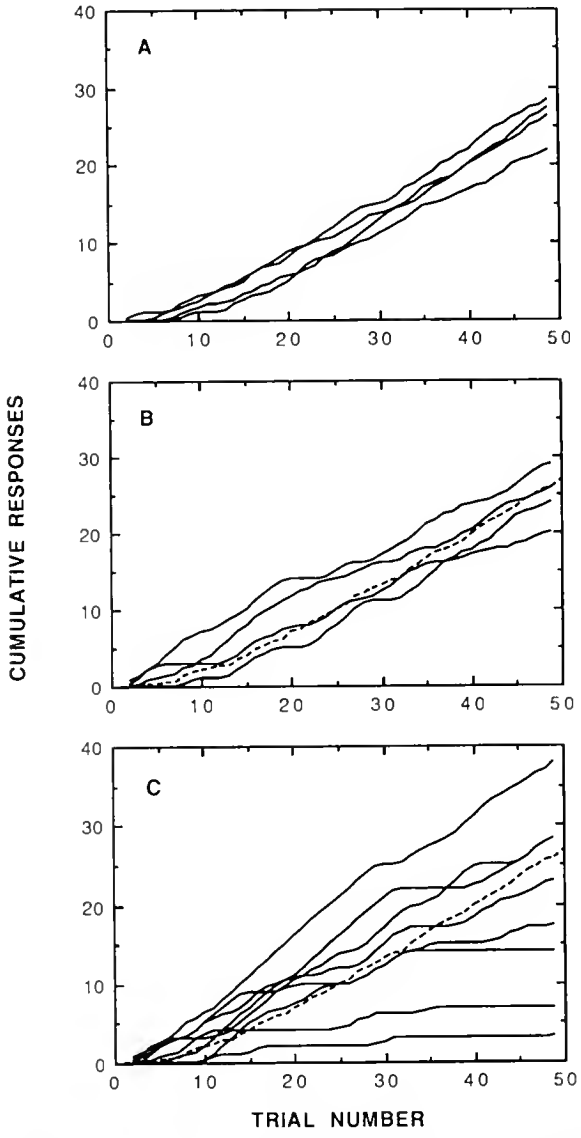

Figure 3. Cumulative record for acquisition of conditioned responses. Results are shown for all experimental (paired CS, US) subjects. A. Normal subjects, unoperated. B. Freely moving eyes with EMG electrodes implanted. C. Animals with EMG leads and conditioned eye immobilized. In B and C, the dotted line represents the average of the records for the four animals in A. Data were smoothed, for graphic clarity, by averaging over three trials at a time.

ports (Abramson and Feinman, 1988). Likewise, controls from day-one now showed a high probability to respond, indicating that there was nothing unusual about this group and that their performance was not repressed by their previous experience as unpaired controls, again consistent with original observations. Figure 2 shows that this day-two acquisition by controls has a very similar time dependence to the day-one acquisition by experimentals (dotted line), indicating that the controls were also not sensitized and had not fortuitously made a CS-US association. This general pattern of responses was similar for both groups: normal animals and those with EMG electrodes.

Electromyographic record of conditioning of a restrained eye

With the behavioral pattern of acquisition, retention, and re-acquisition as background, we next prepared 16 new animals with silver wire electrodes in the eye and now restrained one eye (to be conditioned) with rubber bands. Eight of these animals were subjected to the paired presentation of stimuli as above, while the other eight served as controls and were given specifically unpaired CS, US presentations. Conditioned responses were scored from the EMG record. Activity during CS presentations that resembled those during the US were considered conditioned responses. Figure 1B shows characteristic EMG patterns typical of these animals. Six of the eight experimental animals showed development of a conditioned EMG response in a manner similar to the groups with freely moving eyes. None of the unpaired controls showed the normal acquisition, although one animal gave several responses during the first few trials, presumably due to the sensitizing effect of the manipulations.

Panel C of Figure 3 shows the cumulative records for the eight animals in the experimental paired group. Some animals showed behavior clearly similar to that of animals whose eyes were not restrained (panels A and B), and some are actually sensitized compared to normals. Two animals made few responses, and one initially showed good acquisition but stopped responding at trial 32. Thus, six of the eight animals showed a pattern of responding similar to animals with freely moving eyes for more than 60% of the training session. Figure 5 shows that these six animals also gave more total responses that any unpaired animal in the experiment. Using these arbitrary criteria, we would say that six of the subjects were conditioned. There is also greater variability of individual animals with restrained eyes (first panel of Fig. 5).

The two experimental animals that did not learn (see above; Fig. 3A, B) did show small bursts of phasic activity during the CS presentations. In animals with freely moving eyes, these would correlate with small twitches of the eye, but are not normally scored as full responses. This suggests that even the animals that did not meet the criterion of EMG responses that resembled those to the US may have acquired some association from the training. This idea was strengthened by their subsequent performance in the behavioral tests described below.

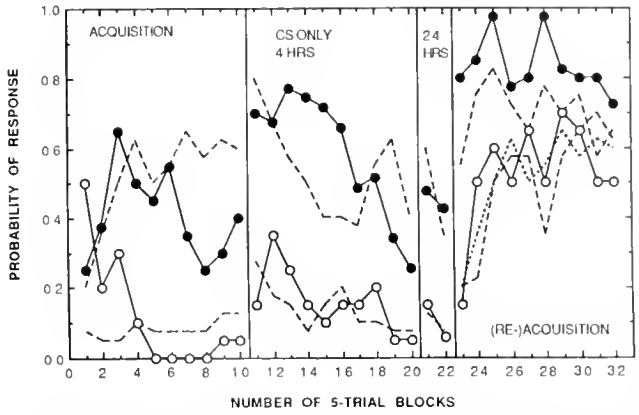

Figure 4. Effect on behavioral performance of immobilizing the eye during acquisition. Group data for animals trained with immobilized eyes compared to animals with freely moving eyes. Data points are averages of eight animals each. Filled symbols: experimentals; open symbols: unpaired controls. Broken line: average of corresponding data from Figure 2 [data from 4 normal and 4 freely moving eye with electrodes were pooled and averaged for each of the two groups (paired and unpaired)]. Data points in ACQUISITION are EMG responses; other data, retention and re-acquisition of classical conditioning, are recorded behaviorally. In RE-ACQUISITION, dotted line is first day performance of the average of experimental animals redrawn for comparison.

Behavioral tests after acquisition

After the acquisition trials, the eyes were freed, the EMG leads were cut, and the animals were returned to their home tanks. They were then tested, as were animals trained with freely moving eyes, for responses in the behavioral tests: retention after 4 h and after 24 h, and reacquisition in a second training session. The results are shown in Figure 4, where they are compared to the averaged data for the two groups trained with freely moving eyes. When the qualitative behavior of the animals trained with restrained eyes is compared for retention and reacquisition to that for animals with freely moving eyes (Figs. 2, 4), similar profiles are found, although, as noted above, the response to CS-only presentations varies substantially. During re-acquisition, behavior of the animals trained with restrained eyes is remarkably like that for animals with moving eyes: all experimentals show enhanced probability of responding, and all controls now subjected to paired training behaved like day-one experimentals. This behavioral performance of the

experimentals suggests that learning took place during day-one acquisition even in the case of the two animals where an EMG response was not evident.

Summary of statistical analysis

The major conclusions bearing on acquisition were that the groups presented with paired stimuli showed an increased probability to respond to the CS when compared to controls, and that the effect of EMG electrodes was somewhat sensitizing in terms of individual performance, although there were no differences over the course of the training. These conclusions are supported by an analysis of variance conducted over the 10 five-trial blocks of acquisition. For normal unoperated animals, differences between paired and unpaired groups was significant, $F(1,60) = 265.08$, $P < 0.0001$, as was the Block effect, $F(9,60) = 5.67$, $P < 0.0001$, and the Group $\times$ Block interaction, $F(9,60) = 5.15$, $P < 0.0001$. For animals with electrodes and freely moving eyes, there was a significant Group effect $F(1,60) = 125.21$, $P < 0.0001$, no significant Block effect $F(9,60) = 1.52$, $P > 0.25$, and no significant Group $\times$ Block interaction $F(9,60) = 0.691$, $P > 0.25$. For animals with electrodes and the eye restrained, there was a significant Group effect $F(1,100) = 24.09$, $P < 0.0001$, no Block effect $F(9,100) = 1.42$, $P > 0.10$ and no Group $\times$ Block interaction, $F(9,100) = 1.39$, $P > 0.10$.

With regard to sensitization, the effect was limited to the initial trials. As training continued, the group differences between animals with electrodes and those without was not significant. As noted above, paired animals with electrodes responded more to the CS at the outset of training than those without electrodes. A somewhat similar trend was observed for unpaired animals: unpaired animals with electrodes and the eye restrained made more responses during the first five CS presentations (mean probability 0.50, SD 0.35) than either the unpaired animals with electrodes and eye freely moving (mean 0.10, SD 0.12) or unoperated unpaired animals (mean .05, SD 0.1). Overall, however, analysis of variance conducted over the 10 five-trial blocks of acquisition revealed no group differences between animals with electrodes and those without: a comparison of animals with electrodes *versus* unoperated animals reveal no Group effect $F(1,60) = 0.631$, $P > 0.25$, a significant Block effect $F(9,60) = 4.15$, $P < 0.005$, and no Group $\times$ Block interaction $F(9,60) = 1.63$, $P > 0.10$. Also, no significant Group, Trial, or Interaction effects ($P > 0.10$) were obtained for animals with electrodes and freely moving eyes versus those with electrodes and the eye restrained. An overall analysis of variance conducted over the 10 five-trial blocks for the three unpaired groups indicated no Group effect $F(2,90) = 1.37$, $P > 0.25$, no Block effect $F(9,90) = 1.45$, $P > 0.05$, but a significant Group $\times$ Block interaction $F(18,90) = 2.19$, $P < 0.01$). The significant interaction reflects the fact that two of the four animals in the unpaired group with electrodes and restrained eyes responded substantially during the first five CS presentations and that such responding decreased over the course of further unpaired training.

The major conclusion about the behavior of animals that had been trained with eyes restrained is that the performance in reacquisition is similar to the groups with freely moving eyes. Also, the unpaired controls with restrained eyes were capable of learning as shown in reacquisition, were not repressed due to unpaired pre-exposure, and had not fortuitously made a CS-US association. The acquisition performance of all paired groups was enhanced during reacquisition. For paired animals without electrodes, analysis of variance indicated significant Group effect $F(1,60) = 17.31$, $P < 0.0001$, a Block effect $F(9,60) = 6.42$, $P < 0.0001$, and a Group $\times$ Block interaction $F(9,60) = 2.73$, $P < 0.01$. Analysis of the reacquisition performance of paired animals with electrodes and the eye free to move revealed a significant Group effect $F(1,60) = 12.64$, $P < 0.005$, no Block effect $F(9,60) = 0.676$, $P > 0.25$, and no Group $\times$ Block interaction $F(9,60) = .676$, $P > .25$. A significant Group effect was also obtained in paired animals with electrodes and the eye restrained $F(1,60) = 96.50$, $P < 0.0001$. There was a Block effect $F(9,60) = 2.02$, $P < 0.05$, but no significant Group $\times$ Block interaction $F(9,60) = 0.546$, $P > 0.25$.

As Figures 2, 4, and 5 suggest, the performance of unpaired animals was greatly enhanced when they received paired training. Analysis of variance of unpaired animals with no electrodes revealed a significant Group effect $F(1,60) = 79.34$, $P < 0.0001$, but no Block effect $F(9,60) = 1.02$, $P > 0.25$, or Group $\times$ Block interaction $F(9,60) = 1.07$, $P > 0.25$. Analysis of unpaired animals with electrodes and the eye free to move indicated a significant Group effect $F(1,60) = 98.97$, $P < 0.0001$, Block effect $F(9,60) = 3.75$, $P < 0.005$, and Group $\times$ Block interaction $F(9,60) = 2.66$, $P < 0.025$. Unpaired subjects with electrodes and the eye restrained (the eye was free to move during the reacquisition phase) also had a significant Group effect $F(1,60) = 93.28$, $P < 0.0001$, no Block effect $F(9,60) = 0.709$, $P > 0.25$, but a significant Group $\times$ Block interaction $F(9,60) = P < 0.0001$.

Discussion

The major goal in this work was to determine the role of eye movement in classical conditioning of the withdrawal reflex. We wanted to determine, first, if eye movement is *necessary* for classical conditioning of the eye withdrawal; that is, whether any animals are capable of

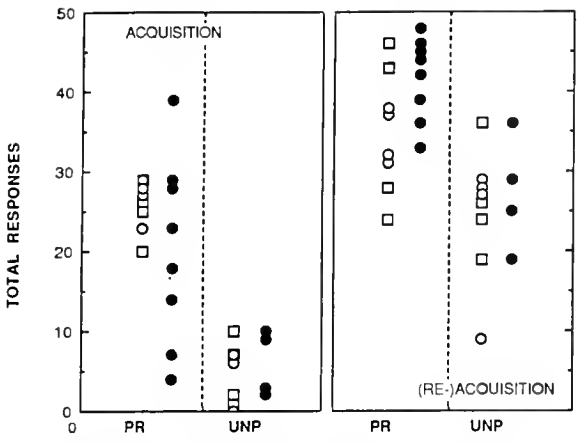

Figure 5. Total responses in acquisition and re-acquisition (50 trials). Data for animals with freely moving eyes are shown with open symbols and includes two subgroups: normal animals (circles) and animals with EMG electrodes (squares). Each experimental population, paired group (PR) and unpaired (UNP), includes 4 normals and 4 EMGs, although some data points overlap. Data for animals with restrained eyes during acquisition are shown as filled circles. There were eight animals in the PR groups and 8 in the UNP group, although some points overlap. Note that the PR group in ACQUISITION is given a second day of training in RE-ACQUISITION, but the group labeled UNP was a control only on the first day. In RE-ACQUISITION it was now presented with paired stimuli as described in the text.

learning when the eye is restrained. Our results show clearly that some animals can, in fact, learn with immobilized eyes. Having established that eye movement is not necessary, we next asked whether any animals ever used signals that arise from eye movement. Two of the eight animals with restrained eyes showed no normal acquisition of the EMG response. Was this because of experimental error, such as damage to the eye from implanting electrodes? Or did these two particular animals normally use a strategy of acquisition that required eye movement accounting for their poor performance when the eye was restrained? Although we cannot rule out an effect of eye movement on these animals, there is evidence that some learning took place even for these animals. When tested behaviorally, all animals performed like normals, particularly in re-acquisition. Also, small EMG bursts were evoked by CSs (but did not appear in the interval between stimuli). Thus, damage to the muscle might have non-specifically reduced the appearance of conditioned responses. Moreover, the eye withdrawal reflex, under normal conditions, proceeds without proprioceptive feedback (Burrows, 1967; Sandeman, 1967), although we do not know whether feedback can affect learning. In the optokinetic response, furthermore, motor output to the eye is driven by the difference in velocity of the eye and of the target (Horridge and Sandeman, 1964; Sandeman *et al.*, 1975; Erber and Sandeman, 1989). This motor output is normally overridden by the eye withdrawal (Burrows and Horridge, 1968), but we cannot exclude the possibility that such a signal could be used by some crabs as part of a strategy in classical conditioning.

Comparison of classical conditioning and signalled avoidance

Our work supports the idea that classical conditioning of the eye withdrawal is simply dependent on the integration of the two sensory stimuli (vibration and air-puff). The results also bear on the study of this reflex in signalled avoidance, and the apparently paradoxical behavior of controls in that procedure. The problem may be summarized as follows. Signalled avoidance is designed as an operant procedure. If the animal makes a response during the presentation of the (signal) CS, the US is omitted, that is, the animal can avoid the aversive stimulus by its own behavior. However, animals that learn in an avoidance procedure may be undergoing a predominantly Pavlovian process; the procedure is identical to a classical conditioning experiment in which some USs have been omitted. Thus, the animal may learn during the CS-US pairings, but may not associate the occasional omission with its own behavior. In our study of signalled avoidance in the eye withdrawal in the crab, we found that animals learned well, but acquisition curves were essentially the same as those for animals in classical conditioning (Abramson *et al.*, 1988), suggesting a Pavlovian interpretation. The apparent paradox is that "yoked" controls presented with the same pattern of CSs and USs (some of which are now omitted) as the experimental animals, but independent of the responses they made, did not perform as well. Since these controls receive the same number of CSs and USs as the experimentals—the only difference is the contingency between stimuli and the animal's behavior—they should do as well (if the mechanism is truly Pavlovian). One of the following hypotheses could explain these seemingly paradoxical results.

One possibility is that learning in both the avoidance procedure and "classical conditioning" procedure is actually the same and substantially operant; reinforcement is provided by attenuation of the air-puff when the eye is retracted during the CR. If this is true, the yoke controls are behaving as per experimental design. The results presented here exclude this mechanism because animals can learn when their eye is retracted and there is no attenuation of the air-puff.

A second hypothesis is that avoidance learning is actually Pavlovian in mechanism; the yoke controls are giving erroneous data due to one of several possibilities. First, it is possible that yoke controls are actually subjected to different stimuli than experimentals as described by Woodward and Bitterman (1973). According

to this theory, there are actually two CSs: CS+ and CS−. These are compound stimuli composed of the vibration and some sensory information about whether the eye is up or down (for example, visual field). For experimentals, CS+ is (the state of eye-up) + vibration, which is predictably followed by the US; CS− is (eye-down) + vibration, predictably followed by an omission; these are randomized when vibration is presented to yoke controls. We have excluded this theory for classical conditioning and, therefore, for a Pavlovian interpretation of avoidance, by showing that animals can be conditioned with the eye restrained.

We favor an alternative explanation: that both classical conditioning and avoidance are Pavlovian in mechanism, but that the process involves two conditioned states, one of which has a higher probability of response than the other and is more resistant to extinction. Such a mechanism resembles the Markov chain model for conditioning (Theios and Brelsford, 1966). Experimental animals in avoidance, then, receive omissions at times when they are most resistant to extinction (high probability state), whereas for yokes, omissions are randomized. A similar explanation for experimental-yoke differences was proposed by Gormezano (1965) for the rabbit nictitating membrane.

Thus, the current work on classical conditioning allows us to exclude two of the possible explanations for signalled avoidance learning in the crab eye. We cannot, however, exclude the possibility that the mechanism of learning is actually different for the two procedures. Possibly the rates of acquisition for avoidance are the same as in classical conditioning because they share a common rate-determining step, probably at the output end of the behavior. For example, there may be a maximum rate of change in properties of the motor neuron. If this were so, the yoke controls would be performing as expected. At this point, we favor the Pavlovian interpretation. From the biological point of view, an all-or-none defensive reflex, such as eye withdrawal, probably does not require the subtle information about the effects of the behavior that an operant mechanism would impart.

In summary, EMGs recorded from muscle 19a of the eye can be used to study the acquisition of classical conditioning in animals with freely moving and immobilized eyes. Experiments using this method show that eye movement is not required for learning.

Acknowledgments

This work was supported in part by grant BNS-8819830 from the National Science Foundation, funds from Scott, Sperry & Hanson, Inc., and funds from the Research Foundation of the State University of New York.

Literature Cited

Abramson, C. I., P. M. Armstrong, R. A. Feinman, and R. D. Feinman. 1988. Signalled avoidance in the eye withdrawal reflex of the green crab. *J. Exp. Anal. Behav.* **50:** 483–492.

Abramson, C. I., and R. D. Feinman. 1987. Operant punishment in the green crab, *Carcinus maenas*. *Behav. Neural Biol.* **48:** 259–277.

Abramson, C. I., and R. D. Feinman. 1988. Classical conditioning of the eye withdrawal reflex in the green crab. *J. Neurosci.* **8:** 2907–2912.

Appleton, T., and J. L. Wilkens. 1990. Habituation and sensitization and the effect of serotonin on the eyestalk withdrawal reflex of *Cancer magister*. *Comp. Biochem. Physiol. A* (in press).

Burrows, M. 1967. Reflex withdrawal of the eyecup in the crab *Carcinus*. *Nature* **215:** 56–57.

Burrows, M., and G. A. Horridge. 1968. Motoneurone discharges to the eyecup muscles of the crab *Carcinus*. *J. Exp. Biol.* **49:** 251–267.

Erber, J., and D. C. Sandeman. 1989. The effect of serotonin and octopamine on the optokinetic response of the crab *Leptograpsus variegatus*. *J. Neurobiol.* **20:** 667–680.

Forman, R., and D. Brumbley. 1980. An improved capacitative position transducer for biological systems. *J. Exp. Biol.* **88:** 399–402.

Gormezano, I. 1965. Yoked comparisons of classical and instrumental conditioning of the eyelid response. Pp. 48–70 in *Classical Conditioning: A Symposium*. Appleton-Century-Crofts, New York.

Horridge, G. A., and D. C. Sandeman. 1964. Nervous control of optokinetic responses in the crab *Carcinus*. *Proc. R. Soc. (B).* **161:** 216–246.

Miall, R. C., and C. J. Hereward. 1988. A simple miniature capacitative position transducer. *J. Exp. Biol.* **138:** 541–544.

Moore, J. W., and I. Gormezano. 1961. Yoked comparisons of instrumental and classical eyelid conditioning. *J. Exp. Psych.* **62:** 552–559.

Sandeman, D. C. 1964. Functional distinction between oculomotor and optic nerve in *Carcinus*. *Science* **201:** 302–303.

Sandeman, D. C. 1967. Excitation and inhibition of the reflex withdrawal of the crab *Carcinus*. *J. Exp. Biol.* **46:** 475–485.

Sandeman, D. C. 1968. A sensitive position measuring device for biological systems. *Comp. Biochem. Physiol.* **24:** 635–638.

Sandeman, D. C. 1969a. Integrative properties of a reflex motoneuron in the brain of the crab *Carcinus maenas*. *Z. Vergl. Physiol.* **64:** 290–464.

Sandeman, D. C. 1969b. The synaptic link between the sensory and motoneurones in the eye-withdrawal reflex of the crab. *J. Exp. Biol.* **50:** 87–98.

Sandeman, D. C., J. Erber, and J. Kien. 1975. Optokinetic eye movements in the crab, *Carcinus maenas*. I. Eye torque. *J. Comp. Physiol.* **101:** 259–274.

Theios, J., and J. W. Brelsford Jr. 1966. A Markov model for classical conditioning: applications to eye-blink conditioning in rabbits. *Psych. Rev.* **73:** 393–405.

Woodward, W., and M. E. Bitterman. 1973. Pavlovian analysis of avoidance conditioning in the goldfish (*Carassius auratus*). *J. Comp. Physiol. Psychol.* **82:** 123–129.

Reference: *Biol. Bull.* **178:** 195–204. (June, 1990)

Behavioral Responses of Crustacean Larvae to Rates of Temperature Change

RICHARD B. FORWARD JR.

Duke University Marine Laboratory, Beaufort, North Carolina 28516 and Zoology Department, Duke University, Durham, North Carolina 27706

Abstract. The ontogeny of behavioral responses of larvae of the crabs *Rhithropanopeus harrisii* and *Neopanope sayi* to rates of change in temperature were analyzed using a video system. A temperature decrease evoked an ascent in both species. The threshold rates of decrease for Stages I and IV zoeae of *R. harrisii*, and Stage I zoeae of *N. sayi*, were 0.06, 0.1, and 0.09°C min^{-1}, respectively. Stage IV zoeae of *N. sayi* were unresponsive to any rate of decrease. Larvae descended upon a temperature increase. For Stages I and IV zoeae of *R. harrisii* and Stage I of *N. sayi* the threshold rates of temperature increase were 0.07, 0.24, and 0.18°C min^{-1}, respectively. Stage IV zoeae of *N. sayi* were again unresponsive. In general, there was an ontogenetic change in responsiveness as Stage IV zoeae of both species were less sensitive than Stage I zoeae. The average absolute amounts of temperature change needed to evoke a response was independent of the rate of change at rates above threshold and ranged from 0.29 to 0.49°C for both species. A consideration of larval sinking rates and ascent speeds, as well as normal environmental temperature gradients, shows that larvae of both species can respond to the rates and amounts of temperature change found in their environments. These responses constitute a negative feedback system that could be used to regulate depth relative to temperature.

Introduction

Temperature change produces measurable alterations in the directional responses to light (phototaxis) and gravity (geotaxis), and the activity of crustacean larvae (for general reviews see Thorson, 1964; Forward, 1976; Sulkin, 1984). In phototactic studies, only narrow beams of light have been used as a stimulus source, rather than a light field that simulates the underwater angular light distribution. For *Callinectes sapidus*, larval phototaxis was not affected by temperature changes of 10°C (Sulkin and Van Heukelem, 1982). The only clear effect on *Rhithropanopeus harrisii* larvae was a slight increase in negative phototaxis by Stage I zoeae upon a temperature increase (Ott and Forward, 1976). Reductions in temperature within the range encountered by larvae did not alter phototaxis in any zoeal stage of *R. harrisii*. Nevertheless, there was a pronounced positive geotaxis by Stage IV zoeae of *R. harrisii* at high temperatures (30 and 35°C) and a sinking response by Stage I zoeae (Ott and Forward, 1976). Similarly, *C. sapidus* descended by passive sinking upon exposure to temperatures of 27.5°C or greater (McConnaughey and Sulkin, 1984).

Activity, as measured by linear swimming speed, has the pattern of an increase in speed with an increase in temperature (Sulkin *et al.*, 1980; Kelley *et al.*, 1982) up to a certain high temperature where inactivity (sinking) occurs (Welsh, 1932; Yule, 1984). In contrast, the swimming speed of Stage I zoeae of *C. sapidus* was not modified by a temperature decrease (Sulkin *et al.*, 1980).

Several studies suggested that responses to high temperatures did not result from sensitivity to a rate of temperature increase but rather to an absolute upper temperature (Ott and Forward, 1976; McConnaughey and Sulkin, 1984). Although the upper temperature may vary with species, this generalization was substantiated by measurements of behavioral responses in sharp thermoclines. If the upper temperature in the thermocline was above this limit, then larvae ascent stopped at the thermocline. Alternatively, larvae ascended through the thermocline if the upper temperature was below the absolute upper limit. Remarkably, 10°C thermoclines had

Received 27 November 1989; accepted 1 March 1990.

no inhibitory effect on an ascent, which has led to the conclusion that, for many species, temperature gradients in nature will not prevent upward movements (Kelley *et al.*, 1982; Sulkin *et al.*, 1983; McConnaughey and Sulkin, 1984).

Considering these past studies, larval crustaceans seem relatively unresponsive to temperature changes. Nevertheless, the behavioral responses that do occur upon changes in temperature can be summarized. A temperature increase to temperatures at and above the absolute upper limit evokes negative phototaxis, positive geotaxis, and sinking, all of which lead to downward movement. An ascent does not occur upon a reduction in temperatures. Activity decreases with decreasing temperature and at extremely low temperatures larvae are totally inactive (*e.g.*, Ott and Forward, 1976).

A limitation of past studies is that larval behavior was studied at very sharp thermoclines and upon exposure to step changes in temperature. Sharp thermoclines can exist in nature, but most often larvae encounter a rate of change in temperature that depends upon the vertical gradient and rates of vertical movement. The present study was undertaken (1) to determine the lowest rates (threshold) of temperature change that evoke ascent and descent responses, (2) to measure the absolute amount of temperature change that must occur before larvae respond, and (3) to compare these rates and absolute amounts to those a larva could encounter in the water column. The study compares larvae of the crabs *Rhithropanopeus harrisii* and *Neopanope sayi* (family Xanthidae). These were selected because both live as adults in estuaries, but the behavior of *R. harrisii* larvae results in retention in upper estuarine areas (Cronin, 1982), whereas *N. sayi* larvae undergo development in lower estuarine and coastal areas (Sandifer, 1975; Dittel and Epifanio, 1982; Salmon *et al.*, 1986). Thus the larval species are taxonomically related, but they develop in different areas where they are potentially exposed to different temperature regimes.

Materials and Methods

Ovigerous specimens of *Rhithropanopeus harrisii* (Gould) were collected from the Neuse River estuary (North Carolina) from July to August 1989. Crabs were placed in 20 ppt seawater, which was passed through a 5-μm filter. Ovigerous *Neopanope sayi* (Smith) were collected from the Newport River estuary (North Carolina) from August to September 1989, and females were held in 32 ppt seawater, which was the approximate salinity at the collection site. Larvae of both species were reared at the same salinity in which the crabs were maintained at a temperature of 25°C. This acclimation temperature was chosen because it approximates the average summer

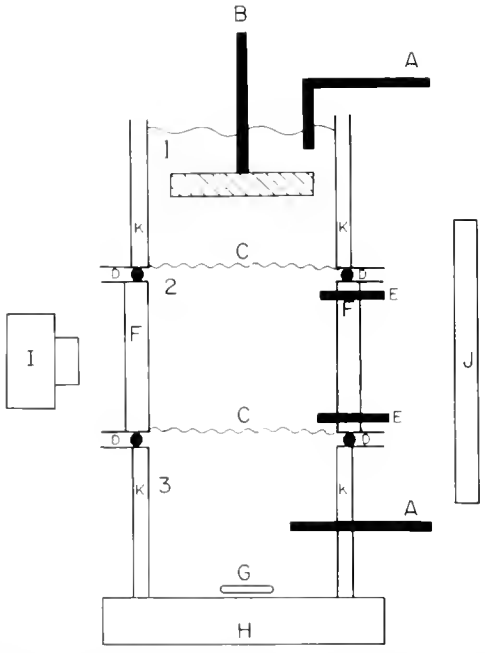

Figure 1. Horizontal view of test chamber consisting of equal size cylindrical upper (1), test (2), and lower (3) sections (not drawn to scale). A—insulated input/output Tygon tubes connected to peristaltic pump; B—stirring paddle connected to a variable speed stirring motor; C—75 μ mesh plankton netting; D—O-ring; E—thermister probe connected to meter with digital readout; F—square water-filled chamber surrounding the test chamber; G—magnetic stirring bar; H—magnetic stirrer; I—video camera; J—far-red illumination light; K—thermal insulation. The video camera and thermisters were oriented perpendicular to each other in the actual chamber.

temperatures where the larvae undergo development (Stefansson and Atkinson, 1967; Kirby-Smith and Barber, 1979).

Specimens were reared in a controlled environmental chamber (Sherer, Model CEL4-4) on a 14:10 LD cycle. Throughout development, larvae were transferred daily to clean seawater and fed newly hatched *Artemia* spp. nauplii. Experiments were conducted with Stages I and IV zoeae, to test for an ontogenetic change in responsiveness because each species has four zoeal stages. All experiments were performed in mid photophase to avoid complications due to biological rhythms in behavior. Larvae were light-adapted to room fluorescent light (intensity = about 1 W m^{-2}) prior to all experiments. In most cases a minimum of five groups of larvae, each from a separate female, were tested in each experimental situation.

Experimental approach

Larval responses to different rates of temperature change were measured in a chamber having three vertical cylindrical sections (section height = 2.5 cm; diameter = 2.5 cm; Fig. 1). For temperature increase, high temperature water (above 25°C) was added to the upper section

and mixed by a slowly rotating paddle. Larvae were confined to the middle section by plankton netting (75 μ mesh) at the upper and lower boundaries; their behavior was monitored and recorded with a closed circuit television system. For viewing, animals were illuminated with far-red light (maximum transmission 775 nm), to which larvae are not responsive (Forward and Cronin, 1979). The lower section was used for temperature decreases. Low temperature water (below 25°C) was added and mixed with a magnetic stirring bar. Preliminary measurements of larval swimming indicated that slow stirring in the upper and lower sections had no apparent effect on movement.

Test water was initially the same water as that used for rearing larvae. This water was pumped through a coil of Tygon tubing situated in a separate water bath (Forma Scientific, Model 2095) and then into the test chamber. The section of tube from the bath to the chamber was insulated with a foam wrap. To insure that there were constant amounts of water in all chamber sections and constant flow through the center section, the waters of different temperature were delivered to the appropriate end section by a variable speed peristaltic pump (Buchler Instruments), and water was extracted at the same rate from the other end section by the same pump. For example, to induce a temperature decrease, low temperature water was pumped into the lower section while water was removed from the upper section at the same rate. Dye studies indicated laminar flow of water through the netting into the center section. Also, the maintenance of constant water levels in all chambers prevented hydrostatic pressure changes during experimentation. This procedure was important because larvae of both species are very sensitive to pressure changes (Forward and Wellins, 1989; Forward *et al.*, 1989).

The rates of temperature change were varied through differences in temperature between the input and acclimation temperature water and pumping rate. In most experiments the temperature difference remained constant and pumping rate was varied. The actual temperatures in the upper and lower subsections of the larval section of the test chamber were measured with two thermister probes (YSI; Model 423; Time constant 1.45 s) connected to separate digital meters (Omega Engineering, Inc.; Model 450-ATH; accuracy 0.1°C). The digital readouts from the probes were viewed by a second video camera and inserted in the video picture with a video screen splitter (Vision Industries, Inc.; Model U2705P). A record of time was also inserted into the picture by a Field/Frame Counter (QSI Systems, Inc.). In this way larval behavior, temperature, and time were recorded simultaneously on videotape. The actual rates of change in temperature were calculated from temperature measurements by the probe closest to the chamber section (upper or lower) where test seawater was added. Measurements by the lower probe were used for temperature decreases and upper probe for temperature increases. Specific rates of temperature change were determined directly from the experimental records. In each experiment the rate of temperature change quickly increased up to the maximum for each flow rate or temperature difference condition and then remained approximately uniform through the time when responses were measured.

Experimental procedures

The same general procedure tested for responses to temperature increases and decreases. Larvae were held in the rearing water in finger bowls (10.3 cm diameter) situated in a separate water bath that was maintained at the acclimation temperature (25°C). The room temperature was also kept at about 25°C. A group of approximately 75 Stage I or 25 Stage IV zoeae was placed in the test chamber in water from the maintenance finger bowl. Thus, the initial temperature in the test chamber was very close to 25°C. The peristaltic pump and videotape recorder were started after 1 min in darkness. Temperature changed at a specific rate and was first detected about 3 min after the pump was activated. The experiment continued until the temperature changed about 1.0°C. Larvae were then removed, the chamber rinsed with water at the acclimation temperature, and a new group of larvae placed in the chamber. The procedure was repeated. Larvae were only tested once at each rate of temperature change. If larvae were retested at a second rate on any particular day, the minimum time between testing was about 2.5 h. Larvae remained at 25°C in the water bath between tests, and there was no obvious change in behavior with multiple tests. To establish that the observed responses were not induced by water flow through the chamber, larvae were tested using the foregoing procedure at the maximum test flow rate with acclimation temperature water. In this way larvae experienced flow but no temperature change. This control also tested for changes in larval distributions over time due to random activity.

Analysis

All experiments were conducted with the test chamber illuminated only with far-red light. Because they were functionally in darkness in this situation, the possible behavioral responses to changes in temperature were changes in activity or geotaxis.

To analyze for behavioral responses, the test (larval) section of the test chamber was divided into three equal horizontal subsections by a template placed over the video screen. The number of larvae in each subsection was counted before (control) and after each 0.1°C

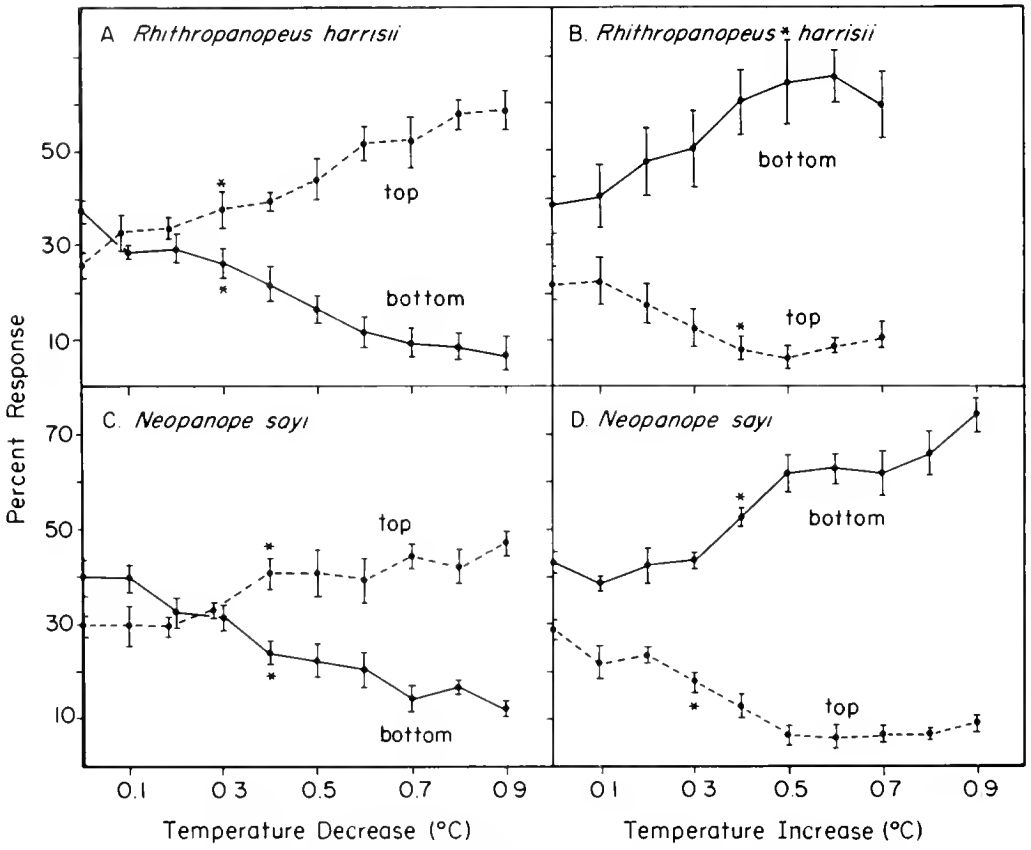

Figure 2. Percentage of Stage I zoeae of *Rhithropanopeus harrisii* (A, B) and *Neopanope sayi* (C, D) in the top (dashed line) and bottom (solid line) subsection of the larval section of the test chamber. Responses were measured after different absolute amounts of temperature change upon temperature decreases (A, C) and increases (B, D). These absolute temperatures are those in the bottom (A, C) and top (B, D) subsections of the test chamber. The rates of temperature change were 0.28 (A), 0.19 (B), 0.23 (C), and 0.28 (D)°C min^{-1}. Means and standard errors are plotted and the replicate sizes are 7 (A, B), 5 (C), and 6 (D). An asterisk indicates the lowest absolute temperature change to evoke a percent response that was significantly different ($P < 0.05$; Dunnett's t-test) from the control level, which is plotted at 0°C.

change. Control counts were made 30 s before the first 0.1°C change in temperature. The percentage of larvae in each subsection was calculated from these data. Response level was considered the percentage of larvae in the subsections after a 0.5°C change in temperature, because responses are clearly evident by this absolute amount of temperature change (Fig. 2).

Ascent and descent responses were expected upon a temperature decrease and increase, respectively. Thus the change in the percentage of larvae in the bottom subsection was monitored upon a temperature decrease, and, in the upper subsection, upon a temperature increase. Arcsine transformed data were used for statistical tests and to calculate means, standard deviations, and standard errors. Back transformed means and standard errors are plotted in the figures. If paired observations were made before (control) and upon stimulation (experimental) of each group of larvae, a t-test for paired comparisons was used to test for differences ($P < 0.05$). In cases where a control was compared to responses at different times after the beginning of stimulation, then the Dunnett's t-test for multiple comparisons with a control was used to test for significant differences ($P < 0.05$; Dunnett, 1964). A Z statistic testing differences between two proportions (Walpole, 1974) was used to test for differences between control and experimental distributions of individual trials.

Results

Response time course

The change in the percentage of larvae in the lower or upper subsections of the experimental chamber, upon an increase or decrease in temperature, respectively, is the response time course. Representative patterns are shown for Stage I zoeae at rates of temperature change that

evoked strong responses (Fig. 2). Initially the larvae were approximately evenly distributed in the test chamber, as the percentage of larvae in the top and bottom subsections was close to 33%. However, because the true values were not always 33%, the initial distribution was determined for each group of larvae, and the mean used as the control level for comparison with percentages upon a temperature change.

An ascent occurred upon a temperature decrease as indicated by a decrease in larvae in the bottom subsection and increase in the top subsection (Fig. 2A, C). For both *R. harrisii* (Fig. 2A) and *N. sayi* (Fig. 2C), significant changes co-occurred in the bottom and top subsections after a 0.3–0.4°C absolute temperature change. Thus, larvae leave the bottom subsection, and ascend to the top subsection, when the temperature decreases (Fig. 2A, C).

With a temperature increase, there was a descent; the percentage of larvae in the top subsection decreased, while it increased in the bottom subsection (Fig. 2B, D). For both species, the percentage of larvae changed significantly in the top subsection after a 0.3°C absolute temperature change, and after a 0.4°C change for larvae in the bottom subsection. This pattern (Fig. 2B, D) indicates that larvae left the top subsection and aggregated in the bottom subsection.

These response patterns were used to establish the analytical methods for the experiments. The percentage of larvae in the bottom subsection was monitored upon a temperature decrease. Because cooled water entered the test chamber at the bottom, larvae in the bottom subsection were initially exposed to the temperature decrease and responded first. Similarly, the percentage of larvae in the top subsection was monitored upon a temperature increase, because warmer water entered the test chamber from above. For both temperature decreases and increases, larval distributions were monitored before (control) and after a 0.5°C absolute change in temperature (experimental). The results shown in Figure 2 indicate that strong responses are evident by this amount of temperature change, and preliminary analysis showed that if larvae had not responded by the 0.5°C change, then they did not respond at greater absolute temperature changes.

Temperature decrease

Responses upon a temperature decrease were not due to fluid flow through the test chamber. Larvae were subjected to the maximum experimental flow rate, but not to a temperature decrease. Distributions were measured at the average time after the beginning of flow for the control and experimental measurements at this flow rate. The mean percentage of larvae in the bottom section never changed significantly with flow. This result also indicates random larval movements did not produce the observed responses.

In contrast, larvae ascended upon a temperature decrease. The lower rates of temperature decrease (threshold) to induce a response by Stages I and IV zoeae of *R. harrisii* (Fig. 3A, C) and Stage I zoeae of *N. sayi* (Fig. 3B) were 0.06, 0.1, and 0.09°C min^{-1}, respectively. A significant response was not displayed by Stage IV zoeae of *N. sayi* at rates up to 0.45°C min^{-1} (Fig. 3D). Thus, there was an ontogenetic change in sensitivity by both species, in which Stage I zoeae were more sensitive than Stage IV.

Temperature increase

Larvae descended upon an increase in temperature (Fig. 4). This response was not due to fluid flow or random movements. Using techniques for measuring responses to flow as described in the previous section, the mean percentage of larvae in the upper section did not change significantly between the control and experimental times (Fig. 4; plotted at rate 0° min^{-1}). The threshold rates for Stages I and IV zoeae of *R. harrisii* (Fig. 4A, C) and Stage I zoeae of *N. sayi* (Fig. 4B) were 0.07, 0.24, and 0.18°C min^{-1}, respectively. Stage IV zoeae of *N. sayi* were not responsive to any rate of temperature increase up to 0.35°C min^{-1} (Fig. 4D). These results indicate that, for both species, Stage I zoeae respond to slower rates of temperature increase than Stage IV zoeae.

Absolute temperature change

The absolute amounts of temperature change necessary to produce a significant response upon temperature decreases and increases were determined for each larval stage (Fig. 5). Determinations were made at those rates that produced a significant response (Figs. 3, 4). For each trial, the proportion of control larvae in the bottom (temperature decrease) or top (temperature increase) subsections was compared to the proportion of larvae after each 0.1°C change, until a significant difference was evident ($P < 0.05$; Z statistic for testing differences between two proportions). Mean absolute temperature values were then calculated for each rate (Fig. 5). Mean values did not vary significantly with rate of temperature change (one-way ANOVA) within each species, zoeal stage, and direction of temperature change. Thus an average value was calculated for a temperature increase and decrease at each zoeal stage (Table I). Mean values varied over a narrow range from 0.28°C to 0.49°C.

Discussion

The general responses of both test species of larvae were an ascent upon a temperature decrease and descent upon a temperature increase. Since all experiments were

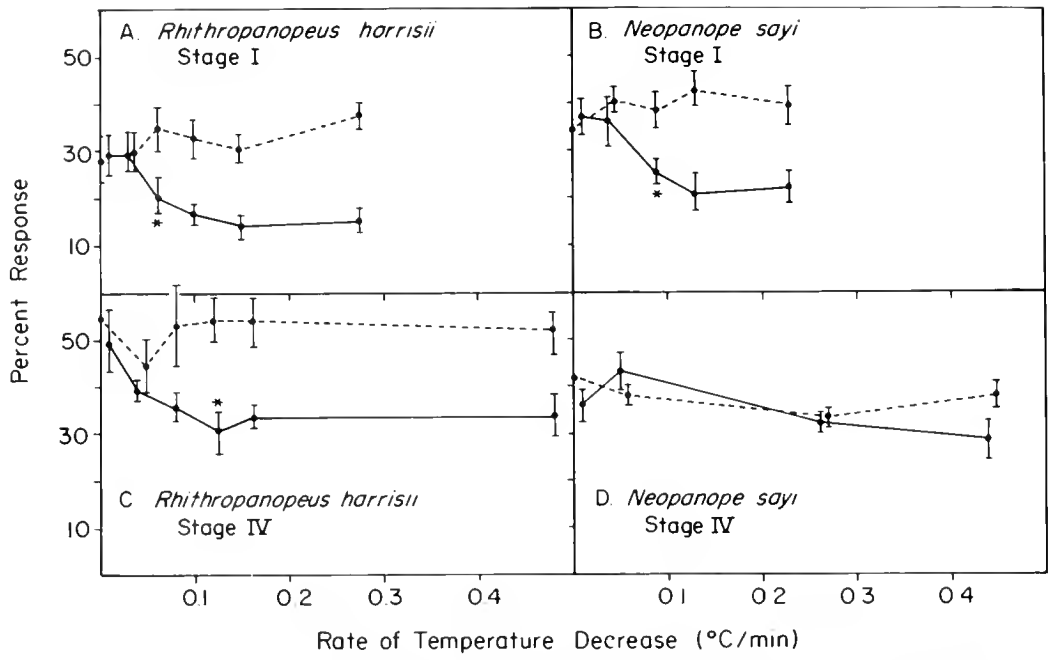

Figure 3. The percentage of Stages I and IV zoeae of *Rhithropanopeus harrisii* (A, C) and *Neopanope sayi* (B, D) in the bottom subsection of the test section before a temperature change (dashed line) and after 0.5°C absolute temperature change (solid line) at different rates of temperature decrease. The control for flow at the fastest test flow rate is plotted at 0°C min^{-1} rate of change. Means and standard errors are plotted and the average replicate size for A, B, C, and D was 6. Asterisks indicate the slowest rate of temperature decrease at which there is a significant difference between mean control and experimental percentages ($P < 0.05$; *t*-test for paired comparison.

conducted in darkness, the ascent could result from an activity increase or negative geotaxis, whereas the descent could involve sinking or positive geotaxis (Forward, 1988). The descent response upon a temperature increase has been observed frequently in past studies, in which larvae were exposed to step changes in temperature, but the ascent response at low temperatures is uncommon (*e.g.*, Ott and Forward, 1976). Because high temperatures usually occur in the upper part of the water column and low temperatures at depth, the behavioral responses of the two test species constitute a negative feedback system that could keep larvae at the acclimatization temperature.

For some crustacean species, such as *Callinectes sapidus*, there is a change in responsiveness to temperature throughout larval development (*e.g.*, Sulkin *et al.*, 1980). Sensitivity decreases with age for both test species. Stage I zoeae of *Rhithropanopeus harrisii* had lower threshold rates for temperature decrease (0.06°C min^{-1}) and increase (0.07°C min^{-1}) than Stage IV zoeae (decrease = 0.1°C min^{-1}; increase = 0.24°C min^{-1}). The ontogenetic change is greater for *Neopanope sayi*, because Stage I zoeae showed pronounced responses to temperature change but Stage IV zoeae were unresponsive to any test rate of temperature increase or decrease, which ranged up to 2.3–5.1 times greater than the threshold rates for Stage I zoeae (Figs. 3, 4).

To respond to a change in temperature, larvae must sense not only a rate of change in temperature but also a particular absolute amount of change. The necessary absolute amounts of temperature change varied slightly with rates of change (above threshold; Fig. 5) and during zoeal development. Average values ranged from 0.28 to 0.49°C (Table I). The fact that rates of change below threshold did not evoke a response (Figs. 3, 4) proves that both a sufficient rate of change and absolute amount of change must be present before a response occurs. At these subthreshold rates, the absolute amount of temperature change (0.5°C) was sufficient for a response, but larvae did not respond.

R. harrisii and *N. sayi* larvae respond at similar threshold rates and after similar absolute amounts of temperature change. An important consideration is whether this sensitivity is adequate for detection of vertical temperature gradients in their environment. Past laboratory studies of other species of crustacean larvae suggest that sharp thermoclines will not impede vertical movements because larvae pass through laboratory thermoclines that are greater than those in their natural environment. Nevertheless, temporary aggregations were observed at ther-

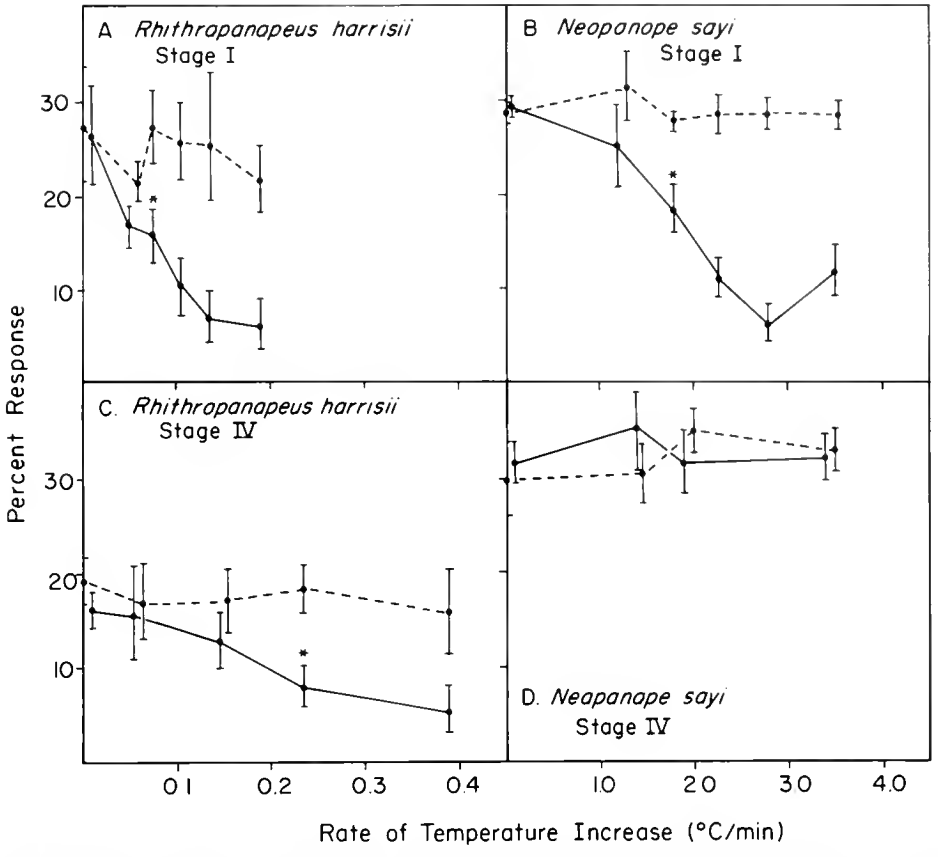

Figure 4. The percentage of Stages I and IV zoeae of *Rhithropanopeus harrisii* (A, C) and *Neopanope sayi* (B, D) in the top subsection of the test section before (dashed line) and after a 0.5°C absolute temperature increase (solid line) at different rates of temperature increase. The control for flow as measured at the fastest test flow rate is plotted at 0°C/min^{-1}. Means and standard errors are plotted. The average replicate size in A, B, C, and D are 6, 6, 7, and 7, respectively. Asterisks indicate the slowest rate of temperature increase at which there is a significant difference between control and test mean percentages ($P < 0.05$; *t*-test for paired comparisons).

moclines during vertical movements by *Eurypanopeus depressus* (Sulkin *et al.*, 1983) and *Callinectes sapidus* larvae (McConnaughey and Sulkin, 1984).

R. harrisii larvae are retained in upper estuarine areas (Cronin, 1982). Kirby-Smith and Barber (1979) measured environmental factors in an area (South River, North Carolina) close to the collection site for ovigerous *R. harrisii* where larvae consistently occur. Daytime temperature at the surface and bottom during the summer reproductive months of July and August (1974–1976) indicate that a temperature difference existed 80% of the measurement times. A conservative assumption is that temperature changed continuously from the surface to the bottom. Under these conditions, the average gradient was 0.9°C m^{-1}.

The threshold rates of detection by larvae and speeds of vertical movement were used to calculate the minimal gradient a larva could perceive. A conservative measure of speed of downward movement is larval sinking speed because larvae can also actively swim down. If *R. harrisii* sink continuously, then the minimal temperature decrease they can detect is 0.32°C m^{-1} for Stage I zoeae and 0.22°C m^{-1} for Stage IV zoeae (Table I). Using average ascent rates, the minimal increase in temperature they could detect is 0.19°C m^{-1} for Stage I zoeae and 0.63°C m^{-1} for Stage IV (Table I). Because these values are below the average gradient calculated from the measurements of Kirby-Smith and Barber (1979), *R. harrisii* larvae can detect changes in temperature in their environment.

N. sayi larvae inhabit low estuarine and coastal environments (Sandifer, 1975; Dittel and Epifanio, 1982; Salmon *et al.*, 1986). Pinschmidt (1963) measured surface and bottom temperatures in the Beaufort Inlet, which connects the Newport River estuary (where ovigerous *N. sayi* were collected) and the coastal waters. Measurements in July and August (1960–1961) indicate temperature differences were present 50% of the time.

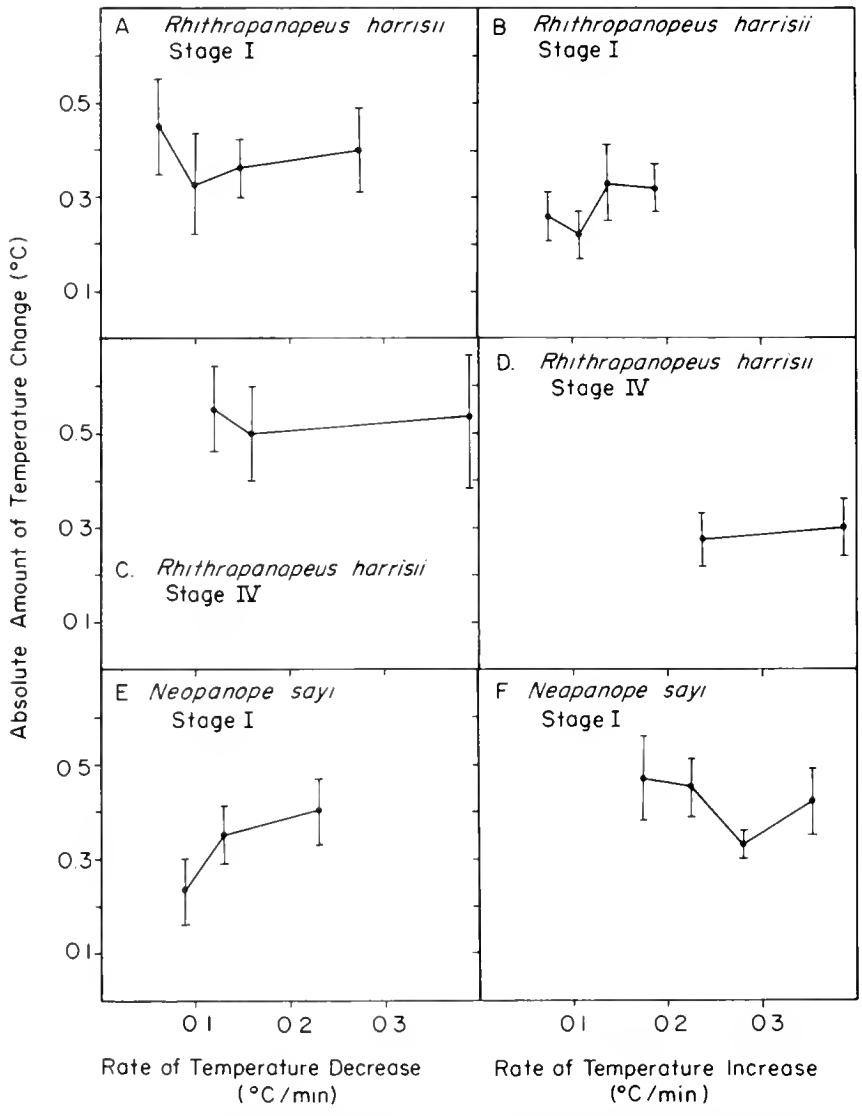

Figure 5. The amount of absolute change in temperature before a response to different rates of temperature decrease and increase by *Rhithropanopeus harrisii* (A, B, C, D) and *Neopanope sayi* (E, F) larvae. Means and standard errors are plotted. The average replicate size for all means was 5.

Again assuming a continuous change in temperature, the average gradient was 0.3°C m^{-1}. Stefansson and Atkinson (1967) extensively measured temperature in the coastal area seaward of the Beaufort Inlet at specific depth intervals. During the summer months, temperature was approximately equal in the upper 10 m, but at times differences approaching those measured by Pinschmidt (1963) were evident at deeper depths.

The gradients that can be perceived by *N. sayi* larvae were calculated using the same procedure as for *R. harrisii* larvae. The detectable gradient in temperature decrease for Stage I zoeae is 0.34°C m^{-1} and for a temperature increase is 0.94°C m^{-1} (Table I). Thus Stage I zoeae of *N. sayi* should be able to detect the average environmental gradients in temperature decrease, but require extreme gradients in temperature increase.

An additional consideration is the functional significance of responses to temperature change. Larvae of both species can respond to a temperature increase and decrease. The threshold rates are in the range of 0.1°C min^{-1} (2×10^{-3}°C s^{-1}), and the necessary absolute amounts of change are less than 0.5°C (Table I). Larvae do not respond to temperatures above some very high absolute upper limit as suggested by past studies (Ott and Forward, 1976; McConnaughey and Sulkin, 1984). These responses could be used to avoid extreme, adverse environmental temperatures. Since high temperatures usually occur near the surface and low temperatures oc-

Table I

Calculation of minimal detectable temperature change per m

Threshold rate temperature decrease ($°C\ s^{-1}$)	Mean sinking rate ($mm\ s^{-1}$)	Minimum detectable gradient of temperature decrease ($°C\ m^{-1}$)	Absolute amount of temperature decrease (°C)
Rhithropanopeus harrisii			
Stage I—1.0×10^{-3}	3.1	0.32	0.38
Stage IV—1.7×10^{-3}	7.8	0.22	0.49
Neopanope sayi			
Stage I—1.5×10^{-3}	4.4	0.34	0.34
Temperature increase	Mean ascent rate ($mm\ s^{-1}$)	Minimum detectable gradient of temperature increase ($°C\ m^{-1}$)	Absolute amount of temperature increase (°C)
R. harrisii			
State I—1.2×10^{-3}	6.3	0.19	0.28
Stage IV—3.9×10^{-3}	6.2	0.63	0.29
N. sayi			
Stage I—3.0×10^{-3}	3.2	0.94	0.41

Threshold rates are from Figures 3 and 4. Mean sinking (Latz and Forward, 1977) and ascent speeds (Forward and Wellins, 1989) for *R. harrisii* are at 20 ppt (rearing salinity), while those for *N. sayi* are at 32 ppt (Forward *et al.*, 1989). The minimum detection rate in $°C\ m^{-1}$ is calculated as (threshold rate/sinking-ascent rate)1000. The absolute amounts of temperature increase are mean values from Figure 5.

cur at depth, the ascent response upon a temperature decrease would move larvae upward out of cool water into warmer water. The opposite responses occur upon a temperature increase. Nevertheless, the high sensitivity of larvae to temperature change suggests that these responses may have an additional function than avoidance of extreme conditions. Temperature could be used as a cue to regulate depth at a particular optimum temperature or as a cue for depth maintenance in a particular water mass that has a characteristic temperature.

With the present study it is possible to evaluate the relationships of larval responses to environmental factors. For *R. harrisii,* responses to rate of change in light (Forward, 1985), hydrostatic pressure (Forward and Wellins, 1989), salinity (Forward, 1989), and temperature (this study) have been determined. Upon descending in a stratified water column, light intensity decreases, pressure increases, salinity increases, and temperature decreases. At rates of change that are within the range larvae can encounter while descending, each of the changes in these environmental factors induces negative geotaxis or an activity increase that results in an ascent.

In contrast, the opposite environmental changes upon an ascent produce weak responses, at best. *R. harrisii* larvae are unresponsive to rates of increase in light intensity (Forward, 1985) and rates of decrease in salinity (Forward, 1989) they are likely to encounter underwater. In darkness, a sinking response occurs upon a pressure decrease, but the threshold rate is much higher than that for a pressure increase (Forward and Wellins, 1989). Similarly, this study indicates larvae can respond to both increases and decreases in temperature, but the thresholds were always higher for responses to a temperature increase (Table I).

For *N. sayi,* responses to rates of changes in salinity (Forward, 1989), pressure (Forward *et al.,* 1989), and temperature (this study) have also been studied. Considering Stage I zoeae, a pronounced ascent is also induced by changes in these factors that are likely to occur upon descending in the water column. The opposite environmental changes produce weaker responses. *N. sayi* larvae are unresponsive to decreases in salinity (Forward, 1989). They respond both to pressures increases and decreases, but the threshold for a pressure increase was lower than that for a pressure decrease (Forward *et al.,* 1989). Finally, this study shows that larvae respond to temperature increases and decreases, but the threshold rate is higher for a temperature increase (Table I). Thus both *R. harrisii* and *N. sayi* larvae have asymmetrical responses to changes in environmental factors. These responses may keep larvae up in the water column and reduce the likelihood that they will encounter the bottom and its associated benthic predators.

Acknowledgments

This material is based on research supported by the National Science Foundation under Grant No. OCE-8603945. I thank Mr. M. Wachowiak for his technical assistance and Dr. D. Rittschof for critically reading the manuscript.

Literature Cited

Cronin, L. W. 1982. Estuarine retention of larvae of the crab *Rhithropanopeus harrisii*. *Estuar. Coast. Sci.* **15:** 207–220.

Dittel, A. L., and C. E. Epifanio. 1982. Seasonal abundance and vertical distribution of crab larvae in Delaware Bay. *Estuaries* **5:** 197–202.

Dunnett, C. W. 1964. New tables for multiple comparisons with a control. *Biometrics* **20:** 282–291.

Forward, R. B., Jr. 1976. Light and diurnal vertical migration: photobehavior and photophysiology of plankton. Pp. 157–209 in *Photochemical and Photobiological Reviews*, Vol. 1, K. C. Smith, ed. Plenum Press, New York.

Forward, R. B., Jr. 1985. Behavioral responses of larvae of the crab *Rhithropanopeus harrisii* (Brachyuran; Xanthidae) during diel vertical migration. *Mar. Biol.* **90:** 9–18.

Forward, R. B., Jr. 1988. Diel vertical migration: zooplankton photobiology and behavior. *Oceanog. Mar. Biol. Annu. Rev.* **26:** 361–393.

Forward, R. B., Jr. 1989. Behavioral responses of crustacean larvae to rates of salinity change. *Biol. Bull.* **176:** 229–238.

Forward, R. B., Jr., and T. W. Cronin. 1979. Spectral sensitivity of larvae from intertidal crustaceans. *J. Comp. Physiol.* **133:** 311–315.

Forward, R. B., Jr., and C. A. Wellins. 1989. Behavioral responses of a larval crustacean to hydrostatic pressure: *Rhithropanopeus harrisii* (Brachyura: Xanthidae). *Mar. Biol.* **101:** 159–172.

Forward, R. B., Jr., C. A. Wellins, and C. U. Buswell. 1989. Behavioral responses of larvae of the crab *Neopanope sayi* to hydrostatic pressure. *Mar. Ecol. Prog. Ser.* **57:** 267–277.

Kelley, P., S. D. Sulkin, and W. F. Van Heukelem. 1982. A dispersal model for larvae of the deep sea red crab *Geryon quinquedens* based upon behavioral regulation of vertical migration in the hatching stage. *Mar. Biol.* **72:** 35–43.

Kirby-Smith, W. W., and R. T. Barber. 1979. The Water Quality Ramifications in Estuaries of Converting Forest to Intensive Agriculture. University of North Carolina—Water Resource Research Institute Report No. 148. Pp. 1–70.

Latz, M. I., and R. B. Forward Jr. 1977. The effect of salinity upon phototaxis and geotaxis in a larval crustacean. *Biol. Bull.* **153:** 163–179.

McConnaughey, R. A., and S. D. Sulkin. 1984. Measurements of the effects of thermoclines on the vertical migration of larvae of *Callinectes sapidus* (Brachyura: Portunidae) in the laboratory. *Mar. Biol.* **81:** 139–145.

Ott, F. S., and R. B. Forward, Jr. 1976. The effect of temperature on phototaxis and geotaxis by larvae of the crab *Rhithropanopeus harrisii* (Gould). *J. Exp. Mar. Biol. Ecol.* **23:** 97–107.

Pinschmidt, W. C., Jr. 1963. Distribution of crab larvae in relation to some environmental conditions in the Newport River estuary, North Carolina. Ph.D. thesis, Duke University, Durham, North Carolina.

Sandifer, P. A. 1975. The role of pelagic larvae in recruitment to populations of adult decapod crustaceans in the York River estuary and adjacent lower Chesapeake Bay, Virginia. *Estuar. Coastal Mar. Sci.* **3:** 269–279.

Salmon, M., W. H. Seiple, and S. G. Morgan. 1986. Hatching rhythms of fiddler crabs and associated species at Beaufort, North Carolina. *J. Crust. Biol.* **6:** 24–36.

Stefansson, U., and L. P. Atkinson. 1967. Physical and Chemical Properties of the Shelf and Slope Waters of North Carolina. Technical Report. Duke University Marine Laboratory. Pp. 1–230.

Sulkin, S. D. 1984. Behavioral basis of depth regulation in the larvae of brachyuran crabs. *Mar. Ecol. Prog. Ser.* **15:** 181–205.

Sulkin, S. D., and W. Van Heukelem. 1982. Larval recruitment in the crab *Callinectes sapidus* Rathbun: an amendment to the concept of larval retention in estuaries. Pp. 459–475 in *Estuarine Comparisons*, V. Kennedy, ed. Academic Press, New York.

Sulkin, S. D., W. Van Heukelem, and W. Kelley. 1983. Behavioral basis of depth regulation in the hatching and post-larval stage of the mud crab *Eurypanopeus depressus*. *Mar. Ecol. Prog. Ser.* **11:** 157–164.

Sulkin, S. D., W. Van Heukelem, P. Kelley, and L. Van Heukelem. 1980. The behavioral basis of larval recruitment in the crab *Callinectes sapidus* Rathbun: a laboratory investigation of ontogenetic changes in geotaxis and barokinesis. *Biol. Bull.* **159:** 402–417.

Thorson, G. 1964. Light as an ecological factor in the dispersal and settlement of larvae of marine bottom invertebrates. *Ophelia* **1:** 167–208.

Walpole, R. E. 1974. *Introduction to Statistics*. Macmillan, New York.

Welsh, J. H. 1932. Temperature and light as factors influencing rate of swimming of larvae of mussel crab *Pinnotheres maculatus* (Say). *Biol. Bull.* **63:** 310–326.

Yule, A. B. 1984. The effect of temperature on the swimming activity of barnacle nauplii. *Mar. Biol. Lett.* **5:** 1–11.

Reference: *Biol. Bull.* **178**: 205–209. (June, 1990)

Food Aversion Learning by the Hermit Crab *Pagurus granosimanus*

KEITH WIGHT, LISBETH FRANCIS, AND DANA ELDRIDGE

Biology Department, Bates College, Lewiston, Maine 04240

Abstract. The common intertidal hermit crab *Pagurus granosimanus* learns in one or two trials to reject an attractive, novel food (beef) when illness is induced by lithium chloride injected one hour after the animal accepts and eats the beef. Crabs fed a familiar food (fish) before lithium chloride injection do not learn to avoid the fish. Nor do they learn to reject beef when injected with a sodium chloride solution, or when punctured with a hypodermic needle one hour after their first and second beef meals. Because many crustaceans are scavengers and generalist feeders, they must commonly encounter a wide variety of toxic foods. Quickly acquired and long-lasting aversion to a new food eaten a few hours before the onset of a serious physiological upset could cause these animals to avoid such hazardous foods in the future. Food aversion learning has never before been reported in a crustacean.

Introduction

From Baja California to Alaska, the common intertidal hermit crab *Pagurus granosimanus* lives on rocky substrates between −1.0 and +0.8 meters, relative to mean lower low water (Nyblade, 1974; Abrams, 1987). Like most hermit crabs, *P. granosimanus* is an omnivorous detritivore that feeds actively on a wide range of plant and animal foods (Orton, 1927; Roberts, 1968; Hazlett, 1981). For an opportunistic feeder living on wave-swept shores, the particular food available, its nutritional value, and the risk of toxicity can vary seasonally, from place to place, and even from tide to tide. This should favor the evolution of sensory capacities and learning mechanisms that allow the animal to be both selective and flexible in its choice of foods.

Food aversion learning is a kind of associative learning that is particularly appropriate for opportunistic feeders (Wilcoxon *et al.*, 1971; Garcia *et al.*, 1974; Garcia and Hankins, 1977; Gustavson, 1977; Zahorik and Houpt, 1981). It is distinguished from classical or operant conditioning on the basis of several distinctive characteristics (reviewed and discussed in Barker *et al.*, 1977). (1) One or a very few conditioning trials are commonly effective. (2) Learning can occur in spite of long delays between ingestion and the resulting illness. (3) The resulting aversion has a long extinction time. (4) Only particular aspects of the food are associated with the illness. (5) Novel foods are much more readily associated with the sickness than are familiar foods.

As generalist feeders and scavengers that distinguish foods primarily by chemoreception (Hazlett, 1968, 1971; Zimmer-Faust, 1987), hermit crabs may benefit from a learning mechanism similar to the taste aversion learning of rats. We demonstrate here that hermit crabs (*Pagurus gransimanus*) quickly learn to reject a novel and attractive food when severe illness is induced by lithium chloride injected about an hour after they first eat that food.

Materials and Methods

Large animals (wet weight 0.48–1.65 grams without the shells) were collected from rockpools at Cattle Point on San Juan Island, Washington, and held in aquaria supplied with running seawater at the Friday Harbor Laboratories. After removing the apex of each shell with a belt sander, we divided the crabs haphazardly into 6 groups of 15 animals each. Each group was held in a plastic mesh (Vexar) cage divided into separate 10 cm square compartments for each animal. The cages were raised 4 cm off the bottom of the aquaria so the animals could not browse on accumulated detritus.

The foods used were fresh ground beef and fresh fish

Received 3 August 1989; accepted 16 March 1990.

(sole) that were frozen raw. Only the amount needed was thawed each day to maintain equal freshness throughout the experiment. The crabs were hand-fed twice a day (morning and evening): we offered them tiny pieces of freshly thawed food on the end of a dissecting probe. Uneaten food that fell through the plastic mesh was removed from the aquaria half an hour later. The crabs were fed fish for at least two days before treatments began. On treatment days we fed them, moved them into separate finger bowls an hour later, and removed them from their shells by gently prodding the abdomens with a thin piece of plastic coated wire inserted through the hole at each shell apex.

Injections were done with a microliter syringe with a fixed needle that was wiped with alcohol between injections. Ten-microliter doses were injected into the thorax dorsally at the joint between the thorax and abdomen. Solutions used were 1.1 *M* lithium chloride (LiCl) and 1.1 *M* sodium chloride (NaCl) in glass distilled water.

On the first day of the experiment (day 0), four of the six groups were fed *beef;* of these, one group was injected one hour later with lithium chloride (LiCl), a second with sodium chloride (NaCl), the third merely pierced with the hypodermic needle but not injected, and the fourth only removed from the shell. The two remaining groups were fed *fish;* and one hour later one group was injected with lithium chloride, and the other with sodium chloride.

Only animals that accepted the test food when it was next offered (24 h after the first treatment) received a second treatment on the following day (day 1).

The crabs' responses to food were tested twice daily for the next 11 days (days 2–12) without further treatment. They were offered bits of fish in the morning and beef at night on the tip of a probe, and each animal's response was scored as either acceptance or rejection (described in the results below).

To reduce the amount of handling during treatment, the animals were not weighed initially. Instead, on day 10 of the experiment, surviving animals were removed from their shells and weighed individually to the nearest hundredth of a gram.

Results

Food acceptance and rejection responses

When accepting food from a probe, hermit crabs usually touch the probe with the second antennae or the dactyls of the walking legs, grasp the food using the chelipeds and sometimes also with the walking legs, then pass it toward the mouth, usually using the minor, left cheliped. Both chelipeds may be used to tear off bits that can be ingested, or the whole mass may be manipulated and held against the inner mouthparts by the third maxillipeds.

When rejecting the food, the crabs generally flick the second antennae back and away after contacting the probe. Sometimes they push the food away vigorously with the chelipeds and back away; and sometimes they hesitantly grasp it with the minor cheliped, pass it to the mouthparts, manipulate it for a few seconds, and then eject it forward and upward using a jet of water.

Dosage and effects of lithium chloride

The mean wet weight overall for the animals was one gram (sd = 0.3, n = 89). To avoid excessive handling, the animals were each given the same size injection; and thus the per weight dose of LiCl varied from 250 to 970 mg/Kg wet weight (per treatment).

This dose of LiCl caused limb trembling, uncontrolled movement, and periods of immobility when the animals usually lay on their backs. All of these animals found and reaccepted their shells within two to three hours. The crabs that were injected with NaCl tended periodically to curl tightly into a ball, sometimes remaining immobile for several minutes; but they reaccepted their shells within half an hour. Those that were stabbed with the needle but not injected returned to their shells within 15 minutes with only occasional periods of immobility; and the crabs that were only removed from their shells usually reaccepted them immediately.

Induced aversion to a novel food

All of the animals injected with LiCl after their first encounters with beef developed an aversion to beef (Figs. 1A, 3A). Two-thirds refused beef after only one LiCl injection. The five that were injected again, after their second beef meal, all refused beef when it was offered for the third time. Without additional injections, the number refusing beef continued to be significantly higher than for the controls through day thirteen (G-test with the Williams correction, $P < .05$). On day 14 the number that refused beef was not significantly higher than in the control groups (G-test, $P > .50$).

As individuals, these animals were also more consistent in refusing beef than were the animals in other treatment groups (Fig. 3). Extinction of the response generally required more than a week—on average, the beef-LiCl treated animals refused beef for 6.9 ± 3.0 consecutive days within the first 11-day period following treatment (days 2 through 12), (Fig. 3A). This was significantly longer than for any other treatment group (t-test, $P \ll .001$). This group rejected beef more consistently than it rejected fish (t-test, $P \ll .001$).

Although about twice as many animals in the beef-NaCl and beef-puncture control groups received a sec-

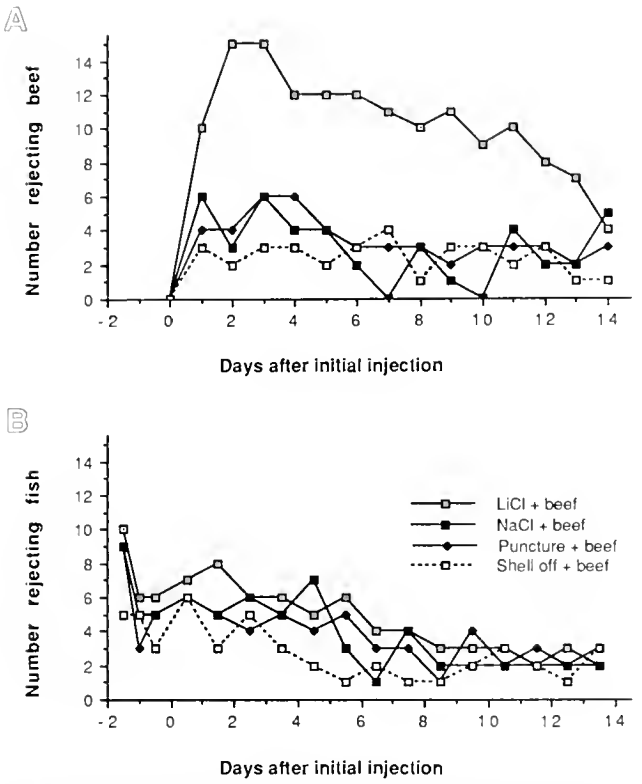

Figure 1. Number of individual hermit crabs (*Pagurus granosimanus*) that rejected daily feedings of (A) beef and (B) fish. The legend applies to both graphs. Four groups of 15 animals each were treated on day zero, one hour after eating a novel food (beef); those that accepted beef the next day received a second treatment. One treatment group was only removed from the shell; a second was also punctured with a hypodermic needle. Two other groups received injections, one with lithium chloride, and the other with sodium chloride.

ond treatment, neither group developed an aversion to beef (Fig. 1A). Significantly more of the animals in the fish-NaCl treatment group rejected beef on first encountering this new food, 12 h after their treatments on day 0 and day 1 (comparison with the beef-shell removal control group; G-test, $P < .01$ and $P < .025$ for day 0 and day 1, respectively; Fig. 2B); however, none of these animals showed a long-term aversion to beef (Fig. 3C).

Consistent acceptance of a familiar food

All of the groups continued to accept fish throughout the test period (Fig. 1B). Of the two groups that were injected after eating this familiar food, neither learned to reject fish (Fig. 2A).

Mortality

Six animals died during the experiment: one from the beef-LiCl group on day 4; three from the fish-NaCl group on days 2, 9, and 10; one on day 11 from the group that was simply removed from the shell; and one from the fish-LiCl group on day 10.

Discussion

When injected with LiCl one hour after their first beef meals, hermit crabs (*Pagurus granosimanus*) learned in one or two trials to avoid this novel food while continuing to eat a familiar food (fish). This aversion to beef commonly lasted for more than a week under laboratory conditions. Hermit crabs rely strongly on chemoreception in locating food (Hazlett, 1968; Zimmer-Faust, 1987). Crustaceans can learn using chemoreception as a cue. Fine-Levy *et al.* (1988) found that the spiny lobster can learn to associate a particular smell with the presence of a predator. It is likely, then, that food is identified and avoided on the basis of chemoreception in response either to water-borne chemicals (smell) or to direct contact (taste). Further work is required to determine what specific food cues are used in this learned avoidance of a specific food.

In laboratory experiments with vertebrates (reviews in

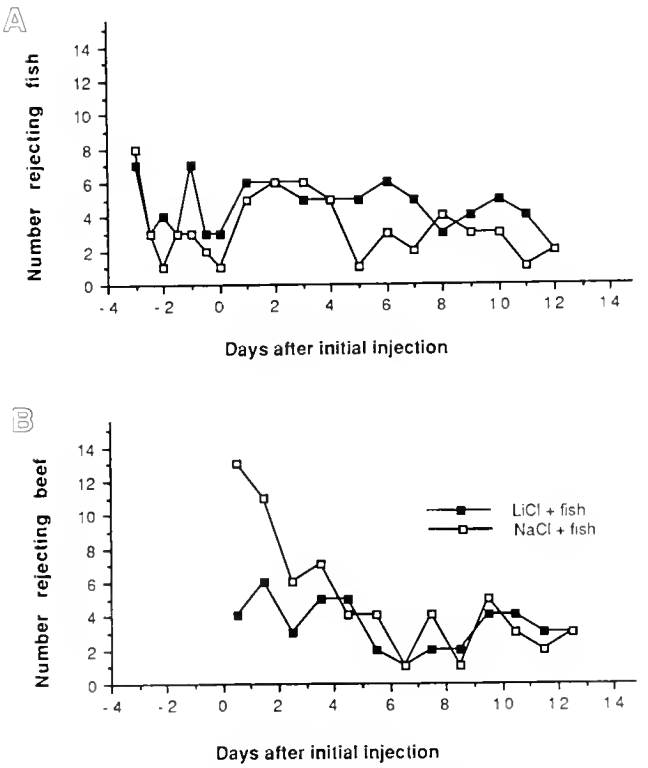

Figure 2. Number of individual hermit crabs (*Pagurus granosimanus*) that rejected (A) fish and (B) beef on each day following treatment. Animals were treated on day zero, one hour after eating a familiar food (fish); those that accepted fish the next day were given a second treatment. The two treatment groups of 15 animals each were injected either with lithium chloride or with sodium chloride.

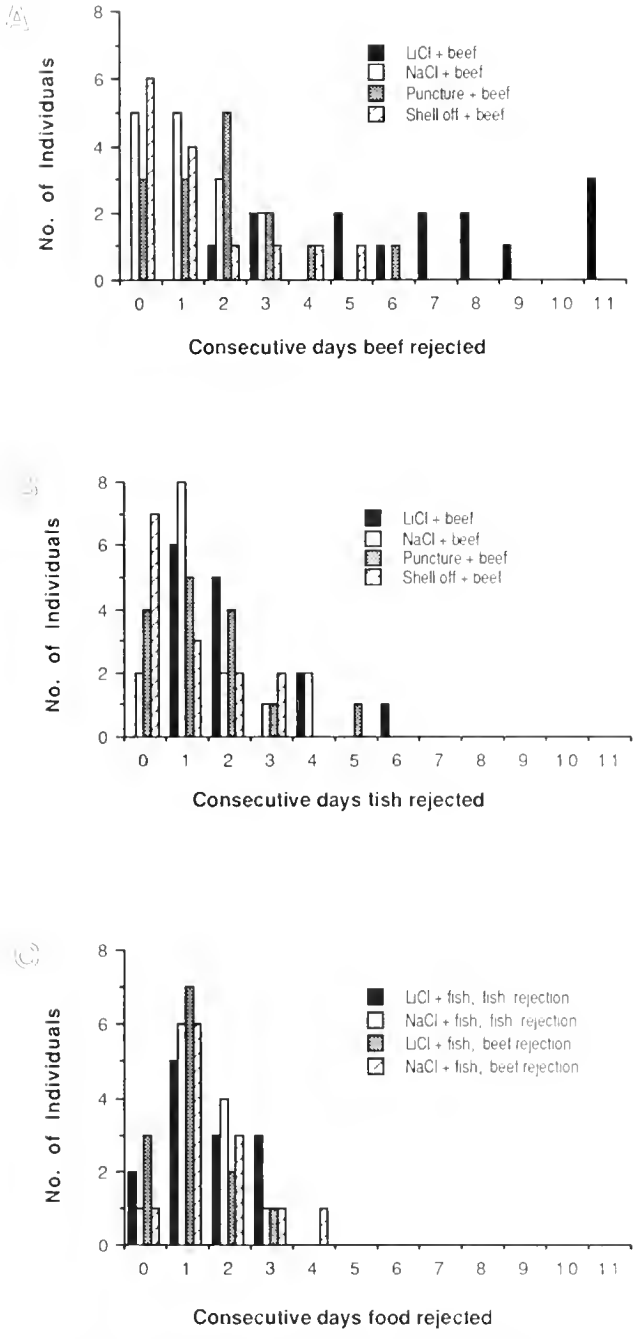

Figure 3. Consistency of food rejection by individual hermit crabs (*Pagurus granosimanus*) in six treatment groups (identified in the legends). Columns show the maximum number of consecutive days that each animal rejected a particular food during the eleven days following treatment: (A) rejection of a novel food (beef) by animals treated one hour after their first beef meal (or after the first and second beef meals, for those that accepted beef on the day after their first treatment), (B) fish rejection by the same animals, and (C) fish and beef rejection by different animals that were treated after eating a familiar food (fish).

Barker *et al.*, 1977), the effects of LiCl injection are generally assumed to mimic the symptoms of illness caused by ingesting a toxic substance. The doses used in our study caused fairly severe and long-lasting general symptoms. Moreover, the food aversion was clearly caused by the effects of the LiCl, and not by osmotic shock or the tonic effects of the injection, because the group injected with the same molar concentrations of NaCl after first eating beef did not develop an aversion to beef. Because animals that developed an aversion to beef continued to accept fish, the aversion is specific, and not merely a generalized, post-trauma avoidance of food. Nor can it be explained as non-specific neophobia (general avoidance of unfamiliar food after an illness), because most of the specimens injected with lithium after a fish meal accepted beef within a few days.

One of the two control groups injected with NaCl solution showed significantly increased rejection of beef for two days following treatment. This response is puzzling because it was inconsistent (*i.e.*, it did not occur in both NaCl injected groups), and because none of the obvious explanations seem to fit. The animals in this group were not significantly smaller than in the other sodium-injected group, which rules out the possibility of unusually high osmotic or tonic stress. If the response were due to non-specific neophobia caused by the treatment, the group injected with lithium after eating fish should also have rejected the beef; but they did not. Whatever the cause of this transient reaction to a new food, it clearly is not long-lasting food aversion of the kind shown by the beef-LiCl treatment group.

Food aversion learning is known to occur commonly among vertebrates (Garcia *et al.*, 1974; Gustavson 1977), and has also been described for a mollusc (Gelperin, 1975) and two insects (Dethier, 1980; Bernays and Lee, 1988). Characteristic of this type of associative learning (Garcia and Hankin, 1977) is rapid aversion to a new food (one or two trials in this case) despite a considerable time lag between ingestion and the onset of illness (in this case, an hour). Also typically, a novel food (in this case, beef) is more readily associated with subsequent internal disorders than is a familiar food (fish). Relatively long extinction times (one or two weeks, here) are also typical.

Most hermit crabs are omnivorous detritivores feeding on fine particles from the sediment as well as on larger morsels of animal matter (Orton, 1927; Roberts, 1968). Thus they are undoubtedly exposed to a wide variety of foods, and presumably also to a wide spectrum of toxins, including rotting debris that can be infested with toxic microorganisms, and macroorganisms that can manufacture or sequester toxins. While food aversion learning has never before been described among crustaceans, many (including the hermit crabs) can learn by classical conditioning (review by Corning *et al.*, 1973). The ability to associate delayed illness with a particular food could be quite advantageous, and might be rather common among the Crustacea.

Acknowledgments

We thank the director of the University of Washington's Friday Harbor Laboratories for use of the facilities, and the faculty, staff, and colleagues there for encouragement and useful discussion.

Literature Cited

Abrams, P. A. 1987. Competitive interactions between three hermit crab species. *Oecologia* **72:** 233–247.

Barker, L. M., M. R. Best, and M. Domjan (eds.) 1977. *Learning Mechanisms in Food Selection.* Baylor University Press, Houston. 632 pp.

Bernays, E. A., and J. C. Lee. 1988. Food aversion learning in the polyphagous grasshopper *Schistocerca americana*. *Physiol. Entomol* **13:** 131–138.

Corning, W. C., J. A. Dyal, and A. O. D. Willows (eds.) 1973. *Invertebrate Learning.* Vol. 2. Plenum Press, New York. 284 pp.

Dethier, V. G. 1980. Food-aversion learning in two polyphagus caterpillars, *Diacrisia virginica* and *Estigmene congrua*. *Physiol. Ent.* **5:** 321–325.

Fine-Levy, J. B., Girardot, M. N., Derby, C. D., and Daniel, P. C. 1988. Differential associative conditioning and olfactory discrimination in the spiny lobster *Panulirus argus*. *Behav. Neural Biol* **49:** 315–331.

Garcia, J., W. G. Hankins, and K. W. Rusiniak. 1974. Behavioral regulation of the *milieu interne* in man and rat. *Science* **185:** 824–831.

Garcia, J., and W. G. Hankins. 1977. On the origin of food aversion paradigms. Pp. 3–43 in *Foraging Behavior*, A. C. Kamil and T. D. Sargent, eds. Garland STPM Press, New York.

Gelperin, A. 1975. Rapid food aversion learning by a terrestrial mollusk. *Science* **189:** 567–570.

Gustavson, C. R. 1977. Comparative and field aspects of learned food aversions. Pp. 23–43 in *Learning Mechanisms in Food Selection*, L. M. Barker, M. R. Best, and M. Domjan, eds. Baylor University Press, Houston.

Hazlett, B. A. 1968. Stimuli involved in the feeding behavior of the hermit crab *Clibanarius vittatus* (Decapoda, Paguridea). *Crustaceana* **15:** 305–310.

Hazlett, B. A. 1971. Chemical and chemotactic stimulation of feeding behavior in the hermit crab *Petrochirus diogenes*. *Comp. Biochem.* **39A:** 665–670.

Hazlett, B. A. 1981. The behavioral ecology of hermit crabs. *Ann. Rev. Ecol. Syst.* **12:** 1–22.

Nyblade, C. F. 1974. Coexistence in sympatric hermit crabs. Ph.D. Thesis, University of Washington, Seattle.

Orton, J. H. 1927. On the mode of feeding of the hermit crab *Eupagurus bernhardus* and some other decapoda. *J. Mar. Biol. Assoc. U.K.* **14:** 909–921.

Roberts, M. H. 1968. Functional morphology of mouth parts of the hermit crabs, *Pagurus longicarpus* and *Pagurus pollicarpis*. *Chesapeake Sci.* **9:** 9–20.

Wilcoxon, H. C., W. B. Dragonin, and P. A. Kral. 1971. Illness induced aversions in rat and quail: relative salience of visual and gustatory cues. *Science* **171:** 826–828.

Zahorik, D. M., and K. A. Houpt. 1981. Species differences in feeding strategies, food hazards, and the ability to learn food aversions. Pp. 289–311 in *Foraging Behavior*, A. C. Kamil and T. D. Sargent, eds. Garland STPM Press, New York.

Zimmer-Faust, R. K. 1987. Crustacean chemical perception: towards a theory on optimal chemoreception. *Biol. Bull* **172:** 10–29.

Reference: *Biol Bull* **178**: 210–216. (June, 1990)

Effect of Calcium on the Stability of the Vitelline Envelope of Surf Clam Oocytes

GEORGE DESSEV AND ROBERT GOLDMAN

Department of Cell, Molecular and Structural Biology, Northwestern University Medical School, 303 East Chicago Avenue, Chicago, Illinois 60611, and Marine Biological Laboratory, Woods Hole, Massachusetts 02543

Abstract. Fertilization and parthenogenic activation of oocytes of the surf clam, *Spisula solidissima*, require the presence of calcium in the extracellular medium. Here we report that the depletion of calcium causes a dramatic increase in the stability of the vitelline envelopes (VE). On the basis of this effect, we have developed a method of isolating intact VE and have studied their morphology, composition, and properties. Experiments using $^{45}Ca^{2+}$ have revealed that isolated VE bind calcium in a weak, but specific way. These findings suggest that the function of calcium may be to maintain the oocyte surface in a fertilization-competent state, while the reactions subsequent to the initial activation event, and leading to nuclear envelope breakdown (NEBD), may not require calcium. In support of this hypothesis, we have demonstrated that hypertonic conditions induce the oocytes to undergo NEBD in the absence of extracellular calcium.

Introduction

Development of the oocytes of most animal species is discontinued at a certain stage of meiosis, usually at the G_2/M border (Masui and Clarke, 1979; Maller and Krebs, 1980; Maller, 1985). The oocytes can remain in a state of arrest for long periods and then resume the meiotic process as a response to external signals. In most vertebrates, these signals are hormone-like substances (Maller and Krebs, 1980; Maller, 1985). In *Spisula*, progress into M-phase is induced by fertilization or by a number of physical or chemical stimuli, such as UV-light or changes in the ionic composition of the medium (Allen, 1953). Whatever the nature of these signals, one of their early biochemical effects is believed to be the activation of a pleiotropic enzymatic system, termed M-phase promoting factor (MPF) (Masui and Markert, 1971; Smith and Eckert, 1971; Wu and Gerhart, 1980; Arion *et al.*, 1988; Draetta *et al.*, 1989; Dunphy *et al.*, 1988; Gautier *et al.*, 1988; Lohka *et al.*, 1988; Murray and Kirschner, 1989). Activation of MPF is supposed to trigger pathways leading to different M-phase specific events (*i.e.*, NEBD, condensation of chromosomes, formation of the mitotic spindle, karyokinesis, etc.).

Fertilization of the oocytes of the surf clam requires the presence of calcium in the extracellular medium (Allen, 1953; Schuetz, 1975; Jaffe, 1983, 1985). The mechanism of action of calcium is not known. Calcium has been put forward as a cofactor of protein kinase C (Dube *et al.*, 1987; Eckberg *et al.*, 1987). Alternatively, generation of the activating signal may require an interaction of calcium with the surface of the oocyte, as shown for other species (Moreau *et al.*, 1976; Schroderet-Slatkine *et al.*, 1976).

The experiments described in this paper were initiated to distinguish between these two mechanisms. We have obtained evidence suggesting that calcium interacts with the oocyte surface. The depletion of calcium has a striking effect on the stability of the vitelline envelope (VE), an extracellular structure surrounding the oocyte and closely associated with the plasma membrane. This finding has allowed us to develop a method of isolating pure VE, and to characterize them by biochemical and ultrastructural methods. Further, we have demonstrated that the isolated VE possess weak calcium-specific binding sites. Our observations suggest that the role of calcium may be to maintain the *Spisula* oocyte surface in a fertilization-competent state, rather than to participate as a co-

Abbreviations: VE, vitelline envelopes; NEBD, nuclear envelope breakdown; MFSW, millipore-filtered seawater; CFSW, calcium-free seawater; MPF, M-phase promoting factor.

factor in the enzymatic pathway leading to NEBD. In agreement with this view, we have demonstrated that treatments with hypertonic solutions of NaCl or glycerol induce the oocytes to resume maturation in the absence of extracellular calcium.

Materials and Methods

Surf clams were supplied by the Department of Marine Resources at the Marine Biological Laboratory (Woods Hole, Massachusetts). The oocytes were obtained by dissection of the ovaries of female animals and were then washed four times with Millipore-filtered seawater (MFSW) (Allen, 1953).

The proportion of oocytes that had undergone NEBD was scored by phase contrast microscopy. For electron microscopy, pellets of isolated VE were fixed in 1% glutaraldehyde in phosphate-buffered saline (pH 7.5), postfixed in OsO_4, embedded in Epon, and sectioned. Proteins were fractionated by SDS PAGE (Laemmli, 1970). Protein was determined by the method of Lowry *et al.* (1951), and carbohydrates by the phenol/sulfuric acid method, as described by Ashwell (1966).

The binding of $^{45}Ca^{2+}$ to isolated VE was studied as follows. The VE were washed 5 times, each time in 200 volumes of binding buffer (0.25 *M* sucrose, 10 m*M* Pipes·NaOH, pH 7.2, 5 m*M* KCl, and 1 mg/ml bovine serum albumin), and resuspended in binding buffer at a protein concentration of 200–250 μg/ml. Aliquots of this suspension were incubated for 30 min at room temperature in the presence of [^{45}Ca]$CaCl_2$ (New England Nuclear; specific radioactivity 20 mCi/mg) at different concentrations of $CaCl_2$. At the end of the incubation, aliquots were taken for determination of the total radioactivity. The samples were then centrifuged in an Eppendorf microfuge for 5 min, and a second set of aliquots was taken from the supernatant to determine the unbound radioactivity. The binding was calculated from the difference between the two measurements. The walls of the tubes adsorbed less than 3% of the radioactivity. The presence of bovine serum albumin, which was necessary to minimize the adhesion of the VE to the plastic, did not affect the results. At all Ca^{2+} concentrations studied, 30 min of incubation was sufficient to reach a constant ratio between free and bound calcium.

Results

Depletion of calcium leads to stabilization of the oocyte VE

In our first experiments, we studied the stability of the VE in the presence or absence of calcium. Oocytes were extensively washed with MFSW or calcium-free seawater (CFSW) and then vigorously homogenized in an all glass homogenizer. After 20 strokes by hand, more than 90% of the oocytes suspended in MFSW were broken and their VE were extensively fragmented. After the same treatment, only about 30% of the oocytes in CFSW were broken and, more important, the VE of the broken cells were nearly intact empty shells. These results suggested that the presence of calcium strongly affects the mechanical stability of the VE.

Table I

Effect of different treatments on the stability of the vitelline envelopes of surf clam oocytes

Treatment of oocytes	State of the VE
10% glycerol, 15 m*M* phosphate buffer, pH 8, 0.5% NP-40	Solubilized in 10 min at 20°C
10% glycerol, 15 m*M* phosphate buffer, 0.5% NP-40, and 20 m*M* EGTA	No lysis
SDS, 0.2%	Solubilized in 10 min at 20°C
SDS, 0.2% in 20 m*M* EGTA	No lysis
4 *M* urea	Solubilized in 10 min at 20°C
4 *M* urea in 20 m*M* EGTA	No lysis

Further experiments revealed that a similar effect could be observed upon treating the oocytes with reagents disrupting protein-protein interactions, such as 4 *M* urea, 0.2% SDS, and with a solution containing 1.4 *M* glycerol, 15 m*M* phosphate, pH 8.0, (with or without 50 m*M* KCl), which destabilizes the VE (Rebhun and Sharpless, 1964; Dessev and Goldman, 1988), followed by 0.5% NP-40. In all these cases, if the samples contained 1–10 m*M* $CaCl_2$, the oocytes lysed and nearly all of the VE were dissolved, as observed by phase contrast optics (Table I). In contrast, when the samples contained 5–10 m*M* EGTA, the cells did not lyse and the integrity of the VE did not seem to be affected (Table I). The EGTA-induced stabilization of the VE was reversible: after addition of $CaCl_2$ to an excess of 10 m*M*, the VE underwent fragmentation over a period of 10–20 min and finally dissolved, which was accompanied by lysis of the oocytes. EGTA caused stabilization of VE when added both before and after the oocytes had undergone NEBD following KCl activation.

These results demonstrate that calcium strongly affects the mechano-chemical properties of the VM: in the presence of EGTA, a marked stabilization of these structures occurs, rendering them resistant to conditions which would completely solubilize them in the presence of calcium.

Isolation of VE

The EGTA-induced stabilization of the VE allowed us to develop the following procedure for their isolation.

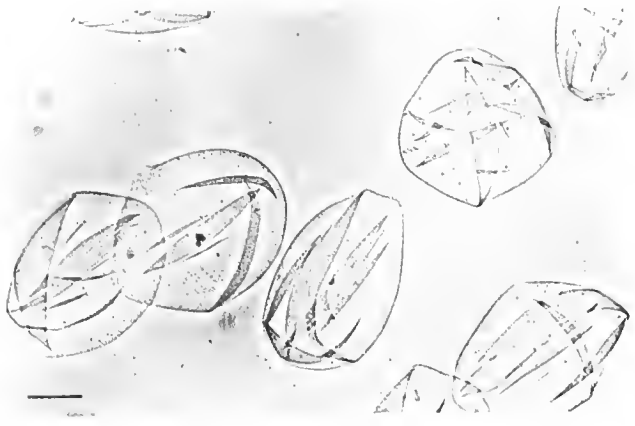

Figure 1. VE isolated as described in the text. Phase contrast. Bar, 20 μm.

Oocytes were sedimented by gravity from 500 volumes of CFSW containing 10 m*M* EGTA, and washed two times with 50 volumes of a solution containing 40 m*M* PIPES (pH 7.2), 100 m*M* NaCl, 10 m*M* KCl, 5 m*M* $MgCl_2$, 50 m*M* EGTA, and 10 m*M* dithiothreitol. The cells were then vigorously homogenized with an all-glass homogenizer in 20 volumes of the same solution at 0°C. The homogenization was continued, with intermittent microscopic control, until virtually all cells were lysed. The homogenate contained empty VE, cytoplasmic granules, and small nuclear fragments. The sample was centrifuged for 10 min at 2000 r.p.m. in a TJ-6 Beckman centrifuge. The crude VE pellet was resuspended in the same solution containing 0.25 *M* sucrose and 0.5% NP-40, and the structures were sedimented again at 2000 r.p.m. The latter step was repeated two more times, yielding a preparation of pure VE (Figs. 1, 2).

If the same procedure was performed on oocytes washed with MFSW, and if the homogenization solution contained 1 m*M* $CaCl_2$ instead of EGTA, then the VE were broken into small fragments, which were impossible to purify.

Ultrastructure

Electron micrographs of isolated VE reveal a structure generally similar to that observed earlier by others (Rebhun, 1962; Longo and Anderson, 1970) on sections of whole oocytes (Fig. 3). The structures consist of a continuous layer of amorphous material, 40–80 nm thick, surrounding the remnants of the microvilli, or spaces formerly occupied by microvilli, located in approximately hexagonal arrays. The inner surface of the VE is associated with smooth sheets or oval-shaped vesicles, which may originate from the oocyte plasma membrane. These sheets, as well as the remnants of the microvilli, probably represent residual, non-lipid, "skeletal" structure of the plasma membrane, as suggested by their resistance to the extensive washing with NP-40.

Our micrographs also reveal an outermost filamentous layer, located above the microvilli, perhaps originating from the oocyte jelly coat. This layer appears less electron-dense than the material surrounding the microvilli. It is separated from their tips by a narrow space which contains a large number of spherical bodies. These bodies are uniform in size (35–40 nm in diameter) and appear to have smooth envelopes.

Composition and properties

The isolated VE contain 55% protein and 45% carbohydrate. They show a complex SDS PAGE pattern (Fig. 4). A treatment of the VE with proteinase K (1 μg/μl at room temperature) leads to their dispersal in less than 1 min, suggesting that protein components are important for their structural integrity. Upon exposure to distilled water, the VE expand up to 50% in diameter. The honeycomb-like structure of the expanded VE can be clearly observed in phase contrast (Fig. 2). Purified VE can be kept frozen at −80°C, which does not affect their morphology or other properties.

Binding of $^{45}Ca^{2+}$ to isolated VE

The stabilizing effect of EGTA described above suggested a direct interaction between the VE and calcium. To verify this, we studied the binding of $^{45}Ca^{2+}$ to isolated VE. Our results showed that at each concentration of Ca^{2+} an equilibrium between free and VE-bound calcium was established, such that between 60% and 70%

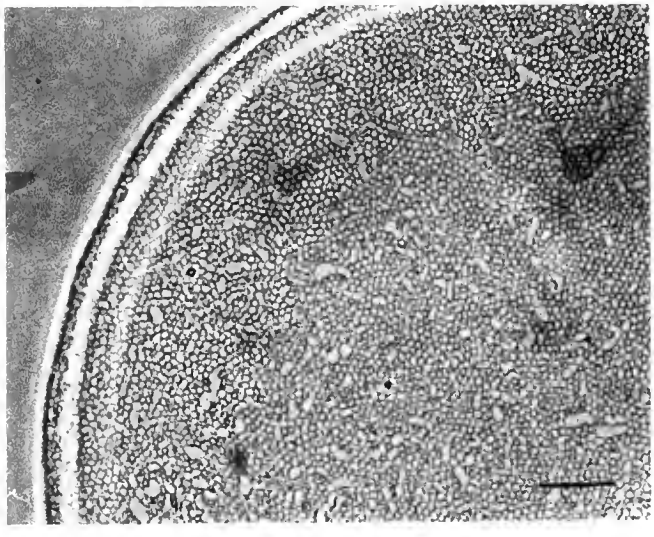

Figure 2. VE isolated as described in the text and resuspended in distilled water for 10 min at room temperature. Phase contrast. Bar, 5 μm.

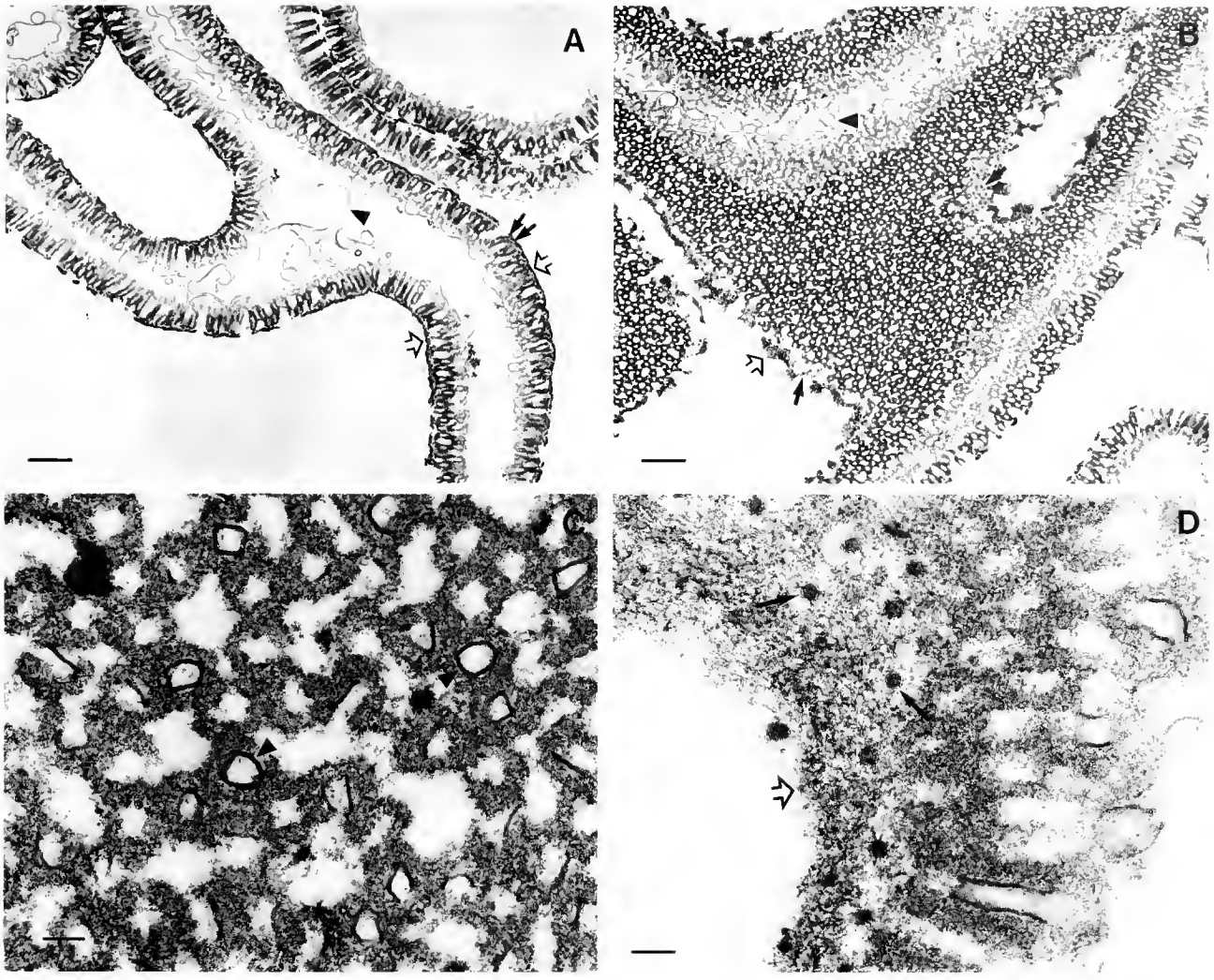

Figure 3. Electron micrographs of sections of isolated VE. (A, B), Bar, 1 μm; (C, D), Bar, 100 nm. A continuous layer of amorphous material, 40–80 nm thick, surrounds the remnants of the microvilli, or spaces formerly occupied by microvilli, located in approximately hexagonal arrays. The inner surface of the VE is associated with smooth sheets or oval-shaped vesicles (arrowheads), which also deliniate the microvilli. A filamentous layer located above the microvilli is seen (open arrows). It is separated from their tips by a narrow space, which contains a large number of spherical bodies, 35–40 nm in diameter, surrounded by smooth envelopes (solid arrows).

of the input calcium cosedimented with the VE at concentrations of Ca^{2+} below 10 μM (Fig. 5). Practically all of the bound radioactivity could be removed by several washings of the pellet with binding buffer. As the concentration of Ca^{2+} increased, the ratio bound Ca^{2+}/input Ca^{2+} declined, and the binding reached an apparent saturation between 10 mM and 40 mM Ca^{2+} at approximately 6 μg bound Ca^{2+} per mg VE-protein (Fig. 6). Despite the low affinity of the VE for Ca^{2+}, the binding was specific, as demonstrated by Mg^{2+} competition experiments (Fig. 7). A 1000-fold excess of Mg^{2+} suppressed the binding of $^{45}Ca^{2+}$ by less than 50%; under the same conditions a much stronger competition by unlabeled calcium was observed (Fig. 7).

Hypertonic conditions induce oocyte activation in the absence of extracellular calcium

Although our results suggested that the action of calcium is restricted to the oocyte surface, they did not preclude the possibility that the stabilization of the VE and the inhibition of oocyte activation are two independent effects of calcium depletion. To obtain more evidence concerning this possibility, we studied the dependence of

Figure 4. SDS PAGE of isolated VE in 7.5% gel. The positions of the molecular weight markers are shown.

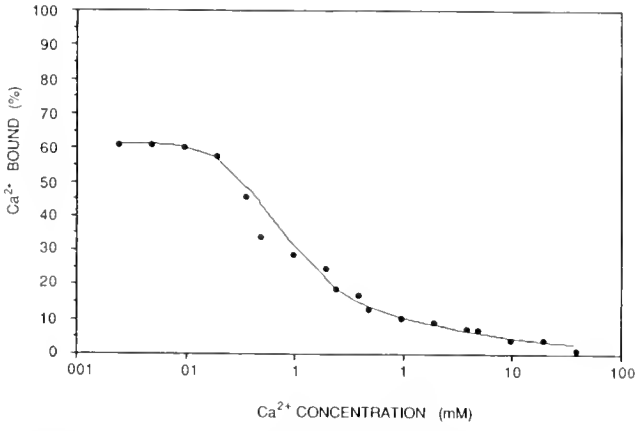

Figure 6. Binding of $^{45}Ca^{2+}$ to isolated VE was determined under the same conditions as in Figure 5, but at Ca^{2+} concentrations up to 40 m*M*

oocyte activation on calcium, using hypertonic solutions (Allen, 1953) such as 1.4 *M* glycerol and 1.2 *M* NaCl as activating agents. The rationale for these experiments was the following.The initial events that induce the oocytes to resume maturation are believed to involve cell depolarization caused by changes in permeability (Finkel and Wolf, 1978; Jaffe, 1983, 1985). Our experiments suggested that calcium, by interacting with the oocyte surface, maintains the latter in a structural state necessary for these events to occur. We hypothesized that unphysiological treatments, such as osmotic shock, might disturb the permeability barrier at the oocyte surface and lead to depolarization and activation in the absence of calcium. Furthermore, glycerol, known to "soften" the VE (Rebhun and Sharpless, 1964), might be expected to counteract the EGTA-induced stabilization which was thought to prevent the oocyte activation.

We found that the oocytes could be activated in CFSW containing glycerol and 50 m*M* KCl. The proportion of activated oocytes did not change linearly with glycerol concentration, but increased abruptly around 10% (1.4 *M*) glycerol, suggesting a correlation between activation and hypertonicity (Fig. 8). No activation occurred in CFSW and 50 m*M* KCl alone. Activation (30–50%) was also observed in solutions containing 1.4 *M* glycerol, 20 m*M* Na-phosphate (pH 8.0), 50 m*M* KCl, and 30–80 m*M* EGTA (not shown).

In another series of experiments, we used a procedure involving concentrated solutions of NaCl to activate the cells (Allen, 1953). Oocytes were extensively washed in CFSW and resuspended in a mixture of CFSW and 0.2 *M* EGTA (1:1). To this sample, 0.25 volumes of 5 *M* NaCl were added to a final NaCl concentration of 1.2 *M*. After 15 min at 18°C, the cells were sedimented and

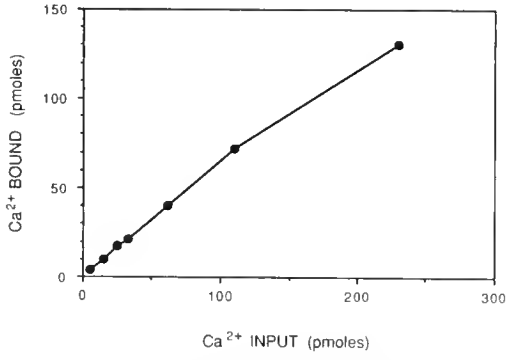

Figure 5. Binding of $^{45}Ca^{2+}$ to isolated VE at low concentrations of Ca^{2+}. VE suspended in binding buffer at a protein concentration of 250 μg/ml were incubated with different amounts of $^{45}Ca^{2+}$ in a final volume of 0.1 ml. The binding was determined as described in Materials and Methods.

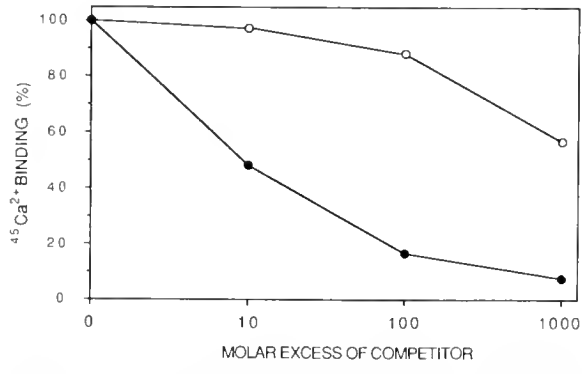

Figure 7. Binding of $^{45}Ca^{2+}$ (initial concentration 0.5 μ*M*) to isolated VE in the presence of increasing concentrations of Mg^{2+} (open symbols) and Ca^{2+} (closed symbols).

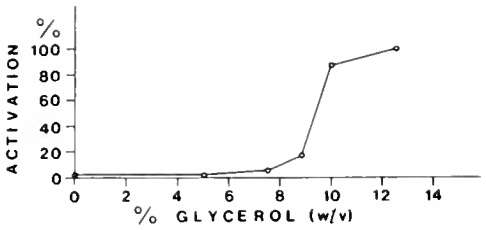

Figure 8. Activation of oocytes in glycerol solutions. Oocytes were suspended in CFSW containing 50 m*M* KCl and glycerol at the indicated concentration. Thirty minutes later, the percentage of oocytes that had undergone NEBD was scored.

resuspended in the same solution without NaCl. Twenty minutes later, the proportion of oocytes that had undergone NEBD was determined. The results varied between 40% and 80% activation in different experiments.

These studies demonstrate that under hypertonic conditions the oocytes can be activated in the absence of extracellular calcium.

Discussion

Our results suggest that calcium interacts with the VE of the surf clam oocytes and that this interaction may be important for maintaining the oocyte surface in a fertilization-competent state. This conclusion is based on the correlation between our experimental findings and the biological properties of the system. Thus, (a) depletion of calcium inhibits fertilization and causes a marked increase in the stability of the VE. Both effects are reversible upon addition of calcium. (b) The weak binding of calcium to isolated VE correlates with the seemingly weak binding of biologically important calcium; a brief washing with a calcium-free medium prevents fertilization or activation of the oocytes. (c) Mg^{2+} does not substitute for calcium in the process of activation, nor does it compete significantly with $^{45}Ca^{2+}$ binding *in vitro*.

A mechanism of action of calcium involving an interaction with the oocyte surface is consistent with studies on other species. Thus, introduction of calcium into zones near the surface of *Xenopus* oocytes leads to their activation, whereas calcium introduced deeper into the oocyte interior has no such effect (Moreau *et al.*, 1976). Similarly, treatment of the *Xenopus* oocyte surface with lanthanum (considered a calcium-mobilizing agent), but not its microinjection into the oocyte, induces maturation (Schorderet-Slatkine *et al.*, 1976).

The effect of phorbol esters on oocyte activation suggests that calcium- and phospholipid-dependent protein kinase C may be involved in the initial stages of maturation (Dube *et al.*, 1987; Eckberg *et al.*, 1987). Schuetz (1975) has concluded that, in the clam, calcium is rapidly equilibrated across the oocyte membrane, and the presence of calcium in the medium is needed to supply intracellular calcium. However, this does not seem to be the case, because hypertonic conditions cause oocyte activation in the presence of EGTA.

These results can be explained in two ways. Either (a) the hypertonic treatment releases calcium from EGTA-inaccessible intracellular sources, or (b) the reactions leading to NEBD do not require calcium. Although we cannot, at present, distinguish between these two explanations, the second one agrees with our finding that NEBD in a *Spisula* oocyte cell-free system does not require calcium (Dessev *et al.*, 1989). Moreover, cytosolic extracts from unstimulated *Spisula* oocytes, which are initially inactive in NEBD *in vitro*, can be activated in the absence of calcium (Dessev, unpub. results). Similarly, the MPF system, which is considered as an universal M-phase regulator, appears to function in a calcium-independent way and is stabilized by EGTA (Wu and Gerhart, 1980; Arion *et al.*, 1988; Dunphy and Newport, 1988; Lohka *et al.*, 1988).

Activation factors, such as fertilization, UV light, and KCl require extracellular calcium (Allen, 1953). We have shown that other agents, such as hypertonic solutions of glycerol and NaCl, are capable of inducing maturation in the absence of calcium. Since glycerol and NaCl are chemically different, they are likely to act via osmotic changes, forcing membrane depolarization to occur even when the surface is structurally altered by depletion of calcium and is not susceptible to the action of other activation factors.

The chemical nature of the calcium binding to the VE, which is both weak and specific, as well as the nature of the structural and functional changes in the VE induced by calcium, remain interesting subjects for further studies.

Acknowledgments

We wish to thank Dr. A. Telser for help in the preparation of the drawings. Research support was provided by NCI.

Literature Cited

Allen, R. D. 1953. Fertilization and artificial activation in the egg of the surf clam, *Spisula solidissima*. *Biol. Bull.* **105:** 213–239.

Arion, D., L. Meijer, L. Brizuella, and D. Beach. 1988. cdc2 is a component of the M phase-specific histone H1 kinase: evidence for identity with MPF. *Cell* **55:** 371–378.

Ashwell, G. 1966. New colorimetric methods for sugar analysis. *Meth. Enzymol.* **8:** 85–95.

Dessev, G., and R. Goldman. 1988. Meiotic breakdown of nuclear envelope in oocytes of *Spisula solidissima* involves phosphorylation and release of nuclear lamin. *Dev. Biol.* **130:** 543–550.

Dessev, G., R. Palazzo, L. Rebhun, and Goldman R. 1989. Disassembly of the nuclear envelope of *Spisula* oocytes in a cell-free system. *Dev. Biol.* **313:** 496–504.

Draetta, G., F. Luca, J. Westendorf, L. Brizuella, J. Ruderman, and D. Beach. 1989. cdc2 protein kinase is complexed with both cyclin A and B: evidence for proteolytic inactivation of MPF. *Cell* **56:** 829–838.

Dube, F., R. Golsteyn, and L. Dufresne. 1987. Protein kinase and meiotic maturation of surf clam oocytes. *Biochem. Biophys. Res. Comm* **142:** 1072–1076.

Dunphy, W. G., L. Brizuella, D. Beach, and J. Newport. 1988. The *Xenopus* cdc2 protein is a component of MPF, a cytoplasmic regulator of mitosis. *Cell* **54:** 423–431.

Dunphy, W., and J. W. Newport. 1988. Mitosis-inducing factors are present in a latent form during interphase in the *Xenopus* embryo. *J. Cell Biol.* **106:** 2048–2056.

Eckberg, W. R. 1983. The effect of quercetin on meiosis initiation in clam and starfish oocytes. *Cell Differ.* **12:** 329–334.

Eckberg, W. R., E. Z., Szuts, and A. G. Carrol. 1987. Protein kinase C activity, protein phosphorylation and germinal vesicle breakdown in *Spisula* oocytes. *Dev. Biol.* **124:** 57–64.

Finkel, T., and D. Wolf. 1978. Fertilization of surf clam oocytes: the role of membrane potential and internal pH. *Biol. Bull.* **155:** 437.

Gautier, J., C. Norbury, M. Lohka, P. Nurse, and J. Maller. 1988. Purified maturation-promoting factor contains the product of a *Xenopus* homolog of the fission yeast cell cycle control gene cdc^{2+}. *Cell* **54:** 433–439.

Jaffe, L. F. 1983. Source of calcium in egg activation: a review and a hypothesis. *Dev. Biol.* **99:** 265–276.

Jaffe, L. F. 1985. The role of calcium explosions, waves and pulses in activating eggs. Pp. 127–165 in *Biology of Fertilization*, Vol. 2, C. B. Metz and A. Monroy, eds. Academic Press, New York.

Laemmli, U. K. 1970. Cleavage of structural proteins during the assembly of the head of bacteriophage T4. *Nature* **227:** 680–685.

Lohka, M. J., M. K. Hayes, and J. L. Maller. 1988. Purification of maturation-promoting factor, an intracellular regulator of early mitotic events. *Proc. Natl. Acad. Sci. USA* **85:** 3009–3013.

Longo, F. J., and E. Anderson. 1970. An ultrastructural analysis of fertilization in surf clam, *Spisula solidissima* I. Polar body formation and development of female pronucleus. *J. Ultrastr. Res.* **33:** 495–514.

Lowry, O. M., N. J. Rosebrough, A. R. Farr, and R. G. Randall. 1951. Protein measurements with the Folin phenol reagent. *J. Biol. Chem.* **193:** 265–275.

Maller, J. L. 1985. Regulation of amphibian oocyte maturation. *Cell Differ.* **16:** 211–221.

Maller, J. L., and E. G. Krebs. 1980. Regulation of oocyte maturation. *Curr. Top. Cell Reg.* **16:** 217–311.

Masui, Y., and H. J. Clarke. 1979. Oocyte maturation. *Int. Rev. Cytol.* **57:** 185–282.

Masui, Y., and C. L. Markert. 1971. Cytoplasmic control of nuclear behaviour during meiotic maturation of frog oocytes. *J. Exp. Zool.* **177:** 349–356.

Moreau, M., M. Doree, and P. Guerrier. 1976. Electrophoretic introduction of calcium ions into the cortex of *Xenopus laevis* oocytes triggers meiosis reinitiation. *J. Exp. Zool.* **197:** 443–449.

Murray, A. W., and M. W. Kirschner. 1989. Dominoes and clocks: the union of two views of the cell cycle. *Science* **246:** 614–621.

Rebhun, L. I. 1962. Electron microscope studies on the vitelline membrane of the surf clam, *Spisula solidissima*. *J. Ultrastr. Res.* **6:** 107–122.

Rebhun, L., and T. K. Sharples. 1964. Isolation of spindles from the surf clam, *Spisula solidissima*. *J. Cell Biol.* **22:** 488–496.

Schorderet-Slatkine, S., M. Schorderet, and E. E. Baulieu. 1976. Initiation of meiotic maturation in *Xenopus laevis* oocytes by lanthanum. *Nature* **262:** 289–290.

Schuetz, A. W. 1975. Induction of nuclear breakdown and meiosis in *Spisula solidissima* oocytes by calcium ionophore. *J. Exp. Zool.* **191:** 443–446.

Smith, L. D., and R. E. Ecker. 1971. The interaction of steroids with *Rana pipiens* oocytes in the induction of maturation. *Dev. Biol.* **25:** 233–247.

Wu, M., and J. C. Gerhart. 1980. Partial purification and characterization of the maturation-promoting factor from eggs of *Xenopus laevis*. *Dev. Biol.* **79:** 465–477.

Reference: *Biol. Bull.* **178:** 217–221. (June, 1990)

Regulation of Tissue Growth in Crustacean Larvae by Feeding Regime

JOHN A. FREEMAN

Department of Biological Sciences, University of South Alabama, Mobile, Alabama 36688

Abstract. Growth of the posterior dorsal carapace, the underlying epidermal cells, and the lateral thoraco-abdominal muscle was examined in the second instar *Palaemonetes pugio* under different feeding regimes. Control larvae (continuous feeding) and larvae fed for the first two days of the molt cycle demonstrated a mean molt increment (MI) of 10.6 and 11.1%, respectively. The muscle in these control larvae grew in width by 6.7%. Starved second instar larvae showed a MI of 3.2% and an increase in muscle width of 1.3%. Larvae fed on only one day of the molt cycle had MIs of 5.5–6.6%—values significantly different from that of the control larvae. Muscle growth in partially fed larvae was intermediate (3.9–4.5%) between those of fed and starved larvae. The increase in the density of the epidermal cells was proportional to the MI for the control and starved larvae, and for larvae fed on day 2; larvae fed only on day 1 or day 3 grew less or more, respectively, than the MI predicted from the increase in cell density. The results show that nutritional state is a strong regulator of tissue growth in shrimp larvae.

Introduction

Food and nutritional state have long been known to affect growth and development of crustacean larvae (Hartnoll, 1982; McConaugha, 1985, for review). Food intake regulates the rate of molting or molt cycle duration (MCD), molt increment (MI, growth at ecdysis), and rate of development in larvae (Knowlton, 1974; McConaugha, 1982; West and Costlow, 1988). In some species, growth, molting, and development are affected differentially by restricted feeding conditions. Several studies have suggested that a hierarchical partitioning of the nutrients for growth, molting, and development may exist, although the mechanism controlling this selection process is not understood (Knowlton, 1974; Anger and Dawirs, 1981; LeRoux, 1982; McConaugha, 1982, 1985; Anger, 1984; West and Costlow, 1988).

Thus far, little is known about the regulatory mechanisms that determine how the level of food consumption may control growth of the integument and tissues. Aspects of growth of the epidermis have been examined in adult shrimp (Tchernigovtzeff, 1965), juvenile crabs (Freeman *et al.*, 1983), larval brine shrimp (Freeman, 1986), and *Daphnia* (Halcrow, 1978). In those studies, the nutritional state and feeding history of the animal were not considered.

To study growth regulation in crustaceans, it will be necessary to determine how the epidermis and muscle—the two tissues with the greatest mass and interaction with the integument—grow during the molt cycle. In this study, instar II *Palaemonetes pugio* larvae were reared under different feeding regimes to examine growth of the epidermis and muscle with respect to feeding and to further define the relationship between the growth of the tissue and the carapace.

Materials and Methods

Larvae were hatched from egg-bearing females collected locally and maintained individually in the laboratory. The artificial seawater, (Instant Ocean, Aquarium Systems, Ohio), was maintained at 15 ppt and at 24°C (room temperature). Under these conditions, the duration of the larval molt cycle was approximately three days.

Instar I (SI) larvae were fed brine shrimp nauplii, and the water was changed daily. Upon ecdysis to instar II (SII), the larvae were placed in containers with or without food for the appropriate test period (see Results); the water was changed daily. The data were excluded where cannibalism (indicated by partially eaten larvae) occurred.

Received 19 December 1989; accepted 28 March 1990.

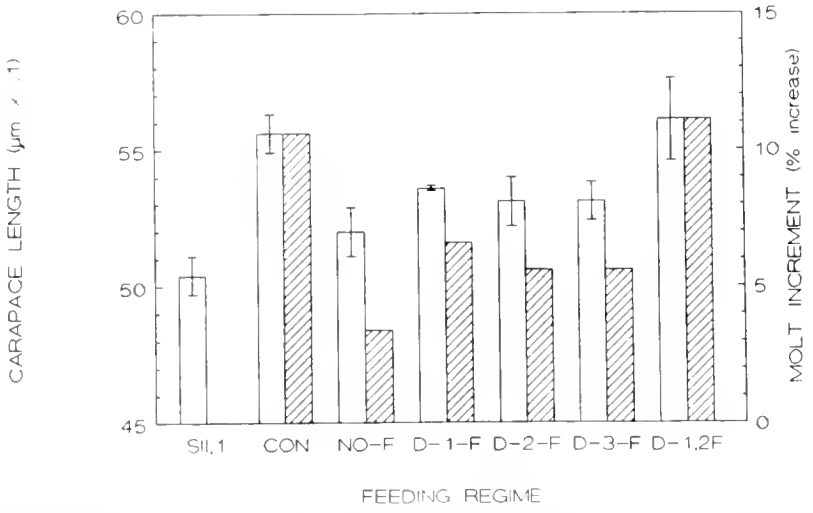

Figure 1. Effect of the instar II feeding regime on the carapace length (open bars; left ordinate) and molt increment (diagonal striped bars; right ordinate) of the resulting instar III larvae. The carapace length of day 1, instar II larvae is shown for comparison (SII, 1; single bar). Each bar represents the mean and one standard deviation of 56–162 larvae. Abbreviations for this and all other figures: CON, control larvae fed throughout the molt cycle; NO-F, starved larvae; D-1-F, D-2-F, D-3-F, D-1,2F, larvae fed, respectively, on day 1, 2, 3, or on days 1 and 2.

Measurement of the carapace length (CL) and muscle width (MW) in living larvae was done with a calibrated ocular micrometer. Larvae were immobilized on a slide in a drop of water. The CL was determined by measuring the distance between the posterior edge of the dorsal carapace and a point even with the posterior edge of the orbit. The width of the lateral thoraco-abdominal extensor muscle was measured at the junction of the muscle with the dorsal carapace. The CL and MW determinations were made between 4 and 8 h after ecdysis to instar II (CL_{SII}) or instar III (CL_{SIII}). These time points are referred to in the Results as day 1, SII or day 1, SIII, respectively. The molt increment (MI) was determined as: $[(CL_{SIII}/CL_{SII}) - 1] \times 100$. Analysis of variance (F-test) was used to determine statistical significance ($P < .05$).

The density of the epidermal cells was measured from specimens fixed in Carnoy's fluid, rehydrated, and stained with the nuclear fluorochrome bisbenzimide (Hoechst 33258, Sigma Chemical Co., St. Louis, Missouri) in phosphate buffered saline (PBS; pH 7.4). The larvae were mounted in PBS or 80% glycerol, with the dorsal carapace up and the long axis of the thorax oriented perpendicular to the axis of the slide. All measurements were made from an image in which the rostrum pointed towards the top of the field of view. The fluorescent image of the epidermal region was captured by a Dage-MTI (Michigan City, Michigan) 67M newvicon video camera mounted on a Leitz Dialux photomicroscope with a PCVISIONplus frame grabber controlled by IMAGEACTIONplus software (both from Imaging Technologies, Inc., Woburn, Massachusetts). A digital rectangle (90 × 109 μm) was superimposed on the posterior dorsal carapace, and the number of nuclei within the rectangle was determined. The cell density was determined on the first and second (and, in some cases, on the third) days of SII, and on the first day of SIII. Because cellular growth leads to expansion in both width and length at ecdysis, the increase in cell number is similar to the potential growth in area of that region of the carapace and therefore approximates the square of the MI in carapace length (Freeman, unpubl.). This "growth potential," or predicted MI (% increase), is defined as: $[(D_{day\ 2}/D_{day\ 1})^{1/2} - 1] \times 100$, where D is the density of epidermal cells in SII on the days indicated.

Results

The feeding regime markedly affected the MI (% increase in carapace length) of the instar II larvae (Fig. 1). Larvae fed throughout the molt cycle (control) or on the first two days of the molt cycle (D-1, 2F) demonstrated MIs of 10.6 and 11.1%, respectively. These values were significantly greater than those of all other groups. Starved larvae (NO-F) showed a MI of 3.4%, which was significantly lower than those of all other groups. An intermediate level of growth (5–7%) was observed in larvae fed only on day 1, 2, or 3 of the molt cycle. There was no significant change in the MCD of starved or partially fed larvae. Many of the larvae that were starved or fed only on day 3 lived for 5 or 6 days without molting.

Reduced carapace growth of larvae maintained on a restricted feeding regime was presumably a result of less

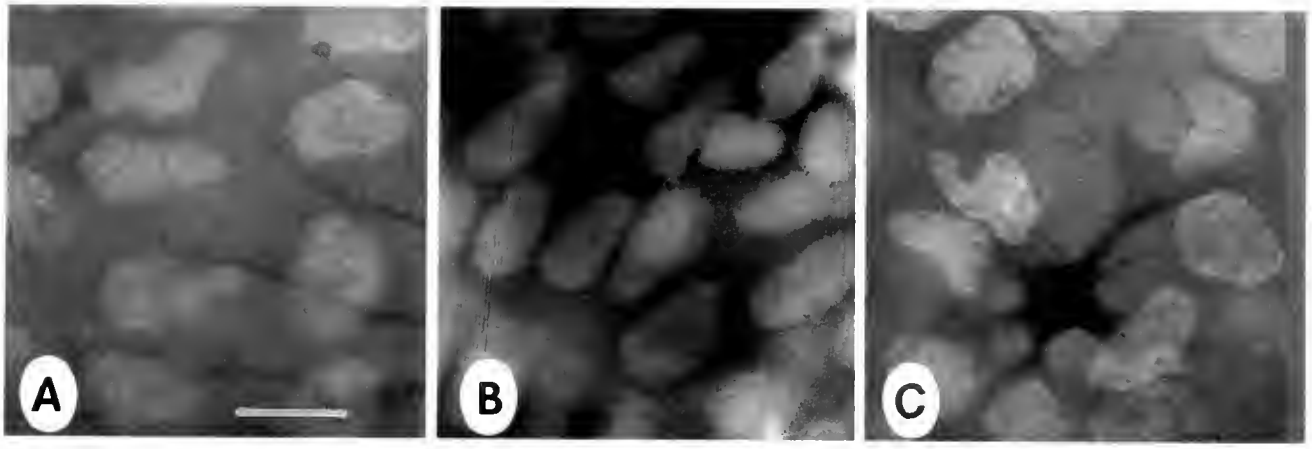

Figure 2. The change in density of the epidermal cells in the posterior dorsal carapace during the second and third instars. The nuclei are stained with bisbenzimide and photographed with epifluorescence optics. A. Carapace epidermal cells in a larva at 6 h after ecdysis to instar II (day 1, SII). The density increased during the first day of the instar, reaching the greatest level by day 2, SII (B). The density decreased when the integument expanded after ecdysis to instar III (C). Bar = 25 μm.

growth of the epidermis which secretes it. To determine if starvation or a restricted feeding regime led to reduced growth of the epidermis, the increase in density of the epidermal cells during SII was determined.

The cell density (nuclei per 90 × 109 μm area) in freshly molted SII larvae was 18.3 cells (Figs. 2, 3). In controls and larvae fed on days 1 and 2, the cell density rose to 22–23 cells (Figs. 2, 3) for a predicted MI of 11–12%. The densities were greater than those for all groups except those fed on day 1. The density returned to 18 by day 1, SIII. Starved larvae showed the least amount of cell growth (1–2 cells), and the predicted MI (2.7%) was very close to the measured MI (3.4%, Fig. 1). The cell density of starved larvae was significantly different from fed larvae (Control) and larvae fed on day 1, or on days 1 and 2, but not significantly different from those fed on day 2 or day 3.

The predicted MI was similar to the mean measured MI (less than one cell difference) for all groups except larvae fed only on day 1 or day 3 ($r = 0.91$, $P = 0.01$, for all groups). The cell density of larvae fed on day 1 was not significantly different from fed larvae, but was significantly greater than larvae fed on day 2 or 3, or starved. Larvae fed on day 1 demonstrated a MI (6.6%) that was well below the predicted MI (9.4%). Conversely, larvae fed on day 3 grew by 5.6%, which was much greater than the predicted value of 3.0%. Not indicated by the value for larvae fed on day 2 (Fig. 3) was the increase in cell density in larvae feeding on day 2. The cell density value on day 2 (before feeding) was 19.9, which would give a predicted MI of 4.3%. There was an increase of one cell during the day of feeding. Thus, without feeding, these larvae would have shown a growth potential similar to larvae fed on day 3.

Since the integument and muscle presumably grow in a coordinated manner, reduced muscle growth would be expected in larvae reared under restricted feeding conditions. Muscle width was measured on day 1 of instar II and compared to the width on day 1 of instar III. Muscle growth was greatest in the control larvae and larvae fed on days 1 and 2 (Fig. 4). The growth in these two groups was significantly greater than all other groups. Significantly less growth was observed in starved larvae than all other groups. Larvae fed only on days 1, 2, or 3 demonstrated intermediate growth levels that were significantly different from the fed and starved groups, although there was no difference among these groups. The growth in muscle width was highly correlated with the MI predicted from epidermal growth ($r = 0.84$, $P = 0.03$) and the measured MI ($R = 0.92$, $P = 0.01$).

Discussion

This study clearly shows that growth of the integument and epidermal and muscle tissue is modulated by feeding regime or nutritional state. In addition, larvae in restricted feeding regimes may demonstrate slightly longer molt cycles, an indication that the low food level affected the molt cycle. The data agree with the findings on this and other species of decapod crustaceans (Knowlton, 1974; Hartnoll, 1982; McConaugha, 1985) and demonstrate, furthermore, that growth can be measured at the cellular level.

The high correlation between epidermal growth in the dorsal carapace and carapace length is consistent with previous findings demonstrating that the size of the cuticle after ecdysis is a result of the amount of cell growth in

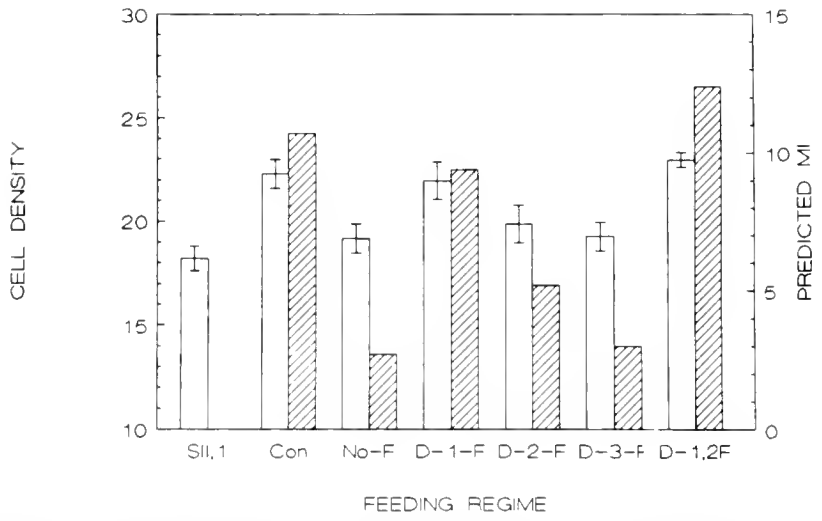

Figure 3. Effect of the feeding regime during instar II on the growth of the epidermis in instar II larvae. The cell density at early day 1 was 18 cells (SII, 1, single bar). The cell density of larvae reared in different feeding regimes was measured on day 2 (open bar; left ordinate). For each group the molt increment predicted by the increase in cell density ($[D_{day\ 2}/18]^{1/2} - 1 \times 100$, where $D_{day\ 2}$ is the density on day 2) is also shown (diagonal striped bar, right ordinate). Abbreviations as in Figure 1. Each open bar represents the mean and 1 SD of 10–45 larvae.

the epidermis during the previous molt cycle (Freeman, 1988, unpubl.). The cell density can be used to predict the MI. The results show a close correlation between the tissue growth and cuticular growth for all groups except those fed on days 1 or 3.

The dissimilar MIs measured in larvae fed only on day 1 or 3 cannot be explained by the experiments from this study. Possibly the cell density of larvae fed only on day 1 (measured on day 2) was later reduced by metabolic requirements, such that, at ecdysis, only a 6.6% increase could be realized. Feeding in shrimp larvae on day 1 may be sufficient to reach the point of reserve saturation (Anger and Dawirs, 1981; Anger, 1984), or a threshold for growth and development (West and Costlow, 1988), but it may not be enough to support the optimal amount of growth.

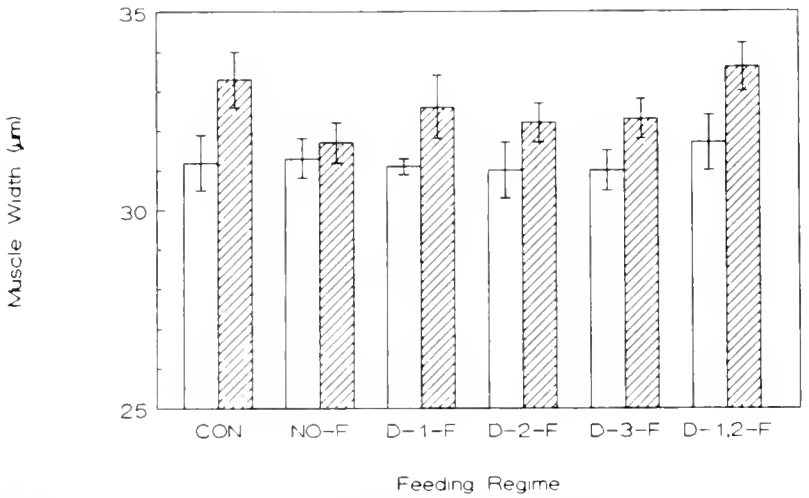

Figure 4. Effect of feeding regime during instar II on growth of the lateral thoraco-abdominal muscle. The width of the muscle in larvae in each feeding regime at the beginning of instar II (open bars) is compared to the width of the muscle in that group on the first day of instar III (diagonal striped bars). The difference in the heights of the paired bars represents the amount of growth of the muscle for that group. Abbreviations as in Figure 1. Each bar represents the mean and 1 SD of 56–162 larvae.

The opposite result was observed in larvae fed on day 3; *i.e.*, the actual MI was greater than that predicted. This result may be explained by the reduced food available for growth and metabolism, as predicted by a day 2 cell density equivalent to a predicted MI of 3.0%. If the integument was in a weakened state, as described for epidermal and muscle tissues of starved crab larvae by Anger (1984), then the stretch at ecdysis due to hydrostatic pressure may have overwhelmed the resistance of the new cuticle, along with the epidermis and muscle, resulting in a MI greater than that set by the growth potential. A similar enhanced growth, or stretch, is seen in eyestalkless larvae (Okazaki *et al.*, 1989). Subsequent feeding on day 3 may have provided only enough energy reserves to complete the molt. The day 3 feeding regime spans the critical "point of no return," as suggested by Anger and Dawirs (1981). The larvae that molted may have received food before this point, while those that remained in SII for extended periods before dying may have resumed feeding beyond this point. Tissue degradation and nutrient depletion may not have been reversed by feeding at this time. The results from larvae fed on day 2 suggest that recovery from the starved condition is possible if feeding resumes during the middle of the molt cycle. This period may be the limit beyond which starvation results in tissue degradation and loss of protein (Anger, 1984; McConaugha, 1985).

Preliminary findings suggest that epidermal growth consists of both cell replication and enlargement of divided cells. The contribution of each phase to the growth process is not understood. Analysis of the cell cycle changes in the epidermal cells is necessary to find the control points of the growth process. There may be several control points where nutritional status may be translated into tissue growth. One may be the entrance to mitosis, and another may be the G1-S transition, both of which have been shown to be control points in many cell types (Murray and Kirschner, 1989; Pardee, 1989). Moreover, the growth process may involve entrance of non-cycling cells into the cycling population.

In this study, the epidermis and the muscle were observed to grow in a coordinated manner, in agreement with earlier studies on muscle growth in crustaceans (Bittner and Traut, 1978; Houlihan and El Haj, 1985). Moreover, muscle growth was affected by nutritional stress in a manner similar to that of the epidermis. These findings would argue that a common mechanism controls the coordinated growth of both tissues. Conversely, the epidermis may control growth of the muscle, possibly through cell-cell interactions. These mechanisms are currently being examined.

Acknowledgments

I thank Dr. Robert K. Okazaki for stimulating discussions and Ms. Dianne Laurendeau for technical assistance. This research was supported by grant no. R11-8996152 from NSF/EPSCoR and the State of Alabama.

Literature Cited

Anger, K. 1984. Influence of starvation on moult cycle and morphogenesis of *Hyas araneus* larvae (Decapoda, Majidae). *Helgol. Wiss. Meeresunters.* **38:** 21–33.

Anger, K., and R. Dawirs. 1981. Influence of starvation on the larval development of *Hyas araneus* (Decapoda, Majidae). *Helgol. Wiss. Meeresunters.* **34:** 287–311.

Bittner, G., and D. L. Traut. 1978. Growth of crustacean muscles and muscle fibers. *J. Comp. Physiol.* **124:** 277–285.

Freeman, J. A. 1986. Epidermal cell proliferation during thoracic development in larvae of *Artemia*. *J. Crust. Biol.* **6:** 37–48.

Freeman, J. A. 1988. Cell growth and the molt cycle in *Palaemonetes* larvae. *Am. Zool.* **28:** 94A.

Freeman, J. A., T. L. West, and J. D. Costlow. 1983. Postlarval growth in juvenile *Rhithropanopeus harrisii*. *Biol. Bull.* **165:** 409–415.

Halcrow, K. 1978. Cell division in the carapace epidermis of *Daphnia magna* Straus (Cladocera). *Crustaceana* **35:** 55–63.

Hartnoll, R. 1982. Growth. Pp. 111–196 in *The Biology of Crustacea*, Vol. 2, L. G. Abele, ed. Academic Press, New York.

Houlihan, D. F., and A. J. El Haj. 1985. An analysis of muscle growth. Pp. 15–29 in *Crustacean Issues 3. Factors in Adult Growth*, A. M. Wenner, ed. Balkema Press, Boston.

Knowlton, R. E. 1974. Larval development processes and controlling factors in decapod Crustacea, with emphasis on Caridea. *Thallasia Jugoslav.* **10:** 138–158.

LeRoux, A. 1982. Les organes endocrines chez les larves des crustacés eucarides. Intervention dans la croissance au cours de la vie larvaire et des premiers stades juvéniles. *Oceanis* **8:** 505–531.

McConaugha, J. R. 1982. Regulation of crustacean morphogenesis in larvae of the mud crab *Rhithropanopeus harrisii*. *J. Exp. Zool.* **223:** 155–163.

McConaugha, J. R. 1985. Nutrition and larval growth. Pp. 127–154 in *Crustacean Issues 2. Larval Growth*, A. M. Wenner, ed. Balkema Press, Boston.

Murray, A. W., and M. W. Kirschner. 1989. Dominoes and clocks: the union of two views of the cell cycle. *Science* **246:** 614–621.

Okazaki, R. K., J. A. Freeman, and D. M. Laurendeau. 1989. Cell growth and cuticle expansion in eyestalk-ablated *Palaemonetes*. *Am. Zool.* **29:** 62A.

Pardee, A. B. 1989. G_1 events and regulation of cell proliferation. *Science* **246:** 603–608.

Tchernigovtzeff, C. 1965. Multiplication cellulaire et régénération au cours de cycle d'intermue des crustacés décapodes. *Arch. Zool. Exp. Gen.* **106:** 377–497.

West, T. L., and J. D. Costlow. 1988. Determinants of the larval molting pattern of the crustacean *Balanus eburneus* Gould (Cirripedia: Thoracica). *J. Exp. Zool.* **248:** 33–44.

Reference: *Biol. Bull.* **178:** 222–230. (June, 1990)

Determination of Alkaline Phosphatase Expression in Endodermal Cell Lineages of an Ascidian Embryo

J. R. WHITTAKER

Laboratory of Developmental Genetics, Marine Biological Laboratory, Woods Hole, Massachusetts 02543

Abstract. *Ciona intestinalis* embryos develop a strong histochemical localization of alkaline phosphatase activity in their known endodermal tissues. Such tissues arise solely from the four vegetal blastomeres at the 8-cell stage and six vegetal blastomeres at the 16-cell stage; these vegetal cells inherit an endodermal lineage cytoplasm. Pairs of blastomeres from the bilaterally symmetrical 8- and 16-cell stages were isolated and reared as partial embryos. Only those partial embryos derived from endoderm-containing lineages developed a histochemically localized alkaline phosphatase activity. From the results of such restricted developmental autonomy (self-differentiation), one can deduce that this enzymic expression of endodermal fate could be specified by events of cytoplasmic segregation that occur during the early cleavages. This conclusion offers additional support to the theory that specification of cell fate in ascidian embryos involves an early differential segregation of histodetermining egg cytoplasmic materials.

Introduction

Elaboration and refinement of cell lineages and the construction of fate maps for certain widely studied animal embryos continue to be important contemporary parts of experimental embryology. Fate maps produced by marking early blastomeres of the embryo indicate what actually happens to each cell or region as it develops, and are an essential component of attempts to interpret the causal relations concerned with eventual regional specializations in the embryo. Yet fate maps do not indicate when, during the succession of cleavages, cells become irreversibly committed to the pathways of differentiation they later exhibit during histodifferentiation. Our one, and still only, radical criterion for discovering whether the prospective fate or "determination" of a blastomere has already been settled during early cleavages is that, when the blastomere is isolated from its usual cellular environment and associations, some or all of its progeny cells then differentiate only in the fixed or limited directions predicted by a fate map (Lillie, 1929). The underlying hypothesis is the presumption that eventual cell fate is determined by certain localized cytoplasmic agents that become differentially segregated only into certain cells (Whittaker, 1987). This paper is such an investigation of specification in the endodermal cell lineages of *Ciona intestinalis*. These embryonic cells eventually become the branchial and digestive tissues of the postmetamorphic juvenile and adult.

The first accurate and extensive cell lineages for ascidian embryos were described by Conklin (1905). Endodermal lineages are segregated at third cleavage (8-cell stage) to the vegetal four cells of the embryo and thereafter become progressively more restricted to certain vegetal regions of the dividing embryo. Based on general characteristics of cytoplasmic morphology and staining (Conklin, 1905, 1911), endodermal lineages appear to inherit a particular kind of cytoplasm. Conklin's original designations of the endodermal lineages have been confirmed recently in studies using injected horseradish peroxidase (HRP) as a cell lineage marker (Nishida and Satoh, 1983, 1985; Nishida, 1987).

Quite early in embryogenesis, beginning at the neurula stage, endodermal tissues develop localizations of an essentially histotypic alkaline phosphatase; other larval tissues lack any significant amount of it (Minganti, 1954a; Whittaker, 1977). In certain species, development of this enzyme is a simple and unequivocal indication of endodermal differentiation. Ascidian embryos, which are di-

Received 28 August 1989; accepted 28 March 1990.

vision-arrested at various early cleavage stages with cytochalasin B, eventually express alkaline phosphatase only in those cells that are known to be of endodermal lineage (Whittaker, 1977; Satoh, 1982). This suggests further that endodermal expression follows a pattern of cytoplasmic localizations. However, in such cleavage-arrested embryos, the enzyme-developing cells are not separated from the influence of their surrounding cells. The present study examines alkaline phosphatase development in partial embryos originating from blastomere pairs of the bilaterally symmetrical embryo isolated from early cleavage stages. Eventual enzyme expression exclusively follows the known endodermal lineages. Such developmental autonomy is likewise consistent with the hypothesis of a differentially segregated cytoplasmic determinant.

Materials and Methods

Organisms

Adult *Ciona intestinalis* (L.) were collected near Woods Hole, Massachusetts, and maintained on sea tables with continuously flowing seawater and under constant light. *Phallusia mammillata* (Cuvier) was obtained from two sources: from the Gulf of Palermo in Sicily by courtesy of the Institute of Zoology at the University of Palermo, and from the coast of Brittany at Roscoff (France) through the kindness of Dr. Lionel Jaffe. Eggs from two or more animals were removed surgically from the oviducts and fertilized with diluted sperm obtained from the sperm ducts of other adults. Embryos were dechorionated manually before first cleavage with sharpened steel needles and cultured at 18 ± 0.1°C in sterile Millipore-filtered (0.2 μm porosity) seawater containing 0.1 m*M* EDTA (Crowther and Whittaker, 1983). Under these conditions, larvae became fully developed by 18 h from fertilization.

Blastomere isolations

Dechorionated embryos of the bilaterally symmetrical 8-cell stage of *Ciona* were the starting point for isolations of various cell pairs at the 8- and 16-cell stages. Blastomeres were separated with agar-coated glass filament needles. Partial embryos from various isolations were then reared in agar-coated Syracuse watch glasses for periods of development up to 20 h before they were processed histochemically for an alkaline phosphatase reaction.

Cleavage inhibition

Exposure to cytochalasin B (Aldrich) (2 μg/ml) prevented cell division in embryos (Crowther and Whittaker, 1983).

Alkaline phosphatase histochemistry

The 80% cold ethanol fixative used previously with chorionated ascidian embryos (Whittaker, 1977) gave satisfactory but often variable results when applied to dechorionated partial embryos. This variability was eliminated by employing the glutaraldehyde-formaldehyde fixative devised by Karnovsky (1965) for electron microscopic histochemistry; it was used here at 0.5% each, half the suggested aldehyde concentrations. One-hour fixation (5°C) and 20-min wash in the recommended sucrose-containing cacodylate buffer (Karnovsky, 1965) produced excellent and reproducible results with the subsequent alkaline phosphatase reaction. Background staining was insignificant under these conditions.

Fixed whole or partial dechorionated *Ciona* embryos were reacted for 24 h (at 18°C) in standard Gomori medium with β-glycerophosphate as substrate and the calcium phosphate product afterwards visualized by a silver reduction technique (Pearse, 1972). This results in a stable brown deposit of reduced silver at the sites of alkaline phosphatase activity. The stained specimens were dehydrated in ethanol, cleared in xylene, and mounted in dammar resin.

Some staining for alkaline phosphatase activity on larvae and dechorionated whole and partial embryos was done with a tetrazolium method using bromochloroindoxyl phosphate (BCIP) as substrate (McGady, 1970, and as described by Whittaker and Meedel, 1989). Both fixation methods were used with this procedure; similar results were obtained with each.

Acetylcholinesterase histochemistry

Assays were done on dechorionated whole and partial embryos after using the same aldehyde fixative described above for alkaline phosphatase. The cholinesterase method of Karnovsky and Roots (1964) was applied as described by Meedel and Whittaker (1984).

Results

Endodermal cell fates predicted by cell lineage studies

The most accurate cell lineage relationships for potential endodermal expression have been obtained from cell marking studies with injected HRP (Nishida and Satoh, 1983, 1985; Nishida, 1987). Figure 1 is a lineage diagram of the cell contributions up to the 16-cell stage: at the 8-cell stage the four vegetal blastomeres (the bilateral pairs of A4.1 and B4.1) contain endodermal lineages; at the 16-cell stage only six of the eight vegetal cells contain endodermal lineages. The sensitivity of the HRP detection method has also permitted an identification of the lineage origins of certain smaller structures of the embryo designated in Figure 1 as secondary. Figure 2 depicts in

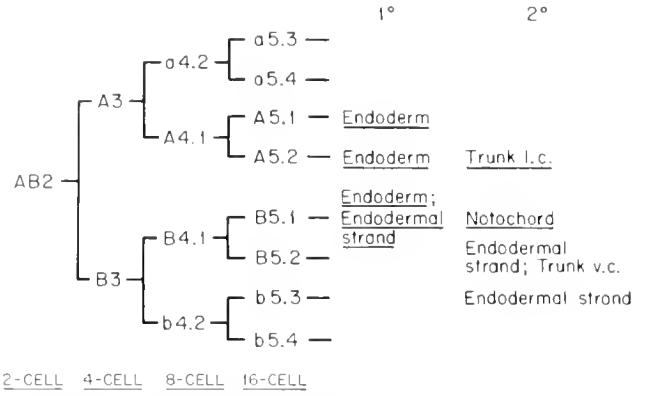

Figure 1. Fate map of endodermal cell lineages in ascidian embryos up to the 16-cell stage, according to Conklin (1905), Ortolani (1954), and Nishida and Satoh (1983, 1985). Cells from one-half of the bilaterally symmetrical embryo are indicated. Primary (1°) and secondary (2°) tissues which ultimately develop alkaline phosphatase are underlined. Nomenclature is that of Conklin (1905).

a middle tailbud stage (11 h) embryo the various "endodermal" regions actually observed by such studies and their respective origins from the bilaterally symmetrical pairs of blastomeres at the 16-cell stage (identified in Fig. 1).

The regions shaded with diagonal lines in the head part of the embryo diagram (Fig. 2) are the locations of the cells that give rise to the endodermal organs of the post-metamorphic juvenile: a branchial basket and the digestive system. These are the fates of the primary endodermal cells in Figure 1. The tail is a strictly larval structure and its tissues, including the endodermal strand (an extension of the main endodermal mass running mid-ventral to the notochord), and the notochord itself are destroyed at the time of larval metamorphosis. Other tissue areas of the embryo-larva (muscle, neural, and epidermal) are not shown.

Questions about the minor endodermal structures identified in Figures 1 and 2 arise from the cell lineage studies. "Trunk lateral cells" (TLC), which occur in two superficial dorsal wing-like accumulations on either side of the mid-tailbud embryo, are undefined in their fate yet still share a major endodermal lineage as late as the 32-cell stage (Nishida and Satoh, 1985); at the 64-cell stage they separate from endoderm as a separate lineage (Nishida, 1987). Two small circular patches of cells, which I have called "trunk ventral cells" (TVC), occur along either side of the embryo ventral midline at the base of the tail. These have been classified as endodermal by Nishida (1987) because of their location in an endodermal region, but they originate after the 128-cell stage from a lineage (B5.2) that is entirely mesodermal from the 16-cell stage onwards. Finally, two short distal segments of the endodermal strand originate from cells (B5.2 and b5.3 cell pairs) which, after the 16-cell stage, are not otherwise endodermal lineages.

Alkaline phosphatase expression in tissues of endodermal lineage

Because differential alkaline phosphatase expression has been regarded as a histotypic indicator of early differentiation in endodermal tissues of some ascidian species (Minganti, 1954a, and others), occurrence of enzyme in the so-called secondary larval tissues (Fig. 2) would be a confirmation of their endodermal specification. The Gomori and BCIP methods of enzyme detection have been applied to 11-h (middle-tailbud stage) *Ciona* embryos and also to embryos cleavage-arrested in cytochalasin B at 11 h and fixed for reaction at 20–28 h postfertilization. Cleavage-arresting dechorionated 11-h embryos has the interesting effect of causing an earlier and more concentrated development of enzyme in cells that might ordinarily divide further. Alkaline phosphatase does not usually occur strongly in endoderm-derived tail tissues until 6–8 h after hatching. Figure 3 shows the BCIP staining of such a cleavage-arrested larva. In previous lineage studies, the middle tailbud stage was used as the reference stage for tissue locations (Nishida, 1987; Nishida and Satoh, 1983, 1985). Cleavage-arrested 11-h embryos (Fig. 3) enable us to make a direct comparison to those results (Fig. 2).

Only tissues arising from lineages that share a primary endodermal lineage until after the 16-cell stage are seen to develop alkaline phosphatase. This includes the eight cells at the tip of the notochord, which have such an endodermal lineage origin but are not structurally or functionally endodermal cells; their lineages first separate from endoderm at the 32-cell stage. The two short terminal segments, which are structurally a part of the endodermal strand, but which do not share endodermal lineages after the earliest cleavages, do not produce alkaline phosphatase.

During the first 30 min of BCIP staining, one can see the TLC reacting strongly against the initially lighter staining of the underlying other endodermal cells. The staining time required to reveal the endodermal strand clearly (2–3 h) soon results in sufficient reaction product in the head region to obscure the TLC. During initial staining, or later, one can not see any differential alkaline phosphatase stain in the TVC region. In normal 11-h embryos, one finds the same differential staining with BCIP in the TLC, but at that time enzyme has not yet developed in the endodermal strand or notochordal tip cells, as it has in the cleavage-arrested embryos reacted after "hatching." Given their sharing of an endodermal lineage, and their expression of alkaline phosphatase, it seems unlikely that the TLC would be the precursors of

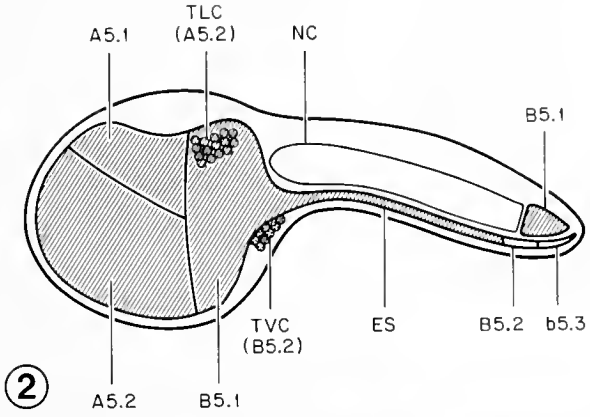

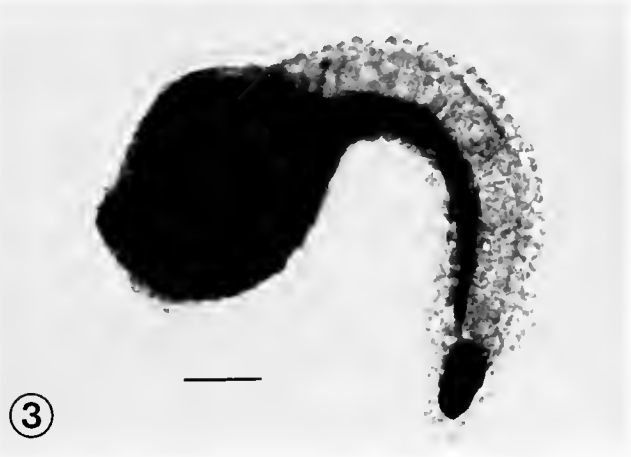

Figure 2. Diagram of the middle tailbud stage (11 h) ascidian embryo showing the endoderm and possibly endodermally related tissues identified from lineage tracing studies (Nishida and Satoh, 1983, 1985; Nishida, 1987). Lineage origins at the 16-cell stage are given for each defined tissue region. Those tissues that eventually express alkaline phosphatase, including the trunk lateral cells (TLC), the proximal endodermal strand (ES), and the distalmost cells of the notochord (NC), are indicated with fine diagonal lines. The (stippled) trunk ventral cells (TVC) develop acetylcholinesterase but not alkaline phosphatase.

Figure 3. Dechorionated 11-h (middle tailbud) *Ciona intestinalis* embryo cleavage-arrested at 11 h with cytochalasin B and reacted at 28 h (after fixation) for alkaline phosphatase with the BCIP reagent. Incubation time is 2 h. Bar = 50 μm.

juvenile blood cells (a presumably mesodermal derivative), as suggested by Nishide *et al.* (1989).

The Gomori stain is much less sensitive than the BCIP stain. It does not reveal any enzyme activity in the endodermal strand, but shows clearly the TLC staining differentially in the head region (not shown). The two bilateral TVC regions stain significantly for acetylcholinesterase, a characteristic expression of differentiating muscle and mesenchyme tissue regions (Meedel and Whittaker, 1979). This TVC staining (not shown) occurs in normal 11-h embryos as well as 11-h cleavage-arrested embryos. By their location, these apparently mesodermal tissues may be the primordia of the juvenile heart. Although the inner distal segment of the endodermal strand originates (at the 64-cell stage) from what is otherwise a mesodermal lineage (B5.2), these tissues do not develop an acetylcholinesterase. They thereby differ from the notochordal tip cells by not expressing a vestige of their secondary origin.

Design of cell isolation experiments

At the 8-cell stage, third cleavage divides the bilaterally symmetrical embryo equatorially across the animal-vegetal axis into a vegetal quartet of cells containing the endodermal lineages and an animal quartet that has no endodermal fate (Fig. 4A). Ortolani (1954) used adhering carbon particles to mark the surface areas of the four vegetal blastomeres which eventually appear in endodermal tissues. Under conditions of appropriate lighting (see below) one can actually observe the endodermal regions indicated in Figure 4A by the diagonal lines, to contain much more yolky material than the other part of the cell, which remains noticeably clearer; these yolky areas have relatively sharp edges. This confirms Conklin's (1905) observations as well. In this investigation, various blastomere pairs have been isolated microsurgically at the 8- and 16-cell stages (Figs. 4B, 4C).

Separation of lineage blastomeres

The *Ciona* 8-cell stage has a very characteristic pattern in lateral aspect (Figs. 4A, 5) by which the four cell pairs can be identified. Often the pair of polar bodies can be seen resting on the a4.2 cells at the animal pole as diagrammed in Figure 4A, but the shapes and apparent sizes of the cells are most diagnostic of their lineage. In doing the isolations, overhead lighting (from a quartz halogen fiber optic lamp) is preferred, with a substage mirror set to reflect back some of this illumination. With properly balanced direct/indirect lighting, the vegetal cell pairs (A4.1 and B4.1), which contain more yolk, appear slightly darker than the others. This facilitates recognition of the A4.1 cells, which thereby appear darkest. The B4.1 cells are somewhat flattened in the animal-vegetal direction and seem to be slightly larger in lateral view than the other pairs of cells.

Animal and vegetal quartets (half-embryos) were isolated by separating the sets as shown in Figure 4B. The cell size and pattern of arrangement in the animal and vegetal quartets (Figs. 6, 7) further simplifies identification of the various cell pairs at the "8-cell stage" in obtaining quarter-embryos (Fig. 4C). Similarly, when the A4.1 and B4.1 blastomere pairs divide again at the "16-cell" stage, there were characteristic sizes and patterns of cells (Figs. 8, 9), which enabled one to isolate the correct lineage pairs.

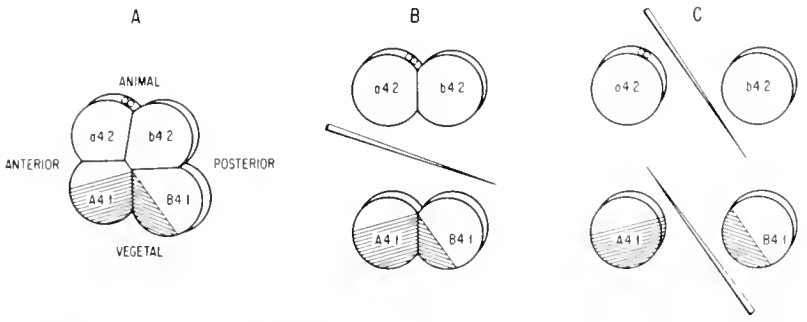

Figure 4. Diagrams of the surgical operations involved in isolating blastomeres from the 8-cell stage (A). Isolation of animal and vegetal quartets (B) and quarter-embryos (C). The endodermal territories as mapped by Ortolani (1954) are indicated by diagonal lines.

Size and pattern of the cells can be learned initially from Conklin's (1905) diagrams, which are exceptionally accurate. One can also observe the shapes, sizes, and positions of cells (*in situ*) when isolated half-embryos divide again in culture. Partial larvae resulting from given blastomere pairs have very distinctive morphologic features by which the accuracy of one's initial selection is easily confirmed.

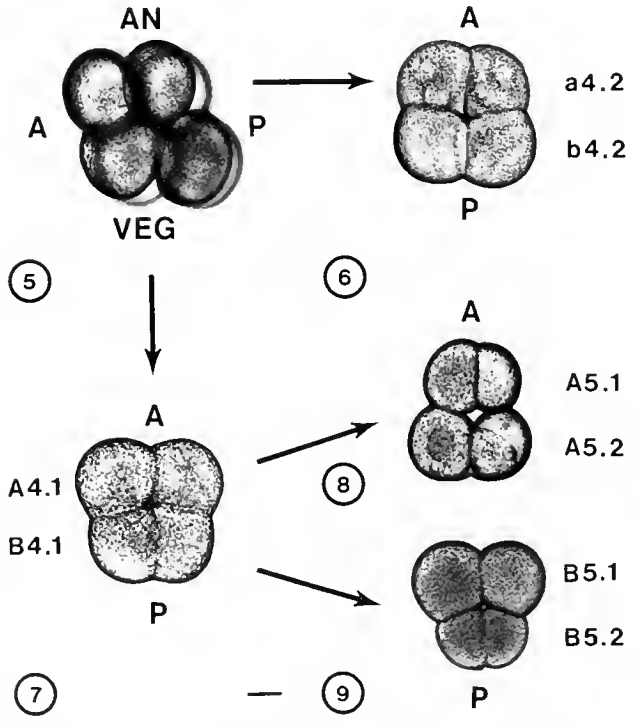

Figures 5–9. *Ciona intestinalis* embryo and isolated blastomeres photographed after brief fixation in the Karnovsky (1965) fixative. Figure 5: 8-cell stage in lateral view as in Figure 4A. Figure 6: Animal quartet of cells from 8-cell stage. Figure 7: Vegetal quartet of cells from the 8-cell stage. Figure 8: Isolated A4.1 cell pair after the next division. Figure 9: Isolated B4.1 cell pair after the next division. The embryo orientation letters are AN (animal), VEG (vegetal), A (anterior), and P (posterior). All magnifications are the same; bar in Figure 7 = 50 μm.

Alkaline phosphatase development in partial embryos

Only partial embryos originating from blastomeres known to contain endodermal lineages (Fig. 1) developed groups of cells containing alkaline phosphatase in the resulting partial larvae (Table I). In larvae developing from dechorionated whole embryos, there was always enzyme staining in the endodermal mass of the head region (Figs. 3, 10). Normal specimens were included as positive controls in each of the various enzyme incubations (Gomori method) with partial embryos. Some larvae show staining in the endodermal strand along the tail and in the few notochordal cells at the tip of the tail; both are evident in Figure 10. Staining of the endodermal strand and notochord did not usually occur until 6–8 h after hatching of controls (18 h), and appeared progressively stronger with time.

Table I

Development of histochemically localized alkaline phosphatase in isolated partial embryos of Ciona intestinalis

Blastomeres isolated	Number of experiments	Embryos examined (positive reaction/total)
8-cell stage		
animal quartet	7	0/155
a4.2 pair	4	0/45
b4.2 pair	4	0/45
vegetal quartet	5	115/115
A4.1 pair	6	73/73
B4.1 pair	6	107/107
16-cell stage		
A5.1 pair	2	42/48
A5.2 pair	2	52/56
B5.1 pair	3	60/62
B5.2 pair	3	1/56

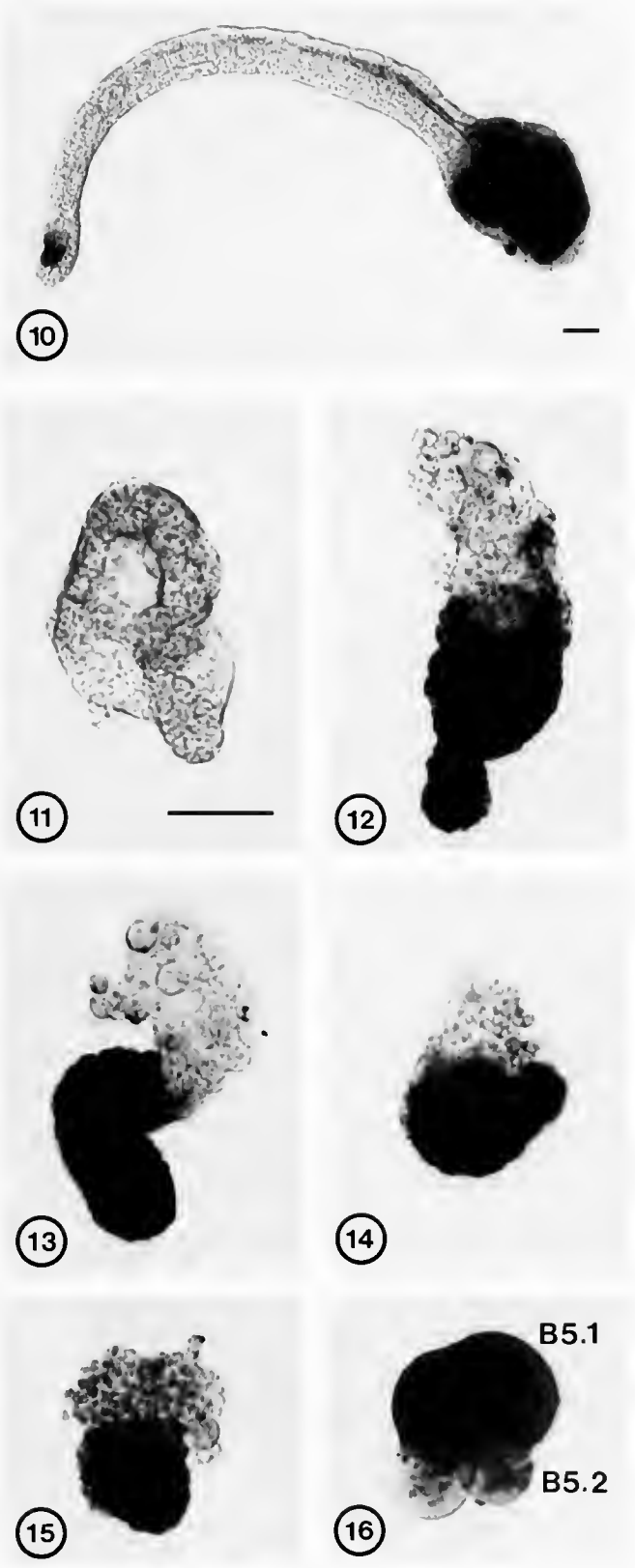

Figures 10–16. *Ciona intestinalis* embryos after 18–20 h of development, reacted for alkaline phosphatase (Gomori). Bar = 50 μm. Figure 10: Larva from dechorionated whole embryo. Figure 11: Animal half-embryo. Figure 12: Vegetal half-embryo. Figure 13:A4.1 quarter-embryo. Figure 14: B4.1 quarter-embryo. Figure 15: B5.1 eighth-embryo. Figure 16: Divided B4.1 embryo (as in Fig. 9), cleavage-arrested in cytochalasin B, and showing the B5.1 and B5.2 cell pairs.

The experimental results presented here were done with isolated blastomeres from embryos with completely normal cleavage patterns. In association with the experiments of Table I, 5 series containing a total of 162 whole dechorionated embryos selected for normal cleavage patterns were reared to "hatching" time. Ninety percent of these embryos developed to fully formed "normal" larvae. In most respects, *Ciona* larvae originating from dechorionated early embryos are normal, but they lack a properly formed tail fin of the translucent test covering (as previously noted with another species by Cloney and Cavey, 1982).

No animal half-embryos developed enzyme (Fig. 11), nor did any quarter-embryos (a4.2 or b4.2) derived from the animal quartet. Vegetal half-embryos always produced enzyme (Fig. 12), as did the A4.1 and B4.1 quarter-embryos (Figs. 13 and 14) prepared from the vegetal half of the 8-cell stage. Partial embryos developing alkaline phosphatase invariably contained tissue staining over a large area of the resulting partial larva (Figs. 12–15). Three experimental "control" series were done in which animal and vegetal quartets were isolated and cultured only until 4 h after fertilization before they were fixed and reacted. These contained no localized enzyme. Ordinarily, experimental and control embryos were cultured for 18–20 h.

Partial embryos from A4.1 and B4.1 vegetal cells prepared after the next cleavage (the "16-cell" stage) also showed alkaline phosphatase development correlated with the segregation of endodermal lineages. Most of the A5.1 and A5.2 ⅛th-embryos produced a mass of enzyme-containing cells. A few embryos did not react. Almost all of the B5.1 ⅛th-embryos developed enzyme (Fig. 15), and essentially none of the B5.2 embryos (Table I). One B5.2 embryo (out of 56) developed some alkaline phosphatase. Because microsurgical preparation of partial embryos from 16-cell stage blastomere pairs necessarily entailed some sequential slight bruising of the cells, the one B5.2 embryo that produced alkaline phosphatase might reasonably have resulted from a missegregation of cytoplasm caused by such trauma.

A striking further illustration of the correlation between alkaline phosphatase development and endodermal lineage segregation occurs with a cleavage-arrested partial embryo. B4.1 pairs were isolated (Fig. 4C) and, before being treated with cytochalasin B, were permitted to undergo an additional cleavage creating an embryo with B5.1 and B5.2 daughter pairs (Fig. 9). Almost all of

these embryos (17 out of 18) had staining in both B5.1 cells and none had staining in the B5.2 cells (Fig. 16). This experiment complements work in a previously published study on expression in cleavage-arrested *Ciona* embryos (Whittaker, 1977).

When the more sensitive BCIP staining method was used to localize alkaline phosphatase in partial embryos, the same strict lineage expressions could be demonstrated as shown above with the Gomori method. However, separating blastomeres before complete closure of the cytoplasmic bridges between daughter cells sometimes caused transfer of very small amounts of cytoplasm, which resulted subsequently in tiny regions of enzyme expression. These expressions could not be detected with the less-sensitive Gomori technique. Such transfers were avoided by a change in isolation techniques. The results will be described in detail elsewhere in another context.

Alkaline phosphatase in Phallusia *embryos*

When hatched *Phallusia* larvae were reacted for alkaline phosphatase uniformly dark Gomori and BCIP staining reaction products occurred in all the tissues, with no indication of localized staining. Similarly, when dechorionated eggs and embryos of early cleavage stages were reacted for enzyme, a same dark reaction product was also found throughout the whole. With each method, this screen of general staining obscured any possibility of seeing a localized specific staining that might otherwise develop in endodermal tissues. These stainings appear to result from the activity of a universally distributed phosphatase enzyme already present in the egg.

Unfortunately, Minganti (1954a) failed to note this staining of *Phallusia* larvae in his survey of several ascidian species. His further observation that partial embryos of *Phallusia* originating from isolated animal and vegetal quartets of the 8-cell stage both have staining (Minganti, 1954b) proves to be correct, but indicative only of enzyme already present and not of new alkaline phosphatase formation in the animal half-embryo during development.

Discussion

The classic study by Reverberi and Minganti (1946) on the fate of blastomere pairs isolated at the 8-cell stage showed that anterior and posterior vegetal pairs (A4.1 and B4.1) give rise to quarter-embryos containing some general histological features of organization resembling early gut tissues. Quarter-embryos arising from the animal blastomere pairs (a4.2 and b4.2) did not have this organization, but unfortunately such histologic characters lack the discrimination and sensitivity for evaluating minor expressions of endodermal differentiation. Except for a predominance of yolk granules in cells of endodermal lineages and some other lineages (*e.g.*, notochordal) derived from the vegetal half of the egg (Mancuso and Dolcemascolo, 1979), there are no simple cytospecific features of endodermal differentiation even at the ultrastructural level. However, a strong alkaline phosphatase development proves to be a simple, sensitive, and essentially histotypic indicator of an early endodermal differentiation, at least in some species. An elevated alkaline phosphatase appears to be a universal constituent of the digestive systems of animals (McComb *et al.*, 1979). As noted in the results, there are ascidians (*Phallusia*) in which any possible differential development of enzyme is obscured by a uniformly distributed strong alkaline phosphatase activity present throughout development, and originating in the egg before development begins.

Results of the present blastomere isolation study indicate that partial embryos derived from "endodermal" blastomeres isolated at 8- and 16-cell stages self-differentiated extensive patches of cells containing high levels of alkaline phosphatase. Embryos obtained from the non-endodermal lineages did not produce alkaline phosphatase, at least at any visual level of differential histochemical staining. These findings are in agreement with the fates indicated by previous lineage studies and with expressions of enzyme observed in cleavage-arrested embryos (Whittaker, 1977, and Fig. 16). A restriction of fate occurs, therefore, in parallel with the lineage. The endodermal lineage map is apparently also a fate map.

The theory behind the early specification of cell fate in ascidian embryos and other so-called mosaically developing organisms is the likelihood of differential segregation of specific egg cytoplasmic materials (Lillie, 1929). Ooplasmic rearrangements that occur immediately after fertilization create visible and presumably chemically distinct regional differences in zygote cytoplasm; these regions become segregated into certain cell lineages as the germ divides (Conklin, 1905, 1911). Cell fate is then ordered by agents or substances (determinants) within these regions of cytoplasmic difference. The present results are consistent with this theory. Some credence can be attached to the theory because muscle lineage fate in ascidians appears to be transferrable to other cells along with myoplasmic cytoplasm (Whittaker, 1987).

One might conclude that endodermal alkaline phosphatase expression is regulated by segregation of an egg cytoplasmic determinant into the major (functional) tissues. Because of their early inclusion in an endodermal lineage, the eight distal notochordal cells that express alkaline phosphatase have probably inherited determinant by segregation. The two distalmost short segments of the endodermal strand are actually not derived from immediate endodermal lineages, do not express enzyme, and would seemingly not have received any determinant.

The unresolved nature of egg cytoplasmic determinants remains an important issue in embryology (Davidson, 1990). In certain cases these agents seem to be masked maternal messenger RNAs for some of the proteins involved in a later developmental change. There is indirect evidence from experiments with actinomycin D and other inhibitors of RNA synthesis that the ascidian alkaline phosphatase determinant could be such a preformed maternal mRNA (Whittaker, 1977; Bates and Jeffery, 1987).

Bates and Jeffery (1987) have observed by histochemistry that "activated" but nonnucleate zygote fragments do not elaborate the endodermal alkaline phosphatase after time. Their results were confirmed by more sensitive quantitative measurements on similar material (Whittaker and Meedel, 1989). Also, aphidicolin, an inhibitor of DNA synthesis, has a time-window effect on *Ciona* alkaline phosphatase development (Satoh, 1982). While such findings do not establish the necessity of a gene transcription, they indicate a possible involvement of nuclear replication events in releasing the expression of alkaline phosphatase. Nuclear division might be related to a mechanism for processing an inactive mRNA.

One possible mRNA processing mechanism to consider is translational activation by polyadenylation of a dormant maternal mRNA. There are some examples in the recent literature of translational activation of dormant mRNAs being accompanied by elongation of their 3′ poly(A) tails (see McGrew *et al.*, 1989). Huarte *et al.* (1987) describe an mRNA for mouse oocyte tissue plasminogen activator that accumulates in the cytoplasm during oocyte growth; translational activation of this mRNA occurs at meiosis and is accompanied by increased 3′-polyadenylation. Actual meiotic changes may be necessary since the mixing of cytoplasm and nucleoplasm at germinal vesicle breakdown is not sufficient to initiate the processing. This meiosis-initiated polyadenylation is insensitive to inhibition of RNA synthesis.

Further speculation about the nature of an alkaline phosphatase determinant would be aided by more direct evidence that there is a differentially segregated egg cytoplasmic factor, and by some information about the conditions under which it functions. The present investigation has established a biological background within which to pursue such questions. A next paper will present evidence that moving endodermal lineage cytoplasm to nonendodermal lineages results in the acquisition of alkaline phosphatase expression.

Acknowledgments

This work was supported by Grant HD-21823 from the National Institute of Child Health and Human Development (NIHHS). I thank Robert J. Crowther and Jane L. Loescher for technical assistance and Drs. Giuseppina Ortolani and Nunzia Farinella-Ferruzza of the University of Palermo for their initial guidance and instruction.

Literature Cited

Conklin, E. G. 1905. The organization and lineage of the ascidian egg. *J. Acad. Nat. Sci. (Philadelphia)* **13:** 1–119.

Conklin, E. G. 1911. The organization of the egg and the development of single blastomeres of *Phallusia mamillata*. *J. Exp. Zool.* **10:** 393–407.

Bates, W. R., and W. R. Jeffery. 1987. Alkaline phosphatase expression in ascidian egg fragments and andromerogons. *Dev. Biol.* **119:** 382–389.

Cloney, R. A., and M. J. Cavey. 1982. Ascidian larval tunic: extraembryonic structures influence morphogenesis. *Cell Tissue Res.* **222:** 547–562.

Crowther, R. J., and J. R. Whittaker. 1983. Developmental autonomy of muscle fine structure in muscle lineage cells of ascidian embryos. *Dev. Biol.* **96:** 1–10.

Davidson, E. H. 1990. How embryos work: a comparative view of diverse modes of cell fate specification. *Development* **108:** 365–389.

Huarte, J., D. Belin, A. Vassalli, S. Strickland, and J.-D. Vassalli. 1987. Meiotic maturation of mouse oocytes triggers the translation and polyadenylation of dormant tissue-type plasminogen activator mRNA. *Genes Dev.* **1:** 1201–1211.

Karnovsky, M. J., and L. Roots. 1964. A "direct-coloring" thiocholine method for cholinesterase. *J. Histochem. Cytochem.* **12:** 219–221.

Karnovsky, M. J. 1965. A formaldehyde-glutaraldehyde fixative of high osmolality for use in electron microscopy. *J. Cell Biol.* **27:** 137A–138A.

Lillie, F. R. 1929. Embryonic segregation and its role in the life history. *Wilhelm Roux's Arch. Entwicklungsmech. Org.* **118:** 499–553.

McComb, R. B., G. N. Bowers Jr., and S. Posen. 1979. *Alkaline Phosphatase.* Plenum Press, New York. 986 pp.

McGady, J. 1970. A tetrazolium method for non-specific alkaline phosphatase. *Histochemistry* **23:** 180–184.

McGrew, L. M., E. Dworkin-Rastl, M. B. Dworkin, and J. D. Richter. 1989. Poly(A) elongation during *Xenopus* oocyte maturation is required for translational recruitment and is mediated by a short sequence element. *Genes Dev.* **3:** 803–815.

Mancuso, V., and G. Dolcemascolo. 1979. Ultrastructural aspects of the endoderm cells of the *Ciona intestinalis* embryo during the tail lengthening phase. *Acta Embryol. Exp.* **1979:** 161–171.

Meedel, T. H., and J. R. Whittaker. 1979. Development of acetylcholinesterase during embryogenesis of the ascidian *Ciona intestinalis*. *J. Exp. Zool.* **210:** 1–10.

Meedel, T. H., and J. R. Whittaker. 1984. Lineage segregation and developmental autonomy in expression of functional muscle acetylcholinesterase mRNA in the ascidian embryo. *Dev. Biol.* **105:** 479–487.

Minganti, A. 1954a. Fosfatasi alcaline nello sviluppo delle Ascidie. *Pubbl. Staz. Zool. Napoli* **25:** 9–17.

Minganti, A. 1954b. Fosfatasi alcaline nei semiembrioni animali e vegetative di Ascidie. *Pubbl. Staz. Zool. Napoli* **25:** 438–443.

Nishida, H. 1987. Cell lineage analysis in ascidian embryos by intracellular injection of a tracer enzyme. III. Up to the tissue restricted stage. *Dev. Biol.* **121:** 526–541.

Nishida, H., and N. Satoh. 1983. Cell lineage analysis in ascidian embryos by intracellular injection of a tracer enzyme. I. Up to the eight-cell stage. *Dev. Biol.* **99:** 382–394.

Nishida, H., and N. Satoh. 1985. Cell lineage analysis in ascidian em-

bryos by intracellular injection of a tracer enzyme. II. The 16- and 32-cell stages. *Dev. Biol.* **110:** 440–454.

Nishide, K., T. Nishikata, and N. Satoh. 1989. A monoclonal antibody specific to embryonic trunk-lateral cells of the ascidian *Halocynthia roretzi* stains coelomic cells of juvenile and adult basophilic blood cells. *Dev. Growth Differ.* **31:** 595–600.

Ortolani, G. 1954. Risultati definitivi sulla distribuzione dei territori presuntivi degli organi nel germe di Ascidie allo stadio VIII, determinati con le marche al carbone. *Pubbl. Staz. Zool. Napoli* **25:** 161–187.

Pearse, A. G. E. 1972. *Histochemistry: Theoretical and Applied,* Vol. 2, 3rd ed. London: Churchill Livingstone, London. 1518 pp.

Reverberi, G., and A. Minganti. 1946. Fenomeni di evocazione nello sviluppo di Ascidie. Risultati dell'indagine sperimentale sull'uovo di *Ascidiella aspersa* e di *Ascidia malaca* allo stadio di otto blastomeri. *Pubbl. Staz. Zool. Napoli* **20:** 199–252.

Satoh, N. 1982. DNA replication is required for tissue-specific enzyme development in ascidian embryos. *Differentiation* **21:** 37–40.

Whittaker, J. R. 1977. Segregation during cleavage of a factor determining endodermal alkaline phosphatase development in ascidian embryos. *J. Exp. Zool.* **202:** 139–153.

Whittaker, J. R. 1987. Cell lineages and determinants of cell fate in development. *Am. Zool.* **27:** 607–622.

Whittaker, J. R., and T. H. Meedel. 1989. Two histospecific enzyme expressions in the same cleavage-arrested one-celled ascidian embryos. *J. Exp. Zool.* **250:** 168–175.

Reference: *Biol. Bull.* **178:** 231–238. (June, 1990)

The Effect of Strontium on Embryonic Calcification of *Aplysia californica*

JOSEPH P. BIDWELL[1], ALAN KUZIRIAN[2], GLENN JONES[3], LLOYD NADEAU[4], AND LISA GARLAND[3]

Howard Hughes Medical Institute, Woods Hole Oceanographic Institution, Woods Hole, Massachusetts 02543

Abstract. During embryogenesis of the marine opisthobranch gastropod *Aplysia californica* Cooper, 1863, there is a brief critical time (window) during which strontium is essential for the onset of calcification. The present study was undertaken to elucidate the role of this element in mineralization. Strontium performed no structural function; deformed shells of strontium-deprived animals had normal atomic crystal structure and the element was excluded during calcification. Calcium deposition and fixation was reduced by approximately 80% in the absence of strontium but was not significantly altered in the presence of sub-optimal concentrations of this metal ion despite dramatic deficits in shell and statolith morphology. This suggests that calcium deficiency *per se* is not responsible for deficits induced by strontium deprivation. The reduced total calcium may be a secondary effect resulting from the complete inhibition of precipitation. Strontium did not modulate total alkaline phosphatase activity or total sulfated mucopolysaccharide synthesis during embryogenesis, and no morphological abnormalities of the organic shell were observed. Although the role of strontium in embryonic calcification of *Aplysia californica* remains enigmatic, these data suggest that strontium affects a highly discrete regulatory component because these more general indicators of calcification and differentiation are unaffected by its absence.

Received 19 July 1989; accepted 26 February 1990.

[1] Present address: Endocrine Research Unit, Mayo Clinic and Foundation, Rochester, Minnesota 55905. To whom requests for reprints and all correspondence should be addressed.

[2] Marine Biological Laboratory, Woods Hole, Massachusetts 02543.

[3] Woods Hole Oceanographic Institution.

[4] Present address: Toxikon, 225 Wildwood Avenue, Woburn, Massachusetts 01801.

Introduction

Strontium is required for the normal embryonic development of a variety of marine molluscs including gastropods (Bidwell *et al.*, 1986), bivalves (Gallager *et al.*, 1989), and cephalopods (Hanlon *et al.*, 1989). Embryos reared in the absence of strontium lack mineralized statoliths or shell, yet the soft-tissues appear normal. There is a critical window for strontium during embryogenesis of the opisthobranch gastropod *Aplysia californica* Cooper, 1863; normal mineralization requires 4 ppm strontium [~45.7 μM, half the concentration of natural seawater (Bruland, 1983)], lower concentrations (1–3 ppm) or exposure to high levels (80 ppm) results in abnormal and incomplete calcification (Bidwell *et al.*, 1986).

The dramatic specificity of the effect of strontium on molluscan embryogenesis affords a unique opportunity to study mineralization, a process only superficially characterized for any organism (Krampitz and Graser, 1988). Is the role of strontium primarily structural, as in the $SrSO_4$ tests of the marine protozoa *Acantharia cantharia spp.* (Anderson, 1981), or is a biochemical mechanism operative?

We report here the effects of varying the strontium concentration of artificial seawater on the atomic crystal structure of the embryonic shell and statoliths of *Aplysia californica*. We also describe the effects of medium strontium concentration on whole embryo levels of calcium, strontium, and magnesium throughout embryogenesis. Finally, we present histochemical analyses of strontium's influence on alkaline phosphatase activity and mucopolysaccharide synthesis.

Materials and Methods

Bioassay

Bioassays were conducted as described previously (Bidwell *et al.*, 1986). Briefly, a fresh egg mass of *Aplysia californica* was washed in basal medium, an artificial seawater consisting of the major salts of natural seawater except $SrCl_2 \cdot 6H_2O$. Stock solutions of $SrCl_2 \cdot 6H_2O$, $CaCl_2 \cdot 2H_2O$, and $MgCl_2 \cdot 6H_2O$ were standardized via flame atomic absorption. The egg mass was cut into strands and distributed among treatments. Natural seawater (NSW) was prefiltered (~1 μm, Millipore) before use and the pH and salinity recorded (pH ~ 8.0, salinity 32‰). All experiments were conducted at 21–22°C under constant illumination. Treatment waters were replaced with fresh media as noted below.

X-ray crystallographic experiments

Embryos were reared in one of three treatments including basal medium plus 3 ppm Sr (strontium, 34.2 μ*M*),[5] basal medium plus 80 ppm Sr (0.913 mM) and NSW. To obtain sufficient material for X-ray analysis, approximately 30 g of egg strands were maintained in 12 l of each test medium. Media were aerated constantly and replenished daily.

At 168 h after oviposition, strands were removed from treatment, rinsed with a 4% solution of ammonium acetate (to pH 8 with ammonium hydroxide), stored at −80°C until lyophilized, soaked in 5% reagent sodium hypochlorite (Baker) for 24 h, and the empty shells rinsed and dried with methanol. Adult shells, removed from the mantle tissue of 20 animals, were prepared as described above.

Samples were analyzed for crystal structure using X-ray diffraction methods. One-quarter to one-half gram of clean shells was backed with 40 mesh granular zinc and press-mounted onto standard Phillips aluminum sample holders using an applied pressure of 2 tons. Data were obtained with a Phillips Model 3500 XRD with a fine-focus Cu-kα X-ray tube operated at 40 kV and 20 ma. A theta compensator slit was placed between the sample and the X-ray tube, and a 0.2° receiving slit and graphite crystal monochrometer were placed between the sample and the scintillation detector.

The X-ray analysis was controlled using an IBM-AT computer and all data were collected and stored digitally. Each sample was scanned from 3 to 60° 2θ (29.45–1.54 Å d-spacing) in 0.03° steps, counting for 3 s between each step.

Calcium, strontium, and magnesium analysis of whole embryos

Egg strands (1 cm) from a single egg mass were distributed randomly between the five treatments of basal medium (0 ppm Sr), 3 ppm Sr, basal medium plus 8 ppm Sr (91.3 μ*M*), 80 ppm Sr, and NSW. Three egg strands were placed in each covered petri dish and its replicate. The test media (50 ml/dish) were replaced twice daily. Throughout development, six strands were collected for each treatment, rinsed with the ammonium acetate solution, transferred to microcentrifuge tubes (1.5 ml), plunged into liquid nitrogen, and stored at −80°C. Egg strands were lyophilized, the individual dry weights recorded, and ashed at 500°C (3 h) for ash weight. The ashed strand was digested to dryness with 50 μl of concentrated nitric acid (EM, Specpure) and stored at 4°C. One hour before analysis the residue was dissolved in 0.1 *N* HCl (EM Specpure)/5 mM $LaCl_3 \cdot 7H_2O$ (Fisher AA grade).

A Perkin Elmer 2280 atomic absorption spectrophotometer equipped with an HGA-400 graphite furnace was used to determine total calcium, magnesium, and strontium [methodology after Delaney (1983)] in whole embryos. Calcium and magnesium were analyzed via flame spectroscopy and strontium was determined with the furnace.

The strontium and magnesium distribution coefficients were determined from these data. The distribution coefficient is defined as:

$$K_M = \frac{[M]/[\text{Ca}]\ \text{tissue}}{[M]/[\text{Ca}]\ \text{medium}}$$

where *M* is the mole concentration of strontium or magnesium (Dodd, 1967). This ratio is a unitless index for characterizing biochemical and/or crystallographic discernment. A value of one indicates a lack of regulation, below one is evidence for discrimination and above one concentration. In this study the [*M*]/[Ca] ratio of the whole embryonic tissue, including the egg strand, was determined rather than the tissue or mineral alone because a clean separation of the embryo, shell, statolith, and egg strand with ultrapure reagents was not successful.

Alkaline phosphatase experiments

Egg strands, from a single egg mass, were maintained either in 2-l erlenmeyer flasks under constant aeration (45, 1 cm strands/flask) or in the petri dishes (3, 1 cm

[5] We express medium ionic concentrations initially in units of parts per million (ppm) and molar (M) but use ppm thereafter. Whole embryo concentrations of calcium, strontium and magnesium are expressed in moles/mg ash because mole units are more descriptive when comparing concentrations of different elements (see Bidwell and Spotte, 1985, for a review of this topic).

strands/dish). Test media were replenished every 48 h for the 2-l flasks and twice daily for the petri dishes. Treatments included NSW, 0 ppm Sr, 8 ppm Sr, and 8 ppm Sr plus 0.09 ppm beryllium (10 μM Be, as $BeSO_4 \cdot 4H_2O$). Be is a potent inhibitor of alkaline phosphatase, both *in vitro* (Aldridge, 1950; Chevremont and Firket, 1951) and *in vivo* (O'Day, 1972). Dose response experiments were conducted with Be (9×10^{-5} to 45 ppm) in the presence of 8 ppm strontium.

Histochemistry. Both the histochemical and biochemical assays for alkaline phosphatase were developed in the laboratory of Richard Whittaker, Marine Biological Laboratory, and kindly made available to us. Embryos were relaxed, while encapsulated, by the addition of 8% $MgCl_2 \cdot 6H_2O$ to the test medium. Egg strands (3–4 mm) were prefixed with 4% formaldehyde (from paraformaldehyde) in 0.2 μm filtered NSW for 30 min (4°C). The strands were incubated in 10 ml of Tris-buffer solution (100 μM Tris-Base, 100 mM NaCl, 5 mM $MgCl_2 \cdot 6H_2O$, pH 9.5) containing 33 μl of nitro blue tetrazolium (Sigma), (50 mg/ml in 70% dimethylformamide) (Sigma), and 33 μl of 5-bromo-4-chloro-3-indoyl phosphate p-toluidine salt (Sigma), (25 mg/ml in 100% dimethylformamide). The color reaction was monitored over 30–60 min with a dissecting scope (21°C). Fixation was continued with 3% glutaraldehyde/1.5% paraformaldehyde in 0.1 M cacodylate buffer (pH 7.4) containing 5 mM EGTA, 5 mM $MgCl_2 \cdot 6H_2O$, and 10% sucrose (4 h to overnight).

Whole mounts were prepared by transferring the egg strands from the cacodylate/sucrose buffer to 0.1 M sodium cacodylate and cutting the capsules to free the embryos. Specimens were rinsed with 50% methanol, dehydrated with dimethoxypropane (DMP, Muller and Jacks, 1975), further rinsed with 100% ethanol, cleared with Histoclear (National Diagnostics, Sommerville, New Jersey) and mounted on a glass slide using Diatex (Scientific Products).

For tissue sections, egg strands were post-fixed in 1% osmium in 0.1 M cacodylate (40–45 min, 21°C), rinsed 3× with 0.1 M cacodylate followed by 50% methanol, and dehydrated in DMP. Following transfer to propylene oxide, the tissues were infiltrated and embedded in Epon/Araldite. The sections were cut (2 μm), heat mounted on clean, untreated slides, and epoxy extracted with a solution of saturated KOH in 100% ethanol for 10 min. These sections were cleared and mounted to check the specific location of the reaction product. Sections and whole mounts were examined using a Zeiss Universal microscope equipped with a polarizing and differential interference contrast (DIC) optics.

Biochemical analysis. Egg strands were transferred to microcentrifuge tubes, plunged into liquid nitrogen, and stored at −80°C until analysis. Samples were thawed on ice and homogenized for 1 h in lysis buffer (4°C) containing 50 mM Tris HCl, 1 mM $MgCl_2 \cdot 6H_2O$, 1 μM $ZnCl_2$, 0.025% (w/v) Triton-X, and 0.0625% (w/v) sodium deoxycholate. The homogenate was centrifuged at $25{,}000 \times g$ for 10 min, 4°C. Alkaline phosphatase activity and total protein of the supernatant were determined colorimetrically via the p-nitrophenol (Sigma) and Bradford (Biorad, microassay) methods, respectively. Modifications of the alkaline phosphatase method included an extended incubation time for color development (16 h *vs.* 15 min) and a lower incubation temperature (21°C *vs.* 37°C, Whittaker, pers. comm.). Alkaline phosphatase activity was normalized to total protein.

SEM analysis. Embryos from Be dose-response experiments were processed for scanning electron microscopy (SEM) as described previously (Gallagher *et al.*, 1989).

Mucopolysaccharide synthesis experiments

Egg strands were maintained in 2-l flasks or petri dishes as described above. Treatments included 0 ppm Sr, 8 ppm Sr, and NSW. Samples were removed from the treatments throughout embryogenesis and analyzed for mucopolysaccharides.

Histochemistry. Following experimental treatment the encapsulated embryos were relaxed with 8% $MgCl_2 \cdot 6H_2O$ and transferred to the complete glutaraldehyde/paraformaldehyde fixative described above supplemented with 0.1% ruthenium red. Fixation lasted 2–4 h (20°C) or overnight (4°C) followed by rinsing and storage in 0.1 M cacodylate buffer plus 25% sucrose. Following routine methods outlined above, the embryos were embedded in epoxy resin. Tissue sections were cut, heat mounted on slides, epoxy extracted and treated with the following stains: Aldehyde fuchsin/alcian blue (pH 2.5) in sequence (Spicer and Meyer, 1960); 0.5% alcian blue (pH 2.5) alone, and 1% alcian blue (pH 1.0) (Lev and Spicer, 1964).

Statistical analysis

Values were log transformed for total calcium, strontium, and magnesium concentrations and alkaline phosphatase-specific activities. A two-way ANOVA was used to compare data from two or more treatments; time and treatment were fixed factors and the significance of the time × treatment interaction was determined. Means and least-square means were compared followed by the Student-Newman-Keuls (SNK) multiple comparison test and pairwise contrasts (adjusted by the Bonferonni method), respectively. The calcium and magnesium concentrations for the 0 ppm Sr treatment were analyzed

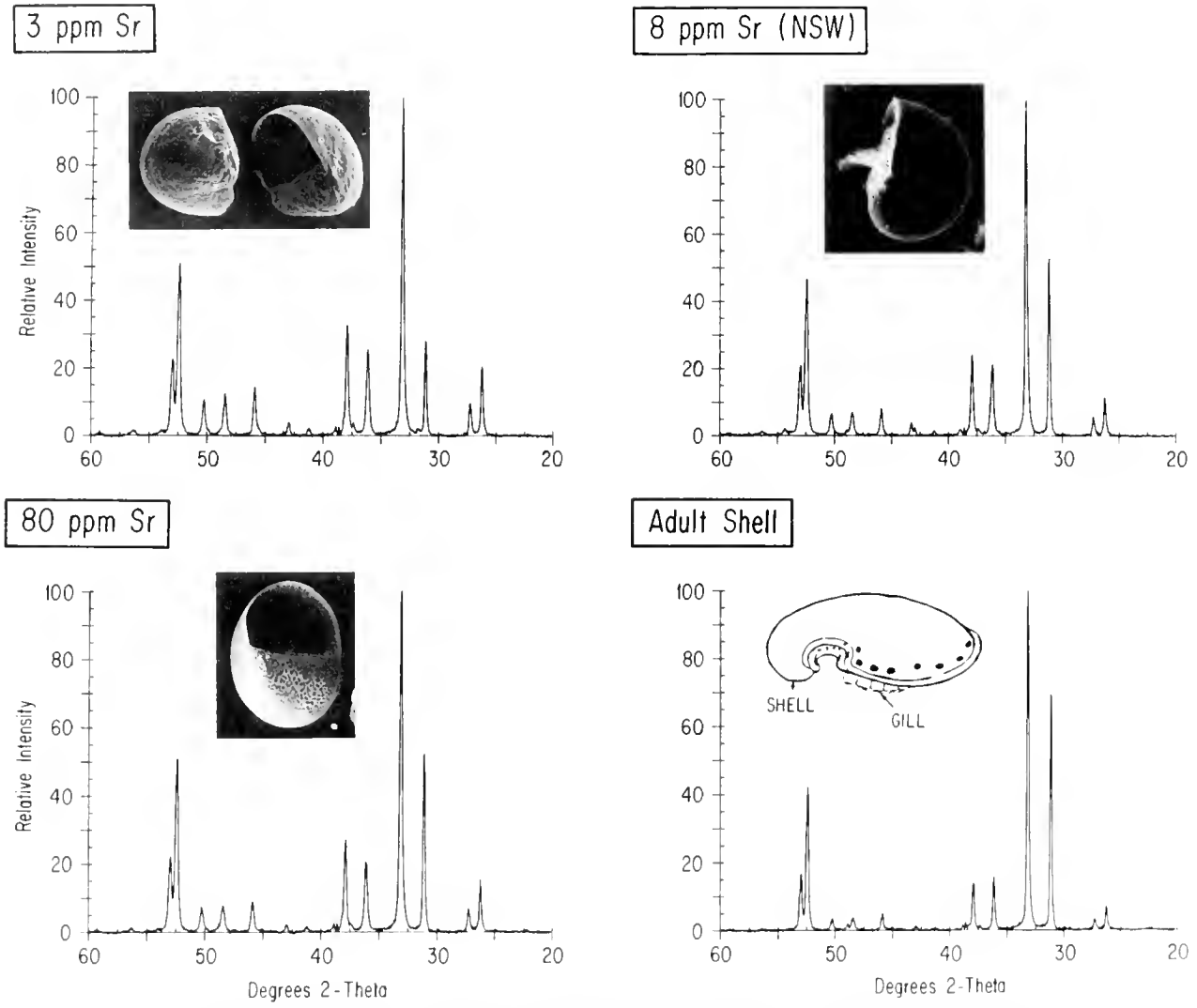

Figure 1. X-ray diffraction spectra of mineralized shell and statolith from indicated treatments. All material was aragonite and there was no evidence of paracrystalline or amorphous material in the deformed shells (3 and 80 ppm Sr).

separately using a one-way ANOVA followed by the SNK. Calculations were performed with SAS.

Results

X-ray crystal structure

Atomic diffraction spectra of abnormal shells and statoliths from embryos reared in the 3 and 80 ppm Sr media were indistinguishable from spectra of normal tissue (Fig. 1). All diffraction peaks observed for each sample were identified as belonging to the aragonite form of calcium carbonate. There were no significant shifts in peak position, changes in peak heights, nor evidence of amorphous or paracrystalline structure in the abnormal mineralized tissue.

Whole embryo concentrations of calcium, strontium, and magnesium

Total calcium at the end of embryogenesis (192 h) was diminished by approximately 80% in those embryos reared in the absence of strontium as compared to those organisms from strontium-containing media; total calcium of embryos from the 3 and 80 ppm Sr treatments were not significantly different from levels of the control organisms (8 ppm Sr, NSW, Fig. 2A). Thus, no correlation between total calcium and shell morphology was evident. Profiles for calcium concentration paralleled mineralization in all media containing strontium (Fig. 2A). At 96 h, a small but statistically significant increase in total calcium was observed coincident with the appear-

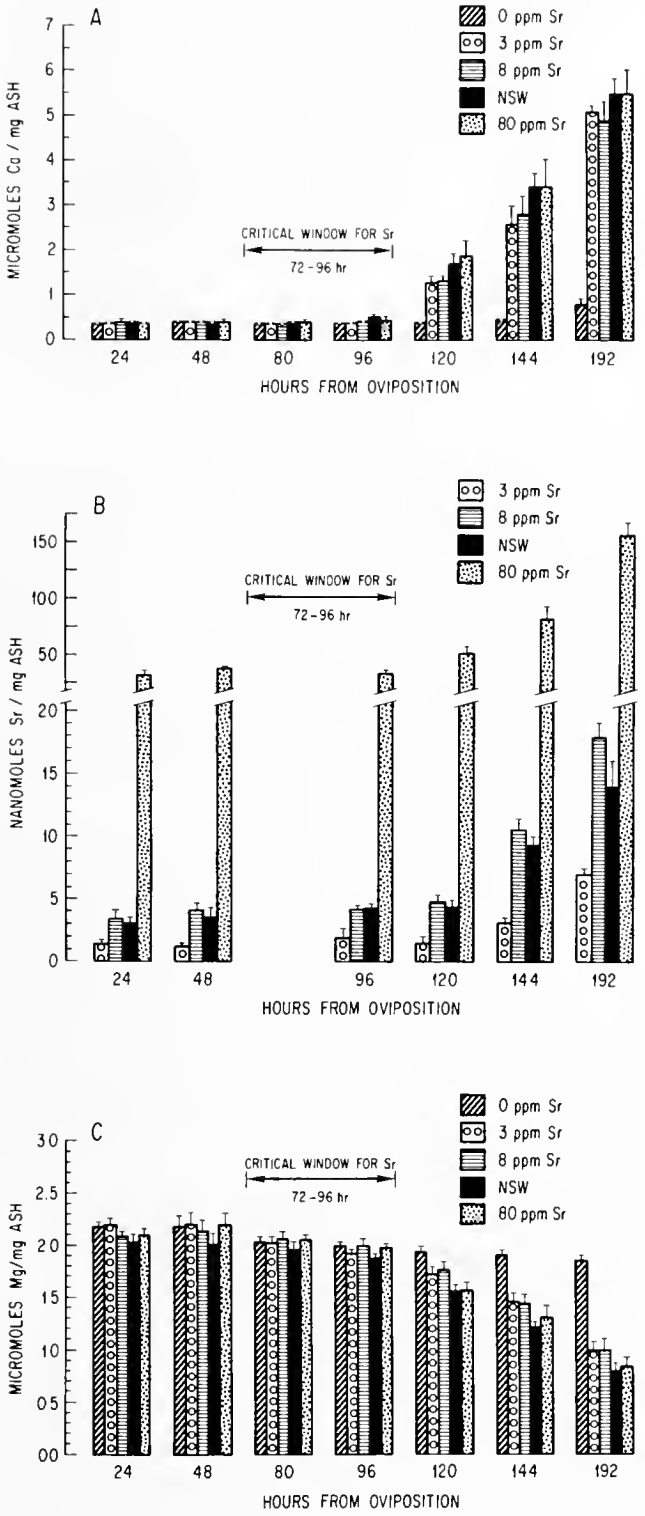

Figure 2. Chemical analysis of whole embryos plus egg strand. (A) Total calcium; a small but statistically significant increase was observed at 96 h (total calcium at 24–80 h = 0.39 ± 0.02 μM/mg ash; total calcium at 96 h = 0.45 ± 0.05, mean of combined treatments 3, 8, 80 ppm Sr and NSW ± S.D., $P < 0.05$. There was no significant difference in total calcium levels nor a significant time × treatment interaction between the 3 ppm and 8 ppm profiles or the NSW and 80 ppm profiles. Planned pairwise comparisons between the ASW treatments 3, 8, and 80 ppm Sr revealed that differences in calcium concentrations were limited to 120 and 144 h ($P < 0.001$). (B) Total strontium; this element was not detected with graphite furnace analysis in organisms from the 0 ppm Sr medium. Strontium samples (80 h) were unsuitable for analysis from this particular experiment. (C) Total magnesium; there was no significant difference between the 3 and 8 ppm Sr profiles but a significant contrast between these two profiles and that for the 80 ppm Sr treatment from 120 h through 192 h ($P < 0.001$). There was also a significant difference between the 80 ppm Sr and NSW profiles ($P = 0.003$) but no difference in magnesium levels at 192 h.

ance of the shell cap and statolith granules. Total calcium was not observed to increase in animals from the basal medium until 144 h, without evidence of mineralization.

Profiles representing total strontium concentration of whole embryos paralleled those for calcium but were proportional to medium levels (Fig. 2B).

Total magnesium concentration of whole embryo decreased during embryogenesis and this decline was attenuated in the absence of strontium (Fig. 2C). Although small, the decrease in whole embryo magnesium concentration over time from the 0 ppm Sr treatment was significant ($P < 0.001$).

Comparison of the strontium distribution coefficients (K_{sr}) over time indicated that the discriminatory mechanism for this element was not acquired until after the critical window. K_{sr} (Fig. 3A) for all treatments containing strontium had values close to one before the onset of mineralization, (1.05 ± 0.01, mean ± S.E., combined means of all treatments containing strontium, 24–96 h, n = 12). An abrupt decrease in the values of K_{sr} (0.34 ± 0.03, mean ± S.E., n = 4) was observed at 120 h as mineralization began. The distribution coefficient for synthetic aragonite prepared from artificial seawater is approximately 1.0 at room temperature (Kinsman, 1969).

The values of the magnesium distribution coefficient, K_{Mg}, for the 0 ppm Sr treatment ranged from 1.16 ± 0.02 at 24 h to 0.45 ± 0.07 at 192 h (mean ± S.D., n = 5 and 6, respectively) indicating discrimination of this element (Fig. 3B). This may represent the biochemical component of the regulatory mechanism for total magnesium because shell formation was absent.

Alkaline phosphatase activity

Positive staining for alkaline phosphatase in whole specimens was coincident with the onset of the critical window (approximately 72 h) and was localized in areas where mineralization was imminent, *i.e.*, the prevelar lobes (statoliths) and the shell field; intensity of the stain was not dependent upon whether the organism had been

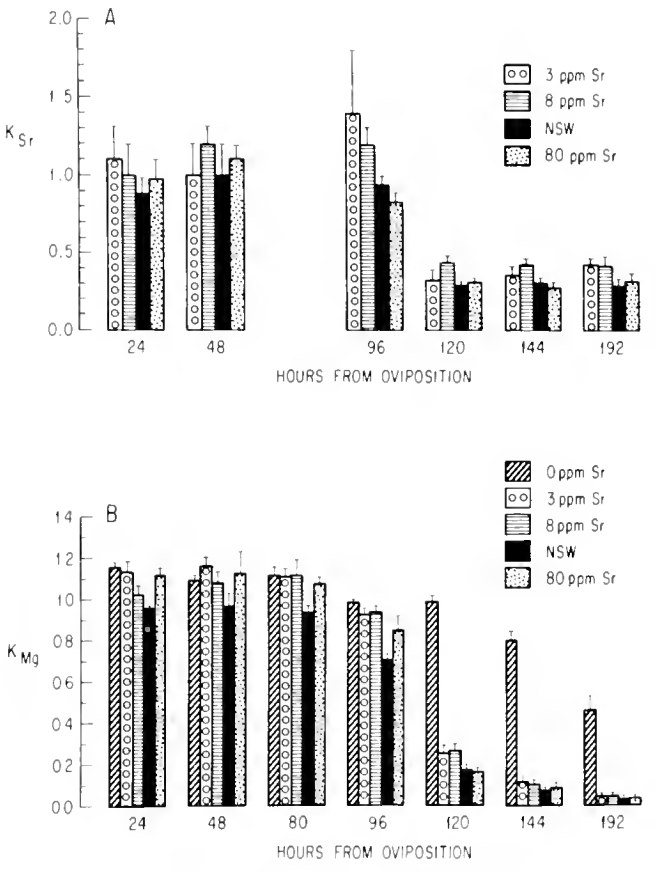

Figure 3. Distribution coefficients for (A) strontium and (B) magnesium for indicated treatments (mean ± S.D., n = 3–6).

reared in the presence of strontium (0 and 8 ppm Sr, Figs. 4A, B). Staining intensified in both treatments as development progressed, encompassing the velum, mantle, and the statoliths (8 ppm Sr) or the empty statocyst cavities (0 ppm Sr).

Exposure to beryllium (0.009–0.09 ppm), a potent inhibitor of alkaline phosphatase (Aldridge, 1950; O'Day, 1972), resulted in abnormalities of the embryonic shell and statoliths similar to those observed for strontium-deprived organisms (Fig. 4C). Nevertheless, this metal ion (0.09 ppm) did not attenuate alkaline phosphatase activity as measured biochemically (Fig. 4D), nor was the measured activity diminished in organisms from 0 ppm Sr.

Mucopolysaccharide synthesis

The presence of strontium had no effect on mucopolysaccharide synthesis as indicated by histochemical analysis, despite the failure of the organic shell to tan in those animals from the basal medium. Whole specimens from both the 0 and 8 ppm Sr treatments stained darkly with ruthenium red during embryogenesis; the indicator appeared evenly dispersed throughout the soft tissue, the organic matrix, and the egg strand. Differential staining with alcian blue and aldehyde fuchin demonstrated the presence of highly sulphated mucopolysaccharides and an absence of the acidic forms; again no differences were detected in embryos from the 0 and 8 ppm Sr treatments. No morphological abnormalities of the organic shell of embryos from the 0 ppm Sr treatment were observed upon examination of thick sections using light microscopy.

Discussion

The marine protozoa *Acantharia spp.*, the only other organisms known to require strontium, use the element for the formation of their $SrSO_4$ tests (Anderson, 1981). Paradoxically, the deficits as a result of strontium deprivation of *Aplysia californica* are specific for calcification, yet the defect is not mineralogical. We have demonstrated that strontium is discriminated against during mineralization and is not required for the stabilization of the aragonite polymorph in seawater. This element prevents the aragonite-to-calcite transition in calcium carbonate preparations (McLester *et al.*, 1970; Yoshioka *et al.*, 1986).

Because strontium is not part of the shell itself, this element may regulate a biochemical pathway vital to the onset of mineralization. Total embryonic calcium was reduced dramatically (~80%) in organisms reared in the absence of strontium, but calcium increase was not abolished. Furthermore, there was no correlation between total calcium levels at the end of embryogenesis and shell morphology in organisms from strontium-containing media. This suggests that calcium deficiency *per se* is not responsible for deficits induced by strontium deprivation. The reduced calcium may be a secondary effect resulting from the complete inhibition of precipitation. The present data do not address whether calcium uptake or transport is modulated by strontium and isotope experiments will be required to investigate this possibility.

Alkaline phosphatase has been implicated as a nucleating agent in precalcifying matrices (Vittur *et al.*, 1984; Marks and Popoff, 1988), and, although the onset of alkaline phosphatase activity was coincident with the critical window, it was not dependent upon the presence of strontium. Beryllium did not diminish this activity, although its presence during embryogenesis resulted in defects remarkably similar to those observed as a consequence of strontium's absence. Beryllium's inhibitory action on alkaline phosphatase is immediately reversible with magnesium in both histo- and biochemical preparations (Raven, 1966; Aldridge, 1950), and therefore mag-

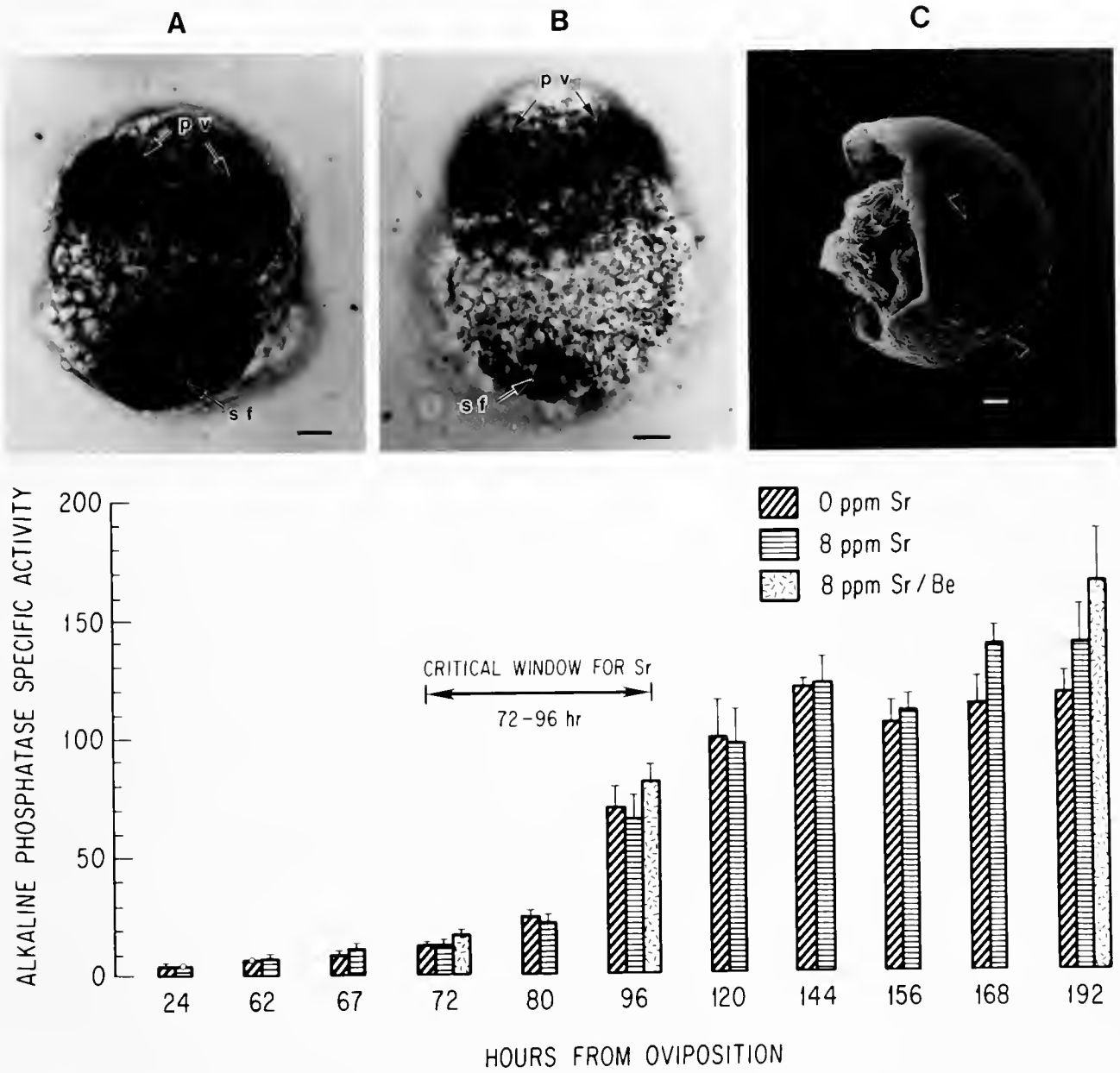

Figure 4. Alkaline phosphatase analysis. (A) Light micrograph showing dark histochemical staining for alkaline phosphatase activity in the, prevelar lobes (pv), and shell field (sf) of *Aplysia californica* embryo, 72 h, from ASW + 8 ppm Sr. (B) as in (A) for 72 h embryo from ASW without Sr. (C) SEM micrograph showing effect of 0.09 ppm Be on shell formation of embryonic *Aplysia californica*, shells were malformed and crenulated (arrowheads). (scales = 10 μm). (Graph) Specific alkaline phosphatase activity (normalized to total protein) of animals from the indicated treatments (mean ± S.D., n = 3). Only three time points were collected and analyzed for the 8 ppm Sr/0.09 ppm Be treatment. The largest increment in total alkaline phosphatase specific activity as measured biochemically was observed during the critical window in organisms from both the 0 and 8 ppm Sr treatments.

nesium may substitute for strontium *in vitro* although the stringent specificity for the latter *in vivo* argues against this possibility.

A defect in the organic matrix could severely limit or inhibit nucleation, but we were unable to demonstrate any morphological abnormalities in the organic shell nor a diminution of sulfated mucopolysaccharide synthesis in those embryos reared in the absence of strontium. The

molluscan matrix is not well characterized and our results do not preclude the formation of other matrix components being strontium-dependent.

Strontium's role and mechanism of action remain enigmatic. While essential for shell formation, the element performs no structural function. Moreover, our preliminary data suggest that strontium affects a highly discrete regulatory component because more general indicators of calcification and embryogenesis, *e.g.*, alkaline phosphatase activity, sulfated mucopolysaccharide synthesis, and soft tissue differentiation, are seemingly unaffected by its absence. Continued histo- and biochemical screening for a strontium-dependent marker will be an appropriate component of future work. Candidates for investigation will include acid phosphatases, Ca^{2+}-ATPase, and lysosomal acid hydrolases—all enzymes associated frequently with mineralization (Linde, 1981). Elucidation of the importance of strontium to seashell formation should contribute to our understanding of the biomineralization processes.

Acknowledgments

We thank Drs. James H. Schwartz and Eric R. Kandel (Columbia University, the Howard Hughes Medical Institute) for their support throughout this research. Donna McPhie (Marine Biological Laboratory) assisted with the histochemical studies. Scott Gallager of the Woods Hole Oceanographic Institution read the manuscript critically and contributed helpful suggestions throughout the work.

Literature Cited

Aldridge, W. N. 1950. Beryllium and alkaline phosphatase. *Nature* **165:** 772.

Anderson, O. R. 1981. Radiolarian fine structure and silica deposition. Pp. 347–379 in *Silicon and Siliceous Structure in Biological Systems*, T. L. Simpson and B. E. Volvani, eds. Springer-Verlag, New York.

Bidwell, J. P., and S. Spotte 1985. *Artificial Seawaters Formulas and Methods* Jones & Bartlett, Inc. Boston. 349 pp.

Bidwell, J. P., J. A. Paige, and A. M. Kuzirian. 1986. Effects of strontium on the embryonic development of *Aplysia californica*. *Biol. Bull* **170:** 75–90.

Bruland, K. W. 1983. Trace elements in seawater. Pp. 157–220 in *Chemical oceanography*, J. P. Riley and G. Skirrow, eds. Academic Press, London.

Chevremont, M., and H. Firket. 1951. Action of beryllium on cells cultivated *in vitro*; effects on mitosis. *Nature* **167:** 772.

Delaney, M. L. 1983. Foraminiferal trace elements: uptake, diagenesis, and 100 M.Y. paleochemical history. Ph.D. thesis. 253 pp. Massachusetts Institute of Technology and the Woods Hole Oceanographic Institution.

Dodd, J. R. 1967. Magnesium and strontium in calcareous skeletons: a review. *J. Paleontol.* **41:** 1313–1329.

Gallager, S. M., J. P. Bidwell, and A. M. Kuzirian. 1989. Strontium is required in artificial seawater for embryonic shell formation in two species of bivalve molluscs. Pp. 349–366 in *Origin, History and Modern Aspects of Biomineralization in Plants and Animals*, R. Crick, ed. Plenum Press, New York.

Hanlon, R. T., J. P. Bidwell, and R. Tait. 1989. Strontium is required for statolith development and thus normal swimming behaviour of hatchling cephalopods. *J. Exp. Biol.* **141:** 187–195.

Kinsman, D. D. J. 1969. Interpretation of Sr^{+2} concentrations in carbonate minerals and rocks. *J. Sediment. Petrol.* **39:** 373–392.

Krampitz, G., and G. Graser. 1988. Molecular mechanisms of biomineralization in the formation of calcified shells. *Agnew. Chem. Int. Ed. Engl.* **27:** 1145–1156.

Lev, R., and S. S. Spicer. 1964. Specific staining of sulphate groups with alcian blue at low pH. *J. Histochem. Cytochem.* **12:** 309.

Linde, A. 1981. On enzymes associated with biological calcification. Pp. 559–570 in *The Chemistry and Biology of Mineralized Connective Tissues*, A. Veis, ed., Elsevier North Holland, Inc.

Marks, S. C., Jr., and S. N. Popoff. 1988. Bone cell biology: the regulation of development, structure, and function in the skeleton. *Am J. Anat* **183:** 1–44.

McLester, M. E., D. F. Martin, and W. H. Taft. 1970. Effects of alkaline-earth metal ions on the transformation of aragonite to calcite in aqueous solution. *J. Inorg. Nucl. Chem.* **32:** 391–399.

Muller, L. L., and T. J. Jacks. 1975. Rapid chemical dehydration of samples for electron microscopic examinations. *J. Histochem. Cytochem* **23:** 107–110.

O'Day, D. H. 1972. An analysis of the effects of cyclic AMP and beryllium on alkaline phosphatase activity during the development of the cellular slime mold. Ph.D. Thesis, University of Delaware. 86 pp.

Raven, C. P. 1966. *Morphogenesis: the Analysis of Molluscan Development.* Pergamon Press, New York. 366 pp.

Spicer, S. S., and D. B. Meyer. 1960. Histochemical differentiation of acid mucopolysaccharides by means of combined aldehyde fuchsin-alcian blue staining. *Am J. Clin. Path* **33:** 453–460.

Vittur, F., N. Stagni, L. Moro, and B. de Bernard. 1984. Alkaline phosphatase binds to collagen; a hypothesis on the mechanism of extracellular mineralization in epiphyseal cartilage. *Experientia* **40:** 836–837.

Yoshioka, S., S. Ohde, Y. Kitano, and N. Kanamori. 1986. Behavior of magnesium and strontium during the transformation of coral aragonite to calcite in aquatic environments. *Mar. Chem* **18:** 35–48.

Reference: *Biol. Bull.* **178:** 239–250. (June, 1990)

Morphologic and Genetic Verification That Monterey *Botryllus* and Woods Hole *Botryllus* are the Same Species

HEATHER C. BOYD[1,*], IRVING L. WEISSMAN[1,2,**], AND YASUNORI SAITO[1,*,***]

[1]*Laboratory of Experimental Oncology, Department of Pathology, Stanford University School of Medicine, Stanford, California 94305, and* [2]*Hopkins Marine Station, Stanford University, Pacific Grove, California 93950*

Abstract. To determine whether Monterey *Botryllus* and Woods Hole *Botryllus* are the same species, comparisons were made of their morphology, biology, and colony specificity. In addition, matings were carried out to ascertain whether fertile [Monterey × Woods Hole] F_1 progeny could be obtained. The morphology and biology of *Botryllus* colonies from Monterey and from Woods Hole are very similar, and fertile F_1 progeny were obtained from interpopulation crosses. Therefore, we conclude that Monterey and Woods Hole *Botryllus* belong to the same species. However, slight differences were observed in the allorecognition reactions (colony specificity) of these two populations. Although there are some inconsistencies among the descriptions of *Botryllus schlosseri* and further extensive studies of *Botryllus* taxonomy are needed, our data indicate that *Botryllus* from Monterey and from Woods Hole may be designated contingently as *B. schlosseri*.

Introduction

Animals of the colonial ascidian genus *Botryllus* are used in scientific research in several different locations around the world, including Japan (Saito and Watanabe, 1982; Taneda and Watanabe, 1982), Italy (Sabbadin, 1977), and the United States (Grosberg, 1981; Scofield *et al.*, 1982; Mackie and Singla, 1983). On the east coast of the United States, *Botryllus* studies have been carried out at Woods Hole, Massachusetts (Milkman, 1967; Scofield and Nagashima, 1983; Grosberg and Quinn, 1986), and on the west coast in Monterey, California (Schlumpberger *et al.*, 1984; Boyd *et al.*, 1986), while some work includes data for *Botryllus* populations from both locations (Scofield *et al.*, 1982). Until now it had not been determined whether *Botryllus* from Monterey and Woods Hole are the same species. This is an important question, especially because of the tendency to apply information and conclusions obtained from experiments on one of these populations to research on the other population.

Woods Hole *Botryllus* has been called *Botryllus schlosseri* (Pallas, 1766) since Bancroft (1903) reported that "*Botryllus* at Woods Hole and at Newport exactly resembles *Botryllus* at Naples." Although this species has been regarded as cosmopolitan, inconsistencies in the literature suggest that *B. schlosseri*, as described thus far, may comprise more than one species. For example, the reported haploid number of chromosomes in the Woods Hole population (seven or eight: Milkman and Therrien, 1965) is half that of the Italian population (16: Colombera, 1969). As noted already (Van Name, 1945; Saito *et al.*, 1981a, b; Saito and Watanabe, 1985), the morphological characteristics of botryllid ascidian adult colonies and blastozooids are very similar from species to species. Therefore, detailed observations of morphology and biology throughout the life cycle are indispensable for the precise identification of the ascidians belonging to the Botryllidae. However, most of the past taxonomic reports on *B. schlosseri* dealt only with the morphological characteristics of adult colonies and blastozooids,

Received 9 November 1989; accepted 23 March 1990.

* H.C.B. and Y.S. are co-principal authors of this study.

** Address reprint requests to I. L. Weissman, Department of Pathology, Stanford University School of Medicine.

*** Present address: Shimoda Marine Research Center, University of Tsukuba, Shimoda-shi, Shizuoka-ken 415, Japan.

whereas the morphology of eggs, embryos, larvae, oozooids, and the blastozooids of very young colonies (as well as other biological characteristics, such as colony specificity) were not included (Van Name, 1945; Tokioka, 1953). These omissions may have contributed to the confusion about the taxonomy of this species. In this study we have identified Monterey and Woods Hole *Botryllus* as members of the same species, and have also described as much about their biology and morphology as possible for future taxonomic studies of *B. schlosseri* and its possible allies.

We used two criteria that define a species in order to ascertain whether Monterey and Woods Hole *Botryllus* belong to the same species (Friday and Ingram, 1985). First, morphological characteristics of individuals from both locations were compared throughout their life cycles, because individuals within a species are more similar to one another than they are to members of other species. Second, we tested the rule that members of the same species can interbreed to produce fertile offspring. We did this by setting up defined crosses between Monterey and Woods Hole colonies in the laboratory, followed by crosses involving their F_1 progeny. We also compared the phenomenon and morphology of colony specificity, a kind of allorecognition manifested by fusion or nonfusion between colonies.

Materials and Methods

Animals

For the observations on morphology, both wild and laboratory-cultured colonies of Monterey and Woods Hole *Botryllus* were used. For the experiments of colony specificity and defined crosses, laboratory-cultured colonies from both populations were used. Monterey *Botryllus* colonies were raised in the laboratory from embryos released or dissected from wild colonies that had been collected from Monterey Marina (Monterey, California). Woods Hole *Botryllus* colonies were raised from embryos dissected from adult colonies that had been collected from the Eel Pond in Woods Hole, or from the Green Pond in Falmouth, Massachusetts, and shipped to our laboratory by the Marine Resources Department of the Marine Biological Laboratory (Woods Hole, Massachusetts). Colonies derived from laboratory intrapopulation crosses (*e.g.*, Woods Hole × Woods Hole) were also used. In these experiments, Woods Hole colonies were held in seawater tanks at 18°C, and Monterey and progeny colonies were held at 20°C. Details of procedures for obtaining larvae and laboratory conditions for raising colonies to sexual maturity have been previously described (Boyd *et al.*, 1986).

Observations on morphology

Living colonies and fixed colonies were observed under a binocular stereomicroscope. For fixation, living colonies were immersed in 0.32 *M* $MgCl_2$ for about 15 min to anesthetize them, and then were transferred to 10% formalin in filtered seawater.

Colony specificity

Colony specificity was examined between colonies of the same population and between colonies of the two different populations by means of the "cut colony assay" (Oka and Watanabe, 1957). A single system (about 15 zooids) was dissected from each of two colonies. The two systems were placed in juxtaposition on a glass slide to allow contact with each other at their growing edges. After incubation for 30–40 min in a moisture chamber, the slide was transferred to a laboratory seawater tank. Observations of the colony specificity reaction were made using a binocular stereomicroscope. The timing and details of tunic fusion, ampullar fusion or deterioration, and blood cell infiltration were recorded as the two colonies underwent fusion or nonfusion.

Defined crosses

To use a genetic marker for verification of successful cross-fertilization in Monterey × Woods Hole crosses, we chose Monterey colonies lacking intersiphonal double bands and Woods Hole colonies having double bands. The parental colonies of a cross were placed in a 4-liter 20°C seawater tank at a time when their sexual stages were appropriately matched so that the sperm of one colony would be ripe when the eggs of its partner were ready to be fertilized. If necessary, the two colonies were held at different temperatures to adjust their reproductive stages prior to the cross.

Periodically during the cross, one or two zooids of each parental colony were dissected to determine the developmental stage of the embryos. Upon maturation, the tadpoles swam out of the maternal colony and attached to a glass settlement slide, where they metamorphosed to become oozooids. Because the *Botryllus* life cycle permits the colonies of a mating pair to alternate as egg and sperm donor for each other, several reciprocal fertilizations and subsequent hatches occurred for each colony pair. The progeny were kept in 4-liter 15°C tanks for two to three weeks, and then were placed in 17-liter 20°C tanks. A subset of the oozooids from each cross was maintained and observed for the presence or absence of the intersiphonal double band marker. The nomenclature used to identify each progeny colony was as follows: [maternal colony × paternal colony]-individual progeny identification number.

Crosses involving [Monterey × Woods Hole] F_1 colonies as parents were also set up in the manner described above.

Results

Biology and morphology

Monterey Botryllus. Colonies of Monterey *Botryllus* are usually found encrusting the surface of pilings, floats, rocks, seaweeds, and other sessile animals, such as *Ascidia ceratodes* (Tunicata) and *Phyllchaetopterus prolifica* (Annelidae), between lower intertidal and shallow subtidal zones in calm water. They compete with colonies of *Botrylloides violaceus* (belonging to the same family as *Botryllus*) in that habitat. In Monterey Marina, many sexually mature colonies are found from March to November; they are scarce in winter. Colonies sometimes grow to 7–8 cm across; the thickness is usually 1.0–1.5 mm. The colony surface is generally flat and free from any foreign matter. The tunic is soft, gelatinous, and transparent. When alive, colonies have orange, red-brown, or dark blue pigmentation. A colony (Fig. 1A) is composed of many zooids called blastozooids, which are arranged in oval or star-shaped systems in a common tunic. These systems are connected to one another, as are the zooids within any system itself, by a common vascular network in the tunic. Each system is composed of 5–15 blastozooids, which share a common cloacal aperture in the center of the system. The periphery of a colony is fringed with sausage-shaped vascular ampullae, each about 700 μm long and 200 μm wide, that project from the tunic's vascular array.

Each colony is founded by a sexually produced yellowish white or pale orange tadpole larva (Fig. 1B), about 1.6 mm long. The trunk of the larva is about 400 μm long, oval in outline, and has the single photolith typical of botryllids. Three adhesive papillae are arranged in a triangle on the anterior end of the trunk, and eight ampullae are arranged in a circular band surrounding the anterior half of the trunk. One or two hours after liberation the larvae attach to a suitable substratum by the adhesive papillae. Each larva extends its eight ampullae to complete attachment, and begins metamorphosis into a primary zooid (oozooid). The larva becomes a functional oozooid by opening its siphons and beginning to feed at 1.5–2 days after attachment.

An oozooid (Fig. 1C) is about 500 μm long and has four long transverse stigmata (protostigmata) on the left side, and four long ones, sometimes accompanied by a rudimental one, on the right side of the branchial sac. There is one inner longitudinal blood vessel on each side of the branchial sac. The stomach of an oozooid is 140 μm long and oval-shaped, with five longitudinal plications. The oozooid makes only one pallial bud, on the right side of the body. After one week, the feeding oozooid is resorbed by the colony and is replaced by its bud, which has developed into a functional zooid (the first blastogenic asexual generation). Buds of the next blastogenic generation develop on both sides of the first blastozooid. Replacement of zooids by new blastozooids of the next generation, called "takeover," occurs about once each week at 18–20°C and synchronously in all feeding zooids of a colony.

The first blastozooid (Fig. 1D, E) is 600–700 μm long and has four stigmatal rows on each side of the branchial sac; the second row does not reach the dorso-median line, and the fourth row is usually rudimentary. There is one inner longitudinal vessel on each side of the branchial sac. The stomach has five longitudinal plications. The first blastozooid usually produces a single bud on each side of the body; after the second blastogenic generation, blastozooids produce one or two buds on each side of their bodies.

The number of stigmatal rows in the blastozooids increases from one asexual generation to the next, ultimately resulting in eight rows. The number of inner longitudinal vessels on each side of the branchial sac also increases from one to three during the first several takeovers (Fig. 1F). Blastozooids of a mature colony (Fig. 2) lie obliquely in a common tunic and are 2.0–2.8 mm long. Branchial tentacles of a blastozooid consist of four large and four small ones, regularly alternating. There are usually eight rows of stigmata on each side of the zooids. The second row of stigmata never reaches the dorso-median line. Around the middle of the branchial sac, stigmata are arranged between the three inner longitudinal vessels as follows: dorsal lamina 5.2.3.4 endostyle (periods represent vessels; Fig. 2B). Many blood cells are deposited along each side of the endostyle in the range from the first to the sixth stigmatal row. The anterior edge of the intestinal loop reaches the level of the fifth or sixth transverse vessel, and the anus opens at the level of the sixth stigmatal row (Fig. 2B). Most of the stomach is exposed posterior to the branchial sac. The stomach is yellowish-orange or orange in fresh specimens, and is furnished with eight longitudinal plications and a long, hooked pyloric caecum.

The testis lies ventro-posterior to the ovary at the level of the 4th–5th stigmatal row on the left side, and at the level of the 6th or 7th stigmatal row on the right side (Fig. 2B, C). It consists of several white opalescent lobes forming a rosette. Eggs mature in the ovary of a bud during bud development and reach a maximum size of 230–250 μm just before takeover (Fig. 2C). Mature eggs are yellowish orange. They are ovulated when new blastozooids open their branchial siphons. The release of sperm occurs about two days after ovulation in the same zooids. Ovulation and sperm release occur synchro-

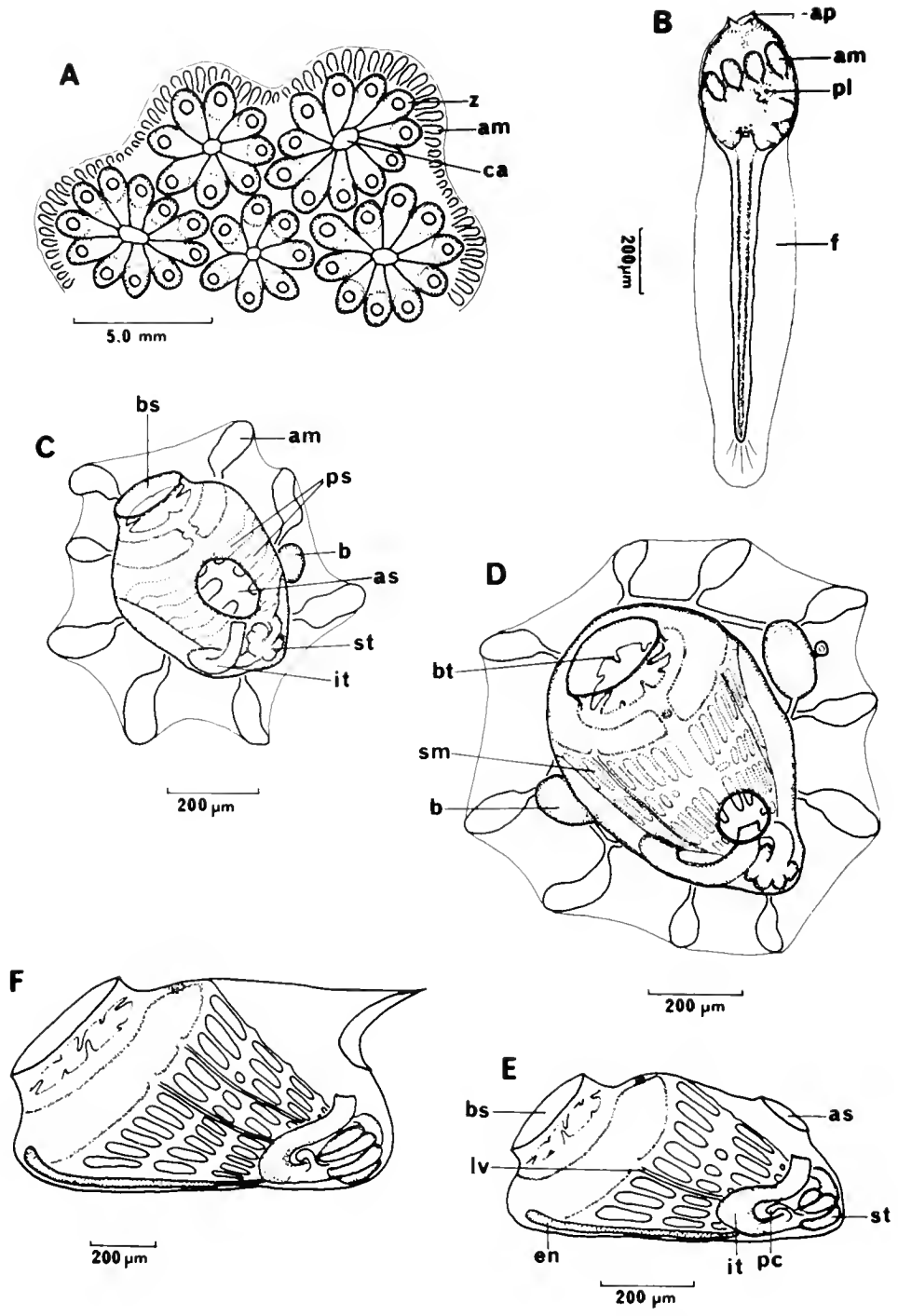

Figure 1. Monterey *Botryllus* (A) Part of a colony. Blastozooids are arranged into oval or star-shaped systems. (B) Larva, left side. (C) Oozooid, dorsal view. (D) First blastozooid, dorsal view, with buds of second blastogenic generation. (E) The same as (D), but left side. (F) Second blastozooid, left side. am, ampulla; ap, attachment process; as, atrial siphon; b, bud; bs, branchial siphon; bt, branchial tentacle; ca, cloacal aperture; en, endostyle; f, fin; it, intestine; lv, longitudinal vessel; pc, pyloric caecum; pl, photolith; ps, protostigmata; sm, stigmata; st, stomach; z, blastozooid.

nously in all zooids of a colony. The blastozooid of a healthy colony has one to three developing embryos supported by oviducal cups on each side of the peribranchial cavity (Fig. 2). The diameter of embryos just before hatching is about 280–300 μm.

Woods Hole Botryllus. We do not have year-round

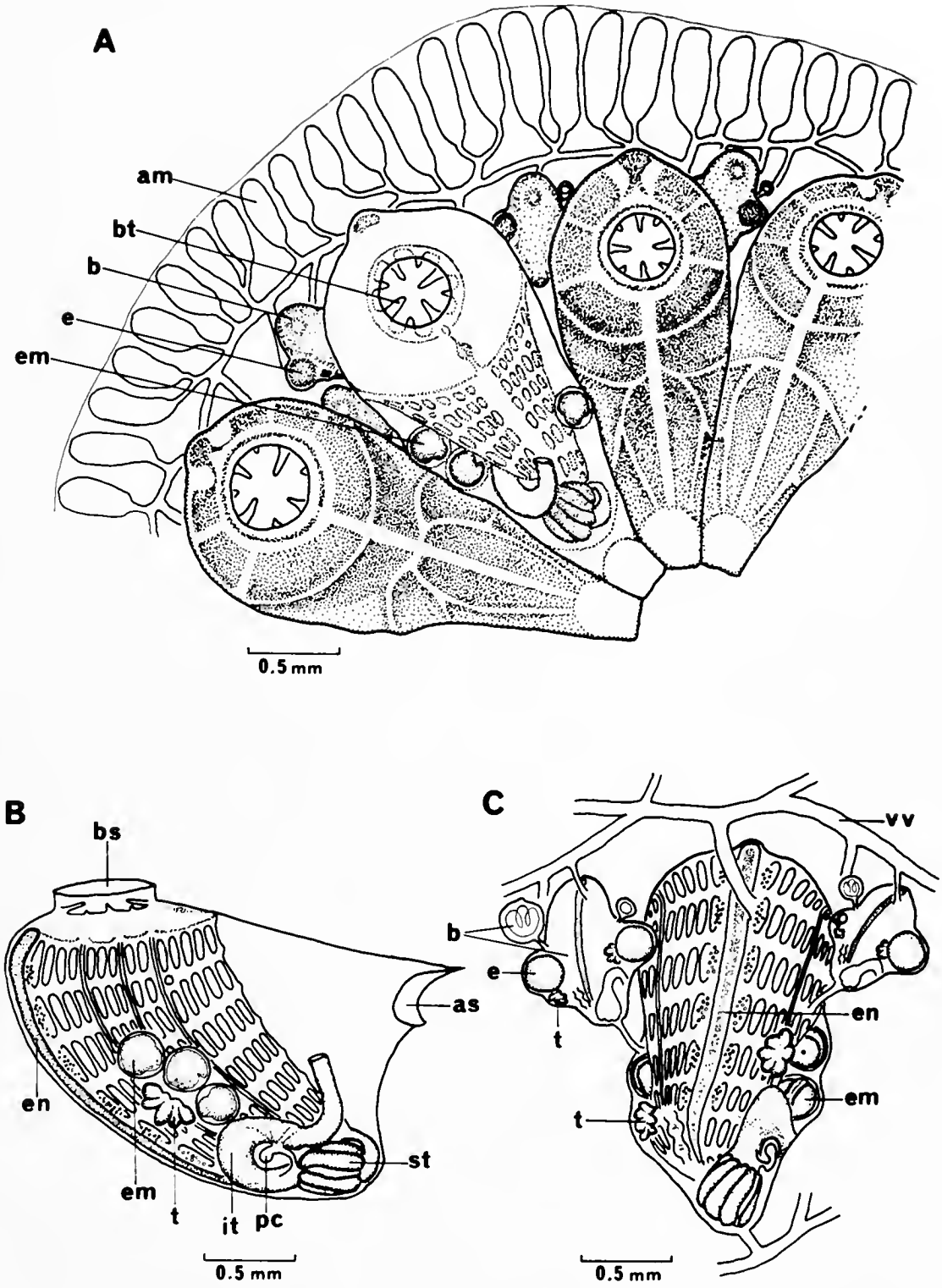

Figure 2. Monterey *Botryllus*. (A) Mature blastozooid, dorsal view. (B) The same as (A), but left side. (C) The same as (A), but ventral view with buds. am, ampulla; as, atrial siphon; b, bud; bs, branchial siphon; bt, branchial tentacle; e, egg; em, embryo; en, endostyle; it, intestine; pc, pyloric caecum; st, stomach; t, testis; vv, vascular vessel.

Table I

Summary of morphology of Monterey and Woods Hole Botryllus

	Monterey[a]	Woods Hole[a]
Colony		
Shape & thickness	Flat, 1.0–1.5 mm	Flat, 0.7–1.6 mm
Color & pigmentation	Orange, blue, brown; double intersiphonal band rarely present on zooids	Many variations; double intersiphonal band often present on zooids
Arrangement of zooid	Oval or star-shaped	Oval or star-shaped
Tunic (=test)	Soft, gelatinous, transparent	Soft, gelatinous, transparent
Larva		
Total length	1.6 mm	1.5–1.7 mm
Trunk shape & size	oval, 400 μm long	oval, 400 μm long
Attachment processes	3	3
Ampullae	8	8
Photolith	1	1
Oozooid		
Protostigmata	L:4, R:4 (+1)	L & R:4
First ampullae	8	8
Longitudinal vessels	L & R:1	L & R:1
Stomach plications	5	5
First buds	R:1	R:1
First blastozooid		
Stigmatal rows	L & R:4	L & R:4
2nd stigmatal row	Incomplete	Incomplete
Longitudinal vessels	L & R:1	L & R:1
Stomach plications	5	5
Number of buds	L:1, R:1	L:1, R:1
Mature blastozooid		
Posture	Obliquely	Obliquely
Size	2.0–2.8 mm long	1.2–2.6 mm long
Branchial tentacles	4 large & 4 small	4 large & 2–4 small
Stigmatal rows	L & R:8	L & R:7–8
2nd stigmatal row	Incomplete	Incomplete
Longitudinal vessels	L & R:3	L & R:3
Stomach plications	8	7
Pyloric caecum	Long, hooked	Long, hooked
Number of buds	L & R:1–2	L & R:1 (lab-culture)
Testis shape & color	Rosette, white opalescent	Rosette, white opalescent
Embryos	L & R:1–3, supported with oviducal cups	L & R:1–3, supported with oviducal cups
Maximum size of embryos	280–300 μm	300 μm
Mature egg number	L & R:1–3	L & R:1–3
size in buds	230–250 μm	220–240 μm
Color of eggs	Yellowish orange	Yellow

[a] L = left; R = right.

ecological data for Woods Hole *Botryllus*. However, we do have observations from a field study at the end of October 1986. According to these data, colonies of Woods Hole *Botryllus* were very common in the Eel Pond, but rare at the shore facing the open sea around the Marine Biological Laboratory. They were encrusting on the surfaces of pilings, floats, rocks, seaweeds, and solitary ascidians (*Styela partita*) in shallow water, and, like Monterey *Botryllus*, apparently were competing with colonies of *B. violaceus* for substrate. At that time, several of the colonies examined had developing embryos and eggs. Under laboratory culture conditions, Woods Hole colonies show the same life history as the Monterey colonies described above.

The detailed data in Table I (from observations on 30 to 100 colonies of each population) show that the morphology of Woods Hole *Botryllus* is similar to that of Monterey *Botryllus*, except for coloration. Therefore, only the few differences that exist between Woods Hole and Monterey colonies will be described here. The

Woods Hole population exhibited many color variations: orange, yellow, blue, green, brown, and mixtures of these colors. In many Woods Hole colonies, blastozooids had intersiphonal bands formed by deposition of white or yellow pigment cells between the branchial siphon and the atrial aperture (see Bancroft, 1903; Watterson, 1945; Sabbadin, 1962). This feature was very rare in Monterey colonies. Woods Hole colonies generally were thinner (0.7–1.6 mm) than Monterey colonies. Oozooids of Woods Hole *Botryllus* had four protostigmata on each side of the body; none (that we observed) had the rudimental fifth stigmata on the right side that was occasionally seen in Monterey colonies. Blastozooids of Woods Hole colonies (1.2–2.6 mm long) were somewhat smaller than those of Monterey colonies. In some adult Woods Hole colonies, blastozooids had four long branchial tentacles and only two small ones, and had seven stigmatal rows on each side of the branchial sac. There were seven stomach plications in Woods Hole colonies. The pattern of increase in the numbers of stigmatal rows, inner longitudinal vessels, and stomach plications during the first several takeovers, and the incompletion of the second stigmatal row, were the same for Woods Hole and Monterey colonies.

Observations on colony specificity

In colonial ascidians, when two colonies come into contact with each other, fusion or nonfusion occurs between them at the contact area. This allogeneic recognition phenomenon is called "colony specificity." Both fusion and nonfusion (allorejection) were observed in colony pairs from Monterey and in pairs from Woods Hole. Interpopulation pairs never fused, and the Woods Hole colony was always damaged by the Monterey colony. In these experiments, each different type of colony specificity reaction was observed in more than ten colony pairs, except for rejection in pairs from Woods Hole (five colony pairs). Within each colony pair, the assay was done in duplicate or triplicate.

The fusion process in both populations proceeded as follows. When two fusible colonies came into contact, vascular ampullae in the tunic of each colony extended toward those of the other colony (Fig. 3, Stage 1). Eventually, the tunic along the contact boundaries of the two colonies fused. The ampullae of each colony continued to grow out into the tunic of the facing colony (Fig. 3A, Stage 2), and finally their tips came into contact with the proximal (not distal) parts of ampullae of the other colony (Fig. 3A, Stage 3). At the contact points, the blood vessels of the two colonies became connected to one another; that is, a common vascular system was formed between the two colonies (Fig. 3A, Stage 4).

As with the fusible colonies, when two nonfusible colonies of the Monterey population came into contact with each other, the ampullae of each colony extended toward those of the other colony (Fig. 3, Stage 1). However, their tunics did not fuse, so the tips of ampullae of both colonies made contact with each other indirectly through the surface layers of their tunics (Fig. 3B, Stage 2). Bright green blood cells gathered near the tips of the ampullae at the contact areas, after which blood cells infiltrated the tunic around the ampullar tips (Fig. 3B, Stage 3). These blood cells changed from bright green to dark brown, and the ampullae of each colony withdrew from the contact areas (Fig. 3B, Stage 4).

When two nonfusible colonies from the Woods Hole population came into contact with each other, ampullae of each colony began to extend toward those of the other colony (Fig. 3, Stage 1). Fusion of their tunics occurred, but the area of tunic fusion was limited to a small space near the ampullar tips (Fig. 3C, Stages 2 and 3). The distal parts of the ampullae penetrating into the facing colony contracted and in some cases, were amputated, while blood cells from these ampullae infiltrated into the tunic (Fig. 3C, Stage 4).

When a Monterey colony and a Woods Hole colony were brought into contact with each other, their ampullae grew toward each other as described above for intraspecies pairs (Fig. 3, Stage 1). However, although the ampullar tips of both colonies came very close to one another, they did not make direct contact because tunic fusion did not occur (Fig. 3D, Stage 2). At the contact area, ampullae of the Woods Hole colony contracted and blood cells infiltrated the tunic from them, but the Monterey colony showed no such response (Fig. 3D, Stage 3). Ampullae of the Woods Hole colony were amputated or withdrew from the contact area, and the infiltrated blood cells in the tunic changed to a dark brown color (Fig. 3D, Stage 4).

Production of F_1 progeny from crosses between Monterey and Woods Hole Botryllus *colonies*

Botryllus colonies from Monterey and from Woods Hole are capable of both self- and cross-fertilization (Scofield *et al.*, 1982). The standard test of species identity requires that fertile F_1 hybrids be produced by cross-fertilization. In our study, two methods were used to demonstrate that cross-fertilization did occur between Monterey and Woods Hole colonies. First, because *Botryllus* colonies are protogynous (Milkman, 1967), eggs in a given colony are ready to be fertilized about two days before the autologous sperm are mature, and thus are fertilized preferentially by mature sperm from a heterologous colony if available (Sabbadin, 1962). Furthermore, the stages of a colony's asexual reproductive (*i.e.*, budding) cycle are interconnected in a predictable way

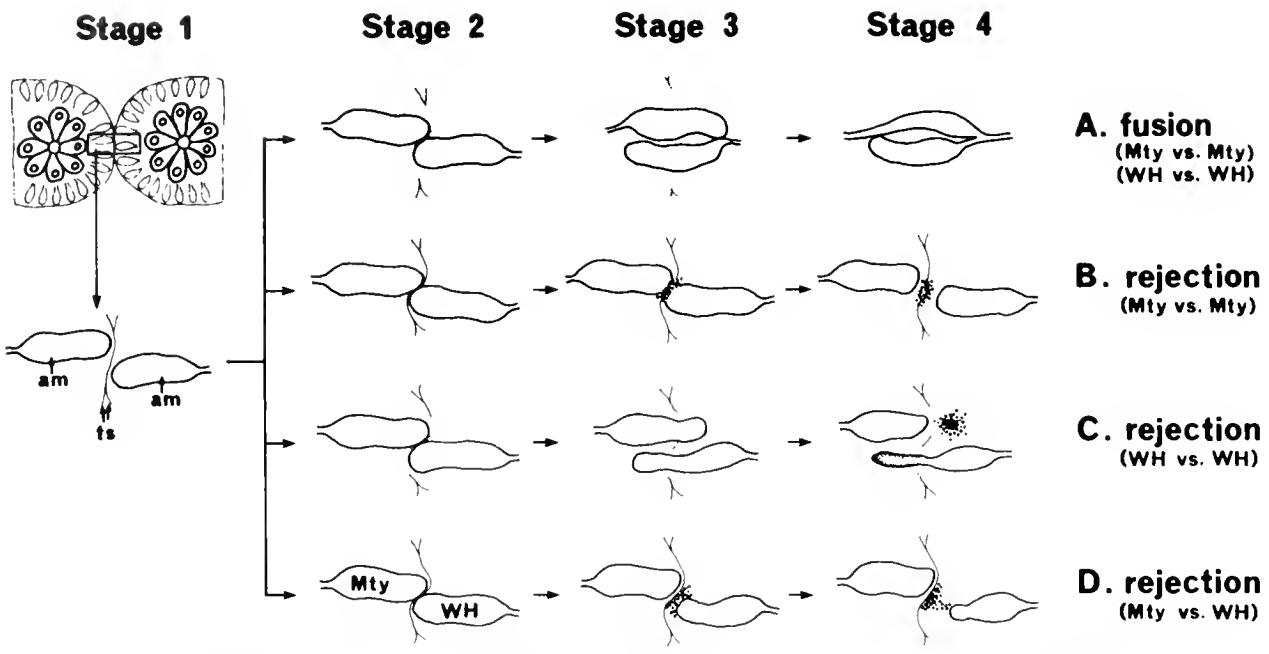

Figure 3. Scheme showing processes of fusion and rejection in Monterey and Woods Hole *Botryllus*. (A) Fusion between Monterey colonies and between Woods Hole colonies. (B) Rejection between Monterey colonies. (C) Rejection between Woods Hole colonies. (D) Rejection between Monterey and Woods Hole colonies. For detail, see text. am, ampulla; ts, tunic surface; Mty, Monterey colony; WH, Woods Hole colony.

with the developmental stages of its cross-fertilized embryos. Considering these traits in combination, we can dissect embryos from the maternal colony and determine whether they arose from self- or cross-fertilization. For example, if mature zooids that are about to undergo takeover (*i.e.*, each having a well-developed primary bud with a secondary bud attached to it via a stalk) contain late "wraparound" stage embryos, then these embryos must be the result of cross-fertilization (also see Milkman, 1967). On the other hand, if these zooids contain much earlier stage embryos, (*e.g.*, gastrulas), these embryos could be the result of self-fertilization. In the two crosses that were set up between Monterey and Woods Hole colonies, observations at selected times during embryonic development verified that reciprocal cross-fertilization had occurred between Monterey and Woods Hole colonies.

The second method for demonstrating that cross-fertilization had occurred depended on a genetically encoded pigmentation marker, the intersiphonal double band. This marker is controlled by a dominant allele at a single gene locus (Sabbadin and Graziani, 1967), and is relatively easy to see with a dissecting microscope (Fig. 4A). Colonies with double bands are more common in Woods Hole than in Monterey (pers. obs.). Therefore, we set up crosses in which one parent was a Monterey colony without double bands (Fig. 4B), and the other parent was a double-banded Woods Hole colony (Fig. 4A). In these cases we could be certain that any double-banded F_1 progeny that were released from the Monterey colony (*i.e.*, maternal colony lacking double bands) must have been derived from Monterey colony eggs fertilized by Woods Hole colony sperm bearing the allele for double bands.

The results of Monterey × Woods Hole crosses are shown in Table II. The numbers in this table are for samples of the progeny that were released. In both crosses, the Monterey and Woods Hole parental colonies each released at least 14 to 32 F_1 progeny, and among these F_1 progeny there were at least 9/32 (28%) to 9/14 (64%) double-banded colonies released from each of the four parents. These data indicate that crosses between Monterey and Woods Hole *Botryllus* colonies can produce viable F_1 offspring.

Monterey × Woods Hole F_1 progeny are fertile

If *Botryllus* colonies from Monterey and Woods Hole belong to the same species, their F_1 progeny should be capable of sexual reproduction. An $F_1 \times F_1$ cross was set up between sibling colonies produced in the second cross in Table II. As shown in part (1) of Table III, both parental F_1 colonies, [Mty 248p.2 × WH 114] – 4 and [WH 114 × Mty 248p.2] – 3, released F_2 progeny. In this

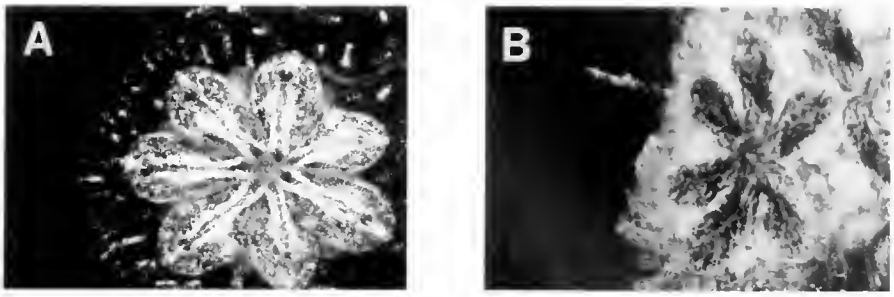

Figure 4. Representative portions of *Botryllus* colonies. (A) Woods Hole colony with intersiphonal double bands. (B) Monterey colony lacking intersiphonal double bands.

cross, the $F_1 - 4$ parent colony was a double-banded colony that was released from Mty 248p.2, which lacked the double band trait (Table II). Therefore, $F_1 - 4$ was definitely an F_1 hybrid resulting from cross-fertilization between Monterey and Woods Hole parental colonies. In this $F_1 \times F_1$ cross, the double band trait could not be used to distinguish between self- and cross-fertilization because both parents expressed it.

In the second cross (part 2, Table III), one parent, the double-banded [Mty 279u × WH 143] − 4 colony, was released from Mty 279u, which lacked the double band trait (Table II). Therefore, this $F_1 - 4$ colony was definitely an F_1 hybrid resulting from cross-fertilization between Monterey and Woods Hole parental colonies. The partner in this cross was a Monterey colony without double bands (Mty 405g). Both parental colonies released F_2 progeny, and at least 6 of 11 progeny released from Mty 405g were definitely the result of cross-fertilization because they expressed the double band trait obtained from the sperm donor $F_1 - 4$ (Table III).

In addition, as in the Monterey × Woods Hole crosses, dissections were performed at several time points during embryonic development in the crosses in Table III. We observed that the relationship between embryo stage and maternal colony asexual stage at given times was consistent with the expected schedule of cross-fertilization rather than self-fertilization. Thus, from this observation and the data in Table III, we conclude that Monterey and Woods Hole colonies can interbreed to produce fertile F_1 offspring, and therefore belong to the same *Botryllus* species.

Table II

Results of crosses between Monterey and Woods Hole colonies

Pairs of parental colonies[a]	Double band in parent	Progeny[b,c]
(1) Mty 279u	−	14 (9)
WH 143	+	29 (18)
(2) Mty 248p.2	−	32 (9)
WH 114	+	16 (6)

[a] Mty = Monterey; WH = Woods Hole.

[b] The progeny on a given line in the table were released from the indicated colony when it was the egg donor (maternal colony) and the other colony of that pair was, therefore, the sperm donor.

[c] These are minimum numbers, because not all progeny that were released were collected and observed. The numbers in parentheses designate the minimum number of progeny, among those observed, that definitely showed the intersiphonal double band.

Discussion

Four or more botryllid ascidians live along the coast of California (Fay and Johnson, 1971; Fay and Vallee, 1979; Abbott and Newberry, 1980), but only two of them have been identified: *Botryllus tuberatus* Ritter and Forsyth 1917 and *Botrylloides diegensis* Ritter and Forsyth 1917. The two unidentified species, one *Botryllus* and

Table III

Results of crosses involving Monterey × Woods Hole F_1 progeny as parents

Pairs of parental colonies[a,b]	Double band in parent	Progeny[c,d]
(1) [Mty 248p.2 × WH 114] − 4	+	22 (11)
[WH 114 × Mty 248p.2] − 3	+	16 (9)
(2) [Mty 279u × WH 143] − 4	+	14 (6)
Mty 405g	−	11 (6)

[a] Mty = Monterey; WH = Woods Hole.

[b] The first three parental colonies in this table were F_1 progeny of Monterey × Woods Hole crosses. The nomenclature used to identify them is: [maternal colony × paternal colony] − individual progeny identification number.

[c] The progeny on a given line in the table were released from the indicated colony when it was the egg donor (maternal colony) and the other colony of that pair was, therefore, the sperm donor.

[d] These are minimum numbers, because not all progeny that were released were collected and observed. The numbers in parentheses designate the minimum number of progeny, among those observed, that definitely showed the intersiphonal double band.

one *Botrylloides*, are commonly found in Monterey Bay. From observations of its morphology and manner of sexual reproduction, we concluded that the latter is *Botrylloides violaceus* Oka 1927 described from Japan (Saito *et al.*, 1981b; Saito and Watanabe, 1985). The unidentified *Botryllus* has been considered to be very similar to *Botryllus schlosseri*, a worldwide species (Berrill, 1950), but Abbott and Newberry (1980) hesitated to call it *B. schlosseri*. Here we have compared the morphology and some other biological characteristics of Monterey *Botryllus* and Woods Hole *Botryllus* (the latter considered to be *B. schlosseri*) in detail, and examined their colony specificity. In addition, we have set up crosses between colonies from these two populations.

As shown in Table I, the morphological characteristics of individuals from both Monterey and Woods Hole populations throughout their life cycles were very similar, except for coloration. Colonies of Monterey *Botryllus* were generally orange, red-brown, or blue, whereas Woods Hole colonies have many color variations, and many colonies have intersiphonal pigment bands. However, differences in colony color or pigmentation markers usually are not of much taxonomic significance in ascidians (Van Name, 1945). In colonies from both populations, blastozooids are arranged into oval or star-shaped systems; this characteristic is seen in *B. schlosseri*, *B. tuberatus*, *Botryllus primigenus* Oka 1928, and *Botryllus communis* Oka 1927.

The number of longitudinal vessels on each side of the branchial sac increases from one to three during the first several blastogenic generations in colonies from both populations. This fact has never been reported in either *B. schlosseri* or other botryllid ascidians, but if detailed observations are carried out in other botryllids the same increase will be found in many of them (pers. obs.). The second stigmatal row never reaches the dorso-median line in either Monterey or Woods Hole *Botryllus*, and this characteristic has already been reported in Japanese *Botryllus* and *Botrylloides* (Tokioka, 1953; Saito *et al.*, 1981a, b; Saito and Watanabe, 1985). This seems to be a common characteristic in botryllids with more than five stigmatal rows. There are some minor differences between Monterey and Woods Hole *Botryllus:* colony thickness, blastozooid length, and numbers of branchial tentacles, of stigmatal rows, and of stomach plications. However, these are differences that plausibly fall within the range of normal intraspecies variation between widely separated populations.

In addition to morphological similarity, members of a species can interbreed to produce fertile offspring (Friday and Ingram, 1985). We developed controlled culture conditions for raising Monterey *Botryllus* colonies from larval release to sexual maturity in the laboratory (Boyd *et al.*, 1986), and these conditions were also suitable for maintaining Woods Hole colonies. Successful laboratory culturing, along with the fact that *Botryllus* colonies reach sexual maturity within a few months and subsequently can breed frequently, permitted us to answer directly whether crosses yield fertile F_1 offspring. As indicated by our data (Tables II, III), Monterey and Woods Hole colonies can interbreed to produce fertile F_1 progeny. The second cross in Table III provides definitive evidence that *cross*-fertilization occurred with the [Monterey $\times$ Woods Hole] F_1 colony. The results of the defined crosses indicate that Monterey and Woods Hole *Botryllus* colonies belong to the same species.

The manner of allorejection in colony specificity has generally been considered to be consistent between colonies of the same species of botryllid (Taneda *et al.*, 1985). However, allorejection between Monterey colonies was distinctly different from that between Woods Hole colonies. Moreover, in interpopulation pairs, only the Woods Hole colony consistently exhibited a rejection reaction. That fusion was not observed between Monterey and Woods Hole colonies in this study is probably related to the frequency and distribution of alleles at the fusibility locus within the two *Botryllus* populations, such that none of the interpopulation pairs happened to include colonies that shared an allele at this locus. Based on the similarity of their morphology and the production of fertile F_1 progeny, it is best to consider that they belong to the same species, although they may be divergent with respect to the allorecognition process. Even though allorejection has never been used as a taxonomic characteristic, this reaction could prove useful for future studies of botryllid taxonomy.

Monterey and Woods Hole *Botryllus* appear to be in the same species, but the question remains whether they are *B. schlosseri*. Although *B. schlosseri* has been called a worldwide species (Van Name, 1945), there seem to be some inconsistencies among reports about this species and our data on Monterey and Woods Hole *Botryllus*. (1) According to Colombera (1969), the haploid number of chromosomes in Italian colonies is 16, whereas it has been reported to be 7 or 8 in Woods Hole colonies (Milkman and Therrien, 1965). (2) In the description by Berrill (1950), an oozooid has eight to nine protostigmata on the right side and six to seven on the left side. However, in Monterey and Woods Hole populations an oozooid usually has four protostigmata on each side. (3) In the same description by Berrill, an oozooid produces one pallial bud of the first blastogenic generation on each side of the body, but in Monterey, Woods Hole, and Italian populations, an oozooid produces a single bud only on the right side of the body (for Italy, see Brunetti and Burighel, 1969; Sabbadin, 1969, 1979). (4) The diameter of mature eggs is about 450 μm in Berrill's (1950) description and 410–430 μm in Korean colonies (Rho, 1971). In

Monterey and Woods Hole colonies, and in some other descriptions (Ärnbäck, 1923; Van Name, 1945; Brewin, 1946), the diameter is 220–265 μm. (5) There is much variation in the eventual number of stigmatal rows, from 6 to 15, among descriptions of *B. schlosseri* (Savigny, 1816; Verrill, 1871; Alder and Hancock, 1912; Michaelsen, 1921; Hartmeyer, 1923; Van Name, 1945; Brewin, 1946; Berrill, 1950; Tokioka, 1953, 1967; Rho, 1971; Kott, 1972; Kott and Goodbody, 1980; Millar, 1982; Ger and Zan, 1983).

These inconsistencies in the basic characteristics of botryllid ascidians suggest that more than two species are currently classified as *B. schlosseri*. In order to clarify this problem, colonies from populations around the world must be used (1) in studies of colony specificity and (2) of zooid morphology throughout the life cycle and (3) for defined crosses to determine whether fertile F_1 progeny can be produced. This taxonomic study would be very important for the several fields of biology using this species for experimental and ecological investigations. In the meantime, researchers should be cautious about applying information and conclusions from experiments on one *Botryllus* population to colonies belonging to other populations. Our present understanding of the taxonomy and genetics of *B. schlosseri* leads us to designate Monterey and Woods Hole colonies as conspecific, but it is premature to definitively call that species *Botryllus schlosseri*. Normally that identification must await comparison of Monterey or Woods Hole specimens with the type-specimen that actually carries the taxon's name—a task that has not yet been undertaken. If that is not feasible, other studies comparable to this one can, at least, ascertain whether the Monterey-Woods Hole taxon is conspecific with populations from *B. schlosseri*'s European type-location (Falmouth, England), and then with other important European populations (*e.g.*, Venice). In fact, this sort of extended comparison would be even preferable, because it permits the live animal breeding experiments that would not be possible in an analysis solely dependent on type-specimens.

Acknowledgments

We acknowledge the excellent technical help of Katherine Ishizuka. We thank John Valois of the Marine Resources Department at the Marine Biological Laboratory (Woods Hole, Massachusetts) for assistance with collection and shipment of *Botryllus* colonies, and Dr. Stephen K. Brown for his critical review of the manuscript. We are especially grateful for the helpful editorial review by Dr. Todd Newberry. Support for this investigation was provided by NIH grant #5R01CA42551 and California Division American Cancer Society Junior Fellowships #J-7-84 (H.C.B.) and #J-46-86 (Y.S.).

Literature Cited

Abbott, D. P., and A. T. Newberry. 1980. Urochordata: the tunicates. Pp. 177–226 in *Intertidal Invertebrates of California.* Stanford University Press, Stanford, California.

Alder, J., and A. Hancock. 1912. *The British Tunicata,* Vol. 3. Ray Society, London.

Ärnbäck-Christie-Linde, A. 1923. Northern and arctic invertebrates in the collection of the Swedish State Museum. *Kungl. Svenska Vet. Acad. Handl.* 63, no. **9:** 1–25.

Bancroft, F. W. 1903. Variation and fusion of colonies in compound ascidians. *Proc. Calif. Acad. Sci.* **3:** 137–186.

Berrill, N. J. 1950. *The Tunicata.* The Ray Society, London.

Boyd, H. C., S. K. Brown, J. A. Harp, and I. L. Weissman. 1986. Growth and sexual maturation of laboratory-cultured Monterey *Botryllus schlosseri. Biol. Bull.* **170:** 91–109.

Brewin, B. I. 1946. Ascidians in the vicinity of the Portobello Marine Biological Station, Otago Harbour. *Trans. R. Soc. N. Z.* **76:** 87–131.

Brunetti, R., and P. Burighel. 1969. Sviluppo dell'apparato vascolare coloniale in *Botryllus schlosseri* (Pallas). *Publ. Staz. Zool. Napoli* **37:** 137–148.

Colombera, D. 1969. The karyology of the colonial ascidian *Botryllus schlosseri* (Pallas). *Caryologia* **22:** 339–349.

Fay, R. C., and J. V. Johnson. 1971. Observations on the distribution and ecology of the littoral ascidians of the mainland coast of southern California. *Bull. So. Cal. Acad. Sci.* **70:** 114–124.

Fay, R. C., and J. A. Vallee. 1979. A survey of the littoral and sublittoral ascidians of southern California, including the Channel Islands. *Bull. So. Cal. Acad. Sci.* **78:** 122–135.

Friday, A., and D. S. Ingram (eds.). 1985. *The Cambridge Encyclopedia of Life Sciences.* Cambridge University Press, New York.

Ger, G., and Y. Zan. 1983. Ascidians of Jiaozou Bay. I. Botryllidae. *J. Shandong Coll. Oceanol.* **13:** 93–100.

Grosberg, R. K. 1981. Competitive ability influences habitat choice in marine invertebrates. *Nature* **290:** 700–702.

Grosberg, R. K., and J. F. Quinn. 1986. Genetic control and consequences of kin recognition by the larvae of a colonial marine invertebrate. *Nature* **322:** 456–459.

Kott, P. 1972. The ascidians of South Australia. I. *Trans. R. Soc. South Australia* **96:** 1–52.

Kott, P., and I. Goodbody. 1980. The ascidians of Hong Kong. *Proceeding of the First International Marine Biological Workshop: The Flora and Fauna of Hong Kong and Southern China.* Hong Kong University Press, Hong Kong.

Hartmeyer, R. 1923. Ascidiacea. *Danish Ingolf Expedition.* Copenhagen, vol. **2,** part 6: 344–361.

Mackie, G. O., and C. L. Singla. 1983. Coordination of compound ascidians by epithelial conduction in the colonial blood vessels. *Biol. Bull.* **165:** 209–220.

Michaelsen, W. 1921. Die Botrylliden und Didemniden der Nordsee und der zur Ostsee fuhrenden Meeresgebiete. *Wiss. Meeresunters.,* Abt. Helgoland, new ser., vol. **14:** 108–112.

Milkman, R. 1967. Genetic and developmental studies on *Botryllus schlosseri. Biol. Bull.* **132:** 229–243.

Milkman, R., and E. Therrien. 1965. Developmental and genetic studies on the compound ascidian, *Botryllus schlosseri. Biol. Bull.* **129:** 417.

Millar, R. H. 1982. The Marine fauna of New Zealand: Ascidiacea. *N. Z. Oceanogr. Inst. Mem.* **85:** 5–117.

Oka, A. 1927. Zur Kenntniss der japanischen *Botryllidae* (Vorlaufige Mitteilung). *Proc. Imp. Acad.* **3:** 607–609.

Oka, A. 1928. Ueber eine merkwürdige *Botryllus*—Art, *B. primigenus* nov. sp. *Proc. Imp. Acad* **4:** 303–305.

Oka, H., and H. Watanabe. 1957. Colony-specificity in compound

ascidians as tested by fusion experiments (a preliminary report). *Proc. Jpn. Acad.* **33:** 657–659.

Pallas, P. S. 1766. Elenchus zoophytorum. Frankfort, p. 355.

Ritter, W. E., and R. A. Forsyth. 1917. Ascidians of the littoral zone of southern California. *Univ. Calif. Publ. Zool.* **16:** 439–412.

Rho, B. J. 1971. A study on the classification and the distribution of the Korean ascidians. *J. Kor. Res. Inst. Bet. Liv.* **6:** 103–160.

Sabbadin, A. 1962. Bande intersifonali di pigmento purinico in *Botryllus schlosseri* (Ascideacea) e loro determinazione genetica. *Boll. Zool.* **29:** 721–726.

Sabbadin, A. 1969. The compound ascidian *Botryllus schlosseri* in the field and in the laboratory. *Pubbl. Staz. Zool. Napoli* **37:** 62–72.

Sabbadin, A. 1977. Linkage between two loci controlling colour polymorphism in the colonial ascidian, *Botryllus schlosseri*. *Experientia* **33:** 876–877.

Sabbadin, A. 1979. Colonial structure and genetic patterns in ascidians. Pp. 433–444 in *Biology and Systematics of Colonial Organisms*, G. Larwood and B. R. Rosen, eds. Academic Press, London and New York.

Sabbadin, A., and G. Graziani. 1967. New data on the inheritance of pigments and pigmentation patterns in the colonial ascidian *Botryllus schlosseri* (Pallas). *Riv. Biol.* **60:** 559–598.

Saito, Y., H. Mukai, and H. Watanabe. 1981a. Studies on Japanese compound styelid ascidians. I. Two new species of *Botryllus* from the vicinity of Shimoda. *Publ. Seto Mar. Biol. Lab.* **26:** 347–355.

Saito, Y., H. Mukai, and H. Watanabe. 1981b. Studies on Japanese compound styelid ascidians. II. A new species of the genus *Botryloides* and redescription of *B. violaceus* Oka. *Publ. Seto Mar. Biol. Lab.* **26:** 357–368.

Saito, Y., and H. Watanabe. 1982. Colony specificity in the compound ascidian, *Botryllus scalaris*. *Proc. Jpn. Acad.* **58:** 105–108.

Saito, Y., and H. Watanabe. 1985. Studies on Japanese compound styelid ascidians. IV. Three new species of the genus *Botryloides* from the vicinity of Shimoda. *Publ. Seto Mar. Biol. Lab.* **30:** 227–240.

Savigny, J. C. 1816. *Memoires sur les Animaux Sans Vertebres*. Paris, part 2.

Schlumpberger, J. M., I. L. Weissman, and V. L. Scofield. 1984. Monoclonal antibodies developed against *Botryllus* blood cell antigens bind to cells of distinct lineages during embryonic development. *J. Exp. Zool.* **229:** 205–213.

Scofield, V. L., and L. Nagashima. 1983. Morphology and genetics of rejection reactions between oozooids from the tunicate *Botryllus schlosseri*. *Biol. Bull.* **165:** 733–744.

Scofield, V. L., J. M. Schlumpberger, L. A. West, and I. L. Weissman. 1982. Protochordate allorecognition is controlled by a MHC-like gene system. *Nature* **295:** 499–502.

Taneda, Y., Y. Saito, and H. Watanabe. 1985. Self or non-self discrimination in ascidians. *Zool. Sci.* **2:** 433–442.

Taneda, Y., and H. Watanabe. 1982. Studies on colony specificity in the compound ascidian, *Botryllus primigenus* Oka. II. *In vivo* bioassay for analyzing the mechanisms of "nonfusion" reaction. *Dev. Comp. Immunol.* **6:** 243–252.

Tokioka, T. 1953. *Ascidians of Sagami Bay*. Iwanami-shoten, Tokyo.

Tokioka, T. 1967. Contributions to Japanese ascidian fauna. XXII. Ascidians from Sado Island. *Publ. Seto Mar. Biol. Lab.* **15:** 239–244.

Van Name, W. G. 1945. The North and South American ascidians. *Bull. Am. Mus. Nat. Hist.* **84:** 219–230.

Verrill, A. E. 1871. Descriptions of some imperfectly known and new ascidians from New England. *Am. J. Sci.* (ser. 3) **1:** 211–212.

Watterson, R. L. 1945. Asexual reproduction in the colonial tunicate, *Botryllus schlosseri* (Pallas) Savigny, with special reference to the developmental history of intersiphonal bands of pigment cells. *Biol. Bull.* **88:** 71–103.

Reference: *Biol. Bull.* **178:** 251–259. (June, 1990)

Behavioral and Metabolic Responses to Emersion and Subsequent Reimmersion in the Freshwater Bivalve, *Corbicula fluminea*

ROGER A. BYRNE[1], ERICH GNAIGER[2], ROBERT F. McMAHON*, AND THOMAS H. DIETZ

*Department of Zoology and Physiology, Louisiana State University, Baton Rouge, Louisiana 70803, and *Section of Comparative Physiology, Department of Biology, The University of Texas at Arlington, Arlington, Texas, 76019*

Abstract. When exposed to air, the freshwater bivalve, *Corbicula fluminea,* displayed valve movement behaviors, such as mantle edge exposure, wider gaping "ventilatory" response, and an escape or "burrowing" response. The proportion of the emersion period spent in these behaviors, relative to valve closure, increased with decreasing temperature. Emersion at 35°C inhibited valve movement behaviors, whereas emersion in a nitrogen atmosphere stimulated ventilatory activity. High rates of aerial oxygen uptake ($\dot{M}_{O_2}$) were associated with initial valve opening and ventilatory behaviors, and lower $\dot{M}_{O_2}$ occurred during bouts of mantle edge exposure. Heart rate was affected by temperature, but not by mantle edge exposure. Heart rate increased during burrowing and ventilatory behaviors suggesting a hydraulic function for hemolymph. Emersed *C. fluminea* had short bursts of heat production followed by longer periods of lower heat flux when measured by direct calorimetry. The mean heat production rate was 1.11 mW (g dry tissue)$^{-1}$, significantly higher than the mean value for clams exposed in a nitrogen atmosphere, 0.50 mW (g dry tissue)$^{-1}$. On reimmersion, *C. fluminea* showed no significant "oxygen debt" until after three days aerial exposure. The bursts of activity, while emersed, may be the result of periodic renewal of oxygen stores followed by immediate oxygen use.

Received 3 November 1989; accepted 20 February 1990.

[1] Present address: Department of Biosciences, University of Calgary, Calgary, Alberta, Canada T2N 1N4.

[2] Present address: Institut Zoophysiologie, Universität Innsbruck, A-6020 Innsbruck, Austria.

Abbreviations: $\dot{M}_{O_2}$—oxygen consumption rate; f_h—heart beat frequency; TW—tapwater; $_t\dot{q}$—weight-specific heat flux.

Introduction

Aerial exposure of marine intertidal bivalves results in a variety of behavioral and metabolic responses (McMahon, 1988; Shick *et al.,* 1988). In general, bivalves inhabiting the shore will either close their valves while emersed and undergo anaerobic metabolism (especially lower shore species such as *Mytilus edulis, Cerastoderma glaucum,* Boyden, 1972a; Widdows *et al.,* 1979), or their valves will periodically gape allowing the maintenance of an aerobic metabolism (predominantly higher shore species, *Cerastoderma edule, Geukensia demissa,* Boyden, 1972a; Widdows *et al.,* 1979).

The intertidal environment is characterized by emersion periods that are predictable and of short duration. In contrast, bivalves inhabiting the shallow regions of freshwater lotic and lentic environments are subject to periods of emersion that are highly unpredictable in their duration, timing, and temperature. Freshwater bivalves can withstand periods of aerial exposure ranging from a few days to months, and will consume oxygen while in air (Dietz, 1974; McMahon and Williams, 1984). To survive such prolonged emergence, bivalves must balance two opposing requirements: to maintain contact with the atmosphere for gas exchange, while minimizing evaporative loss of water.

The Asian freshwater clam, *Corbicula fluminea* (Müller), is commonly found in shallow lakes and streams throughout the United States (McMahon,

1982). A recent invader of freshwater, *C. fluminea* has higher tolerances to emersion than its estuarine relatives, but a relatively low tolerance among other freshwater bivalves (McMahon, 1979; Byrne *et al.*, 1988). It displays several behavior patterns when aerially emersed, such as mantle edge exposure and valve gaping, which are associated with aerial oxygen uptake (McMahon, 1979, 1983; McMahon and Williams, 1984).

In this study, we examined the effects of temperature and hypoxia on the behavioral responses of *C. fluminea* to emersion. Exposure of emersed clams to a N_2 atmosphere allowed us to discriminate between responses to aerial exposure and hypoxia. We examined metabolic responses, including heart rate, aerial oxygen uptake, and heat flux on emersed clams. In addition, the responses to reimmersion after varying periods of aerial exposure were observed.

Materials and Methods

Animals

Specimens of *C. fluminea* were collected, either from the Clear Fork of the Trinity River at its outflow from Lake Benbrook, Tarrant Co., Texas, or from the littoral region of the south shore of Toledo Bend Reservoir on the Texas-Louisiana border. Specimens were maintained, unfed, in aquaria containing either aged tapwater (TW) or artificial pondwater (Dietz and Branton, 1975) at 22–24°C for at least one week prior to use. The animals ranged in size from 19 to 43 mm shell length; 3.8 to 21 g total wet weight; and 0.15 to 0.79 g dry tissue mass. Dry tissue mass was about 8% of total wet body mass, but varies with season (Williams and McMahon, 1989).

Behavioral measurements

The effects of temperature on valve movements of aerially exposed specimens of *C. fluminea* were determined on 5 clams at each of 3 temperatures, 15, 25, and 35°C. In addition, the effects of exposure to a severely hypoxic (N_2) atmosphere ($P_{O_2} \approx 1$ torr) were examined. Measurement of valve movements was made by gluing a monofilament line to a point 1–2 mm from the leading edge of a valve. The opposite valve was attached to a syracuse dish by gently embedding the bivalve, on its side, in modeling clay. The syracuse dish with its attached bivalve was placed inside a 45-ml glass jacketed chamber sealed by a rubber stopper. About 1 ml of distilled water was added to the chamber to maintain relative humidity near saturation. The line was threaded through an 18-gauge hypodermic needle passing through the rubber stopper and was attached tautly to the lever of a displacement transducer. The amplified output was directed to a strip chart recorder. The lever was counterweighted so that little force was exerted on the line attached to the valve, and the line was coated with silicone grease to provide a gas seal but to also allow movement. Temperature inside the chamber was maintained at 15, 25, or 35 $\pm$ 0.1°C by means of a circulating water bath connected to the glass jacket of the respiration chamber. A period of temperature equilibration (30–60 min) was allowed before recording. Depending on the treatment temperature, experiments continued for 24–150 h. The major categories of valve movement behavior were identified by simultaneous observation of behaviors and the tracings.

A hypoxic atmosphere was achieved by flushing the chamber with N_2 gas at a high rate (300 ml/min) for the first 10 min, and at 50–75 ml/min during the experiment. The gas was appropriately temperature equilibrated and humidified before being introduced into the chamber. The P_{O_2} in these chambers was not routinely measured but we have recorded about 1 torr after the 10-min flushing period.

Heart rate

The heart rate of aerially exposed clams was measured simultaneously with valve movements under the three temperature treatments. Measurement of heart beat rate (f_h) was accomplished by a modification of the method of Dietz and Tomkins (1980), a non-invasive technique that records the shadow of the beating heart by means of a photocell attached to the outside of the shell. The photocell (silicon selenium; 5 $\times$ 5 mm) was positioned over the heart and affixed by a small piece of modeling clay or glue to the valve. The clam was prepared for valve movement recording, as described above, and the leads from the photocell were threaded through a hole bored in the stopper and then sealed with rubber cement. The photocell current output was amplified with a Keithly microammeter (100 nA full scale), and was input to an amplifier/chart recorder. Light from a fiber optic lamp was directed through the clam from outside the chamber and adjusted above ambient illumination until the recorder deflection, caused by the movement of the heart, was maximized. Only when the clam was performing burrowing behaviors, were the tracings difficult to interpret.

Aerial oxygen consumption

Aerial oxygen consumption rates (at 25°C) of clams exposed under normoxic conditions, and of clams after an exposure to hypoxic environments, were recorded. The aerial oxygen consumption rate ($\dot{M}_{O_2}$) was measured by the method of McMahon and Williams (1984). Moreover, valve movements and f_h were recorded simultaneously. Clams were prepared for valve movement and

f_h recording as outlined above. Specimens were scrubbed to remove organisms adhering to the shell that might interfere with $\dot{M}_{O_2}$ determinations. A polarographic oxygen sensor (Yellow Springs) was inserted through the rubber stopper sealing the chamber so that its tip was positioned approximately halfway into the chamber. Other openings drilled through the rubber stopper for leads were sealed. After a 30-min equilibration period, simultaneous recordings were made of valve movement, f_h, and P_{O_2}. Reliable determination of $\dot{M}_{O_2}$ could only be made over a period of <24 h as the sensor fluid would need to be replaced. Although $\dot{M}_{O_2}$ measurements were attempted on fifteen specimens, only recordings of individuals displaying valve movements were used in the analyses. $\dot{M}_{O_2}$ was calculated from the decline in percent oxygen saturation and expressed as μmol (g dry tissue · h)$^{-1}$. Sensor drift was measured in an empty chamber and corrections applied to the $\dot{M}_{O_2}$ calculations.

Direct calorimetry

Metabolic heat production by clams exposed in air or nitrogen gas was determined. The heat flux (mW) by emersed clams was measured by direct calorimetry, over periods of 24 to 168 h, with the LKB ThermoMetric 2277 Thermal Activity Monitor microcalorimeter (Suurkuusk and Wadsö, 1982; Gnaiger, 1983; Gnaiger *et al.*, 1989). Small clams (shell length 1.9–2.3 cm) were glued to a specially molded plastic platform (10 × 10 × 10 mm). This platform was designed to present the clam lying on its side in the metabolic chamber (the orientation used previously), while suspending the clam above a 1-ml reservoir of distilled water placed in the chamber to maintain relative humidity near saturation. A 25-cm^3 metabolic chamber was used in all experiments. Rates of heat dissipation were recorded by subtracting the output of a blank chamber (4 ml distilled water, the approximate thermal equivalent mass of the contents of the experimental chamber) from that of the experimental chamber, and recording the result on a strip-chart recorder. As the time-response curve of this larger chamber was not instantaneous, but approximates a first order exponential function (Gnaiger, 1983), the rates of heat dissipation derived from the experiments were averaged over 10-min periods and corrected to give instantaneous heat flux readings.

Heat production of the control chamber (4 ml distilled water replacing the clam) was determined after every two experiments, and an instrument calibration was performed every four experiments, or at least once a week. To determine the effects of emersion in a nitrogen atmosphere, the chamber was flushed for 30 min with humidified N_2 carried in capillary tubing incorporated into the cap of the metabolic chamber containing the experimental animal.

Aquatic $\dot{M}_{O_2}$ on reimmersion

One hundred specimens of *C. fluminea*, individually marked and weighed (±0.0001 g), were aerially exposed in desiccators above a layer of water maintaining relative humidity at near saturation, at 25°C. Five individuals, picked at random, were removed after 1, 2, 3, 5, and 6 days of emersion and used to determine the aquatic $\dot{M}_{O_2}$ upon reimmersion. These clams were immersed in dechlorinated, aged tapwater, and allowed to open their valves and commence siphoning activity for 5 min. The immediate $\dot{M}_{O_2}$ was determined by placing the clams individually into a sealed, temperature controlled respiration chamber (65 ml volume; 25 ± 0.1°C) filled with aerated TW. The clam was supported on a nylon mesh platform above a magnetic stirbar. The decline in chamber dissolved oxygen was measured with a pre-equilibrated oxygen sensor (Yellow Springs) connected to a strip-chart recorder. Rates of oxygen consumption were determined on the basis of the first 10% decline in air saturation, which was usually accomplished in 5–10 min after the method of McMahon and Russell-Hunter (1977). The clams then were returned to aerated TW, and the aquatic $\dot{M}_{O_2}$ remeasured after a total reimmersion period of 1 h to detect any temporal changes in respiratory responses of reimmersed individuals.

Data analysis

Data are expressed as mean ± SEM, and n = the number of animals. Differences were considered significant at $P < 0.05$ with Student's *t*-test, or a one-way ANOVA followed by Duncan's Multiple Range tests.

Results

Behavioral responses to emersion

On emersion, specimens of *C. fluminea* displayed four categories of behavior (Fig. 1). The first was the closed condition with valves clamped shut and no tissues exposed to the environment. The second condition was mantle edge exposure with the valves parted slightly (1–2 mm) and portions of the leading edge of the mantle exposed along the complete extent of the gape. The mantle edges were moist or fused with a hardened mucus over the surface, and no opening into the mantle cavity was evident. On many occasions, the mantle was extended over the edge of the valves, exposing more mantle tissue.

The other two behavioral categories of valve movement on emersion were less common (Fig. 1). After a period of mantle edge exposure, the valves and mantle would part further, forming an opening into the mantle cavity. This position would be maintained for a few minutes followed by rapid valve closure; the opening and closing of valves could continue for some minutes giving

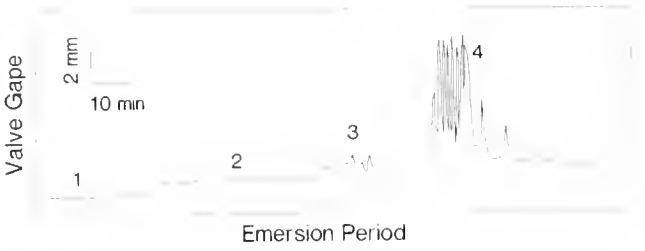

Figure 1. An amalgamation of several recordings to demonstrate the four categories of valve movement behavior in emersed *Corbicula fluminea*. 1. Valves closed. 2. Valves gaping slightly with little valve adduction, characteristic of mantle edge exposure. 3. Valves gaping wider with small medium frequency adductions, often associated with "ventilatory" movements. 4. Valves widely gaping with high frequency adductions indicative of the "escape" or "burrowing" behavior.

the appearance of a form of "ventilation" (category 3 in Fig. 1). The fourth behavior (rare) was a parting of the valves, and an extension of the foot. While the foot was extended, the valves would shut on the foot, then open, and the foot would extend further. This behavior would be repeated until the foot was extended maximally and touching the substratum. This activity resembles the "burrowing" behavior of immersed specimens of *C. fluminea*, and is interpreted as an escape behavior.

Although the patterns of behavior varied extensively between clams, the general progression of valve movement behaviors was similar for all. It began with a period of valve closure which lasted from 8.08 to 17.42 h (11.94 ± 1.98; n = 4) at 15°C, from 7.20 to 27.55 h at 25°C (15.44 ± 3.57; n = 5), and [when valve movement behavior was noted (only 3 of 10 cases)] from 0.33 to 6.52 h at 35°C (3.94 ± 1.86; n = 3). After the initial period of valve closure, bouts of mantle edge exposure were occasionally interspersed with short periods of ventilatory and, rarely, burrowing behaviors. The duration of this period was variable, but ranged from 36.16 to 203.59 h (126.31 ± 35.66; n = 4) at 15°C, from 64.78 to 93.38 h at 25°C (82.71 ± 6.19; n = 5), and 9.00 and 27.55 h at 35°C (n = 2). Following the period of valve movement, the valves remained closed to the end of the experiment, or death.

We determined the percentage of time spent by each clam in each of the behavioral categories with the times spent in ventilatory and burrowing behaviors combined. These values were averaged for each temperature treatment (Table I). An analyses of variance on the transformed values (arcsine of square root of the percentage as a proportion) showed that temperature had a significant effect on the relative time spent in the behavioral categories. The most striking was the inhibition of valve movements at 35°C: only 20% of clams exposed at 35°C displayed any valve movement behavior. Clams exposed at 15°C spent significantly ($P < 0.05$) less time closed and more time in the mantle edge exposure behavior than those clams emersed at 25°C.

Clams exposed to hypoxia in a N_2 atmosphere (25°C) after they began valve movements, spent 40.3 ± 10.1% (n = 3) of the time with mantle edges exposed, and 57.0 ± 7.6% (n = 3) in either ventilatory or burrowing behaviors. After a period of severe hypoxia, and while ventilatory movements were still occurring, the chamber was flushed with humidified air. The result was a significant change in the pattern of valve movement behavior; *i.e.*, clams exposed their mantles 84.6 ± 1.0% (n = 3) of the time and spent 12.1 ± 4.2% (n = 3) of the time in ventilatory behaviors.

Heart rate while emersed

The heart rate of *C. fluminea* was highly variable, and this was true also of emersed specimens of *C. fluminea; i.e.*, for an individual clam in one experiment, the highest values could be more than twice the lowest. Temperature had a significant effect on mean f_h (Table II) with an approximate Q_{10} of 2. As we were interested in the effects of valve movement behaviors on f_h, we determined the heart rate 5 min before the valve movement began, the rate at the onset of valve movements, and f_h at 5 min after valve movement began. Because of individual variability in f_h, the change in f_h was expressed as the fractional change relative to the f_h during the first 5 min of the valve movement (Table III). At 15 and 25°C, the occurrence of mantle edge exposure behavior (Fig. 1, category 2) resulted in no significant change in f_h. The onset of the ventilatory behaviors (Fig. 1, categories 3 and 4) resulted in no change in f_h; however, there was a significant 35% drop in f_h 5 min after the onset of the ventilatory behavior at 15°C. At 25°C, 5 min after the onset of ventilation, f_h declined 13% (Table III). As valve move-

Table I

The effects of temperature on valve movement behaviors in emersed Corbicula fluminea

Temperature (°C)	Valves closed	Mantle edge exposed	Ventilatory and burrowing behaviors
15	29.5 ± 5.9 A	65.8 ± 5.5 A	4.7 ± 1.7 A
25	51.2 ± 4.2 B	43.5 ± 3.8 B	5.3 ± 0.9 A
35	90.5 ± 8.0 C	9.1 ± 7.7 C	0.4 ± 0.3 B

Dissimilar letters after values indicate significant differences between temperature treatments (one-way ANOVA; Duncan's Multiple Range Test; $P < 0.05$; arcsine of square root transformation). Values are the mean ± SEM percentage of the emersion period spent in each behavioral category; ventilatory and burrowing activity were combined (n = 5 for each temperature).

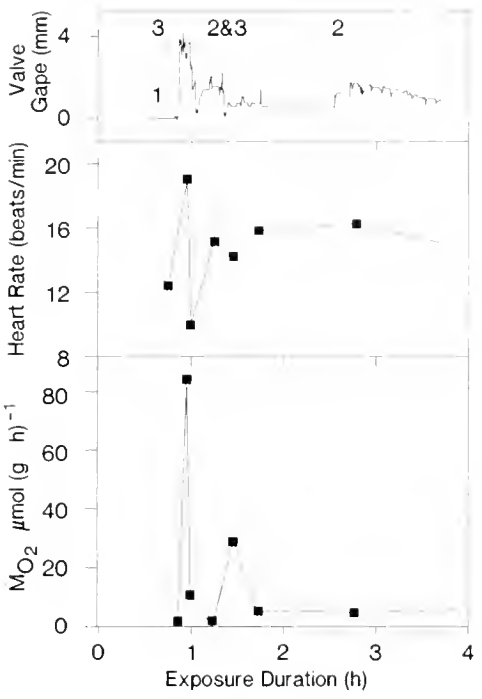

Figure 2. An example of valve movements (upper panel) with the same activity pattern notations as in Figure 1, simultaneous recordings of heart beat rate (middle panel) and aerial oxygen uptake ($\dot{M}_{O_2}$; lower panel) in emersed *Corbicula fluminea*. The initial high rate of oxygen consumption is associated with valve opening and may be the result of oxygen depleted mantle cavity air mixing with the air in the respiration chamber. Heart rate increases during major valve movements.

ment behavior was rare at 35°C, no effects on f_h were measured.

Aerial $\dot{M}_{O_2}$

Of 15 attempts to record simultaneously $\dot{M}_{O_2}$, valve movements, and f_h in aerially exposed clams, measurable $\dot{M}_{O_2}$ was recorded for only three animals. Figure 2 shows an example of O_2 uptake with the concurrent valve movement and f_h recordings. The pattern here, and in the other recordings, was an initial high rate of O_2 uptake coincident with the initial 2–3 min of valve movement, followed by a reduction in oxygen uptake during the period of mantle edge exposure. Further ventilatory movements were associated with elevated rates of oxygen depletion. Oxygen consumption during mantle edge exposure, although low, was measurably greater than when the valves were closed. Oxygen consumption rates integrated over periods of valve movement were 11.1 to 77.5 μmol O_2 (g dry tissue·h)$^{-1}$ (40.4 ± 19.6; n = 3), with most of the oxygen uptake occurring in short bouts. When the valves were shut, $\dot{M}_{O_2}$ ranged from 0 to 0.5 μmol O_2 (g dry tissue·h)$^{-1}$. When ventilatory movements were initiated, the heart rate increased briefly then declined, even though valve movements continued.

Direct calorimetry

The pattern of weight-specific heat flux ($_t\dot{q}$; mW·g^{-1}) in emersed specimens of *C. fluminea* consisted of periods of steady heat flux interspersed with short bursts of relatively high $_t\dot{q}$ (Fig. 3A; Table IV). The peak rates of heat dissipation were between 1.7 and 9 times the average "basal" aerial rate (heat flux between peaks); but the duration of these peaks was less than one hour, and clams had an average of one peak every 7.50 ± 0.89 h (n = 12) of emersion. The time of emersion (in seconds) times the average $_t\dot{q}$ calculated from the continuous recordings over the entire period of emersion [mW (g dry tissue)$^{-1}$ = mJ (g dry tissue·s)$^{-1}$] yields the total energy expenditure over the period of aerial exposure.

Clams exposed to hypoxia did not display the bursts of peak activity noted in clams exposed in normoxia (Fig. 3B). The mean $_t\dot{q}$ of nitrogen-emersed clams was not significantly different from the "basal" level of normoxic emersed clams (Table IV), but was significantly lower than the mean $_t\dot{q}$ (= average energy expenditure) of normoxic emersed clams.

Aquatic $\dot{M}_{O_2}$ on reimmersion

There was an increase in aquatic $\dot{M}_{O_2}$ related to exposure time (ANOVA F = 12.66; $P < 0.001$). However, the effects of aerial exposure were not immediate (Fig. 4). Initial rates of oxygen consumption were not significantly different from control values even after three days of aerial exposure (Duncan's Multiple Range). This suggests that the mussels were not accumulating a significant oxygen debt during three days of emersion. Initial oxygen consumption rose significantly ($P < 0.05$) from a control value of 61.7 ± 5.7 μmol (g dry tissue·h)$^{-1}$ to 135.0 ± 18.2 μmol (g dry tissue·h)$^{-1}$ after 5 days emersion (Fig. 4). $\dot{M}_{O_2}$ continued to rise to 186.1 ± 8.9 μmol (g dry tissue·h)$^{-1}$ after 6 days of exposure. There were no significant differences between initial and 1-h $\dot{M}_{O_2}$ values at any time.

Table II

Effect of temperature on frequency of heart beat (f_h; beats·min^{-1}), in emersed Corbicula fluminea

	Temperature (°C)		
	15	25	35
Heart rate	8.4 ± 0.8 (3) A	14.7 ± 1.8 (6) B	35.8 ± 6.4 (3) C
Q_{10}	1.75	2.44	

Dissimilar letters after the values indicate significant differences (one-way ANOVA; Duncan's Multiple Range; $P < 0.05$). Values for individual clams were averaged, and the grand mean ± SEM (n) for each temperature is presented.

Table III

Change in heart beat frequency (f_h, beats·min^{-1}) associated with valve movements in emersed Corbicula fluminea

	Fractional change in f_h					
	Mantle edge exposed			Ventilatory and burrowing behavior		
Temperature	n	5 min before	5 min after	n	5 min before	5 min after
15°C	5	0.11 ± 0.05	0.10 ± 0.12	10	0.19 ± 0.06	−0.35 ± 0.07*
25°C	14	−0.02 ± 0.02	0.01 ± 0.03	9	0.14 ± 0.03	−0.13 ± 0.02*

The asterisks designate values within a temperature or behavior category significantly different from one another ($P < 0.05$). Values are fractional changes in f_h (±SEM) from 5 min before the onset of the behavior, compared to the f_h at the beginning of the behavior; and the fractional change of the f_h 5 min after the behavior had commenced, compared to the f_h at the onset of the behavior. A positive value indicates an increase in f_h.

By using the oxycaloric equivalent of −450 kJ/mol O_2 (Gnaiger *et al.*, 1989), heat production can be estimated from the $\dot{M}_{O_2}$ of aquatic clams, and is approximately 27 J (g dry tissue·h)$^{-1}$ [= 7.5 mW (g dry tissue)$^{-1}$]. Converting energy flux expressed in units of J·s^{-1} (= mW) to units of J·h^{-1}, the absolute peak values of aerial heat flux were around 22 J (g dry tissue·h)$^{-1}$, or 80% of the aquatic rate. The average peak heat dissipation rate was 9.4 J (g dry tissue·h)$^{-1}$ (34% of the aquatic rate), the overall mean heat flux was 4.0 J (g dry tissue·h)$^{-1}$ (15%) and the basal rate was 2.3 J (g dry tissue·h)$^{-1}$ (9%).

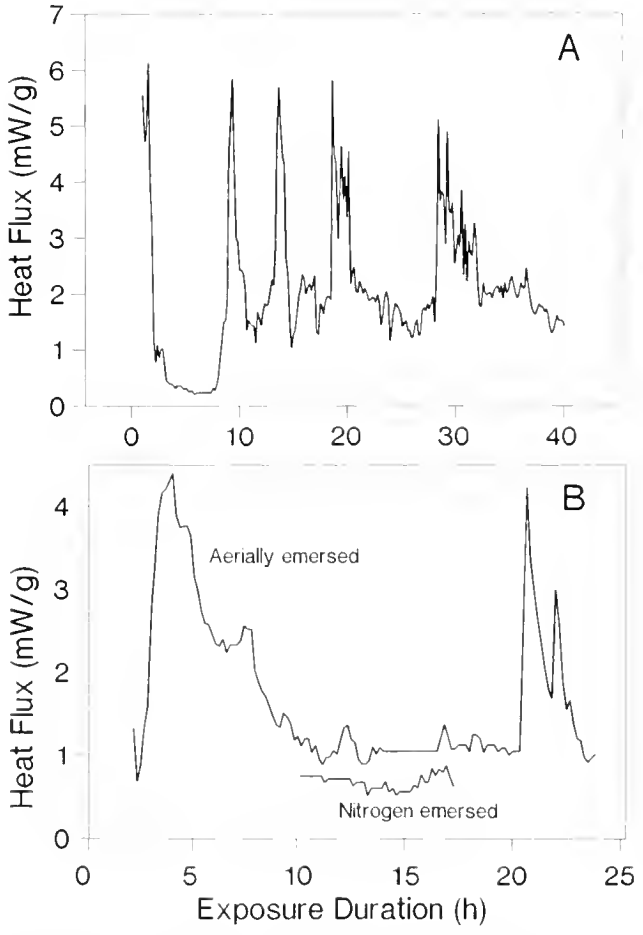

Figure 3. A. Example of the pattern of energy flux for an emersed *Corbicula fluminea* as measured by direct calorimetry. Note the bursts of higher rates of heat dissipation between periods of much lower activity. B. Part of a record of rates of heat dissipation in an emersed specimen of *C. fluminea* exposed in a normoxic and anoxic atmosphere. No burst activity was noted in nitrogen exposed clams.

Discussion

Corbicula fluminea displayed a suite of behavioral responses to emersion: mantle edge exposure; valve ventilatory behavior and burrowing response. These behavioral responses occupied a larger proportion of the total emersion period than had been estimated previously. McMahon and Williams (1984) reported a value for the proportion of time exposing mantle edge at 11.5% in *C. fluminea* emersed at 20°C. In the present study, valve

Table IV

Mean values of rates of heat dissipation (mW·g^{-1}) in emersed Corbicula fluminea

	mW·g^{-1}
Normoxic emersed	
Mean peak rate	2.55 ± 0.29 (12)*
Mean basal rate	0.65 ± 0.12 (12)
Mean heat flux	1.11 ± 0.13 (12)*
Nitrogen emersed	
Mean heat flux	0.50 ± 0.10 (3)

The asterisks indicate significant differences between mean rates of heat flux of nitrogen emersed clams and the aerially emersed bivalves ($P < 0.05$). Peak values are maximum rates sustained during bursts of activity. Mean basal values are average rates of heat dissipation measured during periods of no burst activity. Mean heat flux is the average of all values and approximates the mean energy expenditure of emersed clams. Values are expressed as the mean ± SEM and the number of animals is given in parentheses.

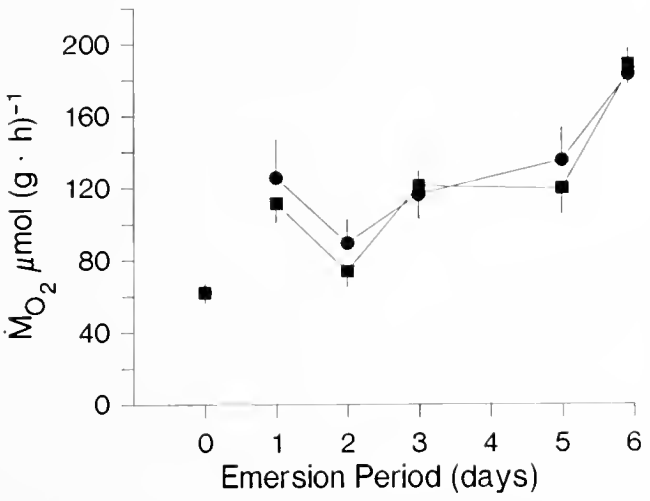

Figure 4. Rates of oxygen consumption ($\dot{M}_{O_2}$) of *Corbicula fluminea* on reimmersion after periods of aerial exposure. Circles represent initial values, within 5–15 min of the initiation of siphoning activity upon reimmersion. Squares are values measured one hour after siphoning activity commenced. The unconnected points represent corresponding initial and 1 h control $\dot{M}_{O_2}$ measurements in tapwater acclimated clams. Bars are standard errors of the means and n = 5 animals for each point.

movements in emersed clams occupied 70% and 49% of the exposure period at 15 and 25°C, respectively. A similar pattern of valve movement behaviors while emersed has been reported for the high estuarine mangrove corbiculid, *Polymesoda erosa*. In *P. erosa*, ventilation of the mantle cavity air space occurred at irregular intervals, interspersed with periods of mantle edge exposure and valve closure (McMahon, 1988).

These behaviors in *C. fluminea* seem to be associated with aerial oxygen uptake (this study; McMahon and Williams, 1984). However, the highest rates of aerial oxygen consumption took place during the first few minutes of valve opening in what was referred to as ventilatory behavior, with lower rates during mantle edge exposure. This is consistent with the hypothesis of a periodically renewed, mantle cavity oxygen store (McMahon and Williams, 1984; Pamatmat, 1984). When the valves first open, the oxygen depleted mantle cavity gas mixes with the air, causing a sudden decline in atmospheric P_{O_2} in the respiration chamber.

Aerial oxygen uptake has been reported for several freshwater bivalves. The unionid clam, *Ligumia subrostrata* was reported to have aerial oxygen uptake rates of between 21–23% of the aquatic rate (Dietz, 1974), and the sphaeriid, *Sphaerium occidentale*, have similar rates of aerial oxygen uptake (Collins, 1967). Heming and coworkers (1988) reported that the freshwater mussel, *Margaritifera margaritifera*, periodically gaped in air with the result that dissolved oxygen levels in the mantle fluid were maintained at approximately half those of immersed bivalves.

Among the intertidal and estuarine bivalves, Lent (1968) suggested that air-gaping in *Geukensia demissa* was an adaptation for air breathing. Non-gaping intertidal bivalves vary from having no measurable aerial O_2 uptake to oxygen consumption rates of 4–17% of the aquatic rate (Widdows *et al.*, 1979). In contrast, the gaping bivalve species have an aerial $\dot{M}_{O_2}$ similar to that in water, or have aerial rates of between 28% and 79% of the aquatic rate (Boyden, 1972a; Booth and Mangum, 1978; Widdows *et al.*, 1979). In general, higher shore bivalve species have higher rates of aerial O_2 consumption associated with valve gaping, whereas lower shore clams, emersed for short periods, tend to remain closed and consequently have lower aerial $\dot{M}_{O_2}$ (McMahon, 1988).

Emersion of *C. fluminea* in a nitrogen atmosphere seemed to stimulate a wider gape response, indicative of ventilatory activity, and the higher level of activity was diminished on return to a normoxic environment. This observation suggests that clam ventilatory behaviors have a respiratory function and may maintain some level of aerobic metabolism while emersed. In addition, a ventilatory loss of CO_2 is also clearly associated with mantle edge exposure (Byrne, 1988) as well as with O_2 uptake, as demonstrated here. The ability to dissipate metabolic CO_2 and maintenance of acid-base balance may be as important as O_2 uptake in the ability of *C. fluminea* to tolerate emersion.

Emersed *C. fluminea* also displayed bursts of heat production interspersed among periods of lower "basal" or quiescent activity. Freshwater bivalves have endogenous rhythms of activity and changes in oxygen consumption (McCorkle *et al.*, 1979). Our calorimetry chamber did not allow concurrent measurements of valve movement. However, emersed specimens of marine bivalves have valve gaping patterns associated with aerial oxygen uptake and elevated heat dissipation rates that are qualitatively similar (Pamatmat, 1984; Widdows and Shick, 1985). The bursts of heat production we observed could have been associated with valve closure or foot movements. However, the duration of valve movement is usually of short duration, but the peak $\dot{q}$ activities we measured was of greater duration making this possibility unlikely. A likely explanation is periodic ventilation and gas exchange during valve gaping episodes resulting in a short-term elevation of aerobic metabolism. Recharging spent phosphagen and ATP stores during short periods of aerobic metabolism would result in increased heat dissipation rates. After valve closure the O_2 availability would be decreasing, even if relatively quiescent, and clams would gradually become anaerobic. Before incurring a significant oxygen debt, however, another bout of valve opening and ventilation would occur. Perhaps the

gradual depression of metabolic rate is due to a decrease in body fluid pH (deZwaan 1983).

Peak values of aerial heat dissipation in *C. fluminea* approached 80% of the aquatic rate. The mean peak rate of heat dissipation was 34% and the overall mean was 15% of aquatic rates in this study. These data correspond well to the aerial O_2 consumption rate being about 20% of the aquatic rate in other freshwater bivalves (Collins, 1967; Dietz, 1974) and *C. fluminea* (McMahon and Williams, 1984). In a N_2 atmosphere, emersed *C. fluminea* did not display bursts of heat production but maintained a low level of $\dot{q}$ similar to the quiescent periods during normoxic exposure. This suggests that the observed bursts of heat flux in normoxia are the result of aerial respiration.

In most cases where bivalves gape while exposed, there is a continuation of heart beat during emersion. Changes in heart rate during emersion are variable, from essentially no change of f_h during emersion in some species, to a distinct bradycardia on emersion in other species (Boyden, 1972b; Coleman and Trueman, 1971). There appears to be no consistent direct effect of valve movement on heart beat frequency; some bivalves show occasional changes in f_h associated with valve movements and others display a suppression of heart activity (Trueman and Lowe, 1971; Coleman, 1976; Dietz and Tomkins, 1980).

Although valve gaping is associated with a respiratory function in emersed bivalves, the importance of circulating blood in the delivery of oxygen to tissues is not certain. Mussel blood typically has no oxygen carrier, and Booth and Mangum (1978) found that only 14% of O_2 in the blood of *Modiolus demissus* was delivered to tissues, leading them to conclude that the circulatory system was not important in this regard. We noted that increases in heart rate in emersed *C. fluminea* were associated mainly with ventilatory and burrowing behaviors. Foot and muscular movements are facilitated by hydraulic pressure and increases in heart rate may be associated with a redistribution of hemolymph among blood sinuses. Alternatively, when clams periodically have bursts in metabolic activity while emersed, the increased f_h may be in response to the momentary increases in perfusion requirements.

When returned to water after three days of emergence, *C. fluminea* had aquatic oxygen consumption rates that were elevated when compared to pre-emersion rates. The increased $\dot{M}_{O_2}$ was evident within 5–10 min of reimmersion and remained elevated 1 h later. Repayment of an "oxygen debt," characterized by an elevated $\dot{M}_{O_2}$, is commonly encountered in marine bivalves reimmersed after periods of aerial exposure (McMahon, 1988; Shiek *et al.*, 1988). Frequently, the size of the oxygen debt is proportional to the duration of the exposure period and is repaid during the first hour of reimmersion (Bayne *et al.*, 1976; deVooys and deZwaan, 1978; Widdows *et al.*, 1979; Widdows and Shiek, 1985). In contrast, oxygen consumption rate in resubmerged *C. fluminea* is not a direct function of exposure time and, indeed, $\dot{M}_{O_2}$ rates did not rise significantly above pre-emersion values until after three days emersion. $\dot{M}_{O_2}$ also did not decline significantly after one hour of reimmersion. Both observations suggest that the elevated $\dot{M}_{O_2}$ observed after three days of emersion was not a typical oxygen debt repayment in *C. fluminea*. Rather, over moderate periods of emersion, *C. fluminea* appears to maintain a sufficient level of aerobic metabolism to be able to avoid dependence on anaerobic metabolism. This corresponds directly with the maintenance of ventilatory and valve movements during the early stages of emergence. Elevated oxygen consumption after three days of emergence may be associated with long-term catabolic and anabolic demands resulting from the emersion stress.

Corbicula fluminea has evolved an additional suite of respiratory and behavioral adaptations, compared to *P. erosa*, an estuarine member of the family Corbiculidae (McMahon, 1988). Although valve gaping and limited emergence tolerance time are similar to high intertidal clams, the novel responses of *C. fluminea* include the exposure of mantle edges alternating with short bouts of valve gaping and ventilatory behavior. These responses would allow rapid exchange of mantle cavity gasses, yet minimize evaporative water loss. After three days of emergence, *C. fluminea* shows evidence of increased O_2 demand on reimmersion, and mortality increases. Although *C. fluminea* does not have the emersion tolerance of the more ancient families of freshwater bivalves (unionids, sphaeriids), it is a successful inhabitant of lakes and streams. Its short-term physiological mechanisms, and high reproductive capacity allow this species to be successful in the variable freshwater habitats.

Acknowledgments

The research was supported by a Sigma Xi Grant-in-aid of Research to R.A.B., the University of Texas at Arlington Research Grants to R.F.M. and NSF grant DCB 87-01504 to T.H.D. E.G. was partially supported by the LSU Department of Zoology and Physiology Visiting Scientist Program and Fonds zur Förderung der wissenschaftlichen Forschung in Österreich, project J0011. This study was part of a dissertation submitted by R.A.B. to the Graduate School of Louisiana State University and A&M College in partial fulfillment of the Ph.D. degree.

Literature Cited

Bayne, B. L., C. J. Bayne, T. C. Carefoot, and R. J. Thompson. 1976. The physiological ecology of *Mytilus californianus* Conrad

2. Adaptations to low oxygen tension and air exposure. *Oecologia (Berl.)* **22:** 229–250.

Booth, C. E., and C. P. Mangum. 1978. Oxygen uptake and transport in the lamellibranch mollusc *Modiolus demissus*. *Physiol. Zool.* **51:** 17–32.

Boyden, C. R. 1972a. Aerial respiration in the cockle *Cerastoderma edule* in relation to temperature. *Comp. Biochem. Physiol.* **43A:** 697–712.

Boyden, C. R. 1972b. The behaviour, survival and respiration of the cockles *Cerastoderma edule* and *C. glaucum* in air. *J. Mar. Biol. Assoc. U.K.* **52:** 661–680.

Byrne, R. A., R. F. McMahon, and T. H. Dietz. 1988. Temperature and relative humidity effects on aerial exposure tolerance in the freshwater bivalve, *Corbicula fluminea*. *Biol. Bull.* **175:** 253–260.

Byrne, R. A. 1988. Physiological and behavioral responses to aerial exposure in the Asian clam, *Corbicula fluminea* (Müller). Ph.D. Dissertation, Louisiana State University, Baton Rouge. 144pp.

Coleman, N. 1976. The aerial respiration of *Modiolus modiolus*. *Comp. Biochem. Physiol.* **54A:** 401–406.

Coleman, N., and E. R. Trueman. 1971. The effect of aerial exposure on the activity of the mussels *Mytilus edulis* L. and *Modiolus modiolus* (L.). *J. Exp. Mar. Biol. Ecol.* **7:** 295–304.

Collins, T. W. 1967. Oxygen-uptake, shell morphology and desiccation of the fingernail clam, *Sphaerium occidentale* Prime. Ph.D. Dissertation, University of Minnesota, Minneapolis. (*Diss. Abstr.* **28B:** 5238).

Dietz, T. H. 1974. Body fluid composition and aerial oxygen consumption in the freshwater mussel, *Ligumia subrostrata* (Say): effects of dehydration and anoxic stress. *Biol. Bull.* **147:** 560–572.

Dietz, T. H., and W. D. Branton. 1975. Ionic regulation in the freshwater mussel, *Ligumia subrostrata* (Say). *J. Comp. Physiol.* **104:** 19–26.

Dietz, T. H., and R. U. Tomkins. 1980. The effect of temperature on heart rate of the freshwater mussel, *Ligumia subrostrata*. *Comp. Biochem. Physiol.* **67A:** 269–271.

Gnaiger, E. 1983. Heat dissipation and energetic efficiency in animal anoxibiosis: economy contra power. *J. Exp. Zool.* **22:** 471–490.

Gnaiger, E., J. M. Shick, and J. Widdows. 1989. Metabolic microcalorimetry and respirometry of aquatic animals. Pp. 113–135 in *Techniques in Comparative Respiratory Physiology an Experimental Approach*, C. R. Bridges and P. J. Butler, eds. Society for Experimental Biology Seminar Series 37, Cambridge University Press.

Heming, T. A., G. A. Vinogradov, A. K. Klerman, and V. T. Komov. 1988. Acid-base regulation in the freshwater pearl mussel *Margaritifera margaritifera*: effects of emersion and low water pH. *J. Exp. Biol.* **137:** 501–511.

Lent, C. M. 1968. Air-gaping by the ribbed mussel, *Modiolus demissus* (Dillwyn): effects and adaptive significance. *Biol. Bull.* **134:** 60–73.

McCorkle, S., T. C. Shirley, and T. H. Dietz. 1979. Rhythms of activity and oxygen consumption in the common pond clam, *Ligumia subrostrata* (Say). *Can. J. Zool.* **57:** 1960–1964.

McMahon, R. F. 1979. Tolerance of aerial exposure in the Asiatic freshwater clam, *Corbicula fluminea* (Muller). Pp. 227–241 in *Proceedings, First International Corbicula Symposium*, J. C. Britton, ed. Texas Christian University Research Foundation, Fort Worth.

McMahon, R. F. 1982. The occurrence and spread of the introduced Asiatic freshwater bivalve, *Corbicula fluminea* (Müller), in North America: 1924–1982. *Nautilus* **97:** 56–58.

McMahon, R. F. 1983. Ecology of an invasive pest bivalve, *Corbicula*. Pp. 505–561 in *The Mollusca*, Vol. 6: *Ecology*, W. D. Russell-Hunter ed. Academic Press, San Diego.

McMahon, R. F. 1988. Respiratory response to periodic emergence in intertidal molluscs. *Am. Zool.* **28:** 97–114.

McMahon, R. F., and W. D. Russell-Hunter. 1977. Temperature relations of aerial and aquatic respiration in six littoral snails in relation to their vertical zonation. *Biol. Bull.* **152:** 182–198.

McMahon, R. F., and C. J. Williams. 1984. A unique respiratory adaptation to emersion in the introduced Asian freshwater clam *Corbicula fluminea* (Müller) (Lamellibranchia: Corbiculacea). *Physiol. Zool.* **57:** 274–279.

Pamatmat, M. M. 1984. Metabolic heat flow patterns in the intertidal mussel *Ischadium* (= *Modiolus* = *Geukensia*) *demissum demissum* during aerial and underwater respiration. *Int. Revue des Gesamten Hydrobiol.* **69:** 263–275.

Shick, J. M., J. Widdows, and E. Gnaiger. 1988. Calorimetric studies of behavior, metabolism and energetics of sessile intertidal animals. *Am. Zool.* **28:** 161–181.

Suurkuusk, J., and I. Wadsö. 1982. A multiple channel modular microcalorimeter. *Chim. Scripta* **20:** 155–163.

Trueman, E. R., and G. A. Lowe. 1971. The effect of temperature and littoral exposure on the heart rate of a bivalve mollusc, *Isognomon alatus*, in tropical conditions. *Comp. Biochem. Physiol.* **38A:** 555–564.

deVooys, C. G. N., and A. deZwann. 1978. The rate of oxygen consumption and ammonia excretion by *Mytilus edulis* after various periods of exposure in air. *Comp. Biochem. Physiol.* **60A:** 343–347.

Widdows, J., B. L. Bayne, D. R. Livingstone, R. I. E. Newell, and P. Donkin. 1979. Physiological and biochemical responses of bivalve molluscs to exposure to air. *Comp. Biochem. Physiol.* **62A:** 301–308.

Widdows, J., and J. M. Shick. 1985. Physiological responses of *Mytilus edulis* and *Cardium edule* to aerial exposure. *Mar. Biol.* **85:** 217–232.

Williams, C. J., and R. F. McMahon. 1989. Annual variations in tissue condition of the Asian freshwater bivalve, *Corbicula fluminea*, in terms of dry weight, ash weight, carbon and nitrogen biomass and its relationship to downstream dispersal. *Can. J. Zool.* **67:** 82–90.

deZwaan, A. 1983. Carbohydrate catabolism in bivalves. Pp. 137–175 in *The Mollusca*, Vol. 1: *Metabolic Biochemistry and Molecular Biomechanics*, P. W. Hochachka ed. Academic Press, San Diego.

Reference: *Biol. Bull.* **178:** 260–266, (June, 1990)

Potentiation of Hypoosmotic Cellular Volume Regulation in the Quahog, *Mercenaria mercenaria*, by 5-hydroxytryptamine, FMRFamide, and Phorbol Esters*

LEWIS E. DEATON

Department of Biology, University of Southwestern Louisiana, Lafayette, Louisiana 70504 and The Whitney Laboratory, University of Florida, 9505 Ocean Shore Blvd., St. Augustine, Florida 32086

Abstract. Ventricles isolated from clams (*Mercenaria mercenaria*) that had been acclimated to 1000 mOsm seawater (SW) release amino acids when incubated in 500 mOsm SW. Taurine, glycine, and alanine account for nearly all of the released amino acids, and total about 37 μmol/g dry tissue weight during a 2-h incubation. The release of amino acids is increased to 69 μmol/g by the addition of 10^{-6} *M* 5-hydroxytryptamine (5HT) to the hypoosmotic SW, and to 83 μmol/g by the addition of 10^{-6} M FMRFamide to the medium. The potentiation of the release by 5HT is blocked by methysergide. The amino acid release is increased by two phorbol esters—phorbol 12,13-diacetate and phorbol 12-acetate, 13-myristate—to 97 and 83 μmol/g, respectively. Forskolin and other cyclic 3′,5′ adenosine monophosphate agonists have no effect on the release of amino acids in hypoosmotic SW. Phorbol esters, 5HT, and FMRFamide have no effect on the release of amino acids from ventricles incubated in 1000 mOsm SW. Ventricles, first isolated from clams acclimated to 1000 mOsm SW, and then transferred to 500 mOsm SW, increase in wet weight by 20–25%. The increase is maintained for 30 min, and the tissues return their original weight in the ensuing 30 min. The addition of 5HT, FMRFamide, or phorbol esters to the hypoosmotic SW decreases the time necessary for the tissues to return to pre-transfer weights. These results implicate protein kinase C in the responses of bivalve tissues to hypoosmotic media, and suggest that these responses may be modified by neuronal or neurohumoral control.

Received 2 January 1990; accepted 19 March 1990.

* This is contribution number 291 from the Tallahassee, Sopchoppy and Gulf Coast Marine Biological Association.

Introduction

In osmoconforming marine bivalves, the restoration of cellular volume in response to changes in the ambient salinity is accomplished by the adjustment of cytoplasmic concentrations of ions and amino acids (Gilles, 1979; Pierce, 1982). The cells of these animals release amino acids when exposed to a hypoosmotic medium, thereby reducing the osmotic gradient between the medium and the cytoplasm (Pierce and Greenberg, 1972; Gainey, 1978; Amende and Pierce, 1980).

The extirpation of particular ganglia in bivalves has been reported to affect the water balance of the animals (Lubet and Pujol, 1963; Nagabushanam, 1964; Durchon, 1967). In both *Crassostrea virginica* and *Mytilus galloprovincialis*, putative neurosecretory cells lost their granular inclusions when the animals were exposed to hypoosmotic media (Lubet and Pujol, 1963; Nagabushanam, 1964). In the opisthobranch *Aplysia californica*, the electrical activity of cell R-15 in the abdominal ganglion is depressed by exposure of the whole animal to dilute seawater (Bablanian and Treistman, 1983). Ninety minutes after homogenates of R-15 were injected into an intact *A. californica*, the animal's wet weight increased by 5% (Kupfermann and Weiss, 1976). The gain in weight induced by the homogenate occurred even in a 5% hyperosmotic medium, in which the animals would be expected to lose water. Hyperpolarization of R-15 in intact animals causes large increases in the free amino acid content of the blood (Bablanian and Treistman,

1985). These observations, while far from conclusive, suggest that neurosecretory products might be involved in the regulation of osmotic balance in molluscs.

This paper describes the effects of known molluscan neurotransmitters and neurohormones on the hypoosmotic volume regulation of isolated ventricles of the clam *Mercenaria mercenaria*. In addition, the effects of cyclic 3′5′ adenosine monophosphate (c-AMP) and protein kinase C agonists on volume regulation have been investigated. The neuropeptide FMRFamide, 5-hydroxytryptamine, and phorbol esters, but not c-AMP agonists, potentiate hypoosmotic volume regulation.

Materials and Methods

Animals and media

Mercenaria mercenaria were collected from several locations in the Intracoastal Waterway in St. Johns County, Florida, or obtained from the Marine Biological Laboratory, Woods Hole, Massachusetts. The animals were maintained, unfed, in either running seawater (SW) (940–1000 mOsm), or in aerated aquaria containing natural SW (1000 mOsm). In all cases, the test media were compounded from vacuum-filtered (0.45 μm) natural SW. The 500 mOsm SW was made by dilution of filtered SW with deionized water.

Concentrated solutions of pharmaceuticals were prepared as follows: forskolin was dissolved in ethanol; phorbol, phorbol 12,13-diacetate, and phorbol 12-acetate,13-myristate were dissolved in dimethylformamide; all others were dissolved in deionized water.

The neural substances tested included the molluscan neuropeptides phenylalanyl-methionyl-arginyl-phenylalanylamide (FMRFamide), phenylalanyl-leucinyl-arginyl-phenylalanylamide (FLRFamide), para-glutamyl-aspartyl-phenylalanyl-leucinyl-arginyl-phenylalanyl-amide (pQDFLRFamide), small cardioactive peptide B (SCP_B), acetylcholine (Ach), and serotonin (5HT). The 5HT receptor blocker methysergide (UML 491) was also used. These drugs were added to either 1000 mOsm or 500 mOsm SW to obtain the desired concentration. Solvent carriers other than water were added to 1000 mOsm or 500 mOsm SW in the same amounts necessary to achieve the desired drug concentrations; such media were used to control for the effect of solvent.

Analysis of the tissue free amino acid pool

Ventricles were removed from animals that had been acclimated to 1000 mOsm SW, and lyophilized. The dried tissues were weighed and homogenized in a small volume of 80% ethanol (1 ml/5 mg dry tissue). The homogenates were centrifuged in a microcentrifuge and 20 μl of the supernatant fluid removed, evaporated to dryness in an oven (60°C), dissolved in 0.02 *N* HCl, and analyzed for amino acids with an amino acid analyzer (Hitachi 835, Na^+ citrate).

Measurement of release of amino acids

Ventricles were dissected from clams, placed in a large volume of 1000 mOsm filtered SW, and incubated for an hour. The ventricles were then placed in 2 ml of either 1000 mOsm or 500 mOsm SW. Preliminary studies of the time course of the release of amino acids from ventricles exposed to 500 mOsm SW showed that the levels of amino acid accumulated in the bath became maximal within 90–120 min. Consequently, a 2-h incubation time was chosen for subsequent experiments.

At the end of the incubation period, a 500-μl sample of the bath fluid was removed, acidified with 5 μl of 0.2 *N* HCl, and analyzed for amino acid content on an amino acid analyzer (Hitachi 835). A protein hydrolysate program was used; quantitation was provided by analyses of a standard mixture of amino acids (Pierce Chemical). Preliminary experiments showed that alanine, glycine, and taurine accounted for over 95% of the total amino acid release; the analysis program was therefore truncated to analyze only those amino acids eluting before cysteine. The amino acid levels are reported in this paper as the sum of alanine, glycine, and taurine, and are reported as μmol/g dry weight. In experiments involving the phorbol esters and the c-AMP agonists, the tissues were incubated in 1000 mOsm SW containing the desired concentration of the agent for 30 min, and were then transferred either to 1000 mOsm or 500 mOsm SW containing the same concentration of these agents.

Measurement of changes in wet weight

The ventricles were removed from clams and incubated in 1000 mOsm SW for an hour. The ventricles were blotted repeatedly on tissue paper until they left no bead of water when touched to a glass plate, and then weighed on an analytical balance (Sartorius 2463). The ventricles were then transferred to test tubes containing 2 ml of the test medium and weighed at intervals. This procedure produced repeatable weights for 3–4 weighings, but with further blotting and weighing, the tissue adhered to the blotting paper and a substantial amount (20–30% wet weight) was lost.

Statistical treatment of the data

Changes in wet weight were expressed as percentages of the original weight of the ventricle; these values were transformed by the arcsin transformation and means and standard deviations were computed. Differences in the mean changes in weight between control and treated

Table I

Amino acid content of ventricles from Mercenaria mercenaria *acclimated to 1000 mOsm seawater*

Amino acid	Content (μmol/g dry weight)
Taurine	415.8 ± 11.9
Aspartic acid	12.0 ± 4.1
Glutamic acid	32.1 ± 5.1
Glycine	27.9 ± 5.5
Alanine	30.9 ± 6.7
Arginine	8.2 ± 0.8
Others	8.0 ± 2.5
Total	534.4 ± 29.7

ventricles were assessed by Student's t test. Student's t test was also used to evaluate differences among the means of treatment groups in the dose-response experiments. The data for the release of amino acids by ventricles were analyzed by a one-way analysis of variance. Differences between treatment groups and the appropriate solvent control groups were assessed by *a priori* F tests.

Results

The amino acid content of ventricles from *Mercenaria mercenaria* is summarized in Table I. Taurine, glutamic acid, glycine, and alanine make up 95% of the total pool. Aspartate and arginine, as well as very small amounts (5 μmol/g or less) of proline, threonine, and serine also contribute to the total pool. Traces of the other neutral and basic amino acids were detected in some, but not all, tissues.

Taurine, glycine, and alanine account for about 80, 10, and 5%, respectively, of the total net loss of amino acids from isolated *Mercenaria* ventricles incubated in either 500 mOsm SW or 1000 mOsm SW. The effects of molluscan neurotransmitters and neurohormones on the release of the three amino acids from ventricles exposed to dilute medium are shown in Figure 1. Ventricles incubated in 500 mOsm SW release 37.1 μmol/g in 2 h. The addition of 10^{-6} *M* 5-hydroxytryptamine (5HT) to the dilute medium increases the net release of amino acids by 87%; the increase is significant ($F_{1,135} = 5.7$; $P < 0.05$). The molluscan neuropeptides FMRFamide, FLRFamide, and pQDFLRFamide, in concentrations of 10^{-6} *M* significantly increase the release of amino acids by 110% or more, but neither SCP_B nor acetylcholine have any effect (Fig. 1). The effect of 5HT on the amino acid release is blocked by the 5HT receptor blocker methysergide (UML); UML alone has no effect on the release of amino acids (Fig. 2).

Dose-response curves for the effects of 5HT and FMRFamide on the release of amino acids by ventricles in hypoosmotic seawater are shown in Figure 3. The difference in amino acids released between control ventricles and those exposed to 5HT and FMRFamide are significant at concentrations of 10^{-10} *M* (for 5HT, $t = 5.78$, $P < 0.001$; for FMRFamide, $t = 2.57$, $P < 0.05$) and above. Concentrations of 5-HT greater than 10^{-8} *M* elicit no further significant increase in the release of amino acids. The amino acid releases elicited by concentrations of FMRFamide from 10^{-10} to 10^{-6} *M* are not

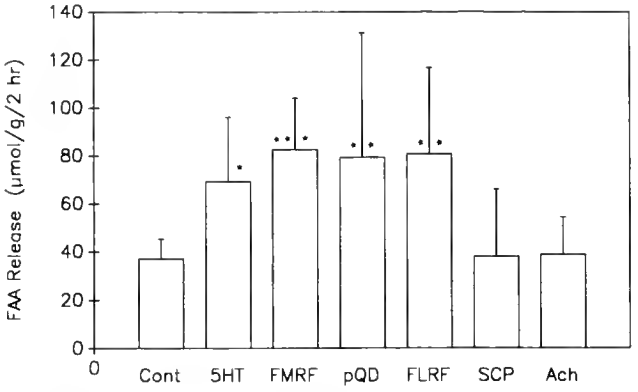

Figure 1. The effects of molluscan neural products on the release of amino acids from *Mercenaria* ventricles transferred from 1000 mOsm seawater to 500 mOsm seawater. Each bar represents the mean of 10 ventricles; error bars are 1 SD. Treatments: Cont = controls; 5HT = 5-hydroxytryptamine; FMRF = FMRFamide; FLRF = FLRFamide; pQD = pQDFLRFamide; SCP = SCP_B; Ach = acetylcholine. The concentration of each agent was 10^{-6} *M*. Each point is the mean ± SD, n = 9. Asterisks indicate treatments significantly different from controls: * = $P < 0.05$; ** = $P < 0.01$; *** = $P < 0.001$.

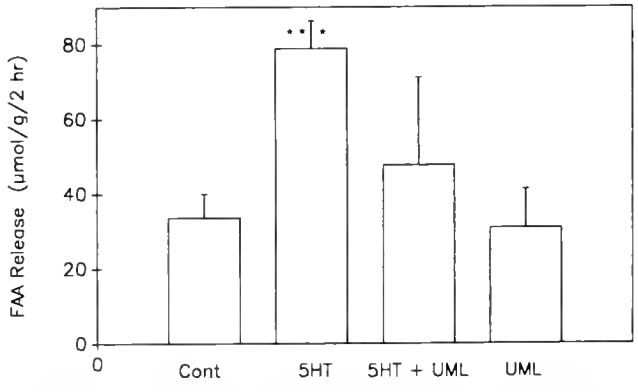

Figure 2. The effect of methysergide and 5-hydroxytryptamine on the release of amino acids from *Mercenaria* ventricles transferred from 1000 mOsm seawater to 500 mOsm seawater. Each bar represents the mean of five ventricles; error bars are 1 SD. Treatments: Cont = controls; 5HT = 5-hydroxytryptamine (10^{-6} *M*); 5HT + UML = 5-hydroxytryptamine (10^{-6} *M*) and methysergide (10^{-5} *M*); UML = methysergide (10^{-5} *M*). The asterisks indicate treatments significantly different from controls: *** = $P < 0.001$.

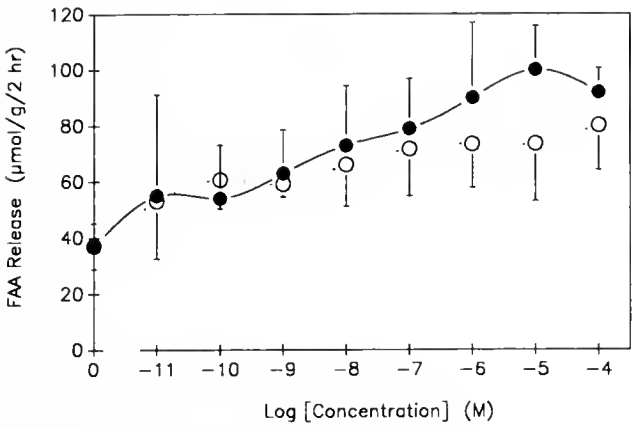

Figure 3. The effects of increasing concentrations of 5-hydroxytryptamine and FMRFamide on the release of amino acids from *Mercenaria* ventricles transferred from 1000 mOsm seawater to 500 mOsm SW. The point at zero on the abscissa represents the release from control tissues. Open circles = 5HT; solid circles = FMRFamide; Each point is a mean (n = 10 for controls, n = 4 for each treatment); the error bars indicate 1 SD.

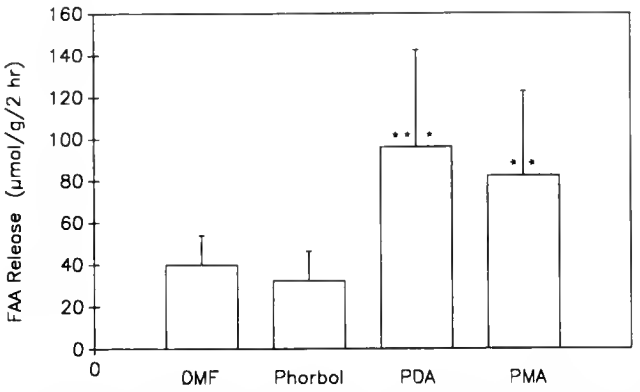

Figure 5. The effects of phorbol esters on the release of amino acids from *Mercenaria* ventricles transferred from 1000 mOsm seawater to 500 mOsm SW. Each bar represents the mean of 10 ventricles; error bars are 1 SD. Treatments: DMF = dimethylformamide (0.01%); Phorbol = 4-β-phorbol (10^{-7} *M*); PDA = phorbol 12,13-diacetate (10^{-7} *M*); PMA = phorbol 12-acetate,13-myristate (10^{-7} *M*). Asterisks indicate treatments that are significantly different from controls: * = $P < 0.05$; ** = $P < 0.01$; *** = $P < 0.001$.

significantly different, but the difference between tissues exposed to 10^{-10} and 10^{-5} *M* is significant (t = 3.22, $P < 0.01$).

The effects of several cyclic 3',5'adenosine monophosphate (cAMP) agonists on the release of amino acids in hypoosmotic seawater are shown in Figure 4. None of these agents affect the amino acid release. The cyclic guanosine monophosphate agonist 8-bromo-cyclic GMP also has no effect on the release of amino acids from ventricles in 500 mOsm SW (data not shown). In contrast, two phorbol esters potentiate the amino acid release, while 4-β phorbol has no effect (Fig. 5). The effective esters, phorbol 12,13-diacetate and phorbol 12-acetate,13-myristate, increase the release of amino acids by 140 and 106%, respectively; the comparisons were made to ventricles incubated in hypoosmotic seawater containing dimethylformamide (1.4 m*M*).

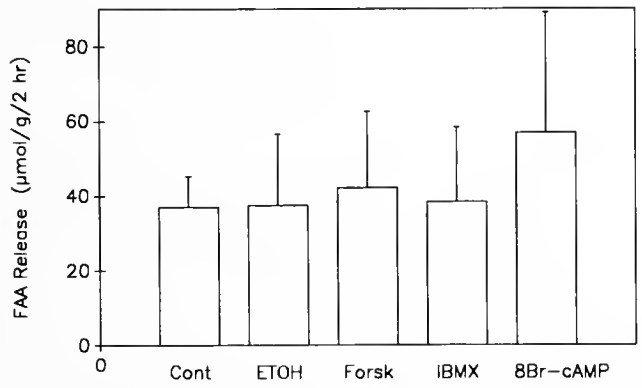

Figure 4. The effects of adenosine 3-'5'cyclic monophosphate agonists on the release of amino acids from *Mercenaria* ventricles transferred from 1000 mOsm seawater to 500 mOsm SW. Each bar represents the mean of 10 ventricles; error bars are 1 SD. Treatments: Cont = controls; ETOH = ethanol (0.1%); Forsk = forskolin (10^{-5} *M*); IBMX = 3-isobutyl-1-methylxanthine (10^{-3} *M*); 8Br-cAMP = 8-bromo-adenosine 3'-5'cyclic monophosphate (10^{-3} *M*).

The effects of 5HT, selected molluscan neuropeptides, and the phorbol esters on the release of amino acids from ventricles incubated in isosmotic seawater for 2 h are shown in Figure 6. The release of amino acids from ventricles in isosmotic SW is considerably lower than that from tissues exposed to hypoosmotic SW. None of the molluscan neural products affects the release of amino acids from tissues in isosmotic medium. The release of amino acids in the presence of phorbol esters and 4-β phorbol is not different from that of ventricles incubated in 1000 mOsm SW containing dimethylformamide (1.4 m*M*). The release of amino acids from ventricles incubated in dimethylformamide is significantly higher than that of control tissues incubated in 1000 mOsm SW.

The changes in wet weight experienced by ventricles incubated in hypoosmotic seawater containing 5HT, FMRFamide, and phorbol esters are shown in Figure 7. Ventricles transferred from 1000 mOsm SW to 500 mOsm SW gained about 20–30% in wet weight within 10 min; this gain is maintained for 30 min, and then gradually decreases to zero over the following 30 min. The addition of FMRFamide (10^{-6} *M*) to the bathing medium reduces the time required by the tissues to regulate volume (Fig. 7a). The changes in wet weight of tissues incubated in media containing FMRFamide are significantly lower than those of control tissues at both 30 (t = 10.1, $P < 0.001$) and 60 min (t = 5.69, $P < 0.001$) after transfer.

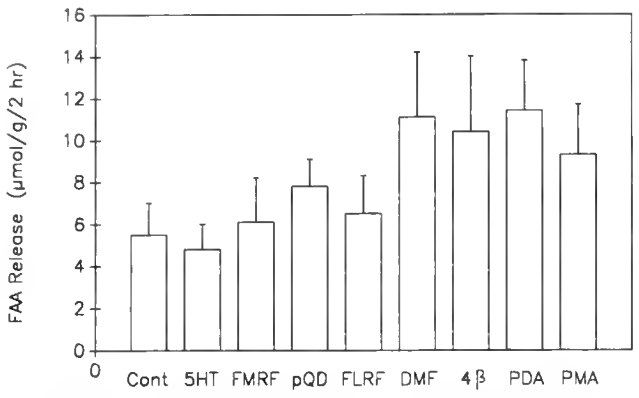

Figure 6. The effects of various agents on the release of amino acids from *Mercenaria* ventricles transferred to isosmotic seawater (1000 mOsm). Each bar represents the mean of five ventricles; error bars are 1 SD. Treatments: Cont = controls; 5HT = 5-hydroxytryptamine (10^{-6} *M*); FMRF = FMRFamide (10^{-6} *M*); pQD = pQDFLRFamide (10^{-6} *M*); FLRF = FLRFamide (10^{-6} *M*); DMF = dimethylformamide (1.4 m*M*); 4β = 4-beta-phorbol (10^{-7} *M*); PDA = phorbol 12,13-diacetate (10^{-7} *M*); PMA = phorbol 12-acetate,13-myristate (10^{-7} *M*).

The wet weights of ventricles incubated in 500 mOsm SW containing 10^{-6} *M* 5HT are lower than control tissues at 10, 30, and 60 min ($t = 9.72$; $P < 0.001$; $t = 10.7$, $P < 0.001$; $t = 3.17$, $P < 0.01$; respectively) (Figs. 7a, b). Ventricles incubated in 500 mOsm SW containing forskolin (10^{-5} *M*) gain significantly more weight than controls in the first 10 min ($t = 63.2$, $P < 0.001$), but there is no difference in wet weight gain 30 and 60 min after transfer (Figs. 7a, b).

Phorbol 12-acetate,13-myristate (10^{-7} *M*) reduces the changes in weight relative to control tissues at 10, 30, and 60 min ($t = 38.3$, $P < 0.001$; $t = 17.9$, $P < 0.001$; $t = 6.55$, $P < 0.001$, respectively) following transfer from 1000 mOsm SW to 500 mOsm SW (Fig. 7c). Tissues transferred from 1000 mOsm SW to 500 mOsm SW containing phorbol 12,13-diacetate show significantly higher ($t = 124.4$, $P < 0.001$) weight gain than control tissues 10 min after transfer, and significantly lower ($t = 7.83$, $P < 0.001$) weight gain 30 min after transfer. There is no significant difference between these tissues and controls 60 min after transfer (Figs. 7a, c).

The changes in wet weight of ventricles transferred from 1000 mOsm SW to isosmotic SW containing FMRFamide, 5HT, and phorbol esters are shown in Figure 8. There is no significant change in wet weight in control tissues following transfer, nor did any of the treatments effect significant differences in weight change relative to control tissues.

Discussion

The release of amino acids from *Mercenaria* cardiomyocytes is potentiated by 5HT and by the molluscan neuropeptide FMRFamide and its naturally occurring analogs. These agents also cause a reduction in the time required for ventricles exposed to hypoosmotic media to

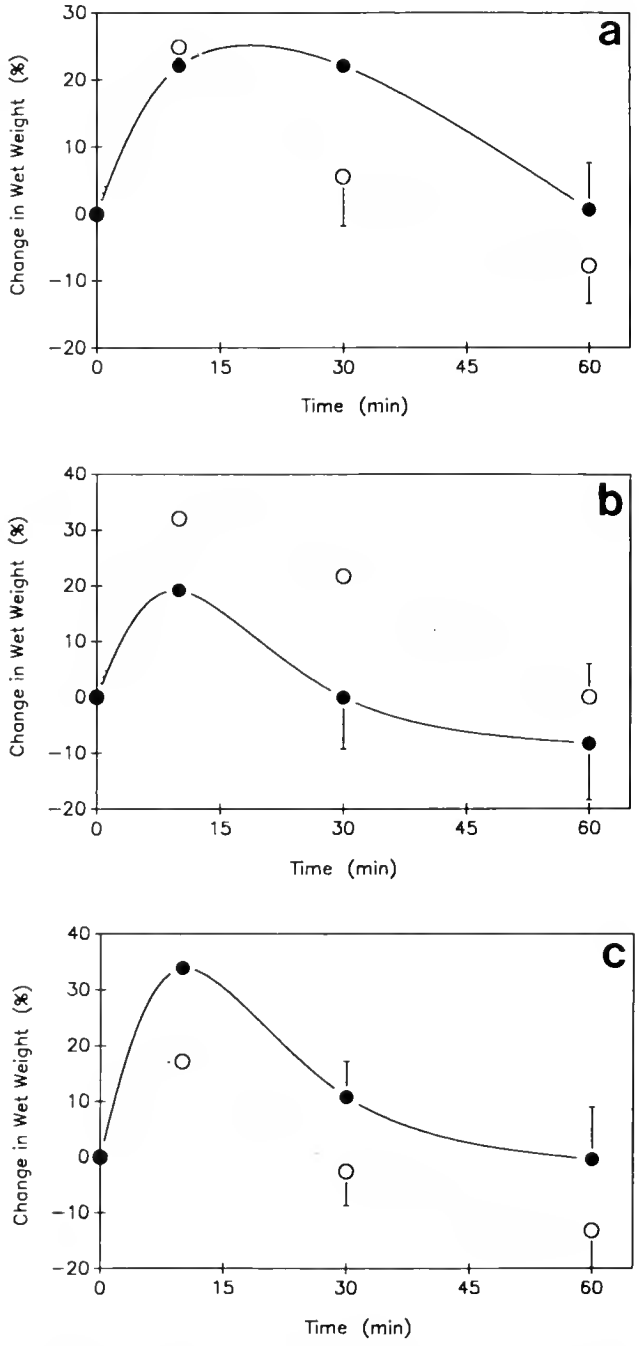

Figure 7. The effects of various agents on the time course of changes in wet weight of *Mercenaria* ventricles transferred from 1000 mOsm seawater to 500 mOsm SW. Each point is the mean of 10 ventricles; error bars are 1 SD. Treatments are indicated as follows: 7a—solid circles = controls, open circles = FMRFamide (10^{-6} *M*); 7b—solid circles = 5-hydroxytryptamine (10^{-6} *M*), open circles = forskolin (10^{-5} *M*); 7c—solid circles = phorbol 12,13-diacetate (10^{-7} *M*), open circles = phorbol 12-acetate,13-myristate (10^{-7} *M*).

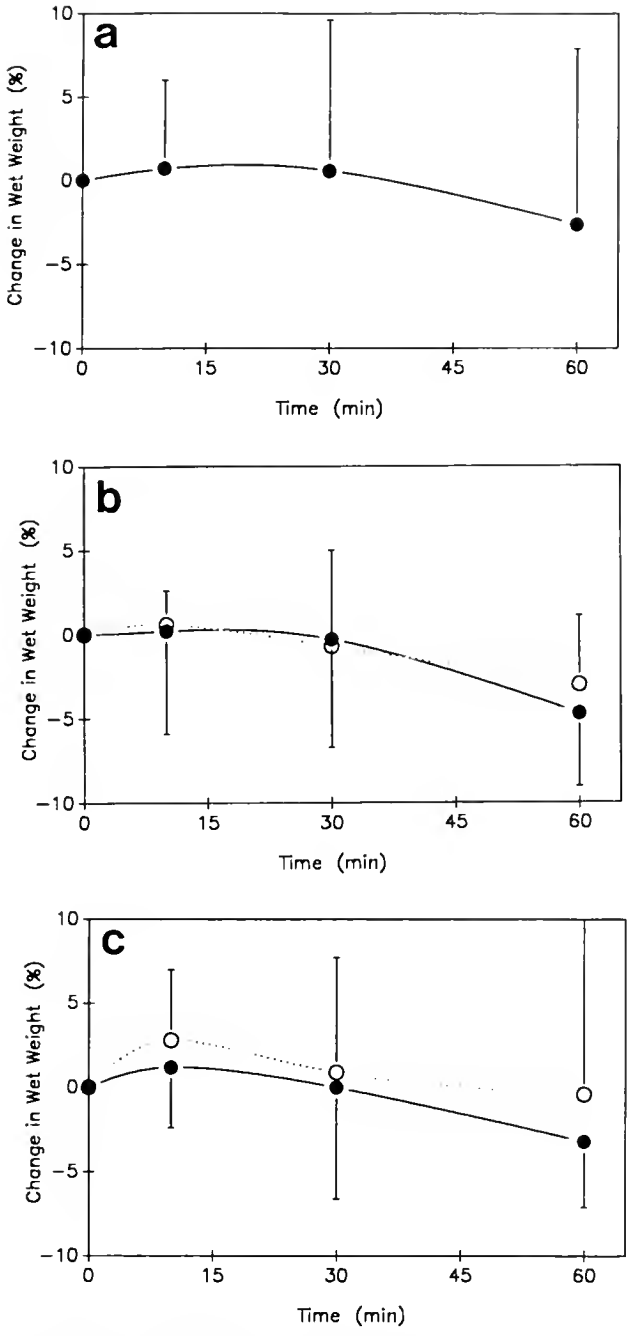

Figure 8. The effects of various agents on the time course of changes in wet weight of *Mercenaria* ventricles transferred to isosmotic seawater (1000 mOsm). Each point is the mean of 10 ventricles; error bars are 1 SD. Treatments are indicated as follows: 8a—solid circles = controls; 8b—solid circles = FMRFamide (10^{-6} *M*), open circles = 5-hydroxytryptamine (10^{-6} *M*); 8c—solid circles = phorbol 12,13-diacetate (10^{-7} *M*), open circles = phorbol 12-acetate,13-myristate (10^{-7} *M*).

volume regulate. The effect of 5HT on amino acid release is mediated by 5HT receptors, since this effect is blocked by UML. The effective concentrations for the potentiation of amino acid release by 5HT and FMRFamide are in the nanomolar range; the concentration of FMRFamide in the hemolymph of the clam *Macrocallista nimbosa* is also in this range (Nagle, 1982).

Both 5HT and FMRFamide stimulate the mechanical activity of isolated *Mercenaria* ventricles (Price and Greenberg, 1980); the cardioexcitatory effects and the potentiation of the volume regulatory response in hypoosmotic media might be due to similar intracellular mechanisms. However, the release of amino acids from ventricles in isosmotic seawater is not affected by either 5HT or FMRFamide. Thus, the chain of events responsible for the cardioexcitatory effects cannot be identical to that responsible for the increase in the release of amino acids and the decrease in the time necessary for the volume regulatory response of the tissues.

Previous studies suggest that stimulation of the mechanical activity of *Mercenaria* ventricles by 5HT and FMRFamide involves an increased sequestration of Ca^{++} ions by the sarcoplasmic reticulum effected by an increase in the intracellular level of c-AMP (Higgins, 1974; Higgins and Greenberg, 1974; Higgins *et al.*, 1978), but the cardioexcitatory effects of 5HT and FMRFamide cannot be completely explained by this mechanism (Paciotti and Higgins, 1985; Deaton and Gray, 1989). The failure of forskolin to affect the release of acids suggests that c-AMP is not involved in the potentiation of this process by 5HT and FMRFamide.

Phorbol esters stimulate protein kinase C, which is also stimulated by diacylglycerol, one component of the phosphoinositol cellular signal transduction system (Nishizuka, 1984; Berridge, 1986). Phorbol esters potentiate the volume regulatory response and increase the release of amino acids of ventricles exposed to dilute media. The phorbol esters only effect increases in the release of amino acids from tissues exposed to hypoosmotic media. The biologically inert compound, 4-β phorbol, also has no effect on amino acid release. The regulatory volume decrease of red blood cells from the clam *Noetia ponderosa* is potentiated by PMA, which appears to affect cytoplasmic K^+ levels (Pierce *et al.*, 1989). Phorbol esters also potentiate the release of amino acids from elasmobranch erythrocytes incubated in hypoosmotic media (Leite and Goldstein, 1987), and mimic the effect of osmotic shrinking on the ion exchangers responsible for adjustment to hyperosmotic stress by cultured lymphocytes (Grinstein *et al.*, 1986). There is, however, no increase in the IP_3 levels in skate red blood cells exposed to hypoosmotic medium (McConnell and Goldstein, 1988). These results suggest that protein kinase C is involved in volume regulation; but the role, if any, of IP_3, is not clear.

Incubation of ventricles from the mussel *Geukensia demissa* in isosmotic medium containing 0.54 m*M* KCl,

which depolarizes the cells by about 60 mV (Wilkens, 1972), increases the release of amino acids from 15 to 21 μmol/g dry wt (Pierce and Greenberg, 1976). These observations raise the possibility that the effects of 5-HT, FMRFamide, and phorbol esters on the release of amino acids might be due simply to depolarization of the cells. This seems unlikely for two reasons. First, there was no increase in the amino acid release from ventricles treated with 5-HT, FMRFamide, or phorbol esters in isosmotic seawater. Second, large doses (10^{-6} *M*) of 5-HT have little effect on the membrane potential of either *G. demissa* or *Mytilus edulis* cardiac muscle cells (Irisawa *et al.*, 1973). However, the effects of FMRFamide and 5-HT on the membrane potential of *Mercenaria* cardiomyocytes are unknown.

In summary, the regulatory volume decrease (RVD) of *Mercenaria* ventricular cells exposed to hypoosmotic media may be mediated by the activation of protein kinase C. The potentiation of the RVD and loss of free amino acids from isolated ventricles by 5-HT and FMRFamide raises the possibility that the response of bivalve tissues to hypoosmotic stress may be modulated by neuronal or neurohormonal control.

Acknowledgments

I thank D. A. Price for assistance with the amino acid analyses and K. H. Hasenstein for help with the figures. This work was supported by funds from the National Science Foundation: PCM 8309314 to M. J. Greenberg and L.E.D. and DCB 8912876 to L.E.D.

Literature Cited

Amende, L. M., and S. K. Pierce. 1980. Cellular volume regulation in salinity stressed molluscs: the response of *Noetia ponderosa* (Arcidae) red blood cells to osmotic variation. *J. Comp. Physiol.* **138:** 283–289.

Bablanian, G. M., and S. N. Treistman. 1983. Sea water osmolarity affects bursting pacemaker activity in intact *Aplysia californica*. *Brain Res.* **271:** 342–345.

Bablanian, G. M., and S. N. Treistman. 1985. The effect of hyperpolarization of cell R15 on the hemolymph composition of intact *Aplysia*. *J. Comp. Physiol. B* **155:** 297–303.

Berridge, M. J. 1986. Cell signalling through phospholipid metabolism. *J. Cell Sci. Suppl.* **4:** 137–153.

Deaton, L. E., and K. R. Gray. 1989. Excitation of the clam heart by phorbol esters. *Comp. Biochem. Physiol.* (in press).

Durchon, M. 1967. *L'Endocrenologie des Vers et des Mollusques.* Masson et Cie, Paris. 241 pp.

Gainey, L. F. 1978. The response of the Corbiculidae (Mollusca: Bivalvia) to osmotic stress: the cellular response. *Physiol. Zool.* **51:** 79–91.

Gilles, R. 1979. Intracellular orgainic osmotic effectors. Pp. 111–153 in *Mechanisms of Osmoregulation in Animals*, R. Gilles, ed. Wiley Interscience, New York.

Grinstein, S., J. D. Goetz-Smith, D. Stewart, B. J. Beresford, and A. Mellors. 1986. Protein phosphorylation during activation of Na^+/H^+ exchange by phorbol esters and by osmotic shrinking. *J. Biol. Chem.* **261:** 8009–8016.

Higgins, W. J. 1974. Intracellular actions of 5-hydroxytryptamine on the bivalve myocardium. I. Adenylate and guanylate cyclase. *J. Exp. Zool.* **190:** 99–110.

Higgins, W. J., and M. J. Greenberg. 1974. Intracellular actions of 5-hydroxytryptamine on the bivalve myocardium. II. Cyclic nucleotide dependent protein kinases and microsomal calcium uptake. *J. Exp. Zool.* **190:** 305–316.

Higgins, W. J., D. A. Price, and M. J. Greenberg. 1978. FMRFamide increases the adenylate cyclase activity and cyclic AMP level of molluscan heart. *Eur. J. Pharmacol.* **48:** 425–430.

Irisawa, H., L. A. Wilkens, and M. J. Greenberg. 1973. Increase in membrane conductance by 5-hydroxytryptamine and acetylcholine on the hearts of *Modiolus demissus demissus* and *Mytilus edulis* (Mytilidae, Bivalvia). *Comp. Biochem. Physiol.* **45A:** 653–666.

Kupfermann, I., and K. R. Weiss. 1976. Water regulation by a presumptive hormone contained in identified neurosecretory cell R-15 of *Aplysia*. *J. Gen. Physiol.* **67:** 113–123.

Leite, M. V., and L. Goldstein. 1987. Ca^{2+} ionophore and phorbol ester stimulate taurine efflux from skate erythrocytes. *J. Exp. Zool.* **242:** 95–97.

Lubet, P., and P. J. Pujol. 1963. Sur l'evolution du system neurosecreuer de *Mytilus galloprovincialis* Lmk. (Mollusque Lamellibranche) lors de variations de la salinitie. *C. R. Seanc. Soc. Biol. Paris* **257:** 4032–4034.

McConnell, F. M., and L. Goldstein. 1988. Intracellular signals and volume regulatory response in skate erythrocytes. *Am. J. Physiol.* **255:** R982–R987.

Nagabushanam, R. 1964. Neurosecretory changes in the nervous system of the oyster, *Crassostrea virginica*, induced by various experimental conditions. *Indian J. Exp. Biol.* **2:** 1–4.

Nagle, G. T. 1982. The molluscan neuropeptide FMRFamide: calcium-dependent release and blood levels in *Macrocallista* (Bivalvia). *Life Sci.* **30:** 803–807.

Nishizuka, Y. 1984. The role of protein kinase C in cell surface signal transduction and tumor promotion. *Nature* **308:** 693–697.

Paciotti, G. F., and W. J. Higgins. 1985. Potential of the 5-hydroxytryptamine-induced increases in myocardial contractility in *Mercenaria mercenaria* ventricle by forskolin. *Comp. Biochem. Physiol.* **80C:** 325–329.

Pierce, S. K. 1982. Invertebrate cell volume control mechanisms: a coordinated use of intracellular amino acids and inorganic ions as osmotic solute. *Biol. Bull.* **163:** 405–419.

Pierce, S. K., and M. J. Greenberg. 1972. The nature of cellular volume regulation in marine bivalves. *J. Exp. Biol.* **57:** 681–692.

Pierce, S. K., and M. J. Greenberg. 1976. Hypoosmotic cell volume regulation in marine bivalves: effect of membrane potential change and metabolic inhibition. *Physiol. Zool.* **49:** 417–424.

Pierce, S. K., A. D. Politis, D. H. Cronkite, L. M. Rowland, and L. H. Smith. 1989. Evidence of calmodulin involvement in cell volume recovery following hypo-osmotic stress. *Cell Calcium* **10:** 159–169.

Price, D. A., and M. J. Greenberg. 1980. Pharmacology of the molluscan cardioexcitatory neuropeptide FMRFamide. *Gen. Pharmacol.* **11:** 237–241.

Wilkens, L. A. 1972. Electrophysiological studies on the heart of the bivalve mollusc, *Modiolus demissus*. I. Ionic basis of the membrane potential. *J. Exp. Biol.* **56:** 273–291.

Reference: *Biol. Bull.* **178:** 267–278. (June, 1990)

Efferent Innervation to *Limulus* Eyes *In Vivo* Phosphorylates a 122 kD Protein

SAMUEL C. EDWARDS*[,1], ANNE W. ANDREWS[1], GEORGE H. RENNINGER[2], ERIC M. WIEBE[1], AND BARBARA-ANNE BATTELLE[1]

[1]*The Whitney Laboratory and the Department of Neuroscience of the University of Florida, 9505 Ocean Shore Boulevard, St. Augustine, Florida 32086, and* [2]*Biophysics Interdepartmental Group, Department of Physics, University of Guelph, Guelph, Ontario, Canada N1G 2W1*

Abstract. Efferent fibers innervate all of the eyes of the horseshoe crab, *Limulus polyphemus.* Driven by a circadian clock located in the central nervous system, the activity of the fibers at night is responsible for anatomical, biochemical, and physiological changes in the eyes, which increase their ability to detect and respond to light. We showed previously that octopamine, a putative efferent neurotransmitter, stimulates the phosphorylation of a 122 kD protein in *in vitro* preparations of both ventral and lateral eyes by means of a cAMP-dependent mechanism. We now report that phosphorylation of the 122 kD protein in the lateral eye is enhanced *in vivo:* (1) at night, in correlation with efferent nerve input activated by the circadian clock; and (2) during the day, in response to electrical stimulation of efferent axons. We show further that the 122 kD protein is enriched in, and may be restricted to, tissues that contain photoreceptors. We postulate that this protein is involved in the efferent-stimulated increase in retinal sensitivity.

Introduction

Retinal efferent neurons project to the eyes of many different vertebrate and invertebrate animals (See Evans *et al.,* 1983; Uchiyama, 1989), and in most species the function of this efferent input is unknown. The best understood of the retinal efferent systems is the one projecting to the eyes of the horseshoe crab, *Limulus polyphemus.* Efferent neurons innervate all of the eyes of *Limulus*—lateral, ventral, and median (Fahrenbach, 1971, 1981; Evans *et al.,* 1983). These neurons are, in turn, driven by a circadian clock located in the central nervous system (Barlow, 1983) such that they become active at night and are silent during the day (Barlow *et al.,* 1977). When the neurons are active, the anatomy, biochemistry, and electrophysiology of cells in the lateral eye change, leading to an increase in the ability of the eye to detect and respond to light (reviewed in Barlow, 1983).

Previous studies provide substantial evidence that the biogenic amine octopamine (OCT) is a neurotransmitter in the efferent neurons (Battelle *et al.,* 1982; Evans *et al.,* 1983; Battelle and Evans, 1984), and that this amine mimicks many of effects of efferent input to the eyes (Kass and Barlow, 1984; Kass and Renninger, 1988; Kass *et al.,* 1988; Pelletier *et al.,* 1984; Renninger *et al.,* 1989). Furthermore, many of these effects may be mediated by an OCT-stimulated increase in the intracellular second messenger, adenosine 3′,5′-monophosphate (cAMP). OCT increases the intracellular concentration of cAMP in lateral eye slices (Battelle and Wishart, unpub. obs.) and in the ventral eye (Kaupp *et al.,* 1982); and analogues of cAMP and agents that increase the level of intracellular cAMP—such as forskolin, a nonspecific adenylate cyclase stimulator (Seamon *et al.,* 1981)—mimic the physiological effects of efferent input or OCT *in situ* and in isolated tissues (Kass and Barlow, 1981, 1984; Kass and Renninger, 1988; Kass *et al.,* 1983, 1988; Pelletier *et al.,* 1984; O'Day and Lisman, 1985; Renninger *et al.,* 1988, 1989; Stieve, pers. comm.). Thus, we suspect that some of the effects of efferent innervation on

Received 3 December 1989; accepted 9 March 1990.

* Corresponding author and the author to whom reprint request should be sent. Present address: Department of Biology, University of South Florida 4202 Fowler Avenue, Tampa, FL 33620.

Abbreviations: cAMP PK, cAMP-dependent protein kinase; ERG, electroretinogram; OCT, octopamine; LON, lateral optic nerve; PAGE, polyacrylamide gel electrophoresis; SEM, standard error of the mean.

visual function may be mediated by an OCT-stimulated increase in cAMP.

Many of the effects of cAMP on cell function are thought to be mediated by the activation of cAMP-dependent protein kinase (cAMP PK) and the phosphorylation of specific substrate proteins (Nestler and Greengard, 1984). In a previous study we identified a 122 kD phosphoprotein, which, in isolated lateral eye slices and ventral eye photoreceptors, is phosphorylated in response to OCT via a cAMP-dependent mechanism (Edwards and Battelle, 1987). This led us to predict that, when efferent fibers become active in the animal, they release OCT into the eyes and stimulate a rise in intracellular cAMP. Cyclic AMP then activates cAMP PK and increases the phosphorylation of the 122 kD protein in retinal cells. To test this prediction we have used a back phosphorylation assay (Valtora *et al.*, 1986) to compare the level of phosphorylation of the 122 kD protein in lateral eyes deprived of efferent input and lateral eyes that received efferent input *in situ*: (1) at night, after efferent neurons were activated by the circadian clock in the central nervous system; and (2) during the day, in response to the electrical stimulation of the efferent axons.

In this back phosphorylation assay, proteins are fractionated by SDS polyacrylamide gel electrophoresis (PAGE), blotted onto nitrocellulose, and incubated in vitro with [γ-^{32}P] ATP and exogenous, purified, catalytic subunit of cAMP PK. The incorporation of $^{32}PO_4$ into specific proteins is then quantified by autoradiography and liquid scintillation spectroscopy. The amount of $^{32}PO_4$ that becomes associated with a protein is a measure of the number of cAMP PK substrate sites that are present in the dephosphorylated form. Thus, a previous increase in the phosphorylation of these sites by endogenous cAMP PK would be reflected as a *decrease* in the amount of radiolabeled phosphate that is incorporated into the protein in the back phosphorylation assay.

The results of our assays show that activation of the efferent axons *in situ*, during the night or during the day, stimulates the endogenous phosphorylation of the 122 kD protein. Furthermore, the tissue distribution of the 122 kD protein suggests that it is a prominent component of photoreceptor cells, and that it is enriched in, and may be restricted to, tissues that contain photoreceptors.

Materials and Methods

Animals

Adult, intermolt *Limulus polyphemus*, collected in the Indian River near Oak Hill, Florida, were maintained in running, natural seawater (15–18°C) on a 12 h light:12 h dark cycle. Animals were fed once a week and allowed to adapt to these conditions for at least two weeks before they were used.

In vitro *experiments*

Both lateral eyes from an animal were removed during the afternoon and placed into MOPS buffered *Limulus* saline (Warren and Pierce, 1982) containing 5 m*M* glucose. The corneas were removed, and small slices (approximately 1 × 2 mm), cut from the central region of the eyes, were placed into individual wells containing 1 ml of saline and incubated at room temperature for 1 h. They were then transferred to either fresh saline or saline containing 2 μM OCT (Sigma, St. Louis, Missouri) or 10 μM forskolin (Calbiochem, San Diego, California) and incubated for an additional 10 min. The tissues were homogenized in Laemmli (1970) SDS buffer, and the resulting homogenates were sonicated in a bath sonicator (Model W-225, Heat Systems-Ultrasonics Inc., Farmingdale, New York) and stored at 4°C pending analysis.

In vivo *experiments*

(1) Endogenous efferent activity. Each experiment was done using a single animal to eliminate animal to animal variation. One of the animal's eyes received endogenous efferent input, while input to the other eye was blocked by transecting the lateral optic nerve (LON) as described below.

An animal was attached to a rigid platform, and the LON of one eye was exposed—through a circular opening (approximately 2 cm in diameter) cut in the carapace just anterior to the eye—and transected. In two of the four experiments, the LON of the other eye was also exposed and served as a sham control; results with sham-operated eyes were the same as those in which the sham operation was not performed. After the opening was closed with gauze and beeswax, the animal was placed in the dark in an aquarium containing enough aerated, natural seawater to keep the book gills submerged. Visual sensitivity was monitored by recording the electroretinogram (ERG) as described by Horne and Renninger (1988). A microcomputer controlled the duration of the light stimulus (a green light-emitting diode, 100 ms), the interval between stimuli (10 min), and the recording of ERG activity.

Four hours after the onset of the animal's subjective night, as determined by an increase in the sensitivity of the eye receiving endogenous efferent innervation, both of its eyes were removed in the dark and immediately placed into liquid N_2. Then, under dim red light, each eye was quickly thawed by immersion in cold saline, the cornea was removed, and the eye was homogenized in SDS buffer with a glass-glass homogenizer. Each sample was sonicated, centrifuged for 5 min at 450 × *g* to remove the insoluble pigment granules, and the resulting supernatant was stored at 4°C until it was analyzed.

(2) Optic nerve stimulation. Early during an animal's

subjective day, it was fixed to a platform, as described above. Both LONs were exposed through circular openings cut in the carapace, and the LON to one eye was prepared for electrical stimulation (Barlow, 1983). Briefly, the LON was drawn into a small, saline-filled recording chamber that fit snugly in the opening in the carapace. The LON was dissected free of the surrounding blood vessel and cut. The cut end of the nerve that was attached to the eye was placed in a suction electrode filled with saline, and the lead of the electrode was connected through a stimulus isolation unit (Grass Model SIU5, Grass Instrument Co., Quincy, Massachusetts) to a pulse stimulator (Grass Model S88). The exposed LON of the other eye was left intact and served as a sham control. ERGs of both eyes were recorded, and the animal was maintained in the dark until the ERG activity stabilized (approximately 2 h). The LON was then electrically stimulated continually for 9 min with 15 or 30 volts DC (4 pulses per s, 2 ms pulse duration). The stimulus was turned off for 1 min while the ERG amplitude of the stimulated eye was monitored. This stimulus paradigm was repeated until the ERG amplitude of the stimulated eye reached a sustained, apparently maximal, level. Then both the stimulated and control eyes were removed from the animal and prepared for analysis, as described in the preceding section.

Back phosphorylation procedure

The level of phosphorylation of the 122 kD protein in *Limulus* visual tissue was examined by means of the back phosphorylation procedure developed by Valtorta *et al.* (1986) for proteins electrophoretically transferred and immobilized on nitrocellulose. Proteins from the lateral eyes were separated by SDS-PAGE (Laemmli, 1970) (7.5% acrylamide separating gel) and then electrophoretically transferred to a sheet of nitrocellulose (Towbin *et al.*, 1979). A prestained form of β-galactosidase (MW 116 kD; Sigma) was loaded into alternate lanes of the SDS gel to help locate the 122 kD protein on the nitrocellulose blot. Using ^{32}P-labeled 122 kD protein that had been prepared by treating lateral eye homogenates with [γ-^{32}P] ATP in the presence of 8-bromo cAMP (Edwards and Battelle, 1987), we determined that the transfer of 122 kD protein present in the gels to nitrocellulose was roughly quantitative and reproducible (coefficient of variation 15% for 5 experiments, data not shown).

Preliminary experiments showed that the ratio of the amount of 122 kD protein per mg total tissue protein varied from eye to eye; thus different volumes of each tissue sample were analyzed by the back phosphorylation procedure. Comparisons were then made between samples containing approximately the same amount of 122 kD protein as determined by Coomassie blue G250 staining of an identical gel, or by fast green staining of the protein on the nitrocellulose blot [0.1% (w/v) in 50% methanol and 10% acetic acid] following the assay.

The assay was usually performed only on the portion of the nitrocellulose blot containing the 122 kD protein, although in one experiment, shown in Figure 3, the level of phosphorylation of other proteins was examined. The blot was rinsed 3 times, for 5 min each, in 50 m*M* Tris and 200 m*M* NaCl at pH 7.4; it was then blocked by incubation for 1 h in the same solution containing, in addition, 0.4% (w/v) Ficol 400 and 0.1% Triton X100 (Valtorta *et al.*, 1986). The blot was then incubated for 1 h at 22°C, with continuous agitation, in a HEPES buffer, 50 m*M* (pH 7.4) containing 25 m*M* NaCl, 10 m*M* $MgCl_2$, 1 m*M* EGTA, 0.1 m*M* 2-mercaptoethanol, 0.1% Triton X100, 0.5 mg BSA, 76 n*M* Tris ATP, 15 μCi/ml [γ-^{32}P] ATP (NEN/Dupont, Wilmington, DE), and 1–5 units/ml of the catalytic subunit of cAMP PK (Sigma). The stock cAMP PK was routinely stored at 4°C in the solution described by Beavo *et al.* (1974). After the incubation, the blot was washed repeatedly, dried, and exposed with Kodak XAR X-ray film. The blotted proteins were then visualized using fast green, the 122 kD protein band was cut from the blot, and the radioactivity associated with it was determined by liquid scintillation spectroscopy.

The amount of labeled phosphate incorporated into the 122 kD protein from the unstimulated eye was expressed as 100%. The relative amount of *endogenous phosphorylation* of the 122 kD protein extracted from eyes receiving efferent nerve input was determined from the difference in the amount of labeled phosphate incorporated into the protein from efferent-stimulated and unstimulated eyes. For example, if the amount of $^{32}PO_4$ incorporated into the protein from the eye receiving efferent nerve input was 60% of that incorporated into the protein extracted from unstimulated eye, the remaining 40% was considered as being due to endogenous phosphorylation.

Validation of the back phosphorylation assay for the 122 kD protein in Limulus *tissue*

The *Limulus* LON contains a relatively large amount of the 122 kD protein that can be phosphorylated in homogenates by activation of endogenous cAMP PK (Edwards and Battelle, 1987; this study). The resulting $^{32}PO_4$ can subsequently be removed from the 122 kD protein by treating the tissue homogenates with alkaline phosphatase (unpub. results). To determine whether the back phosphorylation procedure would detect changes in the phosphorylation of the 122 kD protein, we measured the level of $^{32}PO_4$ incorporation into the blotted protein that had previously been incubated under phosphorylating

conditions, or incubated under phosphorylating conditions and subsequently stripped of phosphates with alkaline phosphatase. Specifically, aliquots of LON homogenates were incubated for 30 min at 30°C in media containing nonradioactively labeled ATP (30 μM) with, or without, 10 μM 8-bromo cAMP (Sigma) (Edwards and Battelle, 1987). At the end of the incubation period, several aliquots were treated with 2X SDS buffer and sonicated as described above. Other aliquots were mixed with an equal volume of 0.2 M Tris HCl (final pH 8.2) containing 2 mM phenylmethylsulfonyl fluoride, 2 mM $ZnCl_2$, 0.2 mM leupeptin, and 100 units/ml aprotinin, and then incubated for 2 h at 37°C with, or without, 81 units/ml calf intestinal alkaline phosphatase (type VII, Sigma) before the addition of SDS buffer. Samples containing the same amount of tissue protein were separated by SDS PAGE, blotted onto nitrocellulose, and the relative level of phosphorylation of the 122 kD protein for each treatment was determined using the back phosphorylation procedure.

Tissue distribution of the 122 kD protein

To determine the tissue distribution of the 122 kD protein in *Limulus*, samples from visual and nonvisual nervous tissues were homogenized in SDS buffer, sonicated and stored at 4°C until they were analyzed. The amount of protein in each sample was determined by a modified Lowry procedure (Peterson, 1977) using bovine serum albumin as the standard. Tissue samples containing an equal amount of protein were subjected to SDS PAGE, and proteins were visualized by silver stain (Heukeshoven and Dernick, 1985).

Results

Validation of the back phosphorylation using LON homogenates

Figure 1 shows that the 122 kD protein from the LON is a substrate for phosphorylation by purified catalytic subunit of cAMP PK and [γ-$^{32}PO_4$] ATP, even after it is separated from other tissue proteins by SDS-PAGE and electrophoretically transferred onto nitrocellulose. Prior treatment of the LON homogenate with 8-bromo cAMP resulted in a substantial reduction in the amount of radiolabeled phosphate ($^{32}PO_4$) associated with the 122 kD protein; subsequent incubation of the cAMP-treated homogenate with alkaline phosphatase returned the level of associated $^{32}PO_4$ to the untreated control level. The amount of 122 kD protein, as determined by fast green staining, was the same in all three samples.

Prolonged incubation (30 min) of the LON homogenate with 8-bromo cAMP did not produce a 100% reduction in the amount of $^{32}PO_4$ that subsequently became

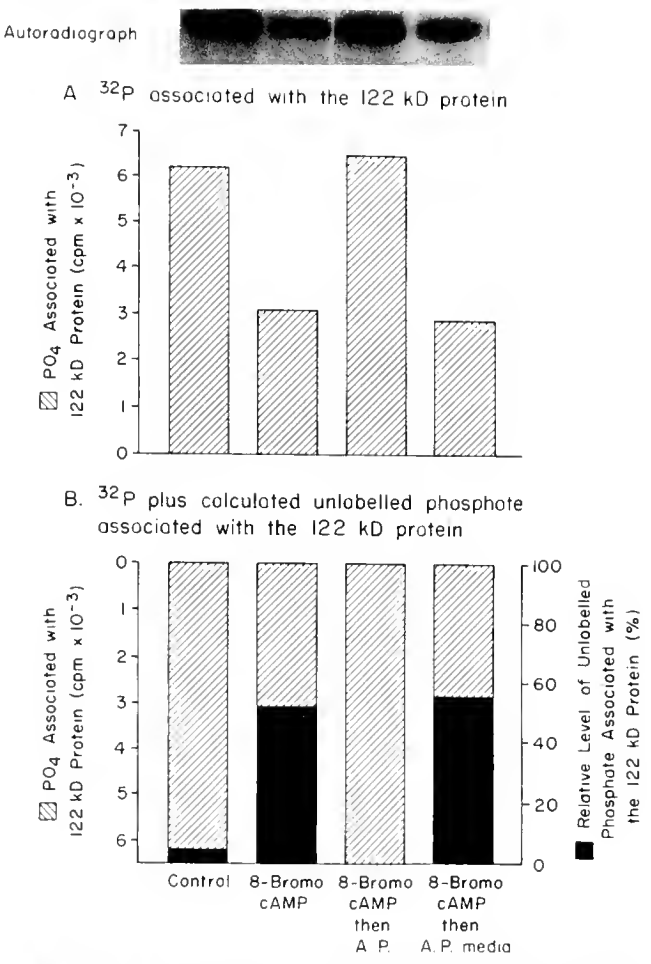

Figure 1. Back phosphorylation of homogenates of the *Limulus* LON demonstrates how the technique can be used to examine the level of cAMP-dependent phosphorylation of the 122 kD protein. Homogenates of LON were prepared and then incubated, as previously described (Edwards and Battelle, 1987), at 30°C in media containing ATP (30 μM) without (Control), or with, 10 μM 8-bromo cAMP. Some aliquots were then mixed with an equal volume of a 0.2 M Tris HCl buffered solution (A.P. media, final pH 8.2) and incubated for 2 h at 37°C with, or without, 81 units/ml calf intestinal alkaline phosphatase (A.P., type VII, Sigma). After all of the samples were solubilized, aliquots of each, containing an equal amount of total tissue protein (20 μg), were fractionated by SDS-PAGE and transferred onto nitrocellulose. The region of the blot containing the 122 kD protein was then subjected to the back phosphorylation procedure (See Methods). The association of $^{32}PO_4$ with the protein was first visualized with autoradiography (top of figure) and then quantified by liquid scintillation spectroscopy (A). The relative level of unlabeled phosphate associated with the protein (B) in each sample was calculated as the difference in the amount of phosphate in that sample compared to the alkaline phosphatase-treated sample. In the experiment shown, the phosphorylation of the 122 kD protein in aliquots incubated with ATP plus 8-bromo cAMP was 52.0% greater than that in aliquots incubated with ATP but without 8-bromo cAMP. In two similar experiments, 8 bromo cAMP stimulated a 23.9% and 28.4% increase in phosphorylation.

In another experiment, samples treated with SDS buffer immediately after homogenization were compared to ones treated with alkaline phosphatase; the amount of $^{32}PO_4$ associated with the 122 kD protein in these two cases was indistinguishable (data not shown). Thus the 122 kD protein seems not to be phosphorylated on cAMP-dependent sites in the intact LON.

associated with the 122 kD protein; the maximum reduction observed was 52% (Fig. 1), and the average percent reduction [± the one standard error of the mean (SEM)] for three separate experiments was 34.8 ± 12.3 (See the legend to Fig. 1). There are at least two possible explanations for this relatively small reduction in the incorporation of $^{32}PO_4$. (1) Sites on the protein normally phosphorylated by cAMP PK in tissue homogenates were not fully occupied by phosphate, even after the homogenate was exposed to 8-bromo cAMP and ATP for 30 min. (2) Treating the 122 kD protein with SDS and blotting it onto nitrocellulose exposes sites for phosphorylation that normally are not available in the protein's native configuration.

We draw two conclusions from these results. First, the reduced incorporation of $^{32}PO_4$ into the 122 kD protein of cAMP-treated homogenates reflects enhanced phosphorylation of the protein prior to the assay. That is, the amount of $^{32}PO_4$ incorporated into the protein on the blot is inversely related to the level of phosphorylation of the protein prior to the assay. Therefore, the back phosphorylation procedure can be used to assay the relative level of phosphorylation of the 122 kD protein. For example, in an experiment similar to that shown in Figure 1, we observed that the level of phosphorylation of the 122 kD protein in an alkaline phosphatase-treated LON homogenate was approximately the same as a sample in which SDS buffer was added immediately following homogenization (data not shown). We interpret this to mean that, at least during the day when all of these experiments were performed, the cAMP PK-dependent phosphorylation sites on the 122 kD protein in the LON are not phosphorylated *in vivo*.

Our second conclusion is that the maximum relative reduction in incorporation of $^{32}PO_4$ into the 122 kD protein that we may expect to observe, using this assay, is approximately 50%. We are assuming here that incubation *in vitro* for 30 min in the presence of 8-bromo cAMP and ATP stimulates the phosphorylation of nearly all of the sites available to cAMP PK in the native 122 kD protein.

OCT- and forskolin-stimulated phosphorylation of the 122 kD protein in slices of the lateral eye

With conventional *in vitro* phosphorylation procedures, we demonstrated an OCT-stimulated phosphorylation of the 122 kD protein in slices of the lateral eye in 3 of 8 (38%) experiments (Edwards and Battelle, 1987). The OCT-stimulated phosphorylation of the 122 kD protein in lateral eye slices is confirmed here using the back phosphorylation procedure (Fig. 2). Furthermore, the OCT-enhanced phosphorylation of the 122 kD protein in lateral eye slices was more reproducible using the back phosphorylation procedure (6 of 8, or 75% of the experiments). At least two factors may contribute to this increased reproducibility. (1) The 122 kD protein may have been extracted more efficiently by the homogenization procedure used in the present experiments (homogenization using a glass-glass homogenizer) as compared to the sonication procedure used previously. (2) Changes in the level of phosphorylation of the 122 kD protein may have been obscured in the conventional experiments due to high background radioactivity in the autoradiographs (See Figure 1a in Edwards and Battelle, 1987).

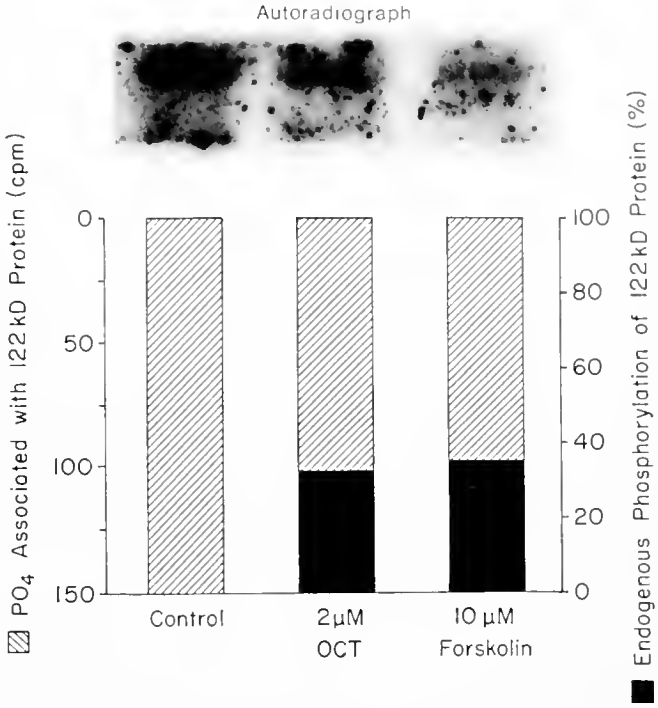

Figure 2. Octopamine- and forskolin-stimulated phosphorylation of the 122 kD protein in *Limulus* lateral eye slices *in vitro* as determined by the back phosphorylation procedure. Isolated tissues were incubated for 10 min in saline (Control), or saline containing 2 μM octopamine (OCT), or 10 μM forskolin (FOR) prior to analysis using the back phosphorylation procedure. This figure presents the results of one experiment. Shown are the autoradiograph, the amount of $^{32}PO_4$, and the calculated relative level of unlabelled PO_4 (endogenous phosphorylation) associated with the 122 kD protein in treated samples containing the same amount of 122 kD protein. The amount of protein as determined by fast green staining on the nitrocellulose blot. The results were similar in four replicates.

The 122 kD protein was also consistently (8 of 8 experiments) phosphorylated in lateral eye slices incubated with forskolin, a nonspecific adenylate cyclase stimulator (Fig. 2).

Changes in the level of 122 kD protein phosphorylation in vivo *in response to:*

(a) Endogenous efferent activity at night. To test our hypothesis that the 122 kD protein becomes phosphory-

lated at night in response to endogenous activation of the retinal efferent neurons, we compared the level of phosphorylation of the 122 kD protein in extracts of lateral eyes that had received endogenous efferent nerve input with those that had been deprived of this input by transection of the LON (Barlow, 1983). Because efferent activity and an increase in the sensitivity of the eye, as measured by an increase in ERG amplitude, are strongly correlated (Barlow, 1983), we monitored the ERG activity of the intact eye to determine when the efferent fibers became active.

In the experiment shown in Figure 3, the ERG amplitude began to increase above the daytime level at approximately 17:00 and continued to increase until it reached a maximum, sustained level 30 min to 1 h later (18:00). At 22:00, both eyes were quickly removed from the animal, processed for SDS-PAGE, and then analyzed for the relative level of endogenous phosphorylation of the 122 kD protein. In this experiment we measured a 34.7% increase in the level of endogenous phosphorylation of the 122 kD protein in the eye receiving efferent input compared to the control eye that had been deprived of efferent nerve activity (See Table IA; animal 1, assay 1). Three separate assays of material from the same animal gave a mean increase (± one SEM 4) of 36 ± 8.4%. Similar results were obtained with two other animals (Table IA).

Similar results were also obtained in an additional experiment in which the eyes of the animal were removed just before the onset of subjective day. In that experiment, the level of endogenous phosphorylation of the 122 kD protein in the eye receiving efferent input was 42% greater than that in the deprived eye. This implies that the level of endogenous phosphorylation of the 122 kD protein remains elevated in response to efferent activity throughout the subjective night.

(b) Optic nerve stimulation during the day. The efferent input to the lateral eye can be activated during the subjective day by electrically stimulating the LON; this also results in an increase in the sensitivity of the eye (Barlow 1983). Therefore, we examined whether electrical stimulation of efferent axons during the day resulted in enhanced phosphorylation of the 122 kD protein in the lateral eye.

The animals were prepared, and one lateral optic nerve was stimulated as described in Materials and Methods. The ERG amplitude began to increase within 10 to 30 min after the onset of stimulation, and continued to increase until it reached a maximum level approximately 40 to 50 min after the onset of the stimulation (Fig. 4). The ERG amplitude of the unstimulated, sham operated eye was unchanged. When the amplitude of the ERG of the stimulated eye reached a stable, maximum level, both the stimulated eye and the unstimulated eye were removed, processed for SDS-PAGE, and the relative level of 122 kD phosphorylation in the two eyes was determined. In the experiment shown in Figure 4, the level of endogenous phosphorylation of the 122 kD protein increased 64.7% in the eye that received electrically stimulated efferent input compared to the intact, daytime, unstimulated eye (See Table IB; animal 2, assay 1). The average increase (± one SEM) measured in four separate assays of material from the same animal was 42.1 ± 2.4%, and in similar experiments performed with 2 other animals, this increase in endogenous phosphorylation measured 47.2 ± 11.2% and 14.5 ± 4.0% (Table IB). Therefore, the increase in endogenous phosphorylation we measured in electrically stimulated eyes during the day was in the same range as what we observed with endogenous efferent input.

Distribution of the 122 kD protein in Limulus *nervous tissue*

The 122 kD protein appears to be restricted to those tissues in *Limulus* involved in visual processes (Fig. 5). It is quantitatively a major protein in the lateral eye, the ventral eye, the lateral and median optic nerves, and the lamina. It is usually observed in the median eye (4 of 6 animals), but its relative abundance in this tissue is variable. It is not a major protein constituent in the medulla, the central body region, or other portions of the brain, more posterior portions of the central nervous system, or the leg nerve. Furthermore, it was not detected in the cardiac ganglion, a tissue in which OCT receptors may also be present (Watson and Augustine, 1982; Groome and Watson, 1987).

Discussion

In this study we present strong evidence that efferent nerve activity stimulates the phosphorylation of a 122 kD protein in *Limulus* lateral eye. Efferent nerve activity could also modulate the amount of 122 kD protein in *Limulus* eyes, but because our assays were done on aliquots of LE extracts that contained the same amount of 122 kD protein, they reveal changes in the level of phosphorylation of the protein and not changes in its absolute amount.

The activity of the efferent nerves that project to *Limulus* eyes is driven by a circadian clock in the central nervous system, and efferent nerve activity causes an increase in the sensitivity of the lateral, ventral, and median eyes to light during the night (Barlow, 1983; Kass and Renninger, 1988). We show that enhanced phosphorylation of the 122 kD protein in lateral eyes *in vivo* correlates with the increased sensitivity of the lateral eye at night. We infer that the phosphorylation of this protein is regulated in a circadian manner, and we speculate

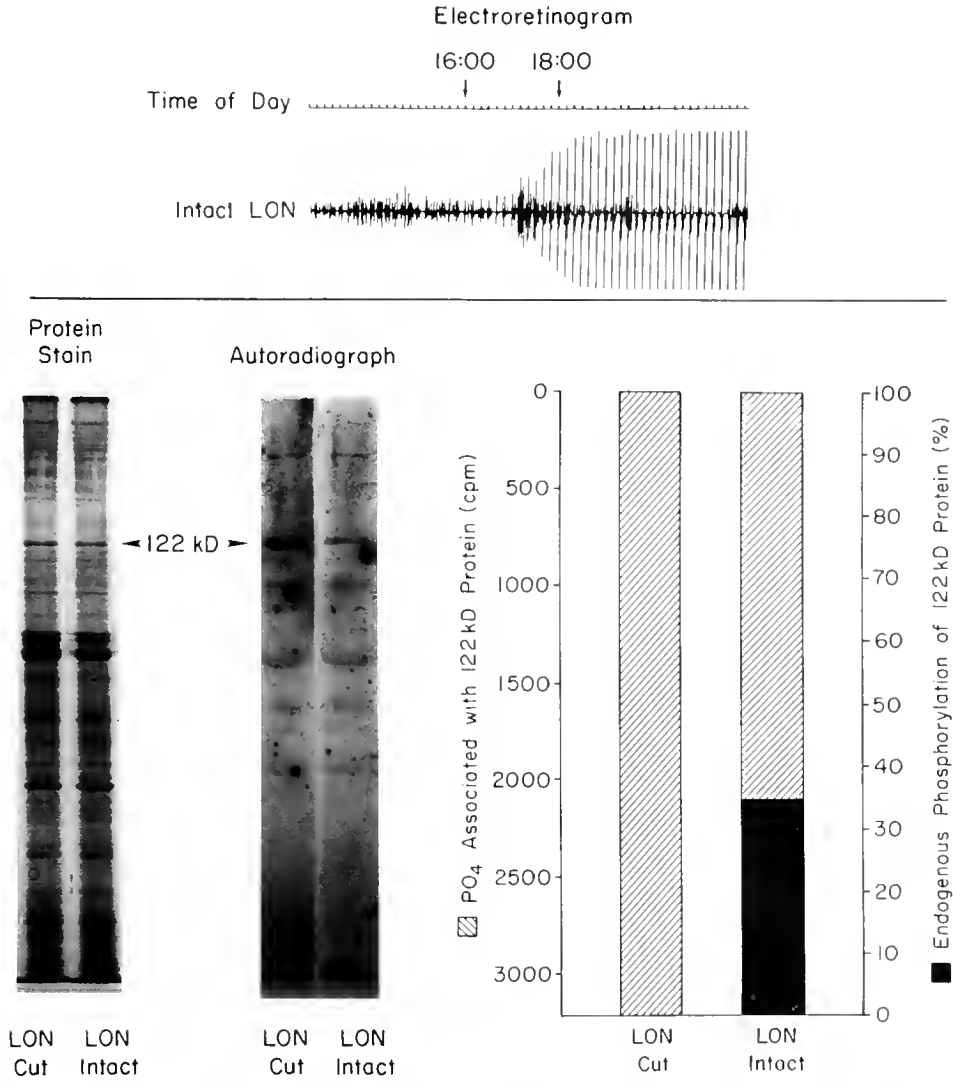

Figure 3. The 122 kD protein is phosphorylated *in vivo* in the *Limulus* lateral eye in response to activation of the efferent neurons by the circadian clock. This figure shows the results of a single assay (Table 1A; animal 1, assay 1). Early in the day, the LON was cut just anterior to one of the eyes to block efferent input to that eye. Input to the other eye was left intact. The animal was then placed into the dark in a standard apparatus for recording the ERG of the intact eye (Barlow, 1983). In the record shown, the ERG amplitudes were recorded every 10 min. Before 16:20, the small ERG amplitudes were partially obscured by voltage noise, probably arising from muscle contractions. After 16:20, the ERG amplitudes were clearly visible, and they began to increase after 17:10 as a result of efferent nerve activity. The ERG amplitudes (light sensitivity) stabilized at an elevated level by 19:00. At 22:00, both eyes were removed from the animal and immediately immersed in liquid N_2. Each eye was then briefly placed in ice cold saline so that the cornea could be removed, the tissue proteins were solubilized, and the amount of endogenous phosphorylation associated with the 122 kD protein from each eye was determined by the back phosphorylation procedure.

The lower portion of this figure shows (left to right): the pattern of proteins visualized by silver stain, (aliquots of solubilized preparations of both eyes contained about the same amount of 122 kD protein); an autoradiograph of a nitrocellulose blot containing larger (4×) aliquots of these samples, subjected to the back phosphorylation procedure; and the amount of $^{32}PO_4$ associated with the 122 kD protein from both eyes. The relative amount of *endogenous phosphorylation* in response to efferent stimulation was determined from the difference in the amount of labeled phosphate incorporated into the protein from efferent-stimulated and unstimulated eyes. The amount of labeled phosphate incorporated into the 122 kD protein from the unstimulated eye was expressed as 100%. The increase in endogenous phosphorylation observed in this assay was 34.7%; the mean increase (± one SEM) determined from three separate assays of material from the same animal was 36.0 ± 8.4%. Experiments with two other animals produced similar results; the results of all of these assays are presented in Table 1A.

Table I

Percent increase in the endogenous phosphorylation of the 122 kD protein following.

A. Endogenous efferent nerve activity[a]

Animal	Assay number[b] 1.	2.	3.	Mean ± SEM[c]
1.	34.7	31.4	32.8	33.0 ± 1.2
2.	28.9	26.4	52.6	36.0 ± 10.0
3.	36.1	48.7	44.7	43.2 ± 4.6

B. Electrically stimulated efferent nerve activity[d]

Animal	Assay number[b] 1.	2.	3.	4.	Mean ± SEM[c]
1.	40.3	41.3	38.7	41.1	42.1 ± 2.4
2.	64.7	33.8	43.2		47.2 ± 11.2
3	18.7	16.6	8.1		14.5 ± 4.0

[a] The experiment was performed on three separate animals exactly as described in the legend to Figure 3.

[b] For each animal studied, the relative level of phosphorylation of the 122 kD protein in homogenates of the unstimulated eye, and the eye receiving efferent input, were compared at least three separate times using the back phosphorylation procedure.

[c] Mean ± one SEM of three or four separate assays of the same set of homogenates.

[d] The experiment was performed on three separate animals exactly as described in the legend to Figure 4.

that the phosphorylation of this protein contributes to some aspects of the structural, physiological, or biochemical changes that occur in *Limulus* eyes in response to efferent nerve activity.

Direct correlation between efferent nerve activity and the phosphorylation of the 122 kD protein

The direct relationship between efferent nerve activity and the phosphorylation of the 122 kD protein is established by the combined results of the experiments done during the night and during the day. The observation that the 122 kD protein was relatively more phosphorylated at night in eyes receiving endogenous efferent nerve input, compared to eyes deprived of input, strongly suggests that enhanced phosphorylation of this protein is due to endogenous efferent nerve activity, but it does not eliminate the possibility that other factors, which may be present at night and not during the day, might also be required for the phosphorylation of the protein. However, results of the experiments in which we electrically stimulated the efferent axons during the day demonstrated that all factors necessary for the lateral eye to respond to efferent input with enhanced phosphorylation of the 122 kD protein are also present during the day.

Tissue distribution of the 122 kD protein

The 122 kD protein is a quantitatively major protein component of many of the tissues of the *Limulus* visual system. Its enrichment in the ventral eye, which consists predominately of photoreceptor cells (Clark *et al.*, 1969), argues that it is enriched in photoreceptor cells. Furthermore, the protein is very likely distributed throughout the photoreceptor cell, because it is found in both cell body- and axon-enriched portions of the ventral eye (Edwards and Battelle, 1987). But the protein may not be found exclusively in photoreceptor cells; much of the volume of the LON, which also contains a large amount of the 122 kD protein relative to other proteins, is composed of the large diameter axons of eccentric cells (Fahrenbach, 1971). It is also found in a high concentration in the first optic ganglia, or laminae, which contain the terminals of photoreceptor and eccentric cells from the lateral eye (Chamberlain and Barlow, 1980). The 122 kD protein may also be present in non-neuronal cells of the lateral eye.

The absence of a conspicuous 122 kD protein band in the medulla was surprising at first, because this tissue is innervated by cells from each of the eyes (Chamberlain and Barlow, 1980). This observation may be explained by a recent finding, which suggests that all photoreceptors from the lateral compound eye terminate in the lamina and do not innervate the medulla (Calman *et al.*, 1990). Thus, compared to the lamina, photoreceptor terminals in the medulla occupy a relatively low percentage of the total volume of the tissue.

The 122 kD protein may be distributed throughout the cells that contain it, but our evidence indicates that it is modified by phosphorylation in the somata of these cells and not in their axons. Previously we showed that activation of cAMP PK stimulated the phosphorylation of the 122 kD protein *in vitro* in portions of the ventral eye enriched in intact photoreceptor cell bodies (Edwards and Battelle, 1987); here we showed that the protein becomes phosphorylated in slices of the lateral eye *in vitro* and in the intact lateral eye *in vivo*. By contrast, in the LON, the 122 kD protein appears not to be a normal substrate of phosphorylation by cAMP PK. It becomes phosphorylated by activation of cAMP PK in broken cell preparations of the LON, but it is not phosphorylated in the LON *in vivo*, at least during the day (See Legend to Fig. 1), nor does it become phosphorylated in intact LON or axons of ventral photoreceptors in response to activation of cAMP PK (Edwards and Battelle, 1987). Consequently we believe that, in the optic nerves, the 122 kD substrate protein is physically separated from the cAMP PK.

The 122 kD protein is quantitatively the major substrate for cAMP PK in broken cell preparations of the

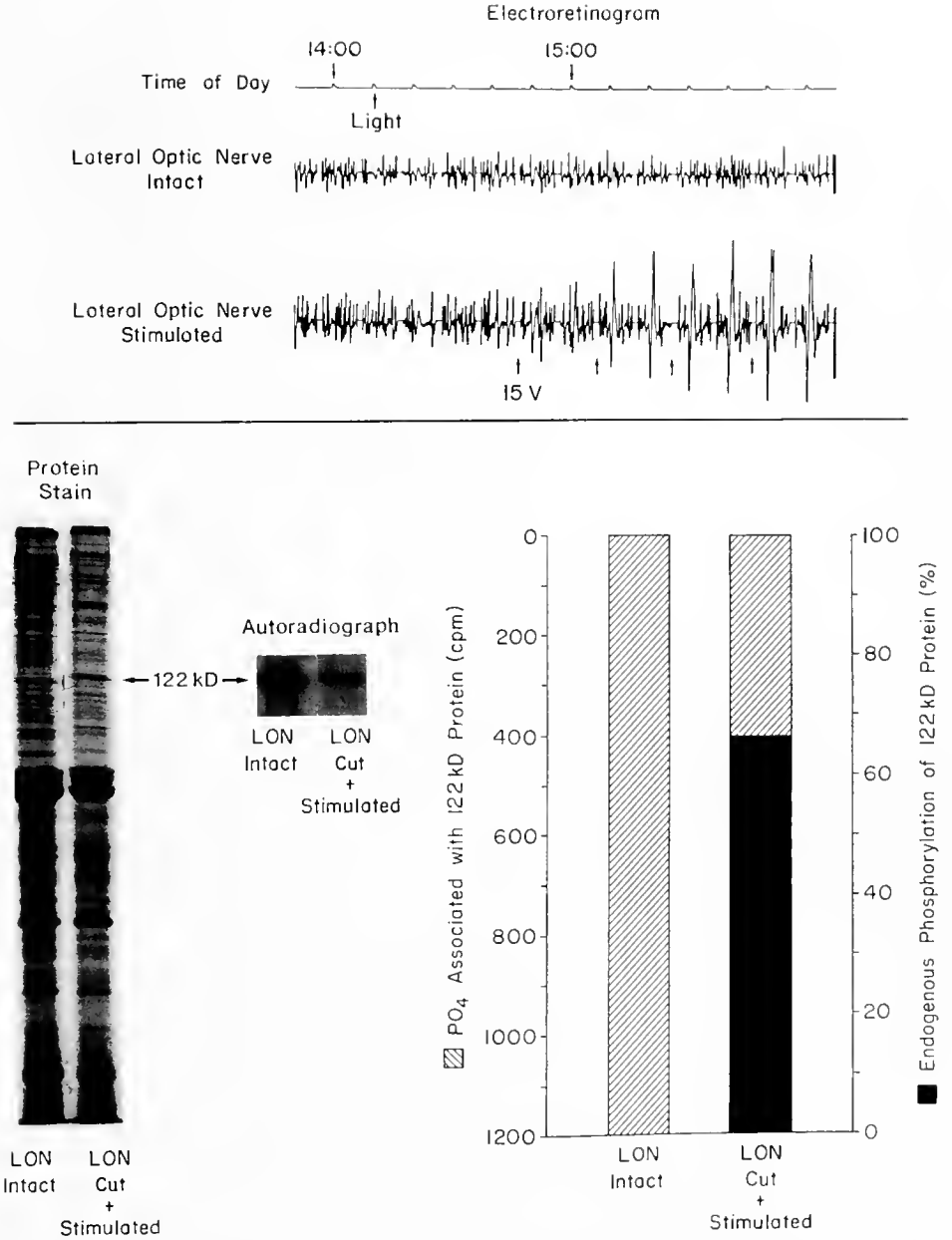

Figure 4. The 122 kD protein is phosphorylated *in vivo* in the lateral eye in response to electrical stimulation of the efferent axons. This figure shows the results of a single assay (Table 1B; animal 2, assay 1). Early in the day, the LON was cut just anterior to one of the eyes. After the animal was placed in the apparatus to record ERG activity, the cut end of the LON that remained with the eye was placed into a suction electrode. The animal was placed in the dark for 2 to 3 h, then the axons of the efferent neurons present in the LON were stimulated continuously with 15 V pulses (4 pps, 2 ms pulse duration) for 9 min (indicated by the arrow); the stimulation was then turned off for 1 min while the ERG amplitude was monitored. This sequence was repeated until the ERG amplitude reached a maximum, at which time both the stimulated and unstimulated eyes were removed and treated as described in Figure 3.

As in Figure 3, the ERG amplitudes of both eyes were initially obscurred by voltage noise. In the lower record, the ERG amplitudes began to increase after the second interval of electrical stimulation. The ERG amplitudes remained small in the upper (control) record.

The lower portion of this figure shows: the protein pattern visualized by silver stain (aliquots of solubilized preparations of both the stimulated and nonstimulated eyes contained about the same amount of 122 kD protein); an autoradiograph of a nitrocellulose blot containing larger (10×) aliquots of these samples, subjected to the back phosphorylation procedure; the amount of $^{32}PO_4$ associated with the 122 kD protein; and the calculated amount of endogenous phosphorylation of the protein in both samples. In the assay shown, we measured a 64.7% increase in endogenous phosphorylation of the 122 kD protein in the stimulated lateral eye of this animal; the average increase (± one SEM), determinated from separate assays of aliquots of the same extract, was 47.2 ± 11.2%. Experiments with two other animals produced similar results. The results of all assays are presented in Table 1B.

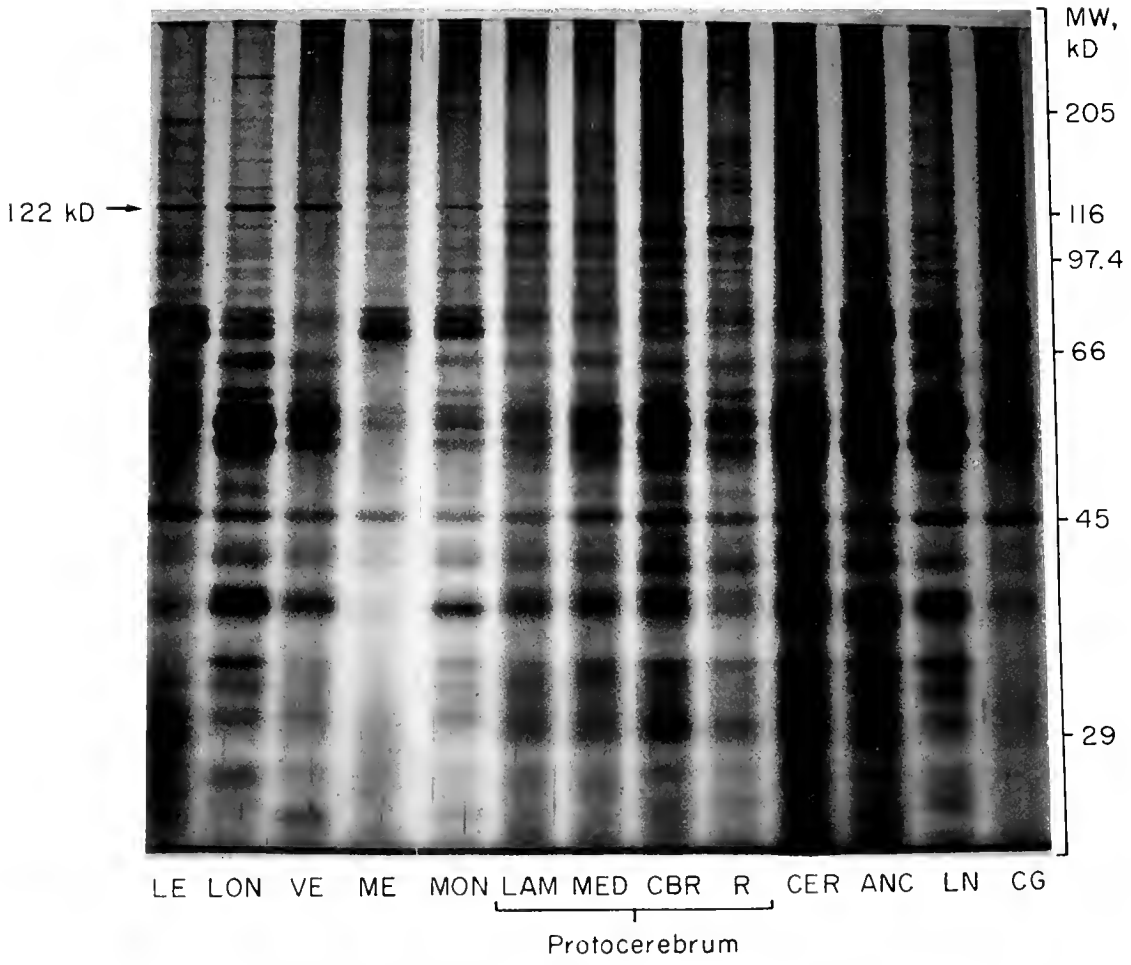

Figure 5. The 122 kD protein is a prominent protein component in *Limulus* eyes and optic nerves, and in the first optic ganglion. It does not appear prominently in other parts of the *Limulus* nervous system. Tissues were homogenized in 1× Laemmli (1970) SDS buffer. After the amount of protein in each sample was determined by a modified Lowry procedure (Peterson, 1977), aliquots containing 1 μg of total tissue protein for each sample were analyzed by SDS-PAGE and silver staining. Abbreviations: lateral eye (LE); lateral optic nerve (LON); ventral eye including P- and A-fractions (VE); median eye (ME); median optic nerve (MON); regions of the protocerebrum—first optic ganglion (lamina—LAM), medulla (MED), central body region (CBR), remaining portions (R); circumesophageal ring (CER); abdominal nerve cord (ANC); peripheral leg nerve (PLN); cardiac ganglion (CG).

lamina as well (data not shown). Because we have not yet examined whether it is phosphorylated in the intact tissue in response to agents that increase intracellular cAMP, the significance of these results are presently unknown.

A model for the regulation of visual function by efferent innervation

Our current model for how efferent nerve activity modulates the function of *Limulus* eyes is presented in Figure 6. The results described in the present study provide support for some aspects of this model.

The circadian nature of the efferent nerve input to *Limulus* eyes is well established (reviewed in Barlow, 1983), and there is convincing evidence that OCT is a neurotransmitter in the efferent axons. OCT is synthesized and stored in the efferent axons that project to the ventral and lateral eyes (Battelle *et al.*, 1982; Evans *et al.*, 1983), and it is released from these axons in a Ca^{2+}-dependent manner *in vitro* in response to veratridine (Battelle and Evans, 1986) or depolarization with high extracellular potassium (Battelle and Evans, 1984). OCT mimics many of the physiological effects of endogenous efferent innervation when applied to the lateral eye in situ (Kass and Barlow, 1984), or to *in vitro* preparations of either the lateral (Kass *et al.*, 1988; Renninger *et al.*, 1989), or ventral eye (Kass and Renninger, 1988). Clo-

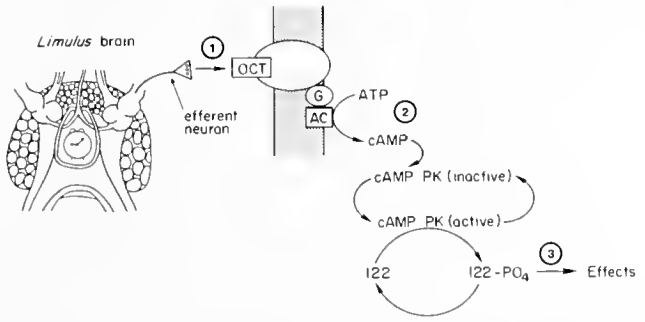

Figure 6. A model for the regulation of visual function by efferent innervation. (1) At night, a circadian clock in the central nervous system activates the efferent fibers innervating *Limulus* eyes, causing the release of the efferent neurotransmitter octopamine (OCT). (2) The interaction of OCT with OCT-specific receptors on the photoreceptors, and perhaps other cell types in the lateral eye, increases the activity of adenylate cyclase, thereby elevating intracellular cyclic AMP levels. (3) This results in the activation of cyclic AMP-dependent protein kinase which phosphorylates the 122 kD protein. We propose that this phosphoprotein is involved in the anatomical, biochemical, and physiological processes responsible for increasing the sensitivity of the eye.

zapine, an OCT-receptor blocker (Dougan and Wade, 1978; Evans, 1981), blocks both the physiological effects of exogenously added OCT and those generated by endogenous efferent activity when it is applied to the lateral eye *in situ* (Kass and Barlow, 1984). Direct evidence for the release of OCT from efferent fibers in response to electrical stimulation or endogenous activation by the circadian clock *in vivo* (Fig. 6, #1) is lacking, but as described below, the results of this study are consistent with this idea.

In the Introduction, we describe the results of many studies that suggest that many of the physiological effects of efferent activity in *Limulus* eyes are mimicked by cAMP. Thus, it is predicted that the release of neurotransmitter from efferent terminals will stimulate an increase in cAMP in *Limulus* eyes (Fig. 6, #2). Here we showed that efferent nerve input enhanced the phosphorylation of a major substrate for cAMP PK, the 122 kD protein (Edwards and Battelle, 1987; this study), at sites specific for purified cAMP PK. Because the 122 kD protein is not a substrate for Ca^{+2}/calmodulin protein kinase (Weibe *et al.*, 1989) or protein kinase C (Weibe, Calman, and Battelle, unpub. obs.), our results provide strong indirect evidence that efferent nerve input increases the intracellular concentration of cAMP in the lateral eye.

OCT, acting apparently through an OCT-specific receptor, stimulates a rise in intracellular cAMP in preparations of ventral and lateral eyes *in vitro* (Kaupp *et al.*, 1982; Battelle and Wishart, unpub. obs.). Thus, our current results are also consistent with the idea that OCT is released in response to efferent fiber activity *in vivo* (Fig. 6, #1). However, we cannot exclude the possibility that the 122 kD protein is phosphorylated in response to another, unidentified neurotransmitter that is released from efferent terminals and acts at a receptor coupled to adenylate cyclase.

Several observations lead us to predict that the 122 kD protein is involved in some aspect of the efferent-stimulated changes in retinal function (Fig. 6, #3). Its phosphorylation is stimulated by efferent innervation, and correlates with efferent stimulated changes in visual sensitivity. It is a major substrate for cAMP PK in *Limulus* eyes, and cAMP is believed to mediate many of the effects of efferent innervation on retinal function. Further analysis of the role of this protein in efferent-stimulated changes in visual function requires a detailed characterization of the protein and its cellular distribution.

Is the 122 kD protein the only protein phosphorylated in response to efferent innervation?

The 122 kD protein was the only detectable substrate for OCT stimulated phosphorylation in intact retinal cells *in vitro* (Edwards and Battelle, 1987), and in the experiment shown in Figure 3 of this study, the 122 kD protein was the only one that showed a detectable change in phosphorylation that correlates with efferent input *in vivo*. However, we wish to emphasize that, in the present study, conditions were optimized specifically to examine changes in the level of phosphorylation of the 122 kD protein, and changes in the phosphorylation of quantitatively more minor protein components may have been missed. Studies with broken cell preparations revealed other potential substrates for cAMP-dependent phosphorylation (Edwards and Battelle, 1987), but it is unclear whether these are relevant substrates in intact cells.

Because the effects of efferent nerve activity, OCT, and cAMP on retinal function in *Limulus* are many and diverse, the 122 kD protein is unlikely to be the only protein that becomes modified. But the 122 kD protein clearly is a major protein substrate in *Limulus* eyes, and it is phosphorylated, and presumably regulated, by cAMP-, OCT-, and efferent innervation.

Acknowledgments

We thank Lynn Milstead and James Netherton for assisting in producing the figures. This work was supported by basic research grants from the National Science Foundation (BNS 86-07660 and BNS 89-09052 to B-A.B.), and undergraduate research training grants from the National Science Foundation (BBS 87-12402) and the Grass Foundation (to E.M.W.).

Contributions of the Authors

S. C. Edwards was principally responsible for designing, conducting, interpreting, and describing this

study; A. W. Andrews performed the back phosphorylation assays; G. H. Renninger provided expertise critical to the performance of the electrophysiological assays; E. M. Wiebe set up the electronics required for monitoring retinal sensitivity and examined the distribution of the 122 kD protein. B-A. Battelle oversaw all aspects of the study, was heavily involved in its design and the interpretation of the data, and, together with G. H. Renninger, contributed significantly to the generation of the manuscript.

Literature Cited

Barlow, R. B., Jr. 1983. Circadian rhythms in the *Limulus* visual system. *J. Neurosci.* **3:** 856–870.

Barlow, R. B., Jr., S. J. Bolanowski Jr., and L. M. Brachman. 1977. Efferent optic nerve fibers mediate circadian rhythms in the *Limulus* eye. *Science* **197:** 86–89.

Battelle, B-A., and J. A. Evans. 1984. Octopamine release from centrifugal fibers of the *Limulus* peripheral visual system. *J. Neurochem.* **42:** 71–79.

Battelle, B-A., and J. A. Evans. 1986. Veratridine-stimulated release of amine conjugates from centrifugal fibers in the *Limulus* peripheral visual system. *J. Neurochem.* **46:** 1464–1472.

Battelle, B-A., J. A. Evans, and S. C. Chamberlain. 1982. Efferent fibers to *Limulus* eyes synthesize and release octopamine. *Science* **216:** 1250–1252.

Beavo, J. A., P. J. Bechtel, and E. G. Krebs. 1974. Preparation of homogeneous cAMP-dependent protein kinase(s) and its subunits from rabbit skeletal muscle. *Meth. Enzymol.* **38:** 299–308.

Calman, B. G., M. A. Lauerman, A. C. Wishart, M. Schmidt, and B-A. Battelle. 1990. A monoclonal antibody to photoreceptor cells in *Limulus*. *Invest. Ophthalmol. Vis. Sci. (suppl.).* **31:** 286.

Chamberlain, S. C., and R. B. Barlow Jr. 1980. Neuroanatomy of the visual afferents in the horseshoe crab (*Limulus polyphemus*). *J. Comp. Neurol.* **192:** 387–400.

Clark, A. W., R. Millecchia, and A. Mauro. 1969. The ventral photoreceptor cells of *Limulus* I. The microanatomy. *J. Gen. Physiol.* **54:** 289–309.

Dougan, D. F. H., and D. N. Wade. 1978. Octopamine receptors and their structural specificity. *Clin. Exp. Pharmacol. Physiol.* **5:** 341–349.

Edwards, S. C., and B-A. Battelle. 1987. Octopamine- and cAMP-stimulated phosphorylation of a protein in *Limulus* ventral and lateral eyes. *J. Neurosci.* **7:** 2811–2820.

Evans, J. A., S. C. Chamberlain, and B-A. Battelle. 1983. Autoradiographic localization of newly-synthesized octopamine to retinal efferents in the *Limulus* visual system. *J. Comp. Neurol.* **219:** 369–383.

Evans, P. D. 1981. Multiple receptor types for octopamine in the locust. *J. Physiol. (Lond.)* **318:** 99–122.

Fahrenbach, W. H. 1971. The morphology of the *Limulus* visual system. IV. The lateral optic nerve. *Z. Zellforsch. Mikrosk. Anat.* **114:** 532–545.

Fahrenbach, W. H. 1981. The morphology of the *Limulus* visual system. VII. Innervation of photoreceptors by neurosecretory efferents. *Cell Tissue Res.* **216:** 655–659.

Groome, J. R., and W. H. Watson III. 1987. Mechanism for amine modulation of the neurogenic *Limulus* heart: evidence for involvement of cAMP. *J. Neurobiol.* **18:** 417–431.

Heukeshoven, J., and R. Dernick. 1985. Simplified method of silver staining of proteins in polyacrylamide gels and the mechanism of silver staining. *Electrophoresis* **6:** 103–112.

Horne, J. A., and G. H. Renninger. 1988. Circadian photoreceptor organs in *Limulus*. I. Ventral, median, and lateral eyes. *J. Comp. Physiol. A* **162:** 127–132.

Kass, L., and R. B. Barlow Jr. 1981. Pharmacological agents partially reproduce the effects of a circadian clock on *Limulus* lateral eye. *Biol. Bull.* **161:** 348.

Kass, L., and R. B. Barlow, R. B. Jr. 1984. Efferent neurotransmission of circadian rhythms in *Limulus* lateral eye. I. Octopamine-induced increases in retinal sensitivity. *J. Neurosci.* **4:** 908–917.

Kass, L., J. L. Pelletier, G. H. Renninger, and R. B. Barlow Jr. 1983. cAMP: a possible intracellular transmitter of circadian rhythms in *Limulus* photoreceptors. *Biol. Bull.* **164:** 378.

Kass, L., J. L. Pelletier, G. H. Renninger, and R. B. Barlow Jr. 1988. Efferent neurotransmission of circadian rhythms in *Limulus* lateral eye. II. Intracellular recordings in vitro. *J. Comp. Physiol. A* **164:** 95–105.

Kass, L., and G. H. Renninger. 1988. Circadian change in function of *Limulus* ventral photoreceptors. *Vis. Neurosci.* **1:** 3–11.

Kaupp, U. B., C. C. Malbon, B-A. Battelle, and J. E. Brown. 1982. Octopamine stimulated rise in cAMP in *Limulus* ventral photoreceptors. *Vis. Res.* **22:** 1503–1506.

Laemmli, U. K. 1970. Cleavage of structural proteins during assembly of the head of the phage T4. *Nature* **277:** 680–685.

Nestler, E. J., and P. Greengard. 1984. *Protein Phosphorylation in the Nervous system.* New York: Wiley.

O'Day, P. M., and J. E. Lisman. 1985. Octopamine enhances dark adaptation in *Limulus* ventral photoreceptors. *J. Neurosci.* **5:** 1490–1496.

Pelletier, J. L., L. Kass, G. H. Renninger, and R. B. Barlow Jr. 1984. cAMP and octopamine partially mimic a circadian clock's effect on *Limulus* photoreceptors. *Invest. Ophthalmol. Vis. Sci.* (Suppl.) **26:** 378.

Peterson, G. L. 1977. A simplification of the protein assay method of Lowry *et al.* which is more applicable. *Anal. Biochem.* **83:** 346–356.

Renninger, G. H., L. Kass, J. L. Pelletier, and R. Schimmel. 1988. The eccentric cell of the *Limulus* lateral eye: encoder of circadian changes in visual responses. *J. Comp. Physiol. A* **163:** 259–270.

Renninger, G. H., R. Schimmel, and C. A. Farrell. 1989. Octopamine modulates photoreceptor function in the *Limulus* lateral eye. *Vis. Neurosci.* **3:** 83–94.

Seamon, K. B., W. Padnett, and J. W. Daly. 1981. Forskolin: unique diterpene activator of adenylate cyclase in membranes and in intact cells. *Proc. Nat. Acad. Sci. U.S.A.* **78:** 3363–3367.

Towbin, H., T. Staehelin, and J. Gordon. 1979. Electrophoretic transfer of proteins from polyacrylamide gels to nitrocellulose sheets. Procedure and some applications. *Proc. Nat. Acad. Sci. U.S.A.* **74:** 4350–4354.

Uchiyama, H. 1989. Centrifugal pathways to the retina: influence of the optic tectum. *Vis. Neurosci.* **3:** 183–206.

Valtorta, F., W. Schiebler, R. Jahn, B. Ceccarelli, and P. Greengard. 1986. A solid-phase assay for the phosphorylation of proteins blotted on nitrocellulose membrane filters. *Anal. Biochem.* **158:** 130–137.

Warren, M. K., and S. K. Pierce. 1982. Two cell volume regulatory systems in the *Limulus* myocardium: an interaction of ions and quaternary ammonium compounds. *Biol. Bull.* **163:** 504–516.

Watson, W. H., and C. J. Augustine. 1982. Peptide and amine modulation of the *Limulus* heart; a simple nervous network and its target tissue. *Peptides*, **3:** 485–492.

Wiebe, E. M., A. C. Wishart, S. C. Edwards, and B-A. Battelle. 1989. Ca^{++}/calmodulin-stimulated phosphorylation of photoreceptor proteins in *Limulus*. *Vis. Neurosci.* **3:** 107–117.

Reference: *Biol. Bull.* **178:** 279–285. (June, 1990)

The Sequencing, Synthesis, and Biological Actions of an ANP-Like Peptide Isolated from the Brain of the Killifish *Fundulus heteroclitus*

D. A. PRICE[1], K. E. DOBLE[1], T. D. LEE[2], S. M. GALLI[3], B. M. DUNN[4], B. PARTEN[4], AND D. H. EVANS[5]

[1]*The Whitney Laboratory, St. Augustine, Florida 32086,* [2]*Division of Immunology, Beckman Research Institute of the City of Hope, Duarte, California 91010,* [3]*Department of Physiology, School of Medicine, University of Florida, Gainesville, Florida 32611,* [4]*Department of Biochemistry, School of Medicine, University of Florida, Gainesville, Florida 32611, and* [5]*Department of Zoology, University of Florida, Gainesville, Florida 32611*

Abstract. We have extracted, purified, and sequenced an ANP-like peptide from the killifish. The peptide was extracted from whole brains with acidic acetone, and the aqueous phase remaining after evaporation of the acetone was subjected directly to HPLC. A pure peak was obtained after three successive HPLC steps. A key part of our purification method was the deliberate oxidation of methionyl residues in the peptide between the second and third HPLC steps. The purified peptide was chemically sequenced, and its molecular weight was determined by fast atom bombardment mass spectrometry (FABms). The peptide is 22 amino acids long and has considerable sequence similarity to the known natriuretic peptides, especially within the disulfide bonded "ring"; but unlike these known peptides it ends immediately after the second half cystine. Though it lacks a C-terminal "tail," the killifish peptide is equipotent to rat ANP in our radioimmunoassay, which employs an antiserum to the rat peptide. Furthermore, this brain peptide is equipotent to eel ANP in relaxing toadfish aortic rings, though both fish peptides are slightly less potent than rat ANP.

Introduction

The natriuretic and diuretic activities of mammalian atrial extracts were first reported in 1981 (DeBold *et al.*, 1981) and were soon ascribed to various atrial natriuretic peptides (ANPs) ranging in molecular weight from 2 kD to about 13 kD. In the past nine years, natriuretic peptides have also been isolated from brain, and the genetic basis of the family has been clarified.

Each mammalian species has two genes encoding ANP-like peptides: an A gene and a B gene. The precursor arising from the A gene is gamma-ANP; it contains 126 amino acid residues (13 kD), and corresponds to the primary gene product minus the signal sequence (Kangawa *et al.*, 1984). Similarly, the B gene gives rise to a precursor designated gamma-BNP (Sudoh *et al.*, 1988, 1989; Kojima *et al.*, 1989; Seilhamer *et al.*, 1989).

Both the A and B genes are expressed in the hearts of all of the mammalian species examined so far, and ANP is present in all of the brains. However, the expression of the B gene in the brain, and the relative abundance of its products in heart and brain, seem to vary with species. In the pig, for example, the B precursor is somewhat (a few fold) more prevalent than the A in brain, whereas the A form is much more common (50 times) than the B in atrium (Aburaya *et al.*, 1989b). In contrast, the B precursor in the rat is not expressed at all in brain and, in fact, accounts for only a minor portion of the activity (compared to ANP) in any tissue (Aburaya *et al.*, 1989a).

The most abundant product of the A gene in atria is gamma-ANP, itself (126 residues), but active peptides as short as 21 amino acids have also been isolated from rat atria (reviewed by Lewicki *et al.*, 1986). All of the smaller peptides corresponded to fragments of gamma-ANP.

Received 23 February 1990; accepted 20 March 1990.

Abbreviations: Atrial Natriuretic Peptide (ANP), Brain Natriuretic Peptide (BNP), Fast Atom Bombardment mass spectroscopy (FABms).

The precursors derived from the B gene in various species have amino acid differences that affect their post-translational processing. In rat atrium, for example, the B gene gives rise to a 45 amino acid peptide and no smaller products have been found (Flynn *et al.*, 1989). However, in the pig brain, gamma-BNP is processed to both 32 and 26 amino acid forms (Sudoh *et al.*, 1988), but these smaller peptides seem not to occur in human brain (Sudoh *et al.*, 1989).

Regardless of size or tissue of origin, all of the biologically active peptides contain a disulfide-linked ring of 17 amino acid residues. This ring is essential for ANP-like biological activity (Misono *et al.*, 1984).

ANPs have also been isolated and sequenced from the atria of sub-mammalian vertebrates (Miyata *et al.*, 1988; Sakata *et al.*, 1988; Takei *et al.*, 1989; sequences are shown in Fig. 5), and ANP-like immunoreactivity occurs in the brain as well. In the toadfish, the total brain levels of ANP-like immunoreactivity are comparable to those of the heart (Galli *et al.*, 1988); in contrast, mammalian heart expresses much higher levels of both ANP and BNP precursors than the brain (Sudoh *et al.*, 1989). This may reflect a relatively greater physiological role for brain ANP in fish compared to mammals, so we thought it important to isolate and sequence an ANP-like peptide from fish brain.

Materials and Methods

Radioimmunoassay (RIA)

We used an antiserum to rat ANP provided by M. I. Phillips (University of Florida), together with iodinated synthetic rat ANP (Peninsula Laboratories), to provide an RIA. Rat ANP was iodinated with chloramine T and separated from unbound iodide on a C18 Sep-Pak (Waters); the methods were basically the same as those used previously with FMRFamide (Price, 1982). Two modifications are important, however: first, contact with metabisulfite must be minimized (5–10 s); second, the peptide should be eluted from the Sep-Pak with 80% aqueous acetonitrile containing 0.1% trifluoroacetic acid, rather than methanol. In some cases, we purified the iodinated peptide by HPLC, but this could be avoided if the metabisulfite contact was sufficiently brief. In the actual assay, we also used the same buffers and charcoal suspension as for the FMRFamide RIA.

When the sequence of eel ANP was determined, some synthetic peptide became available to us (a kind gift from Y. Takei and the Protein Research Foundation of Japan). We have tested it in the RIA with rat ANP trace and have also iodinated it (as above) and used it as trace.

Extraction and purification

Fundulus brains were kindly provided (over the course of weeks) by Peter Lin (Whitney Laboratory) who was dissecting the fish in order to collect the pituitaries. We accumulated the brains (30–40 mg each) in flasks containing acidic (0.1% trifluoroacetic acid) acetone to a final concentration of 2 brains/ml. The flasks were kept at −20°C between successive additions.

When sufficient material had been collected, the acetone was decanted from the brains and clarified by centrifugation. The acetone was removed on a rotary evaporator, leaving an aqueous fraction which was centrifuged, filtered, and neutralized to pH 7.0 with dilute sodium hydroxide solution. The solution was pumped onto an HPLC column (Aquapore Octyl Prep 10, 100 × 10 mm, from Brownlee) at 4 ml/min. After loading, the column was washed with 0.1% aqueous TFA, and then with 16% acetonitrile in 0.1% TFA. Finally, a gradient of acetonitrile (16%–40% over 30 min) was started. Half-minute fractions were collected, and 2 μl aliquots were taken from each fraction for RIA.

The immunoreactive fractions were pooled, diluted with water containing 0.1% TFA (2–3 times the original volume), and applied to an RP-300 (Brownlee) column (220 × 2.1 mm) by pumping at .5 ml/min. Elution of the column was performed with the same gradient as described for the Prep 10 above. The major immunoreactive fraction was oxidized with 1.5% hydrogen peroxide for 15 min and re-run on this same HPLC system.

Sequencing and FAB mass spectrometry (FABms)

The peak immunoreactive fraction from the third HPLC step was divided in half. The half to be used for FABms analysis was dried on a Speed-Vac, and mailed to the mass spectrometry laboratory. There, the residue was redissolved in a very small (few μl) volume of dimethylsulfoxide, and 1–2 μl of this was used for analysis as described previously (Bullock *et al.*, 1988). The remaining half (about 0.1 ml) of the fraction was applied (in 3 portions with intermediate drying) directly to a preconditioned glass-fiber filter disk containing 3 mg of Polybrene. The disk was placed in the sequencer (Applied Biosystems 470A gas-phase sequencer with an on-line 120A PTH analyzer), and the PTH-amino acid derivatives in each cycle were identified by their retention times and quantitated by comparison of the peak areas to standards.

Synthesis

The peptide G-W-N-R-G-C-F-G-L-K-L-D-R-I-G-S-M-S-G-L-G-C was synthesized on an Applied Biosystems 430A peptide synthesizer starting from t-Boc-Cys(4-CH_3-benzyl)-PAM resin (Applied Biosystems) on a 0.1 mmole scale. Each amino acid was added in a double coupling procedure using the manufacturer's programs. The complete resin was recovered in 77% yield

Table I

Amino acid compositions of synthetic ANP

Amino acid	Ratios		
	Crude found	Pure found	Theor.
Glycine	5.93	5.76	6
Leucine	3.14	3.25	3
Arginine	1.90	2.13	2
Methionine	.60	1.02	1
Phenylalanine	.93	.85	1
Serine	1.95	1.97	2
Aspartic acid	2.07	2.13	2
Isoleucine	.99	1.00	1
Lysine	1.05	.83	1
Cystine (1/2)	+	1.98	2

+: Present, but not quantified.

by weight. The peptide was removed from the resin with anhydrous HF/anisole (9/1) at 0°C for 1 h. The peptide was extracted with 10% acetic acid/water and yielded 118 mg after lyophilization. The amino acid analysis is shown in Table I (crude). The formyl group (from the indole ring of Trp) was removed and the disulfide bond formed by bubbling air through a 5×10^{-5} *M* solution of peptide in .5 *M* ammonium bicarbonate, which had been adjusted to pH 8.7 with ammonium hydroxide. The peptide was purified by HPLC and quantitated by amino acid analysis (Table I, pure).

Vasorelaxant activity

Rings cut from the ventral aorta of toadfish (*Opsanus beta*) were suspended in physiological saline and their tension recorded. Peptide solutions were added and the drop in tension recorded (Evans *et al.*, 1989).

Results

Only one major peak of immunoreactivity showed up on the first HPLC fractionation (Fig. 1), but often there were two peaks at the second step separated by about 2 min in elution time (Fig. 2A). We suspected that the earlier-eluting peak might be an oxidation product of the second, and confirmed this by oxidizing the later peak, thereby shifting its retention time to that of the earlier peak (Fig. 2B). This shift is sufficient to move the ANP-like peak out from under the impurities remaining at the second step. We judged the peak to be pure enough for sequencing after the third step. Thus, deliberate oxidation allows purification of the peptide in fewer steps than would otherwise be required.

From about 1500 brains (50 g total) we isolated a peak of immunoreactivity from which we were able to identify 20 of the first 21 amino acid residues from the peptide by sequencing (Fig. 3). At position 6, only dehydro-alanine was present, which is suggestive of the half cystine we would expect by comparison to other ANP-related peptides. In cycle 22, where we expected the other half cystine, no clear signal was observed, nor were any detectable thereafter.

FAB mass spectral analysis showed a prominent protonated molecular ion at m/z 2341.2 (Fig. 4B), which was in good agreement with the value of 2341.1 calculated for the cyclic peptide with a methionine sulfoxide and ending with the second half cystine. The doubly protonated molecular ion was observed at m/z 1171. The ion distribution of the protonated molecular ion cluster was in substantial agreement with that calculated from

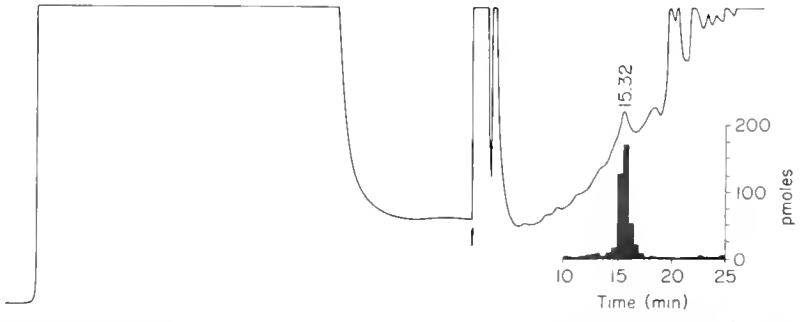

Figure 1. HPLC fractionation of the aqueous fraction remaining after evaporation of acetone from the initial extract (Brownlee Aquapore Octyl column, 100 × 10 mm). The UV absorbance at 210 nm (0.4 AU full scale) is plotted against time, and the immunoreactivity is shown as a histogram. The solvent is pumped at 4 ml/min throughout, and fractions of 0.5 min are collected during the gradient elution. The sample is loaded through the pump inlet and washed in with aqueous HPLC buffer (0.1% TFA); the absorbance remains off-scale during the loading, but drops down during the washing. When the absorbance has leveled off, the flow is switched to 16% ACN in 0.1% TFA, and when this solvent reaches the detector (arrow), a linear gradient is started to 40% ACN at 30 min.

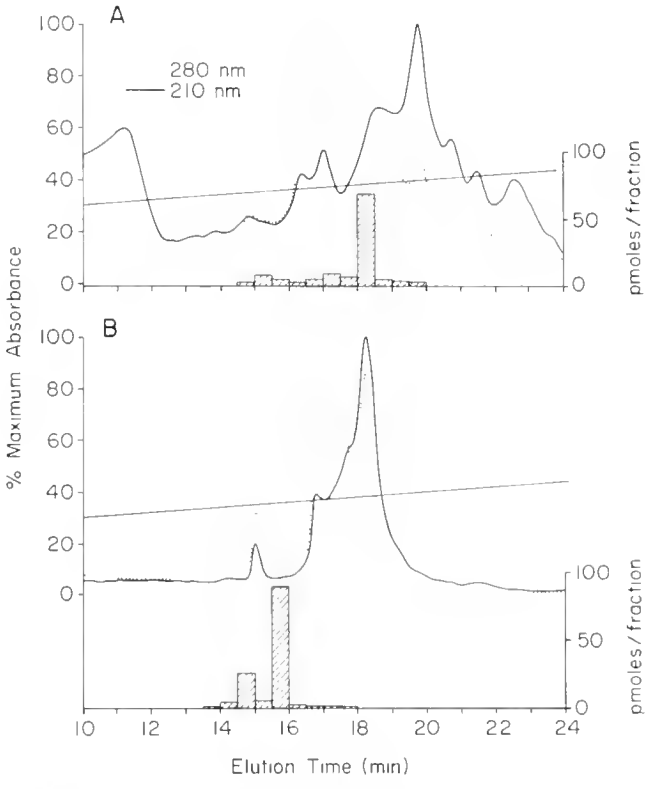

Figure 2. Further HPLC fractionation of the immunoreactive peak from Figure 1 on an Aquapore RP-300 column (220 × 2.1 mm). Loading, gradient and solvents as in Figure 1, but the flow rate is 0.5 ml/min. A. The immunoreactive peak from Figure 1 is diluted with 0.1% TFA and chromatographed. B. The immunoreactive peak from A is oxidized with hydrogen peroxide and chromatographed. A delay of about 0.2 ml (0.4 min) between the UV detector and fraction collector is not corrected for in the figure, so the peak of immunoreactivity corresponds to the UV peak at 15 min.

the elemental composition. The greater than predicted intensities of the higher mass ions (*e.g.*, 2343 and 2344) is probably due to a partial reduction of the disulfide bond during analysis (this would add 2 to the molecular ion).

Similarly, the signal at m/z of 2325 may correspond to a portion of the peptide in which the methionine sulfoxide was reduced back to methionine. Both of these reactions are promoted by the sample matrix, a mixture of dithiothreitol and dithioerythritol made strongly acidic with camphor sulfonic acid.

Taking the FABms data together with the sequence analysis, we conclude that the fish brain peptide has the sequence shown (Fig. 5).

The synthetic *Fundulus* brain peptide had the same elution time as the natural peptide, and the oxidized synthetic material had the same elution time as the oxidized natural peptide, when run under the same HPLC conditions as those used in the purifications. The *Fundulus* brain peptide eluted much later than the synthetic eel heart ANP and slightly later than rat ANP. The oxidized form of the synthetic *Fundulus* peptide has the same retention time as rat ANP.

Vasorelaxant activity

The synthetic *Fundulus* brain peptide is approximately equipotent to eel ANP in relaxing toadfish aortic rings, and both are very similar in potency to rat ANP (Fig. 6).

Immunoreactivity

In the RIA, using either eel ANP or rat ANP as trace, the *Fundulus* ANP peptide is about equiactive to rat ANP, and 3 to 5 fold more active than eel ANP (Fig. 7). All three of the peptides used to generate the curves shown in Figure 7 were quantified by amino acid analysis, so we are confident that the *Fundulus* and rat peptides are very similar in potency, and that both are slightly more potent than the eel peptide. The eel and *Fundulus* peptides consistently gave log/logit slopes of about −1, but the slope with the rat peptide was steeper.

Discussion

We have isolated and sequenced an ANP-like peptide from the brain of *Fundulus heteroclitus*. Like other ANPs and BNPs, this new natriuretic peptide contains a highly conserved, 17-residue disulfide bonded ring; regions outside the ring are, as usual, poorly conserved (Fig. 5). Within the ring, the killifish peptide is most sim-

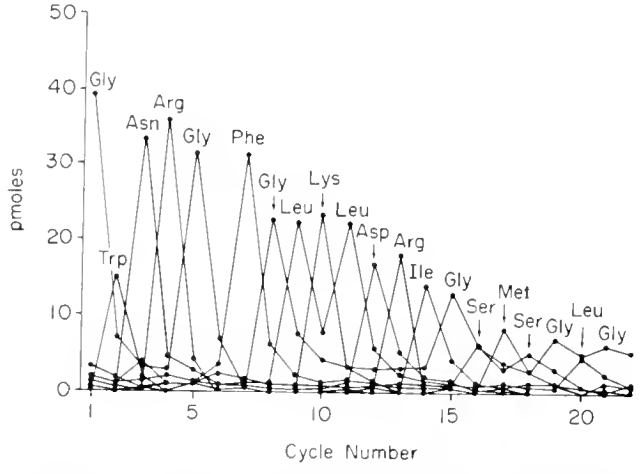

Figure 3. The yields of 11 PTH amino acids at each cycle of the sequencer analysis of the mildly oxidized peptide (Applied Biosystems): the value shown for serine is the sum of serine and dehydroalanine. The assignment for each position is shown. No assignment could be made for position 6, or for 22 and later. An increase in dehydroalanine at position 6 is consistent with this residue being a half cystine, but cystine cannot normally be identified without some pre-sequencing modification.

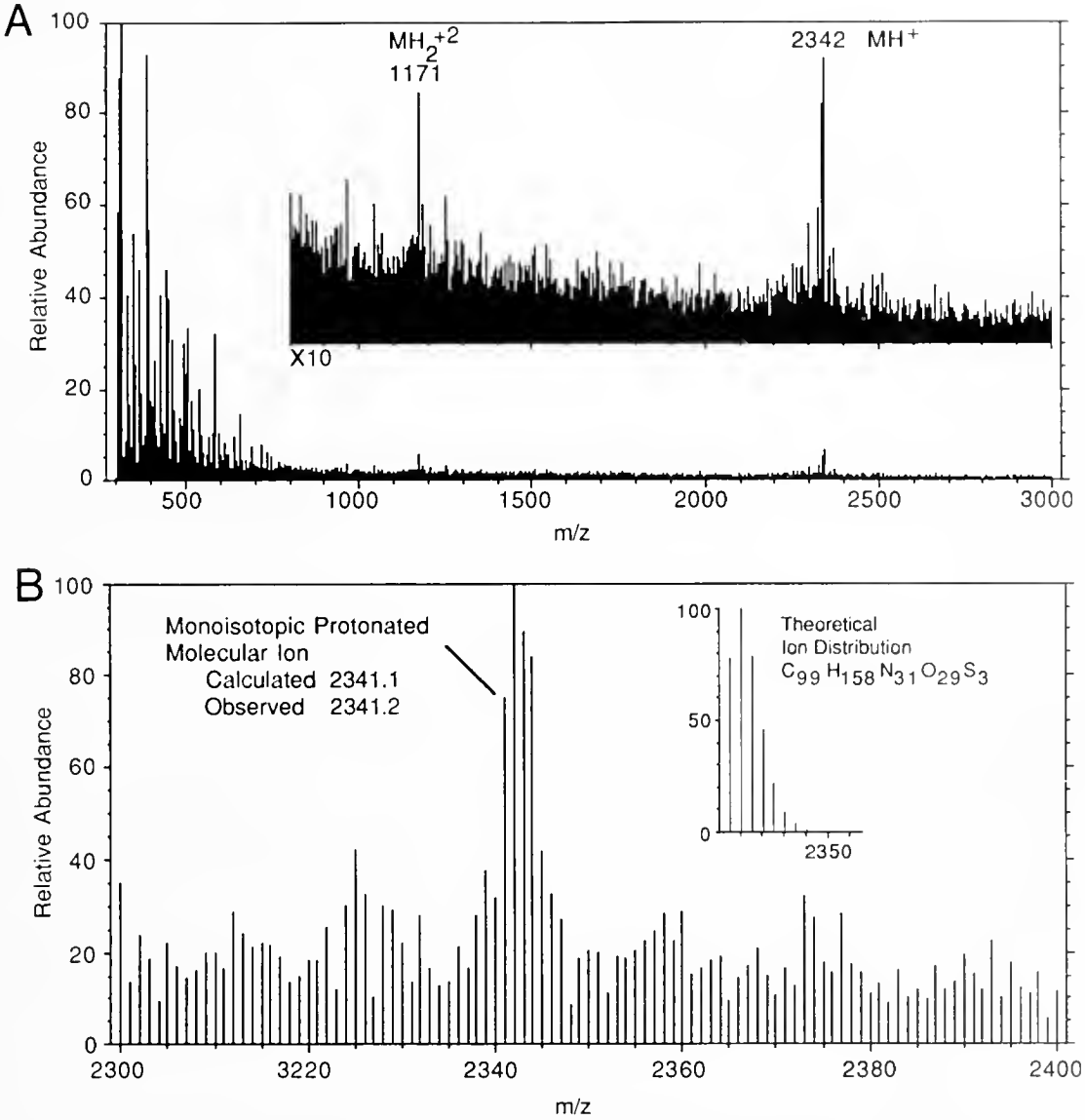

Figure 4. Positive ion FAB mass spectrum of the purified, mildly oxidized peak. A. Scan up to 3000 nominal mass. In the inset the x-axis is unchanged, but the y-axis is expanded 10-fold. The masses shown are rounded to the nearest integer. The two labeled ion clusters are the singly and doubly protonated molecular ions. B. The mass region around 2342, expanded to show the singly protonated molecular ion cluster. The theoretical ion distribution expected for a compound with the elemental composition found is shown in the inset.

ilar to an ANP isolated from eel heart (2 amino acid differences), and both fish peptides are quite similar to a peptide isolated from porcine brain (3 differences within the ring; Fig. 5).

The complete absence of a C-terminal "tail" is a unique feature not previously reported for any natriuretic peptide. The FABms data establish that the peptide sequenced had no tail, but we cannot completely rule out the possibility that a tail was lost by proteolysis during purification. Such degradation is unlikely, however, because the retention time of the immunoreactive peak remains the same when extracts are prepared in other ways (data not shown), and Y. Takei (pers. comm.) has sequenced an eel brain ANP-like peptide that also has no tail. Still, this question will not be settled until the cDNA encoding the precursor has been isolated.

The C-terminal tail seems to be irrelevant to either the relaxing activity of the peptide or its immunoreactivity. Thus, synthetic killifish peptide and eel ANP (which has a C-terminal tail) are equipotent in relaxing toadfish aor-

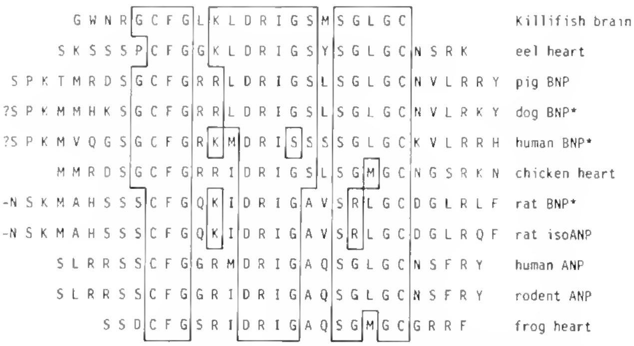

Figure 5. The amino acid sequence of the *Fundulus* brain ANP-like peptide compared to other ANP peptides. The residues in these other peptides that are identical to those in *Fundulus* are boxed. The one-letter abbreviations for the amino acids are used. *Predicted from cDNA sequence. ?Exact length of predominant peptide is unknown. -These peptides are longer than shown.

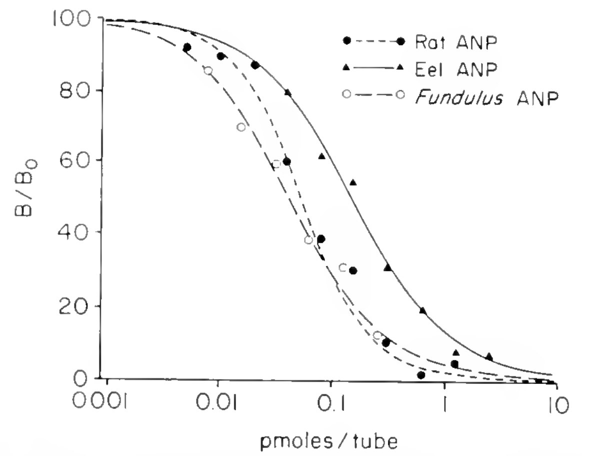

Figure 7. A comparison of the immunoreactivity of rat ANP (1–28), eel ANP, and *Fundulus* brain ANP-like peptide using an RIA with an antiserum to rat ANP and with iodinated eel ANP as trace.

tic rings (Fig. 6). Moreover, the new peptide is as immunoreactive as rat ANP in an RIA which employs the eel ANP as trace. The latter result is surprising since the RIA antiserum was raised to the rat peptide. Finally, we conclude that the apparent functional unimportance of the C-terminal tail is consistent with the dissimilarity of its sequence from one peptide to another (Fig. 5).

In mammals, the levels of ANP-like immunoreactivity in the heart are orders of magnitude higher than those of any other tissue, but such a tissue distribution is not a general characteristic of fish. For example, Galli *et al.* (1988) measured roughly equal levels of immunoreactivity in the brains and hearts of several species of teleosts using the same antiserum employed in our experiments.

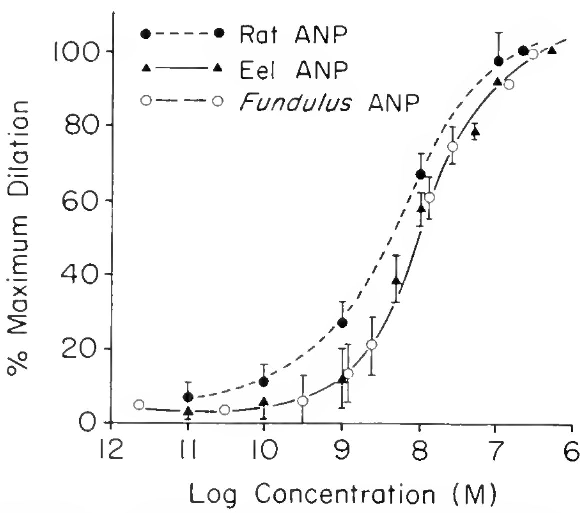

Figure 6. A comparison of the relaxing activity on rings of toadfish (*Opsanus beta*) ventral aorta, of rat ANP (1–28), eel ANP, and *Fundulus* brain ANP-like peptide.

Because this antiserum reacts about equally well with the *Fundulus* and eel peptides (Fig. 7), and because the eel peptide was isolated from heart, and the *Fundulus* from brain, the simplest interpretation of the data of Galli *et al.* (1988) is that heart and brain have roughly equal levels of peptide. Still, the immunoreactivity in the eel heart is (as in mammals) mostly in a high molecular weight form (Takei *et al.*, 1990), and this form may not be as immunoreactive as the smaller molecules that have been isolated and synthesized, and which we have used as standards.

Fish plasma contains ANP-like immunoreactivity, and the levels decrease with adaptation to reduced salinity (Galli *et al.*, 1988; Evans *et al.*, 1989). But neither the identity of the circulating peptide, nor its source, is known with certainty. In rats, even though the heart contains much more immunoreactivity than the brain, changes in hypothalamic and pituitary secretion of ANP markedly affect the blood levels of ANP (Baldissera *et al.*, 1989). Therefore, in species of teleosts like *Fundulus*, where levels of natriuretic peptide are about equal in brain and heart, the brain may be the major source of circulating peptide.

Acknowledgments

We would like to thank M. I. Phillips and B. Kimura for providing antiserum and for help in starting up the RIA for ANP; P. Lin and co-workers for providing so many *Fundulus* brains; Y. Takei and his collaborators at the Protein Research Foundation of Japan for giving us some eel ANP and being so helpful in sharing data on fish ANP-like peptides. We would also like to thank L. Milstead for preparing the figures and M. J. Greenberg for helpful criticism of the manuscript. This work was

partially supported by grants from NIH (HL28440 to D.A.P.), and NSF (PCM-8302621 to D.H.E.).

Literature Cited

Aburaya, M., N. Minamino, J. Hino, K. Kangawa, and H. Matsuo. 1989a. Distribution and molecular forms of brain natriuretic peptide in the central nervous system, heart and peripheral tissue of rat. *Biochem. Biophys. Res. Commun.* **165:** 880–887.

Aburaya, M., N. Minamino, K. Kangawa, K. Tanaka, and H. Matsuo. 1989b. Distribution and molecular forms of brain natriuretic peptide in porcine heart and blood. *Biochem. Biophys. Res. Commun.* **165:** 872–879.

Baldissera, S., J. W. Menani, L. F. Sotero Dos Santos, A. L. V. Favaretto, J. Gutkowska, M. Q. A. Turrin, S. M. McCann, and J. Antunes-Rodrigues. 1989. Role of the hypothalamus in the control of atrial natriuretic peptide release. *Proc. Natl. Acad. Sci. USA* **86:** 9621–9625.

Bulloch, A. G. M., D. A. Price, A. D. Murphy, T. D. Lee, and H. N. Bowes. 1988. FMRFamide peptide in *Helisoma*: identification and physiological actions at a peripheral synapse. *J. Neurosci.* **8:** 3459–3469.

DeBold, A. U., H. B. Bornstein, A. T. Veress, and H. Sonnenberg. 1981. A rapid and potent natriuretic response to intravenous injection of atrial myocardial extract in rats. *Life Sci.* **28:** 89–94.

Evans, D. H., E. Chipouras, and J. A. Payne. 1989. Immunoreactive atriopeptin in plasma of fishes: its potential role in gill hemodynamics. *Am. J. Physiol.* **257:** R939–R945.

Flynn, T. G., A. Brar, L. Tremblay, I. Sarda, C. Lyons, and D. B. Jennings. 1989. Isolation and characterization of iso-rANP, a new natriuretic peptide from rat atria. *Biochem. Biophys. Res. Commun.* **161:** 830–837.

Galli, S. M., D. H. Evans, B. Kimura, and M. I. Phillips. 1988. Changes in plasma and brain levels of atrial natriuretic peptide in fish adapting to fresh water and sea water. *FASEBJ* **2:** A524.

Kangawa, K., Y. Tawaragi, S. Oikawa, A. Mizuno, Y. Sakuragawa, H. Nakazato, A. Fukuda, N. Minamino and H. Matsuo. 1984. Identification of rat gamma atrial natriuretic polypeptide and characterization of the cDNA encoding its precursor. *Nature* **312:** 152–155.

Kojima, M., N. Minamino, K. Kangawa, and H. Matsuo. 1989. Cloning and sequence analysis of cDNA encoding a precursor for rat brain natriuretic peptide. *Biochem. Biophys. Res. Commun* **159:** 1420–1426.

Lewicki, J. A., B. Greenberg, M. Yamanaka, G. Vlasuk, M. Brewer, D. Gardner, J. Baxter, L. K. Johnson, and J. C. Fiddes. 1986. Cloning, sequence analysis, and processing of the rat and human atrial natriuretic peptide precursors. *Fed. Proc.* **45:** 2086–2090.

Misono, K. S., H. Fukumi, R. T. Grammer, and T. Inagami. 1984. Rat atrial natriuretic factor: complete amino acid sequence and disulfide linkage essential for biological activity. *Biochem. Biophys. Res. Commun.* **119:** 524–529.

Miyata, A., N. Minamino, K. Kangawa, and H. Matsuo. 1988. Identification of a 29-amino acid natriuretic peptide in chicken heart. *Biochem. Biophys Res. Commun.* **155:** 1330–1337.

Price, D. A. 1982. The FMRFamide-like peptide of *Helix aspersa*. *Comp. Biochem. Physiol* **72C:** 325–328.

Sakata, J., K. Kangawa, and H. Matsuo. 1988. Identification of new atrial natriuretic peptides in frog heart. *Biochem. Biophys. Res Commun.* **155:** 1338–1345.

Seilhamer, J. J., A. Arfsten, J. A. Miller, P. Lundquist, R. M. Scarborough, J. A. Lewicki, and J. G. Porter. 1989. Human and canine gene homologs of porcine brain natriuretic peptide. *Biochem. Biophys. Res. Commun.* **165:** 650–658.

Sudoh, T., K. Kangawa, N. Minamino, and H. Matsuo. 1988. A new natriuretic peptide in porcine brain. *Nature* **332:** 78–81.

Sudoh, T., K. Maekawa, M. Kojima, N. Minamino, K. Kangawa, and H. Matsuo. 1989. Cloning and sequence analysis of cDNA encoding a precursor for human brain natriuretic peptide. *Biochem. Biophys. Res. Commun.* **159:** 1427–1434.

Takei, Y., A. Takahashi, T. X. Watanabe, K. Nakajima, and S. Sakakibara. 1989. Amino acid sequence and relative biological activity of eel atrial natriuretic peptide. *Biochem. Biophys. Res. Commun.* **164:** 537–543.

Takei, Y., H. Tamaki, and K. Ando. 1990. Identification and partial characterization of immunoreactive and bioactive atrial natriuretic peptide in eel hearts. *J. Comp. Physiol.* (in press).

Reference: *Biol. Bull.* **178:** 286–294. (June, 1990)

Adaptations to the Deep-Sea Oxygen Minimum Layer: Oxygen Binding by the Hemocyanin of the Bathypelagic Mysid, *Gnathophausia ingens* Dohrn

N. K. SANDERS AND J. J. CHILDRESS

Oceanic Biology Group, Marine Science Institute and Department of Biological Sciences, University of California, Santa Barbara, California 93106

Abstract. The bathypelagic mysid, *Gnathophausia ingens* Dohrn, lives aerobically at oxygen partial pressures as low as 6 torr in the oxygen minimum layer off southern California. This study is concerned with the O_2 binding properties of this mysid's hemocyanin and the function of the pigment in O_2 uptake at low P_{O_2}. The effect of temperature on *in vivo* hemolymph pH ($\Delta pH/\Delta T = -0.018$) was measured from 2.5 to 12.5°C. Hemocyanin concentration was estimated to be 24 mg/l, corresponding to an O_2 binding capacity of about 0.3 mmol O_2/l. Freezing of hemolymph samples significantly decreased the affinity and cooperativity of HcO_2 binding, necessitating the use of fresh hemolymph. The HcO_2 affinity was high (P_{50} of 1.4 torr at 5.5°C, pH 7.87), allowing the loading of O_2 even at 6 torr. The cooperativity of HcO_2 binding was also high ($n_{50} = 3.5$ at 5.5°C, pH 7.87); presumably allowing the pigment to function effectively as an O_2 transporter within the small P_{O_2} difference between the environment and the tissues. Temperature differences within the environmental range (2–10°C) had no significant effect on the oxygen affinity ($\Delta H = -6.7$ kJ/mol, pH 7.7) or on the cooperativity of O_2 binding. A large Bohr shift ($\Delta \log P_{50}/\Delta pH = -0.80$ to -0.81) was present at all temperatures. L-lactate produced moderate increases in HcO_2 affinity ($\Delta \log P_{50}/\Delta \log$ [lactate] $= -0.13$ at pH 7.9) and in cooperativity. Regional and ontogenetic comparisons suggest that regional and ontogenetic differences in HcO_2 affinity occur in this species. This mysid has a hemocyanin of unusually high O_2 affinity and cooperativity of O_2 binding for a crustacean living at low temperatures, and this appears to be an adaptation for oxygen loading and transport at the cold, low oxygen conditions in deep-sea oxygen minimum layers. The reduced temperature sensitivity of HcO_2 affinity may also be an adaptation to low oxygen.

Received 31 July 1989; accepted 29 March 1990.

Introduction

Zones of minimum oxygen are found at intermediate depths in most of the world's oceans and, although the oxygen partial pressure in some of these "oxygen minimum layers" is only a few torr, populations of pelagic metazoans exist there (Schmidt, 1925; Sewell and Fage, 1948; Banse, 1964). These oxygen minimum layers are pelagic habitats with stable conditions of continuously low oxygen and low temperature at intermediate depths (400–1000 m depth) over vast areas. Previous studies have shown that most of the pelagic crustaceans living off California, where P_{O_2} at the oxygen minimum is 6 torr, are able to do so aerobically by being unusually effective at extracting O_2 from water (Childress, 1968, 1971, 1975). This remarkable ability has been intensively studied in the lophogastrid mysid *Gnathophausia ingens* Dohrn (Childress, 1968, 1971; Belman and Childress, 1976).

Gnathophausia ingens is the largest entirely pelagic crustacean, and has a circumglobal distribution between 30°N and 30°S latitudes. The mature female (instar 13, estimated duration of 530 days) produces and carries a single brood at depths greater than 800 m (Childress and Price, 1978, 1983). The first two free-living instars (3 and 4, estimated durations of 95 days each) live at depths as shallow as 150–200 m. However, for much of its life (instars 5 to 10, "intermediate instars," estimated durations from 168 to 207 days each), *G. ingens* occurs at depths of about 400–800 m, corresponding to the depth range

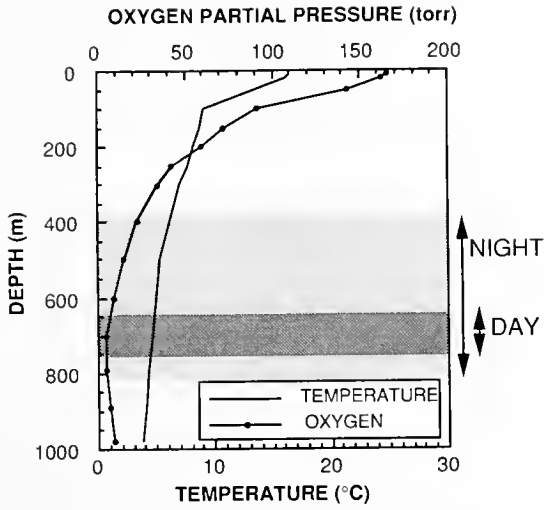

Figure 1. The day and night depth distribution patterns of *Gnathophausia ingens* shown with environmental temperatures and O_2 partial pressures off southern California.

of the oxygen minimum layer off southern California (Fig. 1, 6–20 torr O_2, 4–7°C) (Childress and Price, 1978, 1983). This species has limited anaerobic capacity, and is able to live aerobically at the lowest P_{O_2} it encounters off southern California (Childress, 1968; 1971), although it may use anaerobic metabolism briefly to support high activity levels at the lowest O_2 levels. Its ability to regulate its oxygen consumption to P_{O_2} values as low as 3 torr is due to its ability to maintain a high ventilatory flow (up to 8 body volumes min^{-1}), and simultaneously to remove a large fraction (50–80%) of the oxygen in the inhaled water (Childress, 1971). These abilities are made possible by the highly developed gills and circulatory system (Belman and Childress, 1976). Belman and Childress (1976) also showed that a high affinity, high cooperativity respiratory protein must be present to provide sufficient hemolymph oxygen carrying capacity and unloading at the very low P_{O_2} values at which these mysids live, although at the time of their studies no respiratory protein had been found in the order Mysidacea.

A preliminary report demonstrated the presence, in *Gnathophausia ingens*, of a hemocyanin having a high affinity for oxygen at 20°C (Freel, 1978), but the properties of this hemocyanin were not measured at environmentally appropriate temperatures or pH levels. The report by Freel is the only publication on a hemocyanin in the entire order Mysidacea. The high affinity at high temperature reported by Freel appears anomalous; *i.e.*, the O_2 affinity of hemocyanin normally increases greatly at low temperatures, so how could the hemocyanin be functional at the much lower environmental temperature? In fact, shallow-dwelling crustaceans living at lower temperatures have hemocyanins with lower O_2 affinities as well as lower cooperativities, presumably to maintain a sufficient unloading of O_2 to their tissues (Redmond, 1968; Mangum, 1982; Mauro and Mangum 1982a). In addition, the temperature sensitivity of O_2 binding by hemocyanin is often greater at lower temperatures (Mauro and Mangum, 1982b; Bridges, 1986; Burnett *et al.*, 1988). The hemocyanin of *G. ingens* also seems to have subunits that are quite different electrophoretically from those of decapods (J. E. Reese and C. P. Mangum, pers. comm.), so its properties are of interest for this reason as well.

Although the O_2 binding properties of the hemocyanins of crustaceans inhabiting sometimes hypoxic environments are well studied (Mangum, 1980; Mangum 1983a, b; Morris and Taylor, 1983, 1985; Bridges, 1986), the deep-sea oxygen minima are unique in having stable low oxygen conditions in combination with constant low temperatures. *Gnathophausia ingens*, like most midwater crustaceans, is denser than seawater (Childress and Nygaard, 1974). Therefore, it must swim continuously and cannot cope with low O_2, or other conditions in its habitat, by becoming quiescent. Because it lives in this habitat continuously, its adaptations must be effective in the context of uninterrupted exposure and activity, clearly a different situation from that facing benthic animals in periodically hypoxic habitats.

The present study of the hemocyanin of *Gnathophausia ingens* was undertaken to determine its functional properties, so that its role in oxygen uptake and transport in this species could be elucidated. In addition, the oxygen binding properties of the hemocyanin of *G. ingens* from off Hawaii were measured to gain insight into the poorer regulation of oxygen consumption found in mysids collected from those waters (Cowles, 1987). The functional properties of hemocyanin from brooding female *G. ingens* (instar 13) were also measured to examine possible ontogenetic changes as individuals move to greater depths and higher values of P_{O_2}.

Materials and Methods

Individuals of *Gnathophausia ingens* were collected during 1985–1988 from San Clemente Basin off southern California, and from the leeward side of the Hawaiian island of Oahu from depths of 400–1200 m. Animals were captured with a modified opening-closing Tucker trawl (3.1 m square mouth), and were brought to the surface in a thermally insulated cod end (Childress *et al.*, 1978), which kept the temperature near 5°C. California animals were kept at 5.5°C on board ship, and were housed (within 3 days of capture) in individual 1-liter containers at 5.5°C at the Santa Barbara laboratory until used in experiments. Except where noted (regional comparisons, Fig. 5), all experiments were conducted with

hemolymph samples from mysids collected off California.

Initial sampling

Hemolymph samples were removed from the ventral sinus and ventral abdominal vessel of *Gnathophausia ingens*. In the measurement of pH, a sample of hemolymph was withdrawn with a syringe and, without air exposure, was immediately injected into a Radiometer glass capillary electrode (Radiometer America G298A) in a water jacketed chamber, in conjunction with a reference electrode (Radiometer K171). Precision buffers were used to calibrate the electrode (Radiometer S1500 and S1510). Samples for oxygen equilibrium curves were dialyzed for immediate use, or frozen for later use.

The concentration of hemocyanin in pooled (n = 5) hemolymph samples from *Gnathophausia ingens* (intermediate instar California and Hawaii animals, and brooding females from California) was estimated by measuring the absorbance maximum, near 340 nm, of a 1:100 dilution of hemolymph in 50 mmol/l Tris buffer (pH 8.9) with EDTA (50 mmol/l). Although extinction coefficients have not been determined for mysid hemocyanin, the extinction coefficient for the lobster *Homarus americanus* ($2.69_{1\ cm}^{1\%}$, Nickerson and van Holde, 1971) was used to estimate hemocyanin concentration. The oxygen carrying capacity was estimated from the haemocyanin concentration, assuming a subunit size of 75,000 D.

The concentrations of Na^+, K^+, Ca^{2+}, Mg^{2+}, SO_4^{2-}, and Cl^- in the hemolymph of *Gnathophausia ingens* were measured by single column ion chromatography (Sanders and Childress, 1988), using Wescan cation and anion columns.

The effects of temperature on hemolymph pH in vivo

Individual intermediate instars of *Gnathophausia ingens* were placed in separate 1-liter containers of aerated seawater at 2.5°, 5.0°, 5.5°, 7.5°, 9.0°, or 12°C. After an animal had been maintained at its experimental temperature for 4 h, the pH of its hemolymph was measured. These animals had been captured 1–2 weeks prior to their use.

Oxygen equilibrium curves

To determine the effects of pH and temperature on hemocyanin oxygen binding, dialyzed hemolymph samples were used in a thin-layer spectrophotometric system (Childress *et al.*, 1984; Sanders *et al.*, 1988). Because of the effects of freezing on both affinity and cooperativity (described later), fresh (never frozen) hemolymph samples were used for all measurements except those concerned with freezing and with regional differences in hemocyanin properties.

A small sample of dialyzed *Gnathophausia ingens* hemolymph (5–20 μl) was sandwiched between two layers of teflon membrane (0.006 mm) and placed in a gas-tight, water-jacketed chamber. The absorbance spectrum from 300–800 nm of gas-equilibrated samples was monitored with a Tracor Northern diode array spectrophotometer, and the absorbance at 345 nm was recorded at successively higher oxygen partial pressures. Equilibrium was defined by the absence of further changes in the absorbance spectrum; gas partial pressures around the sample were controlled with a Union Carbide mass flow controller. Oxygen concentrations within the gas-tight sample chamber were monitored with a Systech Instruments Zirconium Cell Oxygen Analyzer. The calibration of the oxygen analyzer was checked frequently with 99.99% oxygen gas, air, and 99.999% nitrogen gas. An additional sample of hemolymph was maintained in a gas-tight, water-jacketed tonometer at the same temperature and gas mixture as the O_2 equilibrium curve sample. The pH of this hemolymph sample was measured near the 50% saturation point at the experimental temperature.

Samples used to determine the effects of temperature and pH on hemocyanin oxygen binding were dialyzed against a physiological saline prepared from the inorganic ion concentrations measured in the hemolymph of intermediate instar *Gnathophausia ingens* from off southern California. Samples were dialyzed for 15–18 h in three changes of physiological saline buffered with 0.05 mol/l Tris buffer (1 part hemolymph to 1000 parts of saline). The effects of L-lactate on O_2 binding by hemocyanin were determined by adding 10 μl of 0, 15, or 150 mmol/l L-lactate in physiological saline to dialyzed 100-μl hemolymph samples. The lactate concentrations in these samples were measured after each experiment using a Boehringer L-lactate test kit.

Data analysis

Results are reported as means and standard deviations unless otherwise noted. Analysis of covariance (ANCOVA) was used to test the significance of differences in the intercepts of regressions only when the slopes did not differ significantly. To examine the properties of this hemocyanin at specific pH values, oxygen equilibrium curves were generated from values of P_{50} and n_{50} interpolated (from regression lines describing $\Delta \log P_{50}/\Delta pH$ and $\Delta n_{50}/\Delta pH$) for those pH values. Software programs for all data analyses were written by Dr. S. Morris.

Results

Concentrations of hemocyanin and inorganic ions in hemolymph

Hemolymph samples from freshly captured intermediate instars of *Gnathophausia ingens* from off California

Table I

The concentrations (mmol/l) of the major inorganic elements in hemolymph from intermediate instars of Gnathophausia ingens *from off California and Hawaii, and from brooding* G. ingens *females from off California*

Ion	California	Hawaii	Brooding females
Na^+	525.2 ± 13.1 (3)	516.3 ± 13.1 (3)	512.8 ± 16.9 (3)
K^+	23.3 ± 2.1 (3)	21.8 ± 1.3 (3)	20.9 ± 1.4 (3)
Ca^{2+}	11.6 ± 3.1 (3)	6.6 ± 0.8 (3)	7.2 ± 1.2 (3)
Mg^{2+}	12.5 ± 1.1 (3)	15.4 ± 1.2 (3)	12.8 ± 1.5 (3)
SO_4^{2-}	10.1 ± 1.7 (4)	4.5 ± 0.9 (3)	8.7 ± 2.1 (3)
Cl^-	532.8 ± 16.3 (4)	525.6 ± 14.4 (3)	530.8 ± 21.2 (3)

Values were determined by ion chromatography and are reported as means ± 1 standard deviation, followed by the number of observations in parentheses.

and Hawaii had a hemocyanin concentration of 24 mg/ml (pooled samples of 5 individuals at each site), while the hemocyanin concentration in hemolymph of brooding females from California was lower (16 mg/ml, 5 individuals pooled). The O_2 carrying capacities of the hemocyanin in the hemolymphs were estimated at 0.32 and 0.21 mmol/l, respectively. Hemolymph ion concentrations were typical for a marine crustacean (Mangum, 1983a) and differed little among California, Hawaii, and brooding female *G. ingens* (Table I).

Temperature/pH relationship in vivo

The regression line calculated from *in vivo* pH measurements *versus* experimental temperature (2.5–12°C) is: pH = 7.95–0.018 (T°C), $r^2 = 0.82$, n = 35. The short term *in vivo* pH change due to temperature in the hemolymph of intermediate instar *Gnathophausia ingens* ($\Delta pH/\Delta T = -0.018$) was similar to the change due to temperature in the neutral pH of water ($\Delta pH/\Delta T = -0.017$, Reeves, 1977). This value is also similar to *in vivo* hemolymph pH changes measured in other crustaceans over physiological temperature ranges (McMahon and Burggren, 1981; Morris *et al.*, 1985, 1988; Morris and Bridges, 1989).

Effects of pH and temperature on oxygen binding by hemocyanin

The effects of pH and temperature (2–15°C) on oxygen binding by hemocyanin in dialyzed, never frozen hemolymph samples from specimens of *Gnathophausia ingens* captured off California are reported in Figure 2. The effect of pH on hemocyanin oxygen affinity was large (Δ log $P_{50}/\Delta pH = -0.80$, 2 to 10°C and −0.81 at 15°C). There was no significant effect of temperature on HcO_2 affinity over the 2–15°C temperature range, as shown by a comparison of the y-intercepts of the regression lines relating log P_{50} to pH at the different temperatures (ANCOVA). Temperature also had no significant effect on cooperativity from 5 to 15°C (ANCOVA), but the slope of the relationship between n_{50} and pH at 2°C was significantly different from those at the higher temperatures. The temperature sensitivity of HcO_2 binding was analyzed by van't Hoff plots (Fig. 3). The data for these plots were obtained by estimating P_{50} values at three constant values of pH from the regression analyses (Δ log $P_{50}/\Delta pH$) of data reported in Figure 2. The low ΔH values at constant pH ($\Delta H = -6.7$ kJ/mol, pH 7.7, 2–10°C) emphasize the lack of temperature sensitivity in this species in the physiological temperature range (Fig. 3).

Effects of L-lactate on oxygen binding by hemocyanin

The effects of L-lactate at 5°C on HcO_2 binding in dialyzed hemolymph (never frozen) of *Gnathophausia ingens* from California are shown in Figure 4. The slopes of the log P_{50} *versus* pH regressions for 0.09 and 14.32 mmol/l L-lactate were not significantly different, but the elevations were ($P < 0.005$, ANCOVA). Thus lactate significantly increases the affinity of this hemocyanin for O_2 (Δ log P_{50}/Δ log [lactate] = −0.17, 5.0°C, pH 7.9). The corresponding regression line at 1.23 mmol/l L-lactate fell in between the other two, but its slope was significantly different from those of the other two ($P < 0.025$). Analysis of covariance showed that cooperativity of oxy-

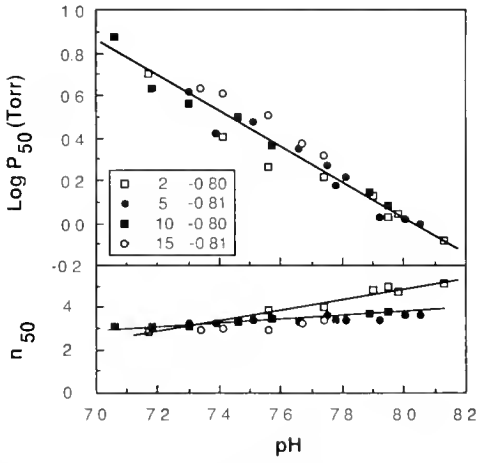

Figure 2. The effects of pH and temperature on HcO_2 binding in dialyzed (never frozen) hemolymph samples from intermediate instar *Gnathophausia ingens* from California. Regression equations for oxygen affinity of hemocyanin: 2°C, Log $P_{50} = 6.04 - 0.80$ pH, $r^2 = 0.96$; 5°C, Log $P_{50} = 6.50 - 0.81$ pH, $r^2 = 0.94$; 10°C, Log $P_{50} = 6.47 - 0.80$ pH, $r^2 = 0.98$; 15°C, Log $P_{50} = 6.59 - 0.81$ pH, $r^2 = 0.98$. Regressions for cooperativity (lines for 2°C and 5°C): 2°C, $n_{50} = -14.83 + 2.47$ pH, $r^2 = 0.96$; 5°C, $n_{50} = -0.89 + 0.56$ pH, $r^2 = 0.70$; 10°C, $n_{50} = -3.22 + 0.88$ pH, $r^2 = 0.98$; 15°C, $n_{50} = -5.50 + 1.14$ pH, $r^2 = 0.76$.

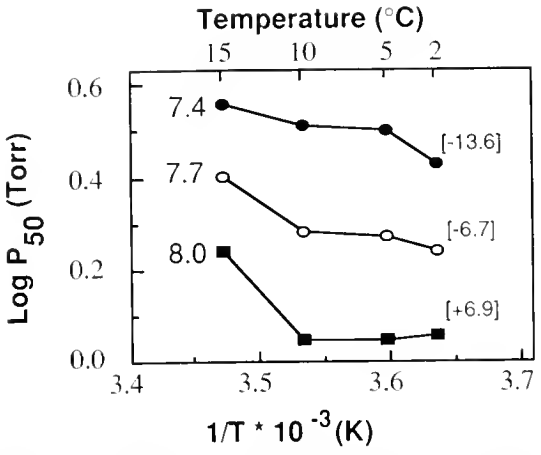

Figure 3. The effect of temperature (2–15°C) on HcO_2 binding of *Gnathophausia ingens* at three constant values of pH (7.4, 7.7, 8.0). Hemolymph samples were taken from intermediate instars of *G. ingens* from California. Numbers in brackets are ΔH values calculated from Log P_{50}/pH data (Fig. 1) at the indicated pH over the 2–10°C temperature range. Points plotted are interpolations from the data in Figure 2.

gen binding by hemocyanin was significantly increased ($P < 0.05$) in the presence of L-lactate (Fig. 4).

Effects of freezing and regional differences on oxygen binding by hemocyanin

When compared with hemolymph samples that had not been frozen, samples from California *Gnathophausia ingens* that had been stored at −80°C for 18–24 months contained hemocyanin with significantly increased O_2 affinity (5°C, $P < 0.05$, ANCOVA, Fig. 5) and significantly decreased cooperativity ($P < 0.05$, ANCOVA). Therefore, we used hemolymph that had never been frozen for all of the other studies on the HcO_2 binding properties of intermediate instar individuals from California. However, because of the availability of frozen but not fresh material, ontogenetic and regional comparisons were made on frozen samples.

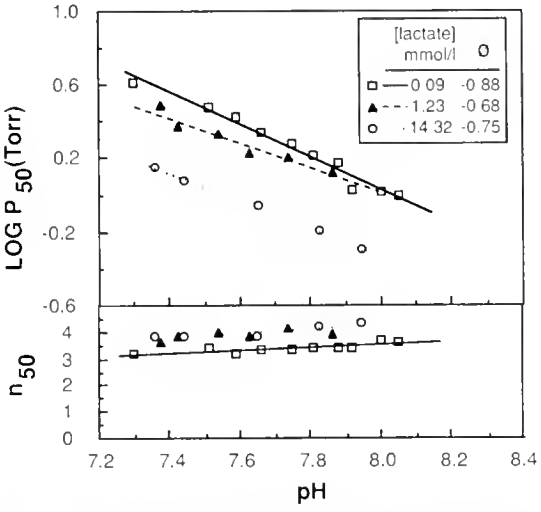

Figure 4. The effects of L-lactate on HcO_2 binding at 5°C of intermediate instars of *Gnathophausia ingens* from California. Regression equations for HcO_2 affinity: 0.09 mmol l^{-1} L-lactate, Log P_{50} = 6.50 − 0.81 pH, r^2 = 0.94; 1.23 L-lactate, Log P_{50} = 3.42 − 0.62 pH, r^2 = 0.89; 14.32 L-lactate, Log P_{50} = 5.70 − 0.75 pH, r^2 = 0.99. Regression equations for cooperativity (lines plotted for 0.09 and 14.32 mmol/l L-lactate): 0.09 mmol l^{-1} L-lactate, n_{50} = −0.83 + 0.55 pH, r^2 = 0.82; 1.23 L-lactate, n_{50} = −2.15 + 0.81 pH, r^2 = 0.79; 14.32 L-lactate, n_{50} = −3.88 + 0.81 pH, r^2 = 0.99.

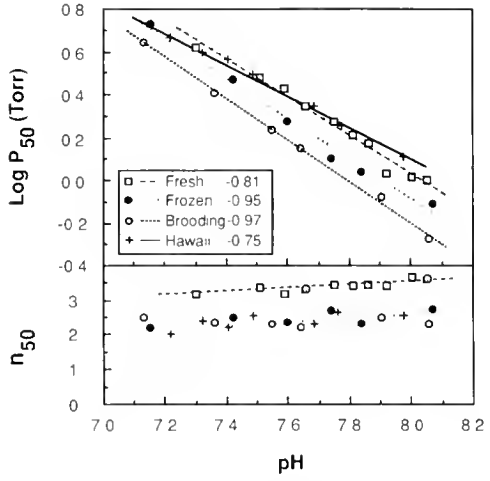

Figure 5. HcO_2 affinity and cooperativity at 5°C in fresh and frozen hemolymph from intermediate instar and brooding female *Gnathophausia ingens* from California, and from intermediate instar Hawaiian *G. ingens*. Regressions for each affinity line: California fresh (fresh), Log P_{50} = 6.50 − 0.81 pH, r^2 = 0.94; California frozen (frozen), Log P_{50} = 7.51 − 0.95 pH, r^2 = 0.99; California brooding female frozen (brood), Log P_{50} = 7.53 − 0.97 pH, r^2 = 0.99; Hawaii frozen (Hawaii), Log P_{50} = 6.06 − 0.75 pH, r^2 = .99. Regressions for cooperativity (lines for California fresh and California frozen): California fresh (fresh), n_{50} = 0.83 + 0.55 pH, r^2 = 0.82; California frozen (frozen), n_{50} = −0.81 + 0.43 pH, r^2 = 0.99; California brooding female frozen (brooding), n_{50} = −0.30–0.07 pH, r^2 = 0.79; Hawaii frozen (Hawaii), n_{50} = −1.93 + 0.57 pH, r^2 = .99

When the HcO_2 binding of frozen, dialyzed hemolymph samples from California brooding females was compared with that of intermediate instars of *G. ingens*, the hemocyanin from the brooding females, had a significantly higher affinity at 5°C, but was not significantly different in cooperativity (ANCOVA, Fig. 5). The hemocyanin in frozen, dialyzed hemolymph samples from Hawaiian intermediate instar *G. ingens* had significantly lower O_2 affinity at 5°C than did that from the California intermediate instars; there was no significant difference, however, in the cooperativity of HcO_2 binding (ANCOVA, Fig. 5). Although the effects of freezing may compromise these results, if freezing had affected all samples equally, then these results would still suggest that ontogenetic changes occur in the hemocyanins of *G. ingens* and that the Hawaiian individuals of this species

living at higher O_2 partial pressures have hemocyanin with a lower O_2 affinity than do California individuals. Studies on fresh material will be necessary to confirm these suggestions.

Discussion

Adaptations to the oxygen minimum layer

Gnathophausia ingens, like most pelagic crustaceans occupying deep-sea oxygen minima, relies primarily on aerobic metabolism, supported by unusually well-developed abilities to remove O_2 from water, to exploit these vast, stable, low O_2 environments (Childress, 1975). Although this species has very little capacity to live without O_2 (it survives for less than 30 min under anoxic conditions), it can regulate its oxygen uptake (P_c as low as 3 torr O_2 at minimal activity) at least to its lowest environmental P_{O_2} (6 torr) when it is routinely active (Childress, 1971). *G. ingens* can regulate its O_2 consumption to such low P_{O_2} values because it maintains a very high ventilatory flow (up to 8 body volumes/min) and a high rate of removal of O_2 from the ventilatory stream (50–80%), even at the lowest P_{O_2} in its environment (Childress, 1971).

The high removal is made possible by great development of the gills and circulatory system in this mysid. The gill surface area is quite large (9–14 cm^2/g wet wt.) for a crustacean, and the oxygen diffusion distance across the branchial epithelium (about 2 μm) is smaller than that measured in most other crustaceans (Belman and Childress, 1976; Taylor, 1982; McMahon and Wilkens, 1983). Therefore, the total oxygen diffusing capacity of the gills of *G. ingens* (as calculated by Belman and Childress, 1976), is much greater than that estimated for other crustaceans, allowing a rate of diffusion of O_2 across the gills that is sufficient even with the very limited O_2 available in its environment. Indeed, a P_{O_2} difference of only about 3–4 torr across the gills was calculated to be sufficient to allow the diffusion of enough O_2 to support routine metabolism. The heart and arterial channels of *G. ingens* are quite large for a crustacean of its size, and the heart also can generate a relatively high systolic pressure for a crustacean of its small size (Belman and Childress, 1976; McMahon and Wilkens, 1983). These properties enable *G. ingens* to generate a high rate of hemolymph flow (55–225 ml/kg/min) as compared to other crustaceans, providing rapid turnover of oxygen depleted venous hemolymph (Belman and Childress, 1976; McMahon and Wilkens, 1983).

However, even with these circulatory adaptations, Belman and Childress (1976) estimated that, without a functional O_2 binding protein in the hemolymph, an unreasonably high value for blood flow (more than 4 times the known maximum values) would be necessary to supply

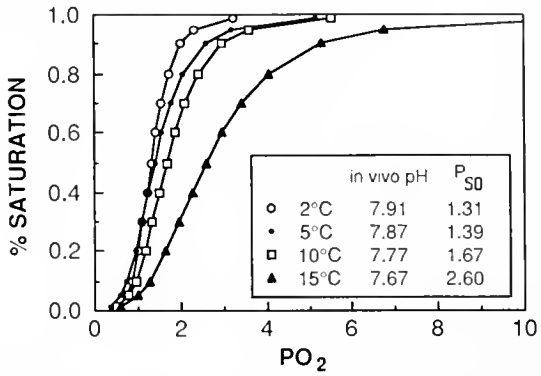

Figure 6. *Gnathophausia ingens* HcO_2 equilibrium curves generated from data in Figure 2, using predicted values of *in vivo* pH [see regression: $\Delta pH/\Delta T$ (°C) in results section] at particular temperatures. The environmentally appropriate temperature for the intermediate instars of this species is 5°C.

the oxygen needed to sustain aerobic respiration in *G. ingens* at 6 torr O_2. To maintain the O_2 consumption rate reported (Childress, 1968, 1971), the mysid would need between 9–36 times greater hemolymph oxygen carrying capacity (0.10–0.78 mmol/l) than could be explained by the maximum dissolved oxygen present at 6 torr (0.011 mmol/l), assuming 100% use of bound O_2 (Belman and Childress, 1976). The hemocyanin oxygen carrying capacity, estimated for California *G. ingens* from measurements of hemocyanin concentration, is 0.32 mmol/l, in good agreement with the estimate of Belman and Childress (1976).

In order to be an effective transporter of O_2, a respiratory protein must be able to load O_2 to near saturation when in the gills, and to unload a large fraction of this O_2 at the tissues. The O_2 binding properties of *G. ingens* hemocyanin can be evaluated for the extent to which they appear to be adaptive in this context. The very high affinity for O_2 should enable the hemocyanin of *Gnathophausia ingens* to bind oxygen from the low P_{O_2} water of the oxygen minimum layer. Because this hemocyanin is 95% saturated at 3 torr O_2 and physiological temperatures (5°C, pH 7.87, Fig. 6), its affinity is high enough to maintain the necessary O_2 gradient of 3 to 4 torr across the gills to support routine metabolism (Belman and Childress, 1976). The high cooperativity at low temperature of this hemocyanin enables it to release most of its bound O_2 with a drop in P_{O_2} of only 2 torr (5°C, pH 7.87, Fig. 6). The large Bohr shift of this hemocyanin would be expected to make this unloading even more effective.

The increase in O_2 affinity by lactate might well be adaptive in this species, as it is in *Callinectes sapidus,* compensating for decreases in affinity resulting from lowered pH during periods of maximal activity, which would have to be partially anaerobically fueled at 6 torr O_2 (Childress, 1971; Booth *et al.* 1982). The concentra-

tion of *G. ingens* hemocyanin is among the lowest ones measured (Mangum, 1983a). However, at the very low P_{O_2} values at which this mysid lives, this O_2 carrying capacity is far greater than the dissolved O_2. The O_2 affinity of *G. ingens* hemocyanin, being temperature insensitive, is unaffected by the small temperature changes within the species' vertical range—a possible adaptation. Given the narrow range of P_{O_2} over which this hemocyanin functions, even small temperature-caused shifts in affinity could have detrimental effects on O_2 transport if the hemocyanin were not temperature insensitive. A low thermal sensitivity of $Hc O_2$ affinity appears to be usual for the hemocyanins of non-hydrothermal vent deep-sea decapods, as well as mysids (Arp and Childress, 1985; Sanders, 1989). Thus, the O_2 binding properties of its hemocyanin appear to be highly adaptive in supporting the uptake and transport of O_2 at the normal low P_{O_2} values in the environment of *G. ingens*.

Patterns of functional properties of hemocyanins

The literature on crustacean hemocyanins deals almost exclusively with shallow water decapods, particularly brachyurans. The oxygen binding properties of hemocyanin have been considered to be conservative in expression (Mangum, 1980), yet plastic in their inherent ability to adapt to environmental conditions. Temperature is an environmental variable with direct and indirect effects on $Hc O_2$ binding, and several generalizations, concerning the effects of temperature on hemocyanins—and based almost entirely on data for shallow living species—have been stated. One such generalization is that the oxygen affinity of hemocyanins is lower in species from "low" temperature environments to offset the usual effect of lower temperature, an increase in the affinity of hemocyanin (Redmond, 1968, Mangum, 1982, Mauro and Mangum, 1982a). The oxygen affinities of hemocyanins from deep-sea pelagic crustaceans do not fit this generalization, however, and they would not be functional in the low oxygen environment found in midwater zones if this were the case (Sanders, 1989). Instead, the quite low P_{O_2} appears to be the selective factor most strongly affecting the functional properties of hemocyanins from O_2 minimum layers, resulting in high $Hc O_2$ affinity and reduced temperature sensitivity. This does support a second generalization concerning temperature and $Hc O_2$ affinity, which suggests an inverse relationship between the Bohr shift (which is large for *Gnathophausia ingens*) and temperature sensitivity (Burnett *et al.*, 1988). Therefore, crustacean hemocyanins seem to have a considerable degree of adaptive plasticity. In those cases that do not follow the expected patterns—*e.g.*, the absence of temperature sensitivity of *G. ingens* Hc, the reverse temperature sensitivity found in *Palaemon elegans* Hc (Morris *et al.* 1985), and hydrothermal vent crab Hc (Sanders *et al.*, 1988; Sanders, 1989)—the hemocyanins appear to be adapted for the particular habitat and habits of the organisms.

Ontogenetic differences

The life history characteristics of *Gnathophausia ingens* are discussed in detail by Childress and Price (1978). Briefly, females of *G. ingens* reproduce only once, and brood the eggs and young in a marsupium for about 530 days. There are 13 distinct instars in this species, and the newly released juveniles (instars 3 and 4) are found at 175–300 m depth (40–100 torr O_2). Intermediate instars (numbers 5 to 10) are found at 650–750 m by day (6–10 torr O_2 off California), and disperse between 400–800 m (6–22 torr O_2) by night. Brooding females (carrying the first 2 instars) live at depths between 800 and 1400 m (10–20 torr O_2). Given the large changes in depth, and therefore temperature and P_{O_2}, during the life of an individual *G. ingens*, one might expect ontogenetic changes in its hemocyanin. The brooding females, in particular, have much lower metabolic rates and live at lower temperatures and slightly higher P_{O_2} values. The hemocyanin concentration of brooding females is reduced relative to that of intermediate instars living at shallower depths and, based on frozen material, the oxygen affinity of the hemocyanin from the brooding female appears to be significantly higher (Fig. 4). The lower O_2 carrying capacity is consistent with the lower metabolic rate and activity of this instar (Childress, 1975).

Regional differences

Gnathophausia ingens is also found off the Hawaiian islands. The depth distribution of the population of *G. ingens* sampled off Oahu was essentially identical to that of *G. ingens* collected in the basins off southern California. Thus, the animals in Hawaiian waters are exposed to much higher P_{O_2} (approximately 20 torr at day-time depths, and greater than 100 torr at night) than those off southern California. Hawaiian individuals of *G. ingens* cannot regulate O_2 consumption as well as can individuals from California (P_c = 10–30 torr, depending upon oxygen consumption rate, for Hawaiian *G. ingens* individuals, Cowles, 1987). Although there is no significant difference in the oxygen consumption rates, the relationship between oxygen consumption and P_c in the two populations is significantly different. A cursory anatomical comparison of the Hawaiian and Californian *G. ingens* individuals revealed no obvious differences in the circulatory system or gills (J. Childress, unpub. obs.). The hemocyanin concentrations in the hemolymphs of *G. ingens* individuals from these two regions are comparable, but the differences in the functional properties of

the hemocyanins (*e.g.*, the apparently lower O_2 affinity of hemocyanin from Hawaiian animals based on frozen material) may explain, at least in part, the observed differences in the regulation of oxygen consumption. Thus, different populations of the same species, *G. ingens*, in different oceanic regions may have adaptive differences in the functional properties of their hemocyanins. Adaptive regional differences in the O_2 affinities of the hemocyanin of *Callinectes sapidus* result from changes in subunit composition due to acclimation (Mangum and Rainer, 1988).

In summary, the high oxygen affinity of the hemocyanin of the mysid *Gnathophausia ingens* appears to be essential for these pelagic, permanent residents of deep-sea oxygen minimum layers. The high affinity and cooperativity of oxygen binding by their hemocyanin, and the previously reported circulatory and ventilatory adaptations, apparently enable the hemocyanin to be fully saturated with oxygen at very low external values of PO_2, and to release a large percentage of the bound oxygen at the tissues with a very small change in PO_2. Offloading is potentially further facilitated by the presence of a large Bohr effect. This hemocyanin clearly shows a different combination of properties than is found in crustaceans from other habitats. However, these HcO_2 binding properties, are highly adaptive for this species in the O_2 minimum layer habitat. While the oxygen binding properties of hemocyanins from shallow-living species are conservative in expression, the inherent adaptive plasticity of crustacean hemocyanins may be considerably greater than has previously been appreciated.

Acknowledgments

This research was supported by N.S.F. grant OCE 8500237 to J.J.C. and a N.S.F. Predoctoral Fellowship to N.K.S. Special thanks to the captains and crews of the research vessels New Horizon and Pt. Sur for assistance with animal collection. We thank A. Alldredge, A. Kuris, S. Morris, and B. Robison for critical review of earlier versions of this manuscript.

Literature Cited

Arp, A. J., and J. J. Childress. 1985. Oxygen binding properties of the blood of the deep-sea shrimp, *Glyphocrangon vicaria*. *Physiol. Zool.* **58:** 38–45.

Banse, K. 1964. On the vertical distribution of zooplankton in the sea. Pp. 53–1225 in *Progress in Oceanography, Volume II*, M. Sears, ed. Pergamon Press, Oxford.

Belman, B. W., and J. J. Childress. 1976. Circulatory adaptations to the oxygen minimum layer in the bathypelagic mysid *Gnathophausia ingens*. *Biol. Bull.* **150:** 15–37.

Bridges, C. R. 1986. A comparative study of the respiratory properties and physiological function of haemocyanin in two burrowing and two non-burrowing crustaceans. *Comp. Biochem. Physiol* **83A:** 261–270.

Booth, C. E., B. R. McMahon, and A. W. Pinder. 1982. Oxygen uptake and the potentiating effects of increased hemolymph lactate on oxygen transport during exercise in the blue crab, *Callinectes sapidus*. *J. Comp. Physiol.* **148:** 111–121.

Burnett, L. E., D. A. Scholnick, and C. P. Mangum. 1988. Temperature sensitivity of molluscan and arthropod hemocyanins. *Biol. Bull.* **174:** 153–162.

Childress, J. J. 1968. Oxygen minimum layer: vertical distribution and respiration of the mysid *Gnathophausia ingens*. *Science* **160:** 1242–1243.

Childress, J. J. 1971. Respiratory adaptations to the oxygen minimum layer in the bathypelagic mysid *Gnathophausia ingens*. *Biol. Bull.* **141:** 109–121.

Childress, J. J. 1975. The respiratory rates of midwater crustaceans as a function of depth of occurrence and relation to the oxygen minimum layer off Southern California. *Comp. Biochem. Physiol.* **50:** 787–799.

Childress, J. J., and M. Nygaard. 1974. The chemical composition and buoyancy of midwater crustaceans as a function of depth of occurrence off southern California. *Mar. Biol.* **27:** 225–238.

Childress, J. J., and M. H. Price. 1978. Growth rate of the bathypelagic crustacean *Gnathophausia ingens* (Mysidacea: Lophogastridae). I. Dimensional growth and population structure. *Mar. Biol.* **50:** 47–62.

Childress, J. J. and M. H. Price. 1983. Growth rate of the bathypelagic crustacean *Gnathophausia ingens* (Mysidacea: Lophogastridae). II. Accumulation of material and energy. *Mar. Biol.* **76:** 165–177.

Childress, J. J., A. J. Arp, and C. R. Fisher. 1984. Metabolic and blood characteristics of the hydrothermal vent tube-worm *Riftia pachyptila*. *Mar. Biol.* **83:** 109–124.

Childress, J. J., A. T. Barnes, L. B. Quetin, and B. H. Robison. 1978. Thermally protecting cod ends for the recovery of living deep-sea animals. *Deep-Sea Res.* **25:** 419–422.

Cowles, D. L. 1987. Factors affecting the aerobic metabolism of midwater crustaceans. Ph.D. dissertation, University of California, Santa Barbara. 228 pp.

Freel, R. W. 1978. Oxygen affinity of the hemolymph of the mesopelagic mysidacean *Gnathophausia ingens*. *J. Exp. Zool.* **204:** 267–273.

McMahon, B. R., and W. W. Burggren. 1981. Acid-base balance following temperature acclimation in land crabs. *J. Exp. Zool.* **218:** 45–52.

McMahon, B. R., and J. L. Wilkens. 1983. Ventilation, perfusion, and oxygen uptake. Pp. 290–372 in *The Biology of the Crustacea, Vol. 5: Internal Anatomy and Physiological Regulation*, L. H. Mantel, ed. Academic Press, New York.

Mangum, C. P. 1980. Respiratory function of the hemocyanins. *Am. Zool.* **20:** 19–38.

Mangum, C. P. 1982. On the relationship between P_{50} and the mode of gas exchange in tropical crustaceans. *Pac. Sci.* **36:** 403–410.

Mangum, C. P. 1983a. Oxygen transport in the blood. Pp. 373–429 in *The Biology of the Crustacea, Vol. 5: Internal Anatomy and Physiological Regulation*, L. H. Mantel, ed. Academic Press, New York.

Mangum, C. P. 1983b. The effect of hypoxia on hemocyanin-oxygen binding in the horseshoe crab *Limulus polyphemus*. *Molec. Physiol.* **3:** 217–224.

Mangum, C. P., and J. S. Rainer. 1988. The relationship between subunit composition and O_2 binding of blue crab hemocyanin. *Biol. Bull.* **174:** 77–82.

Mauro, N. A., and C. P. Mangum. 1982a. The role of blood in the temperature dependence of oxidative metabolism in decapod crustaceans. I. Intraspecific responses to seasonal differences in temperature. *J. Exp. Zool.* **219:** 179–188.

Mauro, N. A., and C. P. Mangum. 1982b. The role of blood in the temperature dependence of oxidative metabolism in decapod crustaceans. II. Interspecific adaptations to latitudinal changes. *J. Exp. Zool.* **219:** 189–195.

Morris, S. M., and A. C. Taylor. 1983. Diurnal and seasonal variation in physico-chemical conditions within intertidal rock pools. *Estuar. Coast Shelf Sci.* **17:** 151–167.

Morris, S. M., and A. C. Taylor. 1985. The respiratory response of the intertidal prawn *Palaemon elegans* (Rathke) to hypoxia and hyperoxia. *Comp. Biochem. Physiol.* **81A:** 633–639.

Morris, S. M., A. C. Taylor, C. R. Bridges, and M. K. Grieshaber. 1985. Respiratory properties of the haemolymph of the intertidal prawn *Palaemon elegans* (Rathke). *J. Exp. Zool.* **233:** 175–186.

Morris, S. M., P. Greenaway, and B. R. McMahon. 1988. Oxygen and carbon dioxide transport by the haemocyanin of an amphibious crab, *Holthuisana transversa*. *J. Comp. Physiol.* **157B:** 873–882.

Nickerson, K. W., and K. E. van Holde. 1971. A comparison of molluscan and arthropod hemocyanin. I. Circular dichroism and absorption spectra. *Comp. Biochem. Physiol.* **39B:** 855–872.

Redmond, J. R. 1968. The respiratory function of hemocyanin. Pp. 5–23 in *Biochemistry and Physiology of Hemocyanins*, G. Ghiretti, ed. Academic Press, New York.

Reeves, R. B. 1977. The interaction of body temperature and acid-base balance in ectothermic vertebrates. *Ann. Rev. Physiol.* **39:** 559–586.

Sanders, N. K. 1989. Functional properties of hemocyanins from deep-sea crustaceans. *Ph.D. thesis, University of California*, Santa Barbara. 209 pp.

Sanders, N. K., and J. J. Childress. 1988. Ion replacement as a buoyancy mechanism in a pelagic deep-sea crustacean. *J. Exp. Biol.* **138:** 333–343.

Sanders, N. K., A. J. Arp, and J. J. Childress. 1988. Oxygen binding characteristics of the hemocyanins of two deep-sea hydrothermal vent crustaceans. *Respir. Physiol.* **71:** 57–68.

Schmidt, J. 1925. On the contents of oxygen in the ocean on both sides of Panama. *Science* **61:** 592–593.

Sewell, R. B. S., and L. Fage. 1948. Minimum oxygen layer in the ocean. *Nature* **162:** 949–951.

Taylor, E. W. 1982. Control and co-ordination of ventilation and circulation in crustaceans: responses to hypoxia and exercise. *J. Exp. Biol.* **100:** 289–319.

Reference: *Biol. Bull.* **178:** 295–299. (June, 1990)

Jelly Layer Formation in Penaeoidean Shrimp Eggs

WALLIS H. CLARK JR.[1], ASHLEY I. YUDIN[2], JOHN W. LYNN[3], FRED J. GRIFFIN[1], AND MURALIDHARAN C. PILLAI[1]

[1]*Bodega Marine Laboratory, University of California at Davis, Bodega Bay, California 94923;* [2]*Department of Reproductive Physiology, University of California at Davis, Davis, California 95616; and* [3]*Department of Zoology and Physiology, Louisiana State University, Baton Rouge, Louisiana 70803*

Penaeoid eggs undergo dramatic cortical rearrangements and extracellular matrix (ECM) alterations in response to activation. Prior to activation, the outermost ECM is a fibrous vitelline envelope (1, 2, 3). Beneath the vitelline envelope invaginations of the oolemma form extracellular crypts in the egg surface that project into the cortex of the egg (1, 2, 3). These crypts contain jelly precursor (JP), previously termed "jelly-like substance" (4) or cortical specializations or rods (1, 2, 5). The presence of JP in both mature ovarian oocytes, and in eggs at spawning, was first reported by Hudinaga (4), but the limitations of light microscopy led him to conclude incorrectly, that the "jelly-like substance" was intraoocytic, a misconception that was perpetuated in subsequent reports (6, 7). Work in our laboratory has clearly demonstrated that JP was housed in extracellular crypts that extended into the cortical cytoplasm (1, 2, 5). We referred to the release of JP during egg activation as a cortical reaction and contrasted it with the exocytosis of cortical vesicles in other systems (1, 2). Although technically correct, since cortical rearrangements accompany JP release, this terminology has apparently caused some confusion. Bradfield *et al.* (8) have cloned cDNA for a major ovarian polypeptide which they clearly localize to JP in the crypts of ovarian oocytes, but which they refer to as a "cortical granule polypeptide." In the present note, we first document the extraoocytic nature of JP in ovarian oocytes of the penaeoid shrimp *Sicyonia ingentis*, and then trace the formation of the jelly layer from JP during egg activation. Lastly a synopsis is presented, in diagrammatic form, of the ECM changes that result from egg activation in penaeoid shrimp.

Received 12 March 1990; accepted 19 March 1990.

Abbreviations: Jelly Precursor (JP), Extracellular Matrix (ECM).

The extracellular crypts that contain JP appear in penaeoid oocytes during the latter stages of oogenesis (5, 9, 10). Oocytes of *S. ingentis* in this stage possess a centrally located germinal vesicle, a large accumulation of yolk in the form of spherical bodies dispersed throughout the ooplasm, and crypts radially arranged around the periphery (Fig. 1A). Figure 1B reveals the fine structural relationship among the oocyte, a crypt, and a follicle cell of an ovarian oocyte at the completion of crypt formation. An invagination in the oolemma forms each crypt (Fig. 1B). Although the mechanisms by which such invaginations are formed have not yet been demonstrated, the crypts at this stage of oogenesis are clearly extracellular, as has been demonstrated for oocytes of *Penqeus aztecus* (5), *P. setiferus* (5), and *P. japonicus* (10). Laterally and basally the crypts are delineated by the oolemma, whereas apically the crypts are not bounded by the oolemma. Instead, the crypts are overlain by the vitelline envelope, the outermost egg investment prior to activation (1, 2, 3, 11). At this stage, near the completion of oogenesis, the oocyte and its investments are still surrounded by a layer of follicle cells (Fig. 1B).

The crypts of *S. ingentis* eggs contain highly organized, tightly packed "bottle-brush" structures (substructural elements of the jelly precursor) similar to the "feathery" substructural elements described for the cortical rods or specializations of oocytes in *P. aztecus* and *P. setiferus* (5). In *P. aztecus*, the "feathery" material constitutes JP that is 25–30% carbohydrate and 70–75% protein (12). "Bottle-brush" structures are also associated with oocytes of the non-penaeoid decapods, *Homarus americanus* and *H. gamarus* (13, 14)). In *H. americanus*, the

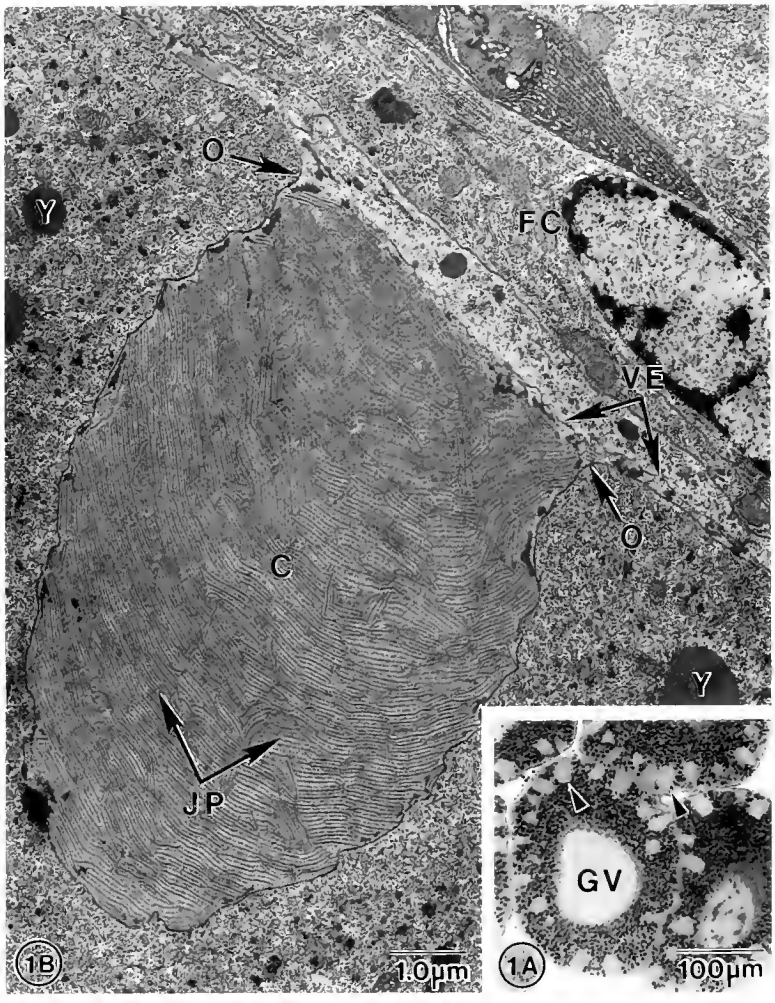

Figure 1. Ovarian oocytes of *Sicyonia ingentis* near the completion of oogenesis. Ovaries of *S. ingentis* were dissected and subsequently fixed and processed according to procedures described by Clark *et al.* (2). A. Light micrograph depicting an oocyte with a germinal vesicle (GV) and radially arranged extracellular crypts (arrow heads). B. Transmission electron micrograph of an extracellular crypt (C) containing jelly precursor (JP). The crypt is separated from the cortical cytoplasm by the oolemma (O) and delimited from the follicle cell layer (FC) by a vitelline envelope (VE). Y = yolk platelet.

Figures 2–5. Jelly precursor (JP) extrusion and jelly layer formation in *Sicyonia ingentis* eggs. Female *S. ingentis* were induced to spawn and eggs collected as described by Pillai *et al.* (18). Eggs were fixed at times described below and processed for light microscopy (A) and transmission electron microscopy (B) as described by Pillai and Clark (3). Eggs spawned into fixative (time "0") still possess JP housed in extracellular crypts (Fig. 2A, arrowheads). In Figure 2B the time "0" egg and its crypts (C) are enveloped by the vitelline envelope (VE). JP, containing "bottle-brush" structures arranged in parallel aggregates, is separated from the cortical cytoplasm by the oolemma (O). Granular material (G), destined to become the surface coat (see ref. 3) lies just beneath the vitelline envelope. Yolk platelets (Y), of two densities, are present in the cortical cytoplasm. At 3–5 min post-spawning, JP extrusion is well underway (Fig. 3A, arrowheads). Although released from the crypts, JP remains predominantly in "bottle-brush" form (Fig. 3B). By 10 min post-spawning, a corona has formed around the egg (Fig. 4A) that consists of a flocculent matrix containing dispersed "bottle-brush" structures (Fig. 4B, arrowheads); Y = yolk platelets. By 15 min, a fully formed jelly layer (JL) is present (Fig. 5A) that is composed entirely of the flocculent matrix (Fig. 5B). In addition, a surface coat (SC) has formed closely apposed to the oolemma.

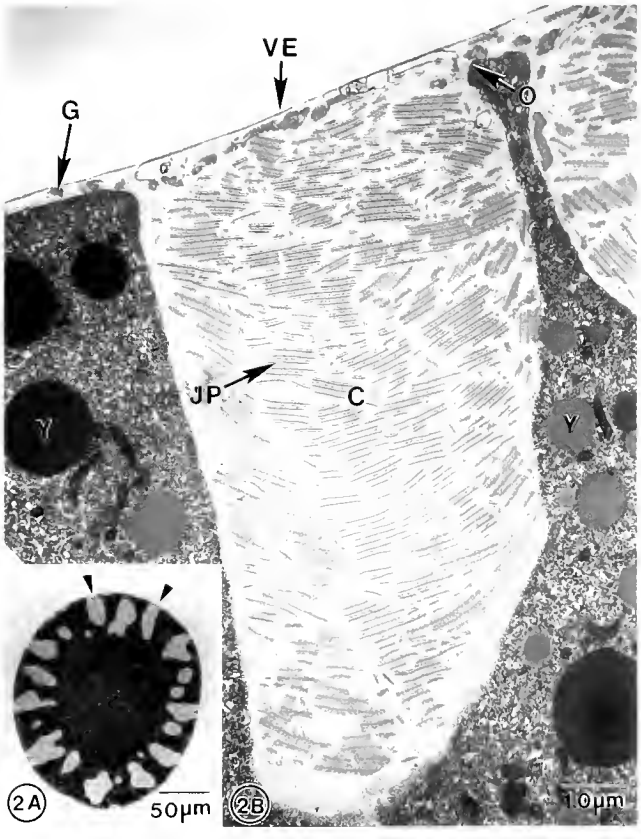
VE
G
O
JP
C
Y
Y
2A
50μm
2B
1.0μm


JP
3A
20μm
3B
1.0μm

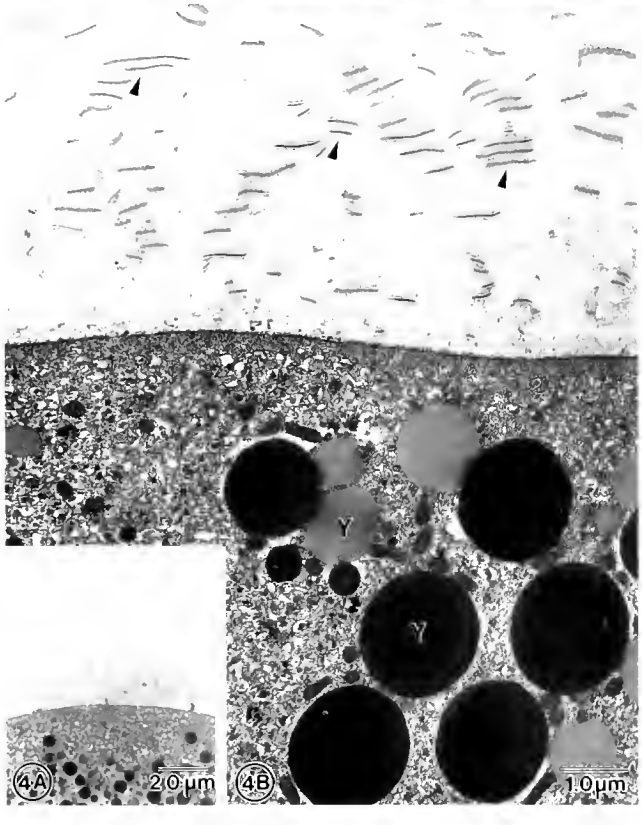
Y
Y
4A
20μm
4B
1.0μm

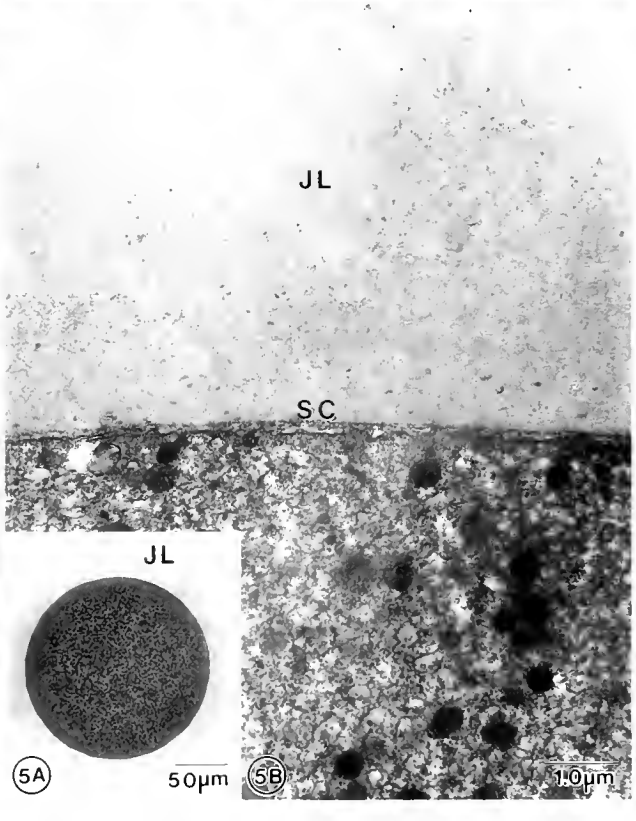
JL
SC
JL
5A
50μm
5B
1.0μm

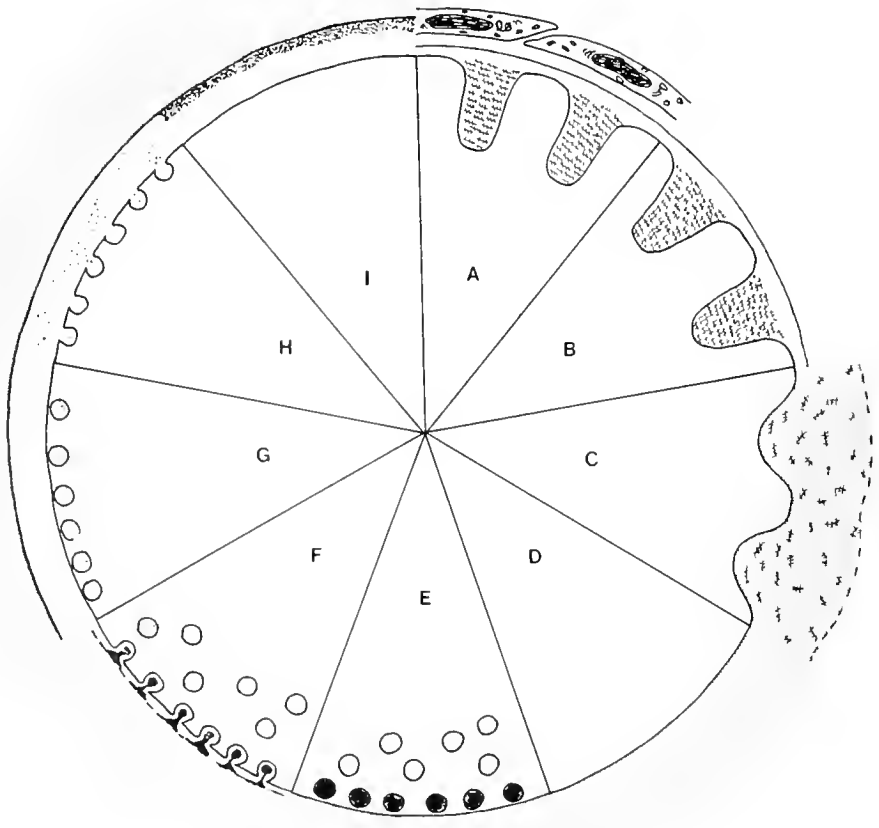

Figure 6. Chronological order of ECM alterations during egg activation. Penaeoid oocytes nearing the completion of oogenesis are enveloped in an acellular vitelline envelope and possess extracellular crypts that contain jelly precursor (JP). The oocytes do not possess cortical vesicles within their cortical cytoplasm (Fig. 6A). At the time of spawning, the JP within the crypts is separated from the surrounding environment by only the vitelline envelope (Fig. 6B). Upon exposure to seawater, the crypts become reduced in size which results in the expulsion of the JP, the lifting and eventual loss of the vitelline envelope, and the establishment of a corona (composed of a flocculent matrix and bottle-brush structures) around the egg (Fig. 6C). Continued transformation or breakdown of the "bottle-brush" structures results in a flocculent jelly layer. By the time the jelly layer has formed, the crypts have vanished (Fig. 6D). Two populations of cortical vesicles (dense vesicles and ring vesicles) arise in the cortical cytoplasm (Fig. 6E). The dense vesicles first undergo exocytosis (Fig. 6F) and give rise to the thin hatching envelope (Fig. 6G). This is closely followed by the exocytosis of the ring vesicles (Fig. 6H). The coalescence of the material from the ring vesicles with the thin hatching envelope results in the formation of a fully formed envelope (Fig. 6I).

"bottle-brush" structures (reported to be of follicular origin) are not contained within crypts, but are rather distributed randomly in the extracellular matrix and contribute to the endochorion of the ovarian oocyte (14). Although the origin of the "bottle-brush" structures of *S. ingentis* oocytes has not yet been documented, preliminary information suggests that they are of oocytic origin (unpub. obs.).

Prior to spawning, *S. ingentis* oocytes undergo germinal vesicle breakdown and ovulation (9). Examination of an egg spawned into fixative (time "0") reveals that neither ovulation nor spawning has caused the expulsion of JP (Fig. 2A). At the fine structural level, the vitelline envelope is evident, overlying the egg and crypts (Fig. 2B). In addition, granular material destined to form the "surface coat" is also closely associated with the oolemma (see also ref. 3). The "bottle-brush" structures in the time "0" egg remain in parallel arrays, apparently attached in groups by their lateral projections. Yolk platelets, although most prevalent deeper in the egg, are

present in the cortical cytoplasm; these are not to be confused with cortical vesicles. In *S. ingentis* eggs, cortical vesicles are not present at the time of spawning, rather they arise approximately 25–30 min after the initiation of egg activation (3, 15).

Contact with seawater, at spawning, initiates egg activation, which includes the release of JP and the establishment of a jelly layer around the egg (3, 11, 16). By 5 min post-spawning, the release of the JP and the coincident decrease in the depth of the crypts are evident (Fig. 3A, B). At approximately 10 min post-spawning, the crypts have disappeared and the JP has formed a corona around the egg (Fig. 4A). The "bottle-brush" structures are dispersed by this time, appear to be reduced in number, and are now embedded in a flocculent matrix (Fig. 4B). By 15 min post-spawning, a jelly layer has formed around the egg (Fig. 5A); this layer is composed entirely of a flocculent matrix with no apparent "bottle-brush" structures remaining (Fig. 5B). In addition, a fibrous surface coat has formed from the granular material that had been closely associated with the oolemma prior to egg activation (see Fig. 2B and also ref. 3).

The hatching envelope of *S. ingentis* eggs forms about 40–45 min post-spawning and is the result of the sequential exocytosis of two populations of cortical vesicles that appear after the initiation of egg activation (3, 16). Not only do the exocytosis of cortical vesicles and the resultant development of the hatching envelope occur after jelly layer formation, but these events also appear to be independent of the presence of the jelly layer. Eggs that have been stripped of the jelly precursor, and thus do not form a jelly layer, develop hatching envelopes that appear identical to those of normal eggs (3). Morphological evidence suggests that the surface coat serves as a template on which the hatching envelope forms (3).

Egg activation in the Penaeoidea initiates a series of cortical changes that coincide with the loss of one ECM (the vitelline envelope) and the formation of three other ECMs (the jelly layer, surface coat, and hatching envelope) (see Fig. 6). The time course of these alterations may differ from one genus, or species, to the next, but the events are consistent for all penaeoids studied to date (1, 2, 3, 11, 15, 17). The jelly layer in penaeoid eggs appears after the onset of egg activation and is formed from JP that is housed in extracellular crypts prior to activation. The hatching envelope is elaborated subsequent to jelly layer formation and is the result of the exocytosis of two populations of cortical vesicles that arise in the cortex of the egg after initiation of activation.

Acknowledgments. This work was supported in part by NOAA, National Sea Grant College Program, Department of Commerce, under grant number NA85AA-D-SG140 project number R/A-61 through the California Sea Grant College Program, grant number NA85AA-D-SG141 project number R/SA-1-PD through the Louisiana Sea Grant College Program, and USDA Competitive Grant number 87 CRCR-1-2514.

Literature Cited

1. **Clark, W. H., Jr., and J. W. Lynn. 1977.** A Mg^{++} dependent cortical reaction in the eggs of penaeid shrimp. *J. Exp. Zool.* **200:** 177–183.
2. **Clark, W. H., Jr., J. W. Lynn, A. I. Yudin, and H. O. Persyn. 1980.** Morphology of the cortical reaction in the eggs of *Penaeus aztecus*. *Biol. Bull.* **158:** 175–186.
3. **Pillai, M. C., and W. H. Clark Jr. 1988.** Hatching envelope formation in shrimp (*Sicyonia ingentis*) ova: origin and sequential exocytosis of cortical vesicles. *Tissue & Cell* **20:** 941–952.
4. **Hudinaga, M. 1942.** Reproduction, development and rearing of *Penaeus japonicus*. *Jpn. J. Zool.* **10:** 305–393.
5. **Duronslet, M. J., A. I. Yudin, R. S. Wheeler, and W. H. Clark Jr. 1975.** Light and fine structural studies of natural and artificially induced egg growth of penaeid shrimp. *Proc. 6th Ann. Workshop, World Maricul. Soc.* **6:** 105–122.
6. **King, J. E. 1948.** A study of the reproductive organs of the common marine shrimp, *Penaeus setiferus* (Linnaeus). *Biol. Bull.* **94:** 244–262.
7. **Cummins, W. C. 1961.** Maturation and spawning of the pink shrimp, *Penaeus durorum* Burkenroad. *Trans. Am. Fish. Soc.* **90:** 462–468.
8. **Bradfield, J. Y., R. L. Berlin, S. M. Rankin, and L. L. Keeley. 1989.** Cloned cDNA and antibody for an ovarian cortical granule polypeptide of the shrimp *Penaeus vanamei*. *Biol. Bull.* **177:** 344–349.
9. **Anderson, S. L., E. S. Chang, and W. H. Clark Jr. 1984.** Timing of post vitellogenic ovarian changes in the ridgeback prawn *Sicyonia ingentis* (Penaeidae) determined by ovarian biopsy. *Aquaculture* **42:** 257–271.
10. **Yano, I. 1988.** Oocyte development in the kuruma prawn *Penaeus japonicus*. *Mar. Biol.* **99:** 547–553.
11. **Clark, W. H., Jr., A. I. Yudin, F. J. Griffin, and K. Shigekawa. 1984.** The control of gamete activation and fertilization in the marine Penaeidae, *Sicyonia ingentis*. *Adv. Invert. Reprod.* **3:** 459–471.
12. **Lynn, J. W., and W. H. Clark Jr. 1987.** Physiological and biochemical investigations of the egg jelly release in *Penaeus aztecus*. *Biol. Bull.* **173:** 451–460.
13. **Talbot, P. 1981.** The ovary of the lobster, *Homarus americanus*. I. Architecture of the mature ovary. *J. Ultrastruct. Res.* **76:** 235–248.
14. **Talbot, P., and M. Goudeau. 1988.** A complex cortical reaction leads to formation of the fertilization envelope in the lobster, *Homarus*. *Gam. Res.* **19:** 1–18.
15. **Pillai, M. C., and W. H. Clark Jr. 1990.** Development of cortical vesicles in *Sicyonia ingentis* ova: their heterogeneity and role in elaboration of the hatching envelope. *Mol. Reprod. Dev.* **26:** (in press).
16. **Pillai, M. C., and W. H. Clark Jr. 1987.** Oocyte activation in the marine shrimp, *Sicyonia ingentis*. *J. Exp. Zool.* **244:** 325–329.
17. **Glass, P. S., J. W. Lynn, and J. D. Green. 1989.** Extracellular assembly of the hatching envelope around *Trachypenaeus similis* eggs in low sodium seawater. *J. Cell Biol.* **109:** 128a.
18. **Pillai, M. C., F. J. Griffin, and W. H. Clark Jr. 1988.** Induced spawning of the decapod crustacean *Sicyonia ingentis*. *Biol. Bull.* **174:** 181–185.

Reference: *Biol. Bull.* **178:** 300–304. (June, 1990)

Revival of Dobell's "Chromidia" Hypothesis: Chromatin Bodies in the Amoebomastigote *Paratetramitus jugosus*

LYNN MARGULIS, MICHAEL ENZIEN*, AND HEATHER I. MCKHANN**

Department of Botany, University of Massachusetts, Amherst, Massachusetts 01003

Multiple fission of a mature *Paratetramitus jugosus* (approx. 10 μm long) resulted in the production of many small, roughly spherical (2–7 μm in diameter) amoebae (1). Our observations of live material and examination of over two hundred micrographs lead us to suggest that DNA-containing membrane-bounded chromatin bodies bud amitotically from the nucleus. DAPI-stained bodies of these were observed in the cytoplasm of amoebae, mastigotes, and cysts, and at least some of these chromatin bodies seemed to be released into the medium. This interpretation revives for *P. jugosus* the "chromidia hypothesis" of Dobell (2). Our data, consistent with the descriptions of Dobell (2), Hogue (3), and Wherry (4), indicate that encysting amoebae may reproduce by chromidia. Dobell's original chromidia concept was limited to amoebae. Others claimed for it far-reaching consequences: "chromidia" were touted as an explanation for embryogenesis and histogenesis of metazoa. Although there is no evidence for chromidia in animals, outright rejection of Dobell's chromidia hypothesis *sensu stricto* as an amitotic multiple fission process in amoebae is unjustified.

Paratetramitus jugosus from microbial mats grows rapidly (5); a small inoculum of this amoebomastigote can lead to a confluent culture populating a petri plate within 2–3 days (6). Small DNA-positive bodies and tiny amoebae are ubiquitous in all *P. jugosus* cultures (1). Chromatin bodies, recognized in electron micrographs (EMs) of *Paratetramitus jugosus* and in the medium, are not present in cytoplasmic buds (1; Fig. 1A), but they are clearly present in the cytoplasm (Fig. 1A, B). After we failed to obtain evidence for sufficiently rapid reproduction by mitosis, budding, or other known reproductive mode, we noticed that chromatin bodies are present in vacuoles (1). Nearly all amoebae are conspicuously vacuolated but, in EMs, water-pumping and food-digesting cytoplasmic vacuoles cannot be distinguished. Cytoplasmic vacuoles generally contain either the chromatin bodies or decomposing bacterial food; both may be present in a single vacuole. The intracellular chromatin bodies themselves show varying morphologies from extremely compact forms to highly vacuolated structures (Fig. 1). Chromatin bodies seem to bud from nuclei in close proximity to vacuoles (Fig. 2). They may pass through heavily vacuolated cytoplasm or be released directly into the medium (Fig. 11 in ref. 1). The tendency to vacuolate is clearly intrinsic to the organism since heavily vacuolated amoebae with degraded cytoplasm (*e.g.*, Fig. 1B) are seen in the same thin sections as well-preserved, entirely intact *P. jugosus* cells. Nuclear budding, vacuolation, release of chromatin bodies, and digestion of bacteria apparently occur in the mastigote as well as the amoeba stage (note in Fig. 11 of ref. 1, the presence of the undulipodium, signifying the mastigote stage; the figure was originally misidentified as an amoeba). The "chromatin bodies" strikingly resemble structures described early in the century by several investigators. Are they "chromidia"?

"Chromidia," by definition, are nucleus-derived bodies composed of the same material as chromatin (*i.e.*, nucleoprotein complexes comprising eukaryotic chromosomes) and capable of producing new cells—or at least new nuclei. Chromidia were defined by Dobell (2) in a description of the life history of *Arachnula impatiens* (Cienkowski):

Received 15 September 1989; accepted 12 March 1990.

* Current address: Department of Biology, Boston University, 5 Cummington Street, Boston, MA 02215.

** Current address: Department of Biology, University of California at Los Angeles, Los Angeles, CA 90024.

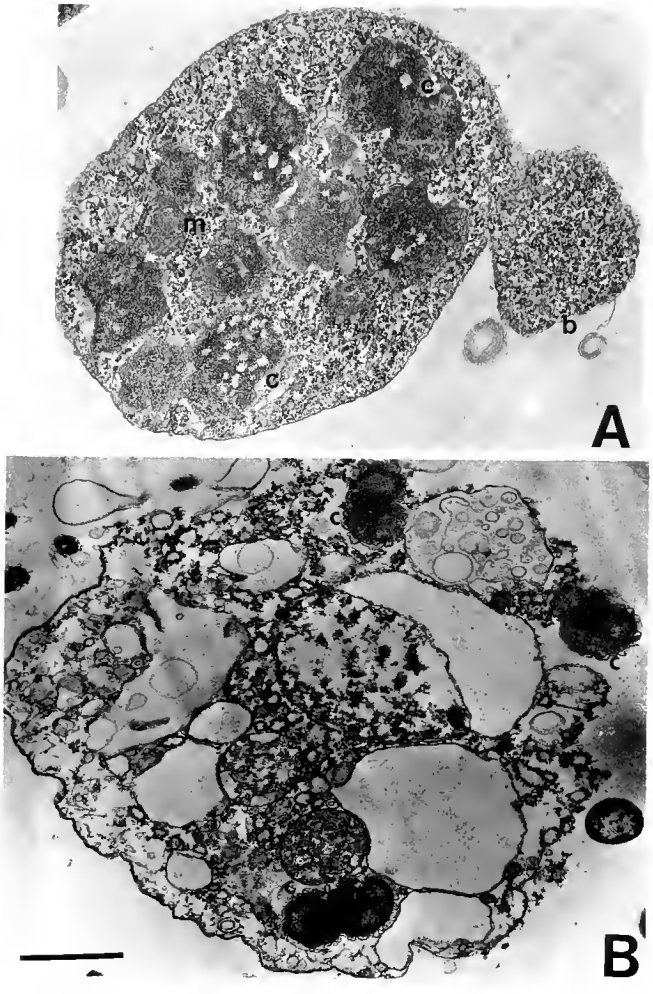

Figure 1. A. Heavily vacuolated cytoplasm containing at least eight chromatin bodies (c) distinguishable from mitochondria (m). Bud or fragment of amoeba (b) (Bar = 1 μm; neg. 1117). B. "Degrading cytoplasm or cystic residue" in which at least three chromatin bodies (c) can be seen (Bar = 1 μm; neg. 2048).

> "Numerous refringent granules can be seen . . . they vary in size, but are mostly of extreme minuteness. Many of them stain deeply with chromatin stains, and for this reason—and for another which will be apparent when I have described other stages in the life cycle—I shall call them chromidia." (2, p. 322)

In reviewing this and other work, Professor E. B. Wilson of Columbia University, writing in the most influential biology text of the early century, concluded that chromidia are

> "small granules or larger irregular clumps of chromatin or a related substance, scattered through the protoplasm without forming a single individualized body [nucleus]." (7, p. 33)

Characterized in part by their staining reactions and resistance to "peptic digestion" (proteolytic enzymes, ref. 7, p. 25), chromidial granules were asserted to multiply by division.

> "Both chromidia and mitochondria formerly belonged to that miscellaneous assemblage of granules known as 'microsomes'. Up to a rather late period the two were often confused and even now considerable uncertainy exists concerning their identification. Theoretically an essential distinction lies in the fact that chromidia are of nuclear origin and composed of 'chromatin' while mitochondria are considered by nearly all recent students of the subject as strictly cytoplasmic; but in practice the determination of the origin of these bodies is not an easy task." (7, p. 700)

Two well-known German zoologists then conferred great meaning on "chromidia." R. Hertwig first suggested, and R. Goldschmidt then developed, an elaborate "chromidial hypothesis," which was reviewed by Wilson (7) (see Wilson for original references).

> ". . . differentiation . . . is largely brought about by a periodic emission of chromatin from the nucleus . . ." (7, p. 703)
>
> "The chromidia hypothesis underwent a sudden expansion with the works especially of Goldschmidt, Popoff and still later of Buchner and of Schaxel by whom an attempt was made to extend it to the Metazoa and to elaborate

Figure 2. Mature amoeba with at least five vacuoles (v); the membranes of at least one are in direct contact with the nucleus (n). (Bar = 1 μm; neg. 3633).

a general theory of the chromidia. Goldschmidt (1904) described in the epithelial, muscular, glandular and connective-tissue-cells a 'chromidial apparatus' consisting of basophilic granules and fibrillar formations which were assumed, mainly because of a general similarity of staining-reactions, to be extruded basichromatin destined to play a particular role in the trophic functions of the cell (p. 726); and Goldschmidt accepted the problem of a similar origin of many other well-known cytoplasmic structures, including the mitochondria, the yolk-nucleus, nebenkern, pseudochromosomes, reticular apparatus, ergastoplasm and cytomicrosomes. These conclusions were extended to the germ-cells by Wassilieff (1907), Popoff (1907), and Bucher (1909, 1910), all of whom concluded that the cytoplasmic granules and filaments aggregated near one pole of the nucleus . . . are chromidia extruded from the nucleus . . ." (7, pp. 702–703)

Most careful observers rejected the attempts of Goldschmidt and others to relate chromidia to theoretical explanations of embryonic development. The case was considered closed by Dogiel and most other protozoologists by 1965.

Chromidia are no longer considered as chromatin inclusions, emerging from the nucleus into the cytoplasm and capable of reproducing new nuclei in the plasma. All the examples of this kind of nucleus formation have been shown to be based on inaccurate and erroneous observations by investigators during the first two decades of the twentieth century. Therefore, the theory of chromidia has been abandoned and, to avoid misunderstanding, the term 'chromidia' should not be used. (8, p. 28)

We, however, find the original "chromidia hypothesis" for reproduction of amoebae to be an attractive explanation for the rapid growth of *P. jugosus* populations (1). Furthermore, Dobell's (2) study of amoeba reproduction accurately describes the salient features of the *P. jugosus* life history. Dobell's light-micrograph-based drawings of *Arachnula* (especially Fig. 343 a, c, g and f; also reproduced in ref. 7, p. 702) are uncannily similar to ours, although *Paratetramitus jugosus* is much smaller and seldom contains more than a single vesicular nucleus.

"Dobell's recent studies of this form show that in its ordinary . . . condition it contains a variable number of vesicular nuclei. During encystment the nuclei are said to give off numerous chromidia to the cytoplasm and finally wholly disappear as such, now being represented only by the scattered chromidial granules (Fig. 343). The cell thereupon breaks up to form a brood (10–20) of small daughter cells, containing chromidia which give rise to a number of vesicular nuclei each of which seems to arise by growth (and multiplication?) of a single granule. (7, pp. 701–702)

Wilson cautiously concludes that increase in number and size of chromidia over the life cycle

". . . has never been sufficiently confirmed by later observers, either in bacteria or other Protista; nevertheless there has been a rather general, more or less tacit, assumption that the chromidia are endowed with such powers." (7, p. 702)

The expanded version of the chromidia hypothesis was justifiably abandoned; chromidial reproduction has not been shown in animals and cannot serve as an explanation of metazoan differentiation. Yet Dobell's original concept was perhaps prematurely rejected for protoctists.

At any stage, one or more chromatin bodies may be present in amoeba cytoplasm. In healthy *Paratetramitus jugosus*, chromatin bodies are apparently released through parental vacuoles, whereas in degenerating amoebae, they may be released from heavily vacuolated parental cytoplasm as it disintegrates, yielding what Dobell called a "cystic residue" (2, p. 333; Fig. 1B, 3). We suggest that the chromatin bodies we are observing are tiny young "chromidia," which contain membranes, ribosomes, and a thin layer of cytoplasm (Fig. 1A; 3A, C); these upon release develop into small amoebae (2–3 μm) which then grow into the typical "limax" amoebae with a vesicular nucleus.

Life histories comparable to Dobell's *Arachnula* were seen in live material for two "vahlkampfiid amoebae," *Vahlkampfia calkensi* (3) and *Vahlkampfia* sp. No. I (4). The figures of Wherry (3, 4, 7 and 9) and Hogue (25–27 and 31) depict remarkably well what we observe in most *P. jugosus* amoebae. Chromidial reproduction stages in vahlkampfiid amoebae (from the Oakland, California, water supply, ref. 4; or symbiotic in oysters from Woods Hole, Massachusetts, ref. 3) were clearly depicted. Hence, Dobell's (2) *A. impatiens* is only one of several amoebae with "chromidial stages." *Arachnula*, now classified with the Granuloreticulosa, is still poorly known; although presumed to be a "naked foraminiferan" (9), it may be related to vahlkampfiid amoebomastigotes.

Chromidia and multiple fission products leading to a 10–20 offspring "brood," amply detailed by Dobell, requires further investigation. Our examination of live material and over 200 micrographs (phase contrast, Nomarski differential interference contrast, scanning and transmission electron micrographs) of Baja California, Cuban, and American Type Culture Collection *Paratetramitus jugosus* cultures lead us to agree with Dobell (2), Hogue (3) and Wherry (4), all of whom claimed that chromidia are normal propagules in the life history of certain mastigote amoebae.

Now that protoctists are excluded from the animal kingdom, which is defined by its blastular embryos, "protozoa" as a phylum no longer exists. We propose reviving the possibility that *Paratetramitus jugosus* and

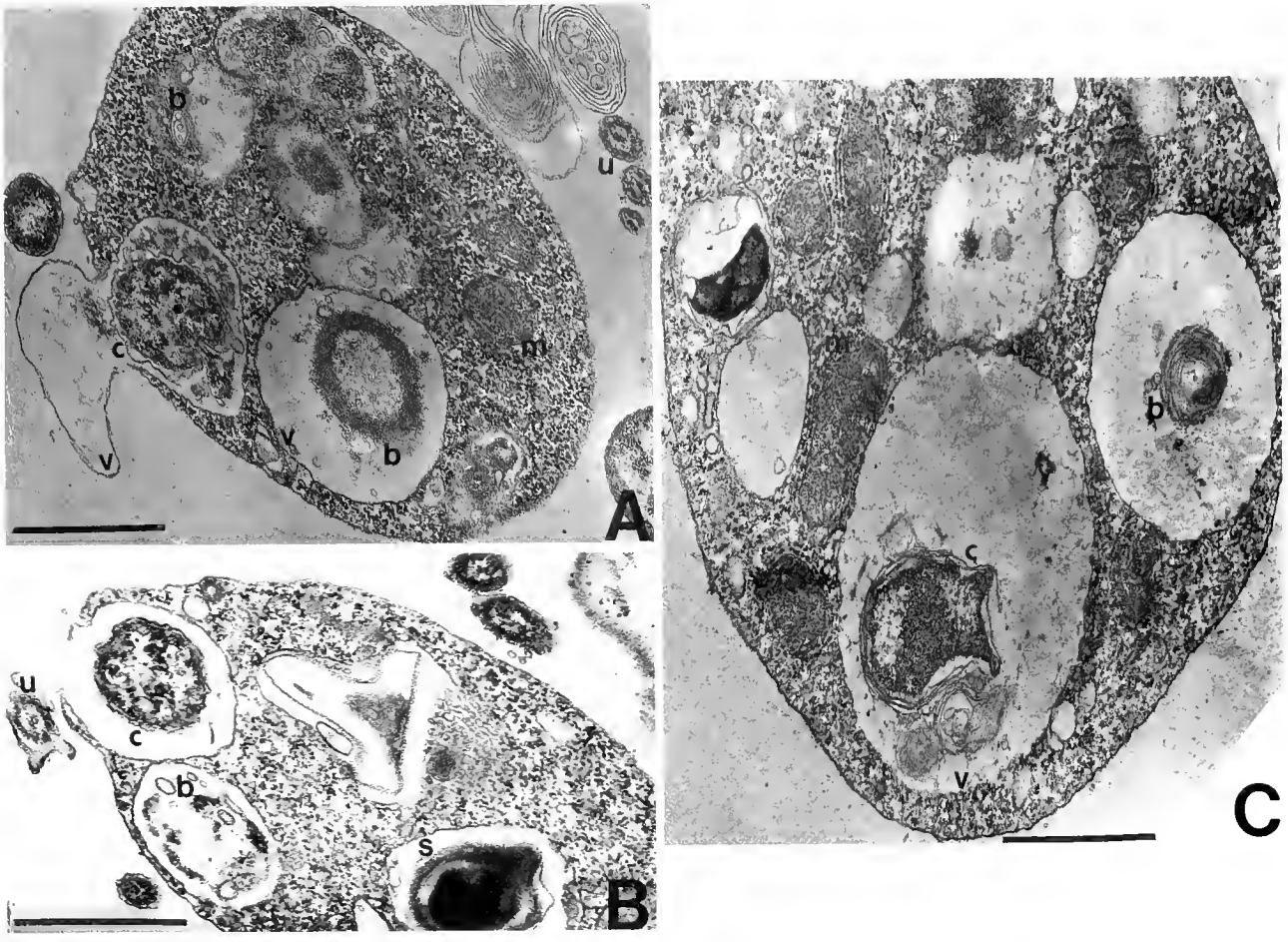

Figure 3. Vacuolated cytoplasm of *Paratetramitus jugosus*. vacuoles may contain either chromatin bodies (c) or bacterial remains (b). A. Swollen vacuole contains coated chromatin body (c); four other vacuoles (v) probably contain bacterial food remnants. Mitochondria (m), not in vacuoles, are distinguishable from chromatin bodies. The [9(2) + 2] axoneme of two undulipodia (u), here and in B, suggest these organisms are mastigotes (neg. 1120). B. Bacterial spore (S) in one vacuole and remains (b) in another with a chromatin body (c) apparently in the process of release (neg. 2155). C. Bacterial remains (b) and membrane-coated chromatin body in large peripheral vacuoles (v) (neg. 1261). All bars = 1 μm.

other protoctists (such as certain vahlkampfiids and *Arachnula*) produce and release chromidia.

That multiple fission, which usually occurs within cysts, can take place entirely independently of encystation was amply demonstrated in *Entamoeba histolytica* by Cleveland and Saunders (10); their "chromatoid bodies," thought to be phosphorus reserves, deserve, like chromidia, re-evaluation in a modern context. Multiple fission, which has long been known in other protoctists, notably suctorian and chonotrich ciliates (11, 12), was recently seen in large *Trichosphaerium*-like marine amoebae which feed on brown algae (*e.g.*, *Sargassum*; ref. 13). These studies with live amoebae demonstrate that electron microscopy and molecular biology enormously aid in the interpretation of live material but can never supplant it.

Anoxia may select for rapid propagule production; chromidia formation seems to be more prevalent than standard amoeba promitosis under conditions of low ambient oxygen as suggested by Wherry (4). Observations of live amoebomastigotes, grown under controlled oxygen concentrations, must be further correlated with their fine structure morphology. Chromidia must be isolated and cloned for study by molecular biological techniques. The qualitative and quantitative relationship of the DNA of chromatin bodies to nuclear DNA must be determined. The nature of the membranes and ribosomes accompanying the DNA of chromatin bodies must be characterized by biochemical techniques. Only after such difficult tasks are accomplished can the existence of chromidia be entirely substantiated. We demonstrate here, however, that the rejection of Dobell's chro-

midial concept by proto- and other zoologists (*e.g.*, ref. 8) was probably premature and prejudicial. Protoctists are not little animals (14, 15, 16). This realization revives claims earlier in this century of the uniqueness of many protoctist structures and processes, including the formation, cytoplasmic passage and vacuolar release of chromidial propagules of amoebomastigotes.

†Note added in proof

A book written in Russian by B. Swarczewsky about the chromidial concept has come to our attention. The transliterated title is *Kromidial'nyiia obrazovaniia u protozoa.* Published in Kiev by the Imperial University Press in 1912, the book is a *Memoire de la Société des Naturalistes de Kieff, Vol. XXII.* A German translation, found on the title page, reads *Die Chromidien der Protozoen und ihre Beziehung zur Chromatindualismushypothese.* From the drawings found in this 176-page book, we infer that some of the phenomena described in the present paper are also discussed in this volume.

Acknowledgments. We are grateful to Floyd Craft for aid with electron microscopy, and to René Fester and Thomas Lang for manuscript preparation; we thank the Lounsbery Foundation, NASA Life Sciences, and research trust funds at the University of Massachusetts for financial support.

Literature Cited

1. **Enzien, M., H. I. McKhann, and L. Margulis. 1989.** Ecology and life history of an amoebomastigote, *Paratetramitus jugosus,* from a microbial mat: new evidence for multiple fission. *Biol. Bull.* **177:** 110–129.
2. **Dobell, C. 1913.** Observations on the life-history of Cienkowski's "*Arachnula.*" *Arch. Protistenkd.* **31:** 317–353.
3. **Hogue, M. 1914.** Studies of the life history of an amoeba of the Limax group. *Arch. Protistenkd.* **35:** 154–163.
4. **Wherry, W. B. 1913.** Studies on the biology of an amoeba of the limax group. *Vahlkampfia* sp. No. 1. *Arch. Protistenkd* **31:** 77–94.
5. **Stolz, J. F. 1990.** Distribution of phototrophs in the flat laminated microbial mat at Laguna Figueroa, Baja California, Mexico. *BioSystems* **23:** 345–357.
6. **Read, L. K., L. Margulis, J. Stolz, R. Obar, and T. K. Sawyer. 1983.** A new strain of *Paratetramitus jugosus* from Laguna Figueroa, Baja California, Mexico. *Biol. Bull.* **165:** 241–264.
7. **Wilson, E. B. 1925.** *The Cell in Development and Heredity,* 3rd edition. The Macmillan Company, New York.
8. **Dogiel, V. A. 1965.** *General Protozoology,* 2nd edition. (Revised by J. I. Poljanskij and E. M. Chejsin.) The Clarendon Press, Oxford, England.
9. **Lee, J. J. 1990.** Granuloreticulosa. Pp. 524–548 in *Handbook of Protoctista: The Structure, Cultivation, Habitats and Life Cycles of the Eukaryotic Microorganisms and Their Descendants Exclusive of Animals, Plants and Fungi.* L. Margulis, J. O. Corliss, M. Melkonian, and D. J. Chapman, eds. Jones and Bartlett Publishers, Boston.
10. **Cleveland, L. R., and E. P. Saunders. 1930.** Encystation, multiple fission without encystment, excystation, metacystic development, and variation in a pure line and nine strains of *Entamoeba histolytica. Arch. Protistenkd.* **70:** 224–266.
11. **Corliss, J. O. 1979.** *The Ciliated Protozoa. Characterization, Classification and Guide to the Literature.* Pergamon, Press, London.
12. **Raikov, I. B. 1982.** *The Protozoan Nucleus: Morphology and Evolution.* Springer Verlag, Vienna and New York.
13. **Polne-Fuller, M. 1987.** A multinucleated marine amoeba which digests seaweeds. *J. Protozool.* **34:** 159–165.
14. **Corliss, J. O. 1990.** Toward a nomenclatural protist perspective. Pp. xxv–xxx in *Handbook of Protoctista: The Structure, Cultivation, Habitats and Life Cycles of the Eukaryotic Microorganisms and Their Descendants Exclusive of Animals, Plants and Fungi.* L. Margulis, J. O. Corliss, M. Melkonian, and D. J. Chapman, eds. Jones and Bartlett Publishers, Boston.
15. **Margulis, L. 1990.** Introduction. Pp. xi–xxiii In *Handbook of Protoctista: The Structure, Cultivation, Habitats and Life Cycles of the Eukaryotic Microorganisms and Their Descendants Exclusive of Animals, Plants and Fungi.* L. Margulis, J. O. Corliss, M. Melkonian, M. and D. J. Chapman, eds. Jones and Bartlett Publishers, Boston.
16. **Margulis, L., and D. Sagan. 1985.** Order amidst animalcules: the Protoctista kingdom and its undulipodiated cells. *BioSystems* **18:** 141–147.

INDEX

E

F

G

H

I

J

K

L

M

N

O

P

Q

R

S

T

U

V

W

X

Y

Z

CONTENTS